Université de Strasbourg

UNIVERSITÉ DE STRASBOURG

École doctorale Sciences de la vie et de la santé | ED 414 Université de Strasbourg

ÉCOLE DOCTORALE DES SCIENCES DE LA VIE ET DE LA SANTÉ

INSERM – U1113 - IRFAC

THÈSE présentée par :

Maria Virginia GIOLITO

soutenue le : **21 Juin 2022**

pour obtenir le grade de : **Docteur de l'université de Strasbourg**

Discipline/ Spécialité : Aspects moléculaires et cellulaires de la biologie

Régulation et fonction du récepteur nucléaire des hormones thyroïdiennes TRa1 dans la biologie des cellules souches cancéreuses des cancers coliques

THÈSE dirigée par :
Mme PLATEROTI Michelina PhD, Université de Strasbourg

RAPPORTEURS :
M MOSCHETTA Antonio NOM Prof, University of Bari "Aldo Moro", Italy.
M DE SANTA BARBARA Pascal DR, Université de Montpellier

AUTRES MEMBRES DU JURY :
M. METZGER Daniel DR, Université de Strasbourg

INVITÉS :
Mme MARTIN Sophie CR, Université de Strasbourg

“A scientist in her laboratory is not a mere technician: she is also a child confronting natural phenomena that impress her as though they were fairy tales.”

Marie Skłodowska-Curie.

Acknowledgements

First of all, I would like to thank Antonio Moschetta and Pascal de Santa Barbara for accepting and taking the time to read and judge my thesis work. I would also like to thank Daniel Metzger and Sophie Martin for being part of my thesis jury and participating in evaluating this thesis during the defence.

I want to thank Michela Plateroti, my thesis supervisor, for taking the risk of choosing a young woman from the other side of the world to do the thesis with her. I am grateful for your trust through these years and for letting me develop the project freely, under your advice and for encouraging me in each step.

I want to thank David Volle and Fabrice Labial for being part of my thesis committee during these years and for their insightful scientific discussions and encouragement.

I especially thank the lab members I had the pleasure of working with during these three years. Some of whom I had the chance to share some months with were Catherine, Gaspard, Matthias, Chloe, Benjamin, Alexis, and Louise. Moreover, to those who had to bear me long enough. Diana, thanks for the talks of life and gossip; Gautier, thanks for following my crazy padawan techniques when doing experiments it made it more fun; Leo, thanks for your help over these years and for making every experiment more fun, and I hope the SEC will continue over time. My biggest thanks go to Theo and Serguei. Without you both, I could not have done as much as I did during this thesis. I am truly grateful. And finally, Carla. You have been a friend since the beginning. Thanks for adopting me as another little sister of yours and always helping me inside and outside the lab.

Thanks to all the people I met in the CRCL and the IRFAC. Thanks to all the people that received us with open arms when we moved. Special thanks to Elisabeth for always answering my questions with a smile and being a listener. Thanks to Isabelle Gross for her counselling and scientific discussions over luciferase experiments, being part of my thesis committee, and her encouragement. I would like to thank Jean-Noel Freund for his discussions of science and much more. I equally thank all students, PhDs and postdocs of the IRFAC for the moments we shared in the cafeteria, in the sun or between experiments. A particular thought to Celine, Chloe, Ourania, Matthieu, Andrea and from downstairs, Sevda and Chloe.

I am thankful to my friends from Argentina that they always made themselves present in one way or another, although being far away. Thanks to my friends from the university, and especially to

my “older” friends: Vicky, Maca and Juli, for always being by my side for years, although now it is by video. Thanks to the friend I met in France, my dear Argentinian, Euge, a great supporter during these years because she knew what it is to be so far away from home. Thanks for the mates and the talks.

Infinite thanks to my family, who supported me in whatever I wanted to do, especially when I decided to go after my dream to the old continent. A particular thanks to my parents, Fanny and Gustavo, and brother Agustín for being my unwavering support, psychologists, and routine video call. Thanks a million for always trusting me. Thanks to Ipa and Amber, my two golden retriever dogs, for always being so crazy and cute that it makes me laugh every time I see them on a video call. Thanks to my grandmothers, Olga and Raquel for always being there and giving me support from a distance. Thanks to my grandfather, Ángel, who takes care of me although he is no longer with us. I always find you when I look at the moon.

Thanks to my French family, who opened me their home during the pandemic and, from then on, took me as one more of them. Many thanks, especially to Yvette, Bruno and Elodie. You have been valuable support during these years.

Finally, the best for the end. My heart and thoughts go to Sébastien for his advice, patience, faith, and encouragement in every step of this thesis because he always understood. He gave me immense stability, without which I would never have been able to get to where I am now. For his infinite tenderness and the countless times he made me laugh. There are not enough words to express my feelings for you, but you already know everything when I look at you. Always.

Table of contents

Table of Figures

List of Tables

Abbreviations

5-FU: 5-fluorouracil
ABC: ATP Binding Cassette
ABCB1: ATP Binding Cassette B family member 1
ABCC1: ATP Binding Cassette C family member 1
ABCC11: ATP Binding Cassette C family member 11
ABCC2: ATP Binding Cassette C family member 2
ABCC3: ATP Binding Cassette C family member 3
ABCC4: ATP Binding Cassette C family member 4
ABCC5: ATP Binding Cassette C family member 5
ABCC6: ATP Binding Cassette C family member 6
ABCG2: ATP Binding Cassette G family member 2
ADME: Absorption, distribution, metabolisation and excretion
ALDH: Aldehyde dehydrogenase
AMP: aadenosinemonophophate
APC: Adenomatous Polyposis Coli
AR: Androgen receptor
ASCL2: Achaete-Scute Family BHLH Transcription Factor 2
ATOH1: Atonal BHLH Transcription Factor 1
ATP: adenosine triphosphate
ATP7: ATPase Copper Transporting
BCRP: Breast cancer resistance protein
BMP: bone morphogenic protein
BMPR: bone morphogenic protein receptor
CAF:cancer-associated fibroblasts
CAR: constitutive androstane receptor
CBC: crypt-base columnar cell
CCND1: cyclin D1
CES: Carboxylesterase
CHGA: chromogranin A
CIMP: CpG island methylator phenotype
CIN: chromosomal instability
CMS: consensus molecular subtype
COX: Cyclooxygenase
CRC: colorectal cancer
CSC: cancer stem cell
CTLA-4: cytotoxic T-lymphocyte antigen-4
CTNNB1: b catenin
CYP: Cytochrome P450 Family
DBD: DNA binding domain
DCLK1: doublecortin-like kinase 1
DHFU: dihydro fluorouracil
DHH: desserthedgehogd
DIO: deiodinase
DIT: diiodotyrosine
DKK: Dickkopf
DLL: delta-like ligand
DNA: deoxynucleic acid
DPYD: dihydropyrimidine dehydrogenase
DPYS: dihydropyrimidinease
DR4: direct repeat 4
DTP: drug-tolerant persister
DTR: diphtheria toxin receptor
DUOX2: NADPH dual oxidase 2
EEC: enteroendocrine cell
EGF: epidermal growth factor
EGFR: epidermal growth factor receptor
EMT: epithelial to mesenchymal transition
ER: estrogen receptor
FACS: Fluorescence-activated cell-sorted
FAP: familial adenomatous polyposis
FBAL: fluoro-beta-alanine
FdUMP: fluorodeoxyuridine monophosphate
FGF: fibroblast growth factor
FUDP: fluorouridine diphosphate
FUDR: fluorodeoxyuridine
FUMP: fluorouridine monophosphate
FUPA: fluoro-beta-ureidopropionate
FUR: fluroridine
FUTP: fluorouridine triphosphate
FZD: Frizzled
GAP: GTPase-activating proteins
GFP: green fluorescent protein
GLI: glioblastoma
GLUT1: glucose transporter 1
GR: glucocorticoird receptor
GREM1: gremlin 1
GSK3: glycogen synthase kinase 3
GST: glutathione-S-transferase
GTP: Guanosine triphosphate
HCC: hepatocellular carcinoma
HES1: Hairy/enhancer of split 1
HH: hedgehog
HIF1: hypoxia-inducible factor 1
HLH: helix-loop-helix
IHH: Indian hedgehog
IL: interleukin
IRES: Internal ribosome entry site
IRI: irinotecan
ISC: intestinal stem cell
JNK: c-JUN N-terminal kinases
KRAS: small GTPase Kirsten sarcoma viral oncogene homolog
KRT20: keratin 20
LAT: large neutral amino acid transporter
LATS: large tumour suppressor kinase
LBD: ligand-binding domain
LGR5: leucine-rich repeat-containing G protein-coupled receptor 5
LRC: label-retaining cell
LRIG1: leucine-rich repeats and immunoglobulin-like domains protein 1
LRP5/6: low-density lipoprotein receptor-related protein 5/6
LV: leucovorin
LXR: liver X receptor
MAPK: mitogen-activated protein kinase
MCT: monocarboxylate transporter

MDR: multigrup resistance
MDR1: multidrug resistance 1
MIT: monoiodotyrosine
MMP2: matrix metalloproteinase 2
MRP: multidrug resistance protein
MSI: microsatellite instability
MSS: microsatellite stable
NICD: notch intracellular domain
NIS: Na+/I- symporter
NOS3: nitric oxide synthase 3
NQO: NADH Quinone Oxidase
NR: nuclear receptor
OATP: organic anion transporter protein
OLFM4: Olfactomedin 4
OXA: oxaliplatin
PC: Paneth cells
PD1: programmed cell death 1
PFKP: phosphofructokinase platelet
PI3K: phosphatidyl-inositol-3-kinase
PLC: phospholipase C
PPAR: peroxisome proliferator-activated receptors
PR: progesterone receptor
PROM1: prominin 1
PTCH: patched
PTGS: Prostaglandin-Endoperoxide Synthase
PXR: Pregnane X Receptor
RAR: retinoic acid receptor
RB: retinoblastoma
RBPJ: Recombination Signal Binding Protein For Immunoglobulin Kappa J Region
RNA: ribonucleic acid
ROS: reactive oxygen species
rT3: reverse triiodothyronine
RXR: Retinoid X Receptor
SC: stem cell
SCNA: somatic copy number alteration
sFRP2: secreted frizzled-related protein-2
SHH: sonic hedgehog
SLC: Solute-like carrier
SLCO: Solute Carrier Organic Anion Transporter Family
T2: diiodothyronine
T3: triiodothyronine
T4: tetraiodothyronine
TA: transit-amplifying
TBG: thyroxine-binding globulin
TCF: T cell factors
TERT: Telomerase Reverse Transcriptase
TG: thyroglobulin
TGF: transforming growth factor b
TH: thyroid hormone
THRA: Thyroid hormone receptor alpha
THRB: Thyroid hormone receptor beta
TKI: tyrosine kinase inhibitor
TME: tumour microenvironment
TOP1: topoisomerase I
TPO: thyroid peroxidase
TR: Thyroid receptor
TRE: Thyroid responsive element
TRH: thyroid releasing hormone
TSH: thyroid-stimulating hormone
TYMP: thymidylate phosphorylase
TYMS: thymidylate synthase
UDP: uridyldiphosphate
UGT: uridine diphosphate glucuronosyltransferase
UMP: uridylmonophosphate
UPB1: beta-ureidopropionase
UTP: uridyltriphosphate
UTR: untranslated region
VDR: vitamin D receptor
VEGF: vascular epidermal growth factor
VEGFR: vascular epidermal growth factor receptor
WIF1: WNT inhibitor factor 1
WT: wild-type
YAP1: Yes-associated protein 1

Chapter 1: Tales from the intestine - to the crypt and beyond

Getting to know the intestine - Intestinal architecture, niche signals in tissue renewal, plasticity, and homeostasis

Intestinal epithelium architecture

The intestine is a long tubular organ consistent in two major parts, the small intestine and the colon (called the large intestine). With its 6 m length, the human small intestine oversees the efficient uptake of nutrients. At the same time, the colon is specialised in water and electrolytes reuptake and elimination of non-digested food and waste. Both the human small intestine and colon specialise in protecting the body from xenobiotics. The small intestine consists of three major anatomical parts: the duodenum (approx. 25 cm long), which is the shortest and widest portion, the jejunum (approx. 2, 5 m long) and finally, the ileum (approx. 3,5 m long). Between the ileum and the colon, we find the caecum, and finally, we have the colon, the rectum and the anal conduct that compose the large intestine. The colon consists of four parts according to its anatomical location, the ascending colon, the transverse, the descendent and the sigmoidal colon [1,2].

The intestinal epithelium has a particular structure that increases the contact surface, facilitating its role in the body. The small intestine has finger-like protrusions into the lumen, called the villi, and invaginations into the submucosa called crypts of Lieberkühn[1–4]. The villi allow increasing the surface area of contact with the nutrients for absorption and is the compartment where non-diving, differentiated cells locate. The length of the villi decreases from the duodenum to the distal ileum. The crypts situate at the bottom of the epithelium. They are the location site for the Paneth cells (PC), proliferating cells: the stem cells (SCs) and a rapidly proliferating subset of progenitors (also known as transit-amplifying (TA) cells). The histology of the colon is quite different, crypts are still present, but there are no villi as a columnar surface epithelium[5,6] replace them (**Figure 1**).

The intestinal epithelium is one of the most intensively self-renewing tissues with a complete renewal every five days, consistent with the entire trajectory of one SC from the crypt base to its final shed-off at the tip of the villi[7]. Briefly, a newborn SC will symmetrically divide to self-renew to expand the SC pool and give rise to a rapidly proliferating subset of progenitors/TA cells that will migrate upwards while differentiating into one of the specialised epithelial lineages. I will introduce each of these cell types below.

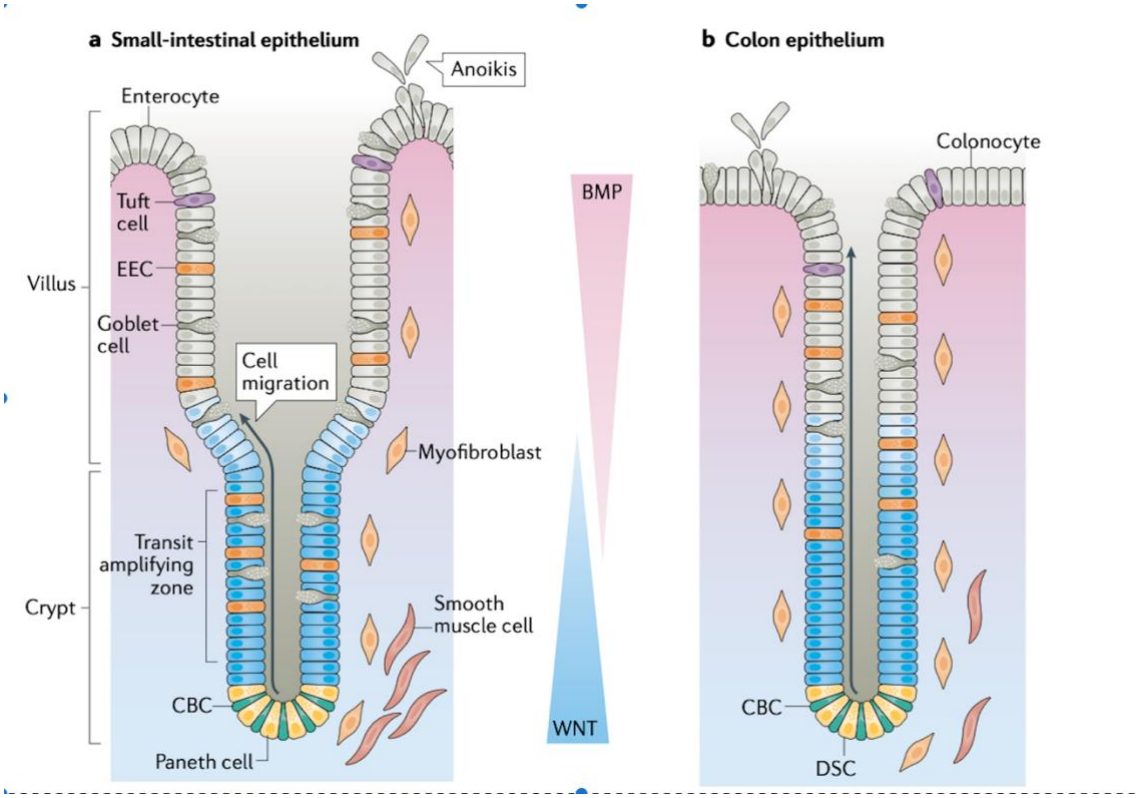

Figure 1 Intestinal epithelium organisation.
A) The small intestinal epithelium is organised in crypts, the proliferation sites where the SCs are located. Paneth cells support the SCs and prevent bacterial infiltration in the crypt by secreting antimicrobial molecules. Stem cell's daughter cells migrate up from the bottom of the crypt to the tip of the villi, where they will die by anoikis. As they migrate upwards, they face decreasing Wnt signals and an increase in the bone morphogenic protein (BMP) signalling. BMPs negatively regulate stemness, and together with Wnt and Notch, these morphogens the borders of the stem cell zone. The opposing Wnt and BMP gradients are established by differential expression along the crypt-villus axis of agonists and antagonists. The crypt also contains transit-amplifying cells that proliferate multiple times before maturation and functional secretory cells (hormone-producing enteroendocrine cells (EECs), mucus-secreting goblet cells and tuft cells that regulate immune responses). In the villi, the nutrient-absorbing enterocytes are found. **B)** The colon lacks villi which a flat surface epithelium has replaced. The colonocytes, the functional equivalents of enterocytes in the small intestine, specialise in water resorption. Most cell types that constitute the small intestine are also present in the colon, except for Paneth cells, which are absent and replaced by deep secretory cells (DSCs) intercalated between SCs and marked by REG4 and cKIT. The figure is taken from 3.

In the quest for intestinal stem cells and beyond

Crypt-columnar stem cells

The SC are undifferentiated cells residing in a specific location (a niche) within a tissue and can self-renew and produce one or more differentiated cell types. The intestinal stem cells (ISCs), located at the bottom of the crypts, divide continually to keep up with the rapid epithelium turnover. The first to have described the presence of slender cells between the Paneth cells (PCs) in the crypt was Joseph Paneth himself in 1887[8]. Every crypt is commonly believed to contain approximately six independent SCs; two schools of thought—the classic model and the SC zone model—define the exact identity of these SCs[9]. The classic model, in the 1950s, proposed using cell tracking experiments predicted that the SCs reside at position +4 relative to the crypt bottom and that terminally differentiated PCs occupy the first three positions.

Potten and colleagues reported that cells could retain a DNA label specifically at the +4 position [10,11]. Additionally, these researchers observed that these +4 cells are unusually radiation-sensitive, a property proposed to functionally protect the SC compartment from genetic damage and be replaced by the first 2-3 generations of progenitor cells which would fall back to the +4 position while regaining SC properties [12]. This finding predicted that the labelled template strand would be retained in the cell destined to remain an SC while the newly synthesised strand is inherited by the daughter cell. This immortal strand theory was considered to protect the SC genome from accumulating potentially dangerous mutations. However, this is only valid if no symmetric cell division occurs and data supporting this model is limited [13].

The second school of thought, the SC zone model, began in the 1970s when Cheng and Leblond initially identified the crypt-base columnar cells (CBCs). These cells are small, undifferentiated, cycling cells interspersed between PCs and can generate all intestinal epithelial lineages. Then, Bjerknes and Cheng continued to champion the CBCs as the adult ISCs with additional but indirect evidence of CBC's multipotency[5,14,15]. According to these authors, CBCs reside in an SC-permissive environment (the SC zone) at the crypt base, and these proliferating SCs regularly generate progeny, which subsequently exit the niche at the ‘‘common origin of differentiation’’ around position +5, where they commit (presumably via committed progenitors) toward the various functional lineages[5,14,15]. Thus, many researchers have tried to study these CBCs, but it was not until the advent of genetic lineage tracing tools that brought final proof of CBCs as SCs. Later in 2007, a landmark study from Clevers' lab showed that the leucine-rich repeat-containing G protein-coupled receptor 5 (LGR5) is a CBC specific bona fide ISC marker[16]. Using *Lgr5EGFP−IRES−CreERT2* mice and crossing them with an *R26R–lacZ* reporter, upon tamoxifen administration in the offspring, activates the Cre-ERT2 fusion enzyme, which removes a transcriptional roadblock and promotes continuous lacZ expression in Lgr5-expressing cells and any future offspring. This activation resulted in ribbons of lacZ-marked cells extending from the bottom of the crypt to the villus within five days. The stripes contained cells of all lineages, and many persisted lifelong. Thus, LGR5+ CBC cells fulfilled both criteria of stemness: generation of multiple lineages and long-term self-renewal [4,16]. Advances in lineage-tracing tools and transcriptomics unveiled many other putative SC markers for CBCs and the other ISC-like located in upper crypt position type, +4. As I mentioned above, they allowed the direct tracking of their progeny. In another study from Clevers' laboratory, Sato and colleagues showed that these LGR5+ cells could establish long-term *ex vivo* organoid cultures containing all the intestinal cell types and recapitulate the *in vivo* epithelial function and structure[17]. Of note, an organoid has been defined, and I quote Hans Clevers, " as a 3D structure grown from SCs and consisting of organ-specific cell types that self-organise through cell sorting and spatially restricted lineage commitment" [18,19].

Fluorescence-activated cell-sorted (FACS) sorted Lgr5GFP cells allowed to determine the gene expression signature of these cells [20] and perform functional analysis of additional SC genes. Thus, Achaete-Scute Family BHLH Transcription Factor 2 *(ASCL2)* [21] and Olfactomedin 4 *(OLFM4)*[22] expression also identify LRG5 ISCs. Actively cycling LGR5 CBCs contribute robustly to intestinal homeostasis[23]. Remarkably, however, genetic ablation of Lgr5+ cells with diphtheria toxin showed that they are dispensable for intestinal homeostasis under basal conditions. Ablation of these highly proliferative ISCs occurs in response to a DNA damaging injury, namely irradiation or chemotherapy[24,25]. Interestingly, diphtheria toxin ablation of Lgr5+ CBCs shortly after or concomitant to a radiation injury revealed that these cells were required for these cells for a robust regenerative response. These data suggested that post-injury *de novo* generated Lgr5+ CBCs and a small fraction of Lgr5+ cells that survive the radiation injury plays an essential role in epithelial regeneration [26]. These LGR5 cells surviving irradiation might be those now known as the LGR5+ slowly-dividing CBCs, marked by MEX3A and resistant to chemotherapy [27]. Indeed, in this same direction, Frau and colleagues [28] showed that treatment of WT animals with 5-FU resulted in the loss of active $Lgr5^{high}$ SCs and significant ablation of the $Lgr5^{low}$ cells with a substantial expansion of the Msi1 compartment. However, interestingly, in Msi1-overexpressing transgenic intestines, 5-FU sensitivity was modified in a cell-dependent manner, and $Lgr5^{low}$ progenitors switched to a resistant phenotype eventually, while $Lgr5^{high}$ SCs remained sensitive. The researchers postulate that there is cellular plasticity promoted by MSI1 upon 5-FU treatment. In resting conditions, Msi1 and Lgr5 cells designate an almost homogeneous population but separate in response to treatment [28]. The expendable nature of $Lgr5^{+}$ CBCs during intestinal homeostasis and the susceptibility of actively cycling CBCs to DNA damage implies the presence of other epithelial cells capable of compensating for CBC loss. For example, as I just mentioned, the subpopulation of Msi1-expressing resistant cells (or MEX3A cells), slow-cycling during homeostasis, can be mobilised to revert to Lgr5+ SCs finally.

Transit amplifying cells

Transit amplifying (TA) cells or TA progenitors are short-lived proliferating cells located between the SCs and the beginning of the differentiated compartment in the intestinal epithelium vertical axis [29]. TAs replicate up to six times with an even shorter cell cycle (~12 h) than CBC cells before entering a postmitotic state and differentiating [30]. The cells entering the transit stage can rapidly produce many differentiated cells. In turn, these TA progenitors will adopt one of the two possible cell lineages of the intestine: absorptive or secretory, as we will see more in detail below.

Reserve stem cells

The identity of the cells that contribute to the epithelium regenerative process and its biological underpinning has been an area of intense investigation and a source of controversy. Initially, the hypothesis was that a quiescent population of SCs residing at the position +4 relative to the base of the crypt [11,12] could withstand damage due to their non-cycling nature.

Intense debate on ISC identity described +4 cells as candidate SC populations in addition to CBCs, focused mainly on the physical positioning in the intestinal crypt. These cells are called +4 cells due to their location between the CBCs and the TA zone [4]. Early DNA labelling experiments showed long-term incorporation and retention of tritiated thymidine in the ISCs that researchers proposed as +4 ISCs populations. These label-retaining cells (LRCs) were slow-cycling and located around cell position 4, just above the differentiated PC in the small intestine [10,12]. Known as reserve SC, "quiescent", "slow-cycling", "revival", or "facultative" SCs [20,23], its name is still in debate.

For consistency in this manuscript, I will refer to them as facultative SC. Moreover, suppose we think about the definition of quiescence as "a state or period of inactivity or dormancy"; this implies that i) quiescent cells have a dormant genome (and thus reside in G0, not G1) and that ii) quiescent cells can re-enter the cycle and act as a stem/progenitor cell. Thus, by this definition, the vast majority of non-dividing cells are not quiescent, and as we will see afterwards, many of these cells are involved in regeneration after damage. That is why hereafter, I will call them facultative.

These cells express several markers: Bmi1[31], Telomerase Reverse Transcriptase (Tert)[32], Hopx[33], leucine-rich repeats and immunoglobulin-like domains protein 1 (Lrig1)[34], musashi1 (Msi1)[35] and later clusterin (Clu)[36] and can reconstitute the intestinal epithelium under injury conditions. As I will describe below, this plastic and dynamic intestinal regeneration capacity are no longer restricted to the +4 facultative SCs.

Plasticity within the hierarchy

Although known for a long time as two independent ISC pools, CBCs and the facultative cells, the properties of these two apparently separate ISC pools were reconciled thanks to the intestinal injury and regeneration models (**Figure 2**). Moreover, using these injury and regeneration models, the TA zone and the committed progenitors took a significant role in the intestine. Several recent studies demonstrated surprising plasticity of the whole epithelium, not only of the cells within the crypt bottom but a more committed progeny of CBCs can re-acquire CBC identity, albeit at a low-frequency [37]. This re-acquisition of a CBC identity has also been observed in the case of non-

physiological injury models (such as genetic ablation of specific cell types), irradiation or chemotherapy[38].

The first evidence of such plasticity arose from studies on LRCs. The first study to test the potential of LRCs to function as SCs in the intestine *in vivo* incorporated a DNA label during a relatively short pulse in a mature animal [37]. Then, they compared the "long-term LRCs" (observed after one month chase or longer) in the small intestine compared with a homogenous population of terminally differentiated PCs downstream of the CBCs[23,37,39]. On the contrary, samples recovered after a "short term chase" (i.e., after 8-12 days chase) presented cells residing at or near the crypt base retained the label. Single-cell expression profiling revealed the latter to be a highly heterogeneous population, including cells with gene expression signatures of PCs, enteroendocrine cells (EECs), and scarce cells with facultative ISC molecular identity[23,37,39]. Moreover, Langner and colleagues observed a small fraction of double-positive cells when using double reporter mice, where Hopx-CreER marked the facultative ISCs and H2B-GFP marked the LRCs and concluded that the facultative ISCs and short-term LRCs/secretory progenitor cells are primarily mutually exclusive populations[39]. Most of the known facultative ISC markers, if not all of them, have been found thanks to irradiation of ablation studies and label-retaining techniques. These cell markers were found in the +4 position and can induce regeneration in the intestine after high-dose irradiation via replenishment of the LGR5+ ISC pool [31–36].

Similarly, in an ablation model with doxorubicin, a chemotherapeutic drug, early progenitors were responsible for intestinal regeneration [40]. In addition, the TA compartment presents developmental plasticity. Short-term label-retaining secretory progenitor cells share functional and molecular properties with cells marked by a delta-like ligand 1 (Dll1) Dll1-CreER allele[41]. These Dll1-CreER-marked cells are the progeny of CBCs, usually generating cells of the secretory lineage, forming organoids *in vitro* in the presence of Wnt3a (not required for organoid formation from CBCs or facultative ISCs), and exhibit rare lineage tracing activity in response to irradiation injury. These findings support a model where CBCs activate Dll1+ cells as they enter the secretory lineage and exit the cell cycle shortly after. These results support the concept that TA secretory precursors are committed to differentiation but are not fully multipotent for all intestinal lineages or ordinarily capable of prolonged self-renewal but can re-acquire stem cell activity within a favourable environment.

A study employing *Bmi1-eGFP* as a marker of EEC cells demonstrated that upon ablation of CBCs, these committed cells undergo chromatin reorganisation reverting to a CBC-like chromatin state, showing functional plasticity at the level of chromatin organisation [42]. Like secretory progenitors, enterocyte committed progenitor cells, marked with Alpi-CreERT2, give rise to entire crypt-villus lineage tracing events at low frequency in response to genetic ablation of CBCs using an Lgr5-DTR allele[43]. Similarly, the generation of small intestinal organoids followed by Lgr5-DTR CBC ablation results in organoid maintenance from an Alpi-CreERT2-

marked population[44]. Several intestinal cell types contribute to crypt homeostasis and injury-induced regeneration. These cells can be enterocytes, EECs, goblet cell precursors, secretory progenitors (expressing *Dll1* or the transcription factor atonal homolog 1 (*Atoh1*)), differentiated $KRT20^{+}$ colonocytes, tuft and PCs [45].

Interestingly, during crypt injury and villous atrophy or injury, researchers have demonstrated that TA cells transiently adopt a unique, differentiated state that incorporates a fetal-like program and can quickly re-establish the epithelial barrier to restore the villus architecture. The Yes-associated protein (YAP) induces this fetal-like regenerative program via an adaptive response. Loss of YAP generates atrophic villi, as observed in pathological conditions. They have called this process "adaptive epithelial differentiation" as engaged goblet, and enterocyte progenitors can replenish the villi [46].

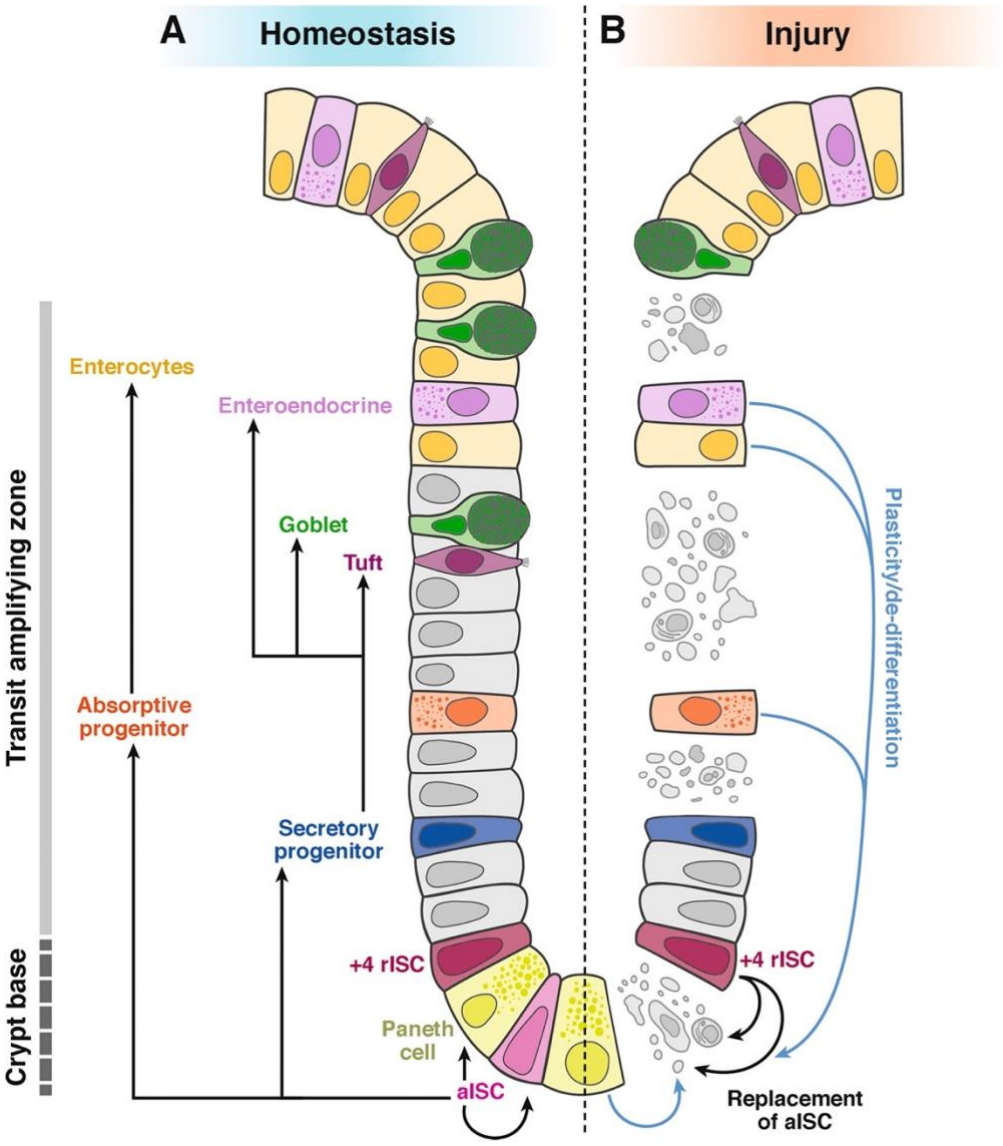

Figure 2 Crypt-localized cells in epithelial homeostasis and injury-induced regeneration.
A) Homeostatic renewal of the intestinal epithelium (comprising ISCs, TA progenitors, enterocytes, PCs, EECs, goblet and tuft cells) is mediated by active ISCs (CBCs) in the crypt base. (B) Injury-induced regeneration, when active ISCs are compromised or lost, rISCs (facultative ISCs) become a primary cell source that mediates regeneration. Committed progenitors can also regenerate epithelial tissue (blue arrows), presumably through an active ISC intermediate generation. The figure is taken from [47].

Specialised cells of the intestinal epithelium

Mature cells of the intestine are present in the crypts and the villi. The intestine has two major specialised progenitors' lineages: absorptive and secretory. Absorptive progenitors will engender enterocytes (or colonocytes in the colon) and microfold cells (M cells). In contrast, secretory progenitors will give rise to PCs, EECs, tuft cells and goblet cells. Figure 3 provides a schematic overview of the hierarchy in cell lineage specification in the intestine. A binary switch controlled by Notch signalling maintains a steady balance between secretory and absorptive cells via lateral inhibition. TA cells require active Notch signalling in a low-WNT environment to commit to their

absorptive fate[30]. Notch ligands are supplied by progenitors of the secretory lineage, which induce absorptive fate in all neighbouring progenitors in a process termed lateral inhibition. Lateral inhibition maintains a stable ratio between the lineages and ensures that most progenitors will assume absorptive fate[8]. In addition, active Notch signalling stimulates the expression of Hairy/enhancer of split 1 (Hes1)[48], a potent repressor for the basic helix-loop-helix (bHLH) transcription factors Atoh1 (also known as Math1) and Neurogenin-3 (Neurog3). The former is essential to produce all secretory cells, and the latter is the key regulator for EEC cell formation (**Figure 3**).

Enterocytes and colonocytes – absorption

The enterocytes are columnar cells with an apical region of microvilli (also called brush border) that helps amplify the absorptive surface [2,30]. These cells specialise in absorbing substances from the intestinal lumen to the circulatory system. Still, they are also secretory cells as they secrete the necessary enzymes for terminal digestion and absorption, as for the secretion of water and electrolytes. The enterocytes are the most prominent cell type of the small intestinal epithelium, representing approximately 80% of the differentiated cells of the intestine. They are responsible for efficient nutrient and water absorption thanks to their brush border that enlarges their cell surface in the apical pole [3]. The colonocytes in the colon are morphologically similar to enterocytes, but they express different proteins, enzymes and transporters according to their function [6]. Enterocytes and colonocytes express many enzymes and transporters to absorb nutrients and protect from daily xenobiotics. The master gene regulator of enterocyte/colonocyte differentiation is HES1.

M cells – Antigen transporting cells

Microfold cells (M cells) are specialised enterocytes that reside in the epithelium overlying Peyer's and transport luminal antigens to underlying immune cells, thereby controlling the immune responses [3,8].

Secretory cells

The secretory progenitors can give rise to PCs, EECs, tuft cells and goblet cells. The master transcription factor ATOH1 regulates this lineage [8]. In contrast to the other differentiated cells, PCs are the only type present in the crypts, as they migrate downwards and situate wedged with SC. They produce antimicrobial compounds and niche factors for the ISC (as discussed below). EECs, the hormone-producing cells of the intestine, secrete hormones that regulate the

physiological processes in response to food intake [49]. Tuft cells are chemosensory and mediate immune responses, and goblet cells secrete mucus, helping protect the intestinal barrier against external factors, including bacteria [3,4].

Paneth cells – the ISC bodyguards

As mentioned before, PCs reside in between CBCs. They are the only differentiated cells of the small intestinal crypts [50], firstly described by Gustav Schwalbe and characterised by Joseph Paneth himself. PCs secrete antimicrobial agents and provide growth factors to ISC such as Wnt3, Notch ligands delta-like (DLL1 and DLL4), and EGF [3,4,51], acting as its guardians. Furthermore, PCs support ISC growth and survival through lactate production [52] and promote ISC self-renewal and proliferation in response to global metabolic changes such as calorie restriction or a high-fat diet [53,54]. *In vitro*, PCs support LGR5+ cells in organoids, providing a niche for the dividing stem population[50]. Thus, PCs seem to have an essential role in the niche. Still, several studies show that its ablation from the epithelium did not cause changes in the homeostatic intestinal renewal, nor CBCs were affected [55,56]. Despite that, PCs are important for regeneration after injury [57].
Tuft cells and EEC can appear between CBCs and serve as Notch signal providers when PCs are absent [58]. The colon lacks typical PCs, but deep crypt secretory cells marked by Reg4 or c-Kit+ fulfil their ISC supportive role [59,60]. Interestingly, a recent study showed the presence of a PC-like lineage in the large intestine, which is mainly involved in inorganic and sulphur metabolism instead of having an antimicrobial function[61]. Furthermore, states of chronic inflammation, such as chronic ulcerative colitis, predispose to colon cancer and give rise to colonic PC metaplasia[62]. Importantly, deep crypt secretory cells do not produce Wnt ligands.

EEC – the hormone-producing cells

EECs are rare epithelial cells endoderm derived that respond to ingested food components by secreting hormones endocrine and paracrine that regulate multiple physiological processes, including gastric emptying, appetite, the release of pancreatic enzymes, mood changes, and insulin release [3]. There are many subtypes of EECs depending on the secreted hormone: D-cells produce somatostatin, K-cells the gastric inhibitory polypeptide, S-cells secretin, I-cells cholecystokinin, L-cells glucagon-like protein 1, N-cells neurotensin, and enterochromaffin cells, serotonin[63]. In addition, differential expression of EEC hormones exists between crypts (e.g. Glp1) and villi (e.g. Secretin), and the BMP4 signals induce hormone switching as EECs migrate up the crypt-villus axis [64].
EECs can have direct luminal contact and sense the intestinal content with microvilli, allowing the direct production of hormones according to the needs. Interestingly, the induction of quiescence of LGR5 SCs could generate several-fold higher levels of chromogranin (CHGA)

positive cells, indicating a fate direction to EECs. The study further concluded that the EEC fate determination needs the combined inhibition of Wnt, Notch and epidermal growth factor receptor (EGFR)/ mitogen-activated protein kinase (MAPK) pathways[63].

Tuft cells – chemosensation and immune mediation

Tuft cells are rare epithelial cells named for the iconic apical cluster of rigid microvilli that project into the lumen of hollow viscera. They are present in the mucosa of numerous epithelia, including the intestine. They represent approximately 0.5% of the murine small intestine and colon epithelial cells, more prevalent in the distal part of the small intestine[65]. These chemosensory cells produce interleukin 25 (IL25) (essential for type 2 immunity), eicosanoids (including certain prostaglandins and leukotrienes) and acetylcholine (Ach) which favour the identification of tuft cells. Furthermore, the characterisation of tuft transcriptional programmes allowed the discovery of unexpected roles of these cells like (a) recovery of the intestinal epithelium from damage and (b) induction of type 2 immune response to parasitic worm intestinal colonization[65,66].

Tuft cells in the intestine share a gene signature with other tuft cells of the body with elements of chemosensory, immune, and neural functions. For example, the doublecortin-like kinase 1 (DCLK1) marker typically identifies tuft cells of the intestine. Other markers used to identify tuft cells include the transcription factor POU2F3, IL-25, Prostaglandin endoperoxide synthase-1 (PTGS1/2), Transient Receptor Potential Cation Channel Subfamily M Member 5, and the choline acetyltransferase (ChAT). However, ChAT and DCLK1 can also be expressed by neurons[66].

Goblet cells – mucus and more

Goblet cells are unicellular glands that secrete mucus all over the intestinal epithelium. The name comes from its apical dilatation due to the accumulation of mucus granules and its basal region straight, giving a goblet structure. Goblet cells are the most abundant secretory cell type in the intestine, increasing numbers from the proximal small intestine to the distal colon as stool becomes compacter [2]. They represent the most abundant cell type in the colon (approx. 80%)[67].

Their primary role involves the secretion of mucins (like MUC2) that self-assemble into a protective mucus layer that coats the apical surface of the epithelial cells. The small intestine has only one layer of unattached mucus. In contrast, the colon has two layers of mucus. The inner layer provides a bacteria-free environment adjacent to the epithelium, and the luminal, less viscous layer harbours the gut microbiota[67]. The continuous mucus secretion limits commensal microbe contact with the epithelium and favours the elimination of more solid waste by reducing mechanical stress[68]. Apart from releasing mucins, goblet cells release other factors (like trefoil factors) in response to stimuli to modulate the gut microbiome leading to expansion and depletion

of gut microbiome populations, which allows the regulation of the intestinal homeostasis and host-microbe interactions[68].

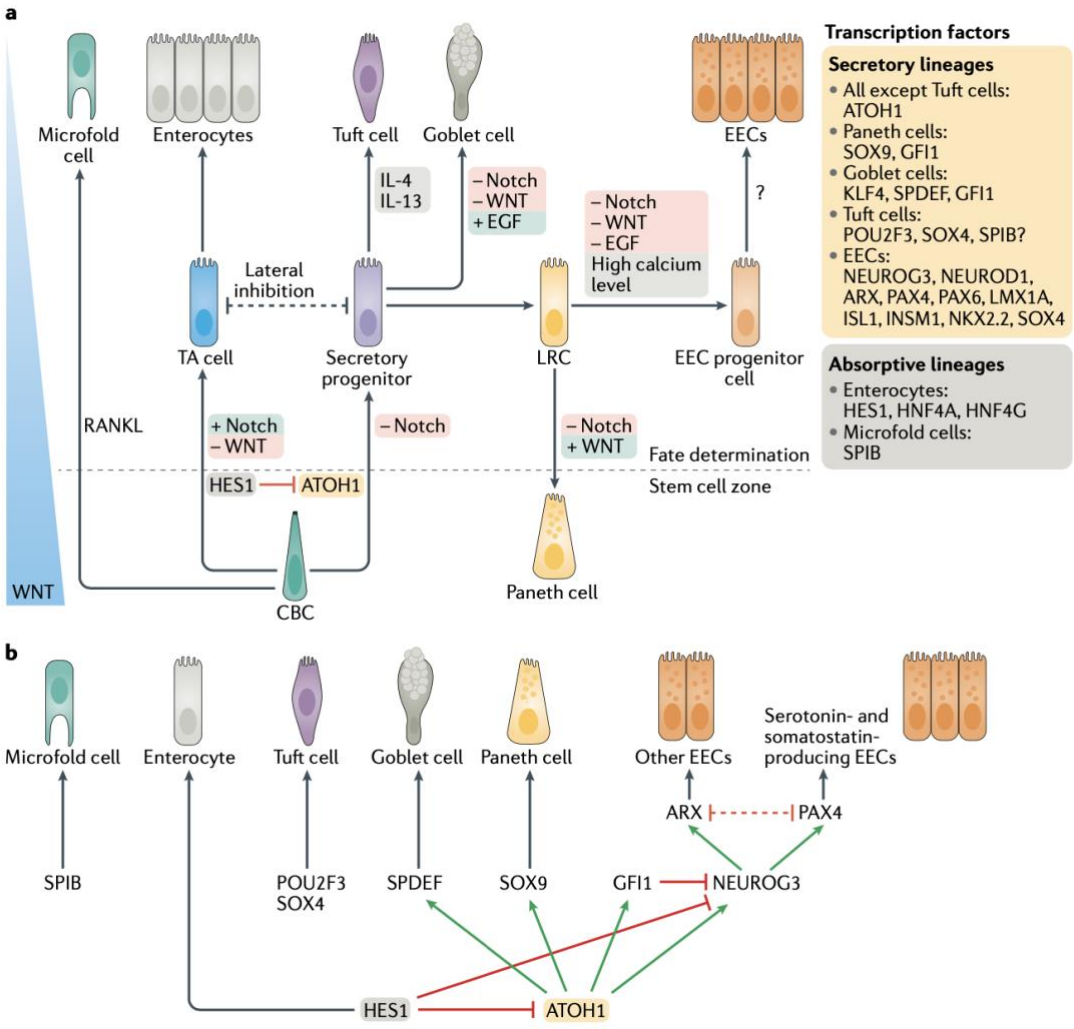

Figure 3 - Lineage specification in the intestine
A) Fate determination of CBCs occurs as progeny cells leave the stem cells zone. Access to Notch signals determines the fate of the cells. Those that stochastically lose Notch are fated towards secretory cells through the derepression of ATOH1. Cells that receive Notch maintain expression of the absorptive master gene Hairy and enhancer of split 1 (HES1) and will continue to mature into enterocytes/colonocytes after completing multiple transit-amplifying divisions. Secretory cells express Notch ligands that signal to enterocyte-fated progenitors, establishing lateral inhibition. In the small intestine, the secretory progenitors that retain sufficient WNT activity after departing the stem cell zone and expressing EphB2/EphB3 will return to the crypt bottom to mature into Paneth cells. Cells that do not receive sufficient WNT proteins mature into either goblet cells or one of the enteroendocrine cell (EEC) lineages. **B)** The transcription factor network that regulates cell fate. Green arrows indicate activation, and red arrows indicate repression. The figure is taken from 3.

Signalling pathways

The intestinal epithelium is highly dynamic and plastic but highly specialised with different cell types and functions. The primary and "classical" signalling pathways involved in the intestinal epithelium's vertical axis organisation include Wnt, Notch and epidermal growth factor (EGF) signalling pathways active in the CBC with a decreasing gradient activity at the top of the vertical axis. In addition, there is the bone morphogenic protein (BMP) signalling, inhibited in CBCs, and

sonic hedgehog (both with higher activity in the upper portion of the vertical axis, decreasing at the crypt bottoms)[29,51]. These signalling pathways control the balance between CBC's self-renewal and commitment in a complex and intricate way. In the following paragraphs, I will try to summarise the main pathways and their interrelation and cell types.

Wnt

Wnt signalling pathways govern cellular functions, including cell proliferation, differentiation, fate specification, migration and polarity [18,69]. As such, Wnt signalling regulation is decisive, and its aberrant activity can lead to developmental defects or various pathogenesis, including cancer [18,69], as we will see in Chapter 2.

The Wnt signalling pathway rules the intestinal epithelium, especially the ISC self-renewal and differentiation. This pathway is well-conserved in flies to humans, where it is involved in many processes during development and homeostasis in adult tissues. It has been at the forefront of ISC research for decades. The Wnt pathway can instruct the organisation of new cells through many signal transduction steps after activation by Wnts, resulting in changes in gene expression and cytoskeleton and the mitotic spindle. In addition, there is the Wnt/β-catenin pathway (a.k.a. the canonical pathway) and the non-canonical Wnt pathway. The latter does not involve the presence of β-catenin.

In the canonical Wnt pathway (**Figure 4**), on the surface of the cells, the Wnt proteins bind to a receptor heterodimeric complex of two molecules: Frizzled (FZDs) and the low-density lipoprotein receptor-related protein 5 (LRP5/6). The central component of the Wnt canonical cascade is the cytoplasmic protein β-catenin. In the absence of Wnts, the scaffolding proteins APC and Axin/Axin2 sequester β-catenin, allowing casein kinase I (CKI) to phosphorylate the N terminus of β-catenin. Subsequently, glycogen synthase kinase 3 β (GSK3β) phosphorylates additional serine and threonine residues. Phosphorylated β-catenin is then ubiquitinated and degraded through the proteasome[70]. Together, these proteins compose the so-called β-catenin destruction complex. As we shall see later in chapter 2, this complex plays a central role in the (de)regulation of intestinal homeostasis. When the Wnts bind to the FZD/LRP heterodimeric receptors, they activate the transduction cascade, inhibiting the cytoplasmatic destruction complex of β-catenin. Then β-catenin translocates to the nucleus to associate with the T cell factors (TCF/LEF) transcription factors family and activate the Wnt target gene expression. However, multiple non-TCF transcription factors can act as alternative transcriptional effectors[18]. Apart from its role as a cytoplasmic effector of canonical Wnt signalling, β-catenin interacts with the cytoplasmic domain of E-cadherin and is also an intracellular component of adhesion junctions[71]. Still, I will not further discuss the non-TCF role of β-catenin in this manuscript.

Extracellular proteins that antagonise the Wnt ligands can naturally inhibit the Wnt pathway. To mention some of them: NOTUM eliminates the palmitoleate from the Wnt, and Dickkopf (DKK)

bind to the LRP5/6 and prevents Wnt induced dimerisation to FZD. In addition, the secreted FZD-related proteins (sFRPs) and the Wnt inhibitory protein (WIF) can bind directly to Wnts and RNF43 and ZNF43, acting as potent negative-feedback regulators of the Wnt signal strength [18]. These Wnt inhibitors are important in the adenomatous expansion of crypts, colorectal cancer development and maintenance, as we will see in chapter 2.

Coming back to the ISC regulation by Wnts, we must recall that one of the Wnt target genes, LGR5, marks the ISCs and that transcriptomic analysis of these LGR5+ cells unveiled multiple Wnt target genes essential for ISC maintenance [20] like EphB2[72] or ASCL2[21]. The initial evidence of the involvement of Wnt in adult SC biology comes from the gene disruption of mouse Tcf4, which lead to the loss of ISCs and the subsequent breakdown of the epithelium [73]. The disruption of the *Tcf7l2* gene (encoding for Tcf4) showed mice lethality after birth. No proliferative compartment was maintained in the prospective crypt regions of the intestinal epithelium, and the neonatal epithelium was composed of differentiated, non-dividing villus cells[73]. Since then, the Wnt pathway has been studied as a central pathway for most SCs types. Thus, the embryonic SC phenotype can be maintained in culture by just two small molecules: the Wnt activating GSK3 inhibitor CHIR [74] and the other purified Wnt proteins that can preserve the embryonic SC pluripotency [75]. But, what about the involvement of Wnt in the physiology of the intestine and the ISCs biology? After the study on mice with genetic ablation of the Tcf4, it was shown that the ectopic expression of the Wnt receptor inhibitor Dickkopf-related protein 1 (Dkk1) reduced the proliferation in the small intestinal epithelium, crypts were lost, secretory progenitors were absent while enterocyte differentiation appeared unaffected[76]. Theis results showed for the first time that Wnt ligands are crucial for driving proliferation in the intestinal epithelium and controlling secretory differentiation[76]. In this direction, another study showed an abolished proliferative capacity of the small intestine and colon when using adenoviral delivery of Dkk1 to achieve a wholly conditional inhibition of canonical Wnt signalling in adult mice. The inhibition of the canonical Wnt led to a severe disruption of intestinal epithelial integrity, including the loss of crypts[77,78]. Later two studies showed that the genetic ablation of β-cateninenin in the intestinal epithelium of adult mice resulted in the loss of crypt and TA cells and induced the terminal differentiation of enterocytes[79,80]. However, markers were required to study adult ISCs and their specific role further. The screen of previously identified β-catenin target genes provided several candidate marker genes enriched in putative adult SCs[81], one of them being the gene Lgr5 which showed a unique expression pattern marking proliferating cells interspersed between PCs in the bottom of intestinal crypts[16].

The discovery of Lgr5 as an SC marker[16] and the establishment of intestinal organoids from purified crypts[17] represented a turning point in the study of ISC biology. In 2009, Sato et al. cultured for the first time murine intestinal organoids from LGR5+ ISC in the absence of mesenchyme and defined what they called “the minimal stromal niche”, consistent with the

minimal necessary signals for the expansion of ISCs. LGR5+ cells can give rise to 3D organoids containing all ISC lineages when supplemented with EGF, R-spondin1 (Wnt signalling amplifier) and Noggin (a bone morphogenic protein (BMP) inhibitor) embedded in an extracellular matrix-like gel, such as Matrigel[17]. Let me introduce another concept studied nowadays, the ISC niche. This ISC niche is a local microenvironment that provides physical support and molecular signals necessary for the proper stem and progenitor cell replication and differentiation [45,51]. The ISCs niche is composed of several cell types: PCs (mentioned above), stromal/sub-epithelial mesenchymal cells (including subepithelial myofibroblasts, non-muscle fibroblasts, telocytes, trophocytes, endothelial cells, pericytes, between others)[82,83], the extracellular matrix, and the complex metabolic signalling observed in the crypt's bottom and surrounding the SCs at the bottom of the crypts.

Nevertheless, later studies on organoids reported that the efficiency of its formation from single $Lgr5^{+}$ cells was significantly increased by adding PCs due to the provision of a Wnt niche[50]. The importance of an epithelial and mesenchymal Wnt-niche in the ISCs maintenance has been challenged. A study reported that impairment of Wnt secretion from the intestinal epithelium or the underlying smooth muscle through conditional knockout of porcupine (*Porcn*) resulted in no apparent defects in the intestinal epithelial structure, Wnt activation or the proliferative rate of ISCs[84]. That study suggested a potential redundant nature of the Wnt ISC niche *in vivo*, later confirmed by a report revealing intestinal defects following global prevention of Wnt secretion through ubiquitous knockout of Wntless[85]. Since then, a growing body of studies has shown a

significant implication of the ISC niche in the maintenance and support of the ISCs. I will not expand on this topic as I have covered it more extensively in the review paper (Paper N°4).

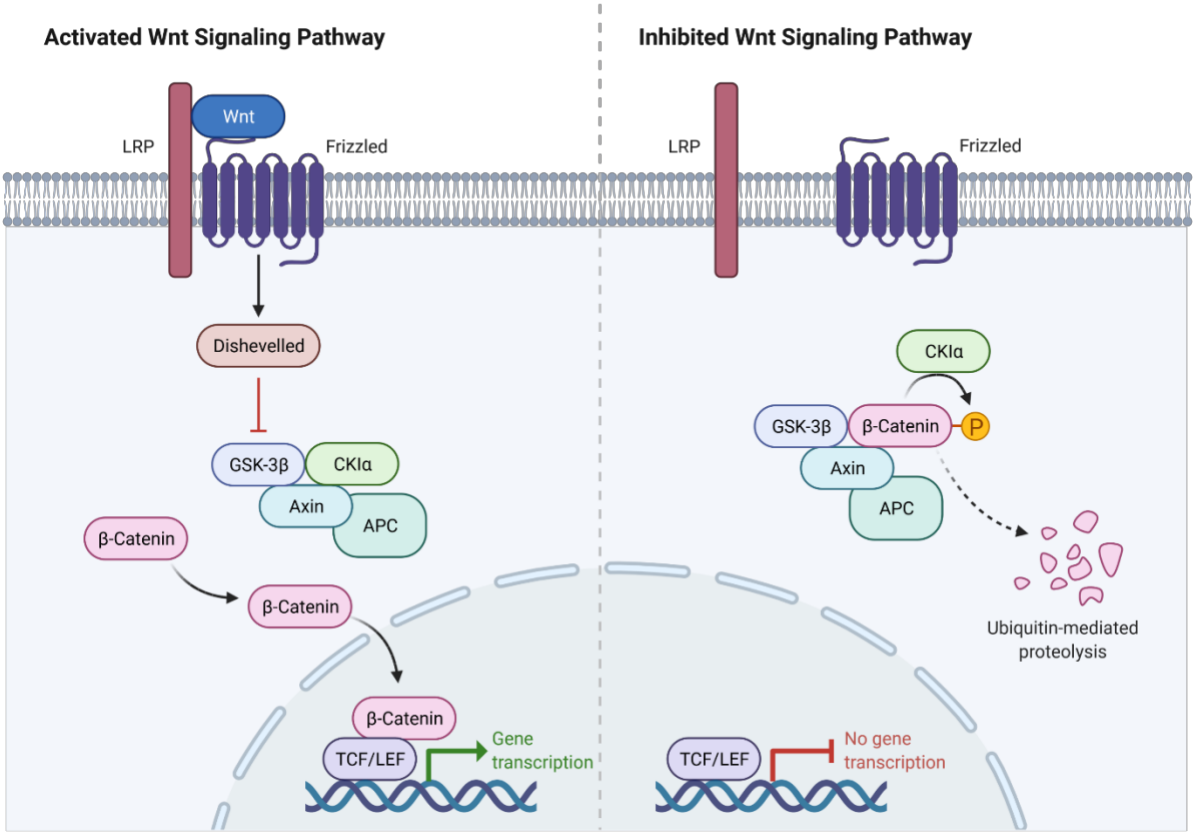

Figure 4 - The canonical Wnt signalling pathway
Left | When the Wnt proteins bind on the surface of the cells to the heterodimeric complex of Frizzled and the low-density lipoprotein receptor-related protein, they activate the transduction cascade, inhibiting the cytoplasmatic destruction complex of β-catenin. Then β-catenin translocates to the nucleus to associate with the T cell factors (TCF/LEF) transcription factors family and activate the Wnt target gene expression. **Right |** In the absence of Wnt ligands, the scaffolding proteins APC and Axin/Axin2 sequester β-catenin, allowing casein kinase I (CKI) to phosphorylate the N terminus of β-catenin. Subsequently, glycogen synthase kinase 3 b (GSK3b) phosphorylates additional serine and threonine residues. Phosphorylated β-catenin is then ubiquitinated and degraded through the proteasome. The figure was created with Biorender.com.

Notch

The Notch signalling pathway, highly conserved between species, directs cell fate in different multicellular organisms. The mammalian Notch family consist of 4 single-span transmembrane Notch receptors (Notch1-4) and five single-span transmembranes Delta/Serrate/Lag2 (DSL) ligands (Jagged (Jag) 1 and 2, delta-like (DLL) 1,3 and 4)[51]. Cell-cell contact triggers Notch signalling (**Figure 5**). The transmembrane bound ligands at the juxtaposed cell membrane bind and activate the Notch receptors, resulting in the initiation of several proteolytic steps that modulate the Notch activity. Finally, the γ-secretase protease releases the Notch intracellular domain (NICD). It translocates to the nucleus to drive gene expression of target genes upon binding to the transcription factors RBPj or CSL (CBF1, suppressor of hairless, Lag1)[51]. Importantly, ubiquitination and endocytosis of Notch receptors on the cell's surface tightly

regulate Notch activity, leading to signalling in the absence of a DSL ligand. Notch receptors can also be recycled back to the membrane or degraded in the lysosome[86].

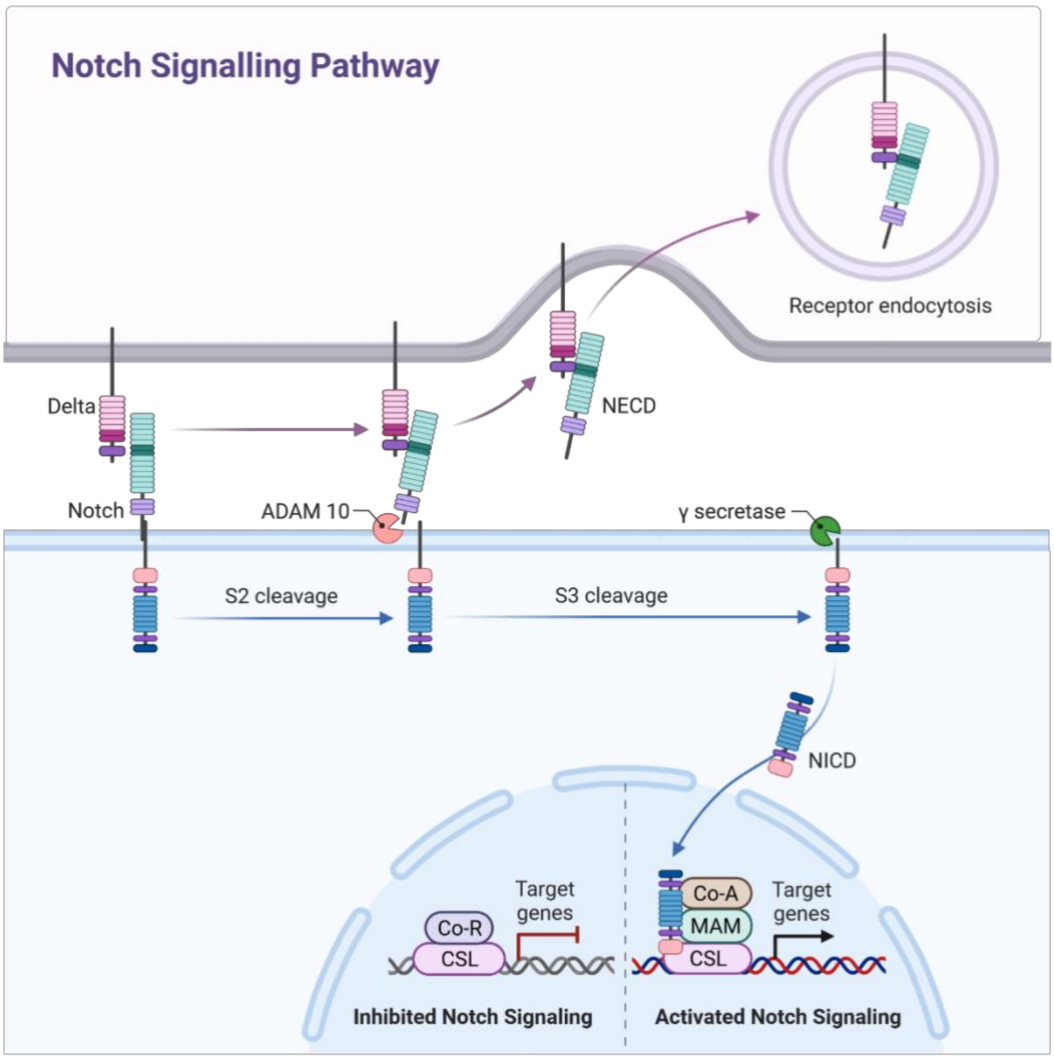

Figure 5 - Notch signalling pathway
When canonical Notch ligands bind to Notch receptors on the adjacent cell surface, they elicit two proteolytic cleavage events, the first by ADAM10 and the second by γ-secretase, that release the Notch intracellular domain (NICD). In the nucleus, NICD interacts with the DNA-binding protein CBF1–Suppressor of Hairless–LAG1 (CSL) and the co-activator Mastermind (MAM) to promote gene transcription [369]. Figure created with Biorender.com

Notch regulates the ISCs' and progenitors' proliferation and cell fate in the intestinal crypt between the two major lineages, absorptive and secretory. Two bHLH transcription factors, HES1 and ATOH1, masters' gene regulators, decide the switch between absorptive and secretory progenitors. HES1, expressed in most proliferative crypt cells, antagonises the transcription of ATOH1, whilst ATOH1 expression is restricted to secretory cells (**See figure 3**)[51]. The activation of secretory differentiation, e.g. goblet cells, is independent of Wnt signals, whereas the proliferative state of crypt cells depends on the integrated action of both Wnt and Notch[86,87]. The latter is an important notion we must keep in mind for future chapters.

So, the question is now, how does Notch signalling affect ISCs? When we talked about the PC, I mentioned that they express Notch ligands DLL1 and DLL4, which provides ligands to activate the Notch pathway in the neighbouring ISCs[88]. Moreover, CBC cells predominantly express Notch1 and Notch2 receptors at the cell surface, and Notch1 receptor mRNA is enriched in these cells, signifying a regulatory role of Notch within the SC compartment [89]. Inhibition of Notch signalling results in rapid loss of CBCs, indicating its requirement for ISC proliferation and survival [90]. In particular, researchers showed that the OLFM4 SC-specific marker is a direct target gene of Notch signalling[22,90]. Moreover, inhibition of Notch leads to the precocious differentiation of progenitors into secretory cell types, mainly PC and goblet cells, in an Atoh1 dependent way[90]. Interestingly, Notch signalling is crucial for intestinal renewal upon irradiation, with PCs that can dedifferentiate, proliferate, and restore all intestinal epithelial cells of the crypt-villus axis. This dedifferentiation capacity of PCs after an injury is due to activated Notch signalling in the PCs[91]. In summary, active Notch signalling is crucial for the maintenance and activity of the ISC pool as it regulates different aspects of intestinal homeostasis, stimulating both SC maintenance and cell fate determination of progenitor cells and induction of PC dedifferentiation upon tissue damage.

EGF

The epidermal growth factor (EGF) is an extracellular ligand that stimulates cell growth, proliferation, and differentiation by binding to the EGFR, a member of receptor tyrosine kinases. Upon binding of EGF, EGFR homodimerises and by stimulating its intrinsic intracellular tyrosine-kinase activity, it autophosphorylates, which drives the activation of the downstream pathway. Its downstream effectors associate with the phosphorylated EGFR and initiate a pro-survival and pro-proliferation signalling cascade that includes the MAPK, phosphatidyl-inositol-3-kinase (PI3K)/AKT, c-JUN N-terminal kinases (JNK), JAK/STAT and phospholipase C (PLC) pathways. The small GTPase Kirsten sarcoma viral oncogene homolog (KRAS) is a central relay in these signalling cascades (**Figure 6**). Unsurprisingly, it is commonly mutated in colorectal cancers, as shown in chapter 2. In the intestine, proliferation and maintenance of ISCs require EGF. The ISC niche (PC and mesenchyme) surrounds the ISCs) produce EGF. PCs and the subepithelial mesenchyme of the niche deliver the required EGF[50,83]. ISCs and TA cells highly and strictly express EGFR [92]. Not surprisingly, as we saw before, EGF is part of the "minimal stromal niche" for maintaining organoids *in vitro*. Also, it was observed that blockade of EGF in organoids converts active ISC into quiescent SCs[63]. Therefore, tight control is necessary to balance the EGF-induced proliferation of ISCs, which express high levels of the EGFR inhibitor – LRIG1 that mediates the ubiquitination and subsequent degradation of the canonical EGFRs. A

negative feedback loop allows SCs to fine-tune their cellular response to EGF ligand-mediated signalling and ensures proper crypt size and tissue homeostasis is created[93].

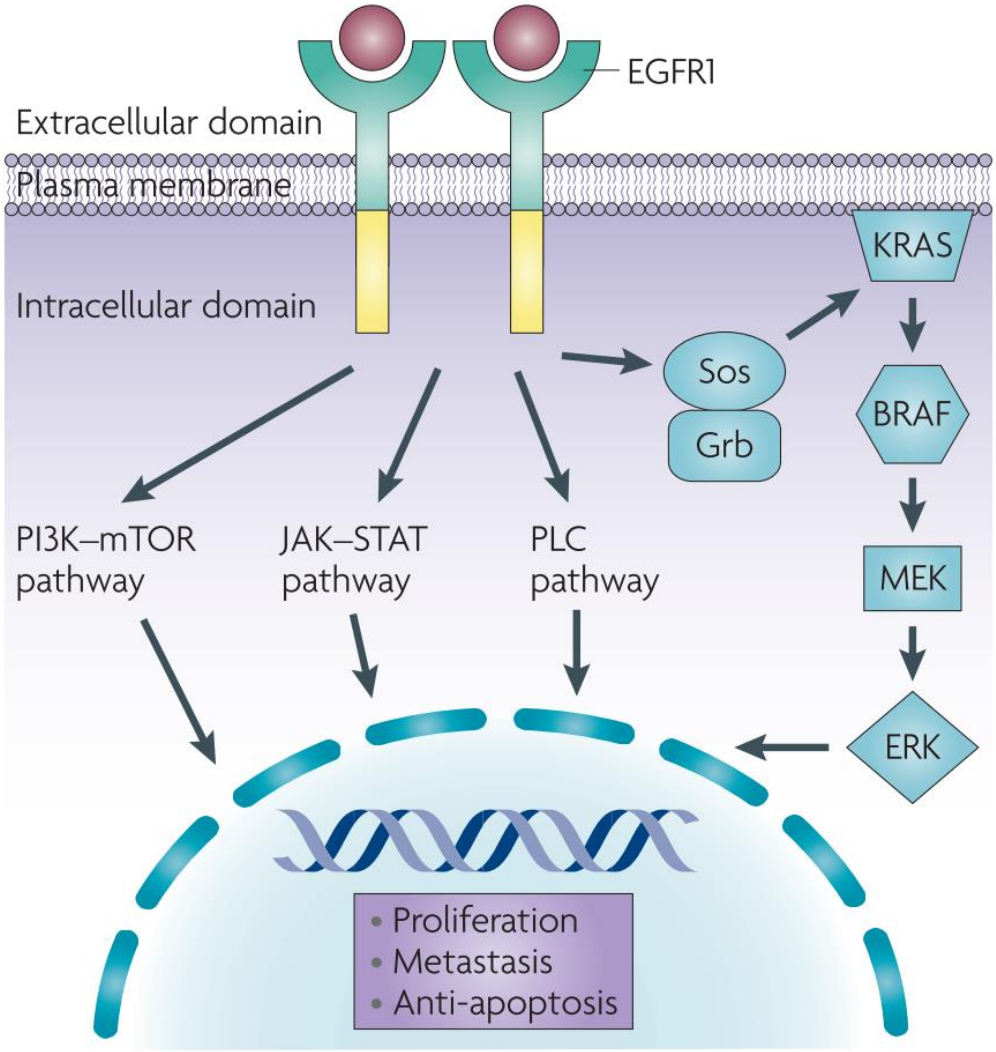

Figure 6 - EGFR pathway
On ligand binding, the epidermal growth factor receptor (EGFR) type 1 homodimerises, leading to the activation of the intracellular kinase domain. The KRAS signalling cascade is activated through the small adaptor proteins Sos and Grb, leading to increased proliferation. The figure was taken from [370].

BMP

Bone morphogenic proteins (BMPs) comprise a class of extracellular signalling molecules that belong to the transforming growth factor β (TGFβ) superfamily. BMPs initiate signal transduction via the canonical SMAD-dependent pathway or the non-canonical pathways. BMPs bind to the type 1 and 2 receptors (BMPR1-2) that form a heterotetrameric complex to initiate the signalling cascade. BMP receptors are transmembrane proteins that carry a serine/threonine kinase activity in the intracellular domain, and upon binding of BMP, the constitutively active BMPR2 phosphorylates the receptor-bound R-SMADS1/5/8[94]. Phosphorylated SMAD1/5/8 associate then with the core mediator SMAD4 and the SMAD complex translocates then to the nucleus to regulate gene expression of target genes like JUNB[51]. The mesenchymal cells produce the main

BMPs in the intestine (including BMP2 and BMP4, which recognise the type 1 receptor BMPR1A). BMPs expression is the highest at the top of the epithelium. In contrast, stromal cells (including myofibroblasts and smooth muscle cells) surrounding the crypt bottom secrete BMP inhibitors, including Noggin, follistatin, chordins and gremlins (GREM) that sequester BMP ligands and thereby block BMP activity[3].

The BMP pathway acts as a negative regulator of crypt formation in the intestine and drives terminal differentiation of the mature intestinal cells[95]. Conditional deletion of BMPR1A or overexpression of Noggin stimulates the formation of ectopic crypts in mice, a phenotype reminiscent of the human juvenile polyposis syndrome caused by inactivating *BMPR1A* and *SMAD4* mutations[96,97]. BMP also restricts the LGR5 SC zone to the bottom of the crypt by suppressing the LGR5 SC signature genes, independently from Wnt/β-catenin signalling via recruitment of histone deacetylases through phosphorylated SMAD[98]. Moreover, apart from its crypt formation and maintenance role, BMPs are also involved in the hormone switching of EECs as they migrate up the intestinal vertical axis *in vivo*[64].

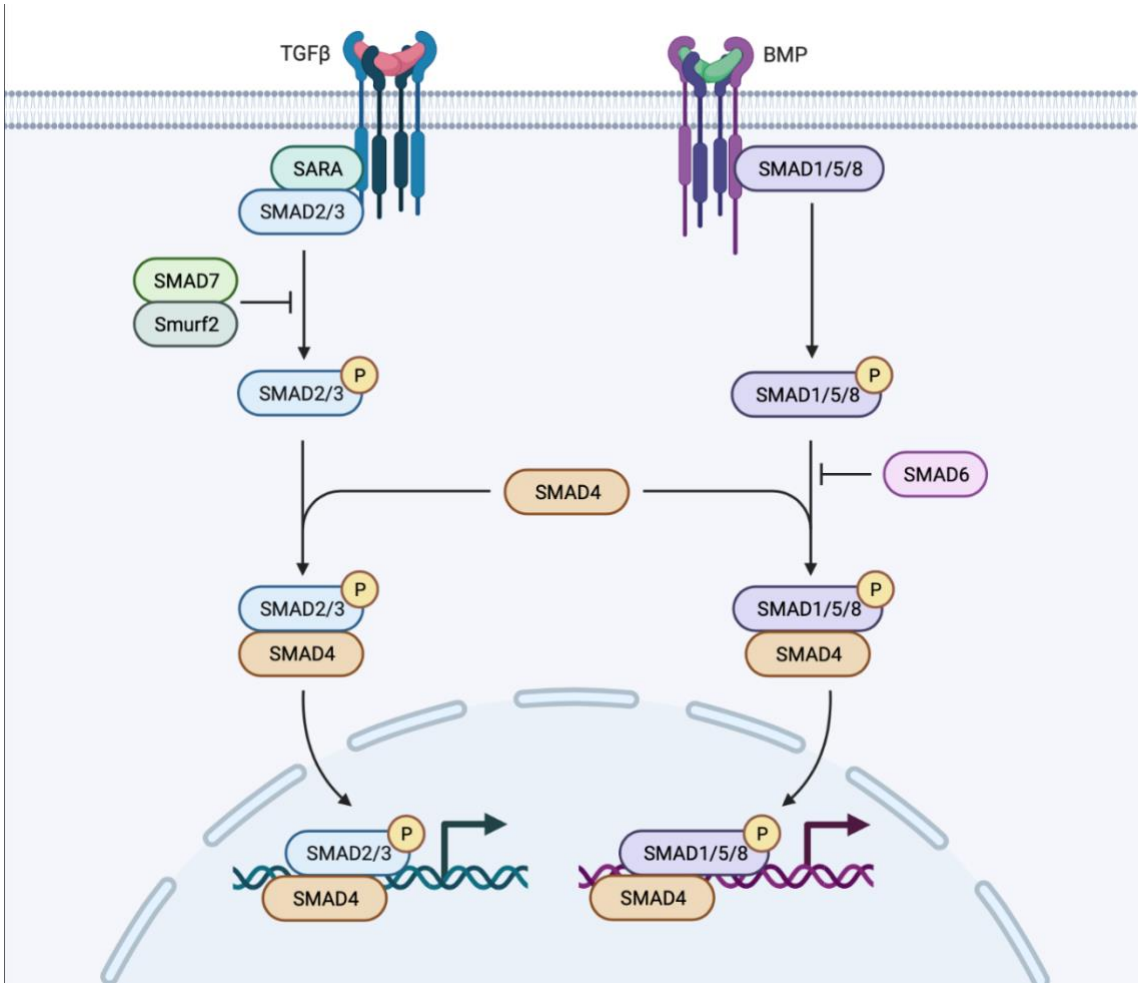

Figure 7 - BMP/TGFβ signalling pathway
The figure was created with Biorender.com

HEDGEHOG

The Hedgehog (Hh) family of secreted ligands consists of three subgroups: desert hedgehog (DHH), Indian hedgehog (IHH) and sonic hedgehog (SHH). HH binds to a transmembrane receptor Patched 1 or 2 (PTCH1/2) and activates the signalling cascade that eventually drives the activation of the zinc-finger transcription factor GLI (GLI1, GLI2 and GLI3), leading to the expression of HH target genes. In the absence of HH ligands, Patch blocks the transmembrane protein activity of Smoothened (Smo), which leads to the proteolytical processing of the full-length GLI proteins into the C-terminally truncated 'GliR' (Gli repressor) and the active repress of HH target genes occurs. The binding of Hh to Ptch causes the loss of Ptch activity and subsequent activation of SMO. The activation of Smo transduces the Hh signal to the cytoplasm and induces the transcription of HH target genes like PTCH1/2, GLI1 and genes that drive proliferation and survival as CCND1, MYC and BCL2[51].

IHH is the main HH expressed in the intestine, while SHH expression is low and localised in the crypt bottom. Epithelial cells of the crypt secrete IHH in a paracrine manner to act in the surrounding niche. Intestinal dendritic cells and macrophages respond to HH signalling[99]. IHH and SHH ligands secreted by TA cells interact with Ptch receptors localised on niche cells to induce BMP production, which negatively regulates ISC proliferation and restricts its number[100,101].

Furthermore, Gli1-positive mesenchymal cells in the niche secrete Wnt ligands essential for ISC renewal in the colon and the small intestine[102]. Overexpression of IHH or deletion of PTCH results in modifications of the intestinal composition and a gain of mesenchymal cells, while deletion of IHH results in complete loss of the villus structure due to the loss of smooth muscle to support the systems. In addition, decreased HH signalling enhances Wnt activity and compromise differentiation which drives crypt hyperplasia[100,103,104]. In summary, HH indirectly affects ISCs via (a) induction of repressive BMP signalling and (b) modulation of adjacent stroma that supports the intestinal structure.

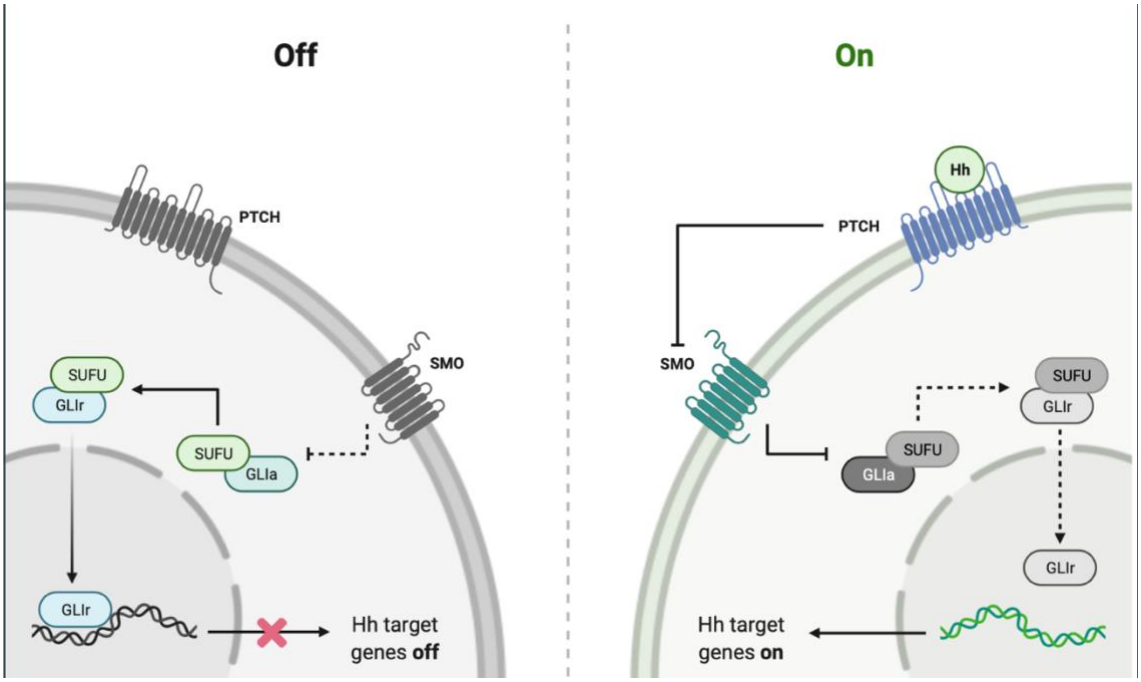

Figure 8 - Hedgehog pathway
The figure was created with Biorender.com

Hippo

During the past years, an increasing body of evidence has put the Hippo pathway at the centre of intestinal regeneration, despite its role in controlling organ size by interpreting mechanical cues. Briefly, the mammalian STE20-like kinase (MST) and large tumour suppressor kinase (LATS) phosphorylate and inactivate the transcriptional regulators Yes-associated protein (YAP; also known as YAP1) and the transcriptional co-activator with PDZ- binding motif (TAZ; also known as WWTR1). In addition, in complex with the transcription factor TEAD, they bind to gene enhancers, interact with chromatin remodelling factors and modulate RNA polymerase II to drive or repress the expression of target genes, including cell cycle, cell fate and cell migration regulators[105].

Surprisingly in the gut, the loss of YAP/TAZ does not affect homeostasis but prohibits regeneration after damage like irradiation or chemical injury[106,107]. Conversely, the gain of YAP/TAZ leads to the extensive expansion of the TA cells and generates crypt hyperplasia[105]. How does YAP activate regeneration in the intestine? As mentioned above, YAP is important during homeostasis, and during regeneration, its expression increases throughout the intestinal epithelium. After damage, the regenerating crypt has increased YAP expression, and it translocates to the nucleus [108]. A recent study showed that YAP-driven crypt expansion during regeneration involves elongation and flattening of the Wnt signalling gradient [109], showing an intricate *modus operandi* of the intestinal epithelium to balance proliferation, homeostasis and regeneration capacity. In addition to this, an EGFR ligand, epiregulin (a YAP target gene), is

upregulated under regeneration, and the Notch pathway reinforces this tight control in the epithelium[3].

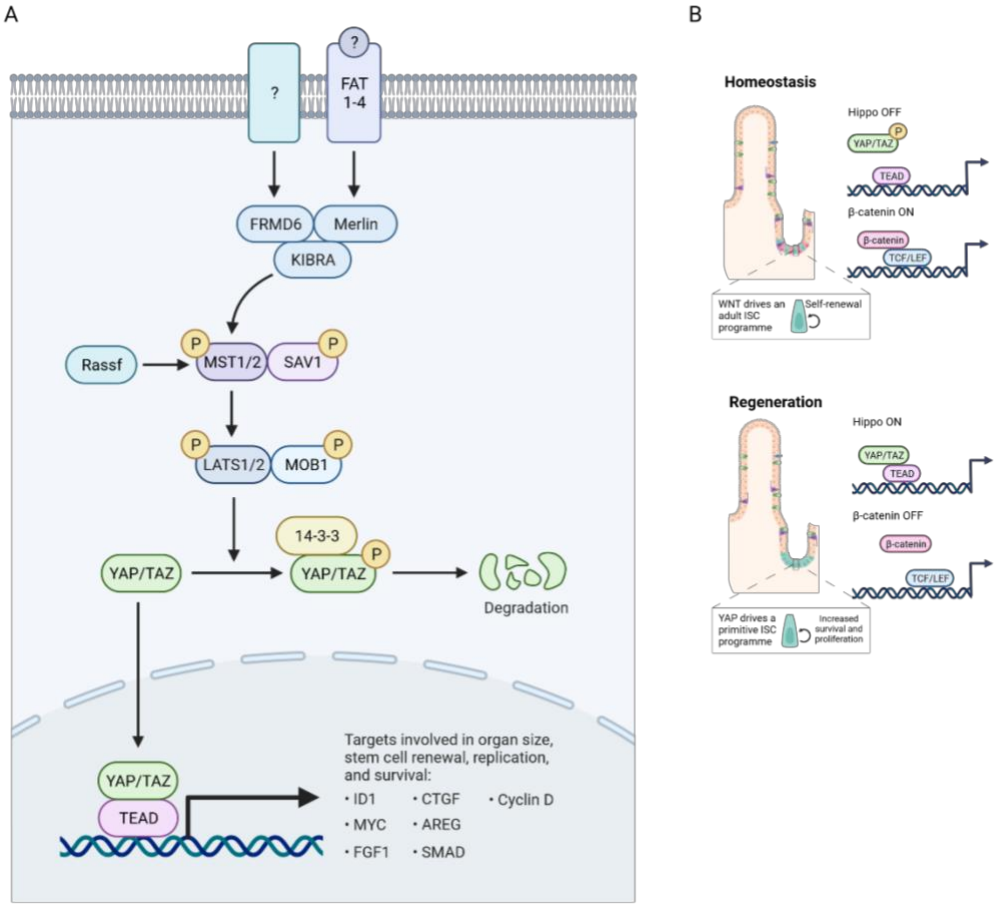

Figure 9 - Hippo pathway

A) The core of the Hippo pathway is defined by an evolutionarily conserved kinase cascade composed of Ste20-like kinase 1 (MST1) and MST2, large tumour suppressor kinase 1 (LATS1) and LATS2, their cofactors, Salvador 1 (SAV1) and MOB1A and MOB1B, the transcription co-activators Yes-associated protein (YAP), transcriptional co-activator with PDZ- binding motif (TAZ) and the TEAD family of transcription factors. Activation of the Hippo pathway is associated with the phosphorylation of the core Hippo kinases, MSTs and LATSs. MSTs are autophosphorylated and subsequently phosphorylate LATSs. Activation of LATSs induces the phosphorylation of YAP and TAZ and inhibits their transcription co-activator function. Phosphorylated YAP/TAZ are exported from the nucleus and degraded in the cytoplasm or sequestered at cellular junctions. When the kinases are not active, YAP/TAZ accumulate in the nucleus, bind to the TEAD transcription factors and promote the expression of target genes. The activity of these core components is regulated by several upstream mechanisms that involve cell junctions through various scaffolding proteins such as neurofibromin 2 (also known as Merlin), kidney and brain protein (KIBRA; also known as WWC1),; cell polarity, mechanical forces through the actin cytoskeleton and integrin signalling from the extracellular matrix; and several cell surface receptors such as G protein-coupled receptors and receptor tyrosine kinases Hippo also cooperates with WNT signalling: both β- catenin and YAP/TAZ associate with the destruction complex and are targeted for degradation

B) Effects of YAP hyperactivation on regeneration and homeostasis of the intestine. Although YAP is enriched in crypt stem cells, it is dispensable for intestinal homeostasis. Upon injury, YAP is activated, enters the nucleus and drives the expression of genes associated with a primitive gut stem cell programme that overrules the WNT-driven stem cell programme that occurs in homeostasis and directs low levels of stem cell self-renewal. This drives the expansion of the intestinal stem cell (ISC) compartment through increased survival of ISCs. Figure created with Biorender.com and adapted from [105].

Chapter 2: COLORECTAL CANCER

Throughout this chapter, I will try to bring some basic notions to help understand my research during this thesis studying colorectal cancer. I will introduce colon cancer SCs and give ideas about cell competition and plasticity during tumour initiation, deregulation of regeneration mechanisms, and resume changes in the signalling pathways that we saw in the past chapter.

Cancer

Cancer is one of the leading causes of death globally, making this non-communicable disease a significant public health problem worldwide [110]. The acquisition of tumorigenic characteristics can occur in any cell in the organism, regardless of its origin. Most adult cancers come from epithelial tissues due to their constant renewal that can favour the acquisition of genetic alterations. As we previously saw, the intestinal epithelium has a renewal time of approximately five days. Furthermore, due to its functions in absorption and xenobiotics' elimination, it is constantly in contact with harmful substances that can further favour a malignant transformation, as we will see below.

Thus, as a first step, a normal cell will undergo a neoplastic transformation, i.e., it will acquire phenotypic characteristics of a cancerous cell, implying a high proliferative capacity, ability to grow independently of growth factors altered metabolism, among others. These characteristics have been named "Cancer Hallmarks" [111]. In the most recent revised version of the Cancer hallmarks, Doug Hanahan postulated incorporating four new hallmarks to the existing ones (**see Figure 10 below**). I want to highlight two of them that may be useful for understanding how tumours can resist the treatments: the unlocking of phenotypic plasticity and the non-mutational epigenetic reprogramming [112].

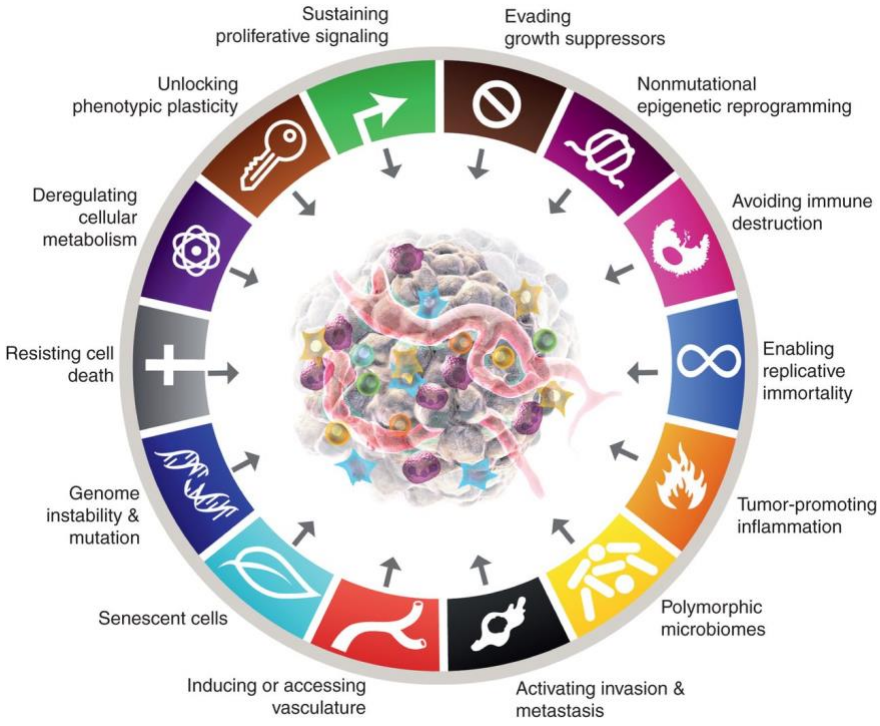

Figure 10 - Hallmarks of cancer

A cell that underwent neoplastic transformation can acquire genetic alterations that will increase the expression of proto-oncogenes (or the activity of their encoded proteins) or inactivate the tumour-suppressor genes. Briefly, proto-oncogenes are generally involved in pathways that promote cellular growth. Therefore, mutations or alterations in the proto-oncogenes that activate them can cause normal cells to become cancerous. Mutations in proto-oncogenes are typically dominant, and the mutated versions of these genes are known as oncogenes [113]. Examples of oncogenes are RAS, PI3K and MYC. Conversely, tumour-suppressor genes are involved in DNA damage repair, cell division inhibition, apoptosis induction, and metastasis suppression. Therefore, loss of tumour-suppressor gene function would result in the onset and progression of cancer. Noteworthy, both alleles of a tumour-suppressor gene must be inactivated or lost to result in tumour development [113]. Examples of tumour-suppressor genes are TP53, RB and APC. As we will see below, APC mutations are common in colon cancer, and APC loss renders intestinal cells insensitive to external Wnt pathway modulation.

The 2020 cancer burden worldwide report from the International Agency for Research on Cancer positions colorectal cancer (CRC) as the 3rd type of cancer in incidence and the 2nd in mortality, with both sexes comprising [114].

Colorectal cancer

Colorectal tumours provide an excellent system to search for and study the genetic alterations involved in the development of a common human neoplasm. Most, if not all, malignant colorectal tumours arise from pre-existing benign growth, allowing the study of these tumours from a small polyp to metastasis. Furthermore, both hereditary and environmental factors contribute to CRC development, allowing the analysis of inherited and somatic genetic alterations. The development of CRC results from a progressive acquisition and accumulation of genetic mutations and epigenetic alterations[115,116], including oncogenes' activation and tumour suppressor genes inactivation [116,117]. Moreover, non-genetic factors, like the tumour microenvironment (TME), can contribute to and promote oncogenic transformation and participate in the evolution of CRCs. Significantly, CRCs are composed of different cell populations, including undifferentiated cancer stem cells (CSCs) and bulk tumour cells displaying some differentiation traits, which constitute a hierarchical structure reminiscent of the organisation of the epithelium in a normal colon crypt[118,119]. These aspects will be detailed below.

As previously mentioned, CRC is the second leading cause of cancer death worldwide, even though there is strong involvement from public health agencies for early detection of this cancer. As I just mentioned, CRC development results from a progressive acquisition and accumulation of genetic mutations and epigenetic alterations. The classical description of colorectal carcinogenesis, the adenoma-carcinoma sequence and multistep tumorigenesis were well described in the '90s by Fearon and Vogelstein[115]. First, colorectal tumours arise due to mutational activation of oncogenes coupled with a predominant loss of tumours suppressor genes by mutational inactivation. Second, multiple gene mutations are required to form a malignant tumour. Fewer changes suffice for benign tumorigenesis. Third, although the genetic alterations often occur according to a preferred sequence, the total accumulation of changes, rather than their order of appearance, is responsible for determining the tumour's biologic properties. Fourth, in some cases, mutations of tumour suppressor genes exert a phenotypic effect even when present in the heterozygous state; thus, some tumour suppressor genes may not be "recessive" at the cellular level [115] (**See figure 11**).

In the adenoma-carcinoma sequence, the premature identifiable lesion is an aberrant crypt focus, a small dysplastic lesion in the colonic epithelium. Two different models propose the origin and growth of dysplastic aberrant crypt foci. Vogelstein and colleagues suggested the "top-down" morphogenesis model in which mutant cells located at the surface of the colonic epithelium spread laterally and downward to form new crypts [120]. An alternative model proposed that adenomas grow initially in a "bottom-up pattern" [121]. Aberrant crypt foci expand over time to develop macroscopically visible adenomatous polyps.

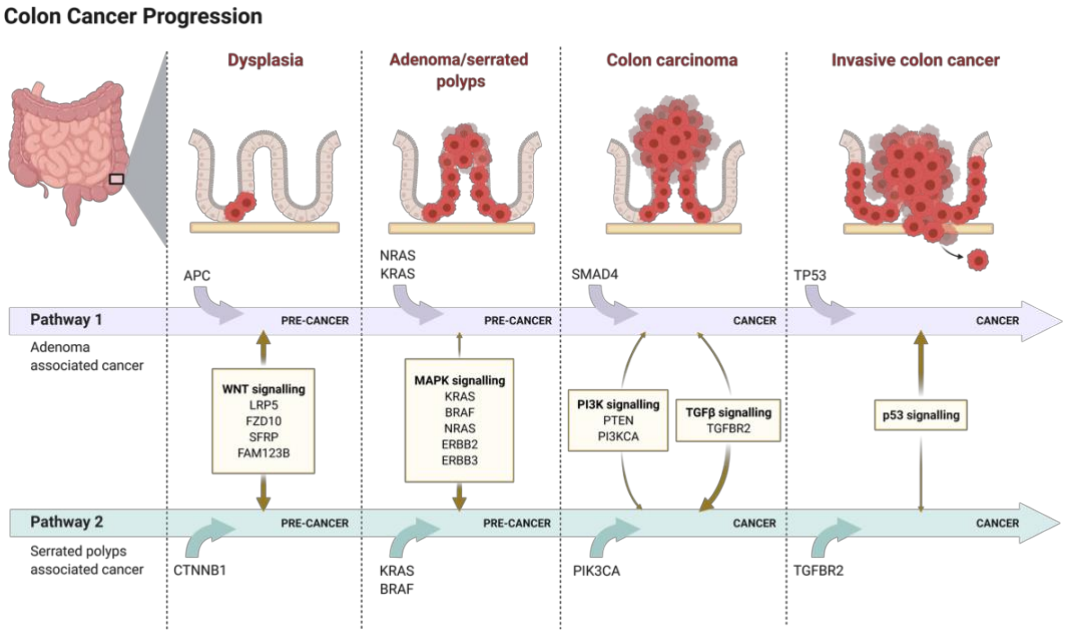

Figure 11 - Colorectal cancer progression

CRC carcinogenesis proceeds via three main genetic pathways. Cancers can arise due to chromosomal instability (CIN), microsatellite instability (MSI), or the serrated neoplasia pathway [122]. Five to ten per cent of CRC cases are inherited in an autosomal-dominant fashion. Hereditary cancer syndromes can be divided into two categories based on the lack or not of polyposis, best exemplified by the two main forms of hereditary CRC: hereditary nonpolyposis CRC and familial adenomatous polyposis (FAP) [117,122]. The hallmark of tumours in hereditary nonpolyposis CRC is chromosomal instability of microsatellites (repeats of short DNA sequences). Microsatellite instability is a measure of the ability of the DNA mismatch repair system to correct errors that often occur during DNA replication. Thus, CRCs can be microsatellite stable (MSS) or unstable (MSI). The latter generates typically serrated polyps, and the former crypt-base conventional adenomas [117,123]. Conversely, FAP patients present several benign epithelial neoplasias (polyps) built from glandular elements (adenomatous). These patients carry one mutant copy of the tumour suppressor gene APC. Of note, APC mutations are present in the hereditary FAP syndrome and may occur in many sporadic adenomas and adenocarcinomas somatically. APC appears as the gatekeeper in the molecular pathogenesis of most sporadic and hereditary forms of CRC.

In the past years, many studies tried to characterise colorectal tumours from a molecular point of view [124]. The advent of new extensive genomic and transcriptomic analyses opened the way to define new criteria and knowledge about the molecular classification of colorectal tumours and have further described the heterogeneity within these cancers by identifying so-called molecular subtypes. Guiney et al.[125] performed an extensive analysis of more than 4000 human CRC tumours that allowed them to classify the CRC types into four consensus molecular subtypes

(CMS) with distinguishing features. The first CMS is CMS1, a group characterised by a serrated morphology, an MSI, a strong CIMP (CpG island methylator phenotype) and hypermutations; it presents mutations in *BRAF* and a strong immune activation and infiltration. That is why it is commonly referred to as the MSI immune CMS. It represents approximately 14% of CRC tumours, and patients with this kind of tumour have a worse survival after relapse. Secondly, there is the CMS2 which represents 37% of CRC tumours and is believed to arrive from the conventional adenoma-carcinoma sequence. They are generally referred to as the canonical CMS; they come from an epithelial origin and are marked by aberrant activation of Wnt and MYC signalling. Third, it is the CMS3 which represents 13% of CRC tumours. They have a low CIN but strong CIMP and *KRAS* mutations. They are so-called metabolic as they present an evident metabolic dysregulation. Finally, the CMS4 tumours are characterised by a high SCNA (somatic copy number alteration) and mesenchymal characteristics, with a prominent TGFβ activation, stromal invasion, and angiogenesis. CMS4 have a heightened metastatic propensity and is inherent to EGFR-blockade therapy. They represent 23% of the CRC tumours, and patients with them have a worse relapse-free and overall survival. It is worth noting that 13% of CRCs remain unclassified by the CMS[122].

CMS1 MSI immune	CMS2 Canonical	CMS3 Metabolic	CMS4 Mesenchymal
14%	37%	13%	23%
MSI, CIMP high, hypermutation	SCNA high	Mixed MSI status, SCNA low, CIMP low	SCNA high
BRAF mutations		*KRAS* mutations	
Immune infiltration and activation	WNT and MYC activation	Metabolic deregulation	Stromal infiltration, TGF-β activation, angiogenesis
Worse survival after relapse			Worse relapse-free and overall survival

Figure 12 - CRC consensus molecular subtypes (CMS)
Proposed taxonomy of colorectal cancer, reflecting significant biological differences in the gene expression-based molecular subtypes. CIMP, CpG island methylator phenotype; MSI, microsatellite instability; SCNA, somatic copy number alteration. The figure is taken from [125].

The cell of origin of CRC? – Cancer stem cells

As we just saw in the CMS classification, CRC tumours can be heterogeneous from a molecular and cellular point of view as they are heterogeneous in composition. Researchers have tried to find the cell of origin of CRCs for many years. They proposed several models to explain the origin and dynamics of the acquisition of tumoral heterogeneity, like the clonal evolution and the emergence of CSCs, as we will see below. For many malignancies, it is assumed that SCs are the

'cell of origin'; that is, a SC acquires the initial mutations that are necessary for malignant conversion. I will try to summarise the discoveries that can help me introduce the concept of CSCs. Since the nineteenth century, tumours have shown explicit histological heterogeneity. However, it was not until 1937 that researchers established that a single cell from a mouse tumour could initiate a new tumour in a recipient mouse [119]. These cells were then known as tumour-initiating cells. Later in a series of landmark experiments, Pierce and colleagues showed that malignant teratocarcinomas contain highly tumorigenic cells that, as single cells, can differentiate into multiple differentiated, nontumorigenic cell types [119]. In the '70s, the focus of cancer research shifted when mutations in oncogenes and tumour suppressor genes were found to cause most human cancers. This new knowledge led Nowell to formulate the clonal evolution concept. He proposed that cancers arise from a single cell of origin and that the tumour's progression results from the acquisition of genetic variability, instability, and the sequential selection of more aggressive populations[126]. Furthermore, later, in 1990, as we saw in the previous paragraphs, Fearon and Vogelstein formulated a clonal evolution model for colon cancer in which the progression from early adenoma to invasive carcinoma reflects the stepwise acquisition of mutations in specific cancer genes[115]. During this same time, studies in acute myeloid leukaemia demonstrated by using FACS and xenografts assays that leukaemia derived hematopoietic SCs could generate tumours when engrafted into immunodeficient mice [118,119]. So, CSCs were found in acute myeloid leukaemia, and after that, CSCs were also found in other solid tumours, including CRC [127–129].

The discovery of colorectal CSCs unveiled an additional layer of intratumoral heterogeneity. CSCs were initially considered a population with well-defined phenotypic and molecular features[130]. However, accumulating evidence suggests that these CSCs are a dynamic population continuously shaped by a convergence of genetic, epigenetic, and microenvironmental factors [118,130]. The concept of ISCs as the colon cancer cell of origin has been challenged by studies showing that CRC may arise from more differentiated cells as the consequence of constitutive NF-kB activation [131] or from a subpopulation of differentiated quiescent tuft cells positive for the marker Dclk1 upon combined *Apc* deletion and chemically induced inflammation[132]. These studies indicate that CRC tumours can originate from both SCs and non-SCs, thus providing an unexpectedly motley picture of the cell of origin in CRC. In this scenario, the view of colorectal CSCs is dealing with a profound transformation during the years, in parallel with a rapidly evolving concept of stemness itself, both in cancer and in normal SCs cells. Stemness is increasingly viewed as a cell-intrinsic characteristic and a property of cell populations that is highly dependent on contextual conditions [130]. Researchers have tried to ablate CSCs, which has been a complex task due to LGR5+ CSCs (re)emergence after depletion and non-CSC dedifferentiation into CSCs[133–135]. This dynamic nature of the CSCs complicates, even more, the identification of the CSCs pool that established CRC[136]. Initial efforts to identify these CSCs

populations relied on the CSC phenotype and activity, and they were identified based on the expression of cell-surface markers: EphB2, LGR5, PROM1, ALDH [72,127,133,137], among others.

CRCs tumours have a high cellular heterogeneity and hierarchy, which resembles the complexity of a normal colon. Similarly to what happens in the normal intestine, in human CRC, different signals directly derived from the TME contribute to the CSC phenotype and functionality and even have a role in the mutational rate of the epithelium, defining the tumour expansion and therapy response. Thanks to the lineage tracing strategies, researchers could show that mutations in the Wnt pathway in crypt cells (whether on Lgr5+, Prom1+ or Bmi1+ cells) can result in adenomatous growth [137]. By contrast, inactivation of Wnt in more differentiated cells only sporadically results in adenoma formation, which requires the acquisition of further mutations in other genes. Thus, as Fearon and Vogelstein stated, a solitary mutation, in this case, in the *APC* gene, is insufficient to initiate an adenomatous expansion. Mutations involved in the malignant transformation of intestinal epithelial cells have been well-defined. Many cases include the mutation of the tumour suppressors *APC* and *TP53* and the oncogene *KRAS*[115]. Later, the Clevers group have elegantly shown that, indeed, the acquisition of multiple sequential mutations in cultured human ISCs gives rise to tumour organoids. Using CRISPR/Cas9, they introduced sequential mutations in the four typical mutated genes in CRC (*APC, TP53, KRAS* and *SMAD4*). Quadruple mutant organoids can be cultured independently of the ISC niche factors mentioned in the past chapter (Wnt, R-spondin, EGF and Noggin). When xenotransplanted in mice, these quadruple mutant organoids could grow as tumours with invasive carcinoma features[138].

With the advent of transcriptomic techniques, many groups have been trying to explain and find the cell of origin of CRC and how the competitive advantage of oncogenic events takes place in the intestinal crypt during the adenoma-carcinoma sequence. Clonal competition recalls Darwinian evolutionary dynamics in which subclones gain an advantageous mutation, which results in increased fitness relative to other subclones. CRC tumours present a high intratumor heterogeneity, and their growth dynamics are different within different tumour regions (border vs central). Interestingly, clonogenic dynamics are higher at the tumour border, where the tumour cells are in contact with the TME[139]. In line with this, another elegant study, using a multicoloured reporter mouse model associated with an oncogene, allowed the tracing of mutant and wild type (WT) cells in the mouse intestinal tissue. They observed that oncogene-expressing mutant crypt cells could alter the organisation of neighbouring WT crypts. Thus, crypts harbouring oncogenic *Kras* or *Pi3k* secrete BMP ligands that suppress local SC activity and the crosstalk with niche stromal cells with changes induced by the *Pi3k* mutated crypts alter the Wnt signalling microenvironment. In summary, oncogene-driven paracrine remodelling of the niche environment becomes detrimental to the maintenance of WT tissue, promoting transformation dominated by oncogenic clones[140].

It is worth mentioning that CSCs compete with normal SCs in the intestinal epithelium. The fast-cycling CBCs are most susceptible to initiating clonal lineages that carry a specific mutation. ISCs that acquire the common mutations in CRC exhibit an advantage over WT SCs. However, this advantage is not absolute. Normal SCs replace the mutant ISCs in stochastic events in homeostasis, which minimises mutated lineages. Written like this seems a simple and strong concept, but as we just saw, the TME in the tumorigenic transformation complexifies the picture. When an ISC acquires an oncogenic mutation in *APC* or *KRAS*, a bias ensues favouring the mutant cells, as I mentioned above. For example, the probability of a *KrasG12D* mutated cell replacing its neighbour ISCs and finally becoming clonal within a crypt is 60–70% compared to 12,5– 20% for non-mutated ISCs[141,142]. Notably, although the mutated ISCs gain a higher probability of niche fixation, these cells are still subjected to replacement by normal ISCs. Another tool that colon CSCs use to eliminate their WT neighbours is the modulation of the Wnt signalling. Earlier studies showed that tumour cells surrounding the niche TME had high Wnt activity, which was necessary for regulating the Wnt signalling in CSCs and restoring a CSC phenotype in more differentiated tumors[143]. Studies have recently dug into this more in detail and showed that *Apc* mutant cells have more transcripts encoding for Wnt inhibitors, mainly *Notum*, than WT in mice and organoids. Furthermore, these actively Notum-secreting mutant clones inhibit WT crypt cells' proliferation and drive their differentiation, acting as supercompetitors in the intestinal epithelium[144,145].

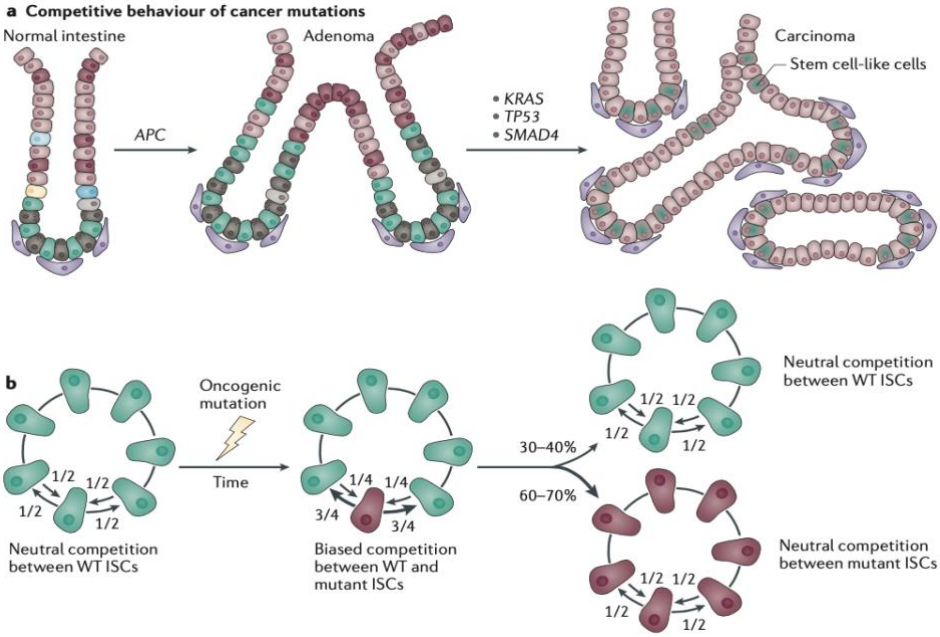

Figure 13 -Competitive behaviour of cancer mutations.
A) Schematic representation of the adenoma-carcinoma formation. Aberrant Wnt activation, via inactivation of APC, underlies adenoma formation and additional mutations in KRAS, TP53 and SMAD4 are associated with progression towards carcinoma *in situ*. **B)** Oncogenic mutations alter the competitive fitness of ISCs to their WT neighbours. As a result, the chance that a mutant ISC will displace a WT-neighbouring ISC (clonal expansion) is higher than the mutant ISC itself displaced (retraction). Therefore, oncogenic mutations frequently colonise the entire niche. Importantly, however, there is still a chance that ISCs with an advantageous mutation will be displaced from the niche and become extinct. Between ISCs containing the same mutation, replacement events are neutral again. The figure is taken and adapted from [146]

Niche-emancipating mutations

In the first chapter, I presented the importance of the Wnt pathway in ISC proliferation and self-renewal and the maintenance of intestinal homeostasis, and I briefly mentioned that deregulation of this pathway was essential for tumorigenesis in the intestine [146].

The tumour suppressor gene APC is mutated in 80% of human CRCs[117] and leads to constitutive Wnt pathway activation. To recall, APC is part of the β-catenin destruction complex. Mutations in the APC gene generate a truncated protein typically in the C-terminal domain, which is the one that in normal conditions binds to and causes the degradation of β-catenin. Indeed, stable β-catenin accumulates to high concentrations in the cytoplasm and nucleus of epithelial cells transformed upon loss of APC function, causing inappropriately active transcriptional activity of TCF/LEF/β-catenin target genes. Mutations in other Wnt pathway components (β-catenin itself or Axin2) led to the recognition of the Wnt/β-catenin pathway as a key effector in CRC initiation [123]. We saw that engineered organoids could recapitulate the adenoma-carcinoma sequence when harbouring cooperating driver-mutations in key CRC pathways (APC, KRAS, TP53, TGFβ, and PI3K) and exhibit a progressive loss of niche dependence, which confers a growth advantage in a hostile milieu[138]. I also mentioned that APC or CTNNB1 (coding for β-catenin) mutations led

to cell-autonomous constitutive activation of the pro-proliferative Wnt signalling, setting niche independence. However, the restoration of APC in invasive carcinoma models can remarkably induce cell differentiation and restore niche homeostasis[147]. Despite the great importance of Wnt in CRC, it is not the only signalling pathway altered, and several pathways interact between them to favour CRC progression. Although activating Notch mutations are rare, elevated Notch pathway components are detected in human CRC[87], but mucinous adenocarcinomas have a reduced Notch1 mRNA expression[148]. Similarly to Wnt activation, Notch activation alone is insufficient to generate adenomas. KRAS mutations are present in approx. 45% of CRC, mostly in codons 12, 13 or 61. These oncogenic mutations render KRAS insensitive to the GAP-mediated GTP hydrolysis and lock KRAS in an active GTP-bound conformation, causing disruption of the downstream pathway and uncontrolled proliferation in ISCs and rendering CSCs insensitive to EGF signals from the microenvironment[149]. Another important pathway in the ISC niche and homeostasis is the BMP pathway. Maybe unsurprisingly, the key components of this pathway are mutated in hereditary and sporadic intestinal cancers, and its inactivation correlates with adenoma progression. Mutations in SMAD4 or BMPR1A are common, same as GREM1 overexpression or BMP2 silencing by methylation, resulting in many colonic tumours due to loss of BMP expression[150,151]. Moreover, experiments in transgenic mice showed the importance of the BMP pathway in intestinal neoplasia. They suggested that this occurs through the influence of the BMP pathway on the Wnt pathway [152]. BMP activity is nevertheless highly context-dependent, and its interplay with the Wnt/β-catenin pathway affects different stages of CRC progression. Early in tumour development, in a WT *SMAD4* context, BMP signalling functions as a tumour suppressor, inhibiting Wnt activity[153] and suppressing stemness genes independently of Wnt/β-catenin[98]. However, loss of *Smad4* converts BMP signalling from a tumour suppressor to a metastasis promoter. The loss of SMAD4 and TP53 mutations and BMP signalling augmented Wnt/β-catenin signalling levels in the CRC cells located in the invasive front of tumours which may be responsible for the stem-like phenotype metastatic capacity and chemoresistance of these cells[153,154]. TGFβ signalling in CRC can also have a dual tumour-suppressing and promoting context-dependent role. It inhibits the onset of tumorigenesis, yet TGF-beta signalling enhances malignant progression and metastasis once tumours are formed. This differential activation status depends on whether the cell retains or loses the functionality of the pathway [155]. CRC advanced tumours with inactivating mutations in the TGFβ-pathway components often display elevated stromal TGFβ-levels and correlate with a poor prognosis [155]. The Batlle laboratory demonstrated in CRC samples, CRC organoids, and patient-derived xenografts from human CRC samples that stromal TGFβ orchestrated a pro-metastatic program, and this stromal TGFβ signature was predictive of disease relapse and metastasis [155,156] as well as immune evasion [157].

Adaptive Evolution: How Cancer Cells Survive Stressful Conditions and Drug Treatment

For many years, there was the conception that the cells that resisted drug treatments were the CSCs. This idea may come from chemotherapy-treated tumours that could regenerate the disease after treatment (relapse). Again, for many years, researchers thought that this relapse was due to the CSCs, and more precisely, those CSCs who adopted a quiescent state reminiscent of the +4 facultative ISCs. Another well-known classical conception of drug resistance was the upregulation of drug-efflux pumps, enhanced DNA repair capability or ROS protection that cancer cells can enhance to survive [118]. For years, the focus of many studies was on better understanding the genetic resistance mechanisms and how quiescent CSCs persisted during and after chemotherapeutic treatment. However, nowadays, the concepts and notions about how cancer cells can persist and resist chemotherapy are vast and extensive. General acceptance considers that intratumor heterogeneity plays a significant role in the emergence of drug resistance. Still, it remains unclear whether yet-to-be-discovered biological features of cancer cells play a role in the therapeutic failures. As we previously saw, the use of mice and diphtheria toxin to ablate Lgr5+ CSCs harbouring a diphtheria-toxin cassette is complicated due to the (re)emergence of Lgr5+ CSCs after the discontinuation of the treatment. Also, we must not forget that the dedifferentiation of non-CSCs to CSCs and the acquisition of phenotypic changes can occur[133–135]. Besides, as many studies showed, several cell types can revert and dedifferentiate after irradiating the epithelium to give rise to ISCs and progenitors [36,40,56,158–161]. Therefore, drug resistance is much more complex than we thought many years ago. Throughout the next part of this chapter, I will try to navigate the growing body of data regarding resistance and persistence to therapies in CRC (and I insist on both terms as they are pretty different, as we will see below). I will try to analyse these concepts and introduce the bases for comprehending part of the work performed during this thesis.

To begin with, I would like to introduce and remind some basic notions. Moreover, the first thing that comes to one's mind when thinking about drug resistance is: what do bacteria and cancer cells have in common? *A priori,* the answer will be not so much, almost anything. Cancer cells' hallmarks and acquired capabilities made them closer to bacteria than we think, especially in response to hostile environments, to protect the global cell population from eradication. Darwinian and Lamarckian selection governs the evolution of tumour cells and sometimes the genetic drift and heritable variations. These will result in a favourable emergence of adapted or fitter subclones that will support the growth and survival in the hostile environment. When facing stressful environments, bacteria deploy rapid and reversible survival programs that foster genetic diversity and facilitate adaptation to changes in the environment [162]. The bacteria rely on

stressful environments, bacteria deploy rapid and reversible survival programs that foster genetic diversity and facilitate adaptation to changes in the environment [162]. The bacteria rely on phenotypic switches to enter a physiologically dormant state displaying transient phenotypic stress tolerance without undergoing genetic changes. The cells that enter this state are called "persisters" [163]. Those persister cells, which are different from permanent genetically resistant cells, can reinitiate growth and regenerate a drug-sensitive population upon the termination of drug treatment (i.e. selective pressure)[163]. Cancer cells are also constantly exposed to stress and, like bacteria, can enter a reversible drug-tolerant persister (DTP) state when exposed to drug treatment [164–166]. A seminal paper by Sharma et al. implied a stochastic, *de novo* acquired, reversible epigenetic transition into a distinct drug-tolerant phenotypic state, enabling tumour cells to survive therapy[164]. This drug-tolerant phenotypic state was reminiscent of the properties of before mentioned antibiotic-tolerant bacterial subpopulations (also called ''persisters''), which similarly exhibit a transient ability to endure potentially lethal stresses[163]. So, these persister cells deploy four main, non-mutually exclusive strategies to survive unnoticed: (1) slowing cell proliferation, (2) adapting cell metabolism, (3) changing cell identity, and (4) hijacking the microenvironment[167] (**Figure 14**). Extended treatment of persister cells would inevitably lead to resistance and consequent treatment failure due to a different type of resistance. However, the acquisition of resistance can occur as a defence mechanism, whether pre-existing or *de novo* generated, especially in response to targeted therapies.

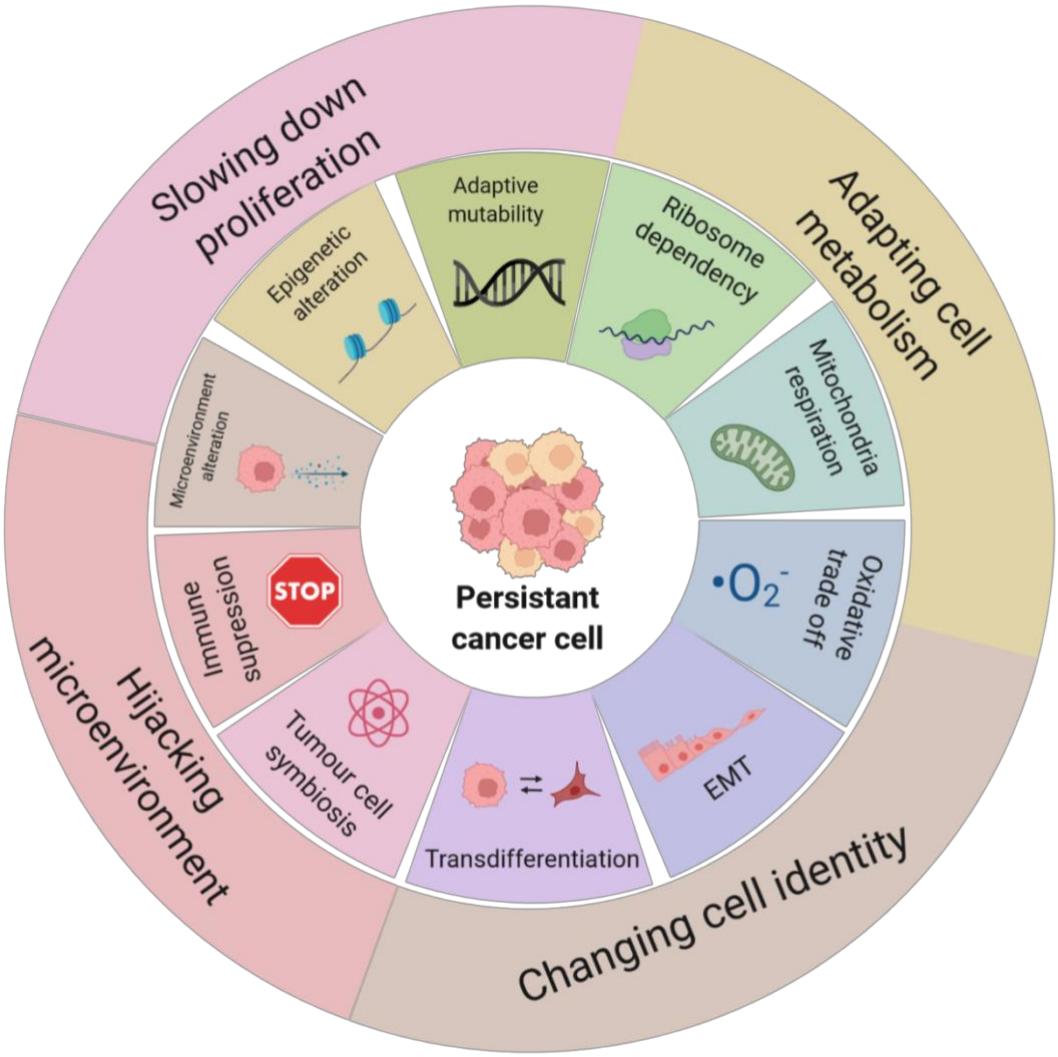

Figure 14 - The Different Ways in which Persistent Cancer Cells Can Evade Treatment
Four non-mutually exclusive main strategies are employed by persistent cancer cells to evade treatment. **A)** Slowing down proliferation: intracellular signalling and epigenetic alterations promote a slow-cycling persistent cell state, including epigenetic changes via histone (de)methylation, DNA methylation, or transcription factor modifications. The slow-cycling status of persistent cells can be related to an adaptive mutability resulting from MMR and HR downregulating and upregulation of error-prone DNA polymerases. **B)** Adapting cell metabolism: increased mitochondrial respiration is observed in various types of persistent cancer cells. Persistent cells can upregulate the membrane expression of fatty acid transport proteins. Increased mitochondrial respiration promotes intracellular reactive oxidant production and lipid peroxidation, which can be neutralised by autophagy or phospholipid hydroperoxidases. Alternative metabolism in persistent cells is associated with mRNA translation reprogramming, depending on the mRNA methylation status. This leads to the translation of a subset of mRNAs, promoting the persistent cell state. Adaptive metabolism is not mutually exclusive with other mechanisms; in particular, key metabolic enzymes are transcriptionally regulated by intracellular signalling and are also involved in slowing down cell proliferation. **C)** Changing cell identity: persistent cancer cells can transit from an epithelial cell state toward a mesenchymal cell state upon anti-cancer treatment, associated with increased expressions of immunosuppressive membrane proteins. Secreted factors from persistent cells that undergo EMT induce an immune-suppressive microenvironment. Additionally, different types of cancer cells can also transdifferentiate into different lineage cell types depending on the origin of the tissue. **D)** Hijacking microenvironment: tumour cells can cooperate to create a metabolic symbiosis with niche cells. Residual cancer cells can also educate other microenvironmental non-tumour cells, for instance, cancer-associated fibroblast, neutrophil, and tumour-associated macrophage. These non-tumour cells can secrete cytokines, chemokines, small RNAs, and metabolites to support the survival of persistent cancer cells upon anti-cancer treatment. The figure was adapted from [167].

Whereas drug tolerance is likely responsible for the ability of tumour cells to survive therapy, clinical relapse requires the acquisition of more robust resistance phenotypes capable of

maintaining net positive tumour growth in the presence of treatment. *Bonafide* resistance can develop from DTP cells by acquiring new genetic mutations, thus requiring new genetic diversification, for example, through adaptive mutability. Adaptive mutability combines stress responses that transiently increase the cell's genomic instability (even during the replicative quiescent state) in response to different environmental stresses, resulting in a stress-induced mutability capacity that promotes stochastic emergence of fitter mutants, leading to higher rates of adaptive evolution [162]. For example, in CRC, adaptive mutability was observed in cells that contained amplification of the *EGFR* gene or gain-of-function mutations in *BRAF* once they were challenged with targeted therapies against those oncogenes. These cells showed the transient repression of key genes involved in regulating the mismatch repair pathway and homologous recombination while increasing the expression of error-prone DNA polymerases[168]. The latter allowed the incorporation of unrepaired mutations into the DNA that increased the chances of the emergence of resistant clones. On the other hand, *bona fide* resistance can also develop from existing but weak resistant populations through a non-genetic mechanism. For example, the resistance to BRAF inhibitor was due to a transient expression heterogeneity in resistance-associated genes, such as *AXL* and *EGFR*, that enabled the survival of subpopulations of tumour cells. However, the development of fully resistant phenotypes involved the acquisition of multiple, partially coordinated gene expression changes[169]. Thus, the DTP state does not limit and may even provide a latent reservoir of cells for the emergence of heterogeneous drug-resistance mechanisms[170].

In all, the origin of therapeutic resistance can be explained either by (i) early selection of preexisting cells that harbour genomic or non-genomic (e.g., transcriptomic, epigenetic) alterations that provide the cancer cell with a clonal advantage to escape the therapeutic pressure, promote resistance and their selection after elimination of sensitive cells; or by (ii) late acquisition of *de novo* resistant alterations as a result of prolonged exposure to therapy [170–173]. In other words, therapeutic resistance can be primary (intrinsic) or secondary (acquired). The lack of objective clinical response following treatment characterises the primary resistance. By contrast, secondary resistance is a local or distal recurrence of the malignance after the clinical response[171]. I will be focusing on this particular type of resistance. Acquired resistance is generally conceived as the genetic evolution of cancer in response to the therapeutic challenge. Still, it is not the sole therapeutic evasion mechanism because, as we just saw, non-genetic priming like the DTP state can contribute too. Within the same patient or even tumour, multiple mechanisms of drug resistance can coexist [170]. Even if I outline the genetic and non-genetic therapeutic resistance (via epigenetic or phenotypic changes) as separate entities, to illustrate the concepts associated with them, it is vital to emphasise that cancers show those therapeutic evasions concurrently and not like mutually exclusive evolutionary trajectories[167,170,171,174]. DTPs can occur as an enrichment of primed persisters following a Lamarckian induction, where this persister state is an adaptive

inheritable state induced by the environmental output. For example, in melanoma, drug-tolerant neural crest SCs appear transiently through active cell transition rather than passive selection [175]. Thus, non-genetic resistance can be stable and heritable via acquiring different transcriptional programmes and cell plasticity to generate the phenotypic switch via epithelial-mesenchymal transition (EMT), transdifferentiation, or reversion of an immature stem/progenitor phenotype, among others. Following the past example and trying to understand how the mechanisms of resistance take place, researchers showed that in melanomas exposed to BRAF and MEK inhibitors, the emergence of a transient neural crest SC population in the DTP state concurs with the development of nongenetic resistance and the activation of the AKT pathway involving the focal adhesion kinase [176]. Ablation of the transient neural crest SC population through inhibition of the focal adhesion kinase delayed the relapse in patient-derived tumour xenografts. Strikingly, they observed that all tumours that ultimately escape this final treatment exhibit resistance-conferring genetic alterations and increased sensitivity to extracellular signal-regulated kinase inhibition[176]. They identified that, at least in melanoma, the nongenetic resistance trajectory could be abolished and demonstrated that the cellular composition of residual tumour cells imposes distinct drug resistance evolutionary paths[176]. Some persister's cells can be more proliferative and lead to rapid clinical progression and early relapse, while others could be less proliferative and correlate with late relapse. Most cancer persisters have an arrested cell cycle in the presence of the drug, while a rare subset can re-enter the cell cycle under constitutive drug treatment [166]. Oren and colleagues developed a high-complexity expressed barcode lentiviral library (watermelon) that enables simultaneous tracking of each cell's clonal origin, proliferative and transcriptional states to understand this phenomenon. Using this model, they showed that cycling and non-cycling persisters arise from different cell lineages with distinct transcriptional and metabolic programs. The latter can poise the persisters to undergo a proliferation-promoting adaptive response and have a chromatin configuration that renders them more likely to transition to an oncogene-independent state following treatment [166]. Any cancer cell can enter a DTP state in response to therapeutic regimens[165]. Altogether, these observations denote the potential contribution of DTP in the emergence and the heterogeneity of acquired resistance observed in the clinic.

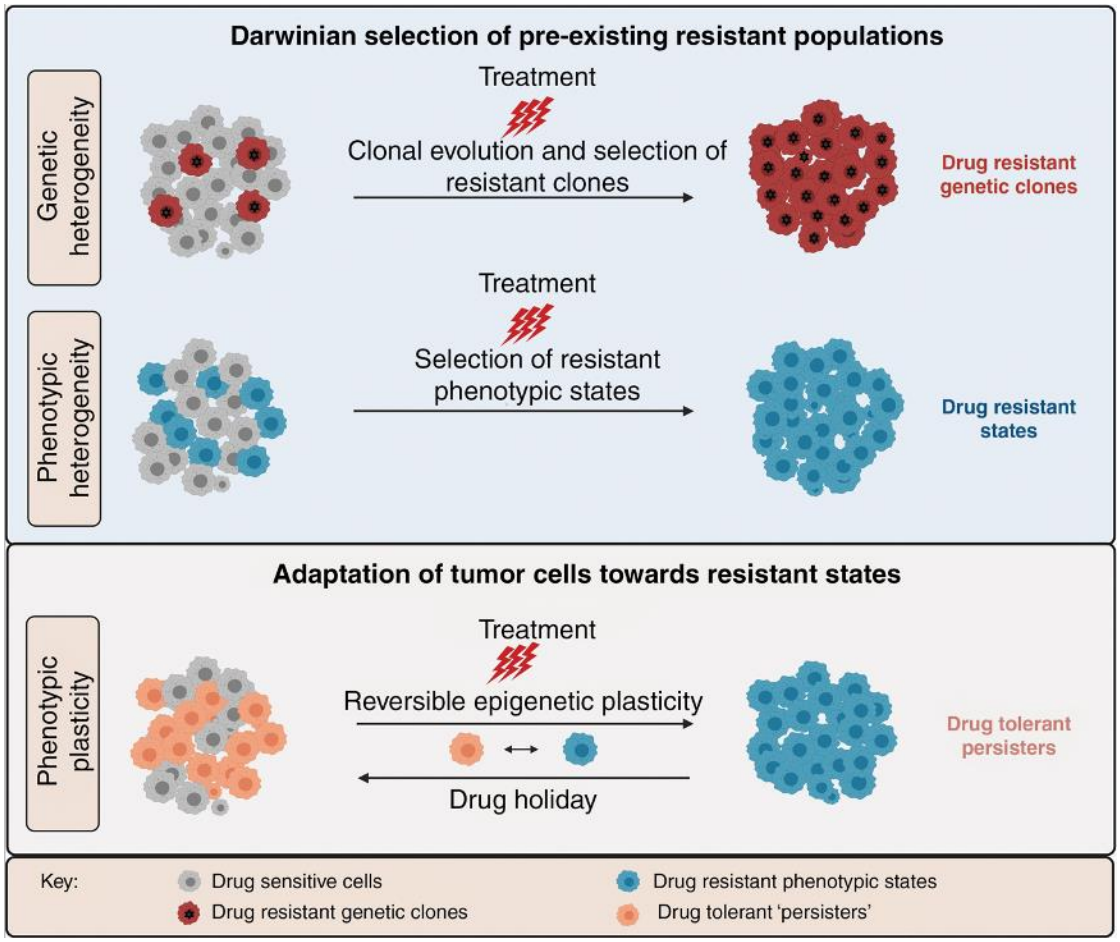

Figure 15 - Tumour heterogeneity and plasticity as resistance mechanisms
Tumours contain cells with varying sensitivity to treatment. Treatment leads to the eradication of drug-sensitive cells. Resistance can be driven by a Darwinian selection of pre-existing resistant cells with advantageous genetic or phenotypic tumour characteristics. Highly resistant genetic clones may also be acquired upon treatment (i.e., clonal evolution and selection). Adaptive resistance is driven by drug-tolerant persisters that survive treatment and adapt towards resistant phenotypic states. Persisters can revert to their initial phenotypic states and recreate phenotypic heterogeneity when released from the treatment (i.e., drug holiday). Drug resistance may thus be a result of reversible epigenetic plasticity combined with irreversible clonal expansion, adapted from [174].

The initial solution to the problem of resistance to single-agent chemotherapy was the combination of agents with non-overlapping mechanisms of action or polychemotherapy to maximise the action spectra. However, it led to complex regimens with increased secondary effects and no response in many tumour types. The necessity of new agents led to the development of targeted therapies that tackle precisely signalling pathways, tyrosine kinases, and nuclear receptors, which resulted in other resistant mechanisms, not necessarily through genetic changes. So, we need to understand how a cancer drug works to know why it is not working and the cells are getting resistant. A cancer drug operates as a three-component system as it needs a therapy regimen, a population of cancer cells and a host environment. Some biological determinants (**summarised in Figure 16**) govern drug resistance [177]. First, there is the tumour burden and growth kinetics where, even if not the rule, bigger tumours contain a higher probability of developing metastasis and having drug-resistant clones. Still, the growth kinetics of the tumour also determine a critical role in response to therapy and resistance. Second, tumour heterogeneity,

as all cells of the tumour are genetically and spatially diverse, makes it hard to tackle all composing cells. Third, the physical barriers. The lack of blood flow in and to the tumour, the spatial gradients surrounding the tumour, hypoxia, and pH can decrease drugs' effectiveness and arrival. Fourth, the TME, like immune cells, stroma, and vasculature, can mediate drug resistance by preventing immune clearance of the tumour cells, hindering drug absorption and secreting growth signal factors to promote cancer growth. Fifth is the presence of non-druggable genomic drivers like *MYC*, *RAS* and *TP53*. Last, the selective therapeutic pressure will enhance the resistance through genetic and non-genetic mechanisms in the cancer cells and the TME [177].

In summary, cancer cells can acquire various mechanisms of resistance, including (a) decreased accumulation of the cytotoxic drug as a result of an increased expression of drug transport proteins, (b) decreased amount of drug uptake by the cell by increasing efflux, (c) insufficient activation of the drug, (d) increased drug inactivation, (e) increased concentration of target enzyme or altered activity of the target, (f) increased utilisation of alternative pathways to the ones inhibited, (g) decreased requirement of the substrate, (h) rapid repair of drug-induced DNA damage and (i) mutations in genes involved in therapy resistance [178,179].

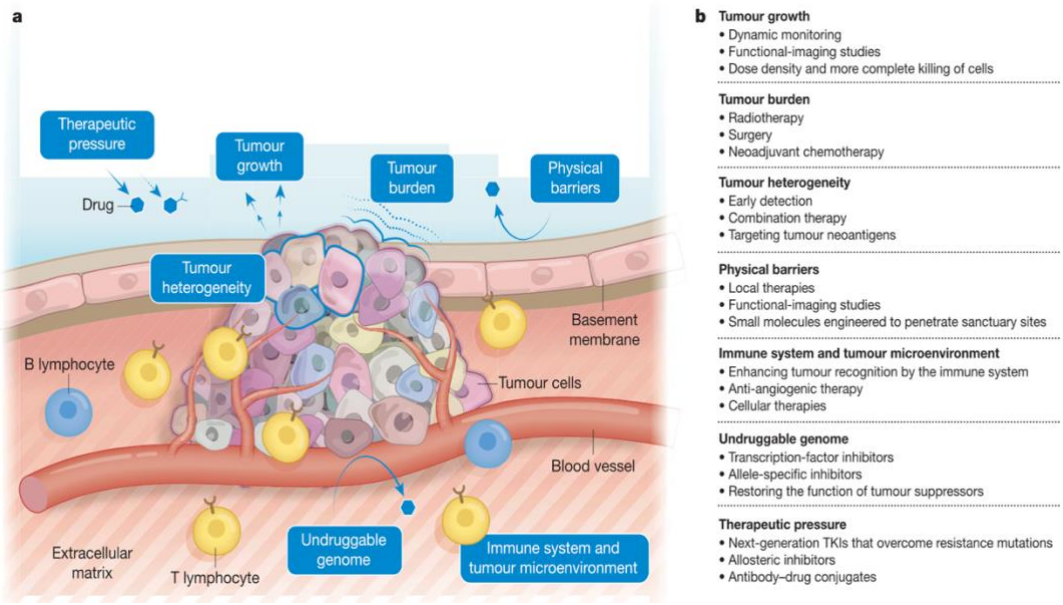

Figure 16 - Understanding drug resistance and its biological determinants

A) Biological determinants of drug resistance. Tumours are heterogeneous and are situated in a milieu that comprises the basement membrane, vasculature, immune cells and tumour microenvironment, among other components. Changes in the physical parameters, genome and surrounding environment of the tumour drive drug resistance. **B)** Standard of care and emerging approaches to managing the biological determinants of resistance. Several clinical diagnostic and therapeutic strategies can target resistance determinants—the figure is taken from [177].

Pharmacological notions

I want to introduce some pharmacological notions and remind others that I will mention below. Pharmacology is the study of the effects of drugs on the function of living systems. It started as a science in the mid-19th century, although apothecaries and pharmacopoeias existed long before, and herbal medicines were widely used. We commonly talk about drugs in cancer, but what is a drug? A drug is a chemical substance of a known structure other than a nutrient or an essential dietary ingredient. When administered to a living organism produces a biological effect [179]. A few points are worth noting. First, drugs may be synthetic chemicals, plant or animal-derived chemicals or products of biotechnology (biopharmaceuticals). Medicine is a chemical preparation and contains other substances (excipients, stabilisers, solvents, etc.) besides the active drug to make it more convenient to use [179]. Insulin and thyroid hormones can be considered drugs when administered intentionally, even if endogenous hormones. Another essential concept is drug dispositioning, divided into four stages and designated by the acronym ADME for Absorption from the administration site, Distribution within the body, Metabolism and Excretion.

I will point out drug metabolism, especially as these notions will help understand the resistance mechanisms. Animals have complex systems to detoxify foreign chemicals (xenobiotics), including carcinogens and toxins. Drugs are a particular case of xenobiotics, and their metabolism involves two kinds of reactions, known as Phase I and Phase II, which often occur sequentially. In addition, enzyme induction and enzyme inhibition are important causes of drug-drug interaction. Phase I reactions (e.g., oxidation, reduction or hydrolysis) are catabolic, and the products are often more chemically active or toxic than the parental drug (**Figure 17**). Moreover, Phase I enzymes often introduce a reactive group, such as hydroxyl, into the molecule, a process known as functionalisation. This group serves as a point of attack for the conjugating enzymes (phase II). Phase I enzymes include the cytochrome P450 superfamily, which are haem proteins related but distinct enzymes referred to as CYP with accompanying numbers and letters [179]. Conversely, Phase II reactions are synthetic (anabolic) and involve conjugating a chemical group glucuronyl, sulphate, methyl or acetyl to the free hydroxyl, thiol or amino group of the drug or conjugating glutathione, which usually results in inactive products (**Figure 17**). These products are eliminated via urine and feces[179]. Another essential notion I want to mention is pharmacokinetics, the branch of pharmacology dedicated to determining the fate of chemical substances administered to a living organism. It involves measuring and interpreting the changes that a drug and its metabolites undergo over time and its concentration in plasma and urine in relation to the dosage. It follows a drug's ADME. In contrast, pharmacodynamics reflects the

differences in drug targets and individual susceptibility to uncommon qualitatively determined differences in enzymes and immune mechanisms[179].

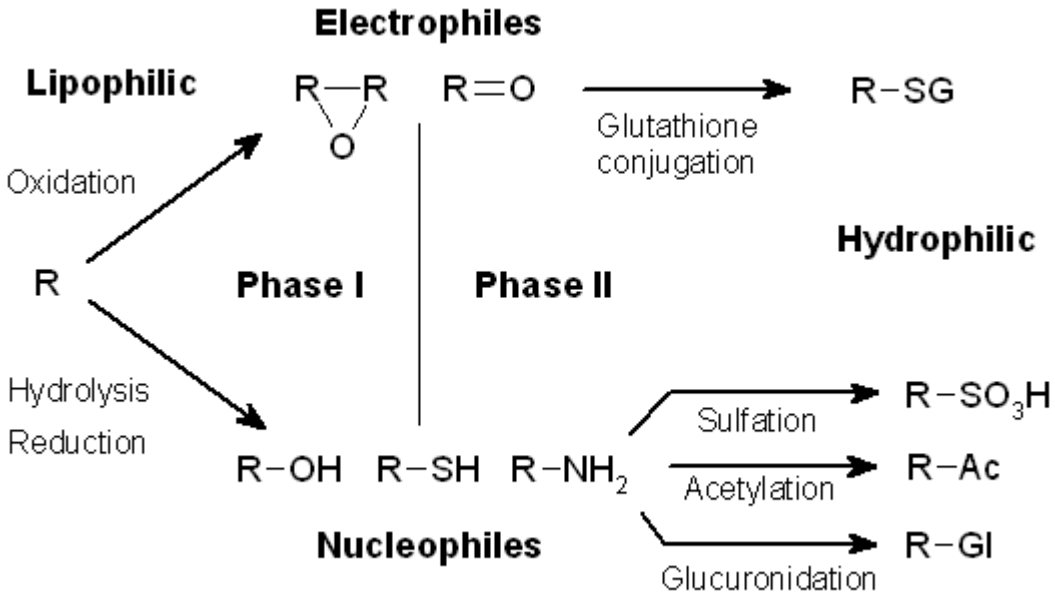

Figure 17 -Phase I and Phase II drug metabolising enzymes

Treatment modalities in CRC

The first treatment for CRC is surgery. The surgeon will eliminate the cancerous tissue/lesion and the adjacent normal tissue. After the surgery, the patient will receive a systemic treatment or radiotherapy as prevention and eliminate any potential cancer cells that may have remained. Chemotherapy can also be administered before the surgery, as it is called neoadjuvant chemotherapy, usually to reduce the size of the tumour before the intervention. Among the modalities of systemic treatment in CRC, chemotherapy has been the most widely used. However, in recent years, targeted therapies have complemented the therapeutic options, especially to treat metastatic CRC. Since the late 50s, fluoropyrimidines have constituted the backbone of CRC chemotherapeutic regimens, with 5-fluorouracil (5-FU) as the most commonly used agent [180]. The addition of folinic acid or leucovorin (LV) to the regimen showed benefits in side effects prevention. The next generation of chemotherapeutic regimens came in the late 90s with the advent of two cytotoxic agents: oxaliplatin (OXA), a platinum derivative, and irinotecan (IRI), a topoisomerase I inhibitor. Thus, the combination of 5-FU/LV with oxaliplatin and irinotecan gave rise to the treatment called FOLFOX and FOLFIRI, respectively. Later, a triple combination, FOLFOXIRI, was also proposed [181].

Over the last two decades, the advent of monoclonal antibodies that targeted the vascular endothelial growth factor (VEGF) pathway (bevacizumab) and the EGFR pathway (cetuximab and panitumumab) moved the therapies one step forward for the treatment of metastatic CRC and

in first-line treatment although always combined with conventional chemotherapy[182]. In patients with unresectable liver metastasis from CRC, systemic doublet or triplet chemotherapy and targeted therapy are standard first-line therapies. However, in metastatic CRC, the use of immune checkpoint inhibitors targeting the programmed cell death 1 (PD1) and its ligand 1 (PD-L1) and the cytotoxic T-lymphocyte antigen-4 (CTLA-4) remain largely ineffective as only a small subset of patients (4–5%), harbouring a deficient mismatch repair system /microsatellite instability-high or mutations in the catalytic subunit of polymerase epsilon can benefit of it[183]. The inter-individual variability limits the use of chemotherapy to treat cancers in drug response and by developing resistance. The liver is the leading metabolisation site for anticancer drugs. Subsequently, in the tumour and TME, drug uptake/efflux transporters modulate intracellular levels of the drug or its active metabolites (conjugated or unconjugated). Therefore, the efficacy of anticancer drugs in tumour cells is dependent on the effective concentrations and the presence and quantity of the drug targets. In addition, inter-individual differences alter enzymes' expression levels and activities, modifying the efficacy and toxicity of anticancer drugs. We will see in the following paragraphs the most used armamentarium to tackle CRC, the modifications in the drugs' ADME that can alter the drug response, and some examples of drug resistance in CRC. In **Table 1** there is a summary of the most commonly used therapies in CRC.

5-Fluorouracil (5-FU)

5-FU belongs to the fluoropyrimidines family, and it has been in use for the last half-century [180]. It is the backbone of all therapies for CRC treatment. It is a fluorinated pyrimidine, analogue to the uracil, that acts primarily through inhibition of thymidylate synthetase (TYMS), the rate-limiting enzyme in pyrimidine nucleotide synthesis, interfering with the formation of 2'-deoxythymidylate, and it is converted into a fraudulent nucleotide, the fluorodeoxyuridine monophosphate (FdUMP)[179]. Leucovorin (LV), a reduced folate that stabilises fluorouracil's interaction with this enzyme, is widely used in combination [179,182]. 5-FU/LV various administration schedules, typically in an intravenous bolus injection, have different toxicities (mainly neutropenia, diarrhoea and stomatitis). Two other drugs, capecitabine and tegafur, can be orally administered and are metabolised to fluorouracil[182]. Recent studies showed another mechanism of action for 5-FU. Many data suggest that apart from its effect on the DNA, 5-FU can also affect RNA and protein synthesis, and both nucleic acids can incorporate fluorinated compounds following 5-FU administration [184]. Moreover, most classes of RNA, including ribosomal RNA (rRNA), incorporate 5-FU. This incorporation generates fluorinated ribosomes (which are still active) that induce changes in the translational activity and modulate the translation of a subset of mRNAs inducing a translational reprogramming [185,186].

Summing up, to exert its cytotoxic effect, 5-FU has to reach the tumour site, enter the cancer cells, and be phosphorylated into its three active metabolites, which are 5-fluorodeoxyuridine

monophosphate (5-FdUMP), 5-fluorodeoxyuridine triphosphate (5-FdUTP) and 5-fluorouridine triphosphate (5-FUTP). Thus, 5-FU ADME is essential for the balance between toxicity and efficacity. As mentioned before, 5-FU administration is intravenous, and the liver metabolises more than 80% of it. Therefore, the metabolism of 5-FU leads to activation and pharmacodynamic actions of the drug. The rate-limiting step of 5-FU catabolism is dihydropyrimidine dehydrogenase (DPYD) conversion of 5-FU to dihydro fluorouracil (DHFU) which is then converted into fluoro-beta-ureidopropionate (FUPA) and subsequently to fluoro-beta-alanine (FBAL) by dihydropyrimidinease (DPYS) and beta-ureidopropionase (UPB1), respectively [187,188]. Therefore, deficiency in enzymes of this pathway can result in severe and even fatal 5-FU toxicity [188]. The primary mechanism of 5-FU activation is conversion to fluorodeoxyuridine monophosphate (FdUMP), which inhibits the enzyme thymidylate synthase (TYMS), an essential part of the folate-homocysteine cycle, purine and pyrimidine synthesis. The conversion of 5-FU to FdUMP can occur via thymidylate phosphorylase (TYMP) to fluorodeoxyuridine (FUDR) and then by the action of thymidine kinase to FdUMP or indirectly via fluorouridine monophosphate (FUMP) or fluroridine (FUR) to fluorouridine diphosphate (FUDP) and then ribonucleotide reductase action to FdUDP and FdUMP [189]. In addition, FUDP and FdUDP can also be converted to fluorouridine triphosphate (FUTP) and FdUTP and incorporated into RNA and DNA, respectively, contributing to the pharmacodynamic actions of fluoropyrimidines[189]. 5-FU enters the cells using several transmembrane proteins known as human nucleoside transporters (**see Figure 18**). The Solute Carrier Organic Anion Transporter Family Member 1B1 (SLCO1B1) uptake 5-FU, but it can also enter the cells by passive transport. ABCC5 and ABCC11, two organic anion transporters ubiquitously expressed in tissues, mediate the efflux of 5-FU through the efflux of 5-FdUMP[189]. An essential consideration when using 5-FU and related drugs is the development of drug resistance. Some mechanisms of resistance involve expression changes in pharmacodynamic and pharmacokinetic gene candidates. Drug resistance can also include changes in drug transport and enzymatic deficiency. 5-FU resistance implicates several transporters, including ABCB1 and ABCG2[189,190], and the ABCC family ABCC3, ABCC4, ABCC5, ABCC6 and ABCC11[189,191]. Additionally, SLC29A1 and SLC22A7 are involved in the increased efflux of 5-FU, favouring resistance.

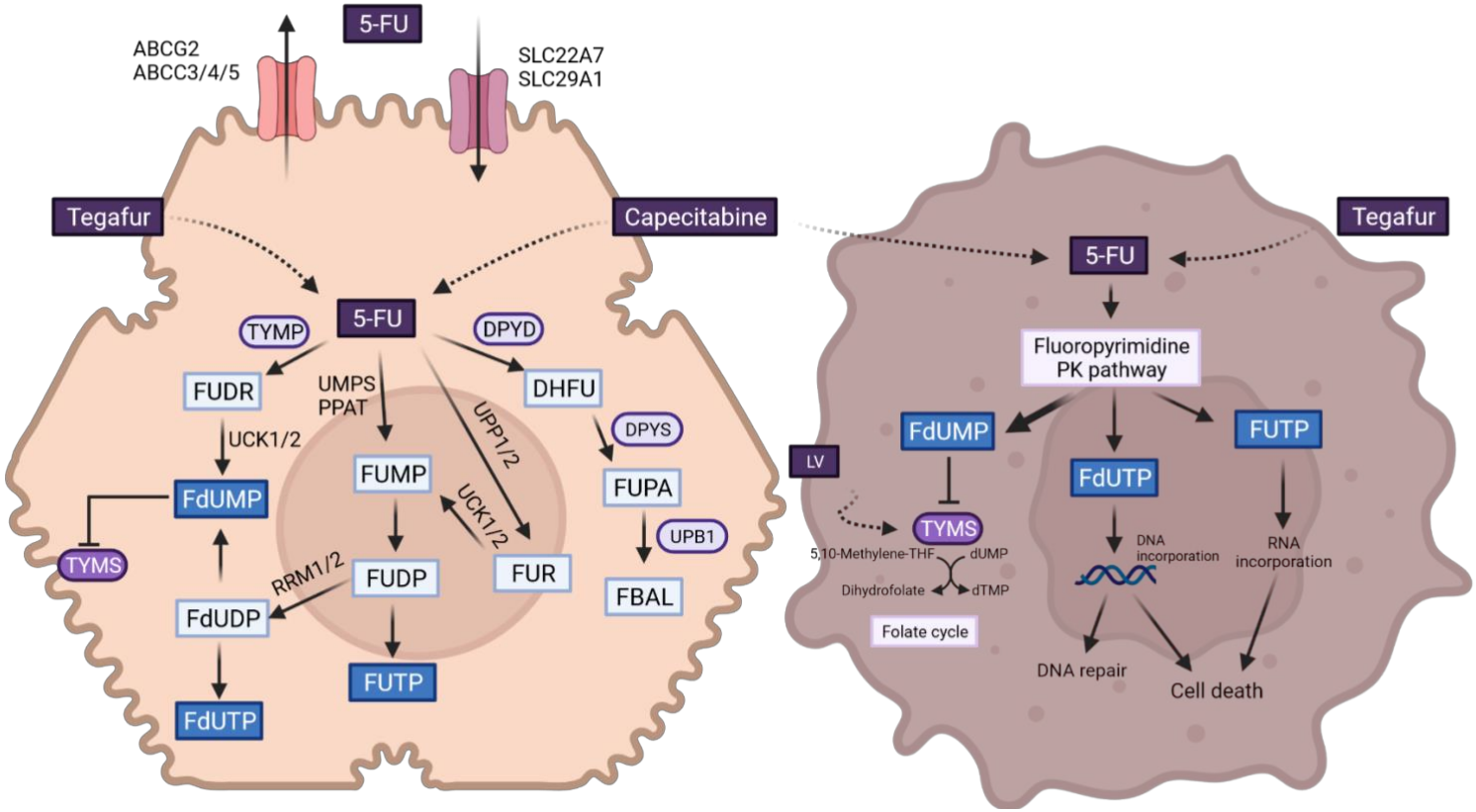

Figure 18 -5-FU pharmacokinetics (PK) and pharmacodynamics (PD)

The scheme shows candidate genes involved in the PK of 5-fluorouracil (5-FU), capecitabine and tegafur (two oral 5-FU prodrugs). There are several routes for the metabolism of 5-FU, some of which lead to the drug's activation and PD actions. The rate-limiting step of 5-FU catabolism is dihydropyrimidine dehydrogenase (DPYD) conversion of 5-FU to dihydro fluorouracil (DHFU). DHFU is then converted to fluoro-beta-ureidopropionate (FUPA) and fluoro-beta-alanine (FBAL) by dihydropyrimidinease (DPYS) and beta-ureidopropionase (UPB1), respectively. Deficiency in these enzymes can result in 5-FU toxicity. The main mechanism of 5-FU activation is conversion to fluorodeoxyuridine monophosphate (FdUMP), which inhibits the enzyme thymidylate synthase (TYMS), an important part of the folate-homocysteine cycle and purine and pyrimidine synthesis. The conversion of 5-FU to FdUMP can occur via thymidylate phosphorylase (TYMP) to fluorodeoxyuridine (FUDR) and then by the action of thymidine kinase to FdUMP or indirectly via fluorouridine monophosphate (FUMP) or fluroridine (FUR) to fluorouridine diphosphate (FUDP) and then ribonucleotide reductase action to FdUDP and FdUMP. FUDP and FdUDP can also be converted to FUTP and FdUTP and incorporated into RNA and DNA, respectively, contributing to fluoropyrimidines' PD's actions. TYMS inhibition is one of the principal mechanisms of fluoropyrimidines' action, but alternative PD pathways acting by incorporating drug metabolites into DNA and RNA were shown. FdUMP forms a covalent complex with TYMS and prevents the binding and conversion of dUMP to dTMP, necessary for pyrimidine and DNA synthesis, and blocks the simultaneous conversion of 5, 10-methylene tetrahydrofolate to dihydrofolate, a key component of the folate pathway. The inhibition of TYMS leads to an imbalance of dUTP and dTTP and a rise in the misincorporation of dUTP into DNA. The complex of FdUMP and TYMS is stabilised by coadministration of leucovorin (LV), a folate analogue that can bind in place of 5, 10-methylene THF. Figure adapted from [189].

Irinotecan

Irinotecan (IRI), CPT-11, is a semisynthetic derivative of the natural alkaloid camptothecin incorporated into the combination 5-FU/LV regimen in the late 90s under the name of FOLFIRI[192]. IRI is a topoisomerase I (TOP1) inhibitor. TOP1 is the enzyme that catalyses the one-strand breakage and rejoining of DNA strands during DNA replication. IRI is a prodrug. Carboxylesterases (CES) metabolise IRI into its active metabolite, SN-38, which causes DNA fragmentation and programmed cell death by binding to the TOP1 and thus preventing the relegation of DNA. CES can metabolise IRI to SN-38 both in the hepatocytes and enterocytes[193,194]. Its rapid interconversion to SN-38 increases the toxic effects. SN-38 can subsequently be detoxified, predominantly by UGT1A1 in hepatocytes and enterocytes, to form inactive SN-38 glucuronide (SN-38G)[193,194]. This SN-38G can also be metabolised to SN-38 by β-glucuronidase of the intestinal microbiota[193]. In the liver, CYP3A4/5 can metabolise IRI into inactive metabolites. In addition to these drug-metabolizing enzymes, several transporters expressed in the liver and intestine imprecate IRI/SN-38 pharmacokinetics (**Figure 19**). A primary active transport system is involved in the permeation of SN-38 across liver canalicular membranes and enterocytes' apical and basal surfaces. The ATP-binding cassette (ABC) transporter family C mainly does this transport where many members are involved. The ABC C subfamily, member 2 (ABCC2), is involved in the biliary excretion of SN-38G, while ABCC3 is involved in its blood excretion from the liver and the intestine. ABC transporter, subfamily G, number 2 (ABCG2), and the ABC transporter, subfamily B, number 1 (ABCB1), play critical roles in mediating IRI/SN-38 and SN-38G biliary excretion in the liver and efflux of SN-38 in the intestine[193,194]. ABCG2 and ABCB1 are important the side effects of IRI and its resistance in CRC. They will be treated in the results section of this thesis.

CRC patients can have pharmacogenetic changes (polymorphisms) in the metabolising enzymes and transporters, resulting in differential availability and toxicity of IRI and increased resistance. Furthermore, besides the molecular targets, other factors like age, organ dysfunction and environment can cause differential action and response to IRI[181,194]. We will see some of them below and in the next chapter.

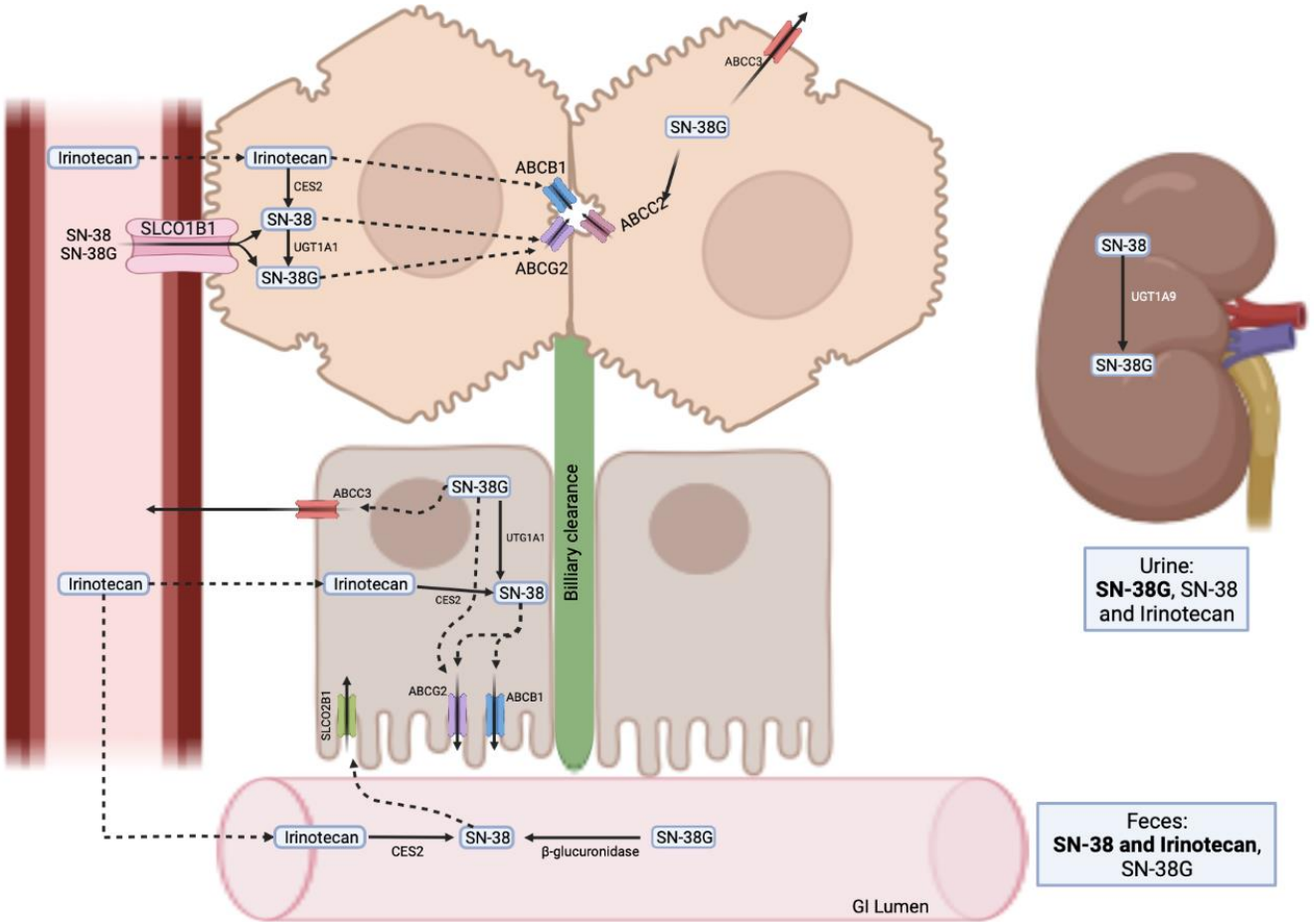

Figure 19 - Irinotecan pharmacokinetics

Irinotecan (IRI) is a prodrug and thus needs metabolisation into SN-38, the active compound, to inhibit the Topoisomerase I (TOP1).-38. IRI uptake and transport into the liver are facilitated by: SLCO1B1, ABCB1, ABCC1, ABCC2, and ABCG2. Specifically, ABCB1 is present on the bile membrane and is responsible for IRI secretion and its metabolites into the liver. IRI is metabolised in the liver and converted to SN-38, the active metabolite and TOP1 inhibitor, by carboxylesterases (CES) mediated hydrolysis (CES1 and CES2). SN-38 is then glucoronized to SN-38 glucuronic acid (SN-38G) and detoxified in the liver via conjugation by the UGT1A1 family, which releases SN-38G into the intestines for elimination. In the intestinal lumen, bacterial β-glucuronidase can reverse the reaction and transform inactive SN-38G back into active SN-38. This is a factor contributing to varied toxicity. Also, the intestinal CES can metabolise IRI into SN-38 in the intestinal lumen. The figure was created with Biorender.com and was adapted from [193].

Oxaliplatin

Oxaliplatin (OXA) was incorporated into the regimen 5-FU/LV in the 2000s under the name of FOLFOX[195,196]. OXA is a diaminocyclohexane platinum compound, a third-generation platinum derivative that forms DNA adducts via inter-and intrastrand crosslinks in DNA and DNA-protein crosslinks leading to impaired DNA replication and cellular apoptosis[181,182,197]. SLC31A1 and SLC22A1/2 regulate the influx of platinum drugs while ABCC2, the copper transporter P-type ATPase ATP7A, and ATP7B regulate their efflux [181]. ABCC transporters are also involved in the elimination of platinum compounds. The increased expression of these transporters, as well as ABCG2, favours oxaliplatin activity *in vitro*[181]. Genes involved in mismatch repairs, such as MSH6 and MLH1, decrease the cell sensitivity to platinum drugs. In addition, XRCC1, ERCC1, ERCC2 and XPA mediate nucleotide excision repair, and known variants in these genes affect a patient's response to platinum-based drugs. These genes act by detecting single-strand breaks and removing proteins from the DNA helix, which becomes more accessible to repair enzymes[197]. Several other genes lower the cellular concentration of platinum compounds [181,198].

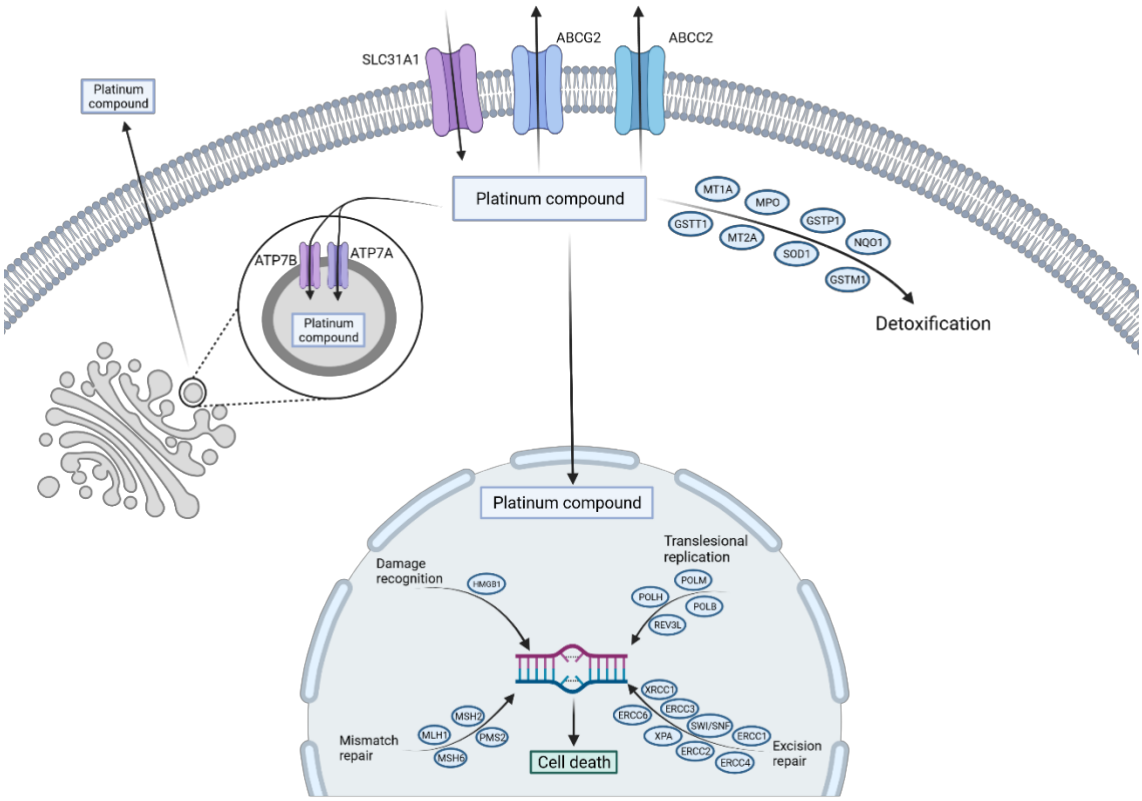

Figure 20 -Oxaliplatin (platinum compound) pharmacokinetics and pharmacodynamics

Platinum-based drugs like oxaliplatin destroy cancerous cells by interfering with the DNA via inter-and intrastrand crosslinks, and DNA-protein crosslinks, preventing cell division and growth.The influx of platinum (Pt) drugs into the cell is regulated by SLC31A1 and the efflux by ABCC2, ABCG2, ATP7A, and ATP7B. ATP7A and ATP7B are involved in the Cu transport from the cytoplasm into the trans-Golgi network, where it serves to export Cu from the cell via the vesicular secretory pathway. Once platinum is inside the cell, the primary anti-tumour mechanism is the formation of Pt-DNA adducts, leading to cell-cycle arrest and apoptosis. HMGB1 is important in the cell recognition of these Pt-DNA adducts and signals cellular response to these adducts. Genes involved in mismatch repair, such as MSH6 and MLH1, decrease the cell sensitivity to these drugs. In addition, nucleotide excision repair is mediated by XRCC1, ERCC1, ERCC2, and XPA. These genes act by detecting single-strand breaks and removing proteins from the DNA helix, which then becomes more accessible to repair enzymes. In addition, several genes, such as MPO, SOD1, GSTM1, NQO1, GSTP1, and MT2A, are responsible for lowering the intracellular concentration of platinum drugs and therefore play a key role in cellular resistance to these drugs. Figure adapted from [197].

Angiogenesis Inhibitor - Bevacizumab

Another strategy used in CRC to control malignant proliferation is preventing neoangiogenesis or new blood vessel formation. The most used strategy in metastatic CRC and when patients fail to respond to conventional chemotherapy is the inhibition of VEGF with monoclonal antibodies such as bevacizumab, in combination with 5-FU/LV FOLFIRI or FOLFOX[199–201].

EGFR Inhibitors – Cetuximab and Panitumumab

In the past chapter, I mentioned that the EGFR is a transmembrane glycoprotein that interacts with signalling pathways affecting cellular growth, proliferation, and cell death. In CRC, 80% of the tumours express EGFR, which is associated with a poorer prognosis[182]. Therefore, researchers

developed antibodies directed against the extracellular domain of EGFR and small molecular inhibitors of its intracellular tyrosine kinase domain. Thus far, in CRC, only the anti-EGFR monoclonal antibodies, cetuximab and panitumumab, have definitively shown efficacy only in combination with conventional chemotherapy[202–204]. Importantly, patients carrying a KRAS mutation appear to be resistant to EGFR inhibition irrespectively of cetuximab or panitumumab[182].

BRAF inhibitor – Encorafenib

BRAF encodes a serine/threonine-protein kinase part of the RAS/RAF/MEK/ERK pathway. Most mutations in *BRAF* result in V600E substitution, and these patients generally have a poor prognosis. Approximately 10% of patients with metastatic colorectal cancer (mCRC) have a *BRAF* mutation and poor prognosis as *BRAF* V600E mutation results in constitutive activation of the MAPK signalling pathway, which drives tumour cell proliferation and survival [205]. Indeed, BRAF inhibitor monotherapy in *BRAF*–mutant mCRC has low response rates due to incomplete inhibition of the MAPK signalling pathway in *BRAF* V600E–mutant CRC cells lines, leading to a rebound in MAPK activation and continued cell proliferation. BRAF and EGFR inhibitor combinations resulted in synergistic inhibition and suggested improved activity compared with single-agent BRAF inhibitors[205]. Encorafenib is a BRAF inhibitor. The doublet combination of the encorafenib and the cetuximab could improve overall survival compared with standard therapy in patients with *BRAF* V600E–mutated mCRC whose disease has progressed after one or two prior lines of treatment compared to the current standard of care. The BEACON CRC trial that studied the combinatorial BRAF/EGFR inhibition therapy marked the first evidence of survival benefit for a chemotherapy-free targeted treatment regimen in prospectively biomarker-defined patients with mCRC, defining a new standard of care for patients with previously treated *BRAF* V600E mCRC[205].

Treatment	Mechanism of action
5-fluorouracil (5-FU)	antimetabolite, TYMS inhibitor
Leucovorin (LV)	Stabilises 5-FU interaction with TYMS
Capecitabine	Prodrug, it is enzymatically metabolised to 5-FU in vivo
Irinotecan (IRI) (CPT-11)	Topoisomerase I inhibitor
Oxaliplatin (OXA)	platinum compound, forms adducts via inter- and intra strand crosslinks in DNA and DNA- protein crosslinks
Bevacizumab	anti-VEGF monoclonal antibody
Cetuximab	anti- EGFR monoclonal antibodies
Panitumumab	
Encorafenib	BRAF inhibitor

Table 1 - Summary of CRC treatments

Resistance to therapy in CRC

In the past chapter, we talked about the intestinal epithelium, its plasticity and the capacity of progenitors and differentiated cells to replenish the epithelium when ISCs are missing after damage [36,40,56,158–161]. In previous paragraphs, we navigated the known mechanisms of drug resistance to anticancer drugs. We talked about the cells that can persist chemotherapy, the DTPs and those who can resist treatment [27,28,165,166,168]. We will now see how this applies to CRCs. Even though, since the late 50s, 5-FU has constituted the backbone of CRC chemotherapeutic regimens, patients' responses to treatment with 5-FU as a single agent are limited; only less than one-third of patients who received 5-FU as a single agent showed some responsiveness. However, combining 5-FU with oxaliplatin-based therapy generates a 50% response rate. Nevertheless, despite the slight increase in chemotherapy response observed with drug combinations and targeted therapies, resistance mechanisms were observed for all CRC treatments in the market. Resistance to FOLFOX and FOLFIRI can be due to alteration of drug metabolism, detoxification, DNA damage repair, adaptation to the stressful condition, and others [206–209]. Furthermore, although cetuximab and panitumumab combined with other agents are very effective, they are not as potent as single agents. Cetuximab and panitumumab alone work in only around 10% of cases besides the increasing number of resistant mechanisms: mutations of the target (i.e. EGFR), downstream signalling reactivation and alternative pathways activation [173,206].

DTPs and resistant populations

As a reminder, the highly proliferative LGR5+ ISCs are not homogenous. A subpopulation of slowly cycling LGR5+ cells can contribute to all intestinal lineages in low outputs during

homeostasis [26]. Undertreatment, several facultative SCs can survive and lead to replenishing the injured epithelium. Several authors have demonstrated the ability of the LGR5+ slow-cycling population and facultative SC to survive, especially with treatment with 5-FU and radiation [27,28,210]. Some studies also claim that the cells that replenish the epithelium after treatment with doxorubicin, a chemotherapeutic agent, are the early progenitors[40], similar to the observations in the irradiation models[23,36].

A recent and elegant study from Catherine O'Brien's lab used CRC patient-derived xenografts models, lentiviral barcoding, next-generation sequencing and mathematical models to show that chemotherapeutic treatment, especially with IRI and FOLFIRI, can generate a particular DTP state which is called diapause-like state. This state is reminiscent of the reversible embryonic developmental state to survive stress by adapting their transcriptional profiling[165]. Furthermore, mathematical models suggested that all cells had an equal probability of entering the DTP state to survive chemotherapy and exit from this state upon IRI or FOLFIRI removal. Importantly, they analysed the clonal complexity of the patient-derived xenografts using a lentiviral barcoding library. They evaluated the treatments that induced a DTP state (IRI and FOLFIRI) and those that did not induce a DTP state (OXA, 5-FU/LV and FOLFOX). There was no loss of barcodes in the CRC cells that underwent a DTP state. Notably, the enriched barcodes were unique for all tumours and treatments, indicating that no pre-existing cell population was selected that gave rise to the persistent phenotype [165]. The researchers then analysed the mechanisms that underlie de IRI induced DTP state. IRI and FOLFIRI treatment did not enrich the CSC pool in the DTP state nor induce loss of intra-tumour heterogeneity. Still, they were characterised by a decrease in the mTOR pathway and an upregulation of the autophagy program genes. Captivatingly, as already mentioned before, IRI induced DTPs are slow-cycling [165]. Many other data suggest that DTP can also arise from epigenetic modifications. Epigenetic regulation happens in many genes implicated in the resistance to DNA damaging agents. For example, drug resistance has been associated with the hypermethylation of promoter regions of pro-apoptotic genes, hypomethylation of drug efflux transporters promoters, and methylation of genes involved in DNA repair [164,206]. Furthermore, global histone modification patterns are also involved in drug resistance [211,212].

Still, resistance to targeted therapies in CRC represents a different persister cells' survival strategy. As I mentioned previously in this chapter, cancer cells and bacterial cultures share a pretty exciting ability to transiently increase the mutability rate (adaptive mutability) to improve the chances of survival by developing resistant clones. In CRC, Russo et al.[168] showed that EGFR/BRAF inhibition generates DTP cells that can down-regulate genes involved in the mismatch repair and homologous recombination DNA repair while concomitantly upregulating genes involved in error-prone polymerases. The EGFR inhibition may cause DNA damage and increase the chances of mutability, allowing cancer cells to evade the therapeutic pressure. Even though genetic *EGFR* and *KRAS* alterations and the acquisition of an adaptive mutability are well-

known causes of EGFR inhibition resistance, researchers surprisingly found in metastatic colorectal cancer that the cetuximab resistance can also arise from non-genetic mechanisms through stromal remodelling. In other words, the stromal niche of the tumours can generate the emergence of cetuximab DTPs in tumours that do not carry genetic alterations in driver genes[213]. More classically, other teams have also observed the emergence of resistant clones, especially to 5-FU in culture, after a long time from the drug withdrawal [207]. Furthermore, another study showed that *in vitro* acquisition of the 5-FU resistance mechanism was due to a stem-cell-like phenotype and a quiescence induction, as seen before in mice[214]. Interestingly, the 5-FU quiescent and resistant cells maintain the stemness through activation of the Hippo pathway through YAP, a pathway involved in regenerating the epithelium after damage [214,215].

Changes in drug targets

Cancer cells can alter the genes and proteins/enzymes involved in the action of the therapeutic agent. For example, known mechanisms of resistance to 5-FU include a higher expression of TYMS, the target enzyme of the 5-FU[207]. On the contrary, the decrease of TOP1, the target enzyme of SN-38, can lead to resistance to IRI, and punctual mutations in the *TOP1* gene can induce conformational changes in the enzyme, which prevents the fixation of SN-38 to its target [216,217]. Regarding targeted therapies, mutations in the *EGFR* can alter the binding of cetuximab to the receptor. Single amino acid substitutions can occur in the EGFR domains, reducing the monoclonal antibody binding affinity [173,218]. Moreover, EGFR overexpression and *KRAS* mutations correlate with poor response to anti-EGFR therapy[182,206]. *RAS* mutations allow CRC cells to grow despite the lack of growth factors and render cells insensitive to the anti-EGFR therapy[173]. Additionally, mechanisms of *de novo* resistance can arise pre-and post-treatment with anti-EGFR, including further alterations in several other genes: *KRAS, NRAS, EGFR, PIK3CA, MET, PTEN, SMAD4* and *TP53*. Mutations in downstream players of EGFR signalling like *BRAF* and *PIK3CA* may be responsible for EGFR therapy failure in *RAS* WT patients [173].

Changes in drug metabolism

Phase I and II enzymes extensively metabolise chemotherapeutic agents. As these enzymes are essential for the activation and inactivation of the chemotherapeutic agents, their alteration represents an evident advantage for the cancer cells to resist. Phase I enzymes, which are primarily involved in the chemical modification of the drug, include the cytochrome P450 superfamily. The CYP3A family is mainly involved in the metabolism of IRI into its inactive metabolites[181,193]. The Phase I enzyme DPYD metabolises 5-FU to an inactive form. Therefore, 5-FU unresponsiveness and increased toxicity are due to DPYD modifications[188,207]. Phase II enzymes are involved in the conjugation of the drug with other molecules that include glutathione,

glutathione-S-transferase (GST), uridine diphosphate glucuronosyltransferases (UGTs) and NADH Quinone Oxidase (NQO). One of the resistance mechanisms to OXA is the elevation of glutathione inactivation, an antioxidant molecule essential for cellular detoxification and prevention of DNA/RNA damage, and the efflux of inactive forms of OXA[209]. UGTs inactivate the active metabolite of IRI, SN-38, by glucuronidation. UGT1A1, one of the central genes involved in SN-38 inactivation, is highly polymorphic. The polymorphisms in this enzyme are associated with the patients' lack of response and an increased toxicity[181,194].

Active efflux of chemotherapeutic agents as a resistance mechanism – ABC superfamily

Hurdles in drug retention impact treatment efficacy after a drug has entered the cell. Drug efflux pumps, including the ATP-binding cassette (ABC) transporters, play a key role in determining drug retention rates within cells. ABC superfamily is the major transporter system and provides one of the drugs' efflux mechanisms in many drug-metabolizing organs like the liver and the intestine. Up to date, there are 49 ABC transporters, classified into seven subfamilies named from A to G. They are composed of a nucleotide-binding domain which hydrolysis ATP to generate the energy to translocate the substance across the transmembrane domain. The ABC transporters regulate cellular levels of several molecules, including hormones, lipids, ions, xenobiotics and other small molecules, by transporting them across cell membranes and serving a range of physiological roles, including intracellular regulation of organelles[219]. Twelve ABC transporters are essential for chemotherapeutic agents' efflux. Still, three of them are widely studied, and I want to point them out in particular ABCB1 (also known as p-glycoprotein or MDR1), ABCG2, also known as breast cancer resistance protein (BCRP) and ABCC family multidrug resistance-associated protein (MRP) (**Figure 21**).

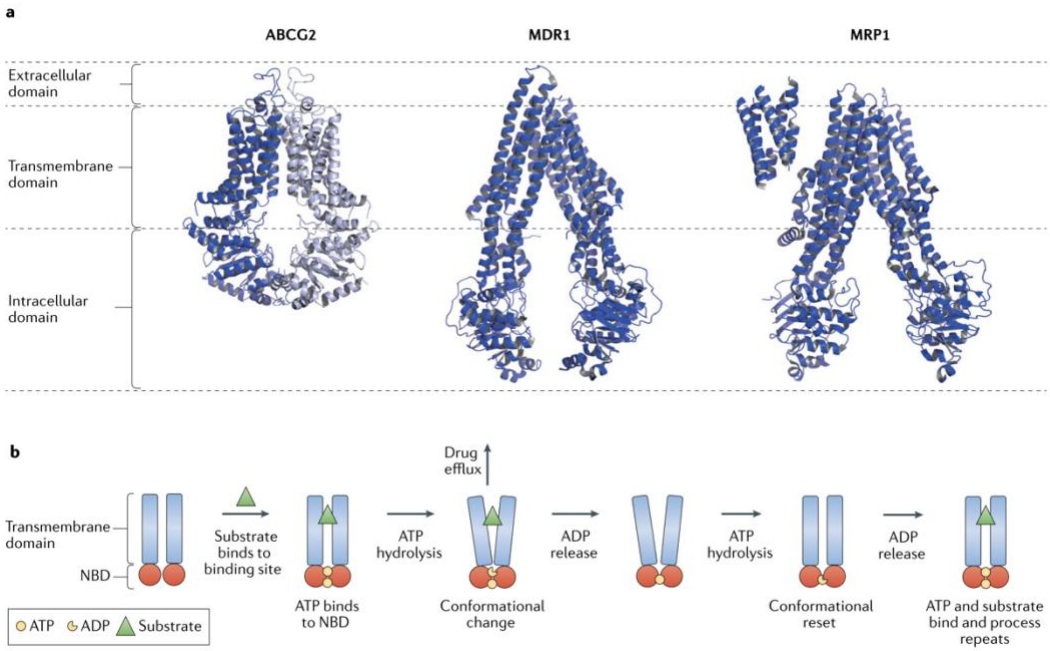

Figure 21 -Structure and mechanism of three ABC transporters important for drug resistance
A) High-resolution 3D structures of ATP Binding cassette superfamily G member 2 (ABCG2), ATP Binding cassette superfamily B member 1 (ABCB1) known as MDR1 and the ATP Binding cassette superfamily C member 1 (ABCC1) known as MRP1. B) Schematic representation of the proposed pumping action of ABCB1, as an example. Figure adapted from [219].

ABCB1 is the most studied ABC transporter. It is highly expressed in the colonic epithelium and overexpressed in numerous cancers, including CRC, and it is known to be associated with chemotherapeutic failure [206,219]. In addition, ABCB1 transports a broad spectrum of drugs, making it a mediator of drug-drug interactions. Notably, a significant part of IRI and SN-38 efflux in the intestine occurs via ABCB1[193], conferring a resistance mechanism via lowering the drug's intracellular concentration and its active metabolite. ABCB1 overexpression may occur by several mechanisms like promoter fusions, modulation by signalling pathways, or drug activation [219]. Moreover, hormones like thyroid hormones can induce the overexpression of ABCB1 and the resistance to drugs[220], as we will see in the next chapter. The ABCC subfamily is involved in the efflux of 5-FU, oxaliplatin and folates. ABCC5 transports monophosphate metabolites in CRC, which bestows the 5-FU efflux and consequently resistance [206], while ABCC2 (also called MRP2) is essential for SN-38G and minor IRI efflux in the intestine[193]. Another well-known multidrug resistance transporter is ABCG2. Similarly to ABCB1, ABCG2 is frequently overexpressed in CRCs. Still, studies show contradictory results about survival and response depending on ABCG2 expression [221]. Efflux of the chemotherapeutic agents used in CRC, 5-FU and IRI is controlled via ABCG2, contributing to the resistance to these agents, among others [221,222]. Moreover, IRI metabolites SN-38 and SN38G are transported via ABCG2[193].

In summary, in this chapter, we saw that cancer cells could take advantage of numerous strategies to survive therapies. They can increase their mutability capacity and acquire DTP states to survive

stressful situations. They can also modulate the drug target genes and enzymes and take advantage of the upregulation of transporters to increase the efflux of drugs and diminish the intracellular concentration of the agents. This armamentarium deployed to increase cells to survive the therapies is quite impressive and still very poorly characterised. *In vivo,* a lot of factors can influence the response to treatment. In this context, the work I performed during my thesis was focused on the function of the thyroid hormones and the nuclear hormone receptor TRα1 in CRCs.

Chapter 3: Thyroid hormones and their receptors

Thyroid hormones (TH) play a critical role in differentiation, growth and metabolism, and the normal functioning of several tissues and organs, including the intestine.

Thyroid hormone synthesis, metabolism and transport

The hypothalamus-pituitary-thyroid axis regulates the synthesis of thyroid hormones (TH). It is one of several hormone regulatory systems, each of them designating an axis from the hypothalamus to the pituitary and ultimately to the peripheral organ targets, in this case, the thyroid gland [223]. The hypothalamus and the pituitary gland are in close anatomical proximity. A negative feedback system exquisitely regulates TH synthesis and secretion[223,224] (**Figure 22**). The paraventricular nucleus of the hypothalamus synthesises the thyrotropin-releasing hormone (TRH) that is transported via axons to the median eminence and then to the anterior pituitary via the portal capillary plexus [223,225]. TRH binds then to the TRH receptors in the pituitary thyrotropes, a subpopulation of pituitary cells that secrete the thyroid-stimulating hormone (TSH). TH negatively regulates both TRH and TSH secretion. TSH, in turn, through the thyroid-stimulating hormone receptor present on the basolateral surfaces of thyrocytes, stimulates the thyroid follicular cells to biosynthesise and secrete the TH. As a result, 80% of the secreted TH is thyroxine or tetraiodothyronine (T4) and 20% triiodothyronine (T3). Additionally, TSH controls the expression of the thyroid-specific genes involved in TH biosynthesis, including Na+/I-symporter (NIS), thyroglobulin (TG), and thyroid peroxidase (TPO) [223,224].

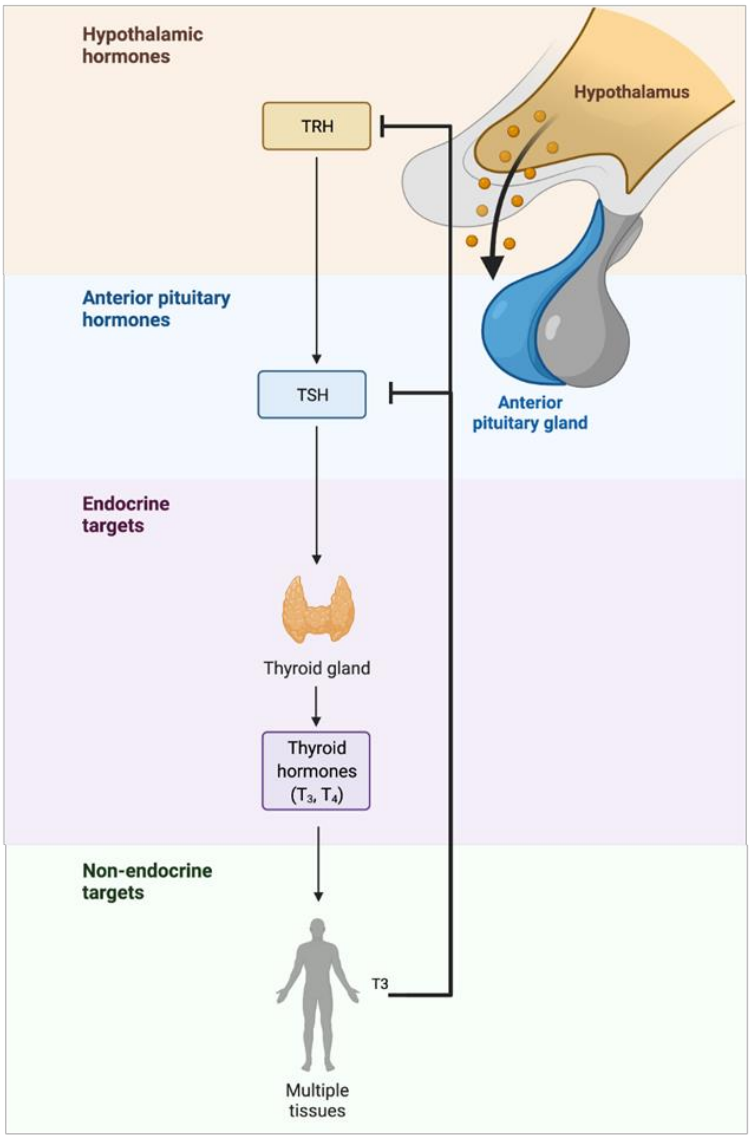

Figure 22 - Hypothalamus - pituitary - thyroid axis

TH biosynthesis comprises a series of specific biochemical reactions that relate to the histological organisation of thyroid tissue. Thyroid follicular cells, also called thyrocytes, are considered the functional units of the thyroid and are formed by a monolayer of polarised follicular epithelial cells organised in a tridimensional ovoid structure surrounding the follicle lumen (**Figure 23**). The interior of the follicle primarily contains the "colloid" due to its high protein contents and the iodinated TG, which are in close contact with the apical plasma membrane of thyrocytes. The basolateral plasma membrane of thyrocytes delimits the exterior of the follicle and is in contact with an extensive network of blood capillaries where intense exchange with the blood occurs[226]. The thyroid gland synthesises both TH, T4 and T3. First, NIS actively transports bloodstream iodide across the plasma membrane into the cytoplasm of thyrocytes, and then, several transporters transfer the iodide to the thyroid follicles' lumen by several transporters. Then, at the outer surface of the apical membranes of thyrocytes, the thyroid peroxidase initiates the biosynthesis of THs using H_2O_2 produced by a NADPH dual oxidase 2 (DUOX2) to oxidise

iodide to iodine radicals and incorporates it into specific tyrosine residues within thyrocyte-secreted thyroglobulin (Tg) molecules[226,227]. After that, TPO couples two residues of diiodotyrosine (DIT) to form thyroxine T4 and one monoiodotyrosine (MIT) to one DIT to generate T3. Mature Tg, containing THs, is stored in the colloid of the follicular lumen. The secretion of THs relies on Tg reabsorption from the lumen by micropinocytosis and its proteolysis by lysosomal enzymes that release THs from the Tg protein. Uncoupled MIT or DIT residues are deiodinated, and iodide is recycled. Finally, the monocarboxylate transporter 8 (MCT8) transports THs outside the basolateral membrane of thyrocytes, from which they reach the bloodstream[227]. The majority of TH release is in the form of T4. The total serum T4 is 40-fold higher than serum T3, and only a few percentages of T3 and T4 are free, unbound to thyroxine-binding globulin (TBG), albumin and thyroid-binding prealbumin. Only the free THs enter the cells to generate the biological response via the TH receptors[224], as we will see in the next section.

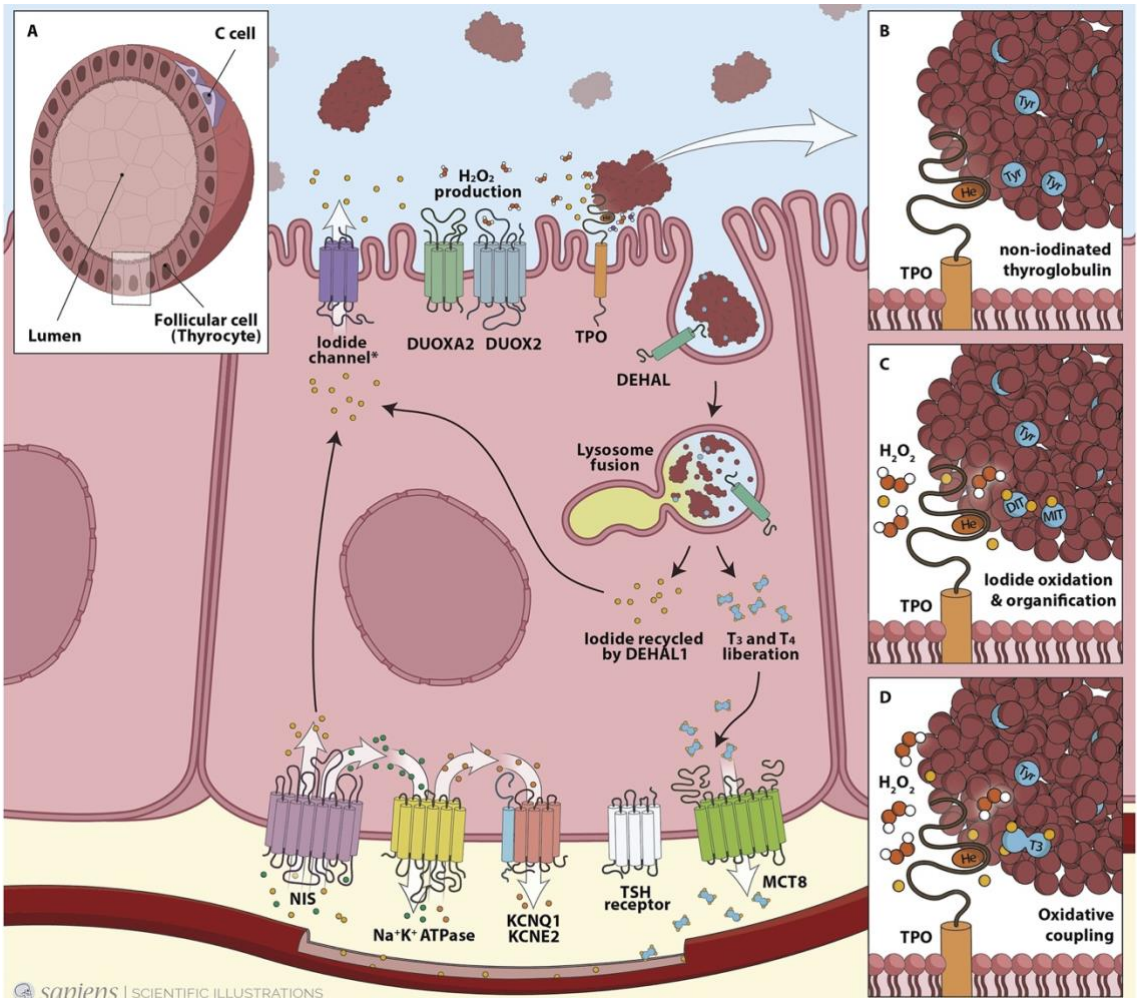

Figure 23 - TH biosynthesis and release

A) Tridimensional structure of the thyroid follicles surrounded by epithelial follicular thyroid cells. C cells are parafollicular cells that produce calcitonin. **B)** TPO: thyroperoxidase, he: heme group of TPO, Tyr: tyrosine residues of thyroglobulin; **C)** iodide oxidation and its incorporation into thyroglobulin depend on the presence of TPO and hydrogen peroxide (H_2O_2) produced by dual oxidase 2 (DUOX2), **D)** the oxidative coupling of iodotyrosines, monoiodotyrosine (MIT) and diiodotyrosine (DIT), depends on the presence of TPO and hydrogen H_2O_2 and lead to the formation of T3 (and mainly T4) that remains bound to the thyroglobulin molecule. NIS: sodium/iodide symporter; KCNQ1 and KCNE2: Voltage-gated K^+ channels; TSHR: thyrotropin receptor; MCT8: SLC16A2 monocarboxylate transporter 8, thyroid hormone transporter; DUOXA2: maturation factor of dual oxidase 2; DEHAL: iodotyrosine dehalogenase. Figure taken from [226].

The primary pathway for T3 production is via 5'-deiodination of the outer ring of T4 by the iodothyronine selenoenzymes, the deiodinases, and specialised enzymes involved in eliminating iodine atoms. It exists three types of deiodinases DIO1, DIO2 and DIO3. DIO1 is mainly present in the liver, kidney and thyroid, and it can deiodinate both the inner and the outer ring of T4 and is essential to generate T3 for circulation. DIO 1 can also catabolise the rT3 in T2 [228,229]. DIO2 locates in the endoplasmic reticulum in the brain, pituitary and brown adipose tissue and converts T4 to T3 for intracellular use, similarly to DIO1 can also catabolise the rT3 in T2 [228,229] (**Figure 24**). TH negatively regulates DIO2 pre- and post-transcriptionally. DIO3 is localised in the plasma membrane and is mainly found in the placenta, brain, and skin; and generates reverse T3 (rT3) and 3,3′- diiodothyronine (T2) inactivating the TH[224,229,230], which are important for the non-genomic actions of TH. In addition, T3 and rT3 can be further deiodinated and conjugated sulfo- or glucuronide-conjugated via Phase II, eliminating enzymes for their excretion, which can affect the elimination of some other molecules or drugs, as we will see.

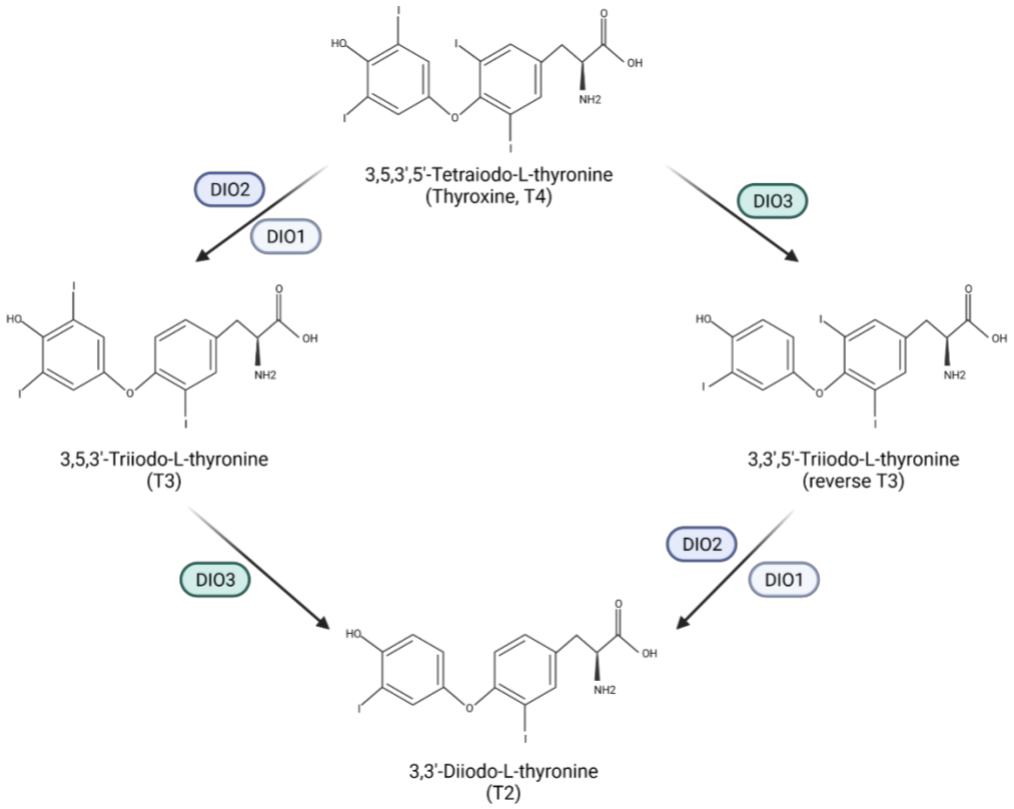

Figure 24 - TH metabolism and deiodinase reactions
Deiodinases type 1, 2 (DIO1 and DIO2) convert T4 to T3 by removing iodine from the outer ring of T4 and T2 by deiodination of rT3. DIO3 generates rT3 and T2 by inner-ring deiodination of T4 and T3, respectively. Adapted from [371] and created with Biorender.com

Transporters can regulate the flux of THs to and from cells, and their expression is tissue-specific. Apart from MCT8, another member of the monocarboxylate transporters family, MCT10, well expressed in the intestine, has been characterised as a TH transporter even if it was initially known

as an aromatic cation transporter [231]. Other well-expressed transporters in the intestine are the organic anion transporter protein 1A2, OATP1A2 and large neutral amino acid transporters LAT1 and LAT2 involved in the transport of neutral amino acids. Notably, the transport of THs and their metabolites follows a specific transport affinity. Thereby, the transport of T3 is higher than T4 or rT3, respectively (T3> T4> rT3~ T2)[231]. Moreover, THs are substrates of the intestinal drug uptake transporter organic anion transporting polypeptide 2B1 (OATP2B1) and are transcriptional regulators of this intestinal transporter[232].

Thyroid hormone receptors

Nuclear hormone receptors

Nuclear hormone receptors (NHR) represent a large family of transcription factors that orchestrate many biological processes. The human NHR superfamily consists of 48 members, including receptors for steroid hormones, TH, retinoic acid, vitamin D, fatty acids, oxysterols (cholesterol metabolites) and some for which no endogenous ligand has been found, called "orphan NHR". Interestingly, *Drosophila melanogaster*, the fruit fly, has only 21 NHR, while *Caenorhabditis elegans* has more than 270 NHR[233].

The NHRs induce transcriptional activation of their target genes after recruiting co-activators in a ligand-dependent or ligand-independent manner. As already implied by their name, NHRs rely on their DNA binding domain (DBD) to transactivate their target genes. However, cotransfection experiments and electrophoretic mobility shift assays showed that the classical steroid receptors (glucocorticoid receptor (GR), estrogen receptor (ER), progesterone receptor (PR) and the androgen receptor (AR) bind as homodimers to their response element, which are arranged in a configuration of two palindromic sequences of six nucleotides separated by three base pairs. On the contrary, non-steroidal NHR (i.e., vitamin D receptor (VDR), thyroid hormones receptor (TR) and retinoic acid receptor (RAR)) bind preferentially to their response element composed of two hexads half-sites arranged as tandem repeats, separated by 3, 4 and 5 nucleotides, respectively. Moreover, VDR, TR and RAR bind DNA as part of a heterodimer with their joint partner, the retinoid X receptor (RXR)[234].

Canonical structure

As already mentioned, NHRs share a common structural organisation. In the N-terminal region, they possess a transactivation region (AF-1), which is variable. The most conserved region is their DBD which contains a P-box, a short motif responsible for the DNA binding specificity on sequences typically containing the AGGTCA motif and its involvement in the NHR dimerisation as homodimers or heterodimers. The 3D structure of the DBD showed that it is composed of two highly conserved zinc fingers. A less conserved region between the DNA-binding and ligand-

binding domains serves as a flexible hinge between these two domains and contains a nuclear localisation signal. Then, there is the ligand-binding domain (LBD), where the corresponding ligand will bind as indicated by its name. Finally, the last domain, AF2 responsible for many functions like transactivation, dimerisation interface, sometimes another nuclear localisation signal and often a repression function[233].

Thyroid hormone receptor

The TH nuclear receptor (TRs) are T3-modulated transcription factors [233]. THs and TRs are involved in multiple processes in organism development, physiology, and, eventually, pathological events[235–238]. From a molecular point of view, they modulate the expression of target genes by binding to TH response elements (TREs) generally present in regulatory regions of target genes. The canonical TRE consensus is a tandem of AGGTCA sequences in direct repetition separated by four base pairs, named direct repeat 4 (DR4) [237]. Other TRE configurations, including palindromic or inverted palindromes arrangements (**Figure 25**), can be found in the promoter regions of some genes and changes in the number of nucleotides that separate the tandem sequences [239].

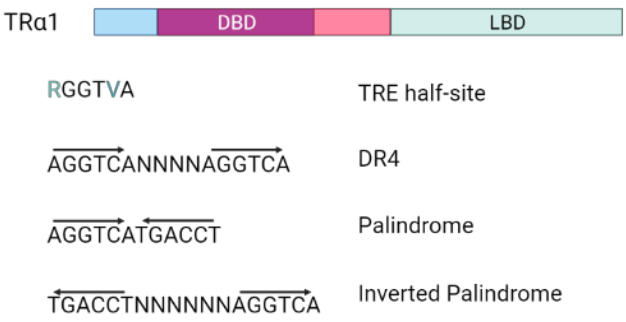

Figure 25 - Different arrangements of the Thyroid Hormone Responsive Elements (TRE). Figure made using Biorender.com.

Upon T3 binding, TRs undergo conformational modification, resulting in activation or repression of the transcriptional machinery [235]. TR binds to T3 with high affinity (Kd ∽ 0.5 nM) [240]. Although I will mainly focus on mammals and briefly mention amphibians, TRs are present in other non-mammalian vertebrates species [241]. In mammals, two genes encode for TRs, *THRA* and *THRB*. The *THRA* locus is situated on chromosome 17 and encodes for four isoforms, TRα1, TRα2, TRΔα1 and TRΔα2, but only TRα1 can bind both T3 and DNA (**Figure 26**). TRα1 and TRα2 are transcribed from the main promoter and result from the alternative splicing of the primary transcript[242]. In contrast, TRΔα1 and TRΔα2 are synthesised from an internal promoter located in the intron 7 [243] and result from the alternative splicing of the primary transcript. All isoforms present a particular structure. Regarding the expression pattern of TRα, it is expressed

in the heart, the brain and the intestinal crypts [244–246]. More precisely, TRα1 and TRα2 have a widespread, ubiquitous expression, whereas the short TRΔα1 and TRΔα2 isoforms display restricted expression patterns [244–246].TRα1 is a true T3 receptor as it has the LBD and DBD. TRα2 presents a shorter LBD that averts the hormone-binding, but it can still bind to the DNA. TRΔα1 and TRΔα2 are truncated isoforms that lack both DNA and ligand biding domains[247].

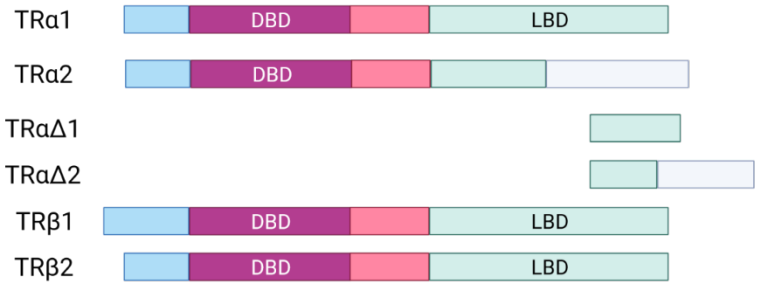

Figure 26 - TRα and TRβ isoforms.
Schematic representation of the various isoforms encoded by THRA and THRB genes and of their structures. DBD (DNA Binding Domain), LBD (Ligand-Binding Domain), which are specifically present in the TRα1, TRβ1 and TRβ2 proteins, as they are bona fide T3 nuclear receptors. The TRα2 isoform lacks the LDB. Adapted from [246,247] and created using Biorender.com.

Experiences using $TR\alpha^{0/0}$ mice where all TRα isoforms are absent and $TR\alpha^{-/-}$ where only the truncated forms of TRα are present showed that TRΔα1 and TRΔα2 behave as antagonists of TRα1 activity on target genes in the intestine[242,243,248]. TRα2 physiological function is still unknown. On the other hand, the *THRB* locus in chromosome 3 encodes for two isoforms, TRβ1 and TRβ2, resulting from different transcriptions start sites[244,249] (**Figure 26**). Of note, only in rats has been shown the existence of a third receptor and its truncated form, TRβ3 and TRΔβ3[250]. TRβ displays a ubiquitous expression and is the main TR isoform expressed in the liver, hypothalamus-pituitary axe, retina and inner ear[244]. As we saw before when we talked about NHRs, from a molecular point of view, TRs heterodimerise with RXR and bind to TRE, generally located within the genomic regions of target genes. In addition, TRs can also heterodimerise with other nuclear receptors like liver X receptors (LXRs) and peroxisome proliferator-activated receptors (PPARs)[240], as well as they can form homodimers[251]. These interactions have only been shown *in vitro*. TRs can present post-translational modifications, including phosphorylation (both in the cytoplasm and the nucleus), acetylation and sumoylation[252]. Phosphorylation of TRs increases the heterodimerisation with RXR and enhances the stability of target genes[253,254]. In addition, acetylation and sumoylation appear to enhance the TR-mediated transcriptional activity[255,256].

Transcriptional activation of TRs

After fixation to the DNA, TRs heterodimerise with RXR. A bimodal switch model is extensively used to describe transcriptional regulation by TRs [257]. In this model, the unliganded TR forms stable, chromatin-bound complexes with transcriptional co-repressors to repress transcription [257]. The binding of T3 induces a conformational change in the receptor resulting in the dissociation of co-repressors and facilitating the recruitment of co-activators to activate transcription of positive positively genes[257] (**Figure 27**). Notably, some genes are negatively regulated by T3, like the gene coding for the TSH and TRH[258]. This negative regulation by TRs/T3 includes altering the basal transcription machinery via corepressor recruitment alteration of the chromatin template. It is essential to highlight that TRs, in addition to hormone-independent TRE occupancy, can be, in a hormone-induced way, recruited to chromatin to induce chromatin remodelling and activate gene transcription in a dynamic process[257]. Liganded TRs can be pioneer factors, opening the chromatin for other transcription factors to access. Four types of transcriptional regulation of TRs have been described[259]. Briefly, Type I regulation accounts for the classical bimodal switch that involves TRs binding to TREs in the target genes. Type II regulation includes the target gene regulation by TRs without direct binding to the DNA. Instead, it binds to another protein or multi-complex protein to bind to the DNA indirectly. In type III transcriptional regulation, TRs recruitment to the DNA is unnecessary to regulate transcription. Finally, in type IV, TH can act independently from the TRs and directly bind to other proteins. We will see more in-depth all these types of regulation when we will talk about the non-genomic actions of THs, but it is important to know that many of these actions have been observed mainly with TRβ[252,259].

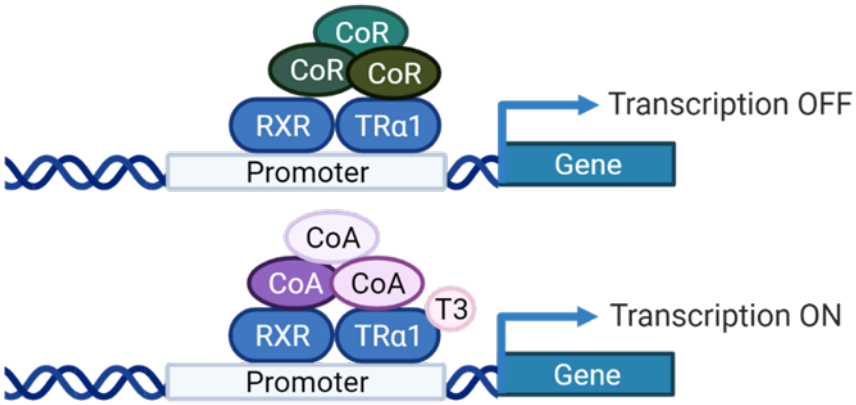

Figure 27 - Molecular mechanisms underlying the modulation of gene transcription by TRs.
In the absence of T3, TRs interact with the TREs present on target genes and forms a heterodimer with Retinoid X Receptors (RXRs). The complex recruits co-repressor (CoRs) proteins that block transcription initiation. In the presence of T3, the CoRs are released, and co-activators (CoAs) are recruited, enabling gene transcription. The figure was adapted from [247] and created with Biorender.com.

Additional mechanisms of transcriptional regulation and non-genomic actions of TRs/THs

I have mentioned earlier that we could consider four types of regulation by TRs and THs. The TR dependent signalling of T3 with direct binding to the DNA describes the canonical or type I regulation. Additionally, the TRα short isoform p43 detected in the mitochondria, which still has the DNA binding domain, can be included in the type one regulation [259]. Type two regulation considers that TR-dependent T3 signalling can occur without direct binding to the DNA. TRs can interact with several chromatin-associated proteins and tether TRs to specific genomic locations, even if not directly contacting the DNA. One way to analyse the DNA-protein complexes in an open genomic regulatory region is to perform DNaseI footprinting. The sequence bound to a regulatory region will be protected from the DNase [260]. A novel variation of this method is called DNase-Seq. The DNA-protein complexes are treated with DNaseI, followed by DNA extraction and sequencing in this updated method. The sequencing provides an accurate representation of the location of regulatory proteins in the genome. So, despite lacking data on TRs protein interaction, DNase-Seq analysis showed, at least in the liver, that after T3 induced chromatin remodelling, there is a *de novo* formation of consensus elements for some transcription factors, besides the specific DR4 TRE consensus elements [257]. The de novo formation of consensus elements for other transcription factors could be explained by an indirect TR-dependent tethering of other transcription factors. Several studies in the intestine and other organs like the liver showed that TH could modulate the expression of other transcription factors, for example, β-catenin. Thus, the TH induced chromatin modulation can be TR dependent or independent. In addition, data suggested that TRs in the cytoplasm could interact with tyrosine kinases found in the plasma membrane, serve as phosphorylation substrates, and participate in the signalling pathway. TRβ1, unlike TRα1, has a critical tyrosine residue and can serve as an intermediate between tyrosine kinase receptors and the PI3K/AKT pathway [261,262]. It was shown that in mice carrying a $TR\beta^{PV/PV}$, a dominant-negative form of the TRβ, the binding of TRβ to the PI3K-regulatory subunit p85 was higher in these mutant mice than in WT mice[261]. The liganded TR Activates PI3K and AKT/PKB, leading to the activation of the PI3K-AKT/PKB-mTOR-p70S6K pathway in the cytoplasmic and nuclear compartments. This activation-induced transcription of several target genes [261,262]. Furthermore, in thyroid tumours, it was observed that the $TR\beta^{PV/PV}$ mutant could be bound to β-catenin[263], indicating that, at least in thyroid cancers, unliganded TRβ can interact with β-catenin and induce the expression of Wnt target genes. Functional interaction between TRα1 and β-catenin/Tcf4 was also observed in CRC[264]. Another short TRα isoform (p30) translated from an internal AUG codon in the TRα1 mRNA is transcriptionally incompetent and localises in a palmitoylated form in the plasma membrane. The p30 isoform can mediate T3 actions in the cell. For example, it can activate the nitric oxide production by the nitric oxide synthase 3 (NOS3) through the direct increase of intracellular Ca^{2+} and indirectly through the

Akt-dependent NOS3 phosphorylation[265]. Those two examples are part of the type III regulation by TRs.

Interestingly, TH can have non-specific downstream effects on gene expression through chromatin-modifying enzymes like DNA methyltransferases and histone acetyltransferases. Different coactivators which act as histone modifiers remodel the chromatin in the presence of T3 and allow the transcription of TR responsive genes[266]. Upon T3 availability, TR binds coactivator complexes containing histone acetyltransferases SRC and histone methyltransferase PRMT1 to facilitate epigenetic modification and gene transcription[266,267]. The final type of regulation consists of TR-independent TH signalling. This type of regulation, commonly known as non-genomic TH signalling, involves a transmembrane receptor called Integrin αvβ3, where T3 and T4 can bind independently of TRs[268], especially in the context of cancer. Integrin αvβ3 has two binding domains and no structural homology with nuclear TRs. Its two domains, S1 and S2, have specific downstream consequences. The S1 domain exclusively recognises T3 and directs Src and the PI3K-mediated trafficking of TRα from the cytoplasm to the nucleus resulting in the transcription of *HIF1A*[268,269]. S2 domain binds both T4 and T3 and regulates MAPK1 and MAPK2, which promotes the nuclear uptake of TRβ1 and leads to tumour cell proliferation[268,269]. Genes regulated by TH-binding to integrin αvβ3 include fibroblast growth factor 2 (FGF2), matrix metalloproteinase 2 (MMP2), HIF1A, and cyclooxygenase 2 (COX2), which associate with cancer development and angiogenesis[268,269]. Moreover, TH binding to intracellular proteins has also been reported, which may impact the transcription of downstream genes. THs can also influence actin *in vitro* polymerisation[224,259].

Thyroid hormones and the intestine

Thyroid hormone action in the intestine – lessons from amphibians and mammals

The role of TH as key regulators in the intestine comes from observations of the amphibian metamorphosis. Indeed, THs strictly and exclusively control amphibian metamorphosis. The gastrointestinal tract undergoes a dramatic remodelling during this process, including the first phase of apoptosis and a subsequent burst in cell proliferation[270,271]. By analogy, further studies unveiled this key role of TH also in the mammals' intestinal postnatal development. During past years, our laboratory has been interested in understanding the role of TH and TRs in the development and homeostasis of the intestine and the context of CRC, as we will see later. The amphibian metamorphosis is a biological process that includes morphological, biochemical, and cellular changes during the postnatal developmental transition from the tadpole state and aquatic life to adult terrestrial life. TH are essential for the initiation and success of this process. THs are secreted after TSH secretion by the pituitary gland in amphibians, similar to mammals[272]. However, not all tadpole tissues respond similarly to the TH signalling. There will be de novo

morphogenesis of some organs (members, jaws, lungs) and remodelling of others like the intestine and the skin, while others will completely disappear like the tail. Altered gene expression accompanies these changes, both general TH-dependent transcriptional programs and tissue-specific[266,270,273,274]. I will point out what happens to the intestine.

The tadpole intestine is a simple lined tube with a monostratified epithelium surrounded by connective tissue and two muscle layers; there are no folds and only one involution. Intestinal remodelling will occur when the TH levels are at their maximum (not all tissues require the same TH levels to start metamorphosis) (**Figure 28**). The tadpole's monolayer epithelium becomes temporally multilayered by the shortening and the constriction of the intestinal diameter[241]. Meanwhile, the extracellular matrix proteins of the lamina propria, located between the epithelial and mesenchymal cells, become thicker and more permeable, allowing the loss of cell-matrix contact that will then induce death by apoptosis[241,275]. As a result, adult epithelial cell proliferation increases transiently. By the end of the metamorphosis process, the muscular and connective tissues are well developed, and the epithelium organises in a monolayered sheet of cells. However, the intestinal epithelium is more complex at that stage and is highly folded into ridges and troughs that more closely resemble the anatomy of a mammalian intestine. Although, the differentiated cells are located in the folds, whereas the proliferative cells localise in the interfold regions. THs also regulate the intestinal niche connective tissue, which is crucial for appropriately developing the epithelium and amphibian ISCs[270,275,276]. Like mammals, the signalling pathways ruling intestinal metamorphosis and ISC self-renewal and maintenance are Wnt, Notch, BMP and SHH[277–280]. This topic has been the focus of a review paper that is included in section 4 of the thesis.

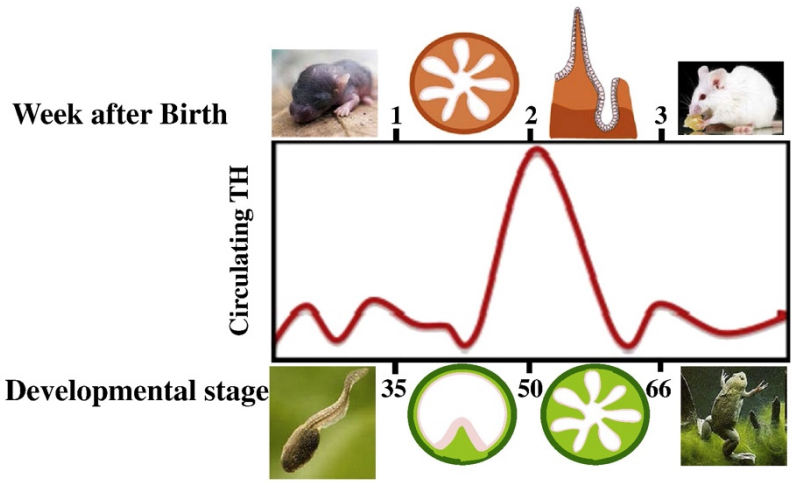

Figure 28 - Postnatal events of the intestinal maturation.
Structural changes depend on TH levels during postnatal development. The lower panel shows the intestinal remodelling during amphibian metamorphosis. Increasing levels of TH characterise the metamorphosis climax. The tadpole intestinal epithelium undergoes dramatic remodelling until it reaches organised compartmentalisation typical of the frog intestine. The upper panel shows the postnatal mouse development where the intestinal epithelium completes the final steps of its maturation. Several factors, including THs, modulate crypt formation and extensive growth. The figure is taken from [241].

In mice, the developmental changes during the endoderm-to-intestinal epithelium maturation occur through significant morphogenetic steps that lead to the remodelling of the primitive gut: i) villus formation during foetal life; ii) crypt formation after birth, and iii) maturation at weaning, which allows the animal to adapt from milk to a solid diet[241] (**Figure 28**). Furthermore, TH levels increase significantly during the first postnatal weeks suggesting the THs role during postnatal intestinal maturation at weaning in rodents. In the following paragraphs, we will explore the current TH/TR role in homeostasis in the intestine and their implication in CRC.

TH signalling in the intestine depends on the cellular availability of TH. As we previously saw, the deiodinases are the enzymes that activate and inactivate the THs. In the mammalian intestine, deiodinases expression levels are low during intestinal development and adult stages[229]. In a normal mouse intestine, only DIO1 has been detected [281], and an increase of DIO3 has been observed in CRC[229]. Both TRs are present in the intestinal epithelium. TRα1 is present exclusively in the intestinal crypts and the smooth muscle layers, while TRβ1 is expressed by the differentiated cells in the top of the villi [246,282–285]. Mouse models have been crucial for determining the role of TH/TRs in the postnatal intestinal epithelium. TRβ$^{-/-}$ mice, which lack all TRβ isoforms, do not present morphological or functional changes in the intestine, compared to TRα$^{-/-}$ (that lacks TRα1 and TRα2) and the double mutant for both receptors, TRα$^{-/-}$β $^{-/-}$. Indeed, TRα$^{-/-}$ and TRα$^{-/-}$β $^{-/-}$ mice presented an impaired small intestinal structure and alterations in cell proliferation a differentiation[282] including the death of the TRα$^{-/-}$ mice within five weeks after birth[286]. These results point out the importance of THs and TRα in postnatal intestinal development and homeostasis.

Indeed, THs mainly regulate the proliferation of crypt epithelial precursors during both maturation at weaning and homeostasis at adulthood via TRα1 activity[241,285] and implicate the activation of specific gene networks and signalling pathways like Wnt, Notch, BMP and SHH[283–285,287]. The genetically modified mouse model TRα$^{0/0}$ mice, where all TRα isoforms are absent, have a decreased crypt proliferation[288], and when exposed to γ-ray irradiation, its intestinal regeneration is firmly impaired [271]. Interestingly, using a 3D organoid model derived from triple transgenic TRami/*Lgr5*-EGFP/*Rosa*-Tomato animals, where the TRα1 loss-of-function can be induced explicitly in crypt cells, Godart and colleagues [285] observed that these mice displayed an impairment to form complex organoids. Instead, they had fewer and shorter buddings, reflecting the negative impact of TRα1 loss on the ISC proliferation and maintenance. TRα$^{0/0}$ organoids presented the same growth impairment and a strong decrease in organoid forming efficacy [285]. Moreover, Godart and colleagues showed that T3 treatment *ex vivo* in organoids surprisingly decreased the expression of SC markers from active and facultative ISC like *Lgr5*, *Olfm4*, *Msi1* and *mTert*. In contrast, other facultative SC markers like *Hopx* and *Clu* are upregulated. Also, T3 treatment in organoids induced a preferential differentiation in goblet cells. RNA-seq confirmed these results and indicated that a short treatment of T3 causes a “thyroid shock” that includes a

complex stress response, metabolic changes and alteration of cell signalling[285]. Of interest, using a hypothyroid zebrafish model, Blitz and colleagues showed that the loss of TH signalling reduces the number of goblet cells in the intestine[289], which can be restored after T3 treatment. Interestingly, *in vivo* in mice, the impact of T3 on ISC was different and in accordance to previous data. T3 treatment increased the number of proliferating cells and increased ISCs, both active and facultative, progenitors, and PCs[285]. In conclusion, this data on T3 and TRα1 on ISCs highlights complex and epithelial cell-autonomous and non-autonomous effects where TRα1 has an immediate and direct impact on the stem and progenitor cells. Therefore, it is essential for ISC maintenance and biology. Furthermore, studies on the role of T3 and TRα1 in the ISC niche are necessary to complete our knowledge of these complex regulations by TH in the intestine; we already have data from the amphibian.

TH, TRs and signalling pathways in intestinal homeostasis and colon cancer

TH and TRα1 signalling are related to the other signalling pathways essential for the intestine's development and homeostasis, and in particular for the ISCs. TRα1 receptor is a direct transcriptional regulator of several components of the Wnt pathway. In intestinal epithelial progenitors, TH–TRα1 increases the level of expression of both *Ctnnb1*, encoding for β-catenin, and the *secreted frizzled-related protein-2* (*Sfrp2*), thanks to the presence of TREs in the regulatory region of those two genes[283,284]. Increased levels of the sFRP2 protein in the extracellular milieu allow stabilisation of β-catenin, resulting in the increased expression of the Wnt target genes and the stimulation of epithelial progenitor proliferation[283,284]. The TRα1 upregulation in the intestinal epithelium in the mouse model *vil-TRα1* generated the apparition of adenomas and an increase of nuclear β-catenin as well as an increase of Wnt target genes Myc, Ccnd1, c-Fos and c-Jun compared to WT mice[281]. In the context of CRC, TRα1 negatively regulates the expression of Wnt inhibitors like Wif1, Frzb and Sox17 [290]. Additionally, T4 treatment increased β-catenin levels in CRC cell lines [291], modulating the balance between the DIO2 and DIO3 and favouring the membrane localisation of β-catenin. However, the latter study also claimed that T3 might have a differentiation-inducing role in CRC cell lines, which may be questionable. Their experiments included long-term culture periods of Caco2 cells that differentiate spontaneously *in vitro*.

In addition to the Wnt pathway, TH levels can modulate the Notch and BMP signalling in intestinal development and homeostasis[287]. Using multiple *in vivo* and *in vitro* approaches, Sirakov and colleagues showed that TH could positively regulate Notch activity through the TRα1 receptor by indirectly controlling the expression of Notch1, Dll1, Dll4 and Hes1 expression and directly modulating the expression of Jag1 by biding to the TRE in *Jag1* promoter[287]. Thus, the complexity of the Notch pathway regulation by TRα1 is achieved through direct control of Jag1 and indirect control of Dll1 and Dll4 expression in PC and progenitor cells and indirect control

of Notch1 and Hes1 on ISCs. Hes1 is the master regulator of enterocyte differentiation. As we previously said, T3 mainly favours the differentiation of the secretory lineages, so this preferential commitment is surely dictated by the crosstalk with the Wnt pathway. In addition, several components of the Notch pathway, including Hes1 and Jag1, have been described as targets of Wnt [87,292,293]. Given that TRα1 activates the Wnt pathway in intestinal crypts and CRC, we cannot exclude the possibility that some of the responses observed for Notch also depend on TRα1-stimulated Wnt activity.

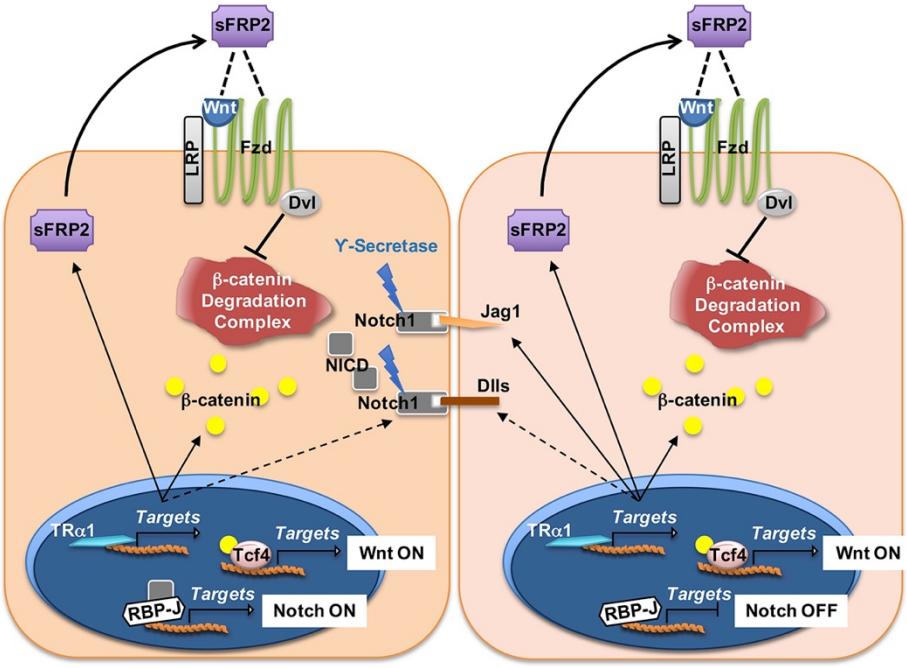

Figure 29 – The proposed molecular model for the action of TRα1 on the Wnt and Notch pathways in intestinal crypt precursors.

In the intestinal crypt cells, TRα1 regulates the expression of several genes involved in the Wnt and Notch pathways. Wnt pathway: the binding of TRα1 to TREs positively regulates the expression of *Ctnnb1* (encoding for β-catenin) and *Sfrp2* genes. In turn, sFRP2 protein, by interacting with the Wnt ligands and Frizzled receptors (Fzd), allows the recruitment of the cytoplasmic protein Dishevelled (Dvl) and blocks the β-catenin destruction complex, stabilising the β-catenin. Indeed, β-catenin can then translocate to the nucleus and form a complex with the Tcf/Lef transcription factor to increase the expression of Wnt target genes. Notch pathway: the action of TRα1 is exerted on two adjacent cells, one expressing Notch receptor(s) (left diagram) and the other expressing Notch ligand(s) (right chart). The cleavage of the Notch1 receptor by the g-secretase into the Notch1-intracellular domain (NICD) induces the expression of Notch target genes, *Jag1, and* the increased expression of Dlls (Dll1 and Dll4) in the ligand-expressing cell and of Notch1 on the adjacent cell. To do so, NICD translocates into the nucleus, where it participates in the transcriptional regulation of Notch-target genes by forming a complex with the transcription factor RBP-J. As a result, TRα1 and Wnt are active in both cells, while only the Notch-expressing cells display an active Notch pathway. Dashed arrows indicate indirect regulation; full arrows indicate direct transcriptional regulation. The figure has been taken from 335.

Another signalling pathway altered by TH is BMP. In the context of CRC and CSC, Catalano and colleagues showed that T3 treatment or DIO3 depletion (which will prevent the degradation of

T3) induced the differentiation of CRC CSC through an increase of BMP4 and its downstream targets. This resulted in the attenuation of the Wnt signalling and reduction of clonogenic capacity and tumorigenic potential [294]. These findings are discordant with our data showing a positive regulation of TH/TRα1 on the Wnt pathway, cell proliferation, tumorigenicity and SC activity. Moreover, the contrasting results between this report and ours may be due to the experimental designs, and the differential BMP response may be due to a different expression pattern of the DIOs in the epithelium and the niche.

Interestingly, during this thesis, we evaluated the role of different transcription factors in regulating the *THRA* gene in CRC (Giolito et al. under revision in Mol. Oncol, see paper Nº2). In this study, we described for the first time the controls of its expression in a tissue and context-specific. Using luciferase assays, we assessed the involvement of various transcription factors in the regulation of *THRA* promoter activity, and we observed that Wnt signalling increases the *THRA* activity. At the same time, Notch decreases or does not change *THRA* activity. Moreover, using different approaches, we validated the direct regulation of *THRA* by Wnt and showed a direct binding of β-catenin/TCF on their two binding sites present within the *THRA* promoter, which contributes to a positive loop between TRα1 and β-catenin.

Thyroid hormones in cancer

Multiple studies have shown a significant connection between TH dysfunction and several types of cancer. Substantial evidence suggests that subclinical and clinical hyperthyroidism increases the risk of several solid malignancies, while hypothyroidism may reduce aggressiveness or delay cancer onset[295]. Studies in which dysregulation of the thyroid hormone axis is secondary to cancer showed that supplementation therapies further support the deleterious effect of altered TH status on cancer outcomes[296,297]. One of the cancer types where the involvement of THs is well known is hepatocellular carcinoma (HCC). Hypothyroidism plays an essential role in liver carcinogenesis, and several studies demonstrated that T3 in HCC downregulates cancer cell proliferation[298]. Also, previous studies have explored the association between the use of levothyroxine and the risk of CRC but have shown conflicting results. Some studies found evidence for a protective effect of levothyroxine, while others found worsening effects or even no association. One of the main problems with the epidemiological studies is that some consider TH supplementation, which aims to normalize TH levels, as a hyperthyroid status, which is perhaps not the case. Other studies separate TH supplementation from thyroid dysfunction. Besides, we must not forget that many epidemiological studies use a particular group of people of a specific ethnicity and generally in a retrospective way, making the data collection tricky and sometimes ambiguous. In the following paragraphs, I will try to explore the controversial data in CRC. If we analyse all epidemiological studies that examine TH supplementation with levothyroxine and risk of the CRC, we find papers claiming TH supplementation in hypothyroid

patients is a protective factor that decreases the risk of CRC[299,300]; reports claiming the worsening role of exogenous TH[297,300–302] and nor risk or benefit [303]. On the other hand, if we analyse the studies that assessed the thyroid status and risk of CRC, we find the dichotomy of papers claiming that both hypothyroid[299,304,305] and hyperthyroid [299,306] patients have a lower risk of CRC (**See Table 2**). As we just saw, hyperthyroidism increases cancer risk in many solid tumours. So, despite the conflicting epidemiological studies, most of them point toward hyperthyroidism as a predisposing risk factor for CRC.

	Cancer type; Organism; Details	Observations and Comments	References
Protection by THs	CRC; Colon and Rectum/sigmoid; Human; Epidemiology; Replacement therapy	Hypothyroid patients received Levothyroxine to normalise TH levels. The reduced risk of CRC is not always significant.	304
	CRC; Human; Epidemiology, replacement therapy	Long term use of levothyroxine is associated with a reduction of CRC risk.	297
	CRC; Human epidemiology; Replacement therapy; Hypothyroid patients	Hypothyroid patients treated with THs replacement have less risk of CRC. Hypothyroid patients had an increased risk of CRCs than those receiving replacement therapy.	300
	Colon; Human epidemiology	Lower risk of colon cancer in hyperthyroid patients	299
	Metastatic CRC; Human; Low circulating T3	High T3 in patients with metastatic CRCs. No causal proof between metastasis and T3.	306
	Human adenomas and adenocarcinomas; D3 and local hypothyroidism	Association between D3 expression and tumours at early stages	307
	CRC; Human primary tumour cells; D3 and intracellular hypothyroidism	*In vitro* T3 increases chemosensitivity.	294

	Cancer type; Organism; Details	Observations and Comments	References
Worsening by THs	Rectal; Human epidemiology	Lower risk of rectal cancer in hypothyroid patients	[299]
	CRC; Human epidemiology; Replacement therapy; Hyperthyroid patients	Hypothyroid patients treated with THs replacement has less risk of CRC. Hyperthyroid patients had an increased risk of CRCs compared with those receiving replacement therapy	[300]
	CRCs; Human epidemiology; Low TSH and high THs	Increased CRC incidence in hyperthyroid patients, but a limited number of cases	[305]
	Tumours	T4 increases tumour number in an AOM-chemical carcinogenesis model	[301]
	CRCs; Human; Transcriptomics	TRα1 increased in several CMS. THs status unknown	[290]
	Intestine and colon cancer; Mouse	TRα1 overexpression in intestinal epithelium induces hyperproliferation and adenomas. TH injections further increase proliferation. In mutant Apc mice, TRα1 overexpression increases the speed of tumour formation, their number and metastatic capacity	[281]
	Colon adenocarcinoma cell lines	THs stimulate the growth of explants and metastasis spreading. Effect mediated by integrin αvβ3 that can be inhibited by TETRAC (competes with T4 and bloc signalling)	[308]
	Colorectal; Human epidemiology; Replacement therapy	Levothyroxine replacement therapy is associated with a higher risk of CRCs in women but not in men	[302]

Table 2 - Summary of studies evaluating the involvement of thyroid status and CRC

Our laboratory has been interested in TH and TRα1 in the intestine and CRC for a long time. Although briefly, we saw that the ectopic expression of TRα1 in the intestinal epithelium using the *vil*-TRα1 mouse model in an Apc-mutated background mouse model (*vil-TRα1/Apc*$^{1638N/+}$) is responsible for an acceleration of tumour appearance, progression and aggressiveness compared to Apc mutants alone (**Figure 30**)[281]. Moreover, TH injections further increased the proliferation of tumors[281]. Later work in the laboratory studied the involvement of TRα1, its expression levels and the link between TRα1 and the Wnt pathway in CRC. Uchuya-Castillo et al. demonstrated for the first time, using various cellular and molecular approaches, the up-regulation of *THRA* and TRα1 in human CRCs. Intriguingly, one of the mechanisms regulating Wnt activity in these tumours relies on a TRα1-linked strong inhibition of Wnt antagonists like WIF1[290]. Concomitant with these results, during my thesis, using another available cohort and by tissue microarray in

CRC and normal samples, we confirmed the upregulation of *THRA* and TRα1 in human CRC, respectively (Giolito et al. under revision in Mol. Oncol, see paper Nº2).

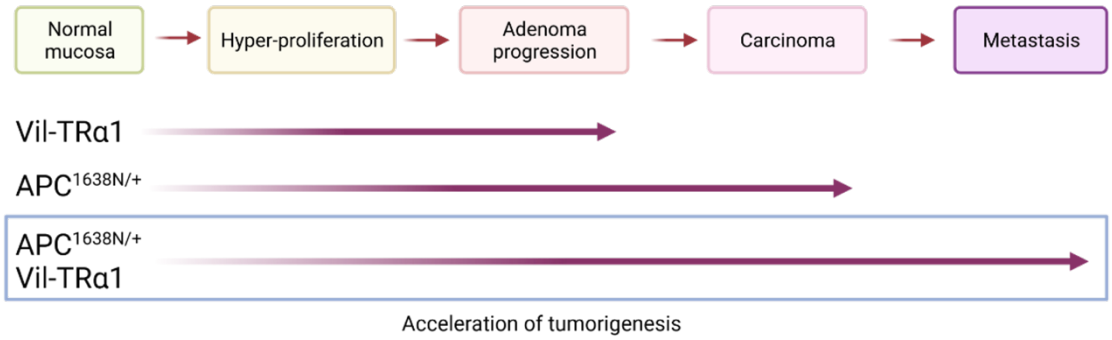

Figure 30 – Influence of TRα1 in the intestinal tumorigenesis

Conversely, as we saw before, papers from the Salvatore group showed that depletion of DIO3 and treatment with T3 for long times in a CRC cell line as Caco2 caused the differentiation of the cells [307]. Of note, Caco2 cells cultured in confluence for several days show characteristics of differentiated enterocytes. Nonetheless, they also observed an association between DIO3 expression and CRC tumours at early stages only, which suggests a protective role of THs. In this same direction, later, they postulated that T3 treatment *in vitro* increases chemosensitivity to 5-FU, OXA and FOLFOX and causes differentiation of colon CSCs[294]. Some discrepancies with our data may arise from different methods, the genes and the proteins evaluated in the different analyses. DIOs can also deiodinate T3, rT3 and T4, and these hormones are found in the serum for the culture medium used in the experiments [309,310].

Another group has studied THs implications in tumours and analysed TH's non-genomic actions of T4 specifically. T4 can induce proliferation and modulate β-catenin expression and activation in CRC cell lines and primary cultures derived from human CRC tumours. In addition, using a siRNA against β-catenin, they showed that its knockdown reverted the T4 induced activation of β-catenin[291]. Thus, they proposed that the contrasting results on tumour proliferation are due to T3-dependent transcription involving the TRs. It was also suggested that the cancer-promoting effects of THs relate to their cell surface receptor, the integrin αvβ3, to which the circulating T4 can bind with higher affinity than T3. CRC patients with a high level of integrin αvβ3-expressing tumour vasculature are associated with the worst prognosis compared to patients with low integrin αvβ3 levels in tumour vasculature, which reinforces the action of TH via the integrin αvβ3[298]. Several years ago, studies in rats using chemical carcinogenesis showed that T4 increased the tumour number[301]. Interestingly, integrin αvβ3 antagonists, which prevent T4 binding, reduce the angiogenesis and metastatic capacity of colon cancer cells[311]. Our studies in mouse models in organoids excluded, however, the involvement of the integrin αvβ3 in response to THs [285].

Thyroid hormones in chemotherapy response

Abnormal hormone levels can profoundly affect liver microsomal drug-metabolizing enzymes in laboratory animals. Concerning the action of THs on drug metabolism, a thyroidectomy (resection of the thyroid gland) or administration of THs has a marked influence on a variety of metabolic reactions[312]. Moreover, THs can influence their own pharmacokinetics and of other hormones like corticosteroids, sex hormones, insulin, and others by regulating their metabolising enzymes. Interestingly, thyroid status can modulate TH metabolism and secretion, and the average half-life of TH is shortened or prolonged in the case of hyperthyroidism and hypothyroidism, respectively [313].

At a molecular level, using the CRC cell line Caco2, Dentice et al. observed that depletion of DIO3 and treatment with T3 for long times induced the differentiation of the cells [307], which, as I previously mentioned, is quite logical as Caco2 cells can differentiate spontaneously if cultured at confluence for long times. Interestingly, results from the same group showed that T3 treatment *in vitro* increases chemosensitivity to 5-FU, OXA and FOLFOX and causes differentiation of colon CSCs[294]. However, we could not observe a tumour differentiating role of T3 during my thesis or from previous work, as discussed earlier.

Although the literature's connection between thyroid function disorders and metabolism is extensive, the data connecting THs and xenobiotic metabolism are sparse. Drug-metabolizing enzymes are an essential barrier to eliminating various xenobiotics and endogenous substances. In addition, these enzymes metabolise common chemotherapeutic agents used in CRC and also THs. Thus, it is logical to think that competition between TH and chemotherapeutic drug metabolism may occur. This competition will further contribute to resistance, given that cancer cells use protective mechanisms to get rid of drugs[206]. UGTs, phase II enzymes involved in the conjugation of drugs like SN-38 (IRI active metabolite), conjugate THs for their elimination. T4 competitively inhibits more than T3 different UGT isoforms (UGT1A1, UGT1A8, UGT1A10 and UGT2B7), which are also SN-38 conjugating enzymes[314]. The inhibition occurs during the metabolisation of THs by UGTs. *In silico* docking, methods showed that a stronger hydrogen bond and hydrophobic interaction occurs between T4 and the activity cavity of UGT1A1 than T3, which contributes to the stronger inhibition by T4 towards UGT1A1 [314].

Cell-based preclinical models showed UGT-associated drug resistance by increasing UGT1A isoforms and drug-induced UGT expression. This increased expression of UGT1A resulted in high extracellular levels of IRI glucuronic conjugate SN-38G. Moreover, as THs are substrates and inhibitors of the UGTs, the THs in the culture medium can favour the increase of UGT expression and compete with SN-38 for its conjugation by UGTs. This competition generates drug-drug interactions, increasing side effects and favour resistance. Additionally, EGFR TKIs like cetuximab and panitumumab, commonly used in CRC patients in combination with FOLFIRI

or FOLFOX, are UGTs inhibitors. Therefore, inhibition of UGTs by TKIs, will further increase the resistance and side effects of IRI and reduce the metabolisation of THs resulting in an increased proliferation of colon CRCs. Strikingly, TKIs and fluoropyrimidines like 5-FU may induce hypothyroidism in patients [315]. Furthermore, as we saw in the past chapter, UGT polymorphisms favour the acquisition of resistance.

In the past chapter, we discussed the increase of drug efflux as an advantageous drug resistance phenotype that cancer cells use to get rid of the treatments. Like UGTs, THs and other endogenous compounds enter and exit the cells via xenobiotics' transporters. Moreover, TH can modulate the expression of some drug efflux pumps, as I briefly mentioned in the past chapter. The most well-known transporter modulated by THs is ABCB1 (p-glycoprotein or MDR1) which can transport hydrophobic chemotherapeutics in the case of CRC, IRI and its metabolites. Two studies, using a Caco2 cell model, evidenced that T3 can regulate the expression and function of ABCB1 in a concentration-dependent manner[316] by binding TR/RXR heterodimers bind to the TREs located 7.9 to 7.8 kb upstream of the transcription start site of ABCB1[317]. The upregulated expression of the transporter resulted in a significantly diminished accumulation of different drugs that are ABCB1 substrates compared with control cells[318,319]. Changes in ABCB1 expression levels under T3 treatment were also associated with acceleration of drug efflux [320]. Another study using Caco2 and LS180 CRC cell lines showed that both T4 and T3 increased the expression of ABCB1 and concluded that the NHR pregnane X receptor (PXR) was not involved in this modulation as these cells do not express this receptor[321]. Siegmund et al.[319] provided data on healthy individuals that oral levothyroxine administration induces elevation of ABCB1 mRNA and protein expression. Therefore, hyperthyroid patients or those receiving exogenous TH may present increased expression of ABCB1 and, consequently, increased efflux of chemotherapeutic drugs like IRI, resulting in drug resistance.

Another ABC transporter essential for drug resistance and transport of IRI is ABCG2. In contrast to ABCB1, there is almost no data about TH and ABCG2 modulation, despite being one of the most studied transporters in cancer cells. In normal small intestine and colon tissue, ABCG2 protein expression localises in the apical membrane of the epithelium. The tissue localisation suggests a crucial role in the absorption, distribution, metabolism, and elimination of endogenous substances and xenobiotics like IRI[221]. ABCG2 is also an SC marker in immature myeloid and leukaemia SCs[322]. In addition, many solid tumours, including CRC, have subpopulations of stem-like cells expressing the ABCG2 side population[221]. Despite being one of the essential transporters in drug resistance, TH modulation of ABCG2 is still unknown. Some studies showed that the Wnt signalling pathway modulates ABCG2 expression[221]. THs modulate the Wnt signalling, as we mentioned earlier in the chapter, via modulation of β-catenin, sFRP2 and even WIF1 inhibition [281,284,290], which can indirectly increase ABCG2 levels. The modulation of ABCG2 and ABCB1 by the Wnt signalling pathway was observed in other cancers like lung cancer and enhanced by

the presence of the chemotherapeutic agent, in this case, cisplatin. Surprisingly, either transporter can efflux cisplatin, but it can improve the efflux of drugs used in combination with it[323].

Similarly, ABCB1 and ABCG2 do not transport THs, but they may induce the efflux of other drugs like IRI, OXA and 5-FU. Overexpression of ABCG2 favours OXA action; thus, TH treatment may increase OXA efficacity[181]. Inhibiting GLI1 decreases ABCB1 and ABCG2 expression[324–326], and TH can indirectly regulate them via hedgehog signalling. Moreover, posttranscriptional variations in the 5′UTR of the mRNA, especially in drug-resistant cell lines, can regulate ABCG2 protein expression [327]. At least in hepatocytes, a binding site for CAR exists in the distal promoter of the *ABCG2* gene [328]. Interestingly, THs were necessary to induce the expression of the NHR CAR and the drug-metabolizing enzyme CYP2B1, even if TH does not directly regulate CAR expression[329]. CAR activation can induce TH glucuronidation and sulfation pathways, facilitating elimination and decreasing THs levels [330]. In CRC, we may expect a similar mechanism, but if we consider that UGT enzymes metabolise IRI, the competition is higher, and the TH elimination will be lower. The latter may also explain why TH levels impact in a lesser manner or even benefit OXA treatment, as UGTs do not metabolise it. The increased TH metabolism by UGTs (that decreases T4 and T3 serum levels) could explain the apparition of hypothyroidism after EGFR inhibition.

Regarding TH action to targeted therapies, there is little information about it. However, we previously saw that integrin αvβ3 and T4 are involved in angiogenesis. Thus, we might expect THs to contribute to the lack of VEGF inhibition response with bevacizumab. As an alternative, bevacizumab administration combined with tetraiodothyroacetic acid (Tetrac), a T4 derivative that competes with T4 for the binding to the integrin, can improve the outcome by further blocking angiogenesis[331]. Tetrac treatment, in combination with the EGFR inhibitor, cetuximab, suppressed the transcription of cell proliferation-associated genes compared to cetuximab alone treatment. In addition, the combination treatment reduced the cell proliferation in a mutant KRAS cell line [308]. So, this combined treatment could improve the outcome of patients carrying the mutation, which generally will not benefit from cetuximab treatment alone. More broadly, TH can affect drug response through their anti-apoptotic actions. TH can affect the transcription of various genes relevant to apoptosis, while tetrac may prevent this action and facilitate apoptosis[332–334]. Of note, T3 and TRα1 are directly involved in apoptosis and DNA damage prevention[271].

Chapter 4: Results

Background. Colorectal cancer (CRC) displays high frequency, strong severity, and relapse to current therapies. Hence, a better knowledge of its biology is needed to develop more efficient treatments. The intestinal epithelium is characterised by its perpetual renewal through adult multipotent stem cells (SC) [3]. Their correct functioning ensures coordinated cell proliferation, migration, and differentiation through complementary Wnt, Notch and BMP signalling pathways. Deregulation of these same pathways is involved in tumorigenesis. It is generally thought that CRC is initiated with the dysfunctioning of SCs and their transformation into Cancer Stem Cells (CSCs), acquiring properties of tumour initiating cells, which may be the basis of tumour relapse and tumour dissemination to form metastases. The CSC concept received strong support in mouse models and human CRC [118,146]. Thus, eliminating CSC is now thought to be a prerequisite for successful therapy. However, it is worth noting that together with these strong indications of CSC-driven tumour development, new data support the notion that non-SC-dependent cell plasticity promotion (de-differentiation and trans-differentiation) allows non-SCs to acquire SCs and CSCs properties.

Our laboratory has contributed to this field by studying the importance of the signal-dependent upon thyroid hormones (THs) in gut development and homeostasis. THs act via the thyroid hormone nuclear receptors TRs, T3-modulated transcription factors. The thyroid hormone T3 and its nuclear receptor TRα1 control gut development and homeostasis through the modulation of intestinal crypt cell proliferation [246,247,335]. The translational potential of our studies in mouse models has been proved in human CRC patients. We observed an increased TRα1 expression in CRC, and, from a molecular point of view, we showed a significant correlation between TRα1 levels and Wnt activity [290]. TRα1 loss-of-function (LOF) and gain-of-function (GOF) in human adenocarcinoma Caco2 cell lines confirmed that TRα1 levels control Wnt activity and demonstrated the role of TRα1 in regulating cell proliferation and migration. Altogether these data strongly suggested the involvement of TRα1 in cancer stem cell biology, similar to what we previously observed in normal intestinal SCs [285]. Despite the progress made, we still lack detailed information on THRA gene regulation, or on TH and TRα1 specific involvement in the intestinal CSC biology including the chemotherapeutic response.

Aims.

(1) Analyse the mechanisms that control THRA gene expression in colon cancer and CSCs.

(2) Study TRα1 in CSCs, including their maintenance, differentiation, and implication on drug resistance.

Methods. For aim 1, we analysed the activity of the *THRA* gene promoter and the mechanisms that control TRα1 expression. For aim 2, we used tumour spheroids based on Caco2 cells developed during this thesis [336]. We evaluated the impact of T3 or altered TRα1 expression in the spheroids formation and growth response to standard CRC chemotherapy.

Results.

Molecular mechanisms of THRA gene regulation

By *THRA* promoter analysis, we demonstrated the presence of binding sites for transcription factors involved in intestinal homeostasis and SC/CSC biology that are also altered in CRC, such as TCF7L2 (Wnt pathway), RBPJ (Notch pathway) and CDX2 (intestinal epithelial cell identity). In addition, an in-depth analysis of the Wnt pathway allowed us to recapitulate the regulation of *THRA* transcription and TRα1 expression by this pathway in human adenocarcinoma cell lines and mouse enteroids (Giolito et al., under revision in Mol. Oncol.).

TRα1 and T3 action on cancer stem cell biology

Using the Aggrewell 400 technology, we developed a new spheroid model from Caco2 cells, well adapted to study the CSCs [336]. Through the analysis of spheroids' growth during the time in the culture, we observed that T3 and TRα1 stimulate while TRα1-knockdown strongly decrease their growth. Furthermore, immunofluorescence and RTqPCR analyses showed changes in cell proliferation in T3 or TRα1-GOF conditions. Interestingly, T3/TRα1 also act as pro-survival factors of spheroids treated with the chemotherapy combinations used in CRC patients.

Conclusion and perspectives. For the first time, our work describes the regulation of the *THRA* gene in specific cell and tumour contexts. We also gained insights into the T3/TRα1-dependent tumour cell behaviour, eventually including their response to chemotherapy.

Paper Nº 1

Article published in JoVE DOI: https://dx.doi.org/10.3791/61783

"A three dimensional model of spheroids to study colon cancer stem cells"

Maria Virginia Giolito[1,2], **Léo Claret**[1,2,] **Carla Frau**[1], **Michelina Plateroti**[1,2]

[1] Département de la recherche, Centre de Recherche en Cancérologie de Lyon, INSERM U1052, CNRS UMR5286, Université de Lyon, Université Lyon 1, Centre Léon Bérard, [2] UMR-S1113 - IRFAC INSERM, Université de Strasbourg

As I just mentioned one of the two aims of my thesis was to study TRα1 in colon CSCs, including their maintenance, differentiation, and implication on drug resistance. For that, the first step was to develop an appropriate tool, a 3D culture system of spheroids, that would allow us to study CSC biology and their response to chemotherapy as a final aim and would be a reliable tool for follow up studies. In this first paper of this thesis, we presented a protocol showing a novel, robust, and reproducible culture system to generate and grow 3D spheroids from Caco2 colon adenocarcinoma cells using a special plate called Aggrewell. The results provide the first proof-of-concept for the appropriateness of this approach to study cancer stem cell biology, including the response to chemotherapy and constituted the basis for all our further works on T3/TRα1 actions on CSC biology. The obtained spheroids grew successfully and their growth and characteristic were followed during the culture time. Furthermore, we could observe that the spheroids obtained with our method (a) actively proliferate, (b) present a very low rate of cell death, (c) organize to form a lumen inside the spheres and (d) the cells retain a differentiation capacity, (e) presented a dynamic expression of CSC markers along the days in culture and representing defined different CSC populations. As the final aim was to study the chemotherapy response, we showed that our spheroids had a heterogeneous response to two different drug combinations used commonly in CRC patients, both morphologically and when analysing different CSC markers involved.

This initial study paved the way for the analysis of T3 and TRα1 in colon CSC biology and their implications in chemotherapy response using this same spheroid model, as can be seen in paper Nº 3.

jove

A Three-dimensional Model of Spheroids to Study Colon Cancer Stem Cells

Maria Virginia Giolito[1,2], **Léo Claret**[1,2], **Carla Frau**[1], **Michelina Plateroti**[1,2]

[1] Département de la recherche, Centre de Recherche en Cancérologie de Lyon, INSERM U1052, CNRS UMR5286, Université de Lyon, Université Lyon 1, Centre Léon Bérard [2] UMR-S1113 - IRFAC INSERM, Université de Strasbourg

Corresponding Author

Michelina Plateroti
plateroti@unistra.fr

Citation

Giolito, M.V., Claret, L., Frau, C., Plateroti, M. A Three-dimensional Model of Spheroids to Study Colon Cancer Stem Cells. *J. Vis. Exp.* (167), e61783, doi:10.3791/61783 (2021).

Date Published

January 22, 2021

DOI

10.3791/61783

URL

jove.com/video/61783

Abstract

Colorectal cancers are characterized by heterogeneity and a hierarchical organization comprising a population of cancer stem cells (CSCs) responsible for tumor development, maintenance, and resistance to drugs. A better understanding of CSC properties for their specific targeting is, therefore, a pre-requisite for effective therapy. However, there is a paucity of suitable preclinical models for in-depth investigations. Although in vitro two-dimensional (2D) cancer cell lines provide valuable insights into tumor biology, they do not replicate the phenotypic and genetic tumor heterogeneity. In contrast, three-dimensional (3D) models address and reproduce near-physiological cancer complexity and cell heterogeneity. The aim of this work was to design a robust and reproducible 3D culture system to study CSC biology. The present methodology describes the development and optimization of conditions to generate 3D spheroids, which are homogenous in size, from Caco2 colon adenocarcinoma cells, a model that can be used for long-term culture. Importantly, within the spheroids, the cells which were organized around lumen-like structures, were characterized by differential cell proliferation patterns and by the presence of CSCs expressing a panel of markers. These results provide the first proof-of-concept for the appropriateness of this 3D approach to study cell heterogeneity and CSC biology, including the response to chemotherapy.

Introduction

Colorectal cancer (CRC) remains the second leading cause of cancer-associated deaths in the world[1]. The development of CRC is the result of a progressive acquisition and accumulation of genetic mutations and/or epigenetic alterations[2,3], including the activation of oncogenes and inactivation of tumor suppressor genes[3,4]. Moreover, non-genetic factors (e.g., the microenvironment) can contribute to and promote oncogenic transformation and thus participate in the evolution of CRCs[5]. Importantly, CRCs are composed of different cell populations, including undifferentiated CSCs

and bulk tumor cells displaying some differentiation traits, which constitute a hierarchical structure reminiscent of the organization of the epithelium in a normal colon crypt[6,7].

CSCs are considered to be responsible for tumor appearance[8], its maintenance and growth, metastatic capacity, and resistance to conventional therapies[6,7]. Within tumors, cancer cells, including CSCs, display a high level of heterogeneity and complexity in terms of their distinct mutational and epigenetic profiles, morphological and phenotypic differences, gene expression, metabolism, proliferation rates, and metastatic potential[9]. Therefore, to better understand cancer biology, tumor progression, and acquisition of resistance to therapy and its translation into effective treatments, human preclinical models capturing this cancer heterogeneity and hierarchy are important[10,11].

In vitro 2D cancer cell lines have been used for a long time and provide valuable insights into tumor development and the mechanisms underlying the efficacy of therapeutic molecules. However, their limitation with respect to the lack of the phenotypic and genetic heterogeneity found in the original tumors is now widely recognized[12]. Moreover, nutrients, oxygen, pH gradients, and the tumor microenvironment are not reproduced, the microenvironment being especially important for the maintenance of different cell types including CSCs[11,12]. To overcome these main drawbacks, several 3D models have been developed to experimentally address and reproduce the complexity and heterogeneity of cancers. In effect, these models recapitulate tumor cellular heterogeneity, cell-cell interactions, and spatial architecture, similar to those observed in vivo[12,13,14]. Primary tumor organoids established from fresh tumors, as well as cell line-derived spheroids, are largely employed[15,16].

Spheroids can be cultured in a scaffold-free or scaffold-based manner to force the cells to form and grow in cell aggregates. Scaffold-free methods are based on the culture of cells under non-adherent conditions (e.g., the hanging-drop method or ultra-low attachment plates), whereas scaffold-based models rely on natural, synthetic, or hybrid biomaterials to culture cells[12,13,14]. Scaffold-based spheroids present different disadvantages as the final spheroid formation will depend on the nature and composition of the (bio)material used. Although the scaffold-free spheroid methods available so far do not rely on the nature of the substrate, they generate spheroids that vary in structure and size[17,18].

This work was aimed at designing a robust and reproducible 3D culture system of spheroids, which are homogenous in size, composed of Caco2 colon adenocarcinoma cells to study CSC biology. Caco2 cells are of particular interest owing to their capacity to differentiate over time[19,20], strongly suggesting a stem-like potential. Accordingly, long-term culture of the spheroids revealed the presence of different CSC populations with different responses to chemotherapy.

Protocol

NOTE: The details of all reagents and materials are listed in the **Table of Materials**.

1. Spheroid formation

1. Spheroid culture media
    1. Prepare basal medium consisting of Dulbecco's Modified Eagle Medium (DMEM) supplemented with 4 mM L-alanyl-L-glutamine dipeptide.
    2. Prepare DMEM complete medium containing 10% fetal bovine serum (FBS) and 1% penicillin-

streptomycin (Pen/Strep) in basal medium from step 1.1.1.

3. Prepare DMEM/basement membrane matrix medium containing 2.5% basement membrane matrix, 10% FBS, and 1% Pen/Strep in basal medium from step 1.1.1.

2. Preparation of plates for spheroid formation

1. Warm basal and DMEM/basement membrane matrix medium at room temperature (RT) for approximately 20 min.

2. Pretreat the wells of a 24-well plate dedicated to spheroid formation by adding 500µL of anti-adherence rinsing solution to each well.
NOTE: In these plates, each well consists of 1,200 microwells.

3. Centrifuge the plate at 1,200 × *g* for 5 min in a swinging bucket rotor with adaptors for plates.
NOTE: If only one plate is used, prepare an additional standard plate filled with water to counterbalance the weight.

4. Rinse each well with 2 mL of warm basal medium, and aspirate the medium from the wells.

5. Observe the plate under the microscope to ensure that bubbles have been completely removed from the microwells. If bubbles remain trapped, centrifuge again at 1,200 × *g* for 5 min to eliminate the bubbles.

6. Repeat the rinsing steps 1.2.4-1.2.5.

7. Add 1 mL of warm DMEM/basement membrane matrix medium to each well.

3. Generation of spheroids

1. Grow the Caco2 cells in a 2D monolayer in DMEM medium supplemented with 10% FBS and 1% Pen/Strep at 37 °C in a humidified atmosphere containing 5% CO_2 (hereafter referred to as 37 °C/5% CO_2).
NOTE: The maximum number of cell passages to be used is 80.

2. When 80% of confluency is reached, wash the cells with phosphate-buffered saline (PBS) 1x (5 mL for a 10 cm dish), add trypsin-ethylenediamine tetraacetic acid (EDTA) (2 mL for a 10 cm dish), and incubate for 2-5 min at 37 °C/5% CO_2.

3. Check cell detachment under the microscope, and neutralize the trypsin by adding 4 mL of DMEM complete medium per 10 cm dish.

4. Count cells using a hemocytometer to determine the total number of cells.

5. Centrifuge the cell suspension at 1,200 × *g* for 5 min. Discard the supernatant, and resuspend the pellet in an appropriate volume of DMEM/basement membrane matrix medium.

6. Refer to **Table 1** to determine the number of cells required per well to achieve the desired number of cells per microwell. Alternatively, calculate the number of cells using the following formula for a 24-well plate, considering each well contains 1,200 microwells
Required number of cells per well = Desired number of cells per microwell × 1,200

7. Add the required volume of the cell suspension to each well to achieve the desired cell number in a final volume of 1 mL.

8. Add 1 mL of DMEM/basement membrane matrix medium to each well to reach the final volume of 2 mL per well (see also step 1.2.7).

NOTE: Be careful not to introduce bubbles into the microwells.

9. Centrifuge the plate immediately at 1,200 × *g* for 5 min to capture the cells in the microwells. If necessary, counterbalance the centrifuge with a standard plate filled with water.

10. Observe the plate under the microscope to verify that the cells are evenly distributed among the microwells.

11. Incubate the plate at 37 °C/5% CO_2 for 48 h without disturbing the plate.

NOTE: According to the original protocol[21], although many cell lines can form spheroids within 24 h, some require a longer incubation time. In this protocol, 48 h are sufficient for spheroid formation.

4. Harvesting the spheroids from the microwells

1. Warm the basal and DMEM/basement membrane matrix medium at RT for approximately 20 min.

2. Using a serological pipette, remove half of the culture medium (1 mL) from each well.

3. Add the medium back onto the surface of the well to dislodge the spheroids from the microwells.
NOTE: Do not touch or triturate the spheroids.

4. Place a 37 µm reversible strainer (or a 40 µm standard strainer) on the top of a 15 mL conical tube to collect the spheroids.
NOTE: If using a 40 µm standard strainer, place it upside down.

5. Gently aspirate the dislodged spheroids (from step 1.4.3), and pass the spheroid suspension through the strainer.
NOTE: The spheroids will remain on the filter; single cells will flow through with the medium.

6. Using a serological pipette, dispense 1 mL of the warm basal medium across the entire surface of the well to dislodge any remaining spheroids and recover them on the strainer.

7. Repeat this washing step 1.4.6 twice.

8. Observe the plate under the microscope to ensure that all spheroids have been removed from the microwells. Repeat the wash if necessary (steps 1.4.6-1.4.7).

9. Invert the strainer, and place it on a new 15 mL conical tube. Collect the spheroids by washing the strainer with DMEM/basement membrane matrix medium.
NOTE: The collected spheroids are ready for downstream applications and analyses.

5. Long-term culture of spheroids

1. Prepare 1.5% agarose solution in basal medium, and sterilize it by autoclaving (standard cycle).

2. While the agarose solution is warm and still liquid, coat the wells of standard culture plates or dishes, as described in **Table 2**.
NOTE: Warming the dish/plate in the oven will facilitate the coating step. Coated dishes/plates can be left at RT for up to 10 days in a sterile environment and protected from the light.

3. Seed the harvested spheroids (from step 1.4.9) in the agarose-coated plates, and add DMEM/basement membrane matrix medium to achieve the final volume depending on the size of the plate.

NOTE: To avoid spheroid aggregates, seed them at the optimal density of 22 spheroids/cm^2. Observe that the coating is not perfectly flat, and it rises towards the edge, creating a light concavity at the center of the plate. If the number of spheroids is too high, they are more likely to adhere to each other.

4. Incubate the plate at 37 °C/5% CO_2 until recovery of the spheroids for specific analyses.

6. Treatment of spheroids with chemotherapeutic drugs

1. Plate spheroids from step 1.5.4, and grow them for 2 days. Starting from day 3 (D3), treat them with FOLFIRI (5-Fluorouracil, 50 µg/mL; Irinotecan, 100 µg/mL; Leucovorin, 25 µg/mL) or with FOLFOX (5-Fluorouracil, 50 µg/mL; Oxaliplatin, 10 µg/mL; Leucovorin, 25 µg/mL) chemotherapeutic regimen combinations routinely used to treat CRC patients[22,23,24,25], or maintain them in (control) not-treated (NT) condition.

2. Collect the spheroids after 3 days of treatment by using a pipette with the tip cut off (1,000 µL tip), ensuring that each condition is represented by at least three replicates. Centrifuge them at 1,000 × *g* for 3 min, and then remove the supernatant.

3. Fix the pellets in 2% paraformaldehyde (PFA) for histological analysis (see section 3), or use the pellets for RNA extraction (see section 4).

4. To analyze cell death, incubate the spheroids from step 1.6.1 in black culture well plates in DMEM/ basement membrane matrix medium for 30 min with a nucleic acid stain (1:5000 dilution) that does not permeate live cells, but penetrates the compromised membranes of dead cells[26]. Measure the accumulation of fluorescence with a microplate reader.

2. Monitoring spheroid growth

1. Using an inverted microscope, acquire representative images of spheroids maintained under different conditions throughout the days in culture.

2. Analyze the images by measuring three different representative diameters of each spheroid using appropriate software.

3. Use the following formula to obtain the estimated sphere volume.

$$\text{Estimated volume } (\mu m^3) = \frac{4}{3}\pi\left(\frac{d_1}{2}\frac{d_2}{2}\frac{d_3}{2}\right)$$

NOTE: The terms, d1, d2, and d3, are the three diameters of the spheroid.

3. Immunofluorescence (IF) and histological staining

1. Fixation and paraffin embedding

1. Collect the spheroids at selected time-points using a pipette with the tip cut off as described in step 1.6.2, and fix them for 30 min at RT in 2% PFA.
NOTE: Alternatively, store the samples at this step at 4 °C until further use.

2. For paraffin embedding, wash the spheroids 3x with PBS 1x, and resuspend them in 70% ethanol. After paraffin inclusion and sectioning, perform hematoxylin & eosin (H&E) staining for histological analysis.

2. Immunolabeling of paraffin sections
NOTE: Use 5-µm-thick sections for indirect immunostaining.

1. Incubate slides at 60 °C for 2 h to melt the wax and improve deparaffinization.
2. Wash the slides twice for 3 min in methylcyclohexane.
3. Wash the slides for 3 min in 1:1 methylcyclohexane:100% ethanol.
4. Wash the slides twice for 3 min in 100% ethanol.
   NOTE: Perform all manipulations for step 3.2.2 to step 3.2.4 in a chemical hood.
5. Wash the slides for 3 min in 90% ethanol.
6. Wash the slides for 3 min in 75% ethanol.
7. Wash the slides for 3 min in 50% ethanol.
8. Wash the slides under tap water.
9. Rehydrate the slides in distilled water for 5 min.
10. Prepare 700 mL of 0.01 M citrate buffer, pH 6.0, and add it to a suitable container (width: 11.5 cm, length: 17 cm, height: 7 cm); submerge the slides in it. Heat the container in the microwave for 9-10 min at 700 W, and when the boiling starts, decrease the power to 400-450 W. Incubate for an additional 10 min.
11. Let the slides cool down in the buffer to RT for approximately 30-40 min.
12. Wash the slides twice in PBS for 5 min.
13. Draw a circle around the sections with a marker pen to create a barrier for liquids applied to the sections.
14. Incubate each section with 50 µL of blocking buffer (10% normal goat serum, 1% bovine serum albumin (BSA), and 0.02% Triton X-100 in PBS) for at least 30 min at RT.
15. Remove the blocking buffer, and add 50 µL of primary antibodies diluted in the incubation buffer (1% normal goat serum, 0.1% BSA, and 0.02% Triton X-100 in PBS). Incubate for 2 h at RT or overnight at 4 °C.
16. Remove the primary antibodies, and wash the slides 3x in PBS for 5 min.
17. Incubate the slides with 50 µL of fluorescent secondary antibodies diluted in the incubation buffer for 1 h at RT.
18. Remove the secondary antibodies, and wash the slides 3x in PBS for 5 min.
19. Add 50 µL of mounting medium with 4′,6-diamidino-2-phenylindole to each section, and place a glass coverslip over the section.

4. RNA extraction, reverse transcription-polymerase chain reaction (RT-PCR), and quantitative RT-PCR (qRT-PCR)

1. Collect spheroids at different time-points, each point represented by at least three replicates. Centrifuge them at 1,000 × *g* for 3 min, and then remove the supernatant.
   NOTE: Pellets can be directly used for RNA extraction or stored at -20 °C until further use.
2. Isolate the total RNA using a commercial RNA isolation kit, according to the manufacturer's instructions.
3. Reverse-transcribe 500 ng of each RNA sample into complementary DNA (cDNA) with a commercial kit according to the manufacturer's instructions.
4. After reverse transcription, perform a PCR analysis on 1 µL of cDNA to amplify a housekeeping gene with primers located in different exons.
   NOTE: This step enables the verification of the absence of any genomic DNA contamination in the RNA

preparations. For this protocol, peptidylprolyl isomerase B (*PPIB)* primers were used.

5. Perform qPCR amplification on 4 µL of previously diluted cDNA (1:10 in RNAse-free double-distilled water) by using primers specific for the genes of interest. In each sample, quantify specific mRNA expression by using the ΔΔCt method and values normalized against a housekeeping gene levels.

   NOTE: For this protocol, β-actin (*ACTB)* was selected. Primers used in this protocol are listed in **Table 3**.

Representative Results

As the lack of homogeneity in the size of spheroids is one of the main drawbacks of currently available 3D spheroid culture systems[13], the aim of this work was to set up a reliable and reproducible protocol to obtain homogenous spheroids. First, to establish ideal working conditions, different numbers of Caco2 cells were tested, ranging from 50 to 2,000 cells per microwell/spheroid using dedicated plates (**Table 1**). In effect, each well in these plates contains 1,200 microwells, enabling the formation of the same number of spheroids per well, and more importantly, the formation of one spheroid per microwell[21]. After two days of culture, the wells containing 2,000 cells per spheroid grew as a monolayer, and 50 cells per spheroid gave rise to small and non-homogenous spheroids (**Figure 1A**). These two conditions were therefore excluded from further analyses. To establish long-term cultures, spheroids were harvested from the microwells and seeded under non-adherent conditions in freshly prepared agarose-coated plates. Spheroid growth was then monitored throughout the experimental time-course by measuring the change in volume. To take into account the non-spherical shape, three different diameters of each spheroid were measured, and the volume formula was applied[27] (**Figure 1B**). Spheroids generated from 100 and 200 cells maintained their initial size over the entire course of the experiment, whereas those containing 1,000 cells disintegrated during harvesting due to their large size and, consequently, presented more variability in their volume. Therefore, as spheroids arising from 500 cells showed the most homogenous increase in size over the experimental time-course, this number of cells was used for spheroid formation.

Second, besides 500 cells per spheroid, additional cell numbers ranging from 300 to 800 cells were studied. Moreover, to improve the non-adherent conditions, the original protocol was modified by pretreating the wells twice instead of applying only one wash. An improvement in spheroid homogeneity and compaction was observed with these changes (**Figure 2A**). The size of the spheroids in each condition was measured at the time of harvest (**Figure 2B**), and their long-term growth was monitored throughout the days in culture in agarose-coated dishes (**Figure 2C**). Based on the results, 500 and 600 cells/spheroid were confirmed as the optimal conditions yielding good growth and low variability. Owing to the more homogenous growth profile throughout the experimental time-course and the compact structures formed, 600 cells per spheroid was selected as the cell number for subsequent experiments. Finally, to further improve the protocol, DMEM complete medium was supplemented with 2.5% of basement membrane matrix, which contains additional growth factors and a large panel of extracellular matrix proteins[28]. Indeed, the multilobular shape of the spheroids could be due to the lack of signals from the microenvironment that may have affected cell polarization[29,30]. The addition of basement membrane matrix enhanced spheroid growth and improved their homogeneity (**Figure 2D**). An example of this improvement can be seen for 500 cells per spheroid. In the absence of the basement membrane matrix (**Figure 1B**), the size of the spheroids was more heterogeneous, doubling from D3 to D7 and then reaching a plateau. However, in the presence of the basement membrane matrix (**Figure 2C**), the size of the spheroids at each time-point was more homogeneous, increasing proportionally over time.

To analyze long-term features of the spheroids, they were recovered at different time-points after culture in agarose-coated dishes for detailed histological and IF analyses on paraffin sections. H&E staining showed that cells within the spheroids underwent changes in their organization and shape over time. Indeed, cells were densely arranged in multilayers at D3, while flattened cells arranged in monolayers were clearly visible at D10. Interestingly, as indicated by the black dotted lines in the images, a lumen appeared within the spheroids from D5 onwards (**Figure 3**). In parallel, cell proliferation and apoptosis were analyzed by IF using the proliferation marker, proliferating cell nuclear antigen (PCNA), and the cell death marker, activated caspase 3. Labeling for PCNA revealed that proliferating cells were often present at the outer surface of the spheroids, sometimes in crypt-like or bud-like structures reminiscent of organoid cultures[15]. In addition, a clear increase in PCNA-positive cells at D5 and D7 was observed that declined by D10 (**Figure 4**, left panels). Surprisingly, activated caspase 3 was observed in very few cells in the spheroids at both D3 and D5 (**Figure 4**, left panels) and over longer periods of time (data not shown). The expression pattern of β-catenin was also evaluated in paraffin sections. Interestingly, high levels of β-catenin expression were observed at each time-point with clear membrane-bound and cytoplasmic staining (**Figure 4**, right panels). It is worth noting that membrane-bound β-catenin participates in cell-cell adhesion by binding to E-cadherin[31]. A high level of ß-catenin labeling was noted in clusters of cells at all time-points. In some cases, cells also displayed clear nuclear ß-catenin localization (**Figure 4**, right panels). Caco2 cells are known to differentiate in vitro in 2D mainly into enterocytes[19,32]. However, the expression of differentiation markers, such as chromogranin A (enteroendocrine cells), lysozyme (Paneth cells) or mucin 2 (MUC 2, goblet cells), was undetectable in these spheroids by IF (data not shown).

However, the potential to differentiate into enterocytes was confirmed, given that the spheroids expressed *ALPI* (alkaline phosphatase) and solute carrier family 2, transcript variant 2 (*SLC2A5)/*glucose transporter 5 (*GLUT5*) mRNAs (**Figure 5**). These mRNA levels increased at D5 and D7, but the difference was either not significant (*ALPI*) or only marginally significant (*SLC2A5*) compared to the levels at D3.

With the final aim of defining whether the spheroids generated and cultured based on this new method are a reliable tool to study CSCs, the expression of CSC markers was analyzed by IF and qRT-PCR. CD133 and CD44 characterize cancer cell populations including CSCs[7,33,34] and are also expressed by SCs in the normal intestine and colon[33,34,35]. Clusters of CD133-positive cells were mainly localized on the external surface of the spheroids at each time-point (**Figure 6A,** left panels). CD44-positive cells were less frequent, but were always associated with CD133-positive cells (**Figure 6A,** right panels), indicating the existence of a population of CD133/CD44 double-positive CSC-like cells and a population expressing only CD133. Olfactomedin 4 (OLFM4) and Musashi 1 (MSI1) were examined as SC/CSC markers; these markers are expressed in a very limited manner in colon crypts[36,37] and also in distinct cell populations[35,38]. Only a few MSI1-positive cells were observed at each time-point (**Figure 7**), whereas OLFM4 remained undetectable (data not shown). Nevertheless, as observed for CD44 and CD133, MSI1-labeled cells were located on the external surface of the spheroids in crypt-like or bud-like structures. The same markers were also analyzed at the mRNA level at the same time-points after culture in agarose-coated dishes. Aldehyde dehydrogenase 1 (*ALDH1a1*), a well-characterized marker of CSCs[39,40], was also included in the study (**Figure 8**). The analysis of prominin-1 (*PROM1* encoding for CD133) and *CD44* mRNAs confirmed the expression of both markers in spheroids at all time-points analyzed. Of note, however, while *PROM1* mRNA levels were quite similar over time in culture, *CD44* levels decreased from D3 onwards. The difference, however, was only marginally significant when comparing the mRNA levels of D10 and D3.

The analysis of *MSI1* mRNA confirmed its expression in spheroids at each time-point, with significantly higher levels at D3 and D5 compared with those at D7 or D10 (**Figure 8**), whereas *OLFM4* mRNA was not detectable (not shown). Finally, *ALDH1a1* mRNA was expressed in spheroids at each time-point and showed an expression profile that declined at D10, the levels being only marginally significant compared to those at D3 (**Figure 8**). To validate the appropriateness of the new model to study cancer cell biology, the response to chemotherapy was analyzed in spheroids treated with FOLFOX or FOLFIRI, combination therapies routinely administered to CRC patients[22,23,24,25]. First, the efficacy of the treatments in inducing cell death was examined by incubating the spheroids with a fluorescent nucleic acid stain that specifically enters into dead cells[26]. Compared to the control NT condition, the treatment with each of the drugs induced significant cell death measured by the accumulation of fluorescence (**Figure 9A**). This observation was also confirmed at the morphological level using live microscopy, which showed that the treatments strongly affected the size and the appearance of the spheroids (**Figure 9B**). Finally, the expression of SC/CSC markers was analyzed by qRT-PCR in spheroids under the same conditions (**Figure 9C**). Intriguingly, a significant decrease in *PROM1* mRNA levels under both FOLFOX and FOLFIRI conditions was observed in comparison to the levels for the control, whereas *MSI1* levels were not affected by the treatments. Furthermore, whereas FOLFOX had no effect

on *ALDH1a1* mRNA expression compared to the control, treatment with FOLFIRI significantly increased its levels. *OLFM4* mRNA was not detected, and *CD44* mRNA levels were extremely low (data not shown).

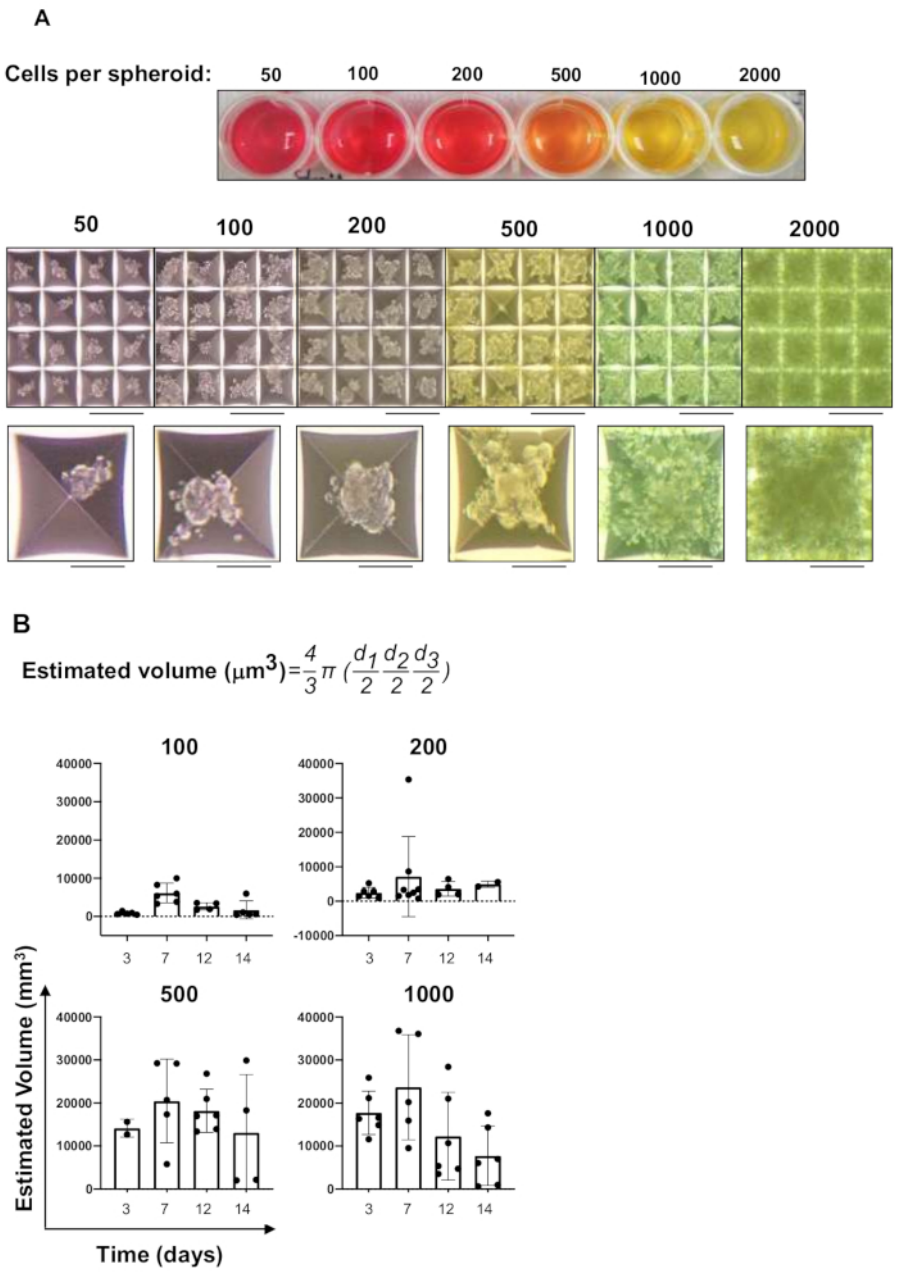

Figure 1: Setup of spheroid cultures. (**A**) Spheroid formation initiated from the indicated concentrations of Caco2 cells per spheroid/microwell. The top panel shows a representative image of a whole culture plate after two days of culture. The bottom panel shows images of selected microwells per condition. Images were taken at 4x magnification (microwell size: 400 µm). Scale bars: low magnification, 100 µm; high magnification, 30 µm. (**B**) Growth characteristics of the spheroids

generated from different number of cells per microwell and analyzed at different time-points. Note that the indicated days include the first two days of culture in the microwells and the subsequent culture of the harvested spheroids in agarose-coated plates. Histograms show mean ± standard deviation, n = 4–6. Black circles show the values for individual spheroids. The formula for the estimated volume is shown in the upper part of the panel, where d1, d2, and d3 indicate the three diameters measured for each spheroid. Please click here to view a larger version of this figure.

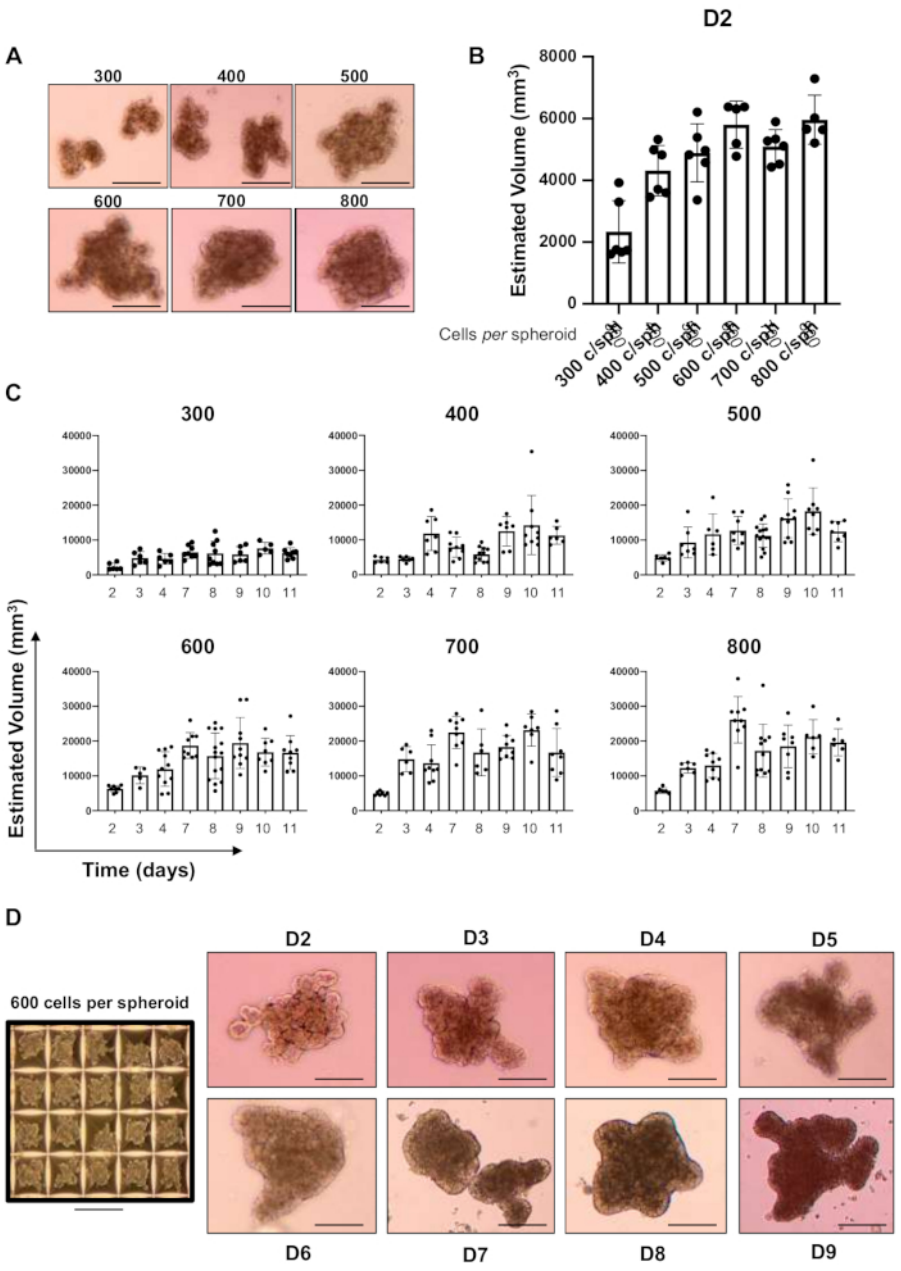

Figure 2: Optimization of the conditions for spheroid formation and culture. (**A**) Representative images of spheroids at D7 after their recovery from the microwells (2 days) and culture in agarose-coated dishes (5 days), using new well preparation and culture medium conditions. Scale bar: 30 µm. (**B**) Estimated volume of the freshly harvested spheroids two days after the start of cell culture in the microwells. Histograms show mean ± standard deviation (SD), n = 4–6. Black circles indicate the size of the individual spheroids. (**C**) Estimated volume of the spheroids in long-term culture based on the newly selected conditions. Graphs show the growth characteristics of the spheroids generated from different number of cells per spheroid and analyzed at different time-points after their harvesting, as indicated. Histograms show mean ± SD, n = 6–10.

Black circles indicate the size of the individual spheroids. (**D**) Representative images of the chosen 600 cells per spheroid condition over the experimental time-course (right panels) and within the microwells (left panel). Images were taken at 4x magnification. Scale bars: low magnification, 100 µm; high magnification, 30 µm. Please click here to view a larger version of this figure.

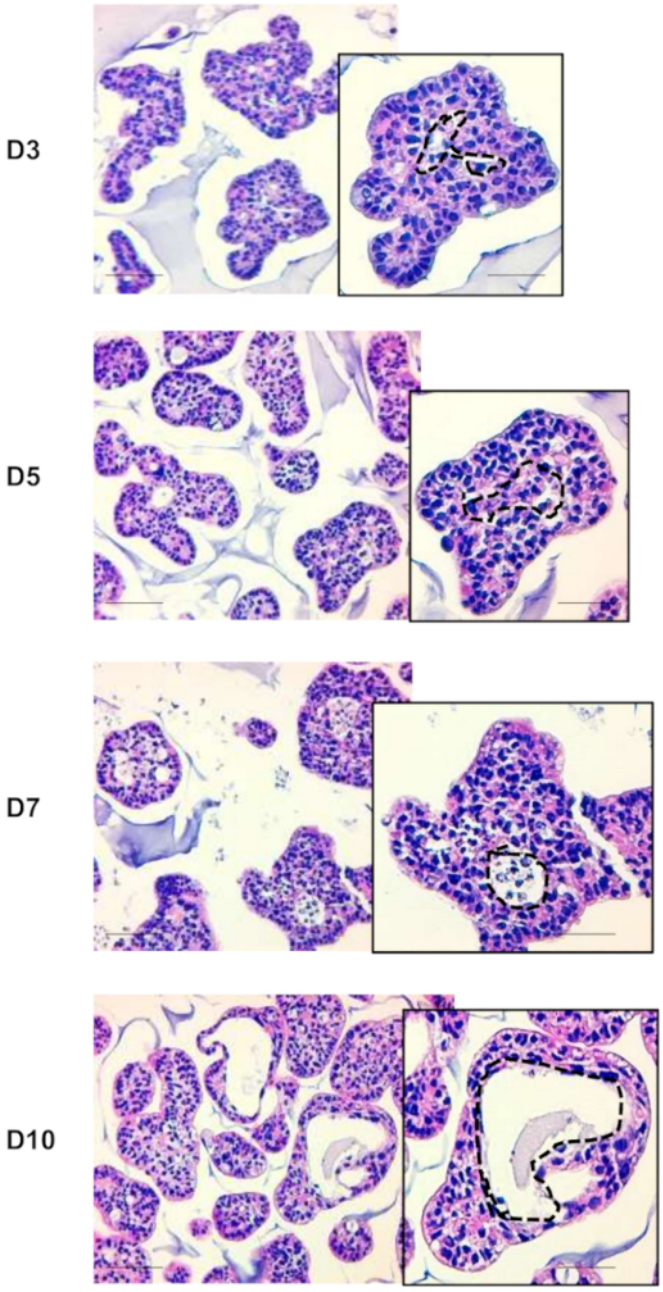

Figure 3: Histological characterization of the spheroids. Histological hematoxylin and eosin (H&E) staining of paraffin sections. Representative images of spheroids at the indicated time-points after harvesting, as indicated. Black dotted lines in each high magnification inset delimit the lumen within the spheroids. Scale bars: low magnification, 30 µm; high magnification, 10 µm. Please click here to view a larger version of this figure.

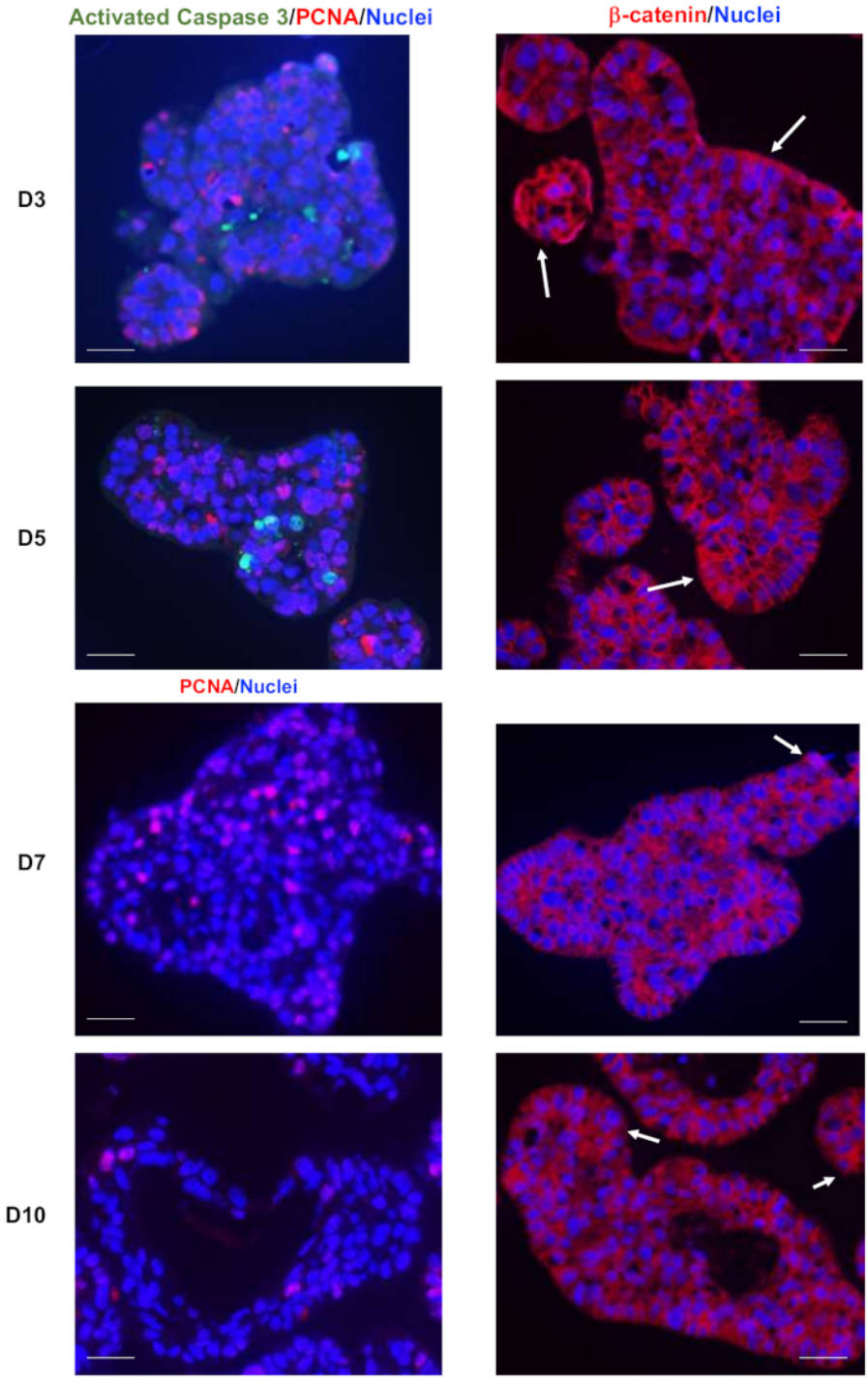

Figure 4: Caco2 spheroid characterization by immunolabeling. Immunostaining of spheroids for proliferation marker, proliferating cell nuclear antigen (PCNA, red), and cell death marker, activated caspase 3 (green) (left panels) and for β-catenin (red) (right panels) at the indicated times. Images show merged labeling of PCNA (red), activated caspase 3 (green), and nuclei (blue) or of β-catenin (red) and nuclei (blue). White arrows point to cells or groups of cells expressing high levels

of β-catenin. Images were taken with a 20x objective. Scale bar: 5 µm. Please click here to view a larger version of this figure.

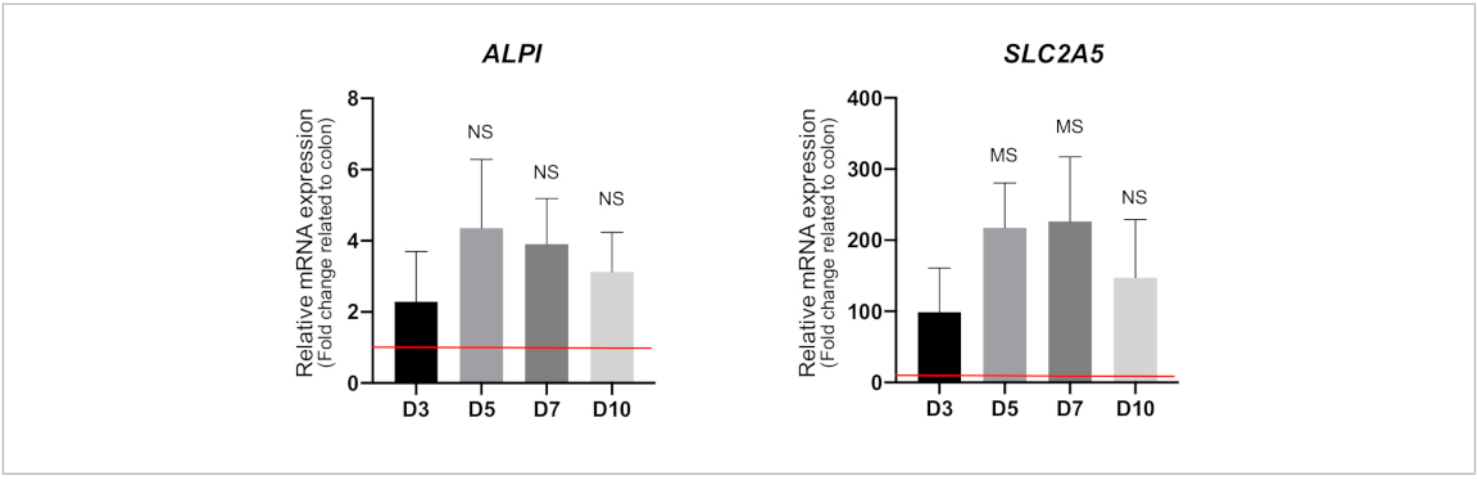

Figure 5: Analysis of enterocyte differentiation markers by qRT-PCR. Analysis of *ALPI* and *SLC2A5* encoding alkaline phosphatase and GLUT5 proteins, respectively. Histograms show mean ± standard deviation, n = 3, after normalization against *ACTB*. Data are represented as fold change relative to normal colon mucosa (red line = 1). NS: not significant; MS: marginally significant compared with D3 by unpaired Student's *t*-test. Abbreviations: qRT-PCR = quantitative reverse transcription-polymerase chain reaction; GLUT5 = glucose transporter 5; SLC2A5 = solute carrier family 2, transcript variant 2; ACTB = β-actin. Please click here to view a larger version of this figure.

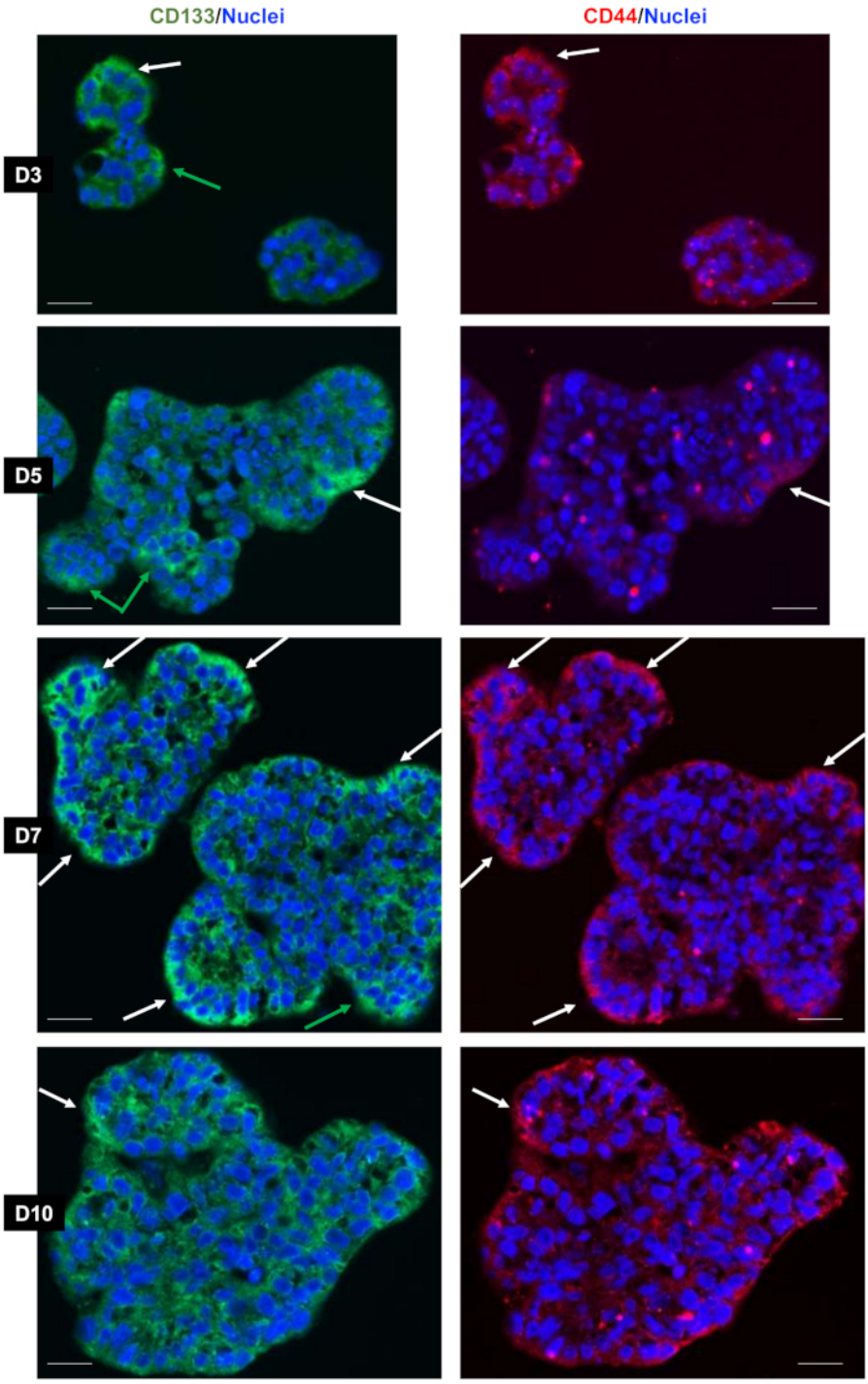

Figure 6: Heterogeneous expression of stem cell markers,CD44 and CD133, in the spheroids. Immunostaining for the stem cell markers, CD133 and CD44, at the indicated times. Images in the left panels show merged labeling of CD133 (green) and nuclei (blue); the same images in the right panels show merged labeling of CD44 (red) and nuclei (blue). Green arrows in the left panels point to CD133-expressing cells, and white arrows in both panels point to cells or groups of cells

expressing CD44 and CD133. Images were acquired with a 20x objective. Scale bar: 5 µm. Please click here to view a larger version of this figure.

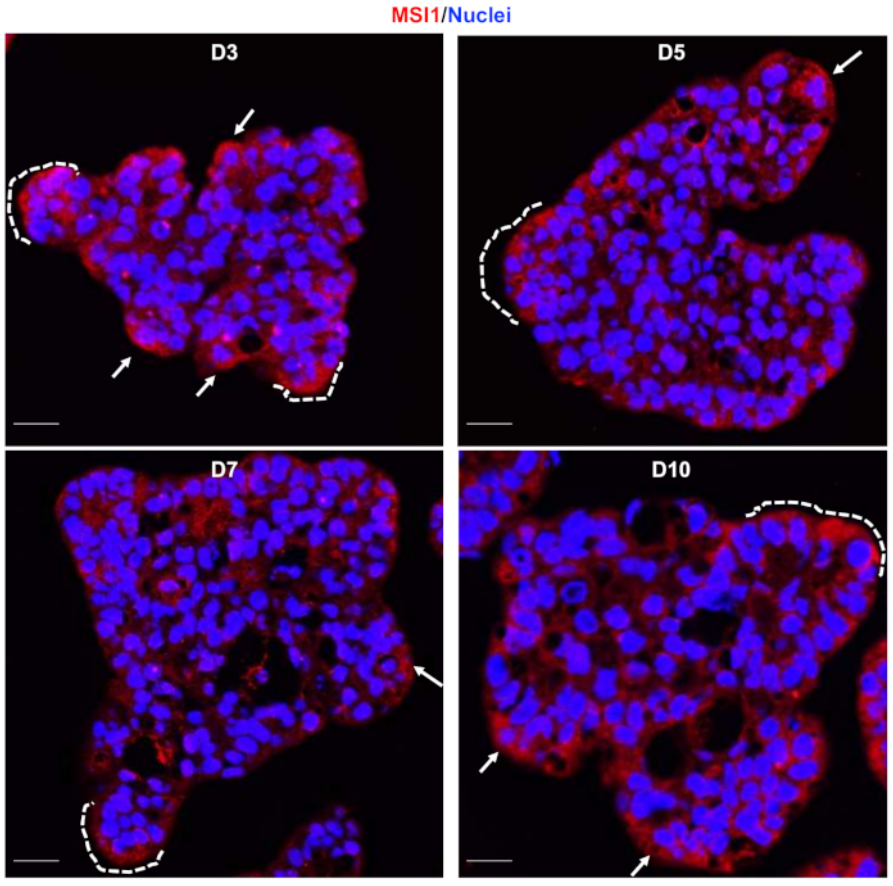

Figure 7: Heterogeneous expression of stem cell marker, MSI1, in the spheroids. Immunostaining for the stem cell marker MSI1 (red) at the indicated times. Images show merged labeling of MSI1 (red) and nuclei (blue). White dotted lines underline some crypt-like structures where cells are positive for MSI1 immunolabeling. Images were taken at 20x magnification. Scale bar: 5 µm. Abbreviation = MSI1 = Musashi 1. Please click here to view a larger version of this figure.

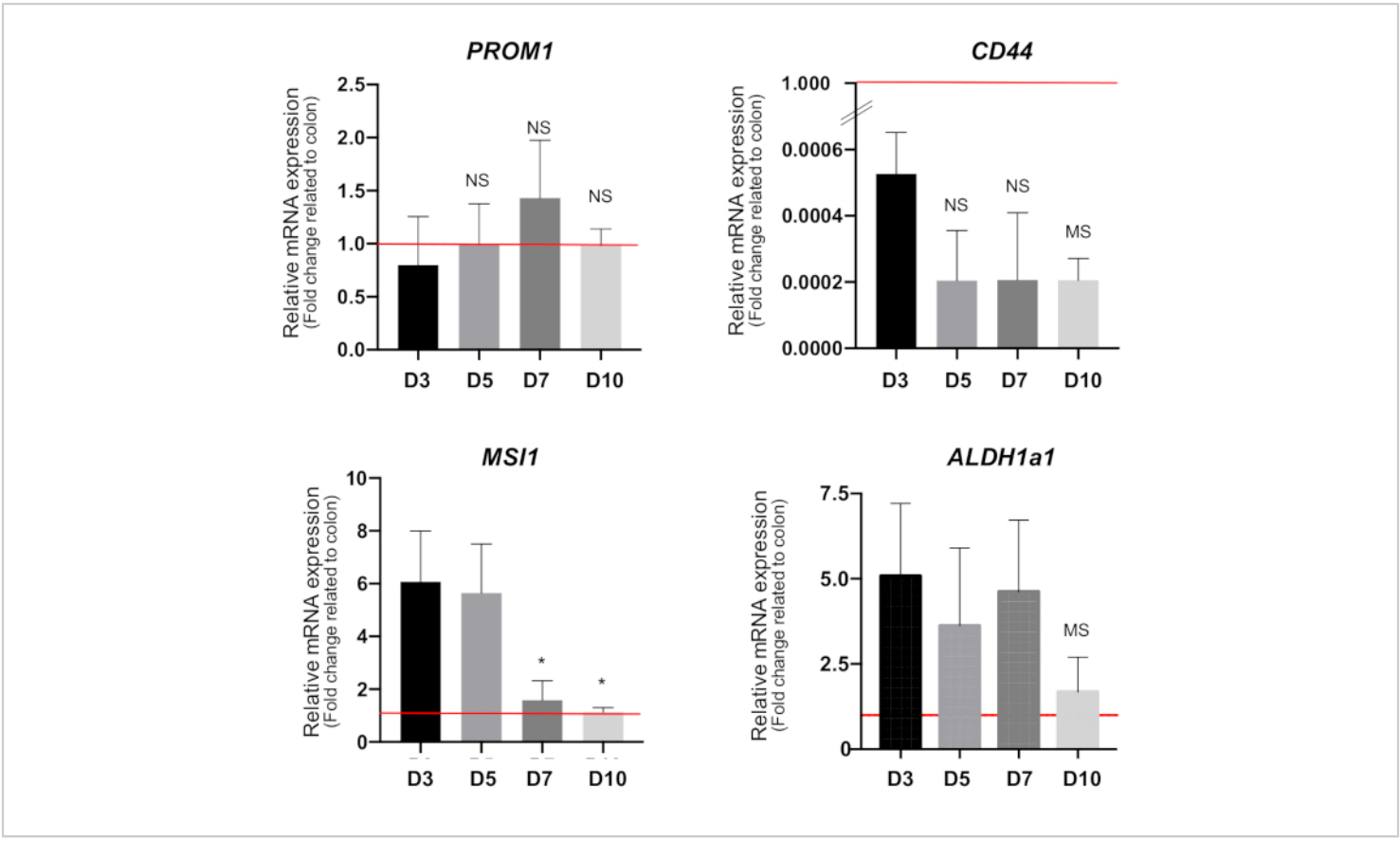

Figure 8: Analysis of stem cell markers by qRT-PCR. Quantification of *PROM1*, *CD44, MSI1,* and *ALDH1a1* levels was performed on mRNA from spheroids at the indicated times. Histograms show mean ± standard deviation, n = 3, after normalization against *ACTB*. Data are represented as fold change relative to normal colon mucosa (red line = 1). NS: not significant; MS: marginally significant compared with D3, using unpaired Student's *t*-test. *: P < 0.05 compared with D3 or D5, using unpaired Student's *t*-test. Abbreviations: qRT-PCR = quantitative reverse transcription-polymerase chain reaction; PROM1 = prominin-1; MSI1 = Musashi 1; ALDH1α1 = aldehyde dehydrogenase 1 alpha; ACTB = β-actin. Please click here to view a larger version of this figure.

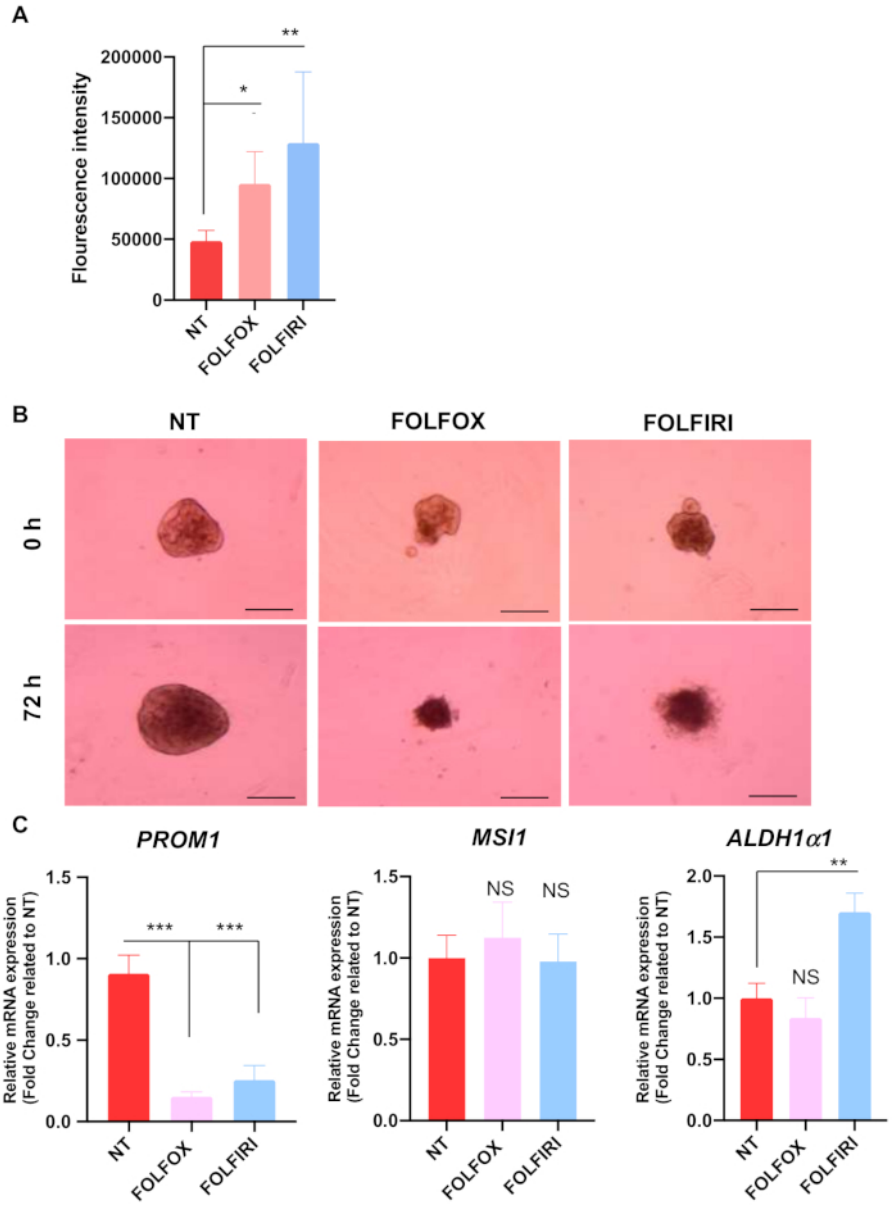

Figure 9: Effect of chemotherapy on spheroids. After harvesting from the microwells, spheroids were cultured in agarose-coated plates and treated for 3 days with FOLFOX or FOLFIRI or were maintained in (control) non-treated (NT) condition. (**A**) Analysis of fluorescence due to labeling of nucleic acid in dead cells. Histograms show mean ± standard deviation (SD), n = 4. (**B**) Morphological features of the spheroids maintained in the different culture conditions. Images were taken with a 4x objective. Scale bar: 400 µm. (**C**) Quantification of *PROM1*, *MSI1,* and *ALDH1a1* mRNAs by qRT-PCR. Histograms show mean ± SD, n = 4, after normalization against *ACTB*. *: NS: not significant; P < 0.05; **: P < 0.01; ***: P < 0.001 compared to the control (NT) condition, using unpaired Student's *t*-test. Abbreviations: FOLFOX = 5-Fluorouracil, 50 µg/mL; Oxaliplatin, 10 µg/mL; Leucovorin, 25 µg/mL ; FOLFIRI = 5-Fluorouracil, 50 µg/mL; Irinotecan, 100 µg/mL; Leucovorin, 25 µg/mL; qRT-

PCR = quantitative reverse transcription-polymerase chain reaction; PROM1 = prominin-1; MSI1 = Musashi 1; ALDH1α1 = aldehyde dehydrogenase 1 alpha; ACTB = β-actin. Please click here to view a larger version of this figure.

Desired number of cells per spheroid	Required number of cells per well
50	6×10^4
100	1.2×10^5
200	2.4×10^5
300	3.6×10^5
400	4.8×10^5
500	6×10^5
600	7.2×10^5
700	8.4×10^5
800	9.6×10^5
1000	1.2×10^6
2000	2.4×10^6

Table 1: Summary of spheroid formation and cell seeding.

	10 mm dishes	6-well plates	12-well plates	24-well plates	96-well plates
Coating Volume	4 mL	300 µL	250 µL	150 µL	50 µL (Down & Up)

Table 2: Volumes of agarose solution for coating of different plates/dishes.

	Genes	Primers	Sequence	Product Length
Differentiation markers	*ALPI*	Forward	CTG GTA CTC AGA TGC TGA CA	81
		Reverse	ATG TTG GAG ATG AGC TGA GT	
	SLC2A5	Forward	TAC CCA TAC TGG AAG GAT GA	94
		Reverse	AAC AGG ATC AGA GCA TGA AG	
Stem cell markers	*ALDH1a1*	Forward	GCC TTC ACA GGA TCA ACA GAG	147
		Reverse	TGC AAA TTC AAC AGC ATT GTC	
	MSI1	Forward	AGT TGG CAG ACT ACG CAG GA	131
		Reverse	TGG TCC ATG AAA GTG ACG AAG	
	PROM1	Forward	GTA AGA ACC CGG ATC AAA AGG	131
		Reverse	GCC TTG TCC TTG GTA GTG TTG	
	CD44	Forward	TGC CTT TGA TGG ACC AAT TAC	160
		Reverse	TGA AGT GCT GCT CCT TTC ACT	
	OLFM4	Forward	TCT GTG TCC CAG TTG TTT TCC	118
		Reverse	ATT CCA AGC GTT CCA CTC TGT	

Housekeeping genes	*ACTB*	Forward	CAC CAT TGG CAA TGA GCG GTT C	134
		Reverse	AGG TCT TTG CGG ATG TCC ACG T	
	PPIB	Forward	ATG ATC CAG GGC GGA GAC TT	100
		Reverse	GCC CGT AGT GCT TCA GTT TG	

Table 3: Primers used for quantitative reverse transcription-polymerase chain reaction.

Discussion

In vitro 3D models overcome the main experimental drawbacks of 2D cancer cell cultures, as they appear to be more reliable in recapitulating typical tumoral features including microenvironment and cell heterogeneity. Commonly used 3D models of spheroids are scaffold-free (cultured in low-attachment conditions) or scaffold-based (using biomaterials to culture cells). These methods present different disadvantages as they depend on the nature of the scaffold used or give rise to spheroids that are variable in structure and size.

The present protocol reports optimized conditions for producing homogeneous spheroids from the colon adenocarcinoma cell line, Caco2, by using a scaffold-free method. The spheroids are easily harvested and contrary to a previously reported study[41], they grow successfully and their growth characteristics during the time in culture can also be analyzed. Moreover, with this new method, the spheroids (a) actively proliferate, (b) present a very low rate of cell death, (c) organize to form a lumen inside the spheres, and (d) exhibit differentiation capacity of the component cells. Given that the final aim of the new approach was its use for studies on CSC biology, the expression of different markers of CSCs was analyzed. Interestingly, the markers presented a dynamic expression pattern depending on the time-point and defined different CSC populations.

Of utmost importance, the spheroids generated through this protocol could be used for analyzing drugs relevant for clinical applications such as the chemotherapeutic regimens, FOLFOX and FOLFIRI. The results also underline a heterogeneous response of cells to the drugs depending on the CSC marker analyzed. This observation is consistent with the current view that heterogeneous and multiple CSC-like cell populations within tumors display diverse chemosensitivity/chemoresistance properties[42,43]. This finding strongly potentiates the applicability of this new method for large scale screening. In addition to the applications reported in this study, the new protocol can also be used for a wider range of analyses (e.g., RNA and/or DNA extraction and large-scale analyses, western blotting, and immunofluorescence). Indeed, the volume of spheroids and growth characteristics can be easily determined by applying the sphere volume formula which, if necessary, also takes into consideration different diameters to counterbalance

deviations from a perfectly spherical form. However, specific parameters should be optimized depending on the cell type (cell line or fresh primary cultures) and growth capacity such as the replication time. Nevertheless, the protocol indicates critical steps that can be easily adjusted.

Some points of concern need to be considered when carrying out spheroid generation described in this article. First, several washing steps should be performed with the anti-adherence rinsing solution to promote the homogeneity and compaction of the spheres. In this case, two washes were necessary. Second, bubbles must be removed from the microwells as this can disturb the correct formation of the spheroids. Third, once the cells are seeded in each microwell after the centrifugation step, the plate must remain undisturbed for two days. Additional considerations and changes in the protocol are needed when studying the early steps of spheroid formation, possibly including an automated visualization and imaging system. Fourth, changing the medium without disturbing the spheroids, given that they are in suspension, can be challenging. Hence, it is recommended to change only half of the volume each time. Fifth, when harvesting the spheroids, it is important to preserve their structure. Hence, the use of serological pipettes or micropipettes with the tips cut off is recommended for all dispensing steps after rinsing in a serum-containing medium or PBS to prevent the spheroids from adhering to the tips.

Some limitations may also be encountered when using this protocol. First, not all cell lines or cell types have the same culture parameters; in some cases, cell heterogeneity and the number of passages/aging of cells may also affect the ability to form spheroids. Second, contrariwise to organoids, it may be difficult to maintain spheroids for a very long time in culture. In addition, they cannot be replicated by simple fragmentation through a micropipette tip[15]. Third, this protocol cannot be adapted for single-spheroid analysis because manually recovering spheroids one by one can be tricky. This technique is more suitable for obtaining high amounts of homogeneous spheroids at the same time. Finally, for studies investigating the effects of growth factors originating from other cell types or analyzing the importance of the microenvironment, it would be important to enrich the model and perform co-culture experiments.

In conclusion, the present methodology describes a new protocol to efficiently generate and culture spheroids from Caco2 cells. The results demonstrate that this method can be applied to the study of tumor heterogeneity and for the analysis of CSCs. This method can also be used for high-throughput drug screening and the study of stem cell biology in cancer and non-cancerous cells.

Disclosures

The authors have nothing to disclose

Acknowledgments

We acknowledge the imaging and Anipath recherche histology platforms (CRCL, CLB). We are indebted to the pharmacy of the Centre Léon Bérard (CLB) Hospital for the kind gift of FOLFOX and FOLFIRI. We also thank Brigitte Manship for critical reading of the manuscript. The work was supported by the FRM (Equipes FRM 2018, DEQ20181039598) and by the Inca (PLBIO19-289). MVG and LC received support from the FRM and CF received support from ARC foundation and the Centre Léon Bérard.

References

1. Bray, F. et al. Global cancer statistics 2018: GLOBOCAN estimates of incidence and mortality worldwide for 36

cancers in 185 countries. *CA: A Cancer Journal for Clinicians.* **68** (6), 394-424 (2018).

2. Fearon, E. R., Vogelstein, B. A genetic model for colorectal tumorigenesis. *Cell.* **61** (5), 759-767 (1990).
3. Rao, C. V, Yamada, H. Y. Genomic instability and colon carcinogenesis: from the perspective of genes. *Frontiers in Oncology.* **3**, 130 (2013).
4. Fearon, E. R. Molecular genetics of colorectal cancer. *Annual Review of Pathology.* **6** (1), 479-507 (2011).
5. Tran, T. Q. et al. α-Ketoglutarate attenuates Wnt signaling and drives differentiation in colorectal cancer. *Nature Cancer.* **1** (3), 345-358 (2020).
6. Batlle, E., Clevers, H. Cancer stem cells revisited. *Nature Medicine.* **23** (10), 1124-1134 (2017).
7. Clevers, H. The cancer stem cell: premises, promises and challenges. *Nature Medicine.* **17** (3), 313-319 (2011).
8. Barker, N. et al. Crypt stem cells as the cells-of-origin of intestinal cancer. *Nature.* **457** (7229), 608-611 (2009).
9. Dutta, D., Heo, I., Clevers, H. Disease modeling in stem cell-derived 3D organoid systems. *Trends in Molecular Medicine.* **23** (5), 393-410 (2017).
10. Bleijs, M., van de Wetering, M., Clevers, H., Drost, J. Xenograft and organoid model systems in cancer research. *The EMBO Journal.* **38** (15), e101654-e101654 (2019).
11. Kawai, S. et al. Three-dimensional culture models mimic colon cancer heterogeneity induced by different microenvironments. *Scientific Reports.* **10** (1), 3156 (2020).
12. Ferreira, L. P., Gaspar, V. M., Mano, J. F. Design of spherically structured 3D in vitro tumor models - Advances and prospects. *Acta Biomaterialia.* **75**, 11-34 (2018).
13. Friedrich, J., Seidel, C., Ebner, R., Kunz-Schughart, L. A. Spheroid-based drug screen: considerations and practical approach. *Nature Protocols.* **4** (3), 309-324 (2009).
14. Chaicharoenaudomrung, N., Kunhorm, P., Noisa, P. Three-dimensional cell culture systems as an in vitro platform for cancer and stem cell modeling. *World Journal of Stem Cells.* **11** (12), 1065-1083 (2019).
15. Sato, T. et al. Single Lgr5 stem cells build crypt-villus structures in vitro without a mesenchymal niche. *Nature.* **459** (7244), 262-265 (2009).
16. Weiswald, L.-B., Bellet, D., Dangles-Marie, V. Spherical cancer models in tumor biology. *Neoplasia.* **17** (1), 1-15 (2015).
17. Nath, S., Devi, G. R. Three-dimensional culture systems in cancer research: Focus on tumor spheroid model. *Pharmacology & Therapeutics.* **163**, 94-108 (2016).
18. Silva-Almeida, C., Ewart, M.-A., Wilde, C. 3D gastrointestinal models and organoids to study metabolism in human colon cancer. *Seminars in Cell & Developmental Biology.* **98**, 98-104 (2020).
19. Chantret, I., Barbat, A., Dussaulx, E., Brattain, M. G., Zweibaum, A. Epithelial polarity, villin expression, and enterocytic differentiation of cultured human colon carcinoma cells: A survey of twenty cell lines. *Cancer Research.* **48** (7), 1936-1942 (1988).
20. Caro, I. et al. Characterisation of a newly isolated Caco-2 clone (TC-7), as a model of transport processes and biotransformation of drugs. *International Journal of Pharmaceutics.* **116** (2), 147-158 (1995).

21. Antonchuk, J. Formation of embryoid bodies from human pluripotent stem cells using AggreWell^{TM} plates. *Methods in Molecular Biology.* **946**, 523-533 (2013).

22. Wolpin, B. M., Mayer, R. J. Systemic treatment of colorectal cancer. *Gastroenterology.* **134** (5), 1296-1310.e1 (2008).

23. Yaffee, P., Osipov, A., Tan, C., Tuli, R., Hendifar, A. Review of systemic therapies for locally advanced and metastatic rectal cancer. *Journal of Gastrointestinal Oncology.* **6** (2), 185-200 (2015).

24. Fujita, K., Kubota, Y., Ishida, H., Sasaki, Y. Irinotecan, a key chemotherapeutic drug for metastatic colorectal cancer. *World Journal of Gastroenterology.* **21** (43), 12234-12248 (2015).

25. Mohelnikova-Duchonova, B., Melichar, B., Soucek, P. FOLFOX/FOLFIRI pharmacogenetics: the call for a personalized approach in colorectal cancer therapy. *World Journal of Gastroenterology.* **20** (30), 10316-10330 (2014).

26. Jordan, N. J. et al. Impact of dual mTORC1/2 mTOR kinase inhibitor AZD8055 on acquired endocrine resistance in breast cancer in vitro. *Breast Cancer Research.* **16** (1), R12-R12 (2014).

27. Mohr, J. C. et al. The microwell control of embryoid body size in order to regulate cardiac differentiation of human embryonic stem cells. *Biomaterials.* **31** (7), 1885-1893 (2010).

28. Hughes, C. S., Postovit, L. M., Lajoie, G. A. Matrigel: A complex protein mixture required for optimal growth of cell culture. *Proteomics.* **10** (9), 1886-1890 (2010).

29. Luca, A. C. et al. Impact of the 3D microenvironment on phenotype, gene expression, and EGFR inhibition of colorectal cancer cell lines. *PLoS One.* **8** (3), e59689 (2013).

30. Petersen, O. W., Rønnov-Jessen, L., Howlett, A. R., Bissell, M. J. Interaction with basement membrane serves to rapidly distinguish growth and differentiation pattern of normal and malignant human breast epithelial cells. *Proceedings of the National Academy of Sciences of the United States of America.* **89** (19), 9064-9068 (1992).

31. Nusse, R., Clevers, H. Wnt/β-catenin signaling, disease, and emerging therapeutic modalities. *Cell.* **169** (6), 985-999 (2017).

32. Sambuy, Y., De Angelis, I., Ranaldi, G., Scarino, M. L., Stammati, A., Zucco, F. The Caco-2 cell line as a model of the intestinal barrier: influence of cell and culture-related factors on Caco-2 cell functional characteristics. *Cell Biology and Toxicology.* **21** (1), 1-26 (2005).

33. Vermeulen, L., Snippert, H. J. Stem cell dynamics in homeostasis and cancer of the intestine. *Nature Reviews Cancer.* **14** (7), 468-480 (2014).

34. van der Heijden, M., Vermeulen, L. Stem cells in homeostasis and cancer of the gut. *Molecular Cancer.* **18** (1), 66 (2019).

35. Barker, N., Bartfeld, S., Clevers, H. Tissue-resident adult stem cell populations of rapidly self-renewing organs. *Cell Stem Cell.* **7** (6), 656-670 (2010).

36. van der Flier, L. G., Haegebarth, A., Stange, D. E., van de Wetering, M., Clevers, H. OLFM4 is a robust marker for stem cells in human intestine and marks a subset of colorectal cancer cells. *Gastroenterology.* **137** (1), 15-17 (2009).

37. Potten, C. S. et al. Identification of a putative intestinal stem cell and early lineage marker; musashi-1. *Differentiation.* **71** (1), 28-41 (2003).

38. Clevers, H. The intestinal crypt, a prototype stem cell compartment. *Cell.* **154** (2), 274-284 (2013).

39. Clark, D. W., Palle, K. Aldehyde dehydrogenases in cancer stem cells: potential as therapeutic targets. *Annals of Translational Medicine.* **4** (24), 518 (2016).

40. Tomita, H., Tanaka, K., Tanaka, T., Hara, A. Aldehyde dehydrogenase 1A1 in stem cells and cancer. *Oncotarget.* **7** (10), 11018-11032 (2016).

41. Zoetemelk, M., Rausch, M., Colin, D. J., Dormond, O., Nowak-Sliwinska, P. Short-term 3D culture systems of various complexity for treatment optimization of colorectal carcinoma. *Scientific Reports.* **9** (1), 7103 (2019).

42. Garcia-Mayea, Y., Mir, C., Masson, F., Paciucci, R., LLeonart, M. E. Insights into new mechanisms and models of cancer stem cell multidrug resistance. *Seminars in Cancer Biology.* **60**, 166-180 (2020).

43. Marusyk, A., Janiszewska, M., Polyak, K. Intratumor heterogeneity: The Rosetta Stone of therapy resistance. *Cancer Cell.* **37** (4), 471-484 (2020).

Paper Nº 2

Article under revision in Molecular Oncology

Regulation of the THRA gene, encoding the thyroid hormone nuclear receptor TRα1, in intestinal lesions

Giolito Maria Virginia[1,2], La Rosa Théo[2,#], Diana Farhat[1,2], Serguei Bodoirat[1], Guardia Gabriela D. A.[3], Domon-Dell Claire[1], Galante Pedro A. F.[3], Freund Jean-Noel[1] and Plateroti Michelina[1,2]

1: Université de Strasbourg, Inserm, IRFAC/UMR-S1113, FMTS, 67200, Strasbourg, France. 2: Centre de Recherche en Cancérologie de Lyon, INSERM U1052, CNRS UMR5286, 69000 Lyon, France. 3: Centro de Oncologia Molecular, Hospital Sírio-Libanês, São Paulo, Brazil. #: current address, Stem-Cell and Brain Research Institute, U1208 INSERM, USC1361 INRA, 69675 Bron, France.

The *THRA* gene, encoding the thyroid hormone nuclear receptor TRα1, is expressed in an increasing gradient at the bottom of the intestinal crypts, overlapping with high Wnt and Notch activities. We know from previous data in the laboratory that the *THRA* gene is upregulated in CRC, particularly in the high-Wnt molecular subtype. However, the basis of this specific and altered expression pattern remained unknown. So then, the first aim of this thesis was to analyse the mechanism that controls *THRA* gene expression in colon cancer. To define the mechanisms controlling *THRA* transcription and TRα1 expression, we used multiple *in vitro,* and *ex vivo* approaches. In accordance with our previous studies, we observed an increased but heterogeneous expression of TRα1 in human colon tumours compared to the normal parts by immunohistochemistry. Moreover, by *THRA* promoter analysis, we demonstrated the presence of binding sites for transcription factors involved in intestinal homeostasis and SC/CSC biology that are also altered in CRC, such as TCF7L2 (Wnt pathway), RBPJ (Notch pathway) and CDX2 (intestinal epithelial cell identity). Specifically, TCF7L2 and CDX2 stimulated *THRA*, RBPJ induced its repression. In previous work, we described complex cross-talk between TRα1 and the Wnt pathway, but whether Wnt could affect THRA/Thra expression was not analysed. So, during this thesis, we focused on analysing more in-depth this cross-talk between Wnt and *THRA*. We showed in cell lines that activating Wnt in all cases and by all approaches resulted in increased *THRA* promoter activity. Additionally, we showed that mutating the putative binding sites for TCF7L2 blunted *THRA* promoter activity, and we validated by chromatin immunoprecipitation that there is a direct β-catenin binding of the promoter regions containing the TCF7L2 binding sites, which strongly supports a direct transcriptional regulation. Importantly, using a physiological model or mouse enteroids where we induced the Wnt stimulation by *Apc* gene mutation increased the expression of TRα1. Altogether, our old and new results suggest a complex regulatory loop and synergy between these endocrine and epithelial-cell-intrinsic signals. Indeed, high Wnt activity and the action of other transcription factors, maintains a basal level of TRα1 expression in normal intestinal crypts, where TRα1 integrates and interacts with different key

pathways, such as Wnt and Notch, as well as CDX2 to participate in intestinal homeostasis. Upon Wnt over-activation in the early stages of tumour development, TRα1 expression increases, which causes a further increase in Wnt activity responsible for crypt hyperplasia and hyperproliferation, observed in CRC. For the first time, our work describes the regulation of the *THRA* gene in specific cell and tumour contexts.

Regulation of the THRA gene, encoding the thyroid hormone nuclear receptor TRα1, in intestinal lesions

Giolito Maria Virginia[1,2], La Rosa Théo[2,#], Farhat Diana[1,2], Bodoirat Serguei[1], Guardia Gabriela D. A.[3], Domon-Dell Claire[1], Galante Pedro A. F.[3], Freund Jean-Noel[1] and Plateroti Michelina[1,2]

1: Université de Strasbourg, Inserm, IRFAC/UMR-S1113, FMTS, 67200, Strasbourg, France. 2: Centre de Recherche en Cancérologie de Lyon, INSERM U1052, CNRS UMR5286, 69000 Lyon, France. 3: Centro de Oncologia Molecular, Hospital Sírio-Libanês, São Paulo, Brazil.
#: current address, Stem-Cell and Brain Research Institute, U1208 INSERM, USC1361 INRA, 69675 Bron, France.

Corresponding author
Mailing address: INSERM U1113, 3 avenue Molière, 67200 Strasbourg – France
Tel: 33 3 88 27 53 56
E-mail: plateroti@unistra.fr

Running title: THRA gene in the intestine

Keywords: Colon cancer; Intestinal organoids; THRA; Thyroid hormone nuclear receptor; TRα1

Abbreviations:
CMS; Consensus Molecular Subtype
CRC; Colorectal Cancer
KO Knock-out
RLU; Relative Luciferase Units
RT; Retro transcription
RTqPCR; Retro transcription quantitative Polymerase Chain Reaction
TH; Thyroid Hormone
TMA; Tissue Microarray Analysis
TR; Thyroid Hormone Receptor

Abstract

The *THRA* gene, encoding the thyroid hormone nuclear receptor TRα1, is expressed in an increasing gradient at the bottom of intestinal crypts, overlapping with high Wnt and Notch activities. Importantly, *THRA* is upregulated in colorectal cancers, particularly in high-Wnt molecular subtype. The basis of this specific and/or altered expression pattern remained unknown.
To define the mechanisms controlling *THRA* transcription and TRα1 expression, we used multiple *in vitro* and *ex vivo* approaches. Promoter analysis demonstrated that transcription factors important for crypt homeostasis and altered in colorectal cancers, such as TCF7L2 (Wnt pathway), RBPJ (Notch pathway) and CDX2 (epithelial cell identity), modulate *THRA* activity. Specifically, while TCF7L2 and CDX2 stimulated *THRA*, RBPJ induced its repression. In-depth analysis of Wnt-dependent increase showed direct regulation of *THRA* promoter in cells and of TRα1 expression in murine enteroids. Given our previous results on the control of Wnt pathway by TRα1, our new results unveil a complex regulatory loop and synergy between these endocrine and epithelial-cell-intrinsic signals. Our work describes, for the first time, the regulation of the *THRA* gene in specific cell and tumor contexts.

Introduction

The thyroid hormone (TH) nuclear receptor TRs are T3-modulated transcription factors belonging to the nuclear hormone receptor protein superfamily [1]. THs and TRs are involved in multiple processes in organism development, physiology, and, eventually, pathological events [2–5]. From a molecular point of view, they modulate the expression of target genes by binding to thyroid hormone response elements (TREs) present in regulatory regions of target genes. Upon T3 binding, TRs undergo conformational modification, resulting in activation or repression of the transcriptional machinery [2].

One well-defined organ target of THs and the receptor TRα1 is the intestine. Indeed, the involvement of TRα1-dependent signaling and/or TH status has been reported in the normal intestine [6–9] and in intestinal tumor biology [6,7,10–12]. Studies in *Thra*- and *Thrb*-knockout animals showed that TRα1 is responsible for TH signaling in intestinal crypts, where it controls the biology of stem cells (SCs) and their fate [13], as well as the balance between cell proliferation and cell differentiation through its actions on the Wnt and Notch pathways (rev in [6,7,10] In accordance with this important role, overexpression of TRα1 in the intestinal epithelium (*vil*-TRα1 mice) in a mutated-Apc background (*vil*-TRα1/Apc$^{+/1638N}$ mice) is responsible for the acceleration of tumor appearance, progression, and aggressiveness compared with Apc-only mutants [14]. Conversely, *Thra* gene loss in the same mutated-Apc background diminishes and slows tumor appearance [15]. Interestingly, the relevance of these observations has been demonstrated in clinics, given that the *THRA* gene and the TRα1 isoform are frequently overexpressed in human colorectal carcinoma (CRC) patients [15].

CRC is the third leading cause of cancer death in the world [16]. CRC development is a multistep process triggered by the accumulation of mutations in oncogenes and tumor suppressors, which, in turn, are responsible for tumor initiation and progression [17]. Crypt hyperplasia, hypertrophy, and stem cell (SC) transformation represent very early events in intestinal tumor development [18–20] and depend on alterations of genes in the Wnt and Notch pathways [21,22]. It is worth noting that these cellular and molecular processes are also affected by TRα1, which synergizes with the Wnt pathway to accelerate neoplastic events [14,15]. Moreover, the expression of the *THRA* gene is upregulated in CRC consensus molecular subtypes (CMS) compared to the normal colon, with significantly higher overexpression in CMS2 [15], which is characterized by high Wnt and Myc signaling activation [23]. However, no information is available on the molecular mechanisms involved in *THRA* regulation in the context of CRC.

Interestingly, the *THRA* gene was characterized in the early 1990s as the cellular homolog of the avian retroviral erytroblastoma virus *v-erbA*, which is involved in neoplastic transformation leading to acute erythroleukemia and sarcomas [24,25], thus suggesting its link with malignancies. However, very few studies have analyzed the genomic organization and transcriptional control of the *THRA* gene [26,27]. Ishida and colleagues [28] observed that the 615-bp 5'-flanking sequence of the *THRA* promoter presented putative binding sites for several transcription factors, including SP1, cAMP-responsive elements (CRE), CREB, AP1, Krow-20, COUP-TF/EAR-3, and retinoid X receptor (RXR) [28]. Another study described the regulation of the *THRA* gene promoter by the orphan nuclear

receptor ERRα [29]. However, these reports did not consider cell type-specific control under physiological or pathological conditions.

In the current study, we investigated the mechanisms underlying *THRA* transcriptional regulation, including the modulation of the TRα1 receptor. *In silico* and molecular approaches identified promoter regions and transcription factors important for *THRA* activity. We demonstrated the presence of binding sites for transcription factors involved in intestinal homeostasis and SC/cancer SC biology that are also altered in CRC [30–32], such as TCF7L2 (Wnt pathway) [33], RBPJ (Notch pathway) [34] and CDX2 (intestinal epithelial cell identity) [35]. Finally, in-depth analysis of the Wnt pathway allowed us to recapitulate the regulation of *THRA* transcription and TRα1 expression by this signaling pathway in human adenocarcinoma cell lines as well as mouse enteroids. This study presents the first extended analysis of *THRA* regulation and its relevance in a patho-physiological context. In addition, it describes, for the first time, the existence of a reciprocal regulatory loop between TRα1-dependent and Wnt-dependent signals in intestinal epithelial cells.

Materials and Methods

Tissue Microarray Analysis (TMA)

TRα1 expression has been analyzed by immunohistochemistry on Tissue Focus Colon Cancer Tissue MicroArray, FFPE, 42x1 mm cores (CT565864, CliniScences). The TMA was composed of 33 tumors at different stages and 9 normal tissues. The study and the score of the labeling were conducted by the Research Pathology Platform (Lyon, France). Briefly, after deparaffinization and dehydration, tissue sections were heated for 50 minutes at 97 °C in 10 mM citrate buffer, pH 6.0. To block endogenous peroxidases, tissue sections were incubated in 5% hydrogen peroxide solution. IHC was performed on an automated immunostainer (Ventana Discovery XT; Roche) using an Omnimap DAB Kit according to the manufacturer's instructions. Sections were incubated with the anti-TRα1 antibody (ab53729, dilution 1:50). The secondary anti-rabbit-HRP antibody was applied to the sections, and staining was visualized with DAB solution with 3,3′-diaminobenzidine as a chromogenic substrate. Finally, the sections were counterstained with Gill's hematoxylin and then scanned with a Panoramic Scan II (3D Histech, Budapest, Hungary) at 20X. The scoring of TRα1 levels (-, negative; +/-, low; + positive; ++, highly positive) was performed independently by two persons.

Bioinformatics analyses of the TGCA CRC Cohort

To analyze the expression levels of THRA in the TCGA cohort, RNA sequencing data from 270 colon adenocarcinoma (COAD) and 41 adjacent normal samples were obtained from the TCGA data portal (https://portal.gdc.cancer.gov/). To obtain Transcripts Per Million (TPM) normalized expression levels of the *THRA* canonical transcript, we used Kallisto [36] with GENCODE (https://www.gencodegenes.org; v29) as reference to the human transcriptome. TCGA samples were also classified according to consensus molecular subtypes (CMSs) [23] using the R package CMS classifier (v1.0.0). Boxplots were created using the R packages ggplot2 (v3.3.2) and ggpubr (v0.4.0), and comparisons between groups were assessed by Wilcoxon tests.

In silico THRA promoter analysis

Analysis of approximately 3500 bp of the *THRA* promoter region upstream the transcription start site (TSS) was performed by the MathInspector library (Genomatix), using Matrix Family Library Version 11.0. Filters were applied to select core matrix similarity > 0.85 (85% of conserved homology) by using the module General Core Promoter Elements (Optimized).

Construction of the *THRA*-luciferase vectors

3238-bp upstream of the transcription starting site of the *THRA* gene were cloned into the pGL3 basic vector (Promega) to construct the pGL3-*THRA*-Luc vector (named pGL3-*THRA*) using MluI (5') and XhoI (3') sites (Figure S1A). A CT>GC mutation was introduced at positions 816 and 2270 of the pGL3-*THRA*-luc vector to mutate the TCF7L2-binding sites and generate the *THRA*-mut-Luc1 and *THRA*-mut-Luc2 vectors (named pGL3-*THRA*-mut-TCF7L2-1 and pGL3-*THRA*-mut-TCF7L2-2, respectively) (Figure S1B, C). For the generation of the double mutant vector (named pGL3-*THRA*-mut-TCF7L2-sites, Figure S1D), both mutant plasmids were digested with AvrII and StuI enzymes (New England Biolabs). The

fragment containing the mutant TCF7L2-1 site was ligated into the vector containing the mutant TCF7L2-2 site, using the DNA quick ligase (M2200L, New England Biolabs). The ligated mix was used to transform competent bacteria and the colonies were recovered for DNA plasmid preparation and sequencing. Gene synthesis, site-directed mutagenesis and sequencing were performed by Eurofins Genomics, Germany.

Cell lines and transfection experiments

The human adenocarcinoma cell lines Caco2, HCT116, and SW480 (from ATCC) were cultured in DMEM Glutamax (4,5 g/l D-Glucose with pyruvate) medium (Gibco) supplemented with 10% heat-inactivated fetal bovine serum (FBS) and 1% penicillin/streptomycin (P/S) (Gibco) at 37 °C in a humidified atmosphere containing 5% CO_2.

For luciferase assays, we seeded each cell line onto 24-well plates (75,000 cells/well) in DMEM supplemented with 10% FBS and 1% P/S. The next day, we transfected the plasmids using PEI Prime™ linear polyethylenimine (Sigma–Aldrich 919012) at a ratio of 1 µg DNA/1.5 µl of PEI at 1 mg/ml. Transfection was performed for 6 h in culture medium without serum. Luciferase activity was measured 48 h after transfection using the Dual-Luciferase Reporter Assay System (Promega). Data represent the normalized beetle-luciferase/renilla-luciferase activities measured in each well to correct for eventual differences in transfection efficiency from well to well. Experiments were performed at least two times with n=6 for each condition.

Luciferase reporter vectors: *THRA*-Luc (200 ng/well), *THRA-mut1-Luc, THRA-mut2-luc and THRA-dmut-luc* (200 ng/well), TopFlash (200 ng/well, Upstate), *RBPJ*-Luc (200 ng/well, [37]), *hLI*-Luc (200 ng/well), pGL3-basic (200 ng/well) and pRL-CMV (10 ng/well, Promega) were used. The generation of *hLI*-Luc was based on a previous publication [38] and consisted of cloning approximately 1 kb of the human LI-cadherin gene promoter into the pGL3 basic vector using Sac1 (5') and HindIII (3') restriction sites.

Expression vectors: β-catenin ΔN (100 ng/well, gift from Pr M. Waterman), TCF1E-EVR2 (100 ng/well) [39], TCF1E-EVR2-DN (300 ng/well) [39], CDX2 (100 ng/well) [40], and NICD (100 ng/well) [37] were used. The amounts of DNA under each condition were normalized by adding the empty pBSK vector. The experiments dealing with Wnt blocking and re-stimulation were performed by transfecting the TCF1-DN vector (dominant negative; 300 ng/well) in the absence or presence of increasing amounts of β-catenin ΔN expression vector (from 50 to 500 ng/well).

siRNA approach: For CDX2 expression modulation by the siRNA approach, we seeded each cell line into 24-well plates (75,000 cells/well) in DMEM supplemented with 10% FBS and 1% P/S. The next day, we removed the medium and added siRNA CDX2 (Silencer® Select siRNA@CDX2 s2876, ThermoFischer) or the siRNA control (Silencer™ Select Negative Control No. 2 siRNA, ThermoFischer #4390846) at a final concentration of 10 nM in a mix containing OPTIMEM medium (Gibco) and lipofectamine RNAiMAX (Invitrogen) for 24 h. In CDX2-KD and control cells, we performed *THRA*-luc transfection assays as indicated above.

Treatments with small molecules: For modulation of the Wnt pathway, we used an approach consisting of treatment with small molecules. Transfected cells, as described above were treated with each molecule 24 h before the end of

transfection. We used the Wnt agonists CHIR99021, 3 µM (Sigma–Aldrich) [41] and the Wnt antagonist IWP4, 5 µM (Tocris) [42]; the Notch agonist Yhhu3792, 2.5 µM (Tocris) [43]; and the Notch antagonists LY411575, 1 µM (Sigma) [44], and DAPT, 10 µM (Tocris) [45]. The effect of the Wnt agonist and antagonist was analyzed on the endogenous TRα1 expression, by treating the cells during 48 h before harvesting.

Chromatin immunoprecipitation (ChIP) and qPCR analysis

For ChIP experiments each cell line was seeded in 6 cm dishes and cells recovered after 2 days of culture. Chromatin crosslink was performed with 1% (vol/vol) formaldehyde for 10 min at room temperature and quenched with 0.125 mol/L glycine for 5 min. ChIP experiments were carried out using the EZ-Magna ChIP G Chromatin Immunoprecipitation kit (Millipore #17-409) as recommended by the supplier. Sonicated chromatin (BioruptorPlus, Diagenod apparatus; 12 cycles of 30s ON/30s OFF on high mode) from $2x10^6$ cells was incubated overnight at 4°C with 4 µg of mouse anti-β-catenin antibody (clone 14, BD Transduction lab) or with immunoglobulin G (IgG) (Upstate Cell Signaling). DNA was quantified by qPCR using SYBR qPCR Premix Ex Taq II (Tli RNaseH Plus, Takara) in a CFX Connect apparatus (Bio–Rad). Primers used for AXIN2, MYC, THRA-1, THRA-2, PPIB and HPRT are listed in Table S1. Antibodies are listed in Table S2. Histograms represent the fold enrichment, normalized to the input, of specific β-catenin DNA binding compared with the IgG condition (=1).

Western Blot

Protein samples from each cell lines (30 µg per lane) were prepared with RIPA buffer as described in [15], separated by SDS-PAGE, and transferred to PVDF membranes 0.2 µm (Bio-Rad). Membranes were blocked with PBS-Tween supplemented with 5% non-fat milk before incubation with primary antibodies. This step was followed by incubation with HRP-conjugated secondary antibodies (Promega). The signal was analyzed using an enzymatic Clarity substrate detection kit and Clarity max ECL (Bio-Rad) and image detection was performed using a Pixie imaging system (Gene-sys), according to manufacturer's protocol. All images were processed using imageJ. Antibodies are listed in Table S2.

Animals, isolation of small intestinal crypts and enteroid cultures

Adult 2- to 4-month-old $Apc^{+/fl}$/Villin-Cre^{ERT2} and $Apc^{+/fl}$ mice [46,47] were maintained in a C57BL/6J genetic background and housed in the same animal facility, where they received standard mouse chow and water *ad libitum*. All experiments were performed in compliance with the French and European guidelines for experimental animal studies and approved by the local committees "Comités d'Éthique Ceccapp" (C2EA55)" the Ministère de l'Enseignement Supérieur et de la Recherche, Direction Générale pour la Recherche et l'Innovation, Secrétariat "Autorisation de projet" (agreement # 13313-2017020210367606).

After sacrifice, we collected the small intestine (from the proximal jejunum to the distal ileum) for crypt preparation and enteroid cultures, using the protocol previously described [13]. Organoids were cultured at 37 °C and 5% CO_2 in IntestiCult Organoid Growth Medium (Stem Cell Technologies). The medium was changed every 3 days, and organoids were replicated approximately 7 days after the beginning of the culture. For all experiments (three independent experiments

from three independent mice), we used organoids after the first replication (R1). Briefly, Matrigel-embedded organoids were grossly dissociated with a micropipette, fragments were washed in PBS and recovered by centrifugation. They were mixed with Intesticult/Matrigel mix (1:1 volume), plated in 50 µL drops, and covered with 900 µL of culture medium in 12-well plates. 24 h after replication, organoids were treated with 4-OH-tamoxifen (0.2 mg/ml, Sigma–Aldrich H6278) or DMSO (control) for 24 h and monitored for several days after treatment. The cultures were recovered on day 5 for genomic DNA (gDNA) and RNA extraction. Pictures were taken over the days of culture using a Zeiss AxioVert inverted microscope with a 10X objective.

Genomic DNA extraction and PCR analysis

We extracted gDNA from $Apc^{+/fl/}$Villin-Cre^{ERT2} and $Apc^{+/fl}$ enteroids at D5 using the Nucleospin Genomic DNA from Tissue kit (Machery Nagel). The presence of the *Apc* mutated allele was detected by PCR using specific primers listed in Table S1.

RNA extraction and RTqPCR

We extracted total RNA using the Nucleospin RNA Kit (Macherey-Nagel). We performed DNase digestion on all samples to remove contaminating gDNA and reverse transcription (RT) of total RNA with iScript reverse transcriptase (Bio–Rad), according to the manufacturer's instructions. We conducted PCR on all preparations to amplify a housekeeping gene (*Hprt/HPRT*) for which the primers are located on different exons of the corresponding gene to further exclude gDNA contamination after RT. For qPCR approaches, we used SYBR qPCR Premix Ex Taq II (Tli RNaseH Plus, Takara) in a CFX Connect apparatus (Bio–Rad). In each sample, specific mRNA expression was quantified using the $\Delta\Delta$Ct method, and values were normalized against *Ppib/PPIB* levels. The primers used are listed in Table S1.

Statistical Analysis

Statistical analyses were conducted using GraphPad Prism software (version 8; GraphPad Software Inc., San Diego, Calif., USA), and the level of significance was established as p-value < 0.05.

Results

Expression of *THRA* in human colorectal cancer

Our previous studies showed increased expression of the TRα1 protein in CRC from patients compared with the normal colon [15]. Here, we enlarged this study and used an approach of immunohistochemistry on a tissue microarray (TMA) to analyze TRα1 expression in a CRC cohort of patients with different tumor stages (Figure 1, Figure S2, Table S3; Table S3 summarizes all known characteristics of the samples). TRα1 labelling intensity has been scored in each sample, including the tumor or normal part as well as the stromal cells and the immune infiltrate (Figure 1B, Table S3). Compared with the normal colon, TRα1 immunolabeling was clearly stronger in almost all tumors and at all tumor stages. Even if there wasn't a clear difference depending on the tumor stages, we noticed that stage II and stage III tumor samples presented frequently TRα1-positive immune infiltrated cells (Figure 1, Table S3), determined by morphological characteristics [48,49]. It is worth emphasizing, however, that evident intratumor heterogeneity was observed, with some cells or tumoral parts strongly labeled and some cells or tumoral zones more lightly labeled or negative. In addition, high-magnification images enabled us to distinguish stromal cells expressing different levels of TRα1 and TRα1-negative cells. In stage IV CRC, we could identify tumors displaying variable levels of TRα1 (*i.e.*, in comparing the two images of stage IV), clearly indicating inter-tumor heterogeneity of TRα1 expression. The expression of the *THRA* gene has also been determined in human TCGA colon adenocarcinoma cohort (Figure S3). Despite the absence of difference when globally comparing CRCs and normal tissues, probably because of the high heterogeneity (Figure S3A), we confirmed increased *THRA* expression in the CMS2 high-Wnt molecular subtype [23] (Figure S3B), as previously described on another cohort [15].
Altogether, these results reinforce our previous data showing that TRα1 is upregulated in human CRC and is correlated with Wnt pathway activity.

THRA promoter analysis

Because of the upregulation of *THRA* in the CRC cohorts and the specific expression of TRα1 in intestinal crypt cells [14], we wanted to determine the molecular basis of its expression regulation. *In silico* analysis of 3238 bp of the *THRA* promoter region showed the presence of several putative binding sites for transcription factors, such as TCF7L2, RBPJ, and CDX2, that are fundamental to intestinal physiology and are altered in CRC [50] (Figure 2). Of note, other studies had also shown β-catenin binding sites in the boundaries of the *THRA* gene [51]. The *THRA* promoter region was cloned into a luciferase reporter vector (*THRA*-luc, Figure S1A), and its activity was analyzed in transient transfection experiments. We implemented two steps to take into account the genetic heterogeneity of CRC and avoid bias in the experiments. First, we performed the study using three different human colon adenocarcinoma cell lines —Caco2, SW480, and HCT116— displaying different mutations of genes or pathways that are more frequently altered in CRC [52–55] (Figure S4A). Second, all cell lines were maintained in culture medium supplemented with the same concentration of serum, ensuring comparable amounts of growth factors that could potentially influence subsequent analyses [56]. We also verified the expression of TRα1 by

RTqPCR and noticed that SW480 presented significantly higher mRNA levels compared with Caco2 and HCT116 cells.
When we started the promoter analysis, we observed *THRA*-dependent luciferase basal activity in every cell line, compared with the pGL3-basic vector (Figure S5A). In addition, upon cotransfected with the Wnt transcriptional regulators β-catenin/TCF1, regardless of the mutational background of the cells, the activity of the *THRA* promoter was significantly increased (Figure 3A-C, left panels). The results on the Notch pathway relative to the *THRA* promoter were more complex, as cotransfection of the Notch intracellular domain (NICD) decreased the luciferase activity in Caco2 and HCT116 cells but had no effect on SW480 cells (Figure 3 A-C, middle panels). When we analyzed the effect of CDX2 on *THRA*, we observed positive regulation of luciferase activity in all cell lines (Figure 3 A-C, right panels). The TopFlash, *RBPJ*-luc and *hLI*-luc vectors were used, respectively, as the positive controls for Wnt, Notch and CDX2 activities. Finally, no effect of the transcription factors could be detected when using the pGL3-basic vector (Figure S5 B).
Taken together, these data show that *THRA* promoter activity is positively regulated by the Wnt/β-catenin pathway and CDX2 in human colorectal adenocarcinoma cell lines. The Notch pathway plays a more complex role and behaves as a negative regulator or has no effect on *THRA* promoter.

Analysis of *THRA* promoter upon modulation of CDX2 expression and signaling pathway activity

To further link *THRA* promoter activity with Wnt, Notch, and CDX2, we used approaches involving modulation by siRNA (CDX2) or small molecules (Wnt and Notch). In the case of CDX2, we confirmed its stimulatory effect on *THRA* activity, which was lost in CDX2-KD cells transfected with siRNA@CDX2 (Figure 4). However, the siRNA@CDX2 *per se* did not decrease *THRA* activity (Figure 4). Treatment of the cell lines with Notch agonists or antagonists confirmed the complex scenario observed in the cotransfection experiments described in the previous paragraph (not shown). We then decided to focus specifically on more in-depth analysis of the Wnt pathway, considering the cross-talk and synergy between TRα1 and Wnt reported in previous studies [14,15,57].
The three cell lines were treated for 24 hours with the Wnt activator CHIR99021 (CHIR) [41] or the Wnt antagonist IWP4 [42]. As expected, CHIR increased the activity of both *THRA*-luc and TopFlash (Figure 5A). IWP4 induced in all cell lines a significant decrease of the TopFlash activity compared with the control (Figure 5B). However, when we analyzed the action of this drug, it clearly inhibited *THRA*-luc activity only in HCT116 cells (Figure 5B). We also evaluated the effect of the Wnt modulators on the endogenous TRα1 expression and compared it with the cotransfection of β-catenin and TCF1 (Figure S6, S7). While we confirmed a certain difference to respond to the Wnt modulators depending on the cell line (Figure S6), the cotransfection of cells with β-catenin/TCF1 resulted in increased TRα1 expression in all cell lines at both mRNA and protein level (Figure S7 A,B). Overall, we confirmed that high CDX2 regulated the *THRA* promoter and that its activity was increased by the Wnt agonist CHIR. In addition, Wnt stimulation also affected the endogenous TRα1 expression.

Mutational and functional analyses of the *THRA* promoter

To definitively link *THRA* promoter activity with the Wnt/β-catenin signaling pathway, we performed experiments on *THRA*-luc construct carrying a mutation in each of the TCF7L2 sites (*THRA*-mut1-luc and *THRA*-mut2-luc vectors) or in both (*THRA*-dmut-luc vector) (Figure S1 B-D). We performed experiments in parallel with *THRA*-luc and the mutated versions in the three cell lines used in the previous experiments, in the presence or absence of cotransfected β-catenin/TCF1 (Figure 6A). In both *THRA*-mut1-luc and *THRA*-mut2-luc, the induction of *THRA*-dependent luciferase activity by β-catenin/TFC1 significantly decreased in the three cell lines compared to that observed with the WT promoter (Figure 6A). This effect was even more important when using the double mutant vector as the induction of *THRA*-dependent luciferase activity by β-catenin/TFC1 was strongly affected in all cell lines. Importantly, the mutations in each or both TCF7L2 sites decreased the *THRA*-dependent luciferase basal activity in all cell lines compared with the non-mutated promoter.

To further confirm the importance of the Wnt activity on the *THRA* promoter, we also performed experiments using a vector expressing a mutated form of TCF1 that acts as a dominant-negative (TCF1-DN) vis-à-vis of the WT protein [58]. By co-transfecting the TCF1-DN vector, we observed a significant decrease of *THRA*-luc activity in Caco2 and HCT116 cells, while only a slight diminution in SW480 cells (Figure 6B). When we re-expressed increasing amounts of β-catenin (from 50 ng to 500 ng) in the suppressed Wnt condition we observed an increased *THRA*-luc activity that was, however, different among the cell lines. In the case of Caco2 cells, a dose-response effect to increased β-catenin amounts was shown. In SW480 and HCT116 cells the luciferase activity increased significantly compared with the TCF1-DN condition, but reached rapidly a plateau and could not be stimulated by higher β-catenin concentrations (Figure 6B). The efficacy of TCF1-DN was validated in the TopFlash control vector (Figure S8).

The above results and those described in the previous paragraphs prompted us to determine whether the regulation of the *THRA* promoter by the Wnt effectors β-catenin/TCF was mediated by a direct binding on chromatin. For this aim we used a chromatin immunoprecipitation (ChIP) approach on the three cell lines. ChIP was performed by using an anti-β-catenin or IgG (negative control). As shown in Figure 7, β-catenin bound to the *THRA* promoter regions containing the TCF7L2 sites. The specificity of β-catenin binding was validated on *AXIN2* and *MYC* positive control promoters (Figure S9) while no specific binding was detected on the *HPRT* or *PPIB* genes (Fig. S9).

These results underline the control of the *THRA* promoter by the Wnt/β-catenin pathway in human colon adenocarcinoma cell lines, which is exerted through the functional TCF7L2 binding sites located in the 3 kb upstream of the transcription start site. In addition, it is achieved by direct binding of β-catenin to the chromatin.

Stimulation of TRα1 expression by activated Wnt in mouse enteroids

The previous results compelled us to investigate the effect of activating Wnt on TRα1 expression in a more complex and physiological model, which eventually recapitulated the steps of Wnt activation in early intestinal lesions. For this purpose, we used $Apc^{+/fl}$/Villin-Cre^{ERT2} and $Apc^{+/fl}$ mice to generate organoids from the small intestine. In $Apc^{+/fl}$/Villin-Cre^{ERT2} enteroids, mutation of the *Apc* gene was induced by the addition of 4-OH-tamoxifen to the culture medium, resulting in the increase of Wnt activity [46]. $Apc^{+/fl}$ enteroids have been used as

negative controls for tamoxifen treatment, given that they do not express the Cre^{ERT2} protein.

Enteroids of different genotypes were freshly prepared and cultured for 7 days before replication. One day after replication, they were treated with tamoxifen or DMSO (control) for 24 h (Figure 8A). The induction of the mutated *Apc* allele by tamoxifen in $Apc^{+/fl}$/Villin-Cre^{ERT2} enteroids was validated by PCR on genomic DNA, while no effect of tamoxifen was observed in $Apc^{+/fl}$ enteroids (Figure 8B). The cultures were monitored under a microscope to follow their growth depending on the genotype and conditions for four days after treatment (Figure 8C). In control condition, independent of the genotype, enteroids underwent typical development during the days in culture, characterized by the outgrowth and lengthening of buds (Figure 8C). Consistent with previous reports [59,60] upon tamoxifen treatment of $Apc^{+/fl}$/Villin-Cre^{ERT2} enteroids, we observed a change in their morphology, with a reduced length of buds and enlargement of the central body because of the lack of the Wnt gradient [61] (Figure 8C, upper panel). On the contrary, tamoxifen treatment of $Apc^{+/fl}$-derived enteroids produced no obvious changes in their morphology (Figure 8C, lower panel). We analyzed in these enteroids the expression of *TRα1* and *Wif1*, a negatively regulated direct TRα1 target gene [15], together with a panel of Wnt-responsive genes. As expected, upon tamoxifen treatment, $Apc^{+/fl}$/Villin-Cre^{ERT2} enteroids displayed increased mRNA levels of the Wnt targets *Ccnd1, cMyc, Axin2,* and *Cd44* (Figure 8D). Importantly, in accordance with the data on the promoter analyses, *TRα1* was significantly stimulated in these mutated-Apc enteroids, and *Wif1* was downregulated (Figure 8D). RTqPCR analysis on $Apc^{+/fl}$ enteroids showed no effect of tamoxifen treatment (Figure S10).

Discussion

It has been more than 50 years since the *THRA* gene was cloned and characterized as a homolog of the *v-erbA* gene, which is involved in neoplastic transformations leading to acute erythroleukemia and sarcomas [24,25], strongly suggesting its link with oncogenesis. Because of this peculiarity, it was quite logical to assume that TRα1, which is produced by this locus, behaves as an oncogene. It has also been speculated that a mutated TRα1 instead of the WT form can have a pro-tumoral function. Indeed, some data has described mutations in the *THRA* gene in gastric cancers (essentially deletions) [62], and mouse models have assigned oncogenic functions to mutated TRα1 [63,64]. Recent studies by our lab, however, clearly indicated the pro-tumoral function of WT TRα1 when overexpressed in the mouse intestine and colon [14]. Studies in human CRC cohorts also allowed us to establish the relevance of observations from mice to human pathology [15]. In this context, the cross-regulations between TRα1 and the Wnt/β-catenin pathway are multiple, and in the case of tumor formation and progression, they depend on mutations in the tumor suppressor gene *Apc*/*APC* [14,15]. Indeed, the *THRA* gene is frequently overexpressed in CRC molecular subtypes, particularly in CMS2 characterized by high Wnt [15]. We would like to emphasize that our previous study also showed its significant association with CMS3, which is characterized by high metabolic status. Differences among the cohorts, in microarray *vs.* RNA-seq analyses and among the normal counterparts analyzed may account for the discrepancy. Higher TRα1 expression was, however, definitively clear when considering the IHC analysis in the TMA of CRCs, where we observed a strong increase in TRα1 expression in tumors at all stages compared with the normal colon. The results also point to great heterogeneity in tumor parts and/or stromal cells strongly or poorly expressing TRα1. In addition to being upregulated in CRCs, in the normal intestine, TRα1 shows a distinct expression pattern that follows the gradient of Wnt and Notch activities [6,14]. However, what determines this specific expression domain was unknown and it was also unknown what are the effectors of its increase in CRCs. Of note, only a few studies have analyzed the molecular basis of *THRA* gene regulation [26–29], and none were performed in the context of cancer. This is the first study analyzing the mechanisms of *THRA* expression regulation in CRCs.

We performed *in silico* analysis on the 3 kb of *THRA* promoter and showed potential binding sites for transcription factors involved in intestinal homeostasis that impact SC biology and CRC development. CDX2 encodes a protein that is a master regulator of intestinal epithelial cell identity [32,65], is involved in SC biology [66,67]. Both tumor inducer and tumor suppressor roles have been indicated for CDX2 [40,68,69] and its downregulation has been very often associated with CRCs [35,40,68,69]. However, new elements also indicate that CDX2 can act as a tumor-inducer depending on its expression levels (Freund, personal communication). We observed here that high CDX2 levels strongly upregulated the *THRA* promoter in all adenocarcinoma cell lines analyzed, despite their different genetics and mutation statuses. *Cdx2*-KO mice display a decreased expression of the *Thra* gene [68], further strengthening our results on the positive control of *THRA* by CDX2. Interestingly, our previous studies showed that *Thra*-KO mice presented increased *Cdx2* mRNA expression and that *CDX2* promoter activity was blunted by TRα1 in transfection experiments [70,71].

Finally, our unpublished observations point to a more complex interplay between *TRα1* and *CDX2* in CRC cohorts, as we observed tumors with opposite expression levels of *TRα1* and *CDX2*, as well as tumors displaying a direct correlation between them (both upregulated or downregulated) (Plateroti and Freund, personal communication). Future studies will surely shed light on the molecular and cellular mechanisms responsible for this complex interrelation.
The Notch pathway showed intriguing action on the *THRA* promoter, which appears to be dependent upon the cellular context. We observed that NICD transfection decreased *THRA* activity in Caco2 and HCT116 cell lines but had a stimulatory function in SW480 cells. Additionally, the use of small molecules, suggested to behave as agonists or antagonists of Notch, was hampered by the difficulty of definitively assigning specific roles as activators or inhibitors to these molecules. According to the literature, it appears clear that each of their roles is much larger and goes beyond the control of the Notch pathway [72–74] [75]. It is also worth noting that the Notch pathway has complex cross-talk with the Wnt pathway, possibly explaining the puzzling results that we observed [22, 37, 76–80]. Given the regulation of *THRA* gene expression by Wnt (also discussed in the next paragraph), we assume that the three cell lines analyzed, which present different levels of Wnt activity (Figure S4), might respond differently to Notch, thus explaining the different effects observed on *THRA* activity.

Our previous work described complex cross-talk between TRα1 and the Wnt pathway [6,7,10], but we did not analyze whether Wnt could affect *THRA*/*Thra* expression. Here, we show that in cell lines, activating Wnt in all cases and by all approaches resulted in increased *THRA* promoter activity. This regulation also applied to the endogenous TRα1 expression upon β-catenin/TCF co-transfection. The direct β-catenin binding of the promoter regions containing the TCF7L2 binding sites strongly supports a direct transcriptional regulation. The effect of the CHIR and IWP4, respectively Wnt agonist and antagonist, on *THRA* activity and on the endogenous TRα1 resulted, however, more complex to analyze. The drugs were chosen based on the literature [41,42] and validated on the Wnt-reporter TopFlash in all cell lines. We speculate that the differences in responsiveness or lack of responsiveness may depend on the different genetic and epigenetic background of the cell lines, and these molecules, as already commented for the Notch agonists and antagonists, could have various targets [72–74]. In relation to the genetic background with respect to the Wnt pathway, Caco2 have a loss-of-function (LOF) mutation of the *APC* gene and a silent mutation of the *CTNNB1* gene (coding β-catenin), SW480 have a LOF mutation of *APC* and a WT *CTNNB1* gene and, finally, HCT116 have a gain of function mutation of *CTNNB1* [54,81]. In addition, they have different status for additional pathways that can also impact on the Wnt [54,55], underlying the complexity when working with these model systems.
Importantly, however, in a physiological context of mouse enteroids, recapitulating the complexity, organization and hierarchy of the intestinal epithelium [82], stimulating Wnt by *Apc* gene mutation increased TRα1 expression. Altogether, considering our previous and new results, we propose the model illustrated in Figure 9. High Wnt, as well as other transcription factors, maintains a basal level of TRα1 expression in normal intestinal crypts, where TRα1 integrates and interacts with other key pathways, such as Wnt and Notch, as well as CDX2 [30–32], to participate in intestinal homeostasis. Upon Wnt over-

activation in the early stages of tumor development, TRα1 expression increases, which in turn causes a further increase in Wnt activity responsible for crypt hyperplasia and hyperproliferation, as shown in *vil*-TRα1 mice [14]. Through its synergy with *Apc*/*APC*-dependent activated Wnt, TRα1 accelerates tumor growth and participates in tumor progression, including cancer spreading [14] and possibly integrating other tumor processes not yet established. The increased aggressiveness of tumors displaying high TRα1/high Wnt might depend on the strong decrease in the Wnt inhibitors *WIF1*/*Wif1*, *SOX17*/*Sox17*, and *FRZB*/*Frzb* that we have shown in mouse models and patient cohorts [15]. All of these proteins are silenced in CRC, and their silencing characterizes advanced stages and/or more aggressive tumors [80].

In conclusion, we showed here that several pathways and transcription factors control the expression of the *THRA* gene in the context of CRC. In particular, we unveiled the complex action of the Wnt pathway on *THRA* promoter activity and TRα1 expression. The significance and clinical relevance of high TRα1 expression are of particular interest when considering CRC patients with altered TH levels [83,84] and/or undergoing chemotherapy treatments that potentially impact thyroid functionality [85,86].

Author contributions

MVG: conception and design, collection and assembly of data, data analyses and interpretation, manuscript writing; **TLR:** collection and assembly of data, data analyses and interpretation; **DF:** collection and assembly of data, data analyses and interpretation; **SB:** collection and assembly of data, data analyses and interpretation; **GDAG**, **PAFG**: collection and assembly of data, data analyses, and interpretation; **CDD**, **JNF**: development of tools, data analyses, and interpretation; **MP**, conception and design, assembly of data, data analyses, and interpretation, manuscript writing, financial support. All authors approved the manuscript.

Acknowledgements

We are grateful to Manon Pratviel, to Pierre Lavogez and Solene Faucheron for the assistance with animal handling and care within the animal facilities (CRCL and IRFAC). We wish to thank Joel Uchuya-Castillo for realizing the very first steps of this work. We are indebted to Nicolas Gadot and the Research pathology platform (CRCL/CLB, Lyon) for the help in performing and analyzing the IHC on TMA. We also thank Isabelle Gross for helpful discussions and suggestions during the revision of the manuscript.

Funding sources

The work was supported by the FRM (Equipes FRM 2018, DEQ20181039598), by the Inca (PLBIO19-289), and by the Ligue Contre le Cancer, Département Grand Est (01X.2020). MVG and TLR received support from the FRM. DF and SB received support from the Inca. GDAG was supported by a fellowship from FAPESP (2017/19541-2).

Conflict of interest

The authors have no competing interests.

References

1 Robinson-Rechavi M, Garcia HE & Laudet V (2003) The nuclear receptor superfamily. *J Cell Sci* **116**, 585–586.

2 Brent GA (2012) Mechanisms of thyroid hormone action. *J Clin Invest* **122**, 3035–3043.

3 Cheng SY, Leonard JL & Davis PJ (2010) Molecular aspects of thyroid hormone actions. *Endocr Rev* **31**, 139–170.

4 Oetting A & Yen PM (2007) New insights into thyroid hormone action. *Best Pract Res Clin Endocrinol Metab* **21**, 193–208.

5 Mullur R, Liu YY & Brent GA (2014) Thyroid hormone regulation of metabolism. *Physiol Rev* **94**, 355–382.

6 Sirakov M, Kress E, Nadjar J & Plateroti M (2014) Thyroid hormones and their nuclear receptors: New players in intestinal epithelium stem cell biology? *Cell Mol Life Sci* **71**, 2897–2907.

7 Frau C, Godart M & Plateroti M (2017) Thyroid hormone regulation of intestinal epithelial stem cell biology. *Mol Cell Endocrinol* **459**, 90–97.

8 Tanizaki Y, Bao L, Shi B & Shi YB (2021) A Role of Endogenous Histone Acetyltransferase Steroid Hormone Receptor Coactivator 3 in Thyroid Hormone Signaling during Xenopus Intestinal Metamorphosis. *Thyroid* **31**, 692–702.

9 Shi YB, Shibata Y, Tanizaki Y & Fu L (2021) The development of adult intestinal stem cells: Insights from studies on thyroid hormone-dependent anuran metamorphosis. *Vitam Horm* **116**, 269–293.

10 Skah S, Uchuya-Castillo J, Sirakov M & Plateroti M (2017) The thyroid hormone nuclear receptors and the Wnt/β-catenin pathway: An intriguing liaison. *Dev Biol* **422**, 71–82.

11 Modica S, Gofflot F, Murzilli S, D'Orazio A, Salvatore L, Pellegrini F, Nicolucci A, Tognoni G, Copetti M, Valanzano R, Veschi S, Mariani-Costantini R, Palasciano G, Schoonjans K, Auwerx J & Moschetta A (2010) The Intestinal Nuclear Receptor Signature With Epithelial Localization Patterns and Expression Modulation in Tumors. *Gastroenterology* **138**, 636-648.e12.

12 Catalano V, Dentice M, Ambrosio R, Luongo C, Carollo R, Benfante A, Todaro M, Stassi G & Salvatore D (2016) Activated thyroid hormone promotes differentiation and chemotherapeutic sensitization of colorectal cancer stem cells by regulating Wnt and BMP4 signaling. *Cancer Res* **76**, 137–1244.

13 Godart M, Frau C, Farhat D, Giolito MV, Jamard C, Le Nevé C, Freund JN, Penalva LO, Sirakov M & Plateroti M (2021) Murine intestinal stem cells are highly sensitive to modulation of the T3/TRα1-dependent pathway. *Dev Camb* **148**.

14 Kress E, Skah S, Sirakov M, Nadjar J, Gadot N, Scoazec JY, Samarut J & Plateroti M (2010) Cooperation Between the Thyroid Hormone Receptor TRα1 and the WNT Pathway in the Induction of Intestinal Tumorigenesis. *Gastroenterology* **138**.

15 Uchuya-Castillo J, Aznar N, Frau C, Martinez P, Le Nevé C, Marisa L, Penalva LOF, Laurent-Puig P, Puisieux A, Scoazec JY, Samarut J, Ansieau S & Plateroti M (2018) Increased expression of the thyroid hormone nuclear receptor TRa1 characterizes intestinal tumors with high Wnt activity. *Oncotarget* **9**, 30979–30996.

16 Global Cancer Statistics 2020: GLOBOCAN Estimates of Incidence and Mortality Worldwide for 36 Cancers in 185 Countries - Sung - 2021 - CA: A Cancer Journal for Clinicians - Wiley Online Library
17 Fearon ER & Vogelstein B (1990) A genetic model for colorectal tumorigenesis. *Cell* **61**, 759–767.
18 Clapper ML, Chang WCL & Cooper HS (2020) Dysplastic aberrant crypt foci: Biomarkers of early colorectal neoplasia and response to preventive intervention. *Cancer Prev Res (Phila Pa)* **13**, 229–239.
19 Aceto GM, Catalano T, Curia MC & Tong Q (2020) Molecular Aspects of Colorectal Adenomas: The Interplay among Microenvironment, Oxidative Stress, and Predisposition. *BioMed Res Int* **2020**.
20 Suzui M, Morioka T & Yoshimi N (2013) Colon preneoplastic lesions in animal models. *J Toxicol Pathol* **26**, 335–341.
21 Barker N, Ridgway RA, van Es JH, van de Wetering M, Begthel H, van den Born M, Danenberg E, Clarke AR, Sansom OJ & Clevers H (2009) Crypt stem cells as the cells-of-origin of intestinal cancer. *Nature* **457**, 608–611.
22 Fre S, Pallavi SK, Huyghe M, Laé M, Janssen KP, Robine S, Artavanis-Tsakonas S & Louvard D (2009) Notch and Wnt signals cooperatively control cell proliferation and tumorigenesis in the intestine. *Proc Natl Acad Sci U S A* **106**, 6309–6314.
23 Guinney J, Dienstmann R, Wang X, De Reyniès A, Schlicker A, Soneson C, Marisa L, Roepman P, Nyamundanda G, Angelino P, Bot BM, Morris JS, Simon IM, Gerster S, Fessler E, De Sousa .E Melo F, Missiaglia E, Ramay H, Barras D, Homicsko K, Maru D, Manyam GC, Broom B, Boige V, Perez-Villamil B, Laderas T, Salazar R, Gray JW, Hanahan D, Tabernero J, Bernards R, Friend SH, Laurent-Puig P, Medema JP, Sadanandam A, Wessels L, Delorenzi M, Kopetz S, Vermeulen L & Tejpar S (2015) The consensus molecular subtypes of colorectal cancer. *Nat Med* **21**, 1350–1356.
24 Thormeyer D & Baniahmad A (1999) The v-erbA oncogene (Review). *Int J Mol Med* **4**, 351–358.
25 Sap J, Muñoz A, Damm K, Goldberg Y, Ghysdael J, Leutz A, Beug H & Vennström B (1986) The c-erb-A protein is a high-affinity receptor for thyroid hormone. *Nature* **324**, 635–640.
26 Laudet V, Begue A, Henry-duthoit C, Joubel A, Martin P, Stehelin D & Saule S (1991) Genomic organization of the human thyroid hormone receptor α (c-erbA-1) gene. *Nucleic Acids Res* **19**, 1105–1112.
27 Laudet V, Hanni C, Coll J, Catzeflis F & Stehelin D (1992) Evolution of the nuclear receptor gene superfamily. *EMBO J* **11**, 1003–1013.
28 Ishida T, Yamauchi K, Ishikawa K & Yamamoto T (1993) Molecular Cloning and Characterization of the Promoter Region of the Human c-erbAα Gene. *Biochem Biophys Res Commun* **191**, 831–839.
29 Vanacker JM, Bonnelye E, Delmarre C & Laudet V (1998) Activation of the thyroid hormone receptor a gene promoter by the orphan nuclear receptor ERRα. *Oncogene* **17**, 2429–2435.
30 Van Der Flier LG & Clevers H (2009) Stem cells, self-renewal, and differentiation in the intestinal epithelium. *Annu Rev Physiol* **71**, 241–260.
31 Gehart H & Clevers H (2019) *Tales from the crypt: new insights into intestinal stem cells* Nature Publishing Group.

32 Freund JN, Domon-Dell C, Kedinger M & Duluc I (1998) The Cdx-1 and Cdx-2 homeobox genes in the intestine. *Biochem Cell Biol* **76**, 957–969.
33 Schepers A & Clevers H (2012) Wnt signaling, stem cells, and cancer of the gastrointestinal tract. *Cold Spring Harb Perspect Biol* **4**, a007989.
34 Kulic I, Robertson G, Chang L, Baker JHE, Lockwood WW, Mok W, Fuller M, Fournier M, Wong N, Chou V, Robinson MD, Chun HJ, Gilks B, Kempkes B, Thomson TA, Hirst M, Minchinton AI, Lam WL, Jones S, Marra M & Karsan A (2015) Loss of the Notch effector RBPJ promotes tumorigenesis. *J Exp Med* **212**, 37–52.
35 Bonhomme C, Duluc I, Martin E, Chawengsaksophak K, Chenard MP, Kedinger M, Beck F, Freund JN & Domon-Dell C (2003) The Cdx2 homeobox gene has a tumour suppressor function in the distal colon in addition to a homeotic role during gut development. *Gut* **52**, 1465–1471.
36 Bray NL, Pimentel H, Melsted P & Pachter L (2016) Near-optimal probabilistic RNA-seq quantification. *Nat Biotechnol* **34**, 525—527.
37 Peignon G, Durand A, Cacheux W, Ayrault O, Terris B, Laurent-Puig P, Shroyer NF, Van Seuningen I, Honjo T, Perret C & Romagnolo B (2011) Complex interplay between β-catenin signalling and Notch effectors in intestinal tumorigenesis. *Gut* **60**, 166–176.
38 Hinoi T, Lucas PC, Kuick R, Hanash S, Cho KR & Fearon ER (2002) CDX2 regulates liver intestine-cadherin expression in normal and malignant colon epithelium and intestinal metaplasia. *Gastroenterology* **123**, 1565–1577.
39 Rezza A, Skah S, Roche C, Nadjar J, Samarut J & Plateroti M (2010) The overexpression of the putative gut stem cell marker Musashi-1 induces tumorigenesis through Wnt and Notch activation. *J Cell Sci* **123**, 3256–3265.
40 Balbinot C, Vanier M, Armant O, Nair A, Penichon J, Soret C, Martin E, Saandi T, Reimund J-MM, Deschamps J, Beck F, Domon-Dell C, Gross I, Duluc I & Freund J-NN (2017) Fine-tuning and autoregulation of the intestinal determinant and tumor suppressor homeobox gene CDX2 by alternative splicing. **24**, 2173–2186.
41 Ying QL, Wray J, Nichols J, Batlle-Morera L, Doble B, Woodgett J, Cohen P & Smith A (2008) The ground state of embryonic stem cell self-renewal. *Nature* **453**, 519–523.
42 Chen B, Dodge ME, Tang W, Lu J, Ma Z, Fan CW, Wei S, Hao W, Kilgore J, Williams NS, Roth MG, Amatruda JF, Chen C & Lum L (2009) Small molecule-mediated disruption of Wnt-dependent signaling in tissue regeneration and cancer. *Nat Chem Biol* **5**, 100–107.
43 Lu H, Cheng G, Hong F, Zhang L, Hu Y & Feng L (2018) A Novel 2-Phenylamino-Quinazoline-Based Compound Expands the Neural Stem Cell Pool and Promotes the Hippocampal Neurogenesis and the Cognitive Ability of Adult Mice. *Stem Cells* **36**, 1273–1285.
44 Pandya K, Meeke K, Clementz AG, Rogowski A, Roberts J, Miele L, Albain KS & Osipo C (2011) Targeting both Notch and ErbB-2 signalling pathways is required for prevention of ErbB-2-positive breast tumour recurrence. *Br J Cancer 2011 1056* **105**, 796–806.
45 Dovey HF, John V, Anderson JP, Chen LZ, Andrieu PDS, Fang LY, Freedman SB, Folmer B, Goldbach E, Holsztynska EJ, Hu KL, Johnson-Wood KL, Kennedy SL, Kholodenko D, Knops JE, Latimer LH, Lee M, Liao Z,

Lieberburg IM, Motter RN, Mutter LC, Nietz J, Quinn KP, Sacchi KL, Seubert PA, Shopp GM, Thorsett ED, Tung JS, Wu J, Yang S, Yin CT, Schenk DB, May PC, Altstiel LD, Bender MH, Boggs LN, Britton TC, Clemens JC, Czilli DL, Dieckman-McGinty DK, Droste JJ, Fuson KS, Gitter BD, Hyslop PA, Johnstone EM, Li W-Y, Little SP, Mabry TE, Miller FD, Ni B, Nissen JS, Porter WJ, Potts BD, Reel JK, Stephenson D, Su Y, Shipley LA, Whitesitt CA, Yin T & Audia JE (2001) Functional gamma-secretase inhibitors reduce beta-amyloid peptide levels in brain. *J Neurochem* **76**, 173–181.

46 Shibata H, Toyama K, Shioya H, Ito M, Hirota M, Hasegawa S, Matsumoto H, Takano H, Akiyama T, Toyoshima K, Kanamaru R, Kanegae Y, Saito I, Nakamura Y, Shiba K & Noda T (1997) Rapid colorectal adenoma formation initiated by conditional targeting of the APC gene. *Science* **278**, 120–133.

47 El Marjou F, Janssen KP, Chang BHJ, Li M, Hindie V, Chan L, Louvard D, Chambon P, Metzger D & Robine S (2004) Tissue-specific and inducible Cre-mediated recombination in the gut epithelium. *Genesis* **39**, 186–193.

48 Mlecnik B, Tosolini M, Kirilovsky A, Berger A, Bindea G, Meatchi T, Bruneval P, Trajanoski Z, Fridman W-H, Pagès F & Galon J (2011) Histopathologic-based prognostic factors of colorectal cancers are associated with the state of the local immune reaction. *J Clin Oncol Off J Am Soc Clin Oncol* **29**, 610–618.

49 Galon J, Costes A, Sanchez-Cabo F, Kirilovsky A, Mlecnik B, Lagorce-Pagès C, Tosolini M, Camus M, Berger A, Wind P, Zinzindohoué F, Bruneval P, Cugnenc P-H, Trajanoski Z, Fridman W-H & Pagès F (2006) Type, density, and location of immune cells within human colorectal tumors predict clinical outcome. *Science* **313**, 1960–1964.

50 Vonlanthen J, Okoniewski MJ, Menigatti M, Cattaneo E, Pellegrini-Ochsner D, Haider R, Jiricny J, Staiano T, Buffoli F & Marra G (2014) A comprehensive look at transcription factor gene expression changes in colorectal adenomas. *BMC Cancer* **14**, 46.

51 Bottomly D, Kyler SL, McWeeney SK & Yochum GS (2010) Identification of β-catenin binding regions in colon cancer cells using ChIP-Seq. *Nucleic Acids Res* **38**, 5735–5745.

52 Cancer Genome Atlas Network (2012) Comprehensive molecular characterization of human colon and rectal cancer. *Nature* **487**, 330–337.

53 Gayet J, Zhou XP, Duval A, Rolland S, Hoang JM, Cottu P & Hamelin R (2001) Extensive characterization of genetic alterations in a series of human colorectal cancer cell lines. *Oncogene* **20**, 5025–5032.

54 Berg KCG, Eide PW, Eilertsen IA, Johannessen B, Bruun J, Danielsen SA, Bjørnslett M, Meza-Zepeda LA, Eknæs M, Lind GE, Myklebost O, Skotheim RI, Sveen A & Lothe RA (2017) Multi-omics of 34 colorectal cancer cell lines - a resource for biomedical studies. *Mol Cancer* **16**.

55 Ahmed D, Eide PW, Eilertsen IA, Danielsen SA, Eknæs M, Hektoen M, Lind GE & Lothe RA (2013) Epigenetic and genetic features of 24 colon cancer cell lines. *Oncogenesis* **2**, e71.

56 Lagziel S, Gottlieb E & Shlomi T (2020) Mind your media. *Nat Metab* **2**, 1369–1372.

57 Hasebe T, Fujimoto K, Kajita M & Ishizuya-Oka A (2016) Thyroid hormone activates Wnt/β-catenin signaling involved in adult epithelial development

during intestinal remodeling in Xenopus laevis. *Cell Tissue Res* **365**, 309–318.

58 Najdi R, Syed A, Arce L, Theisen H, Ting JHT, Atcha F, Nguyen AV, Martinez M, Holcombe RF, Edwards RA, Marsh JL & Waterman ML (2009) A Wnt kinase network alters nuclear localization of TCF-1 in colon cancer. *Oncogene* **28**, 4133–4146.

59 Matano M, Date S, Shimokawa M, Takano A, Fujii M, Ohta Y, Watanabe T, Kanai T & Sato T (2015) Modeling colorectal cancer using CRISPR-Cas9-mediated engineering of human intestinal organoids. *Nat Med* **21**, 256–262.

60 Drost J, Van Jaarsveld RH, Ponsioen B, Zimberlin C, Van Boxtel R, Buijs A, Sachs N, Overmeer RM, Offerhaus GJ, Begthel H, Korving J, Van De Wetering M, Schwank G, Logtenberg M, Cuppen E, Snippert HJ, Medema JP, Kops GJPL & Clevers H (2015) Sequential cancer mutations in cultured human intestinal stem cells. *Nature* **521**, 43–47.

61 Merenda A, Fenderico N & Maurice MM (2020) Wnt Signaling in 3D: Recent Advances in the Applications of Intestinal Organoids. *Trends Cell Biol* **30**, 60–73.

62 Wang CS, Lin KH & Hsu YC (2002) Alterations of thyroid hormone receptor α gene: Frequency and association with Nm23 protein expression and metastasis in gastric cancer. *Cancer Lett* **175**, 121–127.

63 Lin KH, Zhu XG, Shieh HY, Hsu HC, Chen ST, McPhie P & Cheng SY (1996) Identification of naturally occurring dominant negative mutants of thyroid hormone α1 and β1 receptors in a human hepatocellular carcinoma cell line. *Endocrinology* **137**, 4073–4081.

64 Lin KH, Zhu XG, Hsu HC, Chen SL, Shieh HY, Chen ST, McPhie P & Cheng SY (1997) Dominant negative activity of mutant thyroid hormone receptors from patients with hepatocellular carcinoma. *Endocrinology* **138**, 5308–5315.

65 Stringer EJ, Duluc I, Saandi T, Davidson I, Bialecka M, Sato T, Barker N, Clevers H, Pritchard CA, Winton DJ, Wright NA, Freund JN, Deschamps J & Beck F (2012) Cdx2 determines the fate of postnatal intestinal endoderm. *Development* **139**, 465–474.

66 Pereira B, Sousa S, Barros R, Carreto L, Oliveira P, Oliveira C, Chartier NT, Plateroti M, Rouault JP, Freund JN, Billaud M & Almeida R (2013) CDX2 regulation by the RNA-binding protein MEX3A: Impact on intestinal differentiation and stemness. *Nucleic Acids Res* **41**, 3986–3999.

67 San Roman AK, Tovaglieri A, Breault DT & Shivdasani RA (2015) Distinct processes and transcriptional targets underlie CDX2 requirements in intestinal stem cells and differentiated villus cells. *Stem Cell Rep* **5**, 673–681.

68 Balbinot C, Armant O, Elarouci N, Marisa L, Martin E, de Clara E, Onea A, Deschamps J, Beck F, Freund JN & Duluc I (2018) The Cdx2 homeobox gene suppresses intestinal tumorigenesis through non-cell-autonomous mechanisms. *J Exp Med* **215**, 911–926.

69 Singh H, Seruggia D, Madha S, Saxena M, Nagaraja AK, Wu Z, Zhou J, Huebner AJ, Maglieri A, Wezenbeek J, Hochedlinger K, Orkin SH, Bass AJ, Hornick JL & Shivdasani RA (2022) Transcription factor-mediated intestinal metaplasia and the role of a shadow enhancer. *Genes Dev* **36**, 38–52.

70 Plateroti M, Chassande O, Fraichard A, Gauthier K, Freund JN, Samarut J & Kedinger M (1999) Involvement of T3Rα- and β-receptor subtypes in mediation of T3 functions during postnatal murine intestinal development. *Gastroenterology* **116**, 1367–1378.
71 Plateroti M, Gauthier K, Domon-Dell C, Freund J-N, Samarut J & Chassande O (2001) Functional Interference between Thyroid Hormone Receptor α (TRα) and Natural Truncated TRΔα Isoforms in the Control of Intestine Development. *Mol Cell Biol* **21**, 4761–4772.
72 Barat S, Chen X, Bui KC, Bozko P, Götze J, Christgen M, Krech T, Malek NP & Plentz RR (2017) Gamma-secretase inhibitor IX (GSI) impairs concomitant activation of notch and wnt-beta-catenin pathways in CD441 gastric cancer stem cells. *Stem Cells Transl Med* **6**, 819–829.
73 Borggrefe T, Lauth M, Zwijsen A, Huylebroeck D, Oswald F & Giaimo BD (2016) The Notch intracellular domain integrates signals from Wnt, Hedgehog, TGFβ/BMP and hypoxia pathways. *Biochim Biophys Acta - Mol Cell Res* **1863**, 303–313.
74 Krishnamurthy N & Kurzrock R (2018) Targeting the Wnt/beta-catenin pathway in cancer: Update on effectors and inhibitors. *Cancer Treat Rev* **62**, 50–60.
75 Bonfim DC, Dias RB, Fortuna-Costa A, Chicaybam L, Lopes DV, Dutra HS, Borojevic R, Bonamino M, Mermelstein C & Rossi MID (2016) PS1/γ-secretase-mediated cadherin cleavage induces β-catenin nuclear translocation and osteogenic differentiation of human bone marrow stromal cells. *Stem Cells Int* **2016**.
76 Collu GM, Hidalgo-Sastre A & Brennan K (2014) Wnt-Notch signalling crosstalk in development and disease. *Cell Mol Life Sci* **71**, 3553–3567.
77 Hayward P, Balayo T & Arias AM (2006) Notch synergizes with axin to regulate the activity of Armadillo in Drosophila. *Dev Dyn* **235**, 2656–2666.
78 Fendler A, Bauer D, Busch J, Jung K, Wulf-Goldenberg A, Kunz S, Song K, Myszczyszyn A, Elezkurtaj S, Erguen B, Jung S, Chen W & Birchmeier W (2020) Inhibiting WNT and NOTCH in renal cancer stem cells and the implications for human patients. *Nat Commun* **11**, 1–16.
79 Rodilla V, Villanueva A, Obrador-Hevia A, Robert-Moreno À, Fernández-Majada V, Grilli A, López-Bigas N, Bellora N, Albà MM, Torres F, Duñach M, Sanjuan X, Gonzalez S, Gridley T, Capella G, Bigas A & Espinosa L (2009) Jagged1 is the pathological link between Wnt and Notch pathways in colorectal cancer. *Proc Natl Acad Sci U S A* **106**, 6315–6320.
80 Silva A-L, Dawson SNN, Arends MJJ, Guttula K, Hall N, Cameron EAA, Huang TH-MH-M, Brenton JDD, Tavaré S, Bienz M & Ibrahim AEE (2014) Boosting Wnt activity during colorectal cancer progression through selective hypermethylation of Wnt signaling antagonists. *BMC Cancer 2014 141* **14**, 1–10.
81 Ghandi M, Huang FW, Jané-Valbuena J, Kryukov GV, Lo CC, McDonald ER, Barretina J, Gelfand ET, Bielski CM, Li H, Hu K, Andreev-Drakhlin AY, Kim J, Hess JM, Haas BJ, Aguet F, Weir BA, Rothberg MV, Paolella BR, Lawrence MS, Akbani R, Lu Y, Tiv HL, Gokhale PC, de Weck A, Mansour AA, Oh C, Shih J, Hadi K, Rosen Y, Bistline J, Venkatesan K, Reddy A, Sonkin D, Liu M, Lehar J, Korn JM, Porter DA, Jones MD, Golji J, Caponigro G, Taylor JE, Dunning CM, Creech AL, Warren AC, McFarland JM, Zamanighomi M, Kauffmann A, Stransky N, Imielinski M, Maruvka YE,

Cherniack AD, Tsherniak A, Vazquez F, Jaffe JD, Lane AA, Weinstock DM, Johannessen CM, Morrissey MP, Stegmeier F, Schlegel R, Hahn WC, Getz G, Mills GB, Boehm JS, Golub TR, Garraway LA & Sellers WR (2019) Next-generation characterization of the Cancer Cell Line Encyclopedia. *Nature* **569**, 503–508.

82 Sato T, Vries RG, Snippert HJ, van de Wetering M, Barker N, Stange DE, van Es JH, Abo A, Kujala P, Peters PJ & Clevers H (2009) Single Lgr5 stem cells build crypt-villus structures in vitro without a mesenchymal niche. *Nature* **459**, 262–265.

83 Hellevik AI, Åsvold BO, Bjøro T, Romundstad PR, Nilsen TIL & Vatten LJ (2009) Thyroid function and cancer risk: A prospective population study. *Cancer Epidemiol Biomarkers Prev* **18**, 570–574.

84 Iishi H, Tatsuta M, Baba M, Okuda S & Taniguchi H (1992) Enhancement by thyroxine of experimental carcinogenesis induced in rat colon by azoxymethane. *Int J Cancer* **50**, 974–976.

85 Illouz F, Laboureau-Soares S, Dubois S, Rohmer V & Rodien P (2009) Tyrosine kinase inhibitors and modifications of thyroid function tests: A review. *Eur J Endocrinol* **160**, 331–336.

86 Illouz F, Braun D, Briet C, Schweizer U & Rodien P (2014) Endocrine side-effects of anti-cancer drugs: Thyroid effects of tyrosine kinase inhibitors. *Eur J Endocrinol* **171**, R91–R99.

87 Fearon ER & Jones PA (1992) Progressing toward a molecular description of colorectal cancer development. *FASEB J* **6**, 2783–2790.

Figure Legends

Figure 1. Expression of TRα1 in human TMA of colorectal samples. A) Immunohistochemical analysis of TRα1 expression in a CRC cohort of patients with different indicated tumor stages (I, II, III and IV) and in the normal colon. Scale bar: 200 μm (low magnification), 100 μm (medium magnification), 50 μm (high magnification). **B)** Scoring of the TRα1 protein levels: -, negative; +/-, low; +, positive; ++, highly positive. The scoring was performed independently by two persons.

Figure 2. *THRA* promoter *in silico* analysis. *In silico* analysis of 3238 bp of the *THRA* promoter revealed the presence of binding sites for different transcription factors, such as CDX2, TCF7L2 and RBPJ. The insets below the TCF7L2 binding sites shows the changes introduced in the mutant promoters compared to the WT. The approximate location of the binding sites in the scheme is assigned from the 5' part of the promoter. On the right, it is indicated the number of the putative binding sites and the matrix similarity for each of them compared with the canonical binding site (1= 100% similarity).

Figure 3. Modulation of THRA promoter activity in human adenocarcinoma cell lines by Wnt, Notch and CDX2. A-C) Caco2 (**A**), SW480 (**B**) and HCT116 (**C**) cells were transfected with the *THRA*-luc vector alone or cotransfected with different transcription factors. The left panels show results obtained with the Wnt cofactors β-catenin/TCF1; the central panels show results obtained with the Notch pathway activator NICD; and the right panels show results obtained with CDX2. TopFlash, *RBPJ*-luc and *hLI*-luc were used as positive controls for Wnt, Notch and CDX2, respectively. Graphs show the mean ± SD of normalized relative luciferase units (RLU) from at least two independent experiments, each conducted in six replicates. NS: nonsignificant, ***P*<0.01, and ****P*<0.001 by unpaired, two-tailed Student's t-test.

Figure 4. Effect of CDX2-KD on *THRA*-luc activity. Analysis of the effect of silencing CDX2 on the *THRA* promoter activity in the adenocarcinoma cell lines Caco2, SW480 and HCT116, as indicated. Graphs show the mean ± SD of normalized relative luciferase units (RLU) from at least two independent experiments, each conducted in six replicates. NS: nonsignificant and ***P<0.001 by unpaired, two-tailed Student's t-test.

Figure 5. Modulation of *THRA*-luc activity by the Wnt agonist and antagonist. Analysis of *THRA*-luc and TopFlash activity in the presence of the Wnt agonist CHIR99021 (**A)** and the Wnt antagonist IWP4 **(B)** in Caco2, SW480 and HCT116 cells, as indicated. Graphs show the mean ± SD of normalized relative luciferase units (RLU) from at least two independent experiments, each conducted in six replicates. NS: nonsignificant, *: P<0.05, **: P<0.01, and ***: *P*<0.001 by unpaired, two-tailed Student's t-test.

Figure 6. Mutations and Wnt-blocking analyses of *THRA* promoter activity. A) Mutations of the TCF7L2 binding sites. *THRA*-luc or the different *THRA*-mut-luc constructs, as indicated, were transfected alone or cotransfected with β-catenin and TCF1. Experiments were performed in Caco2 (left panel), SW480 (central panel) and HCT116 (right panel) cells. Graphs show the mean ± SD of

normalized relative luciferase units (RLU) from at least two independent experiments, each conducted in six replicates. NS: nonsignificant, *: P<0.05, **: P<0.01, and ***: P<0.001 by comparing the basal activity with the activity after cotransfection. #: P<0.05, ##: P<0.01 and ###: P<0.001 by comparing the *THRA*-luc with the different mutated constructs after cotransfection with β-catenin/TCF1. $: P<0.05, $$: P<0.01 and $$$: P<0.001 by comparing the basal activity of *THRA*-luc with that of the different mutated constructs. Statistics was performed by unpaired, two-tailed Student's t-test. **B)** *THRA*-luc construct was transfected alone or cotransfected with TCF1-DN and different amounts of β-catenin (0, 50, 100, 200, 300 and 500 ng), as indicated. Experiments were performed in Caco2 (left panel), SW480 (central panel) and HCT116 (right panel) cells. Graphs show the mean ± SD of normalized relative luciferase units (RLU) from at least two independent experiments, each conducted in six replicates. NS: nonsignificant, *: P<0.05, **: P<0.01, and ***: P<0.001 compared with the basal promoter activity. NS: nonsignificant, #: P<0.05, ##: P<0.01, and ###: P<0.001 by comparing the activity of the THRA-luc cotransfected with TCF1-DN alone with the activity in the presence of different concentrations of β-catenin. Statistical analysis was performed by unpaired, two-tailed Student's t-test.

Figure 7. Chromatin occupancy of β-catenin in *THRA* gene promoter. ChIP analysis was performed with chromatin prepared from A) Caco2, B) SW480 and C) HCT116 cells and immunoprecipitated using an anti-β-catenin or IgG (negative control). qPCR was performed using specific primers covering each TCF7L2 binding site within the 3 Kb of the *THRA* promoter. Histograms represent the fold enrichment, normalized to the input, of specific β-catenin/DNA binding compared with the IgG condition (=1).

Figure 8. TRα1 modulation by the induction of the Apc mutation in mouse enteroids. A) Schematic diagram of the protocol used for *ex vivo* enteroid cultures. **B)** PCR analysis on gDNA extracted from enteroids of different genotypes and treatments, as indicated, to verify the recombination of the *Apc* gene after tamoxifen treatment. Specific primers recognizing the mutated allele were used. Note that the band corresponding to mutated *Apc* was detected only in $Apc^{+/fl}$/Villin-Cre^{ERT2} tamoxifen-treated organoids. **C)** Bright-field pictures of enteroids obtained from $Apc^{f/+}$/Villin-Cre^{ERT2} and $Apc^{+/fl}$ mice treated with tamoxifen or not treated (control). Pictures were taken at different days of culture, as indicated, using a Zeiss AxioVert inverted microscope with a 10X objective. Scale bar = 10 µm. **D)** RT–qPCR analysis of the indicated genes performed on RNA isolated from $Apc^{+/fl}$/Villin-Cre^{ERT2} enteroids treated with tamoxifen or not treated (control), as indicated. Histograms represent the mean ± SD (n=4), and data are expressed as the fold change relative to the control condition (=1). *Ppib* was used as a reference gene. *: P<0.05, **: P<0.01, and ***: *P*<0.001 by unpaired, two-tailed Student's t-test.

Figure 9. Interplay between TRα1 and the Wnt pathway and correlation with gene deregulation during intestinal tumorigenesis. The picture summarizes the known sequential genetic alterations that are frequently associated with colorectal tumorigenesis in humans. *APC*/*AXIN2*/*CTNNB1* gene mutations, which are responsible for Wnt/β-catenin overactivation, are key events that occur during the early stage of cell transformation. The other indicated mutations are

more frequently associated with later stages [87]. Interestingly, together with the control of the Wnt pathway by TRα1 and its association with the various steps in CRC (hyperproliferation, adenoma progression and carcinoma generation) [14,15], our new data point to regulation of the *THRA* promoter by the Wnt pathway and regulation of TRα1 expression by increased Wnt activity in very early stages of tumor development. LOH = Loss of heterozygosity. The Figure was created with BioRender.com (agreement number: TX23QDYSJV).

Supplementary Figure legends

Figure S1. Schematic representation of the *THRA*-luc constructs. A) *THRA*-luc promoter containing the 3238 bp upstream of the transcription starting site of the THRA gene cloned into the pGL3-basic vector. B-D) *THRA*-mut-luc vectors, including TCF7L2-1-mut (B) containing a CT>GC mutation at 816 bp, TCF7L2-2-mut (C) containing a CT>GC mutation at position 2270 bp and TCF7L2-dmut (D), with mutations in both sites.

Figure S2. Setup conditions for TRα1 IHC in human tissue sections. Two antibodies against TRα1 were used to determine the conditions that produced better efficacy for application in automated TMA analysis. Lab-made anti-TRα1 [14] (dil. 1:100) and commercial anti-TRα1 (ab53729, dil. 1:50), indicated respectively TRα1-a and TRα1-b, were applied to human paraffin sections of the small intestine and colon and colon tumors. In the negative control condition, primary antibody was omitted. Note that the two antibodies produced similar results, with TRα1 expressed in the proliferative/stem cell zone in both the normal small intestine and colon and in a heterogeneous pattern in tumors. Because of the clearer labeling obtained with the commercial antibody, we used it in TMA IHC. Scale bar: 25 μm.

Figure S3. Analysis of THRA expression in a human colorectal cancer cohort. THRA gene expression levels were evaluated in the TGCA Colon Adenocarcinoma (COAD) cohort. A) THRA mRNA levels in normal tissue (NT) vs. cancer samples. B) THRA mRNA expression levels according to the four consensus molecular subtypes (CMS) of CRC. NS= nonsignificant, *: $P<0.05$, and ****: $P<0.00001$ by the Wilcoxon test.

Figure S4. Characteristics of individual cell lines at multiple molecular levels. A) The table shows the microsatellite status and different common CRC mutations in Caco2, SW480 and HCT116 human adenocarcinoma cell lines. The heat map shows standardized single-sample gene set expression enrichment scores for the eight selected pathways indicated at the bottom in the three cell lines, as adapted from [54]. MSS: microsatellite stable, MSI: microsatellite instable, mut: mutated, WT: wild-type, EMT: epithelium-mesenchyme transition, GI: gastrointestinal. B) TRα1 mRNA levels in the three cell lines analyzed by RT–qPCR analysis. Histograms represent the mean ± SD (n=4-6); *PPIB* was used as a reference gene. *: $P<0.05$ by unpaired, two-tailed Student's t-test.

Figure S5. Analyses in pGL3-basic vector. A) Analysis of the *THRA*-dependent luciferase activity in Caco2 (left), SW480 (center) and HCT116 (right) compared to the original vector used for the generation of the THRA-luc construct. Graphs

show the mean ± SD of normalized relative luciferase units (RLU) from at least two independent experiments, each conducted in six replicates. ***P<0.001 by unpaired, two-tailed Student's t-test. B-D) Lack of effect of the Wnt (B) and Notch (C) effectors or of CDX2 (D) on pGL3-basic vector.

Figure S6. Effect of the Wnt agonist and antagonist on the endogenous TRα1 expression. TRα1 mRNA levels in the three cell lines analyzed by RT–qPCR in the different conditions, as indicated. Histograms represent the mean ± SD (n=4-6); *PPIB* was used as a reference gene. NS: not significant, *: P<0.05, **: P<0.01 by comparing the different conditions in each cell line #: P<0.05 and $: P<0.05 by comparing respectively Caco2 control *vs* SW480 control or SW480 control vs HCT116. Statistical analyses were performed by unpaired, two-tailed Student's t-test.

Figure S7. Effect of β-catenin/TCF transfection on the endogenous TRα1 expression. A) WB analysis carried on protein extracts from the three cell lines in control (-) or β-catenin/TCF transfection condition (+). β-catenin was analyzed to confirm the transfection efficacy. The red arrow indicates the truncated form of the transfected β-catenin. The black arrow points to the specific TRa1 band; lower bands represent non-specific signal. MW: molecular weight marker. B) TRα1 and *CTNNB1* mRNA levels in the three cell lines analyzed by RT–qPCR in the different conditions, as indicated. Histograms represent the mean ± SD (n=4-6); *PPIB* was used as a reference gene. NS: not significant, *: P<0.05, **: P<0.01 by comparing the transfected vs the control condition by unpaired, two-tailed Student's t-test.

Figure S8. TopFlash activity is affected in the presence of TCF1-DN. TopFlash was used as the positive control for Wnt activity. Caco2 (left panel), SW480 (central panel) and HCT116 (right panel) cells were transfected with TopFlash alone or cotransfected with β-catenin, TCF1 or TCF1-DN, as indicated. Graphs show the mean ± SD of normalized relative luciferase units (RLU) from at least two independent experiments, each conducted in six replicates. NS: nonsignificant, *: P<0.05, and ***: P<0.001 by comparing basal activity with cotransfection conditions; ###: P<0.001 by comparing TopFlash activity when cotransfected with β-catenin/TCF1 or β-catenin/TCF1-DN by unpaired, two-tailed Student's t-test.

Figure S9. Chromatin occupancy of β-catenin in AXIN2 and MYC promoters. ChIP analysis was performed with chromatin prepared from A) Caco2, B) SW480 and C) HCT116 cells and immunoprecipitated using an anti-β-catenin or IgG (negative control). qPCR was performed using specific primers covering TCF7L2 binding sites within the *AXIN2* and *MYC* promoters (positive controls). Non-specific binding of β-catenin was evaluated using primers for *HRPT* and *PPIB* genes (negative controls). Histograms represent the fold enrichment, normalized to the input, of specific β-catenin/DNA binding compared with the IgG condition (=1).

Figure S10. Complementary analysis on mouse enteroids. RT–qPCR analysis for the indicated genes performed using RNA isolated from $Apc^{+/fl}$ enteroids treated with tamoxifen or not treated (control), as indicated. Histograms

represent the mean ± SD (n=6), and data are expressed as the fold change relative to the control condition (=1). *Ppib* was used as a reference gene. NS: nonsignificant by unpaired, two-tailed Student's t-test.

Giolito et al, Figure 1

A

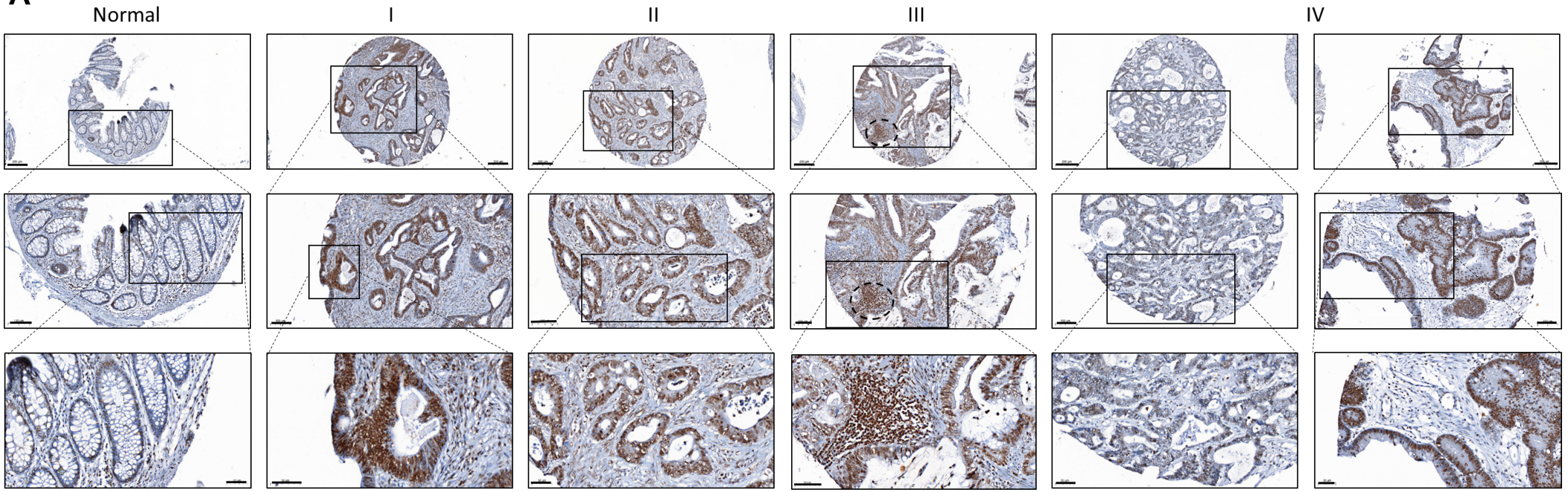

B

TRα1 IHC / Sample, Map	Tumor	Normal	Stroma	Immune Infiltration
Normal colon, I3	NP	+/-	+/-	NI
Stage I, E5	++	NP	++	NI
Stage II, B2	++	NP	++	NI
Stage III, G2	++	NP	+	++
Stage IV, A4	+	NP	+	NI
Stage IV, D2	++	NP	++	NI

NI: not identified
NP: not present

Giolito et al, Figure 2

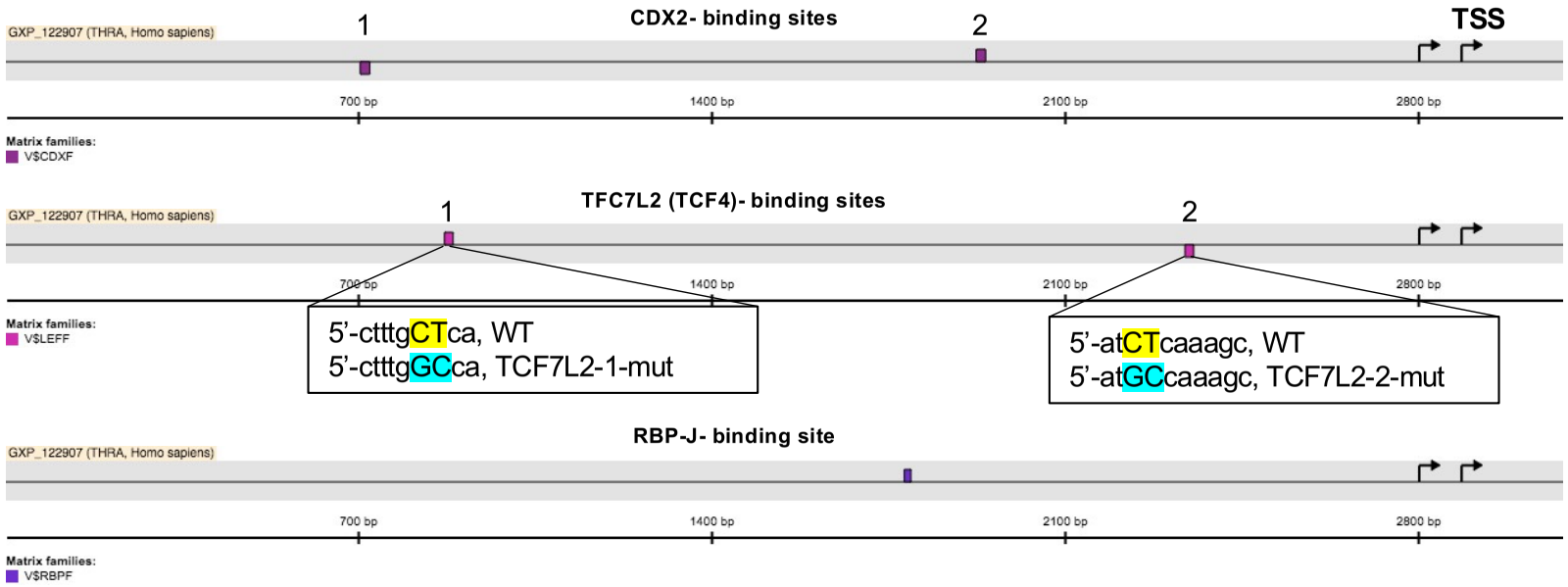

	Number of Binding sites	Matrix similarity
CDX2- binding sites	2	1: 0.995 2: 0.958
TFC7L2 (TCF4)- binding sites	2	1: 0.882 2: 0.921
RBP-J- binding site	1	0.957

Giolito et al, Figure 3

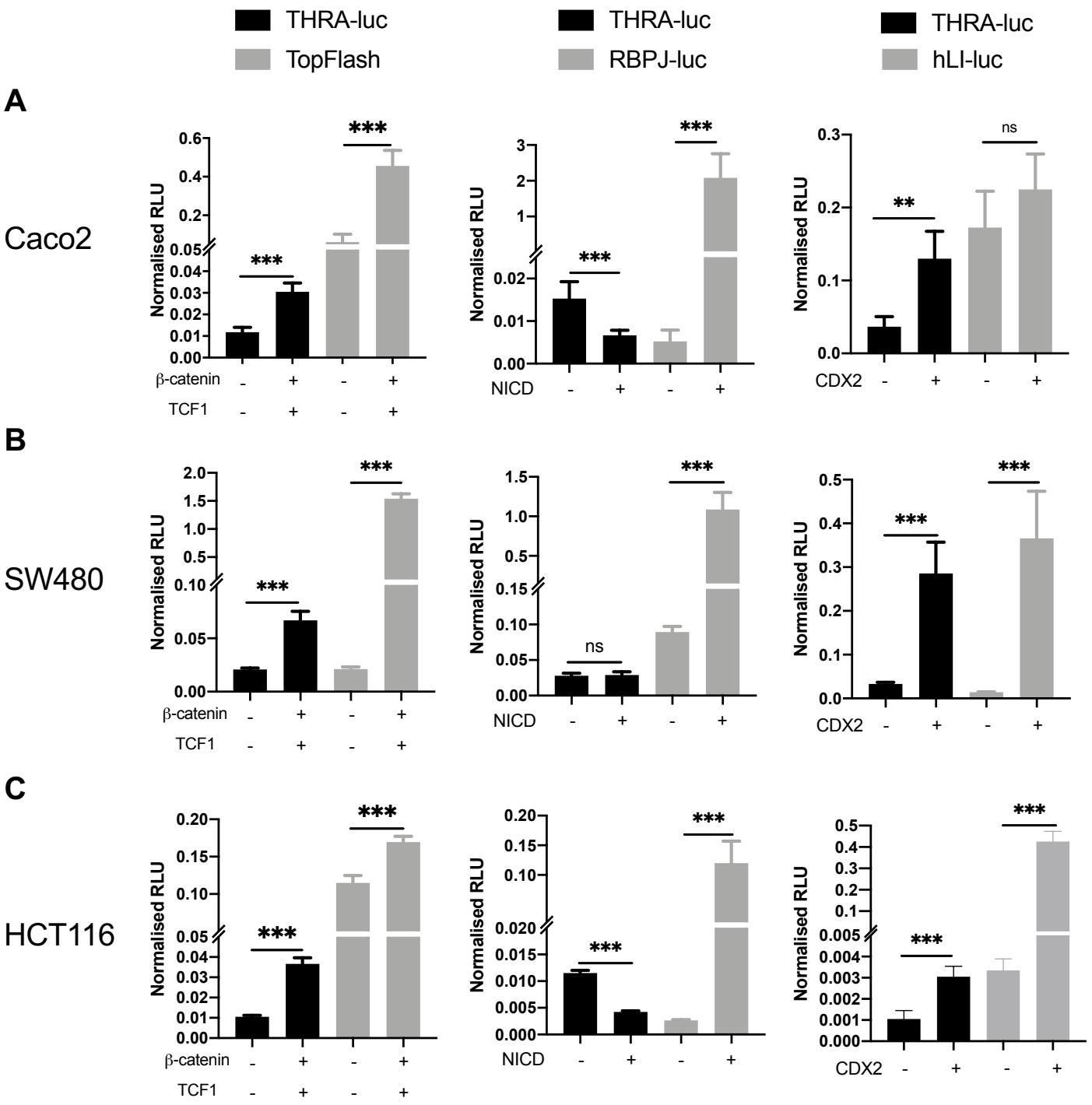

Giolito et al, Figure 4

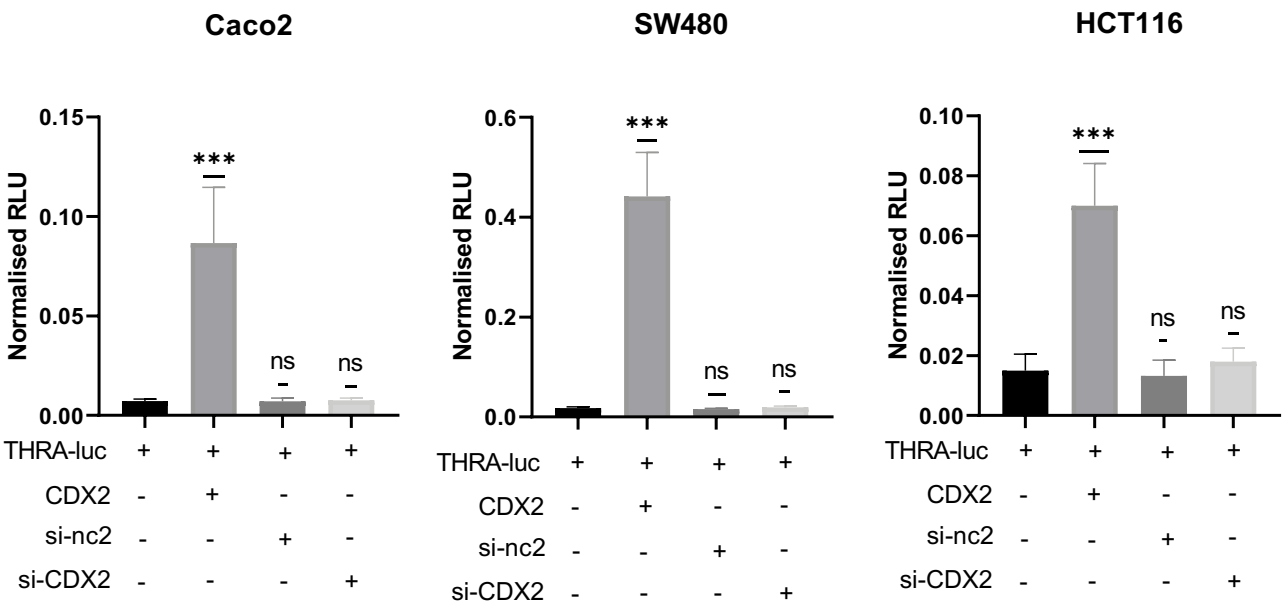

Giolito et al, Figure 5

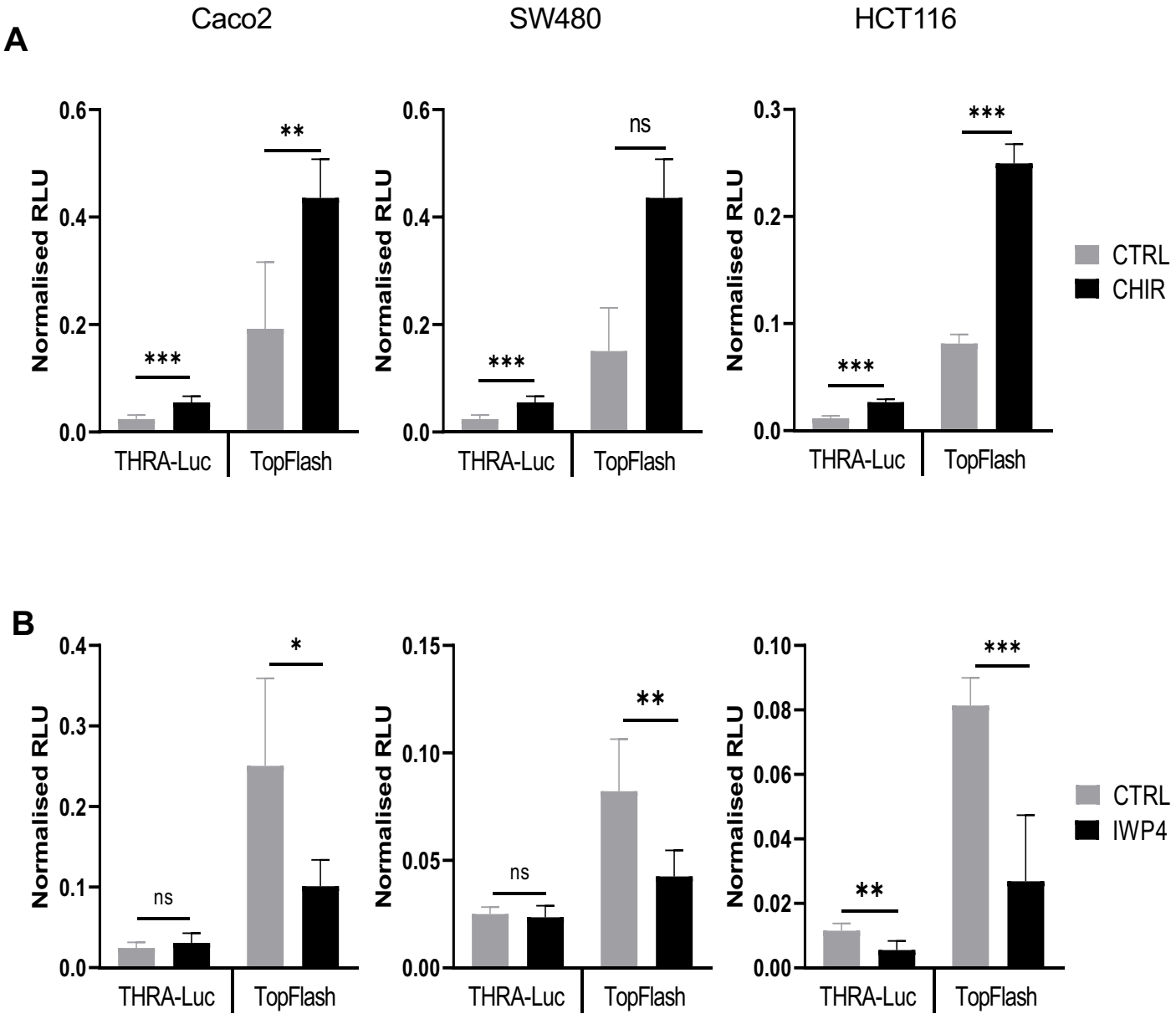

Giolito et al, Figure 6

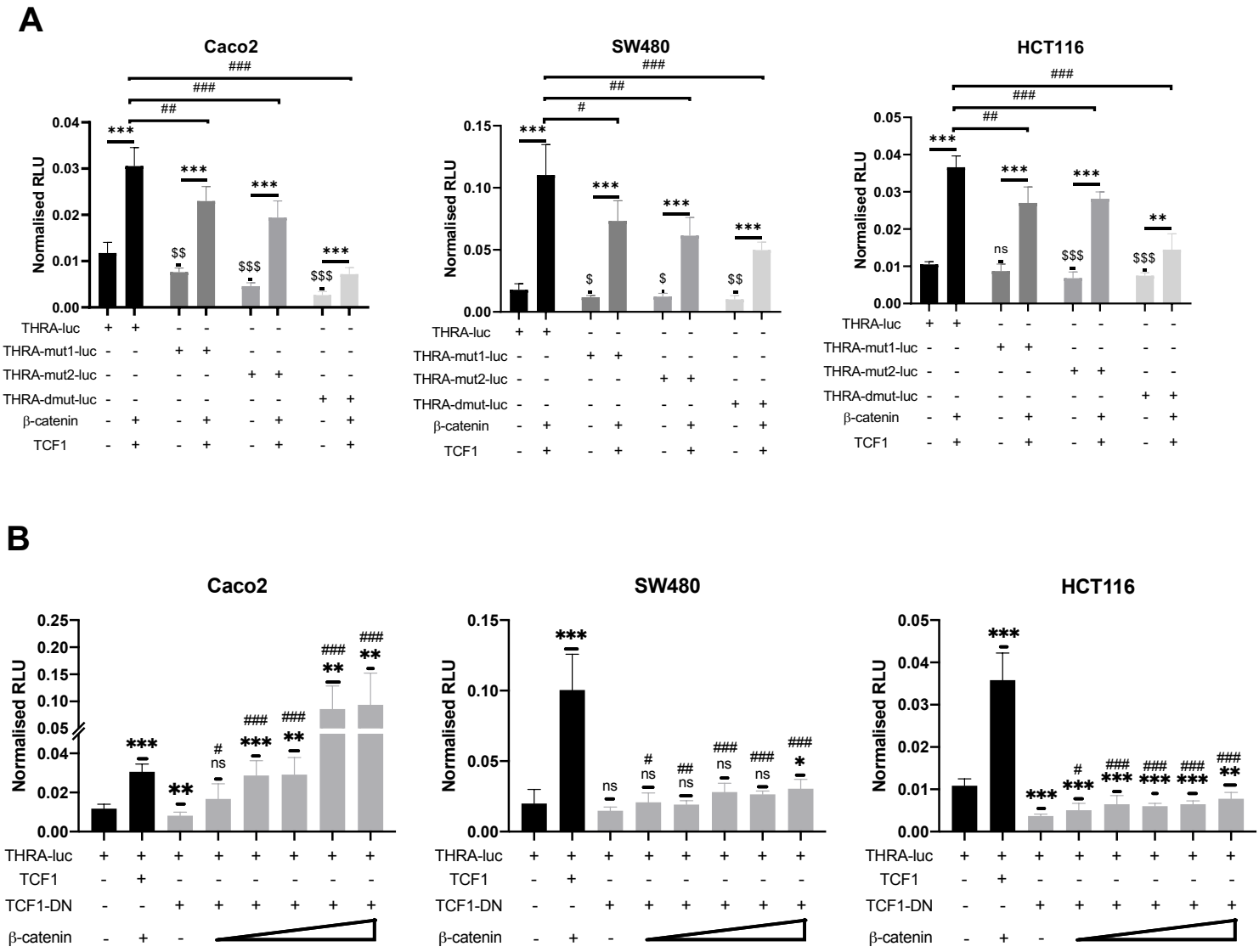

Giolito et al, Figure 7

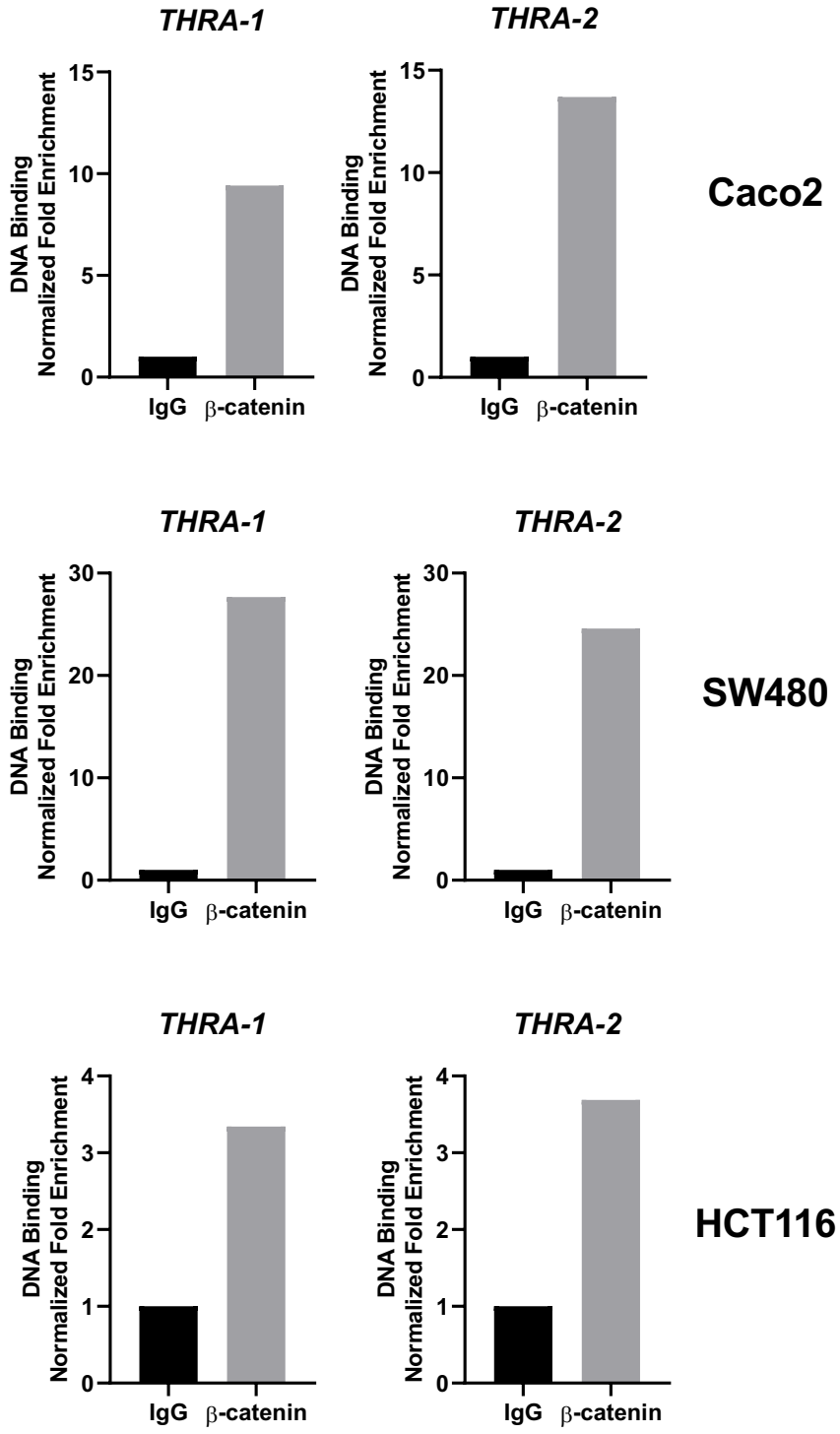

Giolito et al, Figure 8

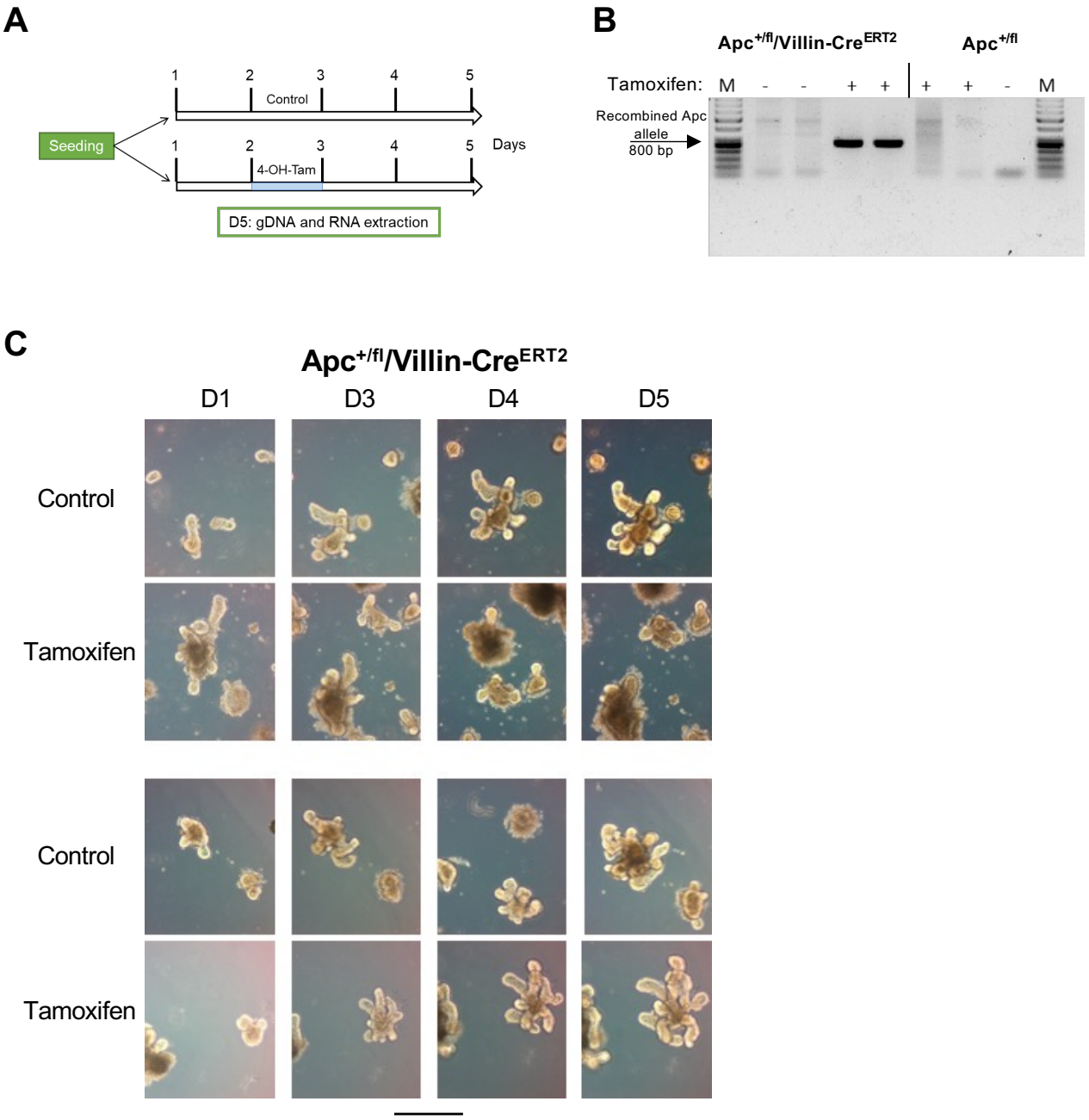

Giolito et al, Figure 9

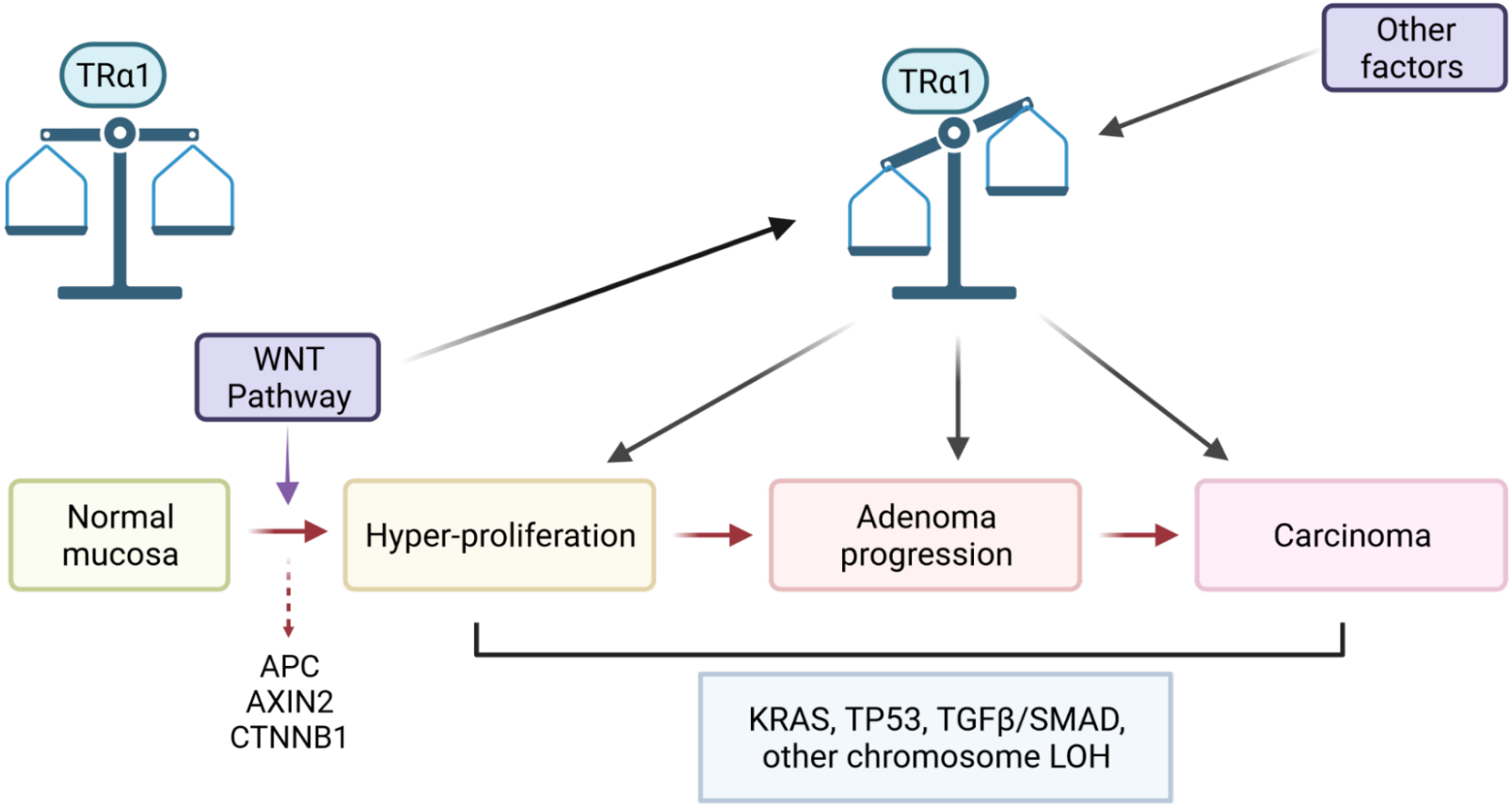

Giolito et al, Figure S1

A

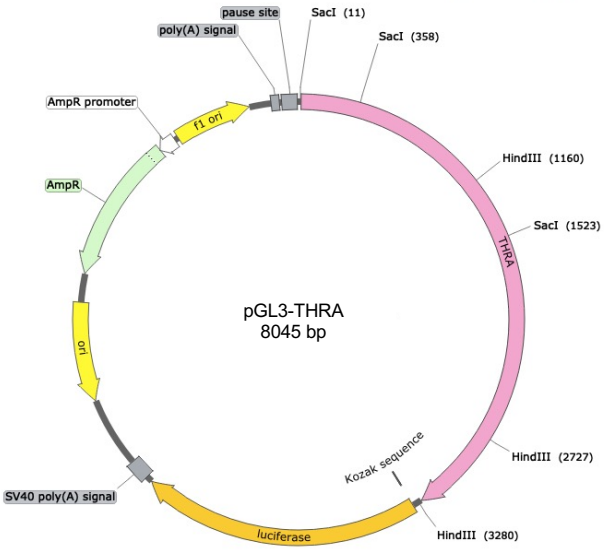

B

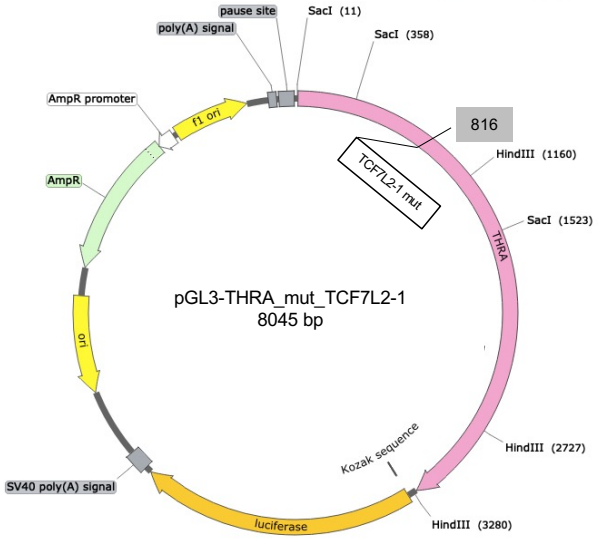

C

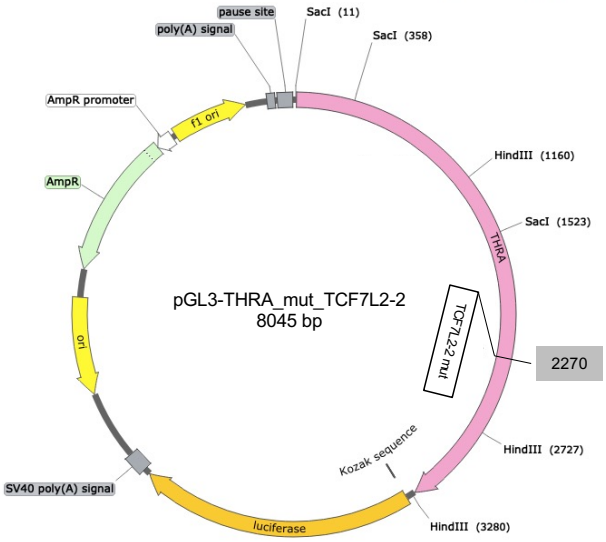

D

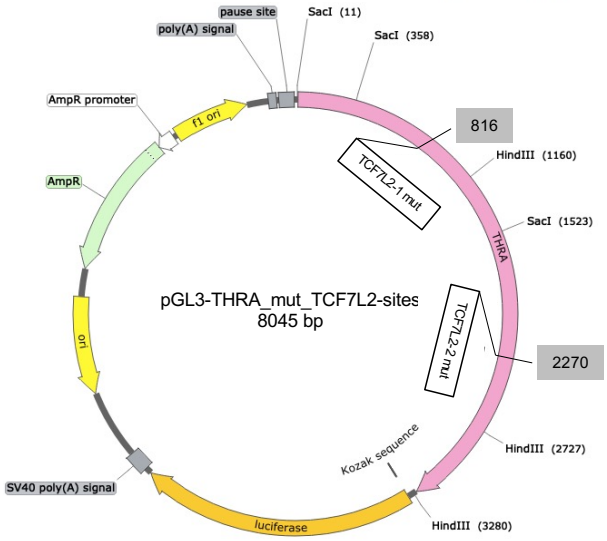

Giolito et al, Figure S2

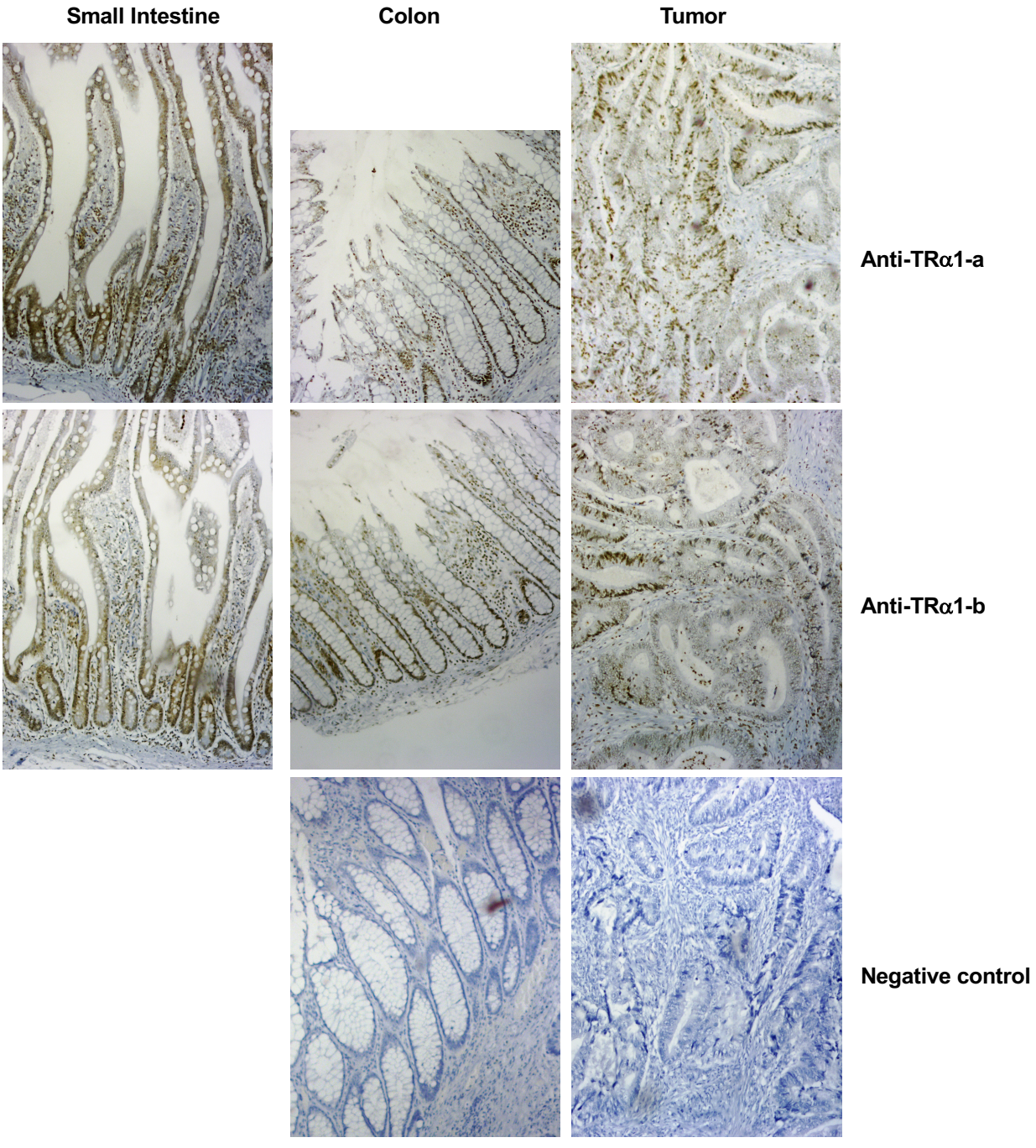

Giolito et al, Figure S3

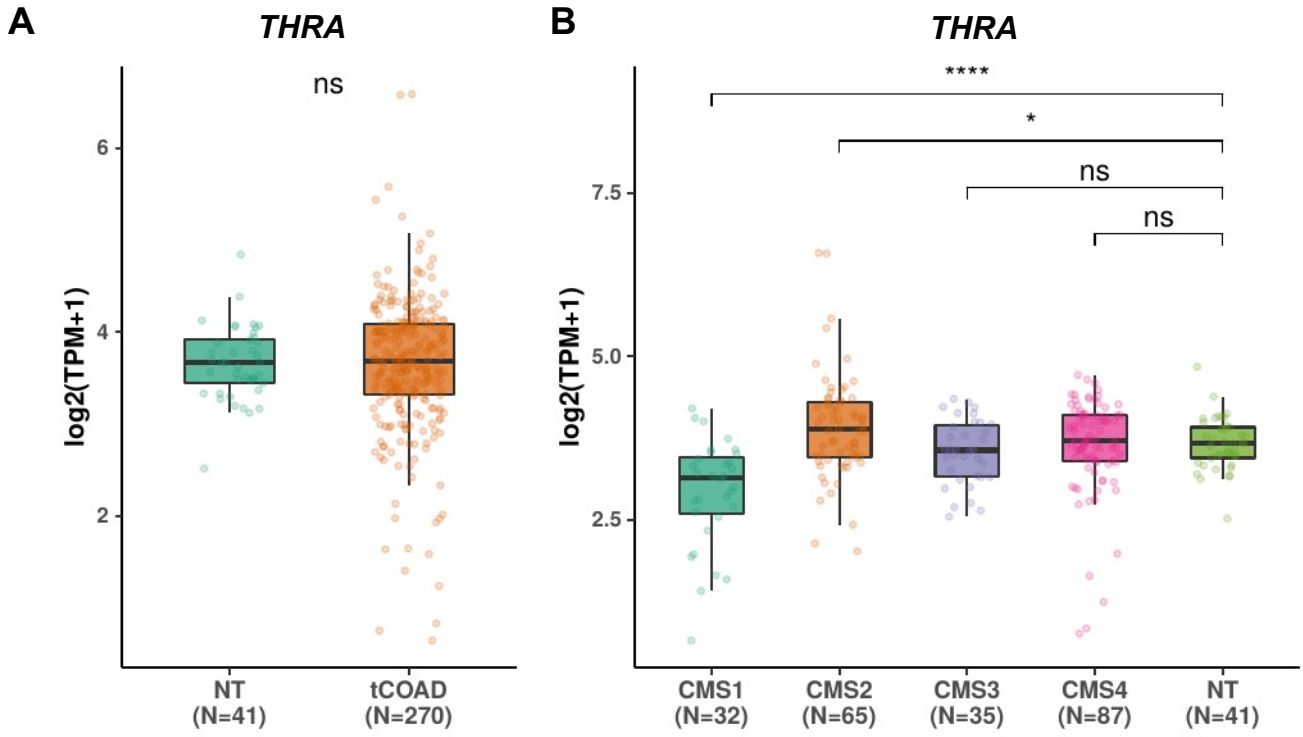

Giolito et al, Figure S4

A

	Microsat. status	*APC*	*CTNNB1*	*TP53*	*KRAS*	*BRAF*	*PI3KCA*	*PTEN*
Caco2	MSS	Mut	Mut	p.E204X	WT	WT	WT	WT
SW480	MSS	Mut	WT	p.R273H; p.P309s	p.G12V	WT	WT	WT
HCT116	MSI	WT	Mut	WT	p.G13D	WT	p.H1047R	WT

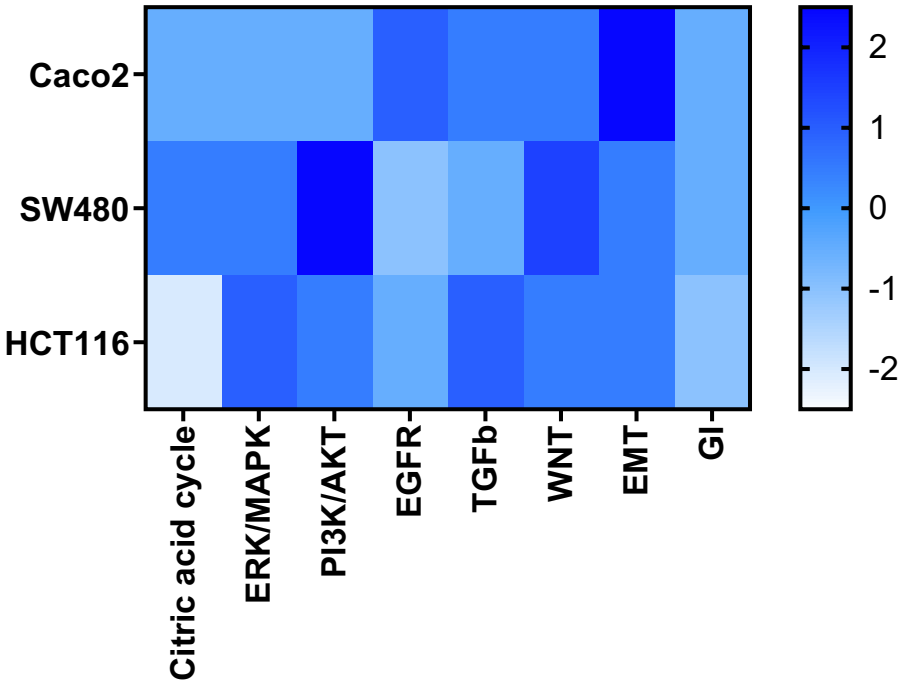

B

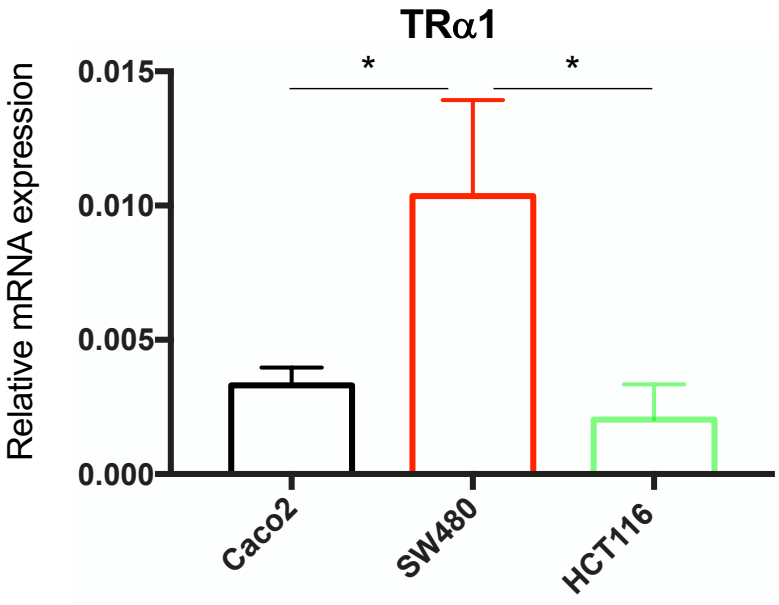

Giolito et al, Figure S5

A

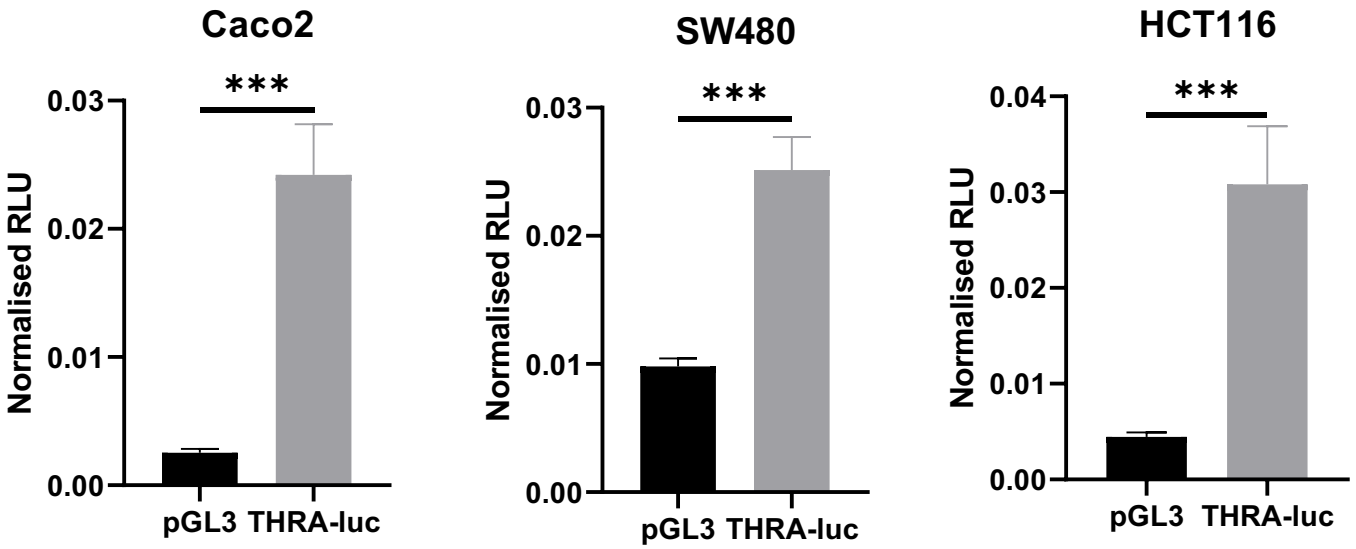

B

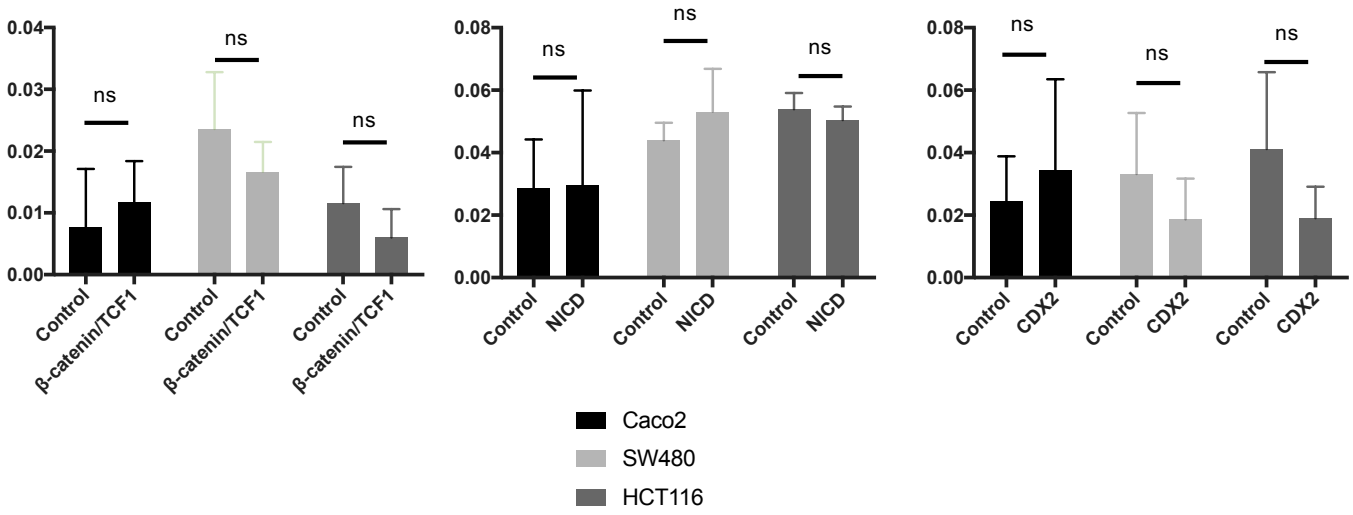

Giolito et al, Figure S6

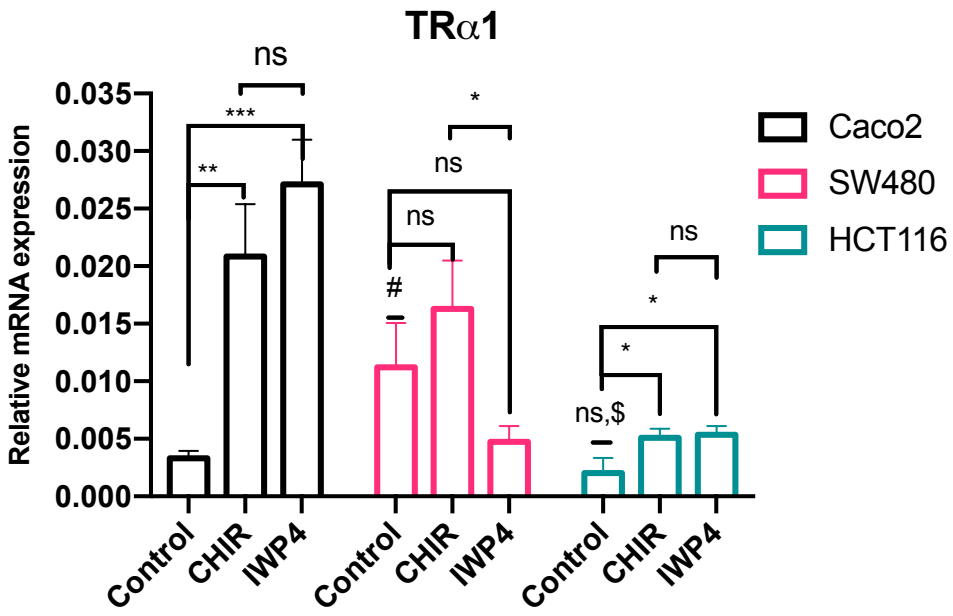

Giolito et al, Figure S7

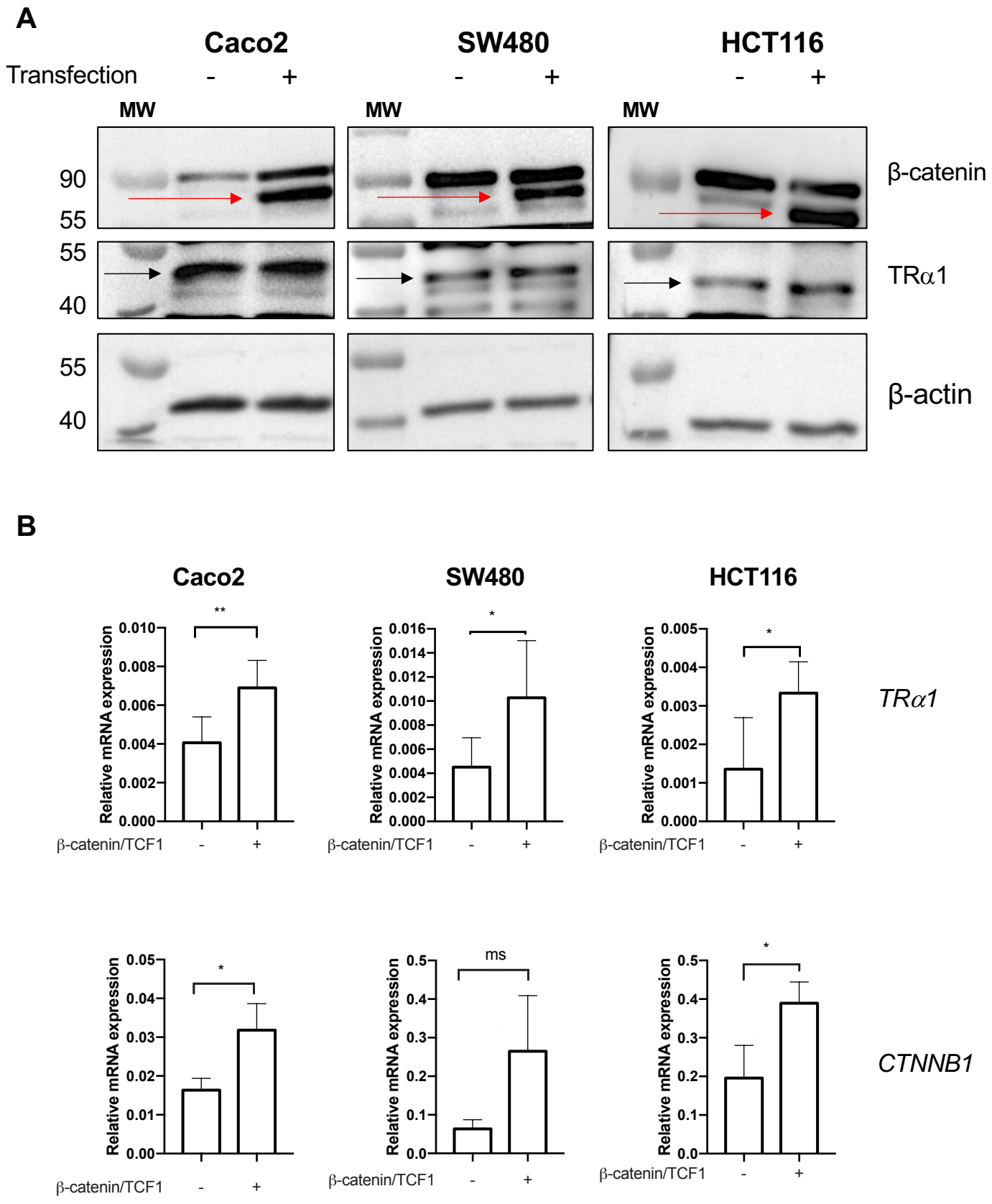

Giolito et al, Figure S8

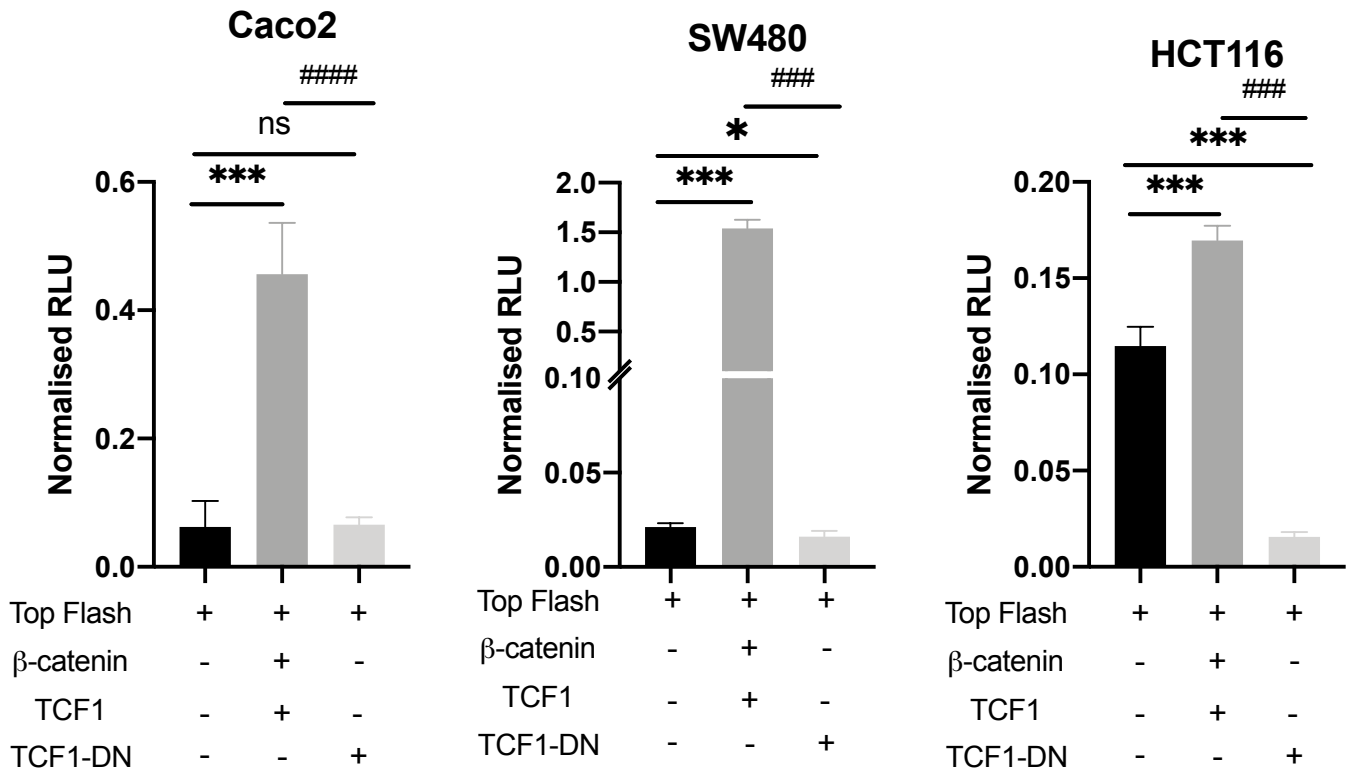

Giolito et al, Figure S9

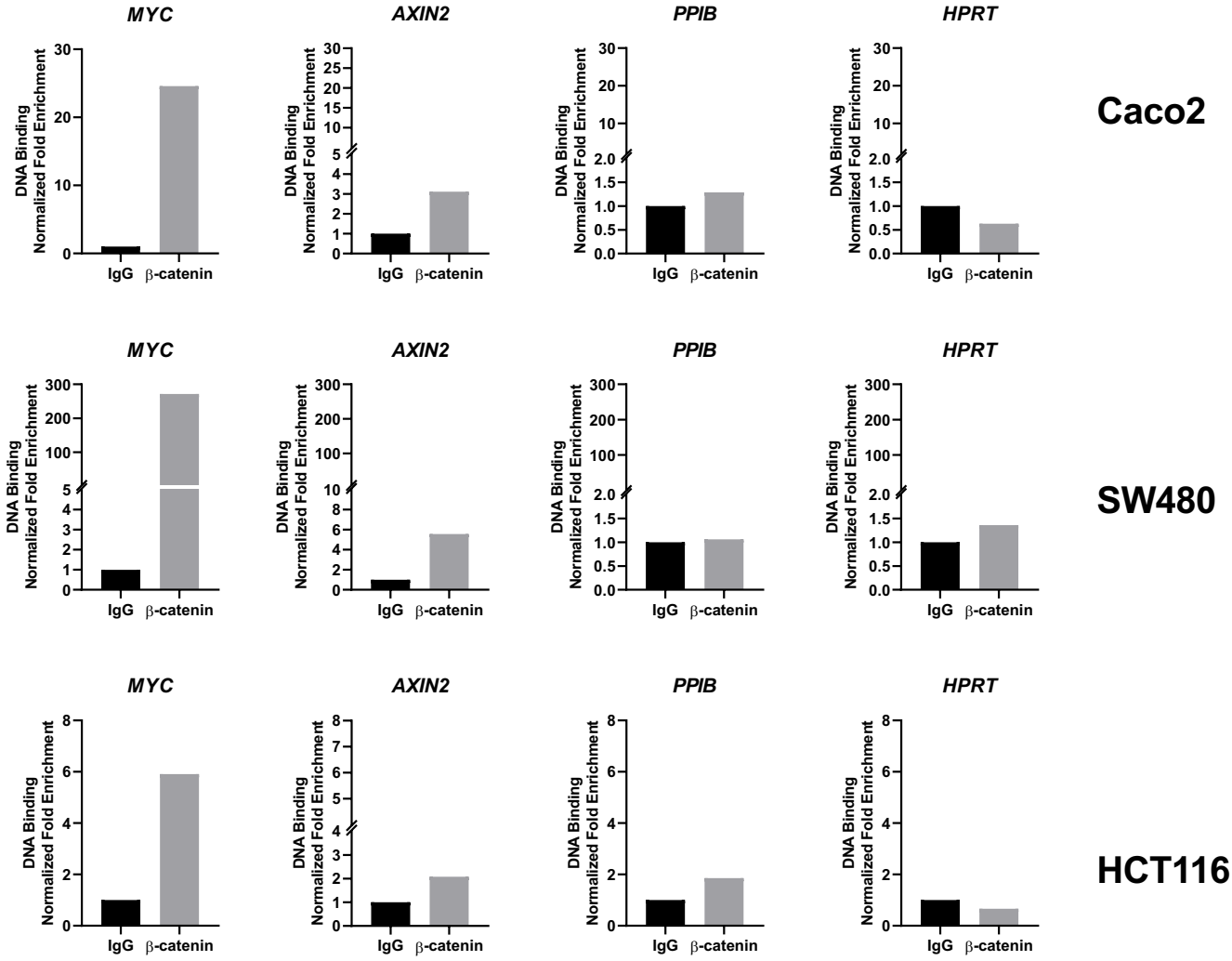

Giolito et al, Figure S10

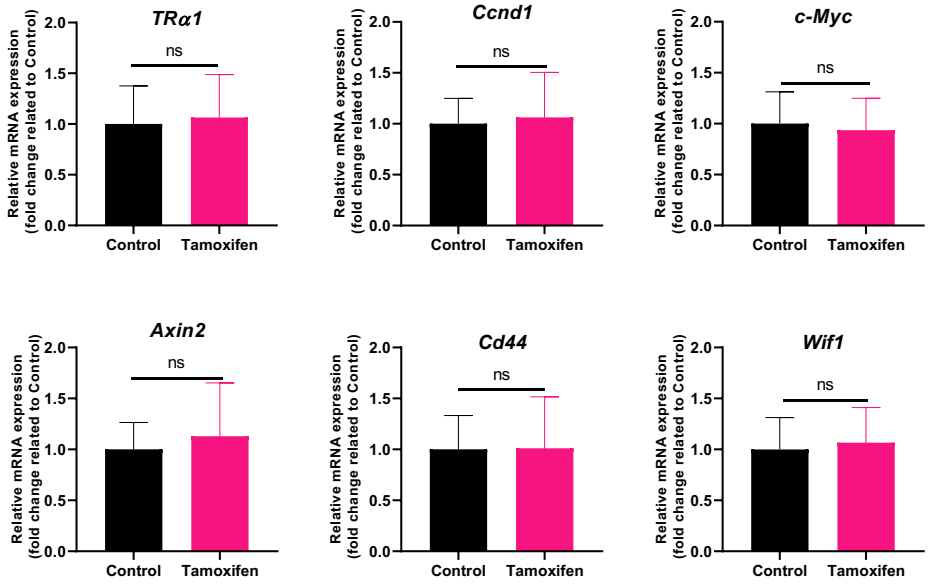

Supplementary Table 1. List of primers

Primers used for RT-qPCR		
Gene	**Sequence**	**Product length**
Axin2	F: ATG CTA GGC GGA ATG AAG ATG	250
	R: GGA GAC AAC GCT GTT GTT CTC	
Ccnd1	F: CAG AGG CGG ATG AGA ACA AGT	180
	R: GCG GTA GCA GGA GAG GAA G	
Cd44	F: GAA TGT AAC CTG CCG CTA	267
	R: GGA GGT GTT GGA CGT GAC	
Hprt	F: GCT GGT GAA AAG GAC CTC T	240
	R: CAC AGG ACT AGA ACA CCT GC	
Myc	F: GTT GGA AGA GCC GTG TGT G	129
	R: CGC TGA TGT TGG GTC AGT C	
Ppib	F: CAC CAA TGG CTC ACA GTT CTT	156
	R: ATG ACA TCC TTC AGT GGC TTG	
TRα1	F: TGC CTT TAA CCT GGA TGA CAC	240
	R: TCG ACT TTC ATG TGG AGG AAG	
Wif1	F: ATG TAT TTG CCC TCC TGG ACT	135
	R: GAG CAC AGG TCT CCT TGG TAA	
CTNNB1	F: TGC CAA GTG GGT GGT ATA GAG	126
	R: CCA TCT CTG CTT CTT GGT GTC	
Primers used for ChIP-qPCR		
THRA-1	F: GTG GTC TCA AAA TCC TGA CCT	154
	R: TGC TCT CCC AGA TTT ATC CTC	
THRA-2	F: AGA ATT GCT TGA ACC CAG GAG	184
	R: TGT CCC TGT TGA GAG GAA ATG	
AXIN2	F: CTG GAG CCG GCT GCG CTT TGA TAA	98
	R: CGG CCC CGA AAT CCA TCG CTC TGA	
MYC	F: GTG AAT ACA CGT TTG CGG GTT AC	304
	R: AGA GAC CCT TGT GAA AAA AAC CG	
HPRT	F: CCA AAG ATG GTC AAG GTC GC	250
	R: CTG CTG ACA AAG ATT CAC TGG	
PPIB	F: ATG ATC CAG GGC GGA GAC TT	102
	R: GCC CGT AGT GCT TCA GTT TG	
Primers used to analyze Apc gene deletion		
ApcΔ14^{fl}	F: GTT CTG TAT CAT GGA AAG ATA GGT GGT C	800
	R: GAG TAC GGG GTC TCT GTC TCA GTG AA	

Supplementary Table 2. List of antibodies

Antibodies used for Western Blot				
Protein	**Brand**	**Reference**	**Species**	**Dilution**
β-actin	Sigma	A5441	Mouse	1/10000
β-catenin	Santa Cruz Biotechnology	sc-7963	Mouse	1/500
β-catenin	BD Transduction	Clone 14	Mouse	1/500
TRα1	Abcam	ab53729	Rabbit	1/500
Anti-mouse IgG HRP conjugate	Promega	W402B	Goat	1/5000
Anti-rabbit IgG HRP conjugate	Promega	W401B	Goat	1/5000

Giolito et al., Table S3

TMA Map Location	Tissue of (Origin/Finding)	Appearance	Sample Pathology from Cytomyx Pathology Verification	Case Diagnosis from Donor Institution Pathology Report	Tumor Grade	TNM	Stage Grouping	TRα1 IHC			
								Tumor	Normal	Stroma	Immune
E3	Colon: right / Colon: right	Tumor	Adenocarcinoma of colon	Adenocarcinoma of colon	AJCC G1: Well differentiated	pT2pN0pMX	I	no tumor	+/-	+	NI
E5	Colon: left / Colon: left	Tumor	Adenocarcinoma of colon	Adenocarcinoma of colon	AJCC G2: Moderately differentiated	pT2pN0pMX	I	++	NP	++	NI
H2	Colon: right / Colon: right	Tumor	Adenocarcinoma of colon	Adenocarcinoma of colon	AJCC G2: Moderately differentiated	pT2pN0pMX	I	+	NP	+/-	NI
B2	Colon: sigmoid / Colon: sigmoid	Tumor	Adenocarcinoma of colon	Adenocarcinoma of colon	AJCC G1: Well differentiated	pT3pN0pMX	IIA	++	NP	++	NI
C2	Colon: right / Colon: right	Tumor	Adenocarcinoma of colon, mucinous	Adenocarcinoma of colon, mucinous	Not Reported	pT3pN0pMX	IIA	-	NP	+/-	++
C4	Colon: right / Colon: right	Tumor	Adenocarcinoma of colon	Adenocarcinoma of colon	AJCC G2: Moderately differentiated	pT3pN0pMX	IIA	+	NP	+	++
D1	Rectum / Rectum	Tumor	Adenocarcinoma of rectum	Adenocarcinoma of rectum	AJCC G2: Moderately differentiated	pT3pN0pMX	IIA	+/-	NP	+	++
D5	Cecum / Cecum	Tumor	Adenocarcinoma of colon	Adenocarcinoma of colon	AJCC G1: Well differentiated	pT3pN0pMX	IIA	+/-,+,++	NP	++	NI
E1	Cecum / Cecum	Tumor	Adenocarcinoma of colon	Adenocarcinoma of colon	Not Reported	pT3pN0pMX	IIA	Section absent			
E4	Colon: right / Colon: right	Tumor	Adenocarcinoma of colon	Adenocarcinoma of colon	AJCC G2: Moderately differentiated	pT3pN0pMX	IIA	++	NP	++	++
F3	Colon: left / Colon: left	Tumor	Adenocarcinoma of colon	Adenocarcinoma of colon	AJCC G2: Moderately differentiated	pT3pN0pM0	IIA	+/-,+,++	NP	++	NI
F4	Colon: hepatic flexure / Colon: hepatic flexure	Tumor	Adenocarcinoma of colon	Adenocarcinoma of colon	AJCC G2: Moderately differentiated	pT3pN0pMX	IIA	++	NP	++	NI
H3	Colon: transverse / Colon: transverse	Tumor	Adenocarcinoma of colon	Adenocarcinoma of colon	AJCC G2: Moderately differentiated	pT3pN0pMX	IIA	+/-,+,++	NP	+	NI
G5	Colon: sigmoid / Colon: sigmoid	Tumor	Adenocarcinoma of colon	Adenocarcinoma of colon	AJCC G1: Well differentiated	pT4pN0pMX	IIB	+/-	NP	+	NI
H5	Colon: sigmoid / Colon: sigmoid	Tumor	Adenocarcinoma of colon	Adenocarcinoma of colon	AJCC G2: Moderately differentiated	pT4pN0pMX	IIB	-	NP	+	+
H1	Colon / Lymph node	Tumor	Adenocarcinoma of colon, metastatic	Adenocarcinoma of colon, metastatic	Not Reported	pTXpN1pMX	IIIA	+	NP	++	++
B1	Colon: sigmoid / Colon: sigmoid	Tumor	Adenocarcinoma of colon	Adenocarcinoma of colon	AJCC G4: Undifferentiated	pT3pN1pMX	IIIB	+	NP	+	NI
C5	Cecum / Cecum	Tumor	Adenocarcinoma of colon	Adenocarcinoma of colon	AJCC G1: Well differentiated	pT3pN1pMX	IIIB	+	NP	+/-	++
E2	Colon: right / Colon: right	Tumor	Adenocarcinoma of colon	Adenocarcinoma of colon	AJCC G2: Moderately differentiated	pT3pN1pMX	IIIB	++	NP	+	NI
F1	Colon / Colon	Tumor	Adenocarcinoma of colon	Adenocarcinoma of colon	AJCC G2: Moderately differentiated	pT3pN1pMX	IIIB	-	NP	+/-	NI
F5	Colon: transverse / Colon: transverse	Tumor	Adenocarcinoma of colon, mucinous	Adenocarcinoma of colon	AJCC G3: Poorly differentiated	pT3pN1pMX	IIIB	Section too damaged			
G4	Cecum / Cecum	Tumor	Adenocarcinoma of colon	Adenocarcinoma of colon	AJCC G3: Poorly differentiated	pT3pN1pMX	IIIB	+/-,+,++	NP	++	NI
C1	Colon: rectosigmoid / Colon: rectosigmoid	Tumor	Adenocarcinoma of colon	Adenocarcinoma of colon	AJCC G2: Moderately differentiated	pT3pN2pMX	IIIC	++	NP	+	NI
D3	Colon: rectosigmoid / Colon: rectosigmoid	Tumor	Adenocarcinoma of colon	Adenocarcinoma of colon	AJCC G2: Moderately differentiated	pT3pN2pMX	IIIC	no tumor	+/-	+/-	++
F2	Colon: left / Colon: left	Tumor	Adenocarcinoma of colon	Adenocarcinoma of colon	Not Reported	pT3pN2pMX	IIIC	+	NP	++	NI
G1	Colon: left / Colon: left	Tumor	Adenocarcinoma of colon	Adenocarcinoma of colon	AJCC G1: Well differentiated	pT4pN2pMX	IIIC	++	NP		NI
G2	Colon: right / Colon: right	Tumor	Adenocarcinoma of colon	Adenocarcinoma of colon	AJCC G1: Well differentiated	pT3pN2pMX	IIIC	++	NP	+	++
G3	Cecum / Cecum	Tumor	Adenocarcinoma of colon, mucinous	Adenocarcinoma of colon, mucinous	AJCC G2: Moderately differentiated	pT3pN2pMX	IIIC	+	NP	+	NI
H4	Cecum / Cecum	Tumor	Adenocarcinoma of colon	Adenocarcinoma of colon	AJCC G1: Well differentiated	pT4pN2pMX	IIIC	++	NP	++	NI
A1	Colon / Liver	Tumor	Adenocarcinoma of colon, metastatic	Adenocarcinoma of colon, metastatic	AJCC G2: Moderately differentiated	pTXpNXpM1	IV	Section absent			
A2	Colon / Liver	Tumor	Adenocarcinoma of colon, metastatic	Adenocarcinoma of colon, metastatic	Not Reported	pTXpNXpM1	IV	Section absent			
A3	Colon: left / Colon: left	Tumor	Adenocarcinoma of colon	Adenocarcinoma of colon	AJCC G2: Moderately differentiated	pT3pN1pM1	IV	+/-,+,++	NP	-	NI
A4	Colon / Liver	Tumor	Adenocarcinoma of colon, metastatic	Adenocarcinoma of colon, metastatic	AJCC G2: Moderately differentiated	pTXpNXpM1	IV	+	NP	+	NI
A5	Colon / Liver	Tumor	Adenocarcinoma of colon, metastatic	Adenocarcinoma of colon, metastatic	Not Reported	pTXpNXpM1	IV	+	NP	+	NI
B3	Colon / Liver	Tumor	Adenocarcinoma of colon, metastatic	Adenocarcinoma of colon, metastatic	Not Reported	pTXpNXpM1	IV	+/-	NP	+	NI
B4	Colon / Liver	Tumor	Adenocarcinoma of colon, metastatic	Adenocarcinoma of colon, metastatic	Not Reported	pTXpNXpM1	IV	+	NP	++	NI
B5	Colon / Liver	Tumor	Adenocarcinoma of colon, metastatic	Adenocarcinoma of colon, metastatic	Not Reported	pTXpNXpM1	IV	-,+/-	NP	-	NI
C3	Colon / Lung	Tumor	Adenocarcinoma of colon, metastatic	Adenocarcinoma of colon, metastatic	Not Reported	pTXpNXpM1	IV	Section absent			
D2	Colon: right / Colon: right	Tumor	Adenocarcinoma of colon	Adenocarcinoma of colon	AJCC G1: Well differentiated	pT3pN0pM1	IV	++	NP	++	NI
D4	Colon / Liver	Tumor	Adenocarcinoma, metastatic, consistent with colon primary	Adenocarcinoma of colon, metastatic	AJCC G2: Moderately differentiated	pTXpNXpM1	IV	Section absent			
I1	Colon / Colon	Normal	Within normal limits	Adenocarcinoma of colon, metastatic	Not Reported	pTXpN1pMX	IIIA	NP	+/-	+/-	NI
I2	Colon: right / Colon: right	Normal	Within normal limits	Adenocarcinoma of colon	AJCC G2: Moderately differentiated	pT2pN0pMX	I	Section absent			
I3	Colon: transverse / Colon: transverse	Normal	Within normal limits	Adenocarcinoma of colon	AJCC G2: Moderately differentiated	pT3pN0pMX	IIA	NP	+/-	+/-	NI
I4	Colon / Colon	Normal	Within normal limits	Adenocarcinoma of colon	AJCC G1: Well differentiated	pT4pN2pMX	IIIC	NP	+/-	+/-	NI
I5	Colon: sigmoid / Colon: sigmoid	Normal	Within normal limits	Adenocarcinoma of colon	AJCC G2: Moderately differentiated	pT4pN0pMX	IIB	Section absent			

NI: Not Identified
NP: Not Present

Paper Nº 3

Original Article in preparation

Impact of the thyroid hormone T3 and of its nuclear receptor TRα1 on colon cancer stem cell biology and response to chemotherapies

Maria Virginia Giolito[1,2], Serguei Bodoirat[1], Theo La Rosa[2,#], Gabriela D. A. Guardia[3], Pedro A. F. Galante[3], Luiz O. F. Penalva[4] and Michelina Plateroti[1,2,*].

1: Université de Strasbourg, Inserm, IRFAC/UMR-S1113, FMTS, 67200, Strasbourg, France. 2: Centre de Recherche en Cancérologie de Lyon, INSERM U1052, CNRS UMR5286, Université de Lyon, 69000 Lyon, France. 3: Centro de Oncologia Molecular, Hospital Sírio-Libanês, São Paulo, Brazil. 4: Children's Cancer Research Institute, University of Texas Health Science Center at San Antonio, USA. 8: Department of Medical Oncology, Centre Léon Bérard, Lyon, France. #: current address, Stem-Cell and Brain Research Institute, U1208 INSERM, USC1361 INRA, 69675 Bron, France.

Colorectal cancers (CRCs) are strongly heterogeneous and show a hierarchical organisation with the presence of CSCs responsible for tumour development, maintenance and resistance to drugs. Our previous studies showed the importance of the thyroid hormone (TH)-dependent signalling on intestinal tumour development and progression through action on stem cells. Also, they showed that the thyroid hormone nuclear receptor TRα1 is up-regulated in human CRCs, including the molecular subtypes associated with CSC features. We took advantage of the spheroid model generated during this thesis (summarised in paper Nº 1) from the human colon adenocarcinoma cell line Caco2. We aimed to study the action of the hormone T3 and TRα1 in the spheroids' formation, growth and response to conventional chemotherapies.

First of all, we analysed the effect of T3 treatment during the spheroids formation by adding it into the medium. Using several cellular and molecular techniques, we observed that the presence of T3 during the formation process increased their size and favoured the appearance of bigger lumens due to increased cell proliferation. We also performed an RNA-seq analysis on the spheroids treated with T3 for 24h. Importantly, we observed that T3 also increased the expression and the number of the ABC-transporters expressing cells (like ABCB1 and ABCG2) and that of ALDH1A1-expressing CSCs.

As a second step, to investigate the role of TRα1 in modulating the spheroid's growth and the CSC biology, we modulated the TRα1 expression in Caco2 cells before using them to generate the spheroids. We obtained TRα1 gain of function (TRα1-GOF) spheroids and TRα1 loss of function spheroids (TRα1-KD). We observed stimulatory functions of TRα1 on the spheroid's development and growth in the TRα1-GOF while the TRα1-KD spheroid's growth was strongly blunted independently of the presence or not of T3. Interestingly, the overexpression of TRα1 induced a compact spheroid morphology organised in multilayered cells that can partially be

reverted by T3 treatment. The TRα1-GOF phenotype is correlated with the increased expression of several CSC markers and, similarly to T3 treatment, the ABC transporters.

As we observed an increase in the expression of two drug efflux transporters in the T3/TRα1-GOF spheroids, we investigated if the T3 and different levels of TRα1 expression may influence the response to the commonly used chemotherapy in CRCs. Therefore, we firstly studied the impact of the T3 treatment (or not) during the spheroid's formation in the chemotherapeutic response to FOLFOX or FOLFIRI. We observed a differential response to FOLFOX and FOLFIRI in the presence or not of T3, both morphologically and at the molecular level. Indeed, FOLFOX-treated spheroids significantly decreased their volume in both CTRL and T3 conditions. On the other hand, FOLFIRI-treated spheroids presented a more conserved structure, whereas T3 FOLFIRI spheroids presented a more conserved morphology than the CTRL FOLFIRI**.** Additionally, we performed a RNA-seq study to define the molecular mechanisms responsible for the phenotype of the spheroids in the presence or absence of T3 in combination with the chemotherapies. Because FOLFIRI combined with T3 resulted in a resistant phenotype, we started a more in-depth analysis of data obtained with FOLFIRI. Interestingly, unique sets of up-regulated genes upon combining T3 with FOLFIRI include genes involved in the control of cell metabolism and energy production, transcytosis/endocytosis, and cell junctions. The uniquely down-regulated genes in T3-FOLFIRI are associated with stress response, cell cycle regulation, cell division and DNA metabolism. Furthermore, similar to aforementioned data, we observed a significantly increased expression of ABC transporters in the T3 NT and T3 FOLFIRI spheroids. We also evaluated the expression of these same markers in the spheroids with different TRα1 expression levels and overall confirmed the results obtained by T3/FOLFIRI treatments, underlining the need for T3 to induce the ABC transporters. Altogether, these studies showed that T3 pre-treatment during the spheroids' formation primes the cells toward a resistant phenotype, linked to increased expression of ABC transporters, responsible for stimulated detoxification. This phenotypical advantage conferred by T3 depends on drug combination, favouring the persistence of CSC-like cells in the presence of FOLFIRI but not of FOLFOX.

Manuscript in preparation

Impact of the thyroid hormone T3 and of its nuclear receptor TRα1 on colon cancer stem cell biology and response to chemotherapies

Maria Virginia Giolito[1,2], Serguei Bodoirat[1], Theo La Rosa[2,#], Gabriela D. A. Guardia[3], Pedro A. F. Galante[3], Luiz O. F. Penalva[4] and Michelina Plateroti[1,2,*].

1: Université de Strasbourg, Inserm, IRFAC/UMR-S1113, FMTS, 67200, Strasbourg, France. 2: Centre de Recherche en Cancérologie de Lyon, INSERM U1052, CNRS UMR5286, Université de Lyon, 69000 Lyon, France. 3: Centro de Oncologia Molecular, Hospital Sírio-Libanês, São Paulo, Brazil. 4: Children's Cancer Research Institute, University of Texas Health Science Center at San Antonio, USA. 8: Department of Medical Oncology, Centre Léon Bérard, Lyon, France. #: current address, Stem-Cell and Brain Research Institute, U1208 INSERM, USC1361 INRA, 69675 Bron, France.

*: Corresponding author
Mailing address: Mailing address: INSERM U1113, 3 avenue Molière, 67200 Strasbourg – France
Tel: 33 3 88 27 53 56
E-mail: plateroti@unistra.fr

ABSTRACT

Colorectal cancers (CRCs) are strongly heterogeneous and show a hierarchical organization with the presence of cancer stem cells (CSCs) responsible for tumor development, maintenance and resistance to drugs. Our previous studies showed the importance of the thyroid hormone-dependent signaling on intestinal tumor development and progression through action on stem cells. This results have a translational value, given that the thyroid hormone nuclear receptor TRα1 is up-regulated in human CRCs, including the molecular subtypes associated with CSC features. We took advantage of a reliable spheroid model generated from the human colon adenocarcinoma cell line Caco2 to study the action of the hormone T3 and of TRα1 in formation, growth and response to conventional chemotherapies. Our results show that T3 treatment and/or increased TRα1 expression in spheroids impair the response to the chemotherapy FOLFIRI and confer a survival advantage. This is achieved through a stimulation of the detoxification pathways that is responsible for an increase in CSCs within the spheroids.

INTRODUCTION

Colorectal cancer (CRC) is the second leading cause of cancer death worldwide [1]. The development of CRC results from a progressive acquisition and accumulation of genetic mutations and epigenetic alterations [2,3], including oncogenes' activation and tumor suppressor genes' inactivation [3,4]. Moreover, non-genetic factors (*e.g.,* the microenvironment) can promote the oncogenic transformation and participate in the evolution of CRCs [5].

A high level of heterogeneity and complexity can be observed within CRCs. The heterogeneity of cells that compose the CRCs, including the undifferentiated cancer stem cells (CSCs) and differentiated tumor-bulk cells, are reminiscent of the normal colon crypt organization [6,7]. CSCs are a dynamic population continuously shaped by a convergence of genetic, epigenetic, and microenvironmental factors [6,8]. Thus, they are responsible for tumor appearance [9], its maintenance and growth, and metastatic capacity [10]. Moreover, the CSCs have also been considered the cells that persisted during and after chemotherapeutic treatment [6,7]. Therefore, a better understanding of cancer biology, tumor progression and acquisition of resistance to therapy is of fundamental importance.

Thyroid dysfunction has been associated with several types of cancer, including CRC [11]. Even though there are conflicting epidemiological studies about the involvement of thyroid hormones (TH) in CRC, most of them point toward hyperthyroidism and TH supplementation as predisposing risk factors for CRC patients [12–15]. Our laboratory has largely contributed to the field, by studying the function of the THs and their nuclear hormone receptor TRα1 in the intestinal physiology and CRC. The targeted expression of TRα1 in the mouse intestinal epithelium in an Apc-mutated background is responsible for accelerating tumor appearance, progression, and aggressiveness compared to the simple Apc mutants alone [16]. Additional work demonstrated for the first time, the up-regulation of the *THRA* gene and of TRα1 receptor in human CRCs as well as the direct correlation between TRα1 and the Wnt pathway in this same context [17]. Only few data, however, described the involvement of THs and TRα1 in the response to chemotherapy.

Resistance to chemotherapeutic treatments in CRC contributes to the bad outcome of this cancer type. Even though, since the late 50s, 5-fluorouracil (5-FU) has constituted the backbone of CRC chemotherapeutic regimens, patients' responses to treatment with 5-FU as a single agent are limited and only less than one-third of patients who received 5-FU as a single agent showed some responsiveness. Combining 5-FU with Oxaliplatin- or Irinotecan-based therapies, named respectively FOLFOX and FOLFIRI [18], ameliorates the responsive rate by 50%. Additionally, targeted therapies like cetuximab and panitumumab alone are efficient only in approximately 10% of cases, but they are more effective when combined with classical chemotherapy. Nevertheless, despite the slight increase in chemotherapy response observed with drug combinations and targeted therapies, resistance mechanisms were extensively observed in CRCs for all type of treatments. Importantly, resistance to FOLFOX and FOLFIRI can be due to several mechanisms including alteration of drug metabolism, detoxification, DNA repair, adaptation to stressful conditions [19–22]. Multidrug resistance is a serious problem and it is considered one of the major causes of chemotherapy

failure and is often associated with the overexpression of ATP-binding cassette (ABC) transporter proteins, such as ABCB1 and ABCG2 [23].

Most of the functions altered in response to treatments, including the expression of the ABC transporters, are regulated by the THs and/or TRs in the intestine or in other organs [24–27]. These observations and the already demonstrated action of this same pathway in intestinal stem cells and in CRCs prompted us to analyze its role in the CSC biology. For this aim we analyzed their interference with the chemotherapeutic response to FOLFOX and FOLFIRI. Taking advantage of a spheroid model developed by our laboratory [28], we evaluated the role of TH and of altered TRα1 levels in spheroid's development and their response to chemotherapy. We observed that T3 treatment or TRα1 up-regulation not only favors the spheroid's formation and growth but also confers a differential response to the chemotherapy regimen FOLFIRI, resulting in the acquisition of a persistent phenotype.

Experiments ongoing. During the last period of this thesis, efforts will focus on the studies of the mechanisms involved in the resistant phenotype, including the analysis of the ABC transporters and the metabolism of the drugs.

MATERIALS AND METHODS

Cell culture

The human adenocarcinoma cell line Caco2 (from ATCC) was cultured in DMEM Glutamax (4,5 g/l D-Glucose with pyruvate) medium (Gibco) supplemented with 10% heat-inactivated fetal bovine serum (FBS) and 1% penicillin/streptomycin (P/S) (Gibco) at 37 °C in a humidified atmosphere containing 5% CO2.

Spheroids culture

Spheroids were generated, cultured, and harvested as indicated in [28]. Briefly, 600 Caco2 cells per spheroids were seeded in an Aggrewell plate (StemCell Technologies) and cultured for 48 hs before harvesting. Then, the spheroids were placed in agarose-coated plates for successive analyses. For the evaluation of T3 response, during the 48 hs of spheroids' formation, 10^{-7} M T3 (Sigma) was added to the spheroids culture medium. After harvesting, all spheroids were cultured in the same spheroid medium (DMEM supplemented with 2.5% Matrigel -Corning-, 10% FBS and 1% P/S).

The growth of spheroids was monitored under a Zeiss Axiovert inverted microscope. Representative pictures of spheroids in the different conditions along the days in culture were analyzed using ImageJ software. Three representative diameters of each structure were measured, and the sphere volume formula was used to obtain the estimated volume of the spheroids, as indicated in [28].

Treatment of spheroids with chemotherapeutic drugs

Spheroids were harvested after 48 hs of formation in the presence or absence of T3 (10-7 M) and plated in agarose-coated plates. One day after harvest from Aggrewell (D3), they were treated with FOLFIRI (5-FU, 50 µg/mL; Irinotecan (IRI), 100 µg/mL; Leucovorin (LV), 25 µg/mL) or with FOLFOX (5-FU, 50 µg/mL; Oxaliplatin (OXA), 10 µg/mL; LV, 25 µg/mL) chemotherapies, routinely used to treat CRC patients [18,29], or maintained in control not treated (NT) condition.

TRα1 expression modulation

The studies were performed on the human colon adenocarcinoma cell line Caco2, clone TC7 [30]. For the loss-of-function experiments, sh-RNA lentiviral vectors Mission-shRNA (derived from pLKO.1-puro, Sigma) were used. The Sh sequences targeting TRα1 are listed in Table S1. For overexpression experiments, the TRα1 cDNA was inserted in Mission® pLKO.1-puro vector (Sigma). The lentiviral particles were produced by the AniRA facility (SFR Biosciences, Lyon). The cells were cultured in the presence of the lentiviral vectors for 24h and maintained for additional 24h before using them to generate the corresponding spheroids.

Immunofluorescence and histological staining.

For histology and immunofluorescence analyses, the spheroids were collected at different time points and fixed in 2% PFA before inclusion in paraffin for sectioning, and hematoxylin & eosin (H&E) staining. Paraffin inclusions and sections were performed by the Anipath Recherche facility (CRCL/CLB). 5-µm thick sections were used for indirect immunostaining. Briefly, the sections were deparaffinized in methylcyclohexane, hydrated in ethanol (100%, 90%, and 75%), and washed with PBS. The slides were subsequently subjected to antigen

retrieval using Tinto Retriever Pressure Cooker (Bio SB) in 0.01 M citrate buffer, pH 6, and incubated for one hour at room temperature with blocking buffer (10% normal goat serum, 1% BSA, and 0.02% Triton X-100 in PBS). The slides were then incubated with primary antibodies overnight at 4°C, followed by incubation with fluorescent secondary antibodies (Alexa Fluor, Life Technologies, 1:1000). Finally, slides were mounted using a fluoro-gel mounting medium with DAPI (Interchim, FP-DT094B). The antibodies used are indicated in Table S2. Fluorescence microscopy and imaging were performed on a Zeiss Axio Apotome 2 Imager M2.

RNA extraction and RTqPCR analysis

Total RNA was extracted using the Nucleospin RNA XS Kit (Macherey-Nagel). To avoid contamination by DNA, DNase digestion was performed on all preparations. According to the manufacturer's instructions, reverse transcription was performed with the iScript reverse transcriptase (Bio-Rad) on 500 ng of total RNA. For qPCR approaches, the SYBR qPCR Premix Ex Taq II (Tli RNaseH Plus) (Takara) was used in a CFX connect apparatus (Biorad). Specific mRNA expression was quantified using the ΔCt/$\Delta\Delta$Ct method, and values were normalized to *PPIB* levels. Primers are listed in Table S1.

Transcriptome analysis

Sample preparation for sequencing. (1) Study the effect of T3 during spheroids formation: we generated the spheroids in Aggrewell plates [28] treated or not with 10^{-7} M T3 for 24 h before recovering them. (2) Study the combined effect of T3 and chemotherapies: for the chemotherapy-treated spheroids, the spheroids were generated in the presence or absence of T3 for 48 h before harvesting them. They were then transferred to agarose coated plates and treatments with FOLFOX or FOLFIRI started 24 h after harvesting for a total of 72 h. Spheroids in the different conditions were recovered as dry pellets and used for RNA extraction and sequencing (Active Motif RNA-seq service; www.activemotif.com). The analyses included: a) Isolation of total RNA, b) Assessment of RNA quality/integrity using an Agilent Bioanalyzer, c) Directional library generation and QC of NGS library, d) Next-generation sequencing using the Illumina platform. The data were successively analyzed to define differentially expressed genes (DEG) by performing different types of comparisons.

Sequencing and Analysis

1. Read Mapping: The paired-end 42 bp sequencing reads (PE42) generated by Illumina sequencing (using NextSeq 500) are mapped to the genome using the STAR algorithm with default settings. Alignment information for each read is stored in the BAM format.
2. Fragment Assignment: The number of fragments overlapping predefined genomic features of interest (e.g. genes) are counted. Only read pairs that have both ends aligned are counted. Read pairs that have their two ends mapping to different chromosomes or mapping to same chromosome but on different strands are discarded. The gene annotations we use were obtained from Subread package. These annotations were originally from NCBI RefSeq database and then adapted by merging overlapping exons from the same gene to form a set of disjoint exons for each gene. Genes with the same Entrez gene identifiers were also merged into one gene.

3. Differential Analysis: After obtaining the gene table containing the fragment counts of genes, we perform differential analyses to identify statistically significant differential genes using DESeq2. The following lists the pre-processing steps before differential calling.
    a. Data Normalization: DESeq2 expects un-normalized count matrix of sequencing fragments. The DESeq2 model internally corrects for library size using their median-of- ratios method. The gene table obtained from Analysis Step 2) is used as input to perform the DESeq2's differential test.
    b. Filtering before multiple testing adjustment: After a differential test has been applied to each gene except the ones with zero counts, the p-value of each gene is calculated and adjusted to control the number of false positives among all discoveries at a proper level. This procedure is known as multiple testing adjustment. During this process, DESeq2 by default filters out statistical tests (i.e. genes) that have low counts by a statistical technique called independent filtering. It uses the average counts of each gene (i.e. baseMean), across all samples, as its filter criterion, and it omits all genes with average normalized counts below a filtering threshold from multiple testing adjustment. This filtering threshold is automatically determined to maximize detection power (i.e. maximize the number of differential genes detected) at a specified false discovery rate (FDR). In the spreadsheet listing the summary of statistics (DESeq2_stats.xlsx), one can refer to "Genes with low counts" to get an idea of how many genes were omitted in the process of multiple testing adjustment. The spreadsheet "DESeq2_results_allgene.csv", lists all genes, including genes with weak signals have valid p-values but "NA" adjusted p-values.
    c. Differential Calling: In an experiment with replicates, differential genes are detected by DESeq2 at 0.1 (or 10%) FDR (i.e. adjusted p-value). In an experiment without replicates, differential genes are defined using shrunkenLog2FC cutoff off 0.3. This 0.3 cutoff is arbitrary, and it is best to interpret the results with prior biological knowledge.

Additional bioinformatics analyses

Differential gene expression analysis. Using FASTq files from RNA-seq assays, we quantified gene expression using Kallisto (v0.43.1) [31] and the R package tximport (v1.0.3) [32]. GENCODE (v37, https://www.gencodegenes.org) was used as reference for the human transcriptome. Differential gene expression analyses between groups were performed with DESeq2 v3.6.2 [33]. Genes with $|\log2FoldChange| \geq 0.5$ and adjusted p-value (FDR) < 0.05 were considered as differentially expressed.

Gene Ontology and Pathway analysis. Genes that were determined to be differentially expressed in the drug treatment (FOLFIRI, FOLFOX or T3) analyses were evaluated with ShinyGO and Metascape to identify enriched biological processes and pathways, and drug treatments producing similar results [34,35].

Statistical Analysis

Statistical analyses were conducted using GraphPad Prism software (version 8; GraphPad Software Inc., San Diego, Calif., USA). The Student t-test (unpaired, 2-tailed) was performed to analyze the statistical significance between groups, and the level of significance was established as a p-value < 0.05.

RESULTS AND DISCUSSION

Effect of the T3 in spheroids' formation and growth

To study the effect of the thyroid hormones T3 in the growth properties of Caco2-derived spheroids, we maintained the cultures in control (CTRL) or treated with 10^{-7}M T3 (T3) during the 48h of spheroids' formation. They were recovered and transferred to agarose-coated plates, and their growth was then followed throughout the experimental time course by measuring their volume [28,36] (experimental plan summarized in **Figure 1A, upper panel**). From the beginning of the monitoring and at each time point, the T3 spheroids presented a significantly higher volume than the CTRL spheroids, with the size increasing during the time in culture (**Figure 1A, 1B).** To further analyze the features of the spheroids, we also recovered them at different time points for a detailed histological and immunofluorescent (IF) analysis on paraffin sections, as well as for molecular analysis. The hematoxylin and eosin (H&E) staining showed that the spheroids underwent changes in their organization and shape over the days. Indeed, both CTRL and T3 spheroids presented cells densely arranged in multilayers at D3, while at D10 several zones were arranged in monolayers. Also, in both cases a lumen appeared within the spheroids from D5 onwards but, accordingly with the volume data (Figure 1B), it was bigger in the T3 compared to the CTRL spheroids (**Figure 1C**).

As the phenotypical differences linked to T3 appeared at early stage of spheroid formation and based in our previous work in mouse enteroids [37], we decided to perform an RNA-seq analysis to have a better appreciation of the molecular events induced by a short period of T3 treatment. For this aim, T3-treated and CTRL spheroids formed during 48 h and received T3 for 24 h before recovering for the RNA-seq. By comparing the T3 *vs* CTRL condition (log2 fold change > 0.5, P-value < 0.05) we retained 227 up-regulated and 67 down-regulated genes. Clustering analysis in **Figure S1** shows the 20 most up- and down-regulated genes. Among the up regulated genes we noticed known TH target genes such as *KLF9* and *HR* [38,39], *DIO1* which is linked to metabolism of THs [40,41] and several ABC transporters. Among the downregulated genes we found genes linked to cell signaling through FGF (*FGF13*) or TGFβ (*LDLRAD4*), lipid metabolism (*MOGAT2*) and calcium ion sensing (*OTOF*). Gene Ontology (GO) and pathways analyses (log2 fold change > 1, P-value < 0.05) are listed in **Table S3** for up-regulated genes while no enrichment was observed for the down-regulated genes with the filters applied.

Complementary RTqPCR and IF analyses completed this study. We already demonstrated that the spheroids are a reliable tool for studying CSC biology [28], so we wanted to determine if the T3 may impact the expression of some CSC markers. For that, we analyzed the mRNA levels of *EPHB2* [42],*TERT* [43] and *ALDH1A1* [44,45]. In addition, we included *ABCG2* and *ABCB1*, two ATP-biding cassette transporters involved in CSC biology and drug resistance [32], and *TRα1,* the T3 nuclear receptor which is present in the intestinal crypts and in CRCs [17,46]. In control NT condition, the expression of the CSC markers *EPHB2, TERT* and *ALDH1A1* changed slightly during the days in culture and a similar behaviour was observed for TRα1. T3 did not affect or decreased their expression at specific time-point. For D7, in particular we observed a decrease in the expression of the CSC markers in the T3 condition that was correlated with a reduction in TR*α*1 expression (**Figure 2A**). The expression of *ABCG2* remained stable during the time in culture and was strongly stimulated by T3 at all-time

points. *ABCB1* mRNA levels strongly increased between D3 and D7 and showed an important up-regulation by T3 at D3 and D5 (**Figure 2A**).
We studied the proliferation and apoptosis in the spheroids by IF using the proliferation marker PCNA and the cell death marker activated-caspase 3, both analyzed at D7. The labeling for PCNA revealed that proliferating cells are located at the external surface of the spheroids, sometimes in crypt-like or bud-like structures reminiscent of the organoid cultures [47] (**Figure 2B upper panels**). In T3 condition there was a higher number of PCNA-positive cells. Surprisingly, very few activated-caspase 3-positive cells were observed in the spheroids, with slightly more apoptotic cells in the CTRL than the T3 **(Figure 2B upper panels).** We then analyzed the CSC marker ALDH1A1 and the ABC transporters ABCG2 and ABCB1. First of all, we noticed that ALDH1A1 positive cells were present all over the spheroids but more strongly associated with the external surface. They were organized in patches, and the levels of expression varied between the cells (**Figure 2B, middle panels**), with more positive cells in the T3 condition than in the CTRL. In accordance to what we observed at the mRNA level, the T3 spheroids presented an increase in ABCG2- and ABCB1-expressing cells, which are localized in both the external surface of the spheroids and in the internal layers surrounding the lumens (**Figure 2B, middle and lower panels**).
Taken together, the presence of T3 during the process of spheroid formation increased their size and favored the appearance of bigger lumens. This is due to the T3-dependent increase of cell proliferation. The increased cell proliferation might be related to the up-regulation of the oncogene FOS (P-value 4.15E-02) and of TERT (P-value 8.62E-14) in T3-spheroids. Importantly, and in accordance with the RNA-seq study, T3 also increased the expression and the number of the ABC-expressing cells as well as that of ALDH1A1-expressing CSCs.

Effect of altered TRα1 levels in spheroids formation and growth
To investigate the role of TRα1 in modulating the spheroid's growth and the CSC biology, we modulated the TRα1 expression in Caco2 cells before using them to generate the spheroids. The parental cell line has been engineered by lentiviral-mediated TRα1 expressing or silencing (Sh-RNA) particles enabling the development of TRα1 gain-of-function (TRα1-GOF) and loss-of-function Caco2 cell lines (Sh1 and Sh2) and their corresponding control conditions (hereafter called, iCTRL and Sh-scr) for the TRα1-GOF and the TRα1-KD respectively.
First, we investigated if the presence of T3 in the forming step of the TRα1-GOF impacted the spheroids' growth, similar to what we observed in the T3 spheroids. Again, we measured the spheroids volume throughout the days in culture and recovered samples for histological and immunolabeling analyses (H&E and IF) and RTqPCR. We observed that the TRα1-GOF *per se* stimulated the growth of the spheroids at all time points and, similar to what we observed previously, the presence of T3 in iCTRL induced the size of spheroids that was further increased in T3-treated TRα1-GOF cultures **(Figure 3A and 3B, Figure S2A and S2B)**. Surprisingly, the TRα1-GOF spheroids showed a compacted multilayered structure at all timepoints with small or absent lumens. However, when T3 was added during the formation of the spheroids, the lumens were evident and bigger (**Figure 3C**). The morphology of the iCTRL spheroids showed the same changes previously shown for the CTRL/T3 spheroids (**Figure S2C**).

RTqPCR analyses confirmed the increase of TRα1 mRNA in TRα1-GOF spheroids and, similar to what observed before, in iCTRL condition *TRα1* expression slightly increased during the days in culture and was down-regulated by T3 at D7. In TRa1-GOF spheroids, the expression of TRa1 was stable at almost all time points with a pick at D5. T3 had any effect at all time points analyzed (**Figure 3D**). When we analyzed the CSC markers, the expression of *EPHB2* showed essentially no changes along the days in culture in iCTRL, iCTRL T3, and TRα1-GOF conditions. However, the presence of T3 in the TRα1-GOF condition increased *EPHB2* levels at all time points. On the other hand, *TERT* expression in both control conditions, iCTRL and TRa1-GOF, increased with the time in culture and was T3-responsive at D10 (**Figure 3D**). *ALDH1A1* mRNA levels were not changed in the different conditions and time in culture. The levels of *ABCB1* and *ABCG2* drug transporters increased over the days, showing a significantly increased expression in the iCTRL T3 and TRα1-GOF T3 conditions at all studied times (**Figure 3D**).

Next, we analyzed by IF whether the TRα1 alteration could affect the proliferation and cell death (D3 and D7) and the expression of ALDH1A1, ABCB1 and ABCG2 (D7). We observed a high number of PCNA-labeled cells at both time points, with a prominent localization in the external surface of the spheroids. T3-treatment increased the number of PCNA-positive cells in both iCTRL and TRα1-GOF conditions (**Figure 4A**). When we analyzed the cell death, more activated-caspase 3-positive cells were present in the spheroids, especially at D7, in particular in the TRα1-GOF compared to the iCTRL **(Figure 4A).** This can be due to the increased size and turnover. The ALDH1A1 labeling was heterogeneous in distribution and intensity in all conditions (**Figure 4B, lower panels**), with no apparent changes observed, similar to what observed at mRNA level (**Figure 3D**). ABCG2- and ABCB1-expressing cells were higher in number in the T3 conditions independently of the TRα1 levels (**Figure 4B, lower and upper panels**). ABCG2-positive cells in TRα1-GOF condition presented a distribution all around the spheroids and not limited to the more external layers (**Figure 4B, lower panels**).

In addition, we analyzed the effect of TRα1 silencing in the spheroids. As expected, we observed that the spheroid's growth was strongly blunted for the Sh1 and Sh2 independently of the presence or not of T3 (**Figure S3A, S3B**). The TRα1 expression levels were diminished in Sh1 and Sh2 compared with the Sh-scr condition. Contrary to what observed before, T3 stimulated TRα1 expression in Sh-Scr organoids **(Figure S3C)**. H&E analysis of the Sh1 and Sh2, compared with the Sh-scr spheroids, revealed smaller and compact multilayered structure un-responsive to T3 **(Figure S3D).** These results correlate with our previous work where we demonstrated, in 2D Caco2 cells, that the depletion of TRα1 levels affected cell growth and migration [17].

Altogether, these results point to the stimulatory functions of TRα1 on development and growth of the spheroids. Interestingly, the overexpression of TRα1 induces a compact spheroid morphology organized in multilayered cells that can partially be reverted by T3 treatment. This phenotype is correlated with the increased expression of several CSC markers and the ABC transporters. It can be speculated that TRα1-GOF condition, under physiological T3 concentration, induces cell proliferation. Supraphysiological levels of T3 in this condition, favours the organization of monolayers of polarized cells.

T3 and TRα1 levels modulate the response to chemotherapy in spheroids

As we observed an increase in the expression of two drug efflux pumps in the T3 spheroids, we investigated if the presence of T3 and different levels of TRα1 expression may influence the response to the commonly used chemotherapy in CRCs. Therefore, we firstly studied the impact of the T3 and treated or not the spheroids in the forming step with T3. 24h after the harvesting (D3), we maintained the spheroids in control not treated (NT) condition or they were treated with FOLFOX or FOLFIRI for 72h. Every 24h hours, we measured the changes in their volume [28,36], compared with the initial volume at D3. The FOLFOX treated spheroids showed a significant decrease in their volume for both CTRL and T3 conditions at 48h and 72h (**Figure 5A, left panel).** Morphologically, after 72h treatment with FOLFOX, in both CTRL and T3 conditions, the spheroids' appeared similarly affected, and detached most probably dead cells, were present in the plates (**Figure 5B, middle panels**). FOLFIRI-treated spheroids in control condition decreased the volume at both 48h and 72h. T3 showed minor and non-significant effect at 24h and 48h but rescued the size at the control level at 72h (**Figure 5A, right panel**). These observations were confirmed at morphological level (**Figure 5B, left panels**).

To better appreciate the histology and the features of the spheroids in the different conditions, we recovered them after 72h of treatment with the chemotherapies for H&E staining and IF analysis on paraffin sections and for molecular analysis. H&E staining showed similar morphology for the NT spheroids as before, with some cells arranged in multilayers and others in flat monolayers with internal lumens (**Figure 5C, right panels**). As already shown, CTRL-NT spheroids present fewer lumens slightly smaller than the T3-NT (**Figure 5C, right panels**). The FOLFOX spheroids, regardless of the condition, presented an amorphous shape with smaller size (**Figure 5C, middle panels**). In the case of FOLFIRI treatment, the CTRL-FOLFIRI spheroids presented a multi-layered morphology with small lumens (**Figure 5C, right panels**). In contrast, the T3-FOLFIRI spheroids maintained an almost intact morphology of mixed multilayered and monolayered zones with the presence of internal lumens **(Figure 5C, right panels).**

To define the molecular mechanisms responsible for the phenotype of the spheroids in the presence or absence of T3 in combination with the chemotherapies we conducted an RNA-seq analysis. Figure S4 summarizes the analyses performed to select the differentially up- and down-regulated genes for FOLFIRI (**Figure S4A, left panels**) or FOLFOX (**Figure S4A, right panels**) regimens. Briefly, in FOLFIRI or FOLFOX conditions, up- or down- regulated genes in CTRL and T3 were compared with the CTRL-NT condition (genes expressed in non-treated spheroids), to obtain shared and unique gene sets. Then the T3 modulated genes in the absence of chemotherapies were compared with the CTRL-NT condition, to define genes which are regulated by T3, independently of the chemotherapies. Because FOLFIRI combined with T3 resulted in a resistant phenotype, we started a more in depth analysis on data obtained with FOLFIRI. GO and Metascape analyses were performed on each unique sets and are shown in **Table S4**. FOLFIRI treatment alone resulted in unique sets of up-regulated genes strongly associated with RNA metabolism, probably due to the effect of the 5-FU in altering RNA structure and translation [48,49]. Downregulated genes in FOLFIRI are linked to membrane transporters. Interestingly, unique sets of up-regulated genes upon combining T3 with

FOLFIRI, include genes involved in the control of cell metabolism and energy production, transcytosis/endocytosis and in cell junctions. The uniquely down-regulated genes in T3-FOLFIRI are associated with stress response, cell cycle regulation, cell division and DNA metabolism. **Figure S4B** shows genes up-regulated in T3-FOLFIRI, coding for ABC-drug transporters, the nuclear hormone receptor CAR that is involved in cell detoxification [50] and the CSC markers *LGR5*, *OLFM4* and *CLU* [9,51,52]. Among the down-regulated genes we noticed *TOP1*, coding for the DNA topoisomerase 1, the enzyme targeted by the irinotecan [53] involved in DNA metabolism, *MEX3a* involved in cell polarity [54,55] and *TYMS/TYMP* that are involved in the cellular action of the 5-FU [56].
To complete the study, we performed RTqPCR on spheroids treated with FOLFIRI and maintained in CTRL or T3 conditions. We analyzed the same CSC markers as for the previous experiments, TRα1 and the ABC transporters. We did not observe any difference in *EPHB2* and *ALDH1A1* expression in the NT condition between the control and T3 spheroids (**Figure 6A**). FOLFIRI-treated spheroids presented a strong decrease in EPHB2 expression that was significantly up-regulated by T3, while ALDH1A1 had an expression level in FOLFIRI similar to NT condition, but its expression was stimulated by T3 (**Figure 6A**). In the case of *TERT*, T3 spheroids showed an increased expression of this marker in both NT and FOLFIRI, even if its expression was down-regulated by FOLFIRI alone (**Figure 6A**). When we evaluated the expression of *TRα1* in the spheroids, we noticed an increased expression induced by FOLFIRI treatment in both NT and T3 conditions, even if there wasn't any differences between CTRL and T3 (**Figure 6A**). Additionally, as seen in the previous experiments, we observed a significant increase in *ABCG2* and *ABCB1* expression in the T3 spheroids in both NT and FOLFIRI, but their levels were not affected by FOLFIRI alone (**Figure 6A**). We also evaluated the expression of these same markers in the spheroids with different TRα1 expression levels and overall confirmed the results obtained by T3/FOLFIRI treatments (**Figure S5**).
Finally, we analyzed the proliferation and apoptosis in the treated spheroids by IF using the proliferation marker PCNA and the cell death marker activated-caspase 3. In chemotherapy conditions we observed a clear decrease of PCNA-expressing cells and an increase in apoptotic cells with a clear presence of higher PCNA-positive cells in the T3 FOLFIRI compared with FOLFIRI alone (**Figure 6B upper panels**). We also analyzed the CSC marker ALDH1A1 and the ABC transporters by IF. The ALDH1A1-positive cells are present in patches in different regions of the spheroids, with variable expression levels. Generally, the NT spheroids had the higher number of ALDH1A1-positive cells compared to the treated FOLFIRI spheroids. (**Figure 6B, lower panels**). According to what observed at the mRNA level, the T3 spheroids present a higher number of cells expressing ABCG2 and ABCB1 compared with the respective control conditions, (**Figure 6B, middle and lower panels**).
Altogether, these studies showed that T3 pre-treatment during the spheroids' formation primes the cells toward a resistant phenotype, linked to increased expression of ABC transporters, responsible for a stimulated detoxification. This phenotypical advantage conferred by T3 depends on drug combination, favoring the persistence of CSC-like cells in the presence of FOLFIRI but not of FOLFOX.

Conclusions and perspectives

Our studies aimed to understand and tackle colon cancer biology, the crosstalk between the thyroid hormones and colon CSC, including their impact on the response to chemotherapy.

We demonstrated that the thyroid hormone T3 and the nuclear hormone receptor TRα1, influence the development and growth of spheroids derived from the Caco2 colon adenocarcinoma cell line and their response to the chemotherapeutic agent used for treating CRC patients, FOLFIRI. These findings shed a new light and provide the first evidence of the prognostic value of analyzing the thyroid hormone status of patients for a better choice of a chemotherapeutic treatment.

We observed that the presence of T3 in the forming step of the spheroids primes them in several ways, resulting in the modification of their morphology and molecular features several days after the exposure. Our previous studies showed a “thyroid shock” in mouse intestinal organoids treated with T3 [37] also responsible for a high metabolic reprogramming and the modifications of SC markers. Similarly, in the T3-spheroids, we observed the induction of a bigger size and differential expression of some CSC markers along the day in culture. The most striking observation in this study is that T3-spheroids increased the expression of two ABC transporters, ABCB1 and ABCG2, well-known drug efflux pumps involved in drug resistance [23,57]. The overexpression of TRα1 in this setting showed similar results and underlined the need of T3 to induce the ABC transporters. Last, but not least, the regulation of ABCB1 by T3/TRα1 has already been shown [26,58,59] but there were no informations regarding ABCG2. An in-silico research of putative nuclear hormone receptor binding sites (Nubiscan), suggested a DR4-type sequence present within 8 Kb of the *ABCG2* promoter. It will be of importance to define if this DR4 is a true TR-binding site.

Author contributions

MVG: conception and design, collection and assembly of data, data analyses and interpretation, manuscript writing; **SB:** collection and assembly of data, data analyses and interpretation; **TLR:** collection and assembly of data, data analyses and interpretation; **GDAG**, **PAFG, LOFP**: collection and assembly of data, data analyses, and interpretation; **MP**, conception and design, assembly of data, data analyses, and interpretation, manuscript writing, financial support.

Acknowledgements

We are grateful to Erwan Pencreach and the pharmacy of the Strasbourg University Hospital for the chemotherapeutic agents. We acknowledge the Anatomopathology recherche platform (CRCL/CLB, Lyon, France). We are grateful to the AniRA lentivectors production facility from the CELPHEDIA Infrastructure and SFR Biosciences (Lyon, France).

Funding sources

The work was supported by the FRM (Equipes FRM 2018, DEQ20181039598), by the Inca (PLBIO19-289), and by the Ligue Contre le Cancer, Département Grand Est (01X.2020). MVG and TLR received support from the FRM and SB by the Inca. GDAG was supported by a fellowship from FAPESP (2017/19541-2).

Conflicts of interest

The authors have no competing interests.

BIBLIOGRAPHY

1 Sung H, Ferlay J, Siegel RL, Laversanne M, Soerjomataram I, Jemal A & Bray F (2021) Global Cancer Statistics 2020: GLOBOCAN Estimates of Incidence and Mortality Worldwide for 36 Cancers in 185 Countries. *CA Cancer J Clin* **71**, 209–249.

2 Fearon ER & Vogelstein B (1990) A genetic model for colorectal tumorigenesis. *Cell* **61**, 759–767.

3 Rao C V & Yamada HY (2013) Genomic instability and colon carcinogenesis: from the perspective of genes. *Front Oncol* **3**, 130.

4 Fearon ER (2011) Molecular genetics of colorectal cancer. *Annu Rev Pathol Mech Dis* **6**, 479–507.

5 Hanahan D (2022) Hallmarks of Cancer: New Dimensions. *Cancer Discov* **12**, 31–46.

6 Batlle E & Clevers H (2017) Cancer stem cells revisited. *Nat Med* **23**, 1124–1134.

7 Clevers H (2011) The cancer stem cell: premises, promises and challenges. *Nat Med* **17**, 313—319.

8 Zeuner A, Todaro M, Stassi G & De Maria R (2014) Colorectal cancer stem cells: From the crypt to the clinic. *Cell Stem Cell* **15**, 692–705.

9 Barker N, Ridgway RA, van Es JH, van de Wetering M, Begthel H, van den Born M, Danenberg E, Clarke AR, Sansom OJ & Clevers H (2009) Crypt stem cells as the cells-of-origin of intestinal cancer. *Nature* **457**, 608–611.

10 Ayob AZ & Ramasamy TS (2018) Cancer stem cells as key drivers of tumour progression. *J Biomed Sci 2018 251* **25**, 1–18.

11 Krashin E, Piekiełko-Witkowska A, Ellis M & Ashur-Fabian O (2019) Thyroid hormones and cancer: A comprehensive review of preclinical and clinical studies. *Front Endocrinol (Lausanne)* **10**, 59.

12 Wu CC, Islam MM, Nguyen PA, Poly TN, Wang CH, Iqbal U, Li YC & Yang HC (2021) Risk of cancer in long-term levothyroxine users: Retrospective population-based study. *Cancer Sci* **112**, 2533–2541.

13 Iishi H, Tatsuta M, Baba M, Okuda S & Taniguchi H (1992) Enhancement by thyroxine of experimental carcinogenesis induced in rat colon by azoxymethane. *Int J Cancer* **50**, 974–976.

14 Wändell P, Carlsson AC, Li X, Sundquist J & Sundquist K (2020) Levothyroxine treatment is associated with an increased relative risk of overall and organ specific incident cancers - a cohort study of the Swedish population. *Cancer Epidemiol* **66**.

15 Boursi B, Haynes K, Mamtani R & Yang YX (2015) Thyroid Dysfunction, Thyroid Hormone Replacement and Colorectal Cancer Risk. *JNCI J Natl Cancer Inst* **107**.

16 Kress E, Skah S, Sirakov M, Nadjar J, Gadot N, Scoazec JY, Samarut J & Plateroti M (2010) Cooperation Between the Thyroid Hormone Receptor TRα1 and the WNT Pathway in the Induction of Intestinal Tumorigenesis. *Gastroenterology* **138**, 1863–1874.

17 Uchuya-Castillo J, Aznar N, Frau C, Martinez P, Le Nevé C, Marisa L, Penalva LOF, Laurent-Puig P, Puisieux A, Scoazec JY, Samarut J, Ansieau S & Plateroti M (2018) Increased expression of the thyroid hormone nuclear receptor TRa1 characterizes intestinal tumors with high Wnt activity. *Oncotarget* **9**, 30979–30996.

18 Wolpin BM & Mayer RJ (2008) Systemic Treatment of Colorectal Cancer.

Gastroenterology **134**, 1296-1310.e1.
19 Briffa R, Langdon SP, Grech G & Harrison DJ (2018) Acquired and Intrinsic Resistance to Colorectal Cancer Treatment. In *Colorectal Cancer - Diagnosis, Screening and Management* IntechOpen.
20 Blondy S, David V, Verdier M, Mathonnet M, Perraud A & Christou N (2020) 5-Fluorouracil resistance mechanisms in colorectal cancer: From classical pathways to promising processes. *Cancer Sci* **111**, 3142–3154.
21 Rajal AG, Marzec KA, McCloy RA, Nobis M, Chin V, Hastings JF, Lai K, Kennerson M, Hughes WE, Vaghjiani V, Timpson P, Cain JE, Watkins DN, Croucher DR & Burgess A (2021) A non-genetic, cell cycle-dependent mechanism of platinum resistance in lung adenocarcinoma. *Elife* **10**.
22 Sazonova E V., Kopeina GS, Imyanitov EN & Zhivotovsky B (2021) Platinum drugs and taxanes: can we overcome resistance? *Cell Death Discov* **7**.
23 Robey RW, Pluchino KM, Hall MD, Fojo AT, Bates SE & Gottesman MM (2018) *Revisiting the role of ABC transporters in multidrug-resistant cancer* Nature Publishing Group.
24 Kurose K, Saeki M, Tohkin M & Hasegawa R (2008) Thyroid hormone receptor mediates human MDR1 gene expression—Identification of the response region essential for gene expression. *Arch Biochem Biophys* **474**, 82–90.
25 Mitin T, Von Moltke LL, Court MH & Greenblatt DJ (2004) Levothyroxine up-regulates P-glycoprotein independent of the pregnane X receptor. *Drug Metab Dispos* **32**, 779–782.
26 Davis PJ, Incerpi S, Lin HY, Tang HY, Sudha T & Mousa SA (2015) Thyroid hormone and P-glycoprotein in tumor cells. *Biomed Res Int* **2015**.
27 Kress E, Rezza A, Nadjar J, Samarut J & Plateroti M (2009) The frizzled-related sFRP2 gene is a target of thyroid hormone receptor α1 and activates β-catenin signaling in mouse intestine. *J Biol Chem* **284**, 1234–1241.
28 Giolito MV, Claret L, Frau C & Plateroti M A Three-dimensional Model of Spheroids to Study Colon Cancer Stem Cells. *JoVE*, e61783.
29 Mohelnikova-Duchonova B, Melichar B & Soucek P (2014) FOLFOX/FOLFIRI pharmacogenetics: the call for a personalized approach in colorectal cancer therapy. *World J Gastroenterol* **20**, 10316–10330.
30 Caro I, Boulenc X, Rousset M, Meunier V, Bourrié M, Julian B, Joyeux H, Roques C, Berger Y, Zweibaum A & Fabre G (1995) Characterisation of a newly isolated Caco-2 clone (TC-7), as a model of transport processes and biotransformation of drugs. *Int J Pharm* **116**, 147–158.
31 Bray NL, Pimentel H, Melsted P & Pachter L (2016) Near-optimal probabilistic RNA-seq quantification. *Nat Biotechnol* **34**, 525–527.
32 Soneson C, Love MI & Robinson MD (2016) Differential analyses for RNA-seq: Transcript-level estimates improve gene-level inferences. *F1000Research* **4**.
33 Love MI, Huber W & Anders S (2014) Moderated estimation of fold change and dispersion for RNA-seq data with DESeq2. *Genome Biol* **15**.
34 Ge SX, Jung D, Jung D & Yao R (2020) ShinyGO: A graphical gene-set enrichment tool for animals and plants. *Bioinformatics* **36**, 2628–2629.
35 Zhou Y, Zhou B, Pache L, Chang M, Khodabakhshi AH, Tanaseichuk O, Benner C & Chanda SK (2019) Metascape provides a biologist-oriented resource for the analysis of systems-level datasets. *Nat Commun* **10**.
36 Mohr JC, Zhang J, Azarin SM, Soerens AG, de Pablo JJ, Thomson JA, Lyons GE, Palecek SP & Kamp TJ (2010) The microwell control of embryoid body

size in order to regulate cardiac differentiation of human embryonic stem cells. *Biomaterials* **31**, 1885–1893.
37 Godart M, Frau C, Farhat D, Giolito MV, Jamard C, Le Nevé C, Freund JN, Penalva LO, Sirakov M & Plateroti M (2021) Murine intestinal stem cells are highly sensitive to modulation of the T3/TRα1-dependent pathway. *Dev* **148**, dev194357.
38 Denver RJ & Williamson KE (2009) Identification of a Thyroid Hormone Response Element in the Mouse Krüppel-Like Factor 9 Gene to Explain Its Postnatal Expression in the Brain. *Endocrinology* **150**, 3935.
39 Chatonnet F, Guyot R, Picou F, Bondesson M & Flamant F (2012) Genome-wide search reveals the existence of a limited number of thyroid hormone receptor alpha target genes in cerebellar neurons. *PLoS One* **7**, e30703.
40 Bianco AC & Kim BW (2006) Deiodinases: Implications of the local control of thyroid hormone action. *J Clin Invest* **116**, 2571–2579.
41 Dentice M, Marsili A, Zavacki A, Larsen PR & Salvatore D (2013) The deiodinases and the control of intracellular thyroid hormone signaling during cellular differentiation. *Biochim Biophys Acta - Gen Subj* **1830**, 3937–3945.
42 Merlos-Suárez A, Barriga FM, Jung P, Iglesias M, Céspedes MV, Rossell D, Sevillano M, Hernando-Momblona X, Da Silva-Diz V, Muñoz P, Clevers H, Sancho E, Mangues R & Batlle E (2011) The intestinal stem cell signature identifies colorectal cancer stem cells and predicts disease relapse. *Cell Stem Cell* **8**, 511–524.
43 Montgomery RK, Carlone DL, Richmond CA, Farilla L, Kranendonk MEG, Henderson DE, Baffour-Awuah NY, Ambruzs DM, Fogli LK, Algra S & Breault DT (2011) Mouse telomerase reverse transcriptase (mTert) expression marks slowly cycling intestinal stem cells. *Proc Natl Acad Sci U S A* **108**, 179–184.
44 Clark DW & Palle K (2016) Aldehyde dehydrogenases in cancer stem cells: potential as therapeutic targets. *Ann Transl Med* **4**, 518.
45 Tomita H, Tanaka K, Tanaka T & Hara A (2016) Aldehyde dehydrogenase 1A1 in stem cells and cancer. *Oncotarget* **7**, 11018–11032.
46 Sirakov M, Kress E, Nadjar J & Plateroti M (2014) Thyroid hormones and their nuclear receptors: New players in intestinal epithelium stem cell biology? *Cell Mol Life Sci* **71**, 2897–2907.
47 Sato T, Vries RG, Snippert HJ, van de Wetering M, Barker N, Stange DE, van Es JH, Abo A, Kujala P, Peters PJ & Clevers H (2009) Single Lgr5 stem cells build crypt-villus structures in vitro without a mesenchymal niche. *Nature* **459**, 262–265.
48 Bash-Imam Z, Thérizols G, Vincent A, Lafôrets F, Espinoza MP, Pion N, Macari F, Pannequin J, David A, Saurin JC, Mertani HC, Textoris J, Auboeuf D, Catez F, Venezia ND, Dutertre M, Marcel V & Diaz JJ (2017) Translational reprogramming of colorectal cancer cells induced by 5-fluorouracil through a miRNA-dependent mechanism. *Oncotarget* **8**, 46219–46233.
49 Chalabi-Dchar M, Fenouil T, Machon C, Vincent A, Catez F, Marcel V, Mertani HC, Saurin J-C, Bouvet P, Guitton J, Venezia ND & Diaz J-J (2021) A novel view on an old drug, 5-fluorouracil: an unexpected RNA modifier with intriguing impact on cancer cell fate. *NAR Cancer* **3**.
50 Timsit YE & Negishi M (2007) CAR and PXR: The Xenobiotic-Sensing Receptors. *Steroids* **72**, 231.
51 van der Flier LG, Haegebarth A, Stange DE, van de Wetering M & Clevers H

(2009) OLFM4 Is a Robust Marker for Stem Cells in Human Intestine and Marks a Subset of Colorectal Cancer Cells. *Gastroenterology* **137**, 15–17.
52 Ayyaz A, Kumar S, Sangiorgi B, Ghoshal B, Gosio J, Ouladan S, Fink M, Barutcu S, Trcka D, Shen J, Chan K, Wrana JL & Gregorieff A (2019) Single-cell transcriptomes of the regenerating intestine reveal a revival stem cell. *Nature* **569**, 121–125.
53 Fuchs C, Mitchell EP & Hoff PM (2006) Irinotecan in the treatment of colorectal cancer. *Cancer Treat Rev* **32**, 491–503.
54 Huang NN & Hunter CP (2015) The RNA binding protein MEX-3 retains asymmetric activity in the early Caenorhabditis elegans embryo in the absence of asymmetric protein localization. *Gene* **554**, 160–173.
55 Pereira B, Sousa S, Barros R, Carreto L, Oliveira P, Oliveira C, Chartier NT, Plateroti M, Rouault JP, Freund JN, Billaud M & Almeida R (2013) CDX2 regulation by the RNA-binding protein MEX3A: impact on intestinal differentiation and stemness. *Nucleic Acids Res* **41**, 3986.
56 Vodenkova S, Buchler T, Cervena K, Veskrnova V, Vodicka P & Vymetalkova V (2020) 5-fluorouracil and other fluoropyrimidines in colorectal cancer: Past, present and future. *Pharmacol Ther* **206**, 107447.
57 Sarkadi B, Homolya L, Szakács G & Váradi A (2006) Human multidrug resistance ABCB and ABCG transporters: Participation in a chemoimmunity defense system. *Physiol Rev* **86**, 1179–1236.
58 Nishio N, Katsura T & Inui K-II (2008) Thyroid hormone regulates the expression and function of P-glycoprotein in Caco-2 cells. *Pharm Res* **25**, 1037–1042.
59 Siegmund W, Altmannsberger S, Paneitz A, Hecker U, Zschiesche M, Franke G, Meng W, Warzok R, Schroeder E, Sperker B, Terhaag B, Cascorbi I & Kroemer HK (2002) Effect of levothyroxine administration on intestinal P-glycoprotein expression: Consequences for drug disposition*. *Clin Pharmacol Ther* **72**, 256–264.

FIGURE LEGENDS

Figure 1: Impact of T3 in the spheroid's formation and growth. A) Representative pictures along the days in culture of the spheroids in different conditions as indicated. Images were taken under a Zeiss Axiovert microscope with a 4X objective. Scale bar: 200 µm. **B)** Estimated volume of the spheroids in culture in the different conditions at different time-points, as indicated. Violin plots show frequency distribution of the data, bold dotted lines indicate the median and light dotted lines indicate the quartiles, n = 12-14. Black spheres indicate the size of individual spheroids. **, *P*<0.01 and ***, *P*<0.001 compared to CTRL condition, by unpaired, two-tailed Student t-test. The result is representative of two independent experiments. **C)** H&E staining of paraffin sections. Representative images of spheroids at the indicated time-points after harvesting as indicated. Scale bar: low magnification: 100 µm; high magnifications: 50 µm.

Figure 2: Characterization of T3-treated spheroids by RT-qPCR and immunolabelling. A) RT-qPCR experiments were performed to analyze the expression of *EPHB2, TERT and ALDH1A1*, TRα1 and the ABC transporters *ABCG2 and ABCB1* in the T3 and CTRL spheroids along the days in culture, as indicated. Histograms represent mean ± SD, N=4, after normalization with *PPIB*. ns, non-significant *, *P*<0.05, **, *P*<0.01 and ***, *P*<0.001 compared to CTRL condition, by unpaired, two-tailed Student t-test. The result is representative of two independent experiments. **B)** Immunostaining of spheroids at D7 for proliferation PCNA (red) and cell death activated-caspase 3 (green) markers (upper panels); ALDH1A1 (green) and ABCG2 (magenta) markers (middle panels); ABCB1 (green) and PCNA (red) markers (lower panels). Images show merged labeling of PCNA (red), activated-caspase 3 (green) and DAPI (nuclei, blue); ALDH1A1 (green), ABCG2 (magenta) and DAPI (nuclei, blue); PCNA (red), ABCB1 (green) and DAPI (nuclei, blue). White dotted lines indicate the cropped parts. Images were taken with a 20X objective under a Zeiss Axio Imager M2 Apotome 2 microscope. Scale bar: 100 µm, cropped images: 50 µm.

Figure 3: Impact of TRα1 overexpression in the spheroid's formation and growth. A) Representative pictures along the days in culture of the TRα1-GOF spheroids in different conditions as indicated. Images were taken under a Zeiss Axiovert microscope with a 4X objective. Scale bar: 200 µm. **B)** Estimated volume of the TRα1-GOF spheroids in long-term culture in the different conditions at different time-points, as indicated. Violin plots show frequency distribution of the data, bold dotted lines indicate the median and light dotted lines indicate the quartiles, n = 12-14. *, *P*<0.05 and **, *P*<0.01 compared to control condition, by unpaired, two-tailed Student t-test. The result is representative of two independent experiments. **C)** H&E staining of paraffin sections. Representative images of spheroids at the indicated time-points after harvesting as indicated. Scale bar: low magnification: 100 µm; high magnifications: 50 µm. **D)** RT-qPCR experiments were performed to analyze the expression of *EPHB2, TERT* and *ALDH1A1*, TRα1 and the ABC transporters *ABCG2 and ABCB1* in the spheroids along the days in culture in the different conditions, as indicated. Histograms represent mean ± SD, N=4, after normalization with *PPIB*. ns, non-significant, *, *P*<0.05, **, *P*<0.01 and ***, *P*<0.001 compared to the respective iCTRL and

TRα1-GOF conditions as shown, by unpaired, two-tailed Student t-test. The result is representative of two independent experiments.

Figure 4: Characterization of TRα1-GOF spheroids by immunolabelling. A) Immunostaining of spheroids at D3 and D7 for proliferation PCNA (red) and cell death activated-caspase 3 (green) markers in the different conditions. Images show merged labeling of PCNA (red), activated-caspase 3 (green) and nuclei (blue). Images were taken with a 20X objective under a Zeiss Axio Imager M2 Apotome 2 microscope. Scale bar: 100 µm. **B)** Immunostaining of spheroids for ALDH1A1 (green) and ABCG2 (magenta) markers (lower panels) or PCNA (red) and ABCB1 (green) markers (upper panels) at D7 in the different conditions. Images show merged labeling of ALDH1A1 (green), ABCG2 (magenta) and DAPI (nuclei, blue) or PCNA (red), ABCB1 (green) and DAPI (nuclei, blue). White dotted lines indicate the cropped parts. Images were taken with a 20X objective under a Zeiss Axio Imager M2 Apotome 2 microscope. Scale bar: 100 µm, cropped images: 50 µm.

Figure 5: Effect of anticancer regimens in CTRL and T3 spheroids. A) Changes in the volume of the spheroids, represented as the percentage of the initial volume, at the indicated time-points of treatment with the drugs, as indicated. Violin plots show frequency distribution of the data, bold dotted lines indicate the median and light dotted lines indicate the quartiles, n = 12-14. **, $P<0.01$ and ***, $P<0.001$ compared to the respective CTRL conditions, by unpaired, two-tailed Student t-test. **B)** Morphological features of the spheroids maintained in the different culture conditions. Images were taken under a Zeiss Axiovert microscope with a 4X objective. Scale bar: 200 µm. **C)** H&E staining of paraffin sections. Representative images of the CTRL and T3 spheroids in not treated (NT) or after 72 h of FOLFOX and FOLFIRI, as indicated. Images were taken using a Zeiss Axio Imager. Scale bar: low magnification (5X): 200 µm; medium magnification (10X): 100 µm; high magnification (20X): 50 µm.

Figure 6: Effect of the FOLFIRI chemotherapy in CTRL and T3 spheroids by RT-qPCR and immunolabelling. A) RT-qPCR experiments were performed to analyze the expression of *EPHB2, TERT and ALDH1A1*, TRα1 and the ABC transporters *ABCG2 and ABCB1* in the CTRL and T3 spheroids in not treated (NT) or after 72 h of FOLFIRI, as indicated. Histograms represent mean ± SD, N=6, after normalization with *PPIB*. *, $P<0.05$, **, $P<0.01$ and ***, $P<0.001$ compared to iCTRL and TRα1-GOF condition, as shown, by unpaired, two-tailed Student t-test. The result is representative of two independent experiments. **B)** Immunostaining of spheroids for ALDH1A1 (green) and ABCG2 (magenta) (lower panels) or PCNA (red) and ABCB1 (green) (middle panels) or PCNA (red) and activated-caspase 3 (green) in the different conditions, as indicated. Images show merged labeling of ALDH1A1 (green), ABCG2 (magenta) and DAPI (nuclei, blue) or PCNA (red), ABCB1 (green) and DAPI (nuclei, blue) or PCNA (red), activated-caspase 3 (green) and DAPI (nuclei, blue). Images were taken with a 40X objective under a Zeiss Axio Imager M2 Apotome 2 microscope. Scale bar: 50 µm.

Supplementary Figure Legends

Figure S1: Comparative transcription profile analysis by RNA-seq of spheroids treated with T3 for 24h during the forming step. A) Heat map shows the 20 most up-regulated or down-regulated genes in T3 vs CTRL condition. **B)** Highlight on selected genes differentially expressed.

Figure S2: Morphological analysis of the iCTRL spheroid's formation and growth. A) Representative pictures along the days of the iCTRL spheroids in different conditions as indicated. Images were taken under a Zeiss Axiovert microscope with a 4X objective. Scale bar: 200 µm. **B)** Estimated volume of the iCTRL spheroids in long-term culture in the different conditions at different time-points, as indicated. Violin plots show frequency distribution of the data, bold dotted lines indicate the median and light dotted lines indicate the quartiles, n = 12-14. *, $P<0.05$ and **, $P<0.01$ compared to control condition, by unpaired, two-tailed Student t-test. The result is representative of two independent experiments. **C)** H&E staining of paraffin sections. Representative images of spheroids at the indicated time-points after harvesting as indicated. Scale bar: low magnification: 100 µm; high magnifications: 50 µm.

Figure S3: Impact of TRα1 down-regulation in spheroids growth. A) Representative pictures along the days of the spheroids in different conditions as indicated. Scale bar: 200 µm. **B)** Estimated volume of the spheroids in the different conditions along the days as mean ± SD. **C)** RT-qPCR experiments were performed to analyze the expression of TRα1 in the different culture conditions, as indicated. Each point in the curve represents the relative mRNA expression levels as mean ± SD, N=4, after normalization with *PPIB*. ns, non-significant, *, $P<0.05$ comparing at D10 Sh-scr vs Sh-scr T3, by unpaired, two-tailed Student t-test. **D)** H&E staining of paraffin sections. Representative images of spheroids at the indicated time-points after harvesting as indicated. Scale bar: 50 µm.

Figure S4: Comparative transcription profile analysis of T3-FOLFIRI vs FOLFIRI treatments in spheroids by RNA-seq. A) Venn diagrams show the overlaps between the up-regulated or down-regulated genes in the different experimental conditions, as indicated. **B)** Highlight of selected differentially up- and down- differentially expressed genes in the T3 FOLFIRI condition compared with NT condition. Genes in bold are modulated by T3 and shared with the T3-NT spheroids; genes marked by * are shared with the CTRL-FOLFIRI condition.

Figure S5: Effect of the FOLFIRI on the expression of different markers in the TRα1-GOF spheroids. RT-qPCR experiments were performed to analyze the expression of *EPHB2, TERT and ALDH1A1*, TRα1 and the ABC transporters *ABCG2 and ABCB1* in the different culture conditions, as indicated. Histograms represent mean ± SD, N=6, after normalization with *PPIB*. *, $P<0.05$, **, $P<0.01$ and ***, $P<0.001$ compared to control condition, by unpaired, two-tailed Student t-test. The result is representative of two independent experiments.

Table S1: Antibodies used for immunolabelling

Table S2: Primers used for RT-qPCR and sequence of the Sh used

Table S3: Unique upregulated GO pathway analysis after 24h T3 treatment in the spheroids

Table S4: Unique GO pathway analysis of up and down regulated genes in CTRL and T3 spheroids

Table S1. Oligos sequences used for RTqPCR and Sh sequences

Gene		Sequence
PPIB	F	ATG ATC CAG GGC GGA GAC TT
	R	GCC CGT AGT GCT TCA GTT TG
TRa1	F	TGC CTT TAA CCT GGA TGA CAC
	R	TCG ACT TTC ATG TGG AGG AAG
EPHB2	F	GTG GAA GAA ACG CTA ATG GAC
	R	TCT CAT CGT AGC CAC TCA CCT
TERT	F	CTC CAT CAG AGC CAG TCT CAC
	R	GTT CAC GTG CAA ATC CAG AAA
ALDH1A1	F	GCC TTC ACA GGA TCA ACA GAG
	R	TGG AAA TTC AAC AGC ATT GTC
ABCG2	F	GTG GTG TGT CTG GAG GAG AAA
	R	TAT CGA GGC TGA TGA ATG GAG
ABCB1	F	AAA CAC CAC TGG AGC ATT GAC
	R	ATT CCT GTC CCA AGA TTT GCT

Sh-RNA sequences against TRa1

	Sequence
Sh1	TTGAGGATCAGGAAGTCTAAA
Sh2	TAGTCATTCTAACTGCACTTT

Table S2 Antibodies used for immunofluorescence

Antibody	Species	Brand	Reference	Dilution
PCNA	mouse	Dako	M0879	1/1000
cleaved-caspase 3 (D175)	rabbit	Cell signalling	#9661	1/100
ALDH1A1 (D9J7R)	rabbit	Cell signalling	#36671	1/400
ABCG2 (BXP-21)	mouse	Santa Cruz Biotechnology	sc-58222	1/200
ABCB1 (E1Y7B)	rabbit	Cell signalling	#13063	1/800
AlexaFluor 568 anti mouse	donkey	ThermoFisher	A10037	1/1000
AlexaFluor 488 anti rabbit	donkey	ThermoFisher	A121206	1/1000

Giolito et al., Figure 1

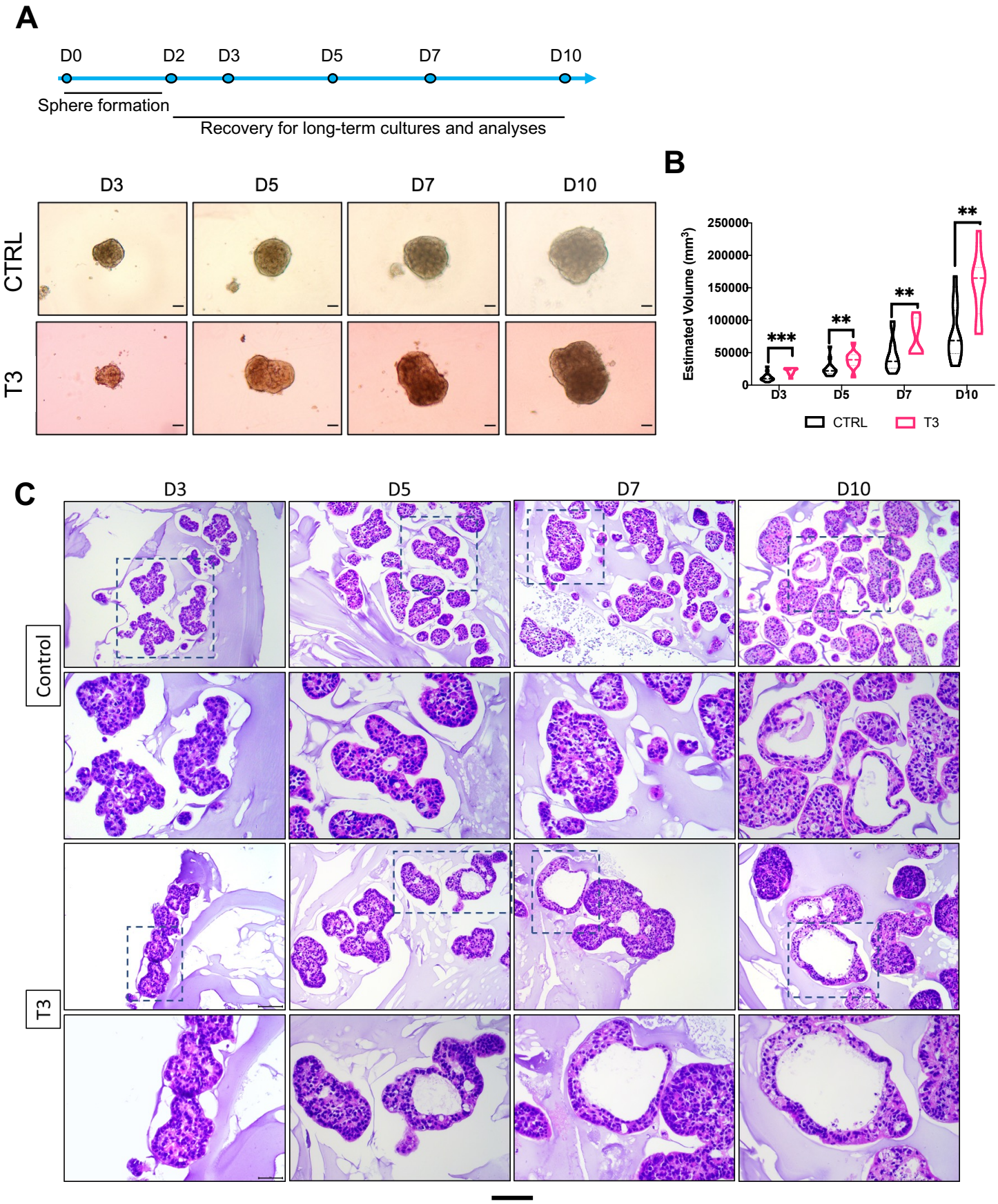

Giolito et al., Figure 2

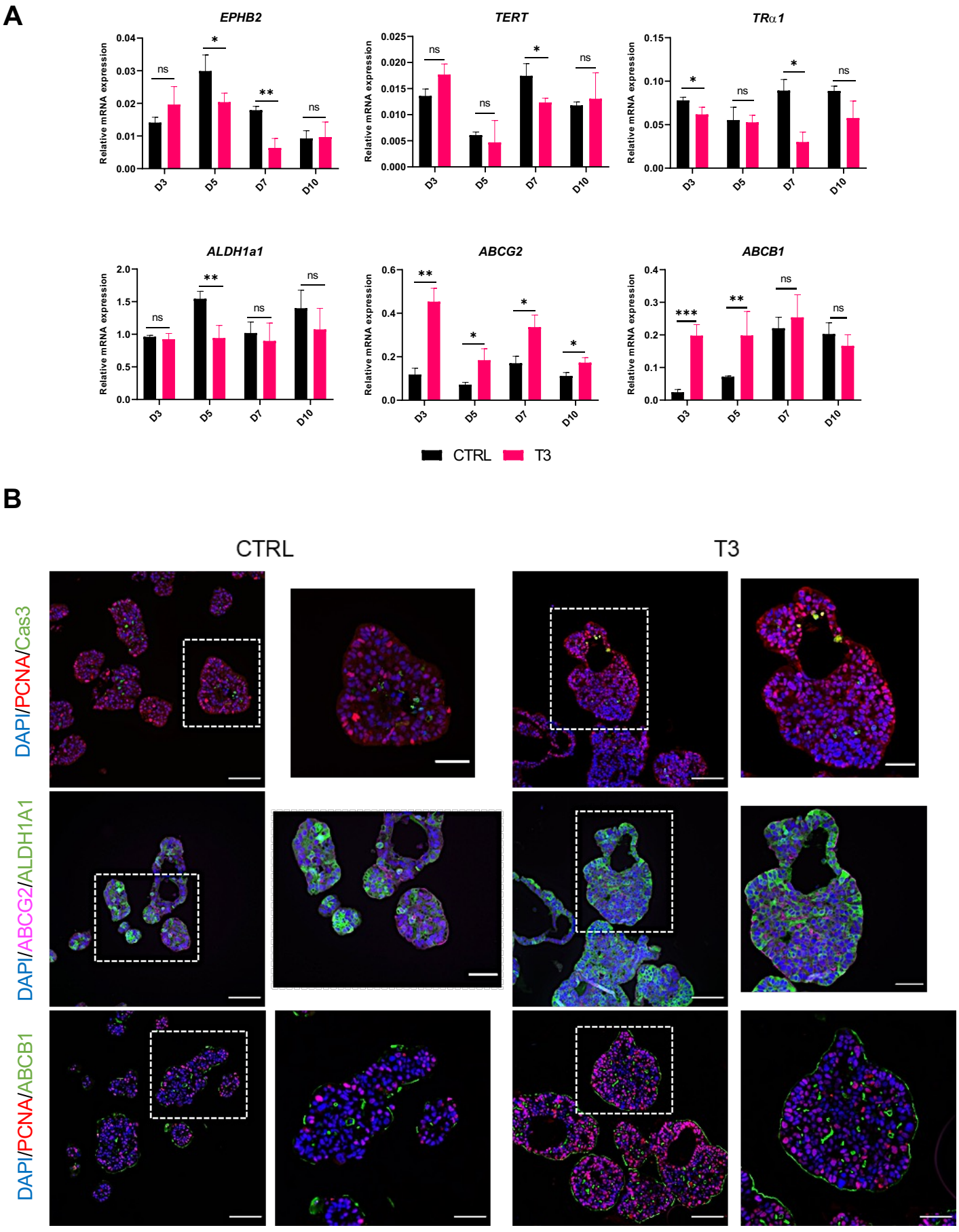

Giolito et al., Figure 3

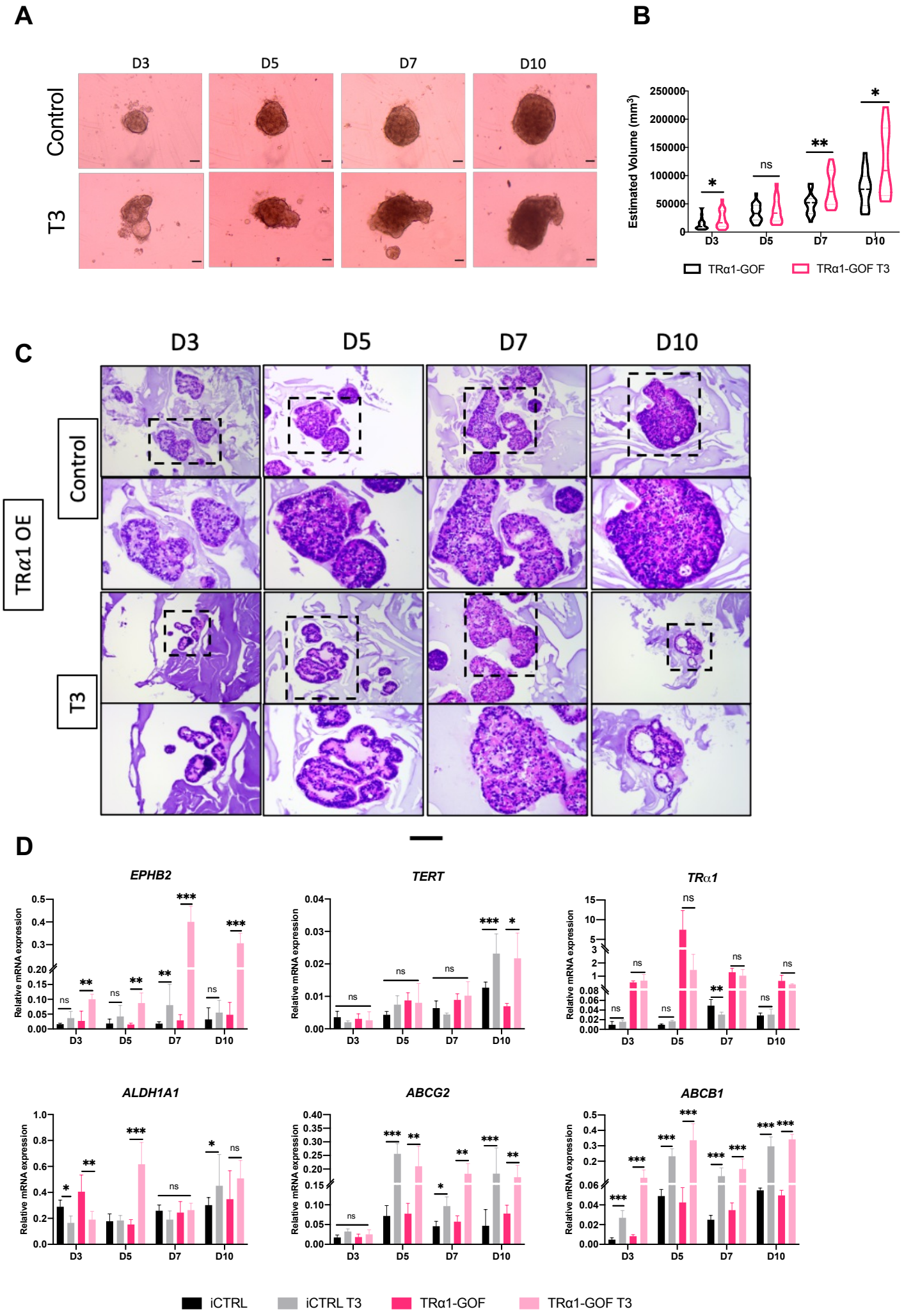

Giolito et al., Figure 4

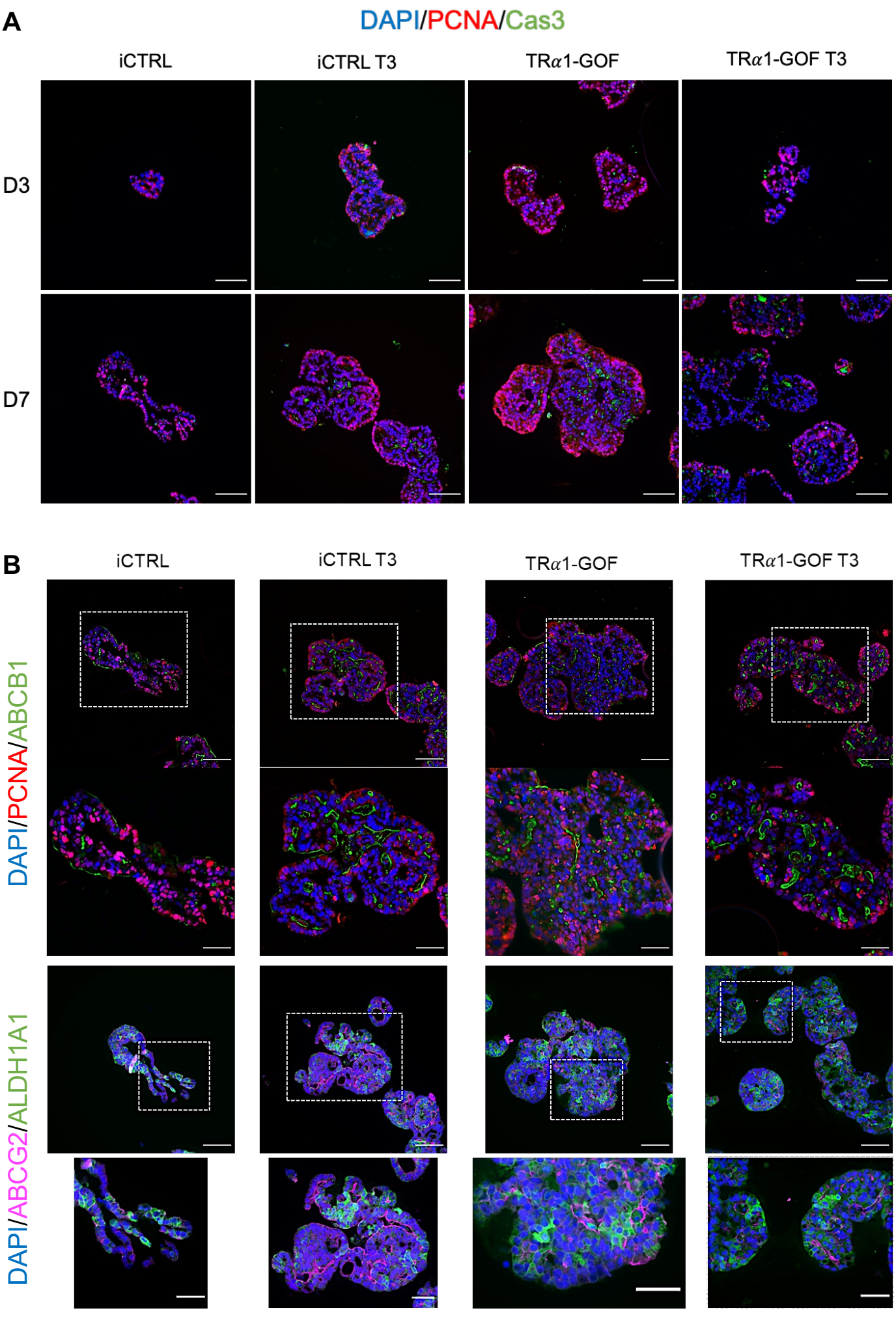

Giolito et al., Figure 5

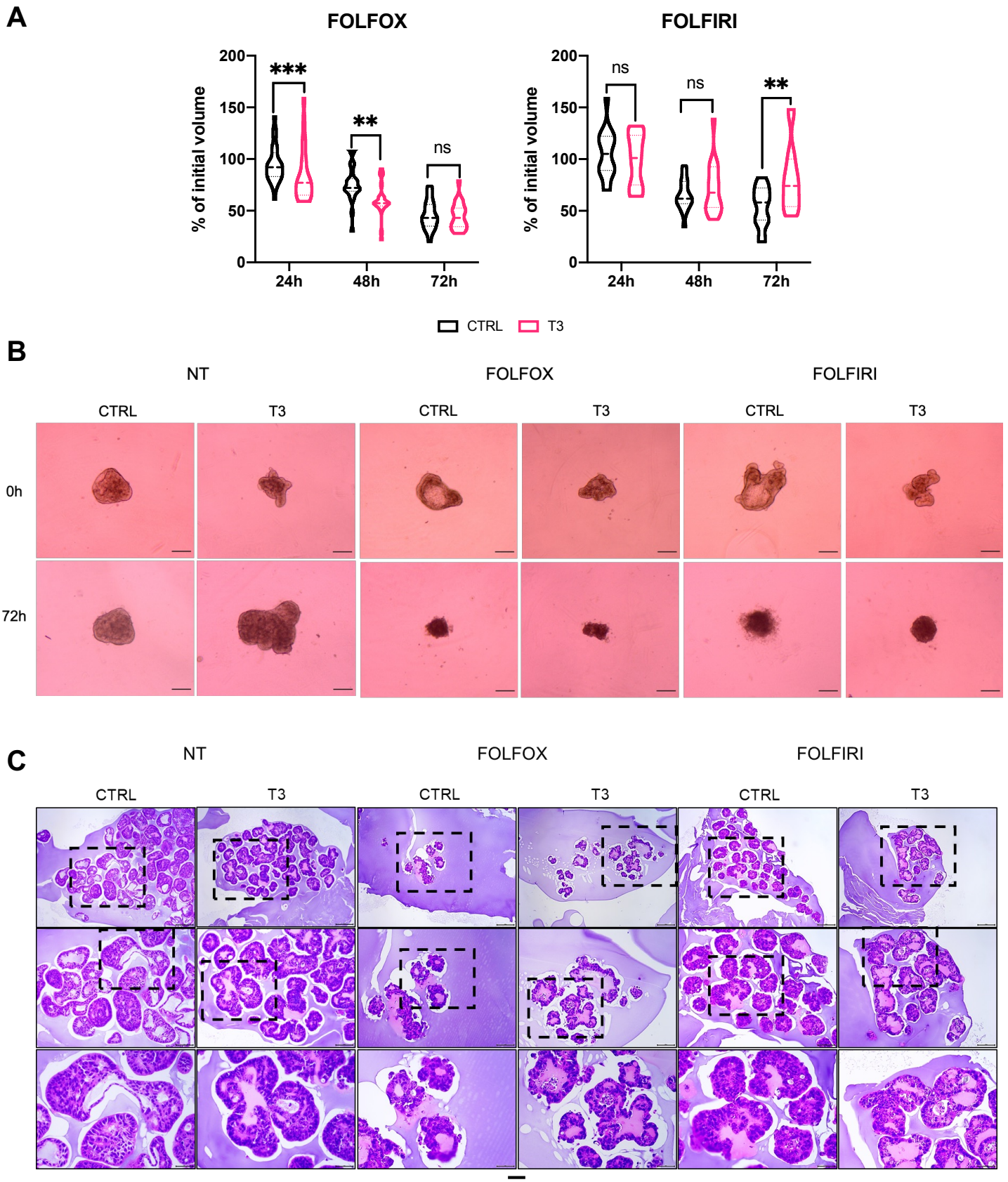

Giolito et al., Figure 6

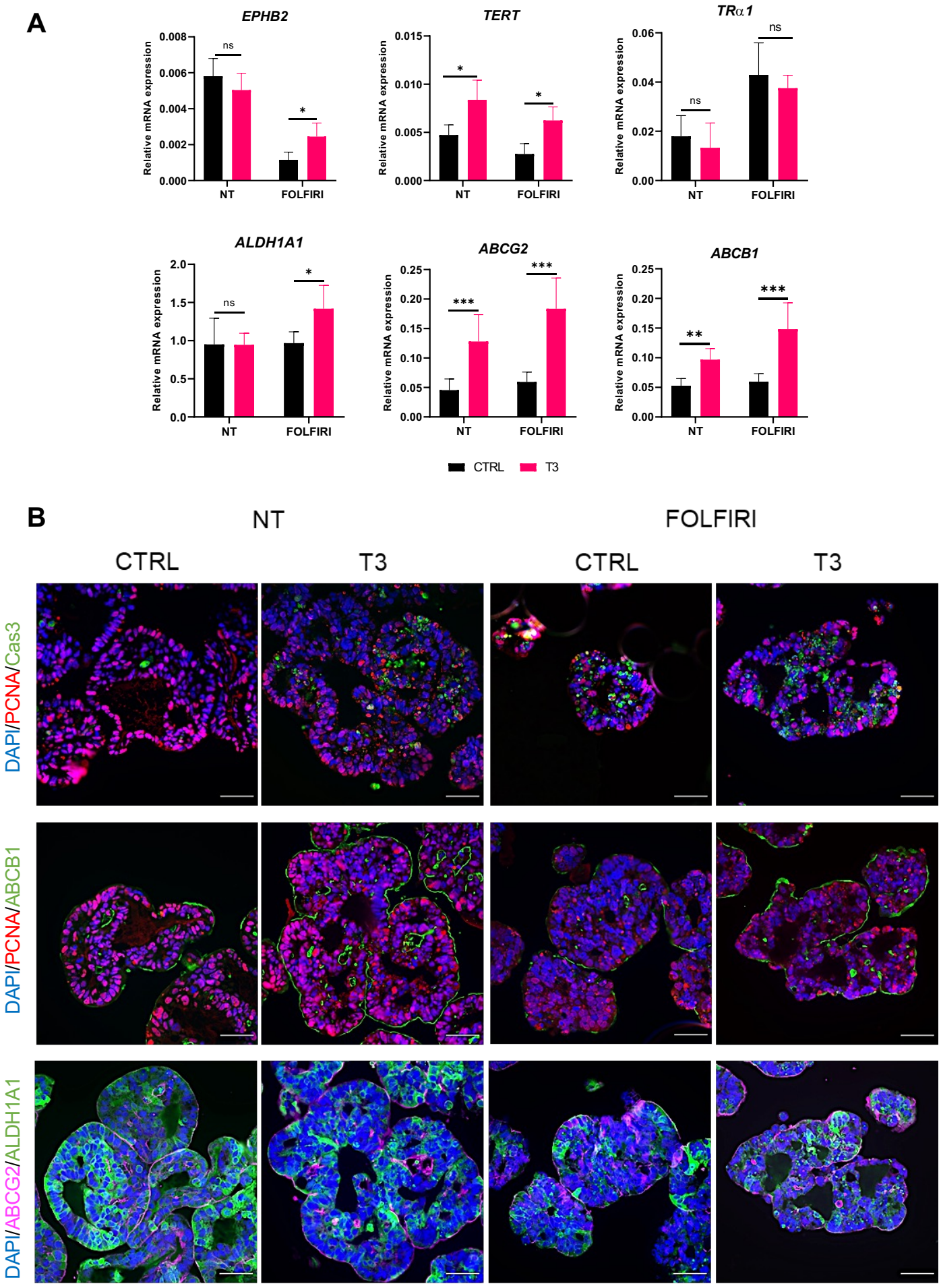

Giolito et al., Figure S1

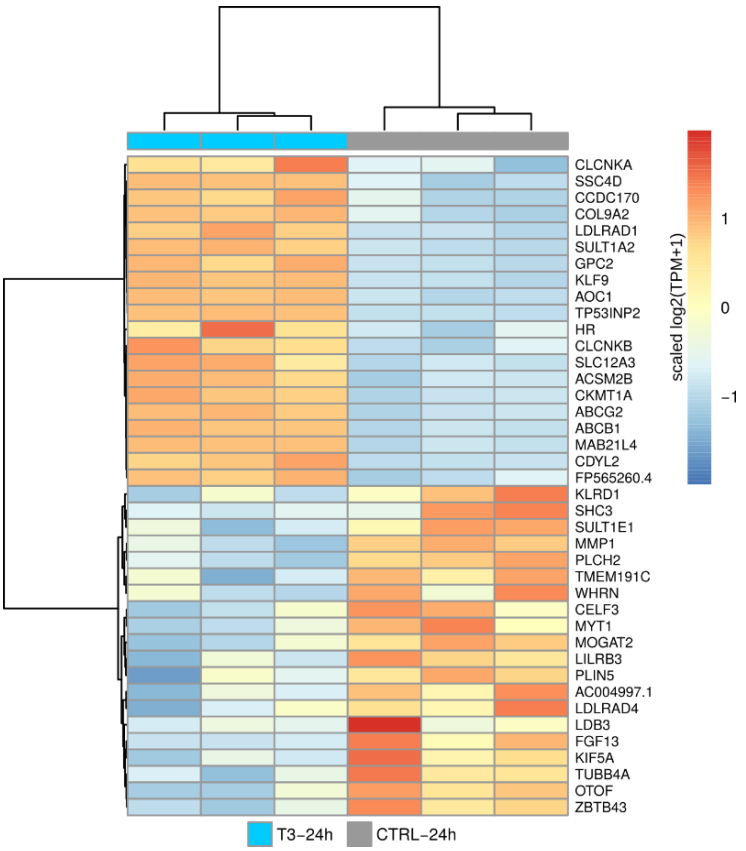

Differentially Expressed Genes	
UP T3 24h	DOWN T3 24h
KLF9	*FGF13*
HR	*LDB3*
ABCG2	*SHC3*
ABCB1	*MOGAT2*
ABCC1	*KIF5A*
DIO1	*LDLRAD4*
SHH	*LILRB3*
UGT1A1	*OTOF*

Giolito et al., Figure S2

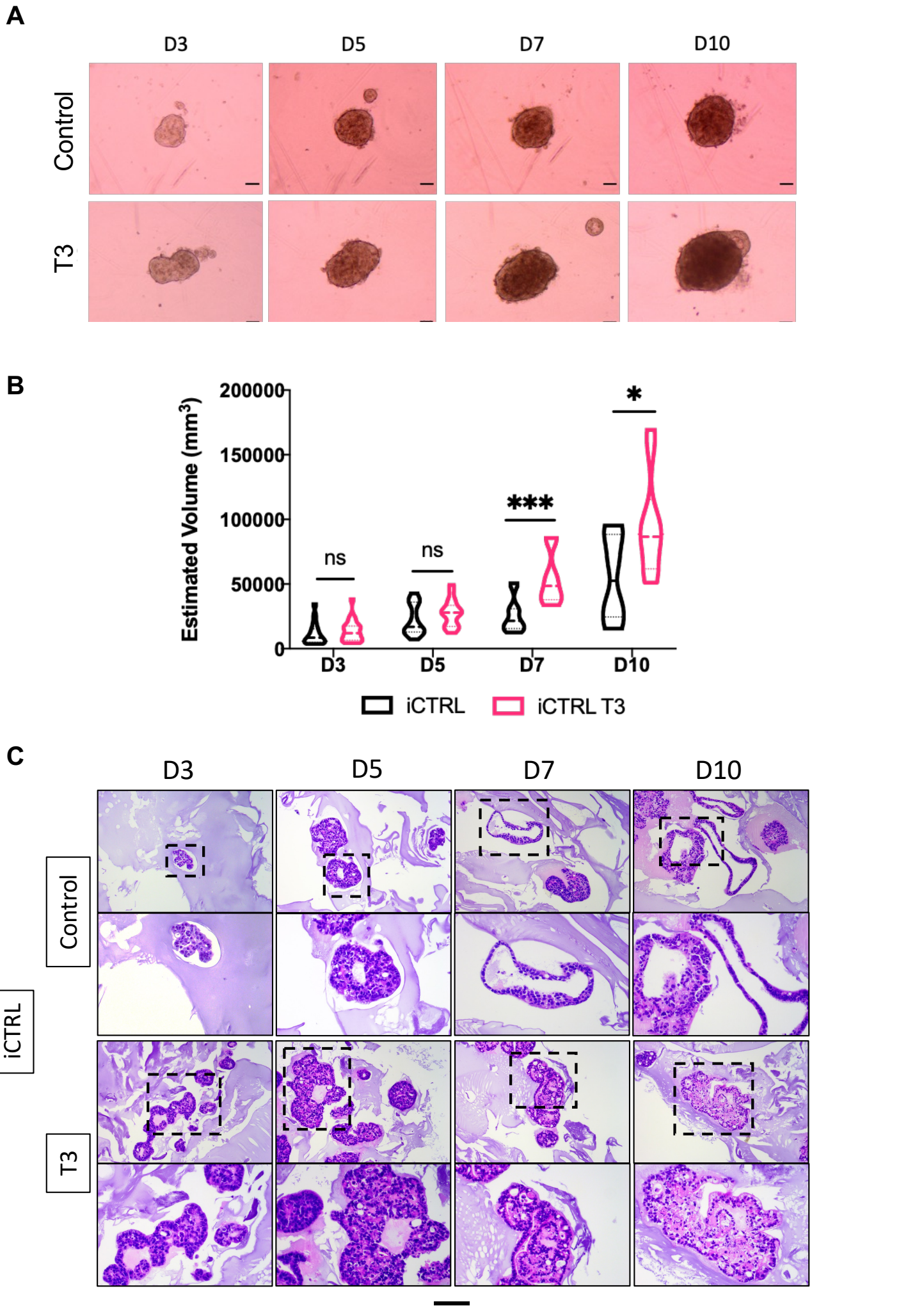

Giolito et al., Figure S3

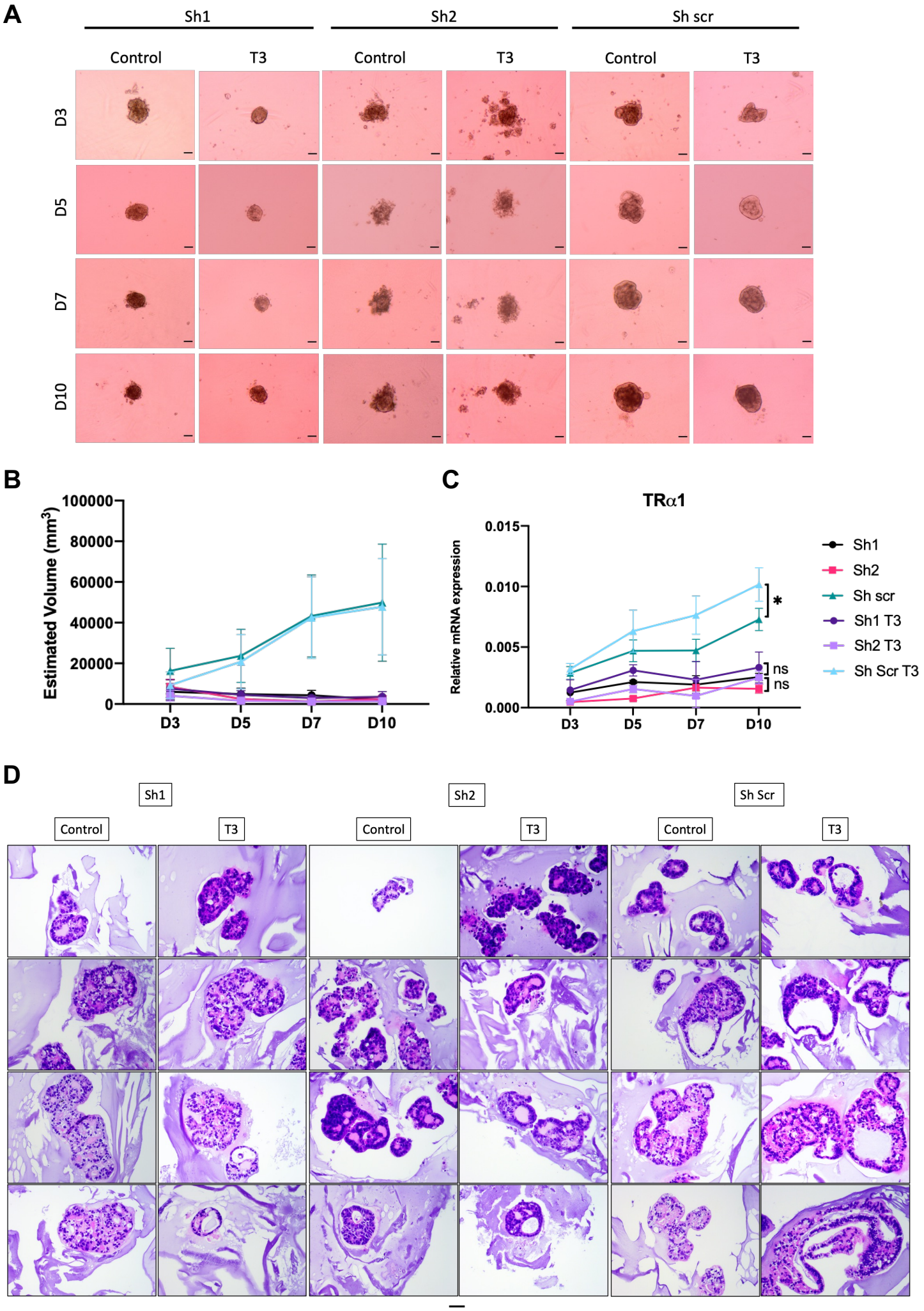

Giolito et al., Figure S4

A

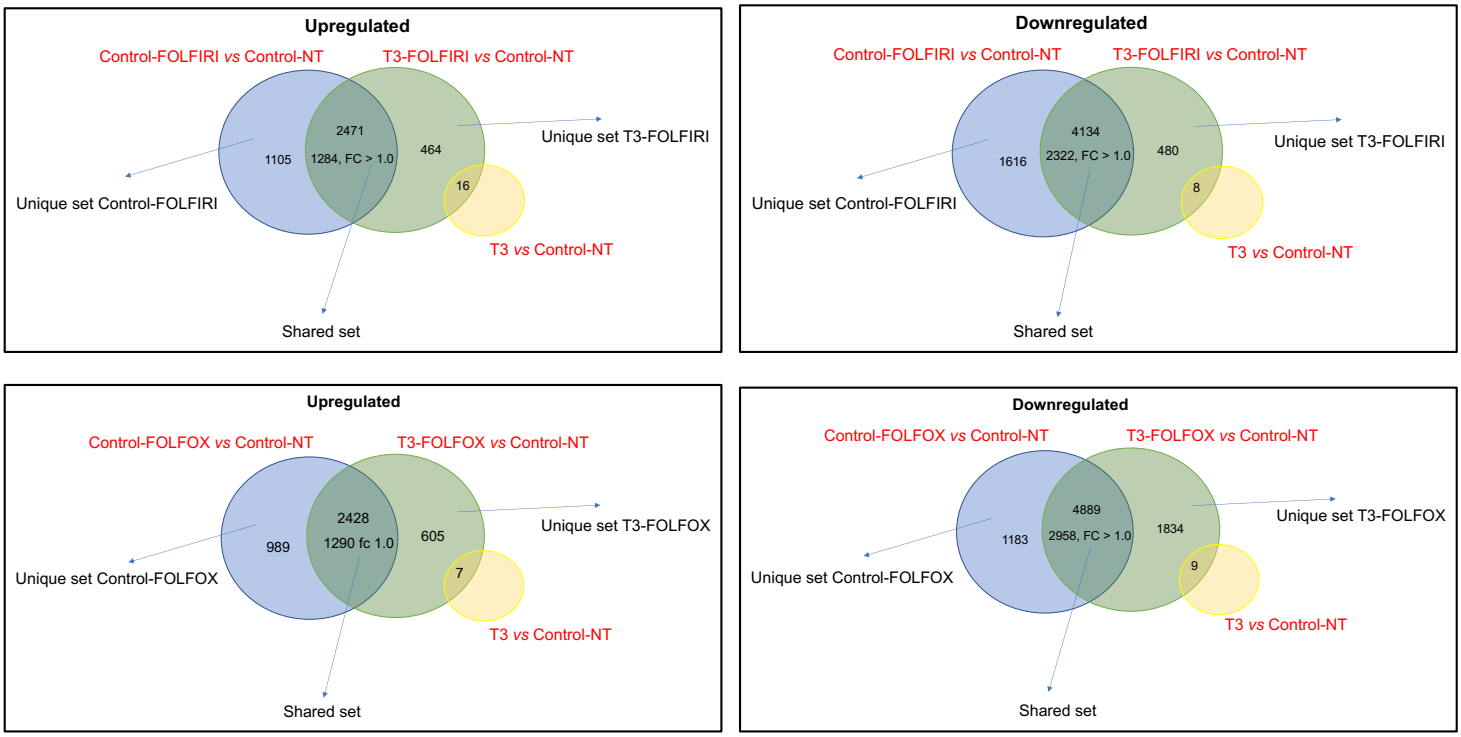

B

Differentially Expressed Genes	
UP T3 FOLFIRI	DOWN T3 FOLFIRI
ABCB4	***KYNU***
ABCB1	*BACH2*
ABCG2	*HIF1A*
DPYS	*TOP1*
KLF9	*MEX3A**
CYP1A1	*TYMP**
SLC7A11	*TYMS**
OLFM4	
NR1I3	
ABCC2	
*UGT1A3**	
*UGT1A5**	
*CLU**	
*LGR5**	
*ABCB11**	

Giolito et al., Figure S5

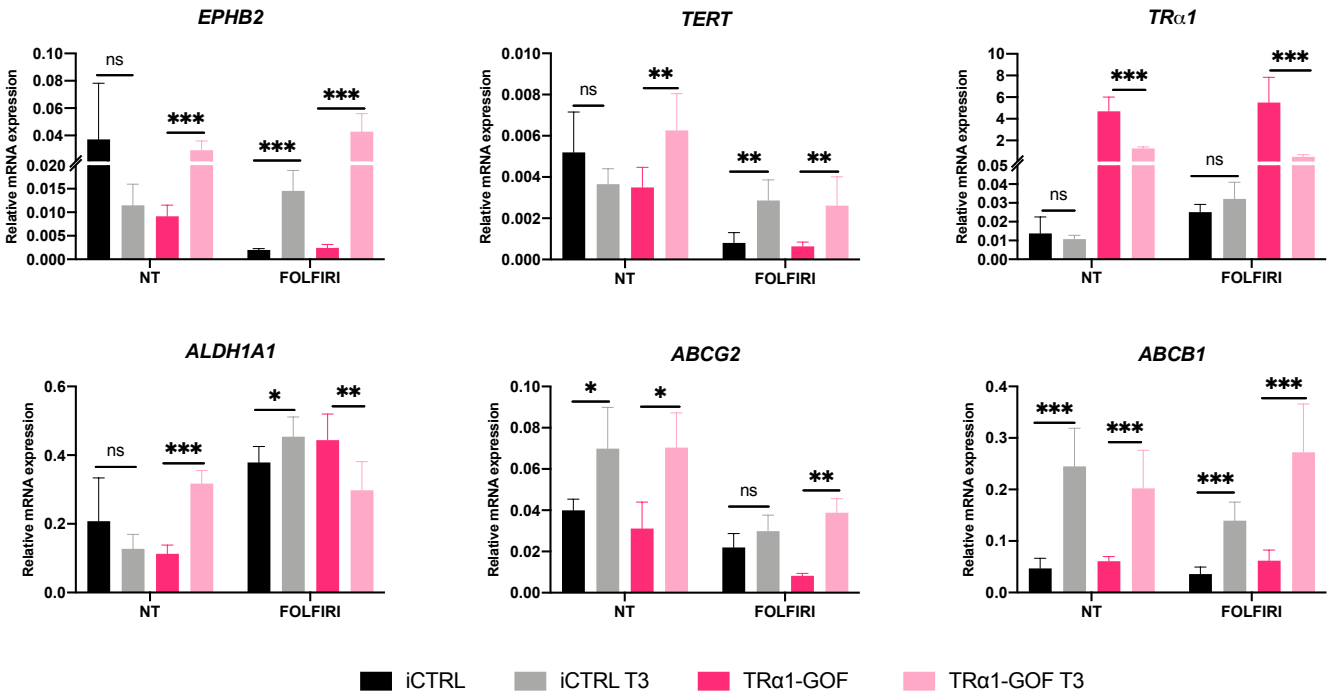

Paper Nº 4

Invited review under review in Cellular and Molecular Life Sciences

"Thyroid hormone signaling in the intestinal stem cells and their niche"

Maria Virginia Giolito[1], **Michelina Plateroti**[1]

[1] UMR-S1113 - IRFAC INSERM, Université de Strasbourg

Thyroid hormones play an important role in stem cell biology via their nuclear hormone receptor TRs, T3-modulated transcription factors. Crosstalk between the epithelium and the underlying mesenchyme is essential for intestinal maturation and stem cell emergence, according to pioneering work on T3-dependent amphibian metamorphosis. Similar findings have begun to be detailed in mammals, where T3 and TRα1 influence physiological and cancer-related stem cell biology, thanks to recent breakthroughs in strong animal models and 3D-organoid cultures. During my thesis, I could participate in the preparation of a review manuscript, which allowed me to navigate the vast and intriguing literature about the intestinal epithelium and its niche and make a huge effort to include what is known about the thyroid hormones in this new perspective. In this review, we have compiled recent results on T3 and TRα1's numerous activities in intestinal epithelial stem cells, cancer stem cells, and their niche. Moreover, we particularly focus on regulating metabolic functions that are directly linked to normal and cancer stem cell biology. These findings could help explain other possible mechanisms by which TRα1 controls stem cell biology beyond the more classical Wnt and Notch signalling pathways.

Thyroid hormone signaling in the intestinal stem cells and their niche

Maria Virginia Giolito[1] and Michelina Plateroti[1,*]

1: Université de Strasbourg, Inserm, IRFAC/UMR-S1113, FMTS, 3 Avenue Molière 67200, Strasbourg, France

***Corresponding author**
Université de Strasbourg, Inserm, IRFAC/UMR-S1113, FMTS
3 avenue Molière, 67200 Strasbourg, France

Tel: 33 3 88 27 77 27
E-mail: plateroti@unistra.fr

Running Title: Thyroid hormones and stem cells

Abstract

Several studies emphasized the function of the thyroid hormones in stem cell biology. These hormones act through the nuclear hormone receptor TRs, which are T3-modulated transcription factors. Pioneer work on T3-dependent amphibian metamorphosis, showed that the crosstalk between the epithelium and the underlying mesenchyme is absolutely required for intestinal maturation and stem cell emergence. With the recent advances of powerful animal models and 3D-organoid cultures, similar findings have now begun to be described in mammals, where the action of T3 and TRα1 control physiological and cancer-related stem cell biology. In this review we have summarized recent findings on the multiple functions T3 and TRα1 in intestinal epithelium stem cells, cancer stem cells and their niche. In particular, we have highlighted the regulation of metabolic functions directly linked to normal and/or cancer stem cell biology. These findings help explain other possible mechanisms by which TRα1 controls stem cell biology, beyond the more classical Wnt and Notch signaling pathways.

Keywords: Colon cancer; Intestinal epithelium; Thyroid hormone; Thyroid hormone receptor; Stem cell; Stem cell niche

1. Introduction

The thyroid hormones (THs) and their nuclear receptors TRs play multiple roles in development, homeostasis and metabolic processes in several organs and organisms [rev. in 1,2]. Their function in intestinal development was described about a hundred years ago based on observations of amphibian metamorphosis. During this postnatal maturation program, increased circulating TH levels are responsible for gut remodeling, including a first phase of apoptosis and shortening of the gut length followed by an increase of cell proliferation [3]. Interestingly, it has been reported that these maturation steps in gut tadpoles depend on complex signaling between different cell types, leading to the emergence of stem cells (SCs) and the establishment of the adult epithelium [4,5]. In the mammalian intestine, it is well established that continuous epithelium renewal and SC maintenance depends on complex cell interactions and on signaling pathways that globally define and contribute to the SC niche [6,7]. Similar to amphibians, TH signaling is also important for mammalian intestinal postnatal development and SC biology and the establishment of a SC niche [8–10]. The focus of this review will be on TH-dependent intestinal SC niche regulation and on how the alteration of this signal can lead to cell transformation and cancer.

1.1. The thyroid hormones and their nuclear receptors

THs are synthesized by the thyroid gland in a process finely regulated by the hypothalamus-pituitary-thyroid axis [11]. The hypothalamus synthesizes and secretes thyrotropin-releasing hormone (TRH) which is transported *via* axons to the pituitary gland where it interacts with its receptor and stimulates the synthesis of thyroid-stimulating hormone (TSH). TSH binds to its receptor located in the follicular cells of the thyroid, inducing the production of the hormones L-Thyroxine (T4) and 3,3',5-Triiodo-L-thyronine (T3). T4 levels tend to be about 40-fold higher compared to T3 [11,12]. TH synthesis is strictly regulated and subject to a negative feedback loop, resulting in TH-dependent negative regulation of TSH and TRH production [11,12]. In addition to the central control of TH production, a local mechanism for controlling hormone levels involves plasma membrane transporters [13,14], which ensure TH entry into cells, and on the presence of the deiodinase selenoenzymes, which activate and/or inactivate the THs [15].

THs are secreted into the blood and transported to distal organs. In the blood, they are carried by proteins present in the serum such as the thyroid binding protein (TBP), transthyretin and albumin [16,17]. Inside the cells THs, in particular T3, act through binding to the nuclear hormone receptors TRs, belonging to a large protein family of transcription factors [18]. T3 is considered the active form of TH since it binds TRs with 10-15 fold higher affinity than T4 [19,20].The TRs have a modular organization, typical of the family members (**Figure 1A**, *upper*) [21]. The A/B N-terminal domain allows the binding of protein co-factors and contains a T3-independent activation function 1 (AF1) region. The C domain contains two zinc finger structural units that bind specific DNA elements within target genes. The D domain is a hinge region linking the C and E domains and also includes a nuclear localization signal. The E domain contains the ligand- and protein co-factor-binding regions, which modulate the downstream transcriptional response. The AF-2 region in this domain allows T3-dependent transcriptional control. The TRs are present in numerous tissues and within several vertebrate

species including mammals, amphibians, fishes, and birds [22]. Inside of cells, they are mainly located in the nucleus and, unlike other nuclear hormone receptors, TRs do not have an “inactive” form in the cytoplasm.
In mammals, the *THRA* and *THRB* genes code for TRα and TRβ protein isoforms. The *THRA* locus is located on human chromosome 17 and encodes for two major isoforms, TRα1 and TRα2, but only TRα1 is a true T3 nuclear receptor because it has DNA- and ligand-binding domains [23, rev. in 24]. The *THRB* locus is located on chromosome 3 and encodes TRβ1 and TRβ2 major isoforms, both acting as T3 nuclear receptors [rev. in 24]. The role of TRα1 is of importance during development [rev. in 10,23] and in certain adult organs such as the heart, brain and intestine [25]. TRβ1 and/or TRβ2 act principally in the liver, retina, developing inner ear and at the level of the hypothalamus-pituitary axis (i.e., TRH neurons and the pituitary gland) [24,26]. TRs modulate the expression of target genes by binding to specific genomic regulatory regions called thyroid hormone response elements (TREs) [26]. TREs consist of repeated hexameric nucleotide sequences organized in half-sites as direct repeats separated by four nucleotides (DR4) or as palindromes, direct or inverted [26] (**Figure 1A**, *lower*). The modulation of gene transcription by TRs involves protein complexes acting as co-activators or co-repressors, depending on the presence or the absence of T3 [27] (**Figure 1B**).

1.2. The intestinal epithelium and its organization

The intestinal epithelium has a peculiar vertical organization all along the anteroposterior axis, that correlates with specific functional compartmentalization [6,28] (**Figure 1C**). Indeed, a proliferation zone is devoted to SC activity and progenitor proliferation, while a differentiation zone defines the region where differentiated cells reside [28,29].
The intestinal SCs have been the focus of active investigations during the last 15 years and we benefited of a strong increase in the knowledge in this field [6,29,30]. They are located at the bottom of the small intestine and colon crypts and cycle rapidly to maintain a continuous turnover of epithelial cells. Crypt-base columnar cells (CBCs), originally described by Cheng and Leblond [31], express the cell surface marker Lgr5 and are now considered the active SCs of the intestinal epithelium [32]. CBCs can generate both a SC or a progenitor that enters the transit-amplifying zone and differentiates while migrating toward the top of the vertical axis. Differentiated cells finally die by apoptosis and are shed into the lumen [28,29]. This entire process is completed within 3-5 days in murine tissue depending on the anterior-posterior intestinal region [28].
The intestinal epithelium hosts two major cell lineages generated from absorptive- and secretory-committed progenitors [6,28]. Absorptive progenitors differentiate into enterocytes/colonocytes which have a brush border that enlarges their cell surface and facilitates efficient nutrient and water absorption [28]. Microfold cells (M cells) sample gut contents and transport, by trans-cytosis, luminal antigens to the underlying immune cells present in the Peyer’s patches, thereby controlling immune responses [6,28]. The secretory progenitors, on the other hand, give rise to Paneth/Paneth-like, enteroendocrine (EEC), tuft and goblet cells [6,28]. Paneth (small intestine) and Paneth-like (colon) cells are the only differentiated cells present at the bottom of the crypts and produce antimicrobial compounds and niche factors important for SC maintenance and activity [33,34]. EECs, the hormone-producing cells of the intestine, secrete

hormones that regulate physiological processes in response to food intake [28,35]. Tuft cells are chemo-sensors and mediate immune responses [36] while goblet cells secrete mucus that helps to protect the epithelium from the aggressive luminal content [28,37].
Interestingly, several studies have described other cell populations within the intestinal epithelium with stem characteristics and these have been collectively called “reserve stem cells” as opposed to the active Lgr5-expressing SCs [28,29]. Depending on the reports, they have been referred to as “quiescent, slow-cycling, revival or facultative”, described and debated as candidate SC-like populations localizing within the SC/progenitor zone [38]. These cells express the markers Bmi1 [39], Tert [40], Hopx [41], Lrig [42], Msi1 [43] and Clu [44] and can regenerate the epithelium after injury and loss of active SCs [39–44]. These plastic and dynamic regeneration capacities are, however, not only restricted to SCs since there is evidence showing that lineage-specific committed progenitors have the capacity to de-differentiate and acquire SC properties [7,45,46].
Finally, it is important to emphasize that several signaling pathways are involved in the organization of the vertical axis of the intestinal epithelium and in defining the SC zone, by actively participating to the SC niche. This includes Wnt, Notch and epidermal growth factor (EGF) pathways which show a higher gradient of activity in the CBC zone [28] (**Figure 1C**). The bone morphogenic protein (BMP) and hedgehog (Hh) pathways show an opposite gradient and are highly active at the top of the axis, where they define a no SC/progenitor zone [7,28]. Collectively, these signaling pathways control the epithelial vertical zonation, the balance between cell proliferation and cell differentiation, as well as between SC self-renewal and commitment [7,28].

1.3. The intestinal epithelium stem cell niche

In 2009, Sato et al. cultured for the first time murine intestinal organoids from isolated Lgr5-expressing crypt SCs [47]. The culture was established in the absence of mesenchymal cells but included growth factors that define “the minimal stromal niche” of necessary signals for the viability and activity of the SCs [47]. Indeed, single Lgr5-expressing cells give rise to 3D multi-budded organoids containing all lineages when supplemented with EGF, R-spondin (a Wnt signaling amplifier) and Noggin (a BMP inhibitor) embedded in an extracellular matrix-like gel [47]. These three niche factors and the complex semi-solid matrix are necessary and sufficient for SC biology and well recapitulated the *in vivo* situation. In fact, *in vivo,* the niche surrounds SCs at the bottom of the crypts and sustains their identity, maintenance and activity by supplying Wnt proteins, R-spondins, EGF and BMP inhibitors [7,28]. The niche is composed of several cell types, including Paneth cells and stromal/sub-epithelial mesenchymal cells (subepithelial myofibroblasts, non-muscle fibroblasts, telocytes, trophocytes, endothelial cells and pericytes) [48–50]. Immune cells may also contribute to the intestinal SC niche through action on Paneth and M cells [49,50]. Moreover, extracellular matrix proteins that form the basal lamina are involved in complex metabolic signaling at the crypt’s bottom and are essential niche elements [51]. Finally, ingested nutrients and diets show a prominent capacity to modulate SCs and this dietary-adaptation capacity has recently been proposed as a hallmark of SC activity [30]. The different cell types and factors described above have been summarized in several reviews [28,29,49,51,52] and will be discussed here only in relation to THs/TRs.

2. TH/TR in intestinal physiopathology

As already mentioned, THs and TRs play an important role in intestinal physiology in amphibians, mice and humans, as well as in intestinal tumor biology. Importantly, several studies have attempted to establish a link between THs and intestinal tumor development. However, a consensus has not been reached, and both anti- or pro-tumoral effects of THs have been described [53,54; rev. in 55–57], as summarized in **Table 1**. Experimental data from models clearly shows a pro-tumoral action of high TH levels [58–61]. Moreover, studies that have monitored the thyroid axis in patients have reported a clear association between low TSH and high THs with cancers, including colorectal cancers (CRCs) [53,54,62]. Finally, some epidemiological studies have been performed in patients treated with either TH-deprivation or TH-supplementation therapies to normalize TH levels and analyzed tumor incidence under these conditions [62–64]. However, these treatments do not mimic hypo- or hyperthyroidism and, paradoxically, show highly diverse results, strongly contributing to the lack of consensus in this matter. Altogether, these findings clearly indicate the complexity of the field and would deserve a specific focus.

Regarding the TRs, it has been shown that mutation or altered expression of TRs may be linked to tumorigenesis [65,66]. Unlike the intestine, TRβ1 has been shown to control cell proliferation in the liver [67], and increased TRβ1 expression is strongly correlated with tumor invasion in hepatic cancer cell lines [68]. In the case of the colon, TRβ1 expression is greatly reduced in cancer due to hypermethylation [69]. Accordingly, TRβ1 is associated with a more differentiated phenotype and its loss of expression is linked to malignant transformation [69,70]. TRα1 has been reported to be associated with the proliferation of pancreatic cells [71], while another study showed that its expression was associated with a poor prognosis in breast tumors with a mutated BRCA1 gene [72]. Interestingly, the expression of TRβ1 in this same study was inversely associated with a favorable prognosis [72]. Our own functional studies of the TRα1 receptor in mouse models highlighted its role in controlling both intestinal development and homeostasis [rev. in 8,10]. These properties result from the ability of TRα1 to regulate the Wnt and Notch pathways and to modulate the expression of various cell division and cell cycle regulators [73,74; rev. in 75]. The importance of these mechanisms was validated by experimentally up-regulating TRα1 expression in intestinal epithelial cells *in vivo* (*vil*-TRα1 mice), and we demonstrated the induction of hyperproliferative and hyperplastic crypts [58]. Moreover, according to the assumption of SC-driven tumorigenesis, the overexpression of TRα1 in an *Apc*-mutated tumor-prone model (*vil*-TRα1/Apc$^{+/1638N}$ mice) increases tumor incidence, accelerates the intestinal tumorigenic process and induces metastasis dissemination [58]. Conversely, loss of TRα1 expression (TRα$^{0/0}$/Apc$^{+/1638N}$ mice) drastically reduces tumor incidence [59]. Among the mechanisms at work, the control of [74,76] or the functional interaction with the Wnt pathway [77] appear to be key processes. Finally, recent findings in human CRCs clearly indicated an up-regulation of *THRA* gene expression in tumors, a direct correlation with Wnt activity and an association with consensus molecular signature CRC subtypes [59] [78]. Collectively, these observations have clear clinical implications.

In the following paragraphs, we will summarize recent findings in the field of TH/TRs and SC biology, including the SC niche in normal intestine and tumors.

2.1. Lessons from amphibian metamorphosis

In amphibians, primary culture approaches have showed that the action of THs in non-epithelial cells is required for the appearance of adult epithelium and the emergence of the intestinal SCs [4,5]. These results underline the importance of TH-dependent epithelial-connective tissue interactions in the establishment of an intestinal SC niche in the developing amphibian intestine [79,80]. Both TRα and TRβ receptors are important for this developmental program [80–83] and finely regulate the cell cycle, apoptosis and the remodeling of the extracellular matrix, notably by the induction of metalloproteases [84].

As described earlier, several signaling pathways are important for intestinal development in mammals, such as Hh, WNT, BMP and Notch pathways. Interestingly, some of them are also necessary for the emergence of SCs in amphibians. For example, Shh is a member of the Hh signaling family and is one of the early T3 responsive genes in the metamorphosing amphibian intestine [85]. It is specifically expressed in the epithelium and highly transiently upregulated during the earliest events of metamorphosis. Some downstream components of Shh signaling, such as the receptors Patched, Smoothened and GLIs, are mainly expressed in the connective tissue, thereby responding to the epithelial-derived Shh signal [86]. In addition to Shh, BMP4 is another T3 target gene in the amphibian intestine, but it is specifically expressed in connective tissue and its expression temporally correlates with adult epithelium differentiation [87]. TH-induced BMP4 represses cell proliferation in connective tissue and promotes differentiation of adult epithelial cells through the epithelial-specific presence of its receptor [88]. Importantly, several TH-modulated genes associated with amphibian metamorphosis belong to the WNT pathway and are expressed in both the epithelium and the mesenchyme, directly participating to the intestinal remodeling [89–91]. Indeed, under the influence of increasing TH levels and in the presence of both TRα and TRβ, the adult epithelium originates from a scattered population of larval absorptive epithelial cells expressing tyrosine kinase-like orphan receptor 2 (Ror2; a receptor for Wnt5a) or Sfrp2 (a Wnt soluble modulator). The non-canonical Wnt5a/Ror2, the canonical sFRP2/Fzd and the hyaluronan/CD44 Wnt signaling, all stimulated by THs, are essential for larval epithelial cells to de-differentiate and generate the adult-type epithelium [89,92,93]. Altogether, the cell-cell interactions that involve WNT, Shh and BMP signaling have an important role in the establishment of the intestinal SC niche that is essential for the neo-generation of SCs of the adult-type epithelium.

Recently, a paper described the importance of TH signaling in tadpole telocytes. These stromal cells in mammalian intestine surround the bottom of the crypts and are characterized by the marker Foxl1 [94,95]. Hasebe *et al*. showed that Foxl1, which is also a marker of telocytes in amphibians, is indirectly upregulated by TH through Shh signaling from the epithelium. This signal exchanges between the epithelium and the Foxl1-expressing niche cells is required for the emergence of SCs in the tadpole intestine [96]. The Notch pathway is activated through ligand-receptor interaction between adjacent cells and is upregulated by TH during metamorphosis [91,97]. Several genes such as Notch1, Hairy1, Delta-like 1 (Dll1) and Jagged 1 (Jag1) are directly or indirectly TH-responsive [97,98]. While Dll1 is expressed in the adult epithelium, Jag1 is present in both larval epithelium and stromal fibroblasts beneath adult progenitor/SCs. These findings suggest

different roles of the Notch elements in the developing or adult intestinal epithelium and SC niche [91,97].

2.2. What do we know in mammals?

Contrary to amphibians, in mammals the role of TH and TRs in intestinal SCs and their niche is much less characterized. Recently, we showed the role of T3 and of TRα1 in murine intestinal SCs *in vivo* and in derived organoids. T3, in a TRα1-dependent manner, induced in organoids an increase in cell turnover affecting the commitment of progenitors into goblet cells [9]. *In vivo,* an increase of crypt cell proliferation upon T3 exposure was also present along with regulation of cell differentiation, but in this case it was directed towards Paneth cells [9]. This study demonstrated for the first time the role of T3 and TRα1 in increasing the number of SCs and their markers, related to an effect on Paneth cells that, as we described in the previous section, are part of the SC niche [33]. TH/TR-dependent cell-cell interactions and instructive signal exchanges between the epithelium and connective tissue have not been formally demonstrated yet. Nevertheless, TH-dependent stimulation of ligands and receptors participating in Wnt, BMP, Hh and Notch pathways has been shown in several reports [59,73,74]. Thus, in the light of these findings, we can hypothesize that THs through TRα1 may also play a role in mesenchymal cells participating to the SC niche. This action might result in direct and indirect modulation of multiple signals in different cell types and tissues, similar to what has been shown in amphibians [94,96].

The local TH/TR signaling has been investigated in the context of intestinal tumors and cancer stem cells (CSCs). The deiodinases, TH metabolizing enzymes, have been well studied both in normal physiology and in cancer [99]. The stroma of *Apc*-mutant mice have elevated expression of Dio2, a T3-activating enzyme. When the expression of Dio2 is inhibited in these cells, or when hypothyroidism is chemically induced, the growth of intestinal tumors is blunted. This is indicative of a crosstalk between the epithelium and the connective tissue mediated by local or systemic TH levels. Importantly, this effect is accompanied by a reduction of angiogenesis [100]. High expression of Dio3, a T3-inactivating enzyme, has been reported in human CRCs [101]. The depletion of Dio3 in adenocarcinoma cell lines or primary tumor cells indicated a pro-differentiation action of T3, through downregulation of Wnt and increase of BMP pathways [101,102, 103]. The contrasting results between these reports may be due to the altered expression of these two enzymes in the stroma (Dio2) or in the epithelial tumor cells (Dio3).

These findings are also discordant with our data showing a positive regulation of TH/TRα1 on the Wnt pathway, cell proliferation, tumorigenicity and on SC activity [9,58,59,74,76]. While we lack explanations for these discrepancies, it is important to note that TH treatment *in vivo* and in organoids have different outcomes. Indeed, organoids are an epithelial-only model where T3 induces a “thyroid shock”, which is not the case when treating the animals and perform analyses on the intestinal epithelium in its integrated physiological context [9].

In addition to mesenchymal derivatives, macrophages also participate in the intestinal SC niche and the CRC tumor microenvironment. In these cells THs regulate the triggering receptor expressed on myeloid cells-2 (TREM2), a cell surface receptor on macrophages and microglia involved in immune-suppression of the tumor microenvironment [104]. This finding is in line with previous data showing the influence of THs as immunomodulators with the potential of

decreasing the physiological response against tumor cells [105]. We can affirm that TH/TRα1 influences intestinal tumor biology through its interaction with the Wnt/β-catenin and other signaling pathways [59,106]. However, we should also consider a possible tumor-promoting role *via* CSC maintenance by an action on the tumor microenvironment (*i.e.*, the CSC niche).
Finally, non-classical TH functions have also been described. These depend mainly on the integrin αVβ3 or the 30 or 43 kDa TRα isoforms and the control of several genes implicated in SC maintenance through the niche [107]. These regulations include COX2, hypoxia-inducible factor 1α (HIF1α), fibroblast growth factor 2, NOS2, MMP9, as well as genes related to glucose and lipid metabolism such as sterol regulatory element-binding protein 1 (SREBP-1) [107] and CD47 [108]. Importantly, actions of THs in the tumor stroma *via* hypoxia induction, tumor microenvironment recruitment and stimulation of angiogenesis have been shown in hepatocellular carcinoma [109,110].

3. TH/TR and metabolic regulations in intestinal SC/CSC and their niche

Several reviews have summarized the roles of signaling pathways in relation to TH/TR in the normal intestine and in cancers [8,10,66,77]. Here we have focused on metabolic regulation, given the increasing interest on the role of metabolism in normal tissues and tumors. In the intestine, particularly in the field of gut SCs and their niche, several studies have shown that nutrient availability and metabolic pathways can directly regulate or instruct cellular function [111–113]. The various cell types within the intestinal crypt and the cells participating in the niche preferentially use different metabolic pathways and, depending on the cell type or on the cell state, a metabolic switch can occur. For instance, active SCs rely highly upon oxidative phosphorylation (OXPHOS) whereas Paneth cells rely on glycolysis (**Figure 2A**) [114,115].
Importantly, THs are critical regulators of metabolic processes and positively or negatively control the transcription of anabolic and catabolic gene subsets that affect energy homeostasis and metabolism [116]. Hyperthyroidism promotes a hypermetabolic state characterized by increased resting energy expenditure, weight loss, reduced cholesterol levels, increased lipolysis and gluconeogenesis. Conversely, hypothyroidism is associated with the opposite effects. THs influence key metabolic pathways that control energy balance by regulating energy storage and expenditure as described in the brain, white fat, brown fat, skeletal muscle, liver and pancreas [116].
In addition to TRs, other nuclear hormone receptors, including peroxisome proliferator-activated receptor alpha (PPARα), PPARγ and liver X receptor (LXR) share a similar structure and mode of action and heterodimerize with the retinoid X receptor (RXR). These similarities have suggested potential functional interactions in the control of metabolic gene expression [117]. PPARs and LXRs are ‘‘permissive’’ RXR partners that bind dietary lipids with low affinity and activate enzymes involved in lipid metabolism [117]. TRs, on the other hand, are "non-permissive" RXR heterodimers, bind to T3 with high affinity and mediate feedback regulation of their ligand [116,117]. T3-liganded TRs dominate the interaction with RXR and may have a stronger effect in co-regulated genes than nutrient signals acting through PPAR and LXR. Furthermore, THs control the expression of SREBPs [118,119], key regulators of lipid metabolism and long-chain fatty acids [120]. It has been shown, at least *in vitro*, that SRPBs can inhibit

T3 binding to TRs, suggesting another level of gene regulation through competition between nutrient signaling and T3 binding to TRs [117].
The role of THs and TRs in lipid and carbohydrate metabolism has been extensively studied in the liver, where TRβ1 is the major TR isoform responsible for these actions [2,117]. In the intestine, TRα1 is the isoform present in the crypt compartment and intestinal SCs, while TRβ is expressed in differentiated cells of the villi [8]. In intestinal tumors, the expression of TRα1 is upregulated [59]while the *THRB* gene is strongly silenced [69,70], indicating that metabolic controls in this context rely exclusively on TRα1.

3.1. Carbohydrate metabolism and mitochondrial activity

TH status influences glucose metabolism. Excess of THs stimulate hepatic glucose production and increases the expression of the glucose transporters GLUT4 and SLGT1 in skeletal muscle and intestine, respectively [116]. Liganded TRα1 impairs glucose-stimulated insulin secretion by acting directly at the level of the pancreatic islets [116]. A further link between glucose metabolism and TH signaling is the T3-dependent induction of the carbohydrate response element-binding protein (ChREBP). This transcription factor stimulates the expression of genes involved in glycolysis and lipogenesis in response to glucose and insulin [117]. In a TRα- and TRβ-dependent manner, THs reduce insulin levels, regulate the expression of genes in the liver and skeletal muscle and stimulate ChREBP expression, which in turn influences glucose response and insulin secretion [117]. In the intestine, THs increase alkaline phosphatase and peptidase activities in a dose-dependent manner *in vivo* and inhibit γ-glutamyltransferase *in vitro* [121,122]. In addition, studies in TRα-knockout animals showed that lactase, sucrase, aminopeptidase and FABP expression and activities are decreased [123], indicating a regulation by the TRα1 receptor of diverse metabolic processes in this organ. More recently, we also showed that T3 impacts the metabolic activity of intestinal organoids by upregulating all enzymes involved in glycolysis, pyruvate metabolism and OXPHOS [9]. This T3-induced metabolic change is parallel to an alteration in SC renewal by favoring secretory progenitor lineages [9]. We can assume that THs *via* TRα1 control the metabolic state of the SCs and, by consequence, regulate their self-renewal capacity and the fate determination of progenitor cells. The fine-tuned mechanisms at the basis of these complex regulations remain, however, to be fully elucidated, as schematized in **Figure 2B, C**.
The Notch/FOXO/mitochondria axis regulates goblet and Paneth cell lineages, with mitochondrial fission as a requisite for inducing differentiation [124]. Mitochondrial dysfunctions are central in the development of inflammatory bowel diseases and cancer, and affect intestinal SCs and Paneth cells by modifying the cellular phenotypes and lineage commitment [125]. Interestingly, THs and TRα1 have been implicated in mitochondrial biogenesis and activity in mammals [126,127] and the mitochondrial fission is also a key process for the amphibian TH-dependent intestinal maturation and the emergence of SCs [128]. The pyruvate dehydrogenase kinase PDK4 gene expression had been shown to be modulated in the rat liver by T3 [129]. This finding suggest that T3, by modulating the mitochondrial metabolic pathways, may direct the differentiation of SCs towards secretory lineages, as it has been shown in mouse organoids [9] (**Figure 2B, C**). Thus, it is possible that in both mammals and amphibians an interplay occurs between classical cell signaling and metabolic pathways and both share

the mitochondria as an essential regulator of SC maintenance and differentiation potentialities.
Aside from direct regulation of target genes, THs can also modulate the expression of several genes by non-genomic actions. TH binding to integrin αVβ3 in colon adenocarcinoma cell lines has been shown to favor an increase of AMPK and the inhibition of mTOR resulting in increased tumor cell aggressivity [130]. In the mitochondria the truncated TRα isoforms or the hormones T3 or T2, generated from deiodination of T3, modulate the activity of several components of the respiratory chain leading to an overall increase in OXPHOS [131]. Moreover, THs can regulate the expression of several enzymes and transporters, like the intestinal fructose transporter GLUT5 [132] and PKM2 enzyme, involved in the generation of acetyl-CoA that favors OXPHOS metabolism [133]. Future research will need to focus on characterizing the cell types in which these regulations take place for a better understanding of the integrated processes.

3.2. Lipid metabolism

Mouse models with TRα and TRβ gene point mutations show a range of metabolic phenotypes, including impairment of cholesterol metabolism, fatty acid oxidation, lipolysis and increased cholesterol and triglyceride serum levels [117]. THs stimulate lipolysis, lipogenesis and cholesterol reduction by regulating the expression of SREBPs. The SREBP-1c isoform, involved in fatty acid synthesis and glucose metabolism, is repressed by THs, while the SREBP-2 isoform, which is a lipid sensor important in cholesterol metabolism, is induced by THs. Also, both TREs and sterol regulatory elements (SREs) are required for the activation of human acetyl–CoA carboxylase [31] and low-density lipoprotein receptor genes [32]. Thus, THs directly regulate SREBPs but also control genes harboring close TREs and SREs in their regulatory regions [134,135]. Interestingly, SREBPs have SC- and tumorigenic- promoting activities in the intestine [136,137], indicating another possible functional link between TRα1 and SREBPs. TRs can also bind to LXR responsive elements in the intestinal ABCA1 gene, affecting the cholesterol efflux through suppression of the LXR-dependent ABCA1 expression [116]. In addition, a crosstalk between TRs and PPARγ has been shown in the regulation of lipid metabolism, in particular the induction of carnitine palmitoyltransferase 1 (CPT1a) enzyme, through peroxisome proliferator-activated receptor gamma co-activator (PGC-1α), a TH-target gene [138]. CPT1a is the key enzyme involved in fatty acid oxidation (FAO) as it exchanges the acyl group of the fatty acid for carnitine, so it can enter the mitochondria to be oxidated [139] (**Figure 2B, C**).
T3 treatment of intestinal organoids causes downregulation of the lipid metabolism pathway, including most of the enzymes involved in FAO, compared to non-treated organoids, with the only exception of CPT1a [9]. AMPK, another major regulator of FAO, is regulated by THs [140] (**Figure 2B, C**). In addition, the mitochondrial trifunction protein (MTP), which catalyzes three FAO reactions, is stabilized and modulated by the TRα p43 isoform [141]. MTP modulation was also observed in intestinal SCs during calorie restriction and fasting [113,142], leading to an increase of SCs, Paneth cells and progenitors, which is similar to what happens in mice when treated with T3 [9]. During calorie restriction, it was shown that mTORC1 inhibition is important for intestinal regeneration and preservation of “reserve SCs” from DNA damage [143]. T3 treatment may have a similar role in this context, as it inhibits mTOR [9]. Moreover, TRα1 protects the

epithelium from DNA damage [144], strongly supporting its role in epithelium regeneration upon injury, through an action on “reserve SCs”.
In the case of the high-fat diet, PPARδ activates the Wnt pathway and increases the intestinal SC number by modulation of metabolic responses and provoking SC self-renewal independently from Paneth cells, through the secretion of Jag1 [111]. A high-fat diet also has a tumor-inducing role *via* increased CPT1a [145], suggesting that THs and TRα1 may have a similar inducing role *via* CPT1a and FAO induction through Wnt or Jag1 modulation [9,73,74].
Altogether, the combination of classical cell signaling with metabolism and diet, nuclear receptors and hormones (like THs) help to maintain SC self-renewal and regulate differentiation through modification of mitochondrial metabolism both in SCs and the cells of their niche. It is worth highlighting that most of the studies to date have focused on the role of metabolism in SCs and Paneth cells. Therefore, additional studies on other cell types within the intestinal SC niche are necessary to fully understand the interrelation between different cell types in this complex metabolic interplay. Towards this end, newer studies have begun to investigate the role of adipocytes in CSCs and intestinal tumorigenesis. As mentioned above, THs have an important role in FAO and SC/CSC metabolism, resulting in increased stemness and tumorigenesis. They are also important in adipose tissue lipidic mobilization [116]. During calorie restriction, SCs and CSCs uptake fatty acids from the nearby adipocytes and promote the expression of CPT1a through PPARγ [146]. This same phenomenon was observed in organoids supplemented with fatty acids [111]. A similar role can be hypothesized for TRs, as both nuclear receptors engage in crosstalk in the regulation of lipid metabolism, adipogenesis, and tumorigenesis [147]. Colon tumors typically grow in an adipose tissue-enriched microenvironment, making adipocytes a key niche component for regulating cancer metabolism. The uptake of fatty acids from adipocytes renders colon cancer cells resistant to nutrient deprivation and favors a high level of Wnt signaling by acetylation of β-catenin [146]. It is therefore likely that THs and TRα1 contribute to the maintenance of CSCs in CRC by a positive induction of the Wnt signaling in CSCs and their niche by upregulating CPT1a and increasing metabolism of fatty acids in adipocytes [9,59,74].

3.4. Chromatin remodelling

As described earlier, changes in nutrient availability can result in the reprogramming of cellular metabolism. Core metabolite pools such as ATP, S-adenosyl methionine, acetyl-CoA, NAD/NADP and α-ketoglutarate underlie a variety of essential metabolic reactions and are used by chromatin modifiers in the establishment of epigenetic signatures [148].
Chromatin remodeling is a requirement for transcription of genes associated with anuran metamorphosis. Intestinal SCs are generally characterized by having open chromatin that allows them to change quickly from self-renewal to differentiation. In amphibians, the presence of different co-activators, which act as histone modifiers, remodel the chromatin in the presence of THs and allow the transcription of TR-responsive genes [149]. Upon T3 availability, TRs bind co-activator complexes containing the histone acetyltransferase SRC and the histone methyltransferase PRMT1 to facilitate epigenetic modification and gene transcription [149,150]. The TRs involved in this histone modification have an important role in cellular reprogramming. As discussed earlier, in mammals TRα1 is expressed in the intestinal crypts while TRβ1 is expressed in the villi. This

specific expression pattern indicates that, like in amphibians, each TR is associated with a unique profile of epigenetic regulation in the different epithelial cells [151].

Large scale studies showed that regulation of gene expression by TRs is not only due to binding of TREs but also to chromatin remodeling in regions close to TREs [135]. This changed the prevailing view that the transition from a repressed to an activated state might not simply work through a switch from co-repressor to co-activator interaction with pre-occupied TRs [135]. In addition, co-activators and chromatin remodelers may also be recruited through ligand-dependent TR occupancy of chromatin, a mechanism already observed for other nuclear hormone receptors [135]. Most T3-activated genes associate with hormone-facilitated TR recruitment to chromatin [135]. For example, some TH target genes fall under epigenomic regulation, which modifies their transcription [149,151,152]. The metabolic state of the intestinal SCs and of the cells participating in the niche may be regulated by sirtuin-mediated epigenetic mechanisms, which are also involved in the regulation of TH target genes [153]. SIRT1 is a NAD-dependent deacetylase that removes the acetyl groups from proteins, such as histones, thereby affecting the expression of genes. Histone deacetylation requires NAD+ and is associated with gene repression [152]. The NAD^+/NADH ratio is important for SIRT1 activity and reflects the metabolic status of the cells. The hormone T2 can activate SIRT1 and induce the deacetylation of PGC1a leading to activation of genes required for FAO [2].

Altogether, THs and TRs can increase the pool of regulated target genes by controlling metabolic fluxes and chromatin remodeling. This, in turn, may affect the metabolic activities of different cell types in both the normal intestine and in tumors. Last, but not least, TH/TR-dependent alterations in the metabolic status influence cell identity (*i.e.*, stem vs non-stem) and behavior (*i.e.*, normal vs tumor).

4. Conclusions

In this review we have highlighted the importance of TH-dependent signaling on intestinal SC physiology, including a direct action on SCs as well as in the SC niche. In addition, since alteration of TH signaling can lead to tumor development, we also discussed new insights into CSC biology and human CRCs.

The *THRA* gene is frequently upregulated in CRC patients [59], in particular in molecular subtypes linked to high metabolic features and elevated Wnt signaling [59]. These results are clearly of high clinical relevance and raise the question of the overall impact of an altered TH/TRα1 axis in CRC biology from tumor initiation to progression and metastasis.

Acknowledgements
MP lab is supported by the FRM (Equipes FRM 2018, DEQ20181039598), by the Inca (PLBIO19-289) and by the Ligue Contre le Cancer, Département Grand Est (01X.2020). MVG received support from the FRM.

References

1 Tata JR (2006) Amphibian metamorphosis as a model for the developmental actions of thyroid hormone. *Molecular and Cellular Endocrinology* **246**, 10–20.

2 Sinha RA, Singh BK & Yen PM (2014) Thyroid hormone regulation of hepatic lipid and carbohydrate metabolism. *Trends in Endocrinology and Metabolism* **25**, 538–545.

3 Brown DD & Cai L (2007) Amphibian metamorphosis. *Developmental Biology* **306**, 20–33.

4 Schreiber AM, Cai L & Brown DD (2005) Remodeling of the intestine during metamorphosis of Xenopus laevis. *Proceedings of the National Academy of Sciences* **102**, 3720–3725.

5 Ishizuya-Oka A & Shi YB (2008) Thyroid hormone regulation of stem cell development during intestinal remodeling. *Molecular and cellular endocrinology* **288**, 71–78.

6 Clevers H (2013) The Intestinal Crypt, A Prototype Stem Cell Compartment. *Cell* **154**, 274–284.

7 Beumer J & Clevers H (2016) Regulation and plasticity of intestinal stem cells during homeostasis and regeneration. *Development (Cambridge)* **143**, 3639–3649.

8 Sirakov M, Kress E, Nadjar J & Plateroti M (2014) Thyroid hormones and their nuclear receptors: New players in intestinal epithelium stem cell biology? *Cellular and Molecular Life Sciences* **71**, 2897–2907.

9 Godart M, Frau C, Farhat D, Giolito MV, Jamard C, le Nevé C, Freund JN, Penalva LO, Sirakov M & Plateroti M (2021) Murine intestinal stem cells are highly sensitive to modulation of the T3/TRα1-dependent pathway. *Development (Cambridge)* **148**, dev194357.

10 Frau C, Godart M & Plateroti M (2017) Thyroid hormone regulation of intestinal epithelial stem cell biology. *Molecular and Cellular Endocrinology* **459**, 90–97.

11 Ortiga-Carvalho TM, Chiamolera MI, Pazos-Moura CC & Wondisford FE (2016) Hypothalamus-pituitary-thyroid axis. *Comprehensive Physiology* **6**, 1387–1428.

12 Feldt-Rasmussen U, Effraimidis G & Klose M (2021) The hypothalamus-pituitary-thyroid (HPT)-axis and its role in physiology and pathophysiology of other hypothalamus-pituitary functions. *Molecular and Cellular Endocrinology* **525**, 111173.

13 Kinne A, Schülein R & Krause G (2011) Primary and secondary thyroid hormone transporters. *Thyroid Research* **4**, S7.

14 Groeneweg S, Van Geest FS, Peeters RP, Heuer H & Visser WE (2020) Thyroid Hormone Transporters. *Endocrine Reviews* **41**, 146–201.

15 Bianco AC & Kim BW (2006) Deiodinases: Implications of the local control of thyroid hormone action. *Journal of Clinical Investigation* **116**, 2571–2579.

16 Bartalena L & Robbins J (1993) Thyroid hormone transport proteins. *Clinics in laboratory medicine* **13**, 583–598.

17 Refetoff S (2000) *Thyroid Hormone Serum Transport Proteins*.

18 Weikum ER, Liu X & Ortlund EA (2018) The nuclear receptor superfamily: A structural perspective. *Protein science : a publication of the Protein Society* **27**, 1876–1892.

19 Apriletti JW, Eberhardt NL, Latham KR & Baxter JD (1981) Affinity chromatography of thyroid hormone receptors. Biospecific elution from support matrices, characterization of the partially purified receptor. *Journal of Biological Chemistry* **256**, 12094–12101.
20 Samuels HH, Tsai JS, Casanova J & Stanley F (1974) Thyroid hormone action. In vitro characterization of solubilized nuclear receptors from rat liver and cultured GH1 cells. *Journal of Clinical Investigation* **54**, 853–865.
21 Germain P, Staels B, Dacquet C, Spedding M & Laudet V (2006) Overview of nomenclature of nuclear receptors. *Pharmacological Reviews* **58**, 685–704.
22 Pascual A & Aranda A (2013) Thyroid hormone receptors, cell growth and differentiation. *Biochimica et Biophysica Acta - General Subjects* **1830**, 3908–3916.
23 Koenig RJ, Lazar MA, Hodin RA, Brent GA, Larsen PR, Chin WW & Moore DD (1989) Inhibition of thyroid hormone action by a non-hormone binding c-erbA protein generated by alternative mRNA splicing. *Nature* **337**, 659–661.
24 Flamant F & Samarut J (2003) Thyroid hormone receptors: lessons from knockout and knock-in mutant mice. *Trends in endocrinology and metabolism: TEM* **14**, 85–90.
25 Jones I, Srinivas M, Ng L & Forrest D (2004) The Thyroid Hormone Receptor β Gene: Structure and Functions in the Brain and Sensory Systems. *https://home.liebertpub.com/thy* **13**, 1057–1068.
26 Yen PM (2001) Physiological and molecular basis of Thyroid hormone action. *Physiological Reviews* **81**, 1097–1142.
27 Brent GA (2012) Mechanisms of thyroid hormone action. *Journal of Clinical Investigation* **122**, 3035–3043.
28 Beumer J & Clevers H (2020) Cell fate specification and differentiation in the adult mammalian intestine. *Nature Reviews Molecular Cell Biology*.
29 Gehart H & Clevers H (2019) *Tales from the crypt: new insights into intestinal stem cells* Nature Publishing Group.
30 Baulies A, Angelis N & Li VSW (2020) Hallmarks of intestinal stem cells. *Development (Cambridge)* **147**.
31 Cheng H & Leblond CP (1974) Origin, differentiation and renewal of the four main epithelial cell types in the mouse small intestine I. Columnar cell. *American Journal of Anatomy* **141**, 461–479.
32 Barker N, Van Es JH, Kuipers J, Kujala P, Van Den Born M, Cozijnsen M, Haegebarth A, Korving J, Begthel H, Peters PJ & Clevers H (2007) Identification of stem cells in small intestine and colon by marker gene Lgr5. *Nature* **449**, 1003–1007.
33 Sato T, Van Es JH, Snippert HJ, Stange DE, Vries RG, Van Den Born M, Barker N, Shroyer NF, Van De Wetering M & Clevers H (2011) Paneth cells constitute the niche for Lgr5 stem cells in intestinal crypts. *Nature* **469**, 415–418.
34 Rothenberg ME, Nusse Y, Kalisky T, Lee JJ, Dalerba P, Scheeren F, Lobo N, Kulkarni S, Sim S, Qian D, Beachy PA, Pasricha PJ, Quake SR & Clarke MF (2012) Identification of a cKit+ colonic crypt base secretory cell that supports Lgr5+ stem cells in mice. *Gastroenterology* **142**, 1195-1205.e6.
35 Beumer J, Gehart H & Clevers H (2020) Enteroendocrine Dynamics - New Tools Reveal Hormonal Plasticity in the Gut. *Endocrine Reviews* **41**, 695.

36 Banerjee A, McKinley ET, Von Moltke J, Coffey RJ & Lau KS (2018) Interpreting heterogeneity in intestinal tuft cell structure and function. *The Journal of Clinical Investigation* **128**, 1711–1719.
37 McCauley HA & Guasch G (2015) Three cheers for the goblet cell: maintaining homeostasis in mucosal epithelia. *Trends in Molecular Medicine* **21**, 492–503.
38 Muñoz J, Stange DE, Schepers AG, Van De Wetering M, Koo BK, Itzkovitz S, Volckmann R, Kung KS, Koster J, Radulescu S, Myant K, Versteeg R, Sansom OJ, Van Es JH, Barker N, Van Oudenaarden A, Mohammed S, Heck AJR & Clevers H (2012) The Lgr5 intestinal stem cell signature: Robust expression of proposed quiescent ′ +4′ cell markers. *EMBO Journal* **31**, 3079–3091.
39 Sangiorgi E & Capecchi MR (2008) Bmi1 is expressed in vivo in intestinal stem cells. *Nature Genetics* **40**, 915–920.
40 Montgomery RK, Carlone DL, Richmond CA, Farilla L, Kranendonk MEG, Henderson DE, Baffour-Awuah NY, Ambruzs DM, Fogli LK, Algra S & Breault DT (2011) Mouse telomerase reverse transcriptase (mTert) expression marks slowly cycling intestinal stem cells. *Proceedings of the National Academy of Sciences of the United States of America* **108**, 179–184.
41 Takeda N, Jain R, LeBoeuf MR, Wang Q, Lu MM & Epstein JA (2011) Interconversion between intestinal stem cell populations in distinct niches. *Science* **334**, 1420–1424.
42 Powell AE, Wang Y, Li Y, Poulin EJ, Means AL, Washington MK, Higginbotham JN, Juchheim A, Prasad N, Levy SE, Guo Y, Shyr Y, Aronow BJ, Haigis KM, Franklin JL & Coffey RJ (2012) The pan-ErbB negative regulator Irig1 is an intestinal stem cell marker that functions as a tumor suppressor. *Cell* **149**, 146–158.
43 Yousefi M, Li N, Nakauka-Ddamba A, Wang S, Davidow K, Schoenberger J, Yu Z, Jensen ST, Kharas MG & Lengner CJ (2016) Msi RNA-binding proteins control reserve intestinal stem cell quiescence. *Journal of Cell Biology* **215**, 401–413.
44 Ayyaz A, Kumar S, Sangiorgi B, Ghoshal B, Gosio J, Ouladan S, Fink M, Barutcu S, Trcka D, Shen J, Chan K, Wrana JL & Gregorieff A (2019) Single-cell transcriptomes of the regenerating intestine reveal a revival stem cell. *Nature* **569**, 121–125.
45 Seishima R & Barker N (2019) A contemporary snapshot of intestinal stem cells and their regulation. *Differentiation* **108**, 3–7.
46 Sheahan BJ, Freeman AN, Keeley TM, Samuelson LC, Roper J, Hasapis S, Lee CL & Dekaney CM (2021) Epithelial Regeneration After Doxorubicin Arises Primarily From Early Progeny of Active Intestinal Stem Cells. *Cmgh* **12**, 119–140.
47 Sato T, Vries RG, Snippert HJ, van de Wetering M, Barker N, Stange DE, van Es JH, Abo A, Kujala P, Peters PJ & Clevers H (2009) Single Lgr5 stem cells build crypt-villus structures in vitro without a mesenchymal niche. *Nature* **459**, 262–265.
48 Powell DW, Pinchuk I V., Saada JI, Chen X & Mifflin RC (2011) Mesenchymal cells of the intestinal lamina propria. *Annual Review of Physiology* **73**, 213–237.

49 McCarthy N, Kraiczy J & Shivdasani RA (2020) Cellular and molecular architecture of the intestinal stem cell niche. *Nature Cell Biology* **22**, 1033–1041.
50 Pinchuk I V., Mifflin RC, Saada JI & Powell DW (2010) Intestinal mesenchymal cells. *Current Gastroenterology Reports* **12**, 310–318.
51 Spit M, Koo BK & Maurice MM (2018) Tales from the crypt: Intestinal niche signals in tissue renewal, plasticity and cancer. *Open Biology* **8**.
52 Sphyris N, Hodder MC & Sansom OJ (2021) Subversion of niche-signalling pathways in colorectal cancer: What makes and breaks the intestinal stem cell. *Cancers* **13**, 1–55.
53 L'Heureux A, Wieland DR, Weng CH, Chen YH, Lin CH, Lin TH & Weng CH (2019) Association Between Thyroid Disorders and Colorectal Cancer Risk in Adult Patients in Taiwan. *JAMA Network Open* **2**.
54 Hellevik AI, Åsvold BO, Bjøro T, Romundstad PR, Nilsen TIL & Vatten LJ (2009) Thyroid function and cancer risk: A prospective population study. *Cancer Epidemiology Biomarkers and Prevention* **18**, 570–574.
55 Brown AR, Simmen RCM & Simmen FA (2013) The role of thyroid hormone signaling in the prevention of digestive system cancers. *International Journal of Molecular Sciences* **14**, 16240–16257.
56 Moeller LC & Führer D (2013) Thyroid hormone, thyroid hormone receptors, and cancer: A clinical perspective. *Endocrine-Related Cancer* **20**.
57 Goemann IM, Romitti M, Meyer ELS, Wajner SM & Maia AL (2017) Role of thyroid hormones in the neoplastic process: An overview. *Endocrine-Related Cancer* **24**, R367–R385.
58 Kress E, Skah S, Sirakov M, Nadjar J, Gadot N, Scoazec JY, Samarut J & Plateroti M (2010) Cooperation Between the Thyroid Hormone Receptor TRα1 and the WNT Pathway in the Induction of Intestinal Tumorigenesis. *Gastroenterology* **138**, 1863–1874.
59 Uchuya-Castillo J, Aznar N, Frau C, Martinez P, Le Nevé C, Marisa L, Penalva LOFF, Laurent-Puig P, Puisieux A, Scoazec J-YY, Samarut J, Ansieau S & Plateroti M (2018) Increased expression of the thyroid hormone nuclear receptor TRα1 characterizes intestinal tumors with high Wnt activity. *Oncotarget* **9**, 30979–30996.
60 Lee YS, Chin YT, Yang YCSH, Wei PL, Wu HC, Shih A, Lu YT, Pedersen JZ, Incerpi S, Liu LF, Lin HY & Davis PJ (2016) The combination of tetraiodothyroacetic acid and cetuximab inhibits cell proliferation in colorectal cancers with different K-ras status. *Steroids* **111**, 63–70.
61 Iishi H, Tatsuta M, Baba M, Okuda S & Taniguchi H (1992) Enhancement by thyroxine of experimental carcinogenesis induced in rat colon by azoxymethane. *International Journal of Cancer* **50**, 974–976.
62 Rennert G, Rennert HS, Pinchev M & Gruber SB (2010) A Case–Control Study of Levothyroxine and the Risk of Colorectal Cancer. *JNCI: Journal of the National Cancer Institute* **102**, 568–572.
63 Wändell P, Carlsson AC, Li X, Sundquist J & Sundquist K (2020) Levothyroxine treatment is associated with an increased relative risk of overall and organ specific incident cancers - a cohort study of the Swedish population. *Cancer epidemiology* **66**.
64 Boursi B, Haynes K, Mamtani R & Yang YX (2015) Thyroid Dysfunction, Thyroid Hormone Replacement and Colorectal Cancer Risk. *JNCI Journal of the National Cancer Institute* **107**.

65 Sirakov M & Plateroti M (2011) The thyroid hormones and their nuclear receptors in the gut: From developmental biology to cancer. *Biochimica et Biophysica Acta - Molecular Basis of Disease* **1812**, 938–946.
66 Kim WG & Cheng SY (2013) Thyroid hormone receptors and cancer. *Biochimica et Biophysica Acta - General Subjects* **1830**, 3928–3936.
67 Kowalik MA, Perra A, Pibiri M, Cocco MT, Samarut J, Plateroti M, Ledda-Columbano GM & Columbano A (2010) TRβ is the critical thyroid hormone receptor isoform in T3-induced proliferation of hepatocytes and pancreatic acinar cells. *Journal of Hepatology* **53**, 686–692.
68 Lin K huei, Lin Y wen, Lee H fang, Liu WL, Chen ST, Chang KSS & Cheng S yann (1995) Increased invasive activity of human hepatocellular carcinoma cells is associated with an overexpression of thyroid hormone β1 nuclear receptor and low expression of the anti-metastatic nm23 gene. *Cancer Letters* **98**, 89–95.
69 Markowitz S, Haut M, Stellato T, Gerbic C & Molkentin K (1989) Expression of the ErbA-beta class of thyroid hormone receptors is selectively lost in human colon carcinoma. *The Journal of clinical investigation* **84**, 1683–1687.
70 Hörkkö TT, Tuppurainen K, George SM, Jernvall P, Karttunen TJ & Mäkinen MJ (2006) Thyroid hormone receptor β1 in normal colon and colorectal cancer–association with differentiation, polypoid growth type and K-ras mutations. *International Journal of Cancer* **118**, 1653–1659.
71 Furuya F, Shimura H, Yamashita S, Endo T & Kobayashi T (2010) Liganded thyroid hormone receptor-α enhances proliferation of pancreatic β-cells. *Journal of Biological Chemistry* **285**, 24477–24486.
72 Heublein S, Mayr D, Meindl A, Angele M, Gallwas J, Jeschke U & Ditsch N (2015) Thyroid hormone receptors predict prognosis in BRCA1 associated breast cancer in opposing ways. *PLoS ONE* **10**, e0127072.
73 Sirakov M, Boussouar AA, Kress E, Frau C, Lone IN, Nadjar J, Angelov D & Plateroti M (2015) The thyroid hormone nuclear receptor TRα1 controls the Notch signaling pathway and cell fate in murine intestine. *Development (Cambridge)* **142**, 2764–2774.
74 Kress E, Rezza A, Nadjar J, Samarut J & Plateroti M (2009) The frizzled-related sFRP2 gene is a target of thyroid hormone receptor α1 and activates β-catenin signaling in mouse intestine. *Journal of Biological Chemistry* **284**, 1234–1241.
75 Skah S, Uchuya-Castillo J, Sirakov M & Plateroti M (2017) The thyroid hormone nuclear receptors and the Wnt/β-catenin pathway: An intriguing liaison. *Developmental Biology* **422**, 71–82.
76 Plateroti M, Kress E, Mori JI & Samarut J (2006) Thyroid Hormone Receptor α1 Directly Controls Transcription of the β-Catenin Gene in Intestinal Epithelial Cells. *Molecular and Cellular Biology* **26**, 3204–3214.
77 Sirakov M, Claret L & Plateroti M (2021) Thyroid Hormone Nuclear Receptor TRα1 and Canonical WNT Pathway Cross-Regulation in Normal Intestine and Cancer. *Frontiers in Endocrinology* **12**, 1653.
78 Guinney J, Dienstmann R, Wang X, De Reyniès A, Schlicker A, Soneson C, Marisa L, Roepman P, Nyamundanda G, Angelino P, Bot BM, Morris JS, Simon IM, Gerster S, Fessler E, De Sousa .E Melo F, Missiaglia E, Ramay H, Barras D, Homicsko K, Maru D, Manyam GC, Broom B, Boige V, Perez-Villamil B, Laderas T, Salazar R, Gray JW, Hanahan D, Tabernero J, Bernards R, Friend SH, Laurent-Puig P, Medema JP, Sadanandam A,

Wessels L, Delorenzi M, Kopetz S, Vermeulen L & Tejpar S (2015) The consensus molecular subtypes of colorectal cancer. *Nature Medicine* **21**, 1350–1356.
79 Hasebe T, Buchholz DR, Shi YB & Ishizuya-Oka A (2011) Epithelial-connective tissue interactions induced by thyroid hormone receptor are essential for adult stem cell development in the Xenopus laevis intestine. *Stem Cells* **29**, 154–161.
80 Shi YB (2021) Life Without Thyroid Hormone Receptor. *Endocrinology* **162**, 1–12.
81 Wen L & Shi YB (2016) Regulation of growth rate and developmental timing by Xenopus thyroid hormone receptor α. *Development, Growth & Differentiation* **58**, 106–115.
82 Shibata Y, Tanizaki Y & Shi YB (2020) Thyroid hormone receptor beta is critical for intestinal remodeling during Xenopus tropicalis metamorphosis. *Cell and Bioscience* **10**, 1–15.
83 Shibata Y, Tanizaki Y, Zhang H, Lee H, Dasso M & Shi YB (2021) Thyroid Hormone Receptor Is Essential for Larval Epithelial Apoptosis and Adult Epithelial Stem Cell Development but Not Adult Intestinal Morphogenesis during Xenopus tropicalis Metamorphosis. *Cells 2021, Vol 10, Page 536* **10**, 536.
84 Tanizaki Y, Shibata Y, Zhang H & Shi YB (2021) Analysis of Thyroid Hormone Receptor α-Knockout Tadpoles Reveals That the Activation of Cell Cycle Program Is Involved in Thyroid Hormone-Induced Larval Epithelial Cell Death and Adult Intestinal Stem Cell Development during Xenopus tropicalis Metamorphos. *Thyroid* **31**, 128–142.
85 Shi YB & Brown DD (1993) The earliest changes in gene expression in tadpole intestine induced by thyroid hormone. *Journal of Biological Chemistry* **268**, 20312–20317.
86 Hasebe T, Kajita M, Fu L, Shi YB & Ishizuya-Oka A (2012) Thyroid hormone-induced sonic hedgehog signal up-regulates its own pathway in a paracrine manner in the Xenopus laevis intestine during metamorphosis. *Developmental Dynamics* **241**, 403–414.
87 Ishizuya-Oka A, Ueda S, Amano T, Shimizu K, Suzuki K, Ueno N & Yoshizato K (2001) Thyroid-hormone-dependent and fibroblast-specific expression of BMP-4 correlates with adult epithelial development during amphibian intestinal remodeling. *Cell and Tissue Research* **303**, 187–195.
88 Ishizuya-Oka A, Hasebe T, Shimizu K, Suzuki K & Ueda S (2006) Shh/BMP-4 signaling pathway is essential for intestinal epithelial development during Xenopus larval-to-adult remodeling. *Developmental Dynamics* **235**, 3240–3249.
89 Ishizuya-Oka A, Kajita M & Hasebe T (2014) Thyroid hormone-regulated wnt5a/ror2 signaling is essential for dedifferentiation of larval epithelial cells into adult stem cells in the xenopus laevis intestine. *PLoS ONE* **9**.
90 Hasebe T, Fujimoto K, Kajita M & Ishizuya-Oka A (2016) Thyroid hormone activates Wnt/β-catenin signaling involved in adult epithelial development during intestinal remodeling in Xenopus laevis. *Cell and Tissue Research* **365**, 309–318.
91 Ishizuya-Oka A (2017) How thyroid hormone regulates transformation of larval epithelial cells into adult stem cells in the amphibian intestine. *Molecular and Cellular Endocrinology* **459**, 98–103.

92 Hasebe T, Fujimoto K, Kajita M & Ishizuya-Oka A (2016) Thyroid hormone activates Wnt/β-catenin signaling involved in adult epithelial development during intestinal remodeling in Xenopus laevis. *Cell and tissue research* **365**, 309–318.
93 Ishizuya-Oka A (2017) How thyroid hormone regulates transformation of larval epithelial cells into adult stem cells in the amphibian intestine. *Molecular and cellular endocrinology* **459**, 98–103.
94 Kaestner KH (2019) The Intestinal Stem Cell Niche: A Central Role for Foxl1-Expressing Subepithelial Telocytes. *Cmgh* **8**, 111–117.
95 Kondo A & Kaestner KH (2019) Emerging diverse roles of telocytes. *Development (Cambridge)* **146**.
96 Hasebe T, Fujimoto K & Ishizuya-Oka A (2020) Thyroid hormone-induced expression of Foxl1 in subepithelial fibroblasts correlates with adult stem cell development during Xenopus intestinal remodeling. *Scientific Reports* **10**, 1–11.
97 Hasebe T, Fujimoto K, Kajita M, Fu L, Shi YB & Ishizuya-Oka A (2017) Thyroid Hormone-Induced Activation of Notch Signaling is Required for Adult Intestinal Stem Cell Development During Xenopus Laevis Metamorphosis. *Stem Cells* **35**, 1028–1039.
98 Ishizuya-Oka A, Shimizu K, Sakakibara SI, Okano H & Ueda S (2003) Thyroid hormone-upregulated expression of Musashi-1 is specific for progenitor cells of the adult epithelium during amphibian gastrointestinal remodeling. *Journal of Cell Science* **116**, 3157–3164.
99 Salvatore D (2018) Deiodinases and stem cells: an intimate relationship. *Journal of Endocrinological Investigation* **41**, 59–66.
100 Kojima Y, Kondo Y, Fujishita T, Mishiro-Sato E, Kajino-Sakamoto R, Taketo MM & Aoki M (2019) Stromal iodothyronine deiodinase 2 (DIO2) promotes the growth of intestinal tumors in ApcΔ716 mutant mice. *Cancer Science* **110**, 2520–2528.
101 Dentice M, Luongo C, Ambrosio R, Sibilio A, Casillo A, Iaccarino A, Troncone G, Fenzi G, Larsen PR & Salvatore D (2012) β-Catenin Regulates Deiodinase Levels and Thyroid Hormone Signaling in Colon Cancer Cells. *Gastroenterology* **143**, 1037–1047.
102 Catalano V, Dentice M, Ambrosio R, Luongo C, Carollo R, Benfante A, Todaro M, Stassi G & Salvatore D (2016) Activated thyroid hormone promotes differentiation and chemotherapeutic sensitization of colorectal cancer stem cells by regulating Wnt and BMP4 signaling. *Cancer Research* **76**, 137–1244.
103 Dentice M, Marsili A, Zavacki A, Larsen PR & Salvatore D (2013) The deiodinases and the control of intracellular thyroid hormone signaling during cellular differentiation. *Biochimica et Biophysica Acta - General Subjects* **1830**, 3937–3945.
104 Ferrara SJ, Chaudhary P, DeBell MJ, Marracci G, Miller H, Calkins E, Pocius E, Napier BA, Emery B, Bourdette D & Scanlan TS (2021) TREM2 is thyroid hormone regulated making the TREM2 pathway druggable with ligands for thyroid hormone receptor. *Cell Chemical Biology* **0**.
105 De Luca R, Davis PJ, Lin HY, Gionfra F, Percario ZA, Affabris E, Pedersen JZ, Marchese C, Trivedi P, Anastasiadou E, Negro R & Incerpi S (2021) Thyroid Hormones Interaction With Immune Response, Inflammation and

Non-thyroidal Illness Syndrome. *Frontiers in Cell and Developmental Biology* **8**, 1775.
106 Lee YS, Chin YT, Shih YJ, Nana AW, Chen YR, Wu HC, Yang YCSH, Lin HY & Davis PJ (2018) Thyroid Hormone Promotes β-Catenin Activation and Cell Proliferation in Colorectal Cancer. *Hormones and Cancer* **9**, 156–165.
107 Davis PJ, Goglia F & Leonard JL (2016) Nongenomic actions of thyroid hormone. *Nature Reviews Endocrinology* **12**, 111–121.
108 Davis PJ, Leonard JL, Lin H-Y, Leinung M & Mousa SA (2018) Molecular Basis of Nongenomic Actions of Thyroid Hormone. In *Vitamins and Hormones* pp. 67–96. Academic Press.
109 Schmohl KA, Mueller AM, Dohmann M, Spellerberg R, Urnauer S, Schwenk N, Ziegler SI, Bartenstein P, Nelson PJ & Spitzweg C (2019) Integrin αvβ3-Mediated Effects of Thyroid Hormones on Mesenchymal Stem Cells in Tumor Angiogenesis. *Thyroid* **29**, 1843–1857.
110 Schmohl KA, Müller AM, Nelson PJ & Spitzweg C (2020) Thyroid Hormone Effects on Mesenchymal Stem Cell Biology in the Tumour Microenvironment. *Experimental and Clinical Endocrinology and Diabetes* **128**, 462–468.
111 Beyaz S, Mana MD, Roper J, Kedrin D, Saadatpour A, Hong SJ, Bauer-Rowe KE, Xifaras ME, Akkad A, Arias E, Pinello L, Katz Y, Shinagare S, Abu-Remaileh M, Mihaylova MM, Lamming DW, Dogum R, Guo G, Bell GW, Selig M, Nielsen GP, Gupta N, Ferrone CR, Deshpande V, Yuan GC, Orkin SH, Sabatini DM & Yilmaz ÖH (2016) High-fat diet enhances stemness and tumorigenicity of intestinal progenitors. *Nature* **531**, 53–58.
112 Rodríguez-Colman MJ, Schewe M, Meerlo M, Stigter E, Gerrits J, Pras-Raves M, Sacchetti A, Hornsveld M, Oost KC, Snippert HJ, Verhoeven-Duif N, Fodde R & Burgering BMT (2017) Interplay between metabolic identities in the intestinal crypt supports stem cell function. *Nature* **543**, 424–427.
113 Yilmaz ÖH, Katajisto P, Lamming DW, Gültekin Y, Bauer-Rowe KE, Sengupta S, Birsoy K, Dursun A, Onur Yilmaz V, Selig M, Nielsen GP, Mino-Kenudson M, Zukerberg LR, Bhan AK, Deshpande V & Sabatini DM (2012) MTORC1 in the Paneth cell niche couples intestinal stem-cell function to calorie intake. *Nature* **486**, 490–495.
114 Alonso S & Yilmaz ÖH (2018) Nutritional regulation of intestinal stem cells. *Annual Review of Nutrition* **38**, 273–301.
115 Calibasi-Kocal G, Mashinchian O, Basbinar Y, Ellidokuz E, Cheng CW & Yilmaz ÖH (2021) Nutritional Control of Intestinal Stem Cells in Homeostasis and Tumorigenesis. *Trends in Endocrinology and Metabolism* **32**, 20–35.
116 Mullur R, Liu YY & Brent GA (2014) Thyroid hormone regulation of metabolism. *Physiological Reviews* **94**, 355–382.
117 Liu YY & Brent GA (2010) Thyroid hormone crosstalk with nuclear receptor signaling in metabolic regulation. *Trends in Endocrinology and Metabolism* **21**, 166–173.
118 Yin L, Zhang Y & Bradley Hillgartner F (2002) Sterol Regulatory Element-binding Protein-1 Interacts with the Nuclear Thyroid Hormone Receptor to Enhance Acetyl-CoA Carboxylase-α Transcription in Hepatocytes *. *Journal of Biological Chemistry* **277**, 19554–19565.
119 Shin DJ, Plateroti M, Samarut J & Osborne TF (2006) Two uniquely arranged thyroid hormone response elements in the far upstream 5′ flanking region confer direct thyroid hormone regulation to the murine cholesterol 7α hydroxylase gene. *Nucleic Acids Research* **34**, 3853–3861.

120 Bertolio R, Napoletano F, Mano M, Maurer-Stroh S, Fantuz M, Zannini A, Bicciato S, Sorrentino G & Del Sal G (2019) Sterol regulatory element binding protein 1 couples mechanical cues and lipid metabolism. *Nature Communications 2019 10:1* **10**, 1–11.
121 Jumarie C & Malo C (1994) Alkaline phosphatase and peptidase activities in Caco-2 cells: Differential response to triiodothyronine. *In Vitro Cellular & Developmental Biology - Animal* **30**, 753–760.
122 Hodin RA, Chamberlain SM & Upton MP (1992) Thyroid hormone differentially regulates rat intestinal brush border enzyme gene expression. *Gastroenterology* **103**, 1529–1536.
123 Plateroti M, Chassande O, Fraichard A, Gauthier K, Freund JN, Samarut J & Kedinger M (1999) Involvement of T3Rα- and β-receptor subtypes in mediation of T3 functions during postnatal murine intestinal development. *Gastroenterology* **116**, 1367–1378.
124 Ludikhuize MC, Meerlo M, Gallego MP, Xanthakis D, Burgaya Julià M, Nguyen NTB, Brombacher EC, Liv N, Maurice MM, Paik J hye, Burgering BMT & Rodriguez Colman MJ (2020) Mitochondria Define Intestinal Stem Cell Differentiation Downstream of a FOXO/Notch Axis. *Cell Metabolism* **32**, 889-900.e7.
125 Urbauer E, Rath E & Haller D (2021) Mitochondrial Metabolism in the Intestinal Stem Cell Niche—Sensing and Signaling in Health and Disease. *Frontiers in Cell and Developmental Biology* **8**, 1520.
126 Lesmana R, Sinha RA, Singh BK, Zhou J, Ohba K, Wu Y, Yau WW, Bay BH & Yen PM (2016) Thyroid hormone stimulation of autophagy is essential for mitochondrial biogenesis and activity in skeletal muscle. *Endocrinology* **157**, 23–38.
127 Zhou J, Gauthier K, Ho JP, Lim A, Zhu XG, Han CR, Sinha RA, Cheng SY & Yen PM (2021) Thyroid hormone receptor α regulates autophagy, mitochondrial biogenesis, and fatty acid use in skeletal muscle. *Endocrinology (United States)* **162**, 1–11.
128 Na W, Fu L, Luu N & Shi YB (2020) Thyroid hormone directly activates mitochondrial fission process 1 (Mtfp1) gene transcription during adult intestinal stem cell development and proliferation in Xenopus tropicalis. *General and Comparative Endocrinology* **299**, 113590.
129 Attia RR, Connnaughton S, Boone LR, Wang F, Elam MB, Ness GC, Cook GA & Park EA (2010) Regulation of pyruvate dehydrogenase kinase 4 (PDK4) by thyroid hormone role of the peroxisome proliferator-activated receptor γ coactivator (PGC-1α). *Journal of Biological Chemistry* **285**, 2375–2385.
130 Lin HY, Chin YT, Yang YCSH, Lai HY, Wang-Peng J, Liu LF, Tang HY & Davis PJ (2016) Thyroid Hormone, Cancer, and Apoptosis. *Comprehensive Physiology* **6**, 1221–1237.
131 Bassett JHD, Harvey CB & Williams GR (2003) Mechanisms of thyroid hormone receptor-specific nuclear and extra nuclear actions. In *Molecular and Cellular Endocrinology* pp. 1–11.
132 MATOSIN-MATEKALO M, MESONERO JE, LAROCHE TJ, LACASA M & BROT-LAROCHE E (1999) Glucose and thyroid hormone co-regulate the expression of the intestinal fructose transporter GLUT5. *Biochemical Journal* **339**, 233–239.

133 Choi J, Moskalik CL, Ng A, Matter SF, Buchholz DR, J C, CL M, A N, SF M & DR B (2015) Regulation of thyroid hormone-induced development in vivo by thyroid hormone transporters and cytosolic binding proteins. **222**, 69–80.
134 Weinhofer I, Kunze M, Rampler H, Forss-Petter S, Samarut J, Plateroti M & Berger J (2008) Distinct modulatory roles for thyroid hormone receptors TRα and TRβ in SREBP1-activated ABCD2 expression. *European Journal of Cell Biology* **87**, 933–945.
135 Grøntved L, Waterfall JJ, Kim DW, Baek S, Sung MH, Zhao L, Won Park J, Nielsen R, Walker RL, Zhu YJ, Meltzer PS, Hager GL & Cheng SY (2015) Transcriptional activation by the thyroid hormone receptor through ligand-dependent receptor recruitment and chromatin remodelling. *Nature Communications* **6**, 1–11.
136 Wang B, Rong X, Palladino END, Wang J, Fogelman AM, Martín MG, Alrefai WA, Ford DA & Tontonoz P (2018) Phospholipid Remodeling and Cholesterol Availability Regulate Intestinal Stemness and Tumorigenesis. *Cell Stem Cell* **22**, 206-220.e4.
137 Wen YA, Xiong X, Zaytseva YY, Napier DL, Vallee E, Li AT, Wang C, Weiss HL, Evers BM & Gao T (2018) Downregulation of SREBP inhibits tumor growth and initiation by altering cellular metabolism in colon cancer article. *Cell Death and Disease* **9**.
138 Zhang Y, Ma K, Song S, Elam MB, Cook GA & Park EA (2004) Peroxisomal proliferator-activated receptor-γ coactivator-1α (PGC-1α) enhances the thyroid hormone induction of carnitine palmitoyltransferase I (CPT-Iα). *Journal of Biological Chemistry* **279**, 53963–53971.
139 Jackson-Hayes L, Song S, Lavrentyev EN, Jansen MS, Hillgartner FB, Tian L, Wood PA, Cook GA & Park EA (2003) A thyroid hormone response unit formed between the promoter and first intron of the carnitine palmitoyltransferase-Iα gene mediates the liver-specific induction by thyroid hormone. *Journal of Biological Chemistry* **278**, 7964–7972.
140 Sayre NL & Lechleiter JD (2012) Fatty acid metabolism and thyroid hormones. *Current trends in endocrinology* **6**, 65–76.
141 Sandra Chocron E, Sayre NL, Holstein D, Saelim N, Ibdah JA, Dong LQ, Zhu X, Cheng SY & Lechleiter JD (2012) The trifunctional protein mediates thyroid hormone receptor-dependent stimulation of mitochondria metabolism. *Molecular Endocrinology* **26**, 1117–1128.
142 Mihaylova MM, Cheng CW, Cao AQ, Tripathi S, Mana MD, Bauer-Rowe KE, Abu-Remaileh M, Clavain L, Erdemir A, Lewis CA, Freinkman E, Dickey AS, La Spada AR, Huang Y, Bell GW, Deshpande V, Carmeliet P, Katajisto P, Sabatini DM & Yilmaz ÖH (2018) Fasting Activates Fatty Acid Oxidation to Enhance Intestinal Stem Cell Function during Homeostasis and Aging. *Cell Stem Cell* **22**, 769-778.e4.
143 Yousefi M, Nakauka-Ddamba A, Berry CT, Li N, Schoenberger J, Simeonov KP, Cedeno RJ, Yu Z & Lengner CJ (2018) Calorie Restriction Governs Intestinal Epithelial Regeneration through Cell-Autonomous Regulation of mTORC1 in Reserve Stem Cells. *Stem Cell Reports* **10**, 703–711.
144 Kress E, Rezza A, Nadjar J, Samarut J & Plateroti M (2008) The thyroid hormone receptor-α (TRα) gene encoding TRα1 controls deoxyribonucleic acid damage-induced tissue repair. *Molecular Endocrinology* **22**, 47–55.
145 Mana MD, Hussey AM, Tzouanas CN, Imada S, Barrera Millan Y, Bahceci D, Saiz DR, Webb AT, Lewis CA, Carmeliet P, Mihaylova MM, Shalek AK &

Yilmaz ÖH (2021) High-fat diet-activated fatty acid oxidation mediates intestinal stemness and tumorigenicity. *Cell Reports* **35**.
146 Xiong X, Wen Y-AA, Fairchild R, Zaytseva YY, Weiss HL, Evers BM & Gao T (2020) *Upregulation of CPT1A is essential for the tumor-promoting effect of adipocytes in colon cancer* Nature Publishing Group.
147 Lu C & Cheng SY (2010) Thyroid hormone receptors regulate adipogenesis and carcinogenesis via crosstalk signaling with peroxisome proliferator-activated receptors. *Journal of Molecular Endocrinology* **44**, 143–154.
148 Boon R, Silveira GG & Mostoslavsky R (2020) Nuclear metabolism and the regulation of the epigenome. *Nature Metabolism* **2**, 1190–1203.
149 Fu L, Yin J & Shi YB (2019) Involvement of epigenetic modifications in thyroid hormone-dependent formation of adult intestinal stem cells during amphibian metamorphosis. *General and Comparative Endocrinology* **271**, 91–96.
150 Tanizaki Y, Bao L, Shi B & Shi YB (2021) A Role of Endogenous Histone Acetyltransferase Steroid Hormone Receptor Coactivator 3 in Thyroid Hormone Signaling during Xenopus Intestinal Metamorphosis. *Thyroid* **31**, 692–702.
151 Hasebe T, Fujimoto K, Buchholz DR & Ishizuya-Oka A (2020) Stem cell development involves divergent thyroid hormone receptor subtype expression and epigenetic modifications in the Xenopus metamorphosing intestine. *General and Comparative Endocrinology* **292**, 113441.
152 Anselmo J & Chaves CM (2020) Physiologic Significance of Epigenetic Regulation of Thyroid Hormone Target Gene Expression. *European Thyroid Journal* **9**, 114–123.
153 Suh JH, Sieglaff DH, Zhang A, Xia X, Cvoro A, Winnier GE & Webb P (2013) SIRT1 is a Direct Coactivator of Thyroid Hormone Receptor β1 with Gene-Specific Actions. *PLOS ONE* **8**, e70097.

Figure Legends

Figure 1. TRα1 action and location within the small intestine and colon epithelia. A) (*Upper*) Modular organization of the TRα1 nuclear receptor, including DNA-binding (DBD) and ligand-binding (LBD) domains. (*Lower*) Typical organization of thyroid hormone responsive elements (TREs) on target genes constituted by two repetitions of half-sites organized in different manners, as indicated. **B)** Model of TR action on target genes. For a gene positively regulated by T3, in the absence of T3, co-repressors are recruited resulting in the inhibition of transcription. Upon T3 binding, co-activators bind to TR inducing transcription. **C)** Organization of the intestinal mucosa in small intestine (*upper* panel) and colon (*middle* panel), showing the vertical epithelial axis. At the bottom of the axis reside stem/progenitor cells while in the higher part of vertical axis are located differentiated cells. It is interesting to note that TRα1 has a gradient of expression similar to Wnt and Notch pathway activities, while BMP pathway presents an opposite gradient. In the *bottom* panel are depicted the different cell types present in the mucosa, including epithelial and mesenchymal-derived cells. The Figure was created with BioRender.com (agreement number: QC23PTXLWH).

Figure 2. Proposed models recapitulating the integration of classical signaling and metabolic pathways depending on TH/TRα1 in intestinal crypts and colon cancer cells. A) Differential outcome in stem cells (SCs) or in Paneth cells in response to T3, possibly inducing metabolic shifts. Accumulating data suggest that T3 through the TRα1 receptor modulates the stemness in crypts *via* regulation of the Wnt and Notch pathways. However, recent data also point to the induction of metabolic challenges stimulated by high glucose and high lipid metabolism, acting on the balance between self-renewal and differentiation [7,28,33]. Importantly, T3 also induces an increase of Paneth cells in the intestinal crypts [9]. Paneth cells are well known to act on stemness through Wnt and Notch, but also to produce lactate that once up-taken by SCs contributes to the oxidative phosphorylation (OXPHOS) metabolic pathway [112], participating in the maintenance of the stem phenotype. **B)** Overview of the integrated glucose and lipid metabolism in the intestinal SCs under T3 treatment. We speculate that T3 might mimic a high glycolysis and high lipolysis condition increasing OXPHOS. Upon oxidation of fatty acids, stimulated OXPHOS can induce reactive oxygen species (ROS) and p38 expression. The stemness, stimulated by Wnt and Notch, or the differentiation induced by ROS/p38, depend on the balance between these two events. **C)** Integrated view of the action of T3/TRα1 in a cancer context. Adipocytes are strongly mobilized in the cancer environment and considered as part of the cancer stem cell niche [52,146,147], releasing high levels of lipids that can be absorbed by cancer cells. The T3-induced transcriptional program includes genes involved in fatty acid oxidation, OXPHOS, and stemness together with mitochondrial turnover. The balance between these major events determines the extent of stem potential *versus* their differentiation. The Figure was created with BioRender.com (agreement number: PO23PTXM00).

Giolito and Plateroti, Table 1

Table 1. Representative literature on TH/TR and CRCs

	Cancer type; Organism; Details	Observations and Comments	TR involved	References
Protection by THs	CRC; Colon and Rectum/sigmoid; Human; Epidemiology; Replacement therapy	Hypothyroid patients received Levothyroxine to normalize TH levels. Reduced risk of CRC, not always significant	ND	Rennert et al. J Natl Cancer Inst. 2010 Apr 21;102(8):568-72. Friedman et al. J. Natl. Cancer Inst. 2011 Nov 2;103(21):1637-9.
	CRC; Human; Epidemiology	Patients suffering Grave's disease (hyperthyroid). Patients very probably treated to cure hyperthyroidism	ND	Cheng et al. Thyroid 2013, 23(7):879-84.
	CRC; Human epidemiology; Replacement therapy; Hypothyroid patients	Hypothyroid patients treated with THs replacement have less risk of CRC. Hypothyroid patients had increased risk of CRCs compared with those receiving replacement therapy	ND	Boursi et al. J Natl Cancer Inst. 2015, 107(6):djv084.
	Colon; Human epidemiology	Lower risk of colon cancer in hyperthyroid patients	ND	L'Hereux et al. JAMA Network Open 2019, 2(5):e193755.
	Metastatic CRC; Human; Low circulating T3	High T3 in patients with metastatic CRCs. No causal proof between metastasis and T3	ND	Rose et al. Arch. Intern. Med. 1981, 141:116-1164.
	Human adenomas and adenocarcinomas; D3 and local hypothyroidism	Association between D3 expression and tumors at early stages	ND	Dentice et al. Gastroenterology 2012, 143(4):1037-47.
	CRC; Human primary tumor cells; D3 and intracellular hypothyroidism	In vitro T3 increases chemosensitivity	TRα1	Catalano et al. Cancer Research 2016, 76(5):1237-44.
	CRC; Human	Strong TRβ1 down-regulation	TRβ1	Markowitz et al. J. Clin. Investig.1989, 84:1683-1687.
	CRC; Human	Higher TRβ1 expression in more differentiated tumors	TRβ1	Horkko et al. Int. J. Cancer 2006, 118(7):1653-9.
Worsening by THs	Rectal; Human epidemiology	Lower risk of rectal cancer in hypothyroid patients	ND	L'Hereux et al. JAMA Network Open 2019, 2(5):e193755.
	CRC; Human epidemiology; Replacement therapy; Hyperthyroid patients	Hypothyroid patients treated with THs replacement has less risk of CRC. Hyperthyroid patients had increased risk of CRCs compared with those receiving replacement therapy	ND	Boursi et al. J Natl Cancer Inst. 2015, 107(6):djv084.
	CRCs; Human epidemiology; Low TSH and high THs	Increased CRC incidence in hyperthyroid patients, but limited number of cases	ND	Hellevik et al. Cancer Epidemiology, Biomarkers & Prevention 2009, 18:570–574.
	Colon; Rat; Chemical induced tumors	T4 increases tumor number in an AOM-chemical carcinogenesis model	ND	Iishi et al. Int. J. Cancer 1992, 50:974–976.
	CRCs; Human; Transcriptomics	TRα1 increased in several CMS. THs status unknown	TRα1	Uchuya-Castillo et al. Oncotarget 2018, 9(57):30979-30996.
	Intestine and colon cancer; Mouse	TRα1 overexpression in intestinal epithelium induces hyperproliferation and adenomas. Proliferation is further increased by TH injections. In mutant Apc mice, TRα1 overexpression increases speed of tumor formation, their number and metastatic capacity	TRα1	Kress et al. Gastroenterology 2010, 138(5):1863-74.
	Colon adenocarcinoma cell lines	THs stimulates growth of explants and metastasis spreading. Effect mediated by integrin avb3 that can be inhibited by TETRAC (competes with T4 and blocks signaling)	ND	Lin et al. Steroids 2016, 114:59-67.
	Colorectal; Human epidemiology; Replacement therapy	Levothyroxine replacement therapy is associated with higher risk of CRCs in women but not in men	ND	Wandell et al. Cancer Epidemiology 2020, 66:101707.

ND: not determined

Giolito and Plateroti, Figure 1

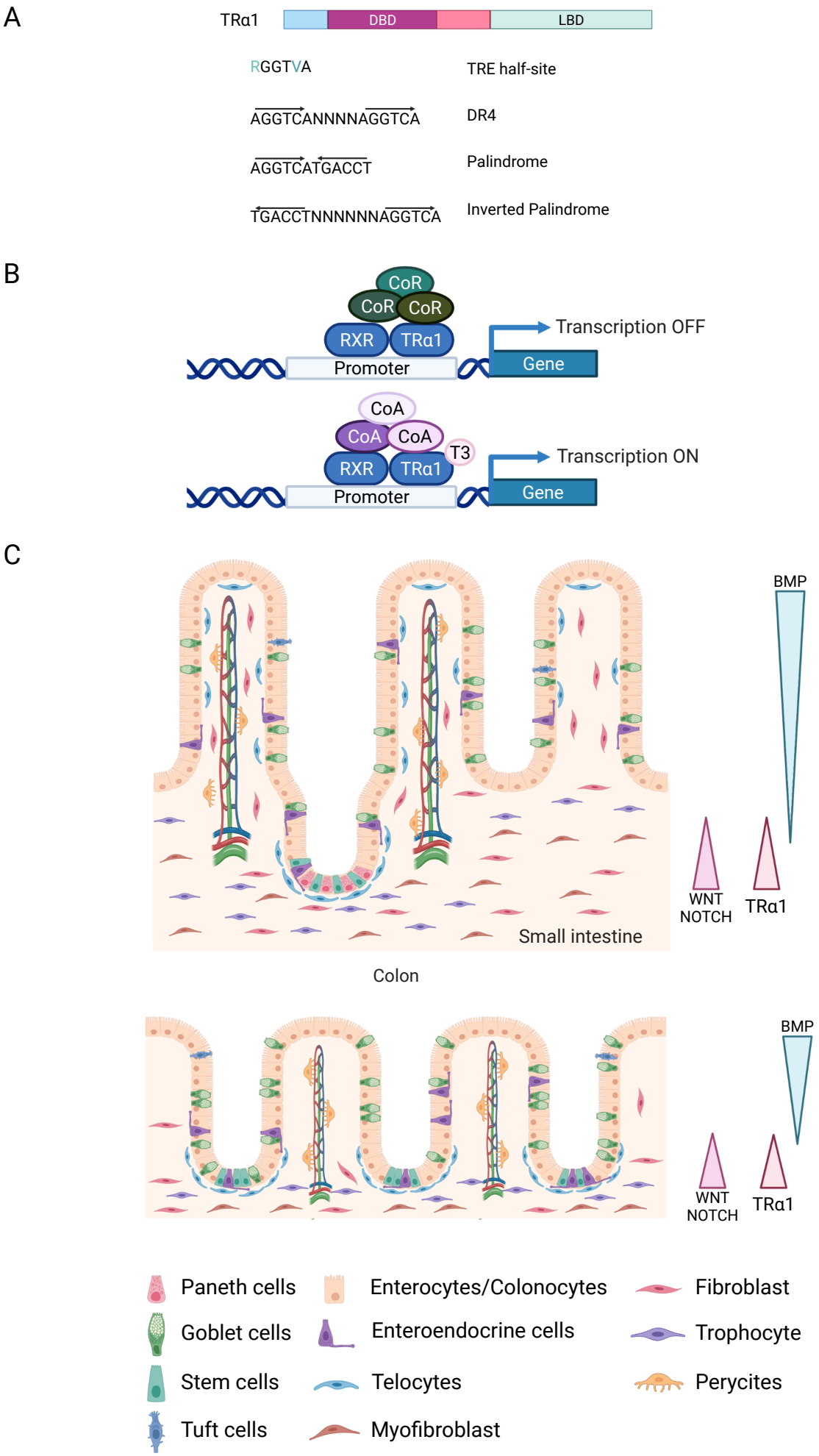

Giolito and Plateroti, Figure 2

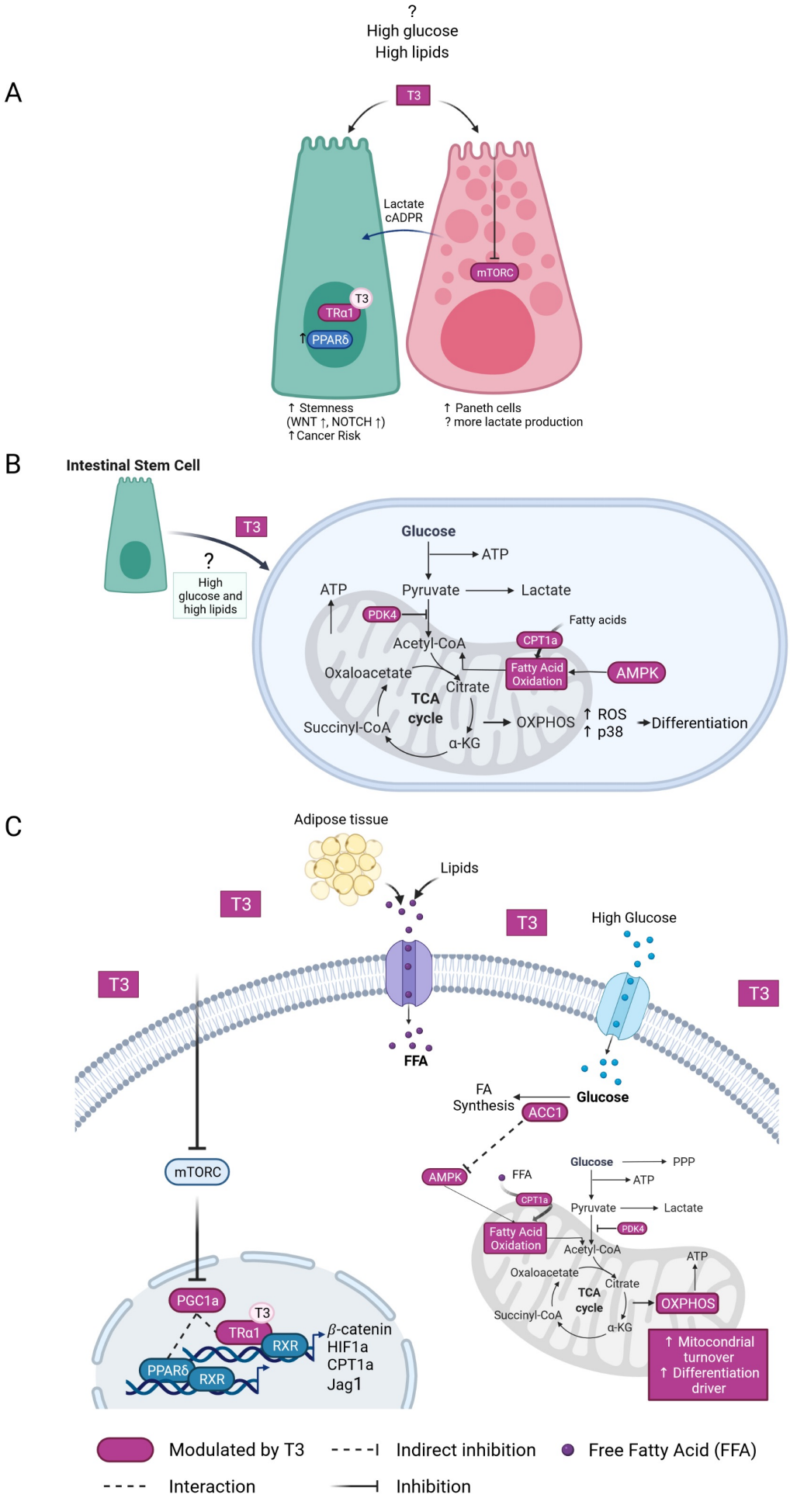

Chapter 5: Discussion

As extensively seen in this thesis, CRC is the second leading cause of death by cancer worldwide. Despite the huge effort from researchers and clinicians to understand the disease, to prevent and tackle it, it is still the third cancer for incidence worldwide (in both sexes) [114]. CRC provides a valuable system to study the involvement of genetic mutations (hereditary or acquired) in the development of the neoplasm. As the colon is constantly impacted by environmental factors, both external and internal (including hormones, xenobiotics, daily nutrients, pollutants, etc.), it is also a good model to study the contribution of these factors to CRC development, allowing the analysis of inherited and acquired somatic genetic alterations [115,116]. Moreover, CRCs are composed of different cell populations, including the CSC and the bulk tumour cells displaying some differentiation traits, constituting a hierarchical structure reminiscent of the normal colon crypt epithelium [118,119]. This complexity and heterogeneity impact the response to the treatments given to CRC patients regardless of their nature (chemotherapies or targeted therapies).

This thesis mentioned that resistance and persistence to chemotherapy are not synonyms and cannot be interchanged. One of the reasons for this is that the acquisition of this capacity to evade the chemotherapeutic treatment can be intrinsic (primary resistance linked to an inherited genetic advantage) or acquired (secondary resistance, which can go through a *de novo* mutation, an epigenetic change or a phenotypic adaptation in response to the presence of the selective pressure) [167,171]. In other words, persistence to therapy and the apparition of DTP (drug-tolerant persister) cells can be considered an acquired resistance mechanism in which all cells have the same probability of evading treatment, and the selection of the persistent clones is made in a Lamarckian selection rather than in a classic Darwinian selection, as is the case for the intrinsic resistance. However, as I mentioned in Chapter 2, these two types of therapeutic evasion and their selection process are not an on/off mechanism. They are not mutually exclusive and can co-exist. Long before this new way of thinking, for many years and in several cancers, the cells that exhibited a therapy resistance were shown to have features of CSCs and to be endowed with increased xenobiotic resistance [323,337–339]. This supported the idea of the high plasticity of the tolerant state by acquiring CSC-like features. However, tumour recurrence may be caused by surviving cells that do not *a priori* exhibit an increased tumour-initiating capacity. Recent studies in several cancers showed that the fraction of cells surviving chemotherapy *in vivo* and in patients do not display enrichment of SCs, suggesting that CSC functionality is not a fixed DTP property but can be induced under stress conditions [165,166,168,172,340–343]. Still, throughout the treatment course, tumour cells could acquire the phenotypic features of CSCs (by dedifferentiation, for example) and result in the continuous replenishment of the CSC pool [344,345]. This capacity is one of the most important in the intestinal epithelium, as we saw in Chapter 1. After damage,

facultative SCs, progenitors or differentiated cells can dedifferentiate to replenish the ISC pool and regenerate the epithelium [36,40,56,158–161]. Even though there is quite an impressive number of techniques to address many biological questions nowadays, it is still hard to answer how the resistance, especially the epigenetic and transcriptional changes, is occurring to give rise to the resistant phenotype. One of the main problems is how the assays are performed. They are done at the population level (with classical molecular biology techniques or bulk RNA-Seq) or the single-cell level with the advent of single-cell omics. Nonetheless, both assays give a snapshot of what is happening at a precise time and do not track the resistant cells and their adaptive changes in a kinetic manner. Indeed, if we were able to analyse every persistent and resistant cell throughout the time and monitor their changes in the presence of the drug and the environmental factors, we would be able to design and rationally tackle these DTP and resistant cells, hopefully for the last time.

Another important characteristic that was observed in the DTPs is their slow-cycling feature. It was shown in lung cancer that some cells could enter a slow-cycling DTP state that enables proliferative capacity even in the presence of a drug. Using an elegant barcoding model called watermelon, Oren and colleagues showed that cycling and non-cycling persister cells arise from different cell lineages with distinct metabolic and transcriptional programs. Moreover, these cells upregulated an antioxidant gene expression and the fatty acid oxidation metabolism associated with the persister state[166]. In the intestinal epithelium, it was already shown that the LGR5 SC population is not homogenous. There are slow-cycling and highly-cycling LGR5 cells that can be distinguished by the expression of the MEX3A marker[27]. Besides, LGR5+ slow-cycling cells, which also express PROX1, were responsible for the chemoresistance in CRC after IRI treatment [210]. So, this heterogeneity within the CBCs could contribute to the differential sensitivity when those cells are exposed to the chemotherapeutic treatments. Likewise, the presence within the ISC compartment of the facultative SCs, progenitors, and differentiated cells that could resist therapy respond in case of injury taking over the maintenance of the epithelium complicates the picture. The latter may explain why we do not still have a clear explanation for the therapeutic resistance in CRC despite all efforts.

The intestine is also a quite particular organ as, due to its function of absorption is constantly exposed to xenobiotics, daily nutrients and hormones, among other things. Indeed, the presence of these molecules encountered can shape the response of this organ on a normal basis and, thus, in tumours. One of the hormones that can impact the organ's everyday functions is thyroid hormones (THs). THs are important for regulating the metabolism and thus the absorption of nutrients; they are important for several functions, including intestinal motility and the development of the intestine, the complexification of the epithelium, and the transitioning between milk and solid food[241,346,347]. THs and their nuclear receptor TRα1 have been linked to worse prognosis in intestinal and colorectal tumours from mouse models, human patient samples

[281,290] and epidemiological studies (linking hyperthyroidism and exogenous thyroid hormone supplementation) [296,299]. Several questions came into our minds. We knew that *THRA*/TRα1 is upregulated in CRC, but we did not know how this upregulation occurs. The obvious question was then, what are the mechanisms that control *THRA* gene expression in colon cancer and CSCs. Moreover and as I just mentioned, THs' and TRα1's link with poor prognosis in CRC has been demonstrated. So, during this thesis, we aimed to get more in-depth and focus on understanding the role of the THs and its receptor TRα1 in CRC CSCs and how THs can impact the chemotherapeutic response.

For the first part of this thesis, we decided to evaluate in an available cohort of CRC patients, both *in silico* and in tumour and normal samples, the expression of *THRA* and TRα1, respectively. These experiments confirmed the upregulation of *THRA* and TRα1 in CRC. The results also showed great heterogeneity in TRα1 expression in tumour parts and that stromal cells can strongly or poorly express TRα1. In addition to being upregulated in CRCs, TRα1 in the normal intestine shows a gradient expression, high in the bottom of the crypts and decreasing along the vertical axis, similar to that of the Wnt and Notch pathways. So then, our question was, what regulates the *THRA* expression in CRC?

An analysis of the 3Kb upstream the transcription starting site of the *THRA* gene demonstrated the presence of putative binding sites for transcription factors known to be altered in cancer, including CDX2, RBPJ and TCF7L2. Indeed, other transcription factors' putative binding sites were found that may impact the transcription of *THRA*, but the matrix score (the similarity with the canonical sites) were lower. By consequence, we decided to focus on those three. We observed an increased THRA-luciferase dependent expression when co-transfecting with CDX2 and β-catenin/TCF. The co-transfection with NICD decreased or did not change THRA-luciferase dependant expression, which seems context-dependent. Additionally, when we evaluated the action of agonists and antagonists of the Notch pathway, the intricated responses we observed made it difficult to assign their specific roles correctly. Also, according to the literature, it appears clear that the roles of the molecules are much larger and go beyond the control of the Notch pathway. Moreover, it is also worth noting that the Notch pathway has a complex cross-talk with Wnt, resulting in an additional complexity in the analysis of the results. In animal models, it has been shown that activated Notch synergises with Wnt to induce intestinal tumorigenesis and that both are involved in the intestinal SC and CSC biology [86,87,293,348]. Given the regulation of *THRA* gene expression by Wnt, it may be reasonable to think that the differences observed in the three cell lines analysed regarding their levels of Wnt and mutational backgrounds might influence the response to Notch. Consequently, this would impact the response in the *THRA* gene, explaining the different effects observed on its activity.

Due to this complex response and, as it was already shown in the laboratory that TRα1 could modulate the Wnt signalling pathway, we decided to perform a more comprehensive study on the

possible implications of this pathway in the regulation of *THRA*. Firstly, I will like to point out and discuss the Wnt signalling and the heterogeneity of expression of TRα1 in tumours and cell lines. As I mentioned in Chapter 2, we know from previous work in our laboratory that TH-TRα1 in the intestinal crypts induces the level of expression of several genes involved in the Wnt signalling pathway, including its effector *Ctnnb1*, encoding for β-catenin, and *sFRP2*, as well it negatively regulates the expression of Wnt inhibitors (Wif1, Frzb and Sox17) in CRC [281,283,284,290]. So, we wondered if a regulatory loop might exist and if the Wnt pathway could be able to modulate the expression of *THRA* in CRC cell lines.

Using different molecular and cellular approaches (Paper Nº2), we showed that β-catenin could increase the expression of *THRA* using a THRA-luciferase dependent model. Additionally, a point mutation on each of the binding sites for TCF7L2 blunted the transactivation dependent on the presence of β-catenin/TCF/LEF. Indeed, ChiP analysis showed that the β-catenin could bind to the *THRA* promoter in the three cell lines analysed. These results showed that not only the Wnt pathway positively controls the *THRA* expression but that this control is achieved through a direct β-catenin binding on the promoter. We also observed that mutations in the *Apc* gene in a physiological model of mouse enteroids stimulated TRα1 expression. All this data suggests a positive cross-talk and feedback between the Wnt signalling pathway (notably through β-catenin) and THRA/TRα1, favouring CRC progression (Figure 9 paper Nº2). TRα1 expression, as I mentioned, even though higher in tumours, is heterogeneous. Researchers have been focusing on analysing the expression of their genes of interest in the different CMS groups when the disparity of expression within the tumours is so big. A similar diversity can be observed in the CRC cell lines. In addition, the Wnt pathway is frequently hyperactivated in CRC and CRC-derived cell lines. The use of different approaches as mentioned above allowed us to demonstrate the positive regulation of *THRA*/TRα1 by Wnt. Nevertheless, the effect of CHIR and IWP4 (Wnt agonist and antagonist, respectively) on *THRA* activity and the endogenous TRα1 resulted in more complex analysis. The drugs were chosen based on the literature [349,350] and validated on the Wnt-reporter TopFlash in all cell lines. We speculate that the differences in responsiveness or lack of responsiveness may arise from the different genetic and epigenetic backgrounds of the cell lines used [351] and the fact that the molecules are not specific and could have various targets [352–354]. Moreover, the differentia status of the cell lines in other signalling pathways in the cell lines could also impact the Wnt [355,356], which renders the whole picture more complex when using these models.

The single-cell omics can be a powerful tool to analyse the heterogeneity of CRC cancer tumours deeply. It may help explain the involvement of the TRα1 present in the stroma in the CRC progression and maintenance. When I looked at some single-cell analyses publicly available (https://singlecell.broadinstitute.org/single_cell), I was able to see the heterogeneity as mentioned earlier in tumours in a clearer way. Indeed, the cells that express high levels of *THRA* in CRC

tumours are those that have an SC/progenitor identity, which is not surprising if we consider that in a normal colon, TRα1 expression is localised at the bottom of the crypts and that they are also the cells with a high Wnt activity, reinforcing our results. However, the heterogeneity also comes from the stroma (as observed in the immunohistochemistry of tumour samples). In the review paper currently under review (Paper Nº4), we evidenced an important role of the intestinal niche in maintaining the normal epithelium SCs and CSCs in CRC.

THs, as we extensively mentioned, are key actors in intestinal development and impact the metabolic features of SC and niche cells and favour the crosstalk between the epithelium and the stroma and even the immune system. More studies analysing the involvement of THs and TRα1 in the tumour microenvironment are needed, both in bulk tumour cells and at a single cell level, to try to explain and understand the complex interplay between the tumour and its niche. Understanding the heterogeneity and how THs can impact each cell type may give light to new potential targets for therapies.

I wanted to point out the heterogeneity before discussing the second part of my thesis. This complexity found in many cancers, including CRC, is one of the main reasons why the therapeutics are not efficient. Nowadays, we also focus on developing a personalised medicine approach for each patient and each type of tumour, ideally more efficient and with fewer side effects. Many cancer treatments still in use are indeed chemotherapies whose mechanism of action is not cell-specific as they normally target diving cells, causing many undesired effects. As I mentioned in Chapter 2 and above, cancer cells have developed many mechanisms to evade the therapy. The factors contributing to the therapeutic evasion can be intrinsic to the cancer cells through an acquired mutation, a phenotypic feature acquired in the presence of the therapy (and other molecules, like hormones, for example, TH) or a combination of both at the same time [167,171,177]. The most classical and known mechanisms of resistance in pharmacology include (a) a decreased accumulation of the cytotoxic drug as a result of an increased expression of drug efflux proteins, (b) insufficient activation of the drug, (c) increased drug inactivation, (d) decreased concentration of target enzyme or altered activity of the target, (e) increased utilisation of alternative pathways to the ones inhibited, (f) decreased requirement of the substrate, (g) rapid repair of drug-induced DNA damage and (h) mutations in genes involved in therapy resistance [178,179]. The mechanisms listed from (a) to (g) are phenotypic features that cancer cells that persist chemotherapy use to survive treatment. These cells are called “persisters” or drug-tolerant persisters (DTPs).

Abnormal hormone levels, for example, TH levels, were shown to affect the microsomal drug-metabolizing enzymes in laboratory animals profoundly [312]. Although the literature's connection between thyroid function disorders and metabolism is extensive [312,313], the data connecting THs and xenobiotic metabolism and drug resistance are sparse. The thyroid status of patients is not monitored before and during the administration of the treatments, except for patients receiving

tyrosine kinase inhibitors, as it is known that they impact the thyroid status, resulting in patients' hypothyroidism [357,358]. During this thesis, we tried to evaluate the involvement of THs in the chemotherapeutic response, notably to FOLFOX and FOLFIRI, two main chemotherapeutic regimes used to treat CRC patients. Firstly, we took advantage of a novel 3D culture model of spheroids, also developed during this thesis [336], that allowed us to study CSCs and the impact of THs (specifically T3) and the TRα1 levels on the spheroid's formation and development. We observed that T3 and TRα1-gain of function (TRα1-GOF) stimulate while TRα1-loss of function strongly decreases the spheroids' growth. Despite stimulating the spheroids' growth, we did not observe significant changes in the SC markers in the T3 treated spheroids. We know from previous work in mouse organoids that T3 could induce a "thyroid shock" [285] and modify the expression of several genes. So, as we observed differences in the size of those spheroids treated with T3 during their formation, we decided to perform an RNA-seq analysis during spheroid formation, treated or not with T3, for 24 hs. Apart from the well-known T3 targets like KLF9 and hairless (HR), it was surprising to observe deferentially expressed upregulated genes belonging to the ABC-transporter family, *ABCB1* and *ABCG2*. This was interesting because, as I extensively mentioned in this thesis, both genes code for the two well-known drug efflux transporters involved in drug resistance [219]. So we supposed that if T3 can induce the expression of these transporters, it might contribute to a chemotherapeutic resistance or differential response to the treatments. We then treated the spheroids, previously generated in control or T3 condition, with FOLFOX and FOLFIRI (or no treatment), and we performed several molecular and cellular analyses (some still ongoing). We observed a differential response to the two chemotherapeutic regimens from a morphological point of view. Thus, we conducted an RNA-seq analysis to have unbiased results on the molecular mechanisms responsible for the differential response. Indeed, spheroids treated with FOLFIRI were more resistant than those treated with FOLFOX, and among the FOLFIRI treated spheroids, those generated in the presence of T3 had a further survival advantage. A potential explanation came from the RNA-seq data. T3-treated spheroids have an increased expression of *ABCB1* and *ABCG2*. The upregulation of those two efflux pumps gives a clear phenotypic advantage to the spheroids; as I mentioned before, one of the known pharmacological evasion mechanisms contributing to persistence is the decreased accumulation of the cytotoxic drug via an increased expression of drug efflux proteins [178,179]. Therefore, IRI (and their metabolites) and 5-FU are transported via these efflux pumps and are easily excluded from the cells, impeding their action. Emmink and colleagues suggested that the ABCB1 expressing cells are differentiated cells that protect and give resistance by increasing the drug efflux to preserve the ALDH1+ tumour-initiating cells from irinotecan[359]. This seems not to be precisely our case, as even if we are still analysing the data, the presence of differentiated cells in our spheroid model is moderate. Indeed, this difference may depend on the use of a spheroid model derived from liver metastasis and not a primary tumour. However, we cannot deny or

exclude that ABCB1 and ABCG2 protect both undifferentiated and differentiated cells present in our spheroid model. Most importantly, the presence of the T3 only at the stage of spheroids' formation primes the cells for this phenotypic advantage, given that the chemotherapies are given after T3 treatment. As I mentioned in Chapter 2, ABCB1 is modulated by THs [316,320], and TRs can bind to the *ABCB1* promoter [317] to modulate its expression. At the same time, there is almost no data about the regulation of ABCG2 by THs and TRs. *ABCG2* is modulated by the Wnt signalling and hedgehog pathway[219,338], which may suggest that THs/TRs may be able to modulate this transporter through their actions in those pathways. Interestingly, when we generated TRα1-GOF spheroids and treated them with the chemotherapy, we did not observe a further increase in the ABCB1 or ABCG2 expression without the previous treatment with T3, indicating that the TRα1-liganded receptor is necessary for the regulation of these genes.

Several xenobiotic enzymes, transporters and the xenobiotic nuclear receptor CAR (NR1I3) have been shown to be upregulated by TH/TRs [360]. Accordingly, CAR is upregulated in the T3/FOLFIRI condition in our RNA-seq study. The upregulation of CAR can explain the modulation observed in T3-treated spheroids of several detoxification genes where a direct regulation by TRs has not been shown [361,362]. Although modulation of CAR by TH levels was shown through transcriptional regulation of DIO1, no data described its control by TRs [362,363]. Of note, much of this data comes from studies in the liver, so analysis of the regulation of the xenobiotic enzymes via the THs/TRs in the intestine may be different and requires further studies. Finally, CAR can also modulate the THs' metabolism, suggesting that a regulation loop occurs between THs and CAR [330].

We also obtained other interesting results, specifically in the spheroids treated with T3 and FOLFIRI, suggesting other mechanisms favouring persistent cells to therapy: increased drug inactivation and a decreased concentration of target enzyme [178,179]. First, the RNA-seq data of T3 FOLFIRI spheroids revealed an upregulation of the UGTs enzymes and *DPYS*. UGTs are phase II enzymes involved in the conjugation of drugs like SN-38 (IRI active metabolite) into its inactive form SN-38G for its elimination and are also involved in drug resistance [364,365]. THs are also metabolised via UGTs for their elimination, favouring resistance due to direct drug-drug interaction with IRI and contributing to the magnification of the side effects and toxicity linked to SN-38 action in the intestine (i.e. diarrhoea) [314,366]. In addition to their role in detoxification and drug resistance, for example, in prostate cancer, UGTs may also impact cancer progression and metastasis development thanks to their role in modulation of steroidal hormones elimination [365]. The other interesting enzyme modulated is *DPYS*, an enzyme implicated in the catabolism of 5-FU. DPYS is less known than the other 5-FU catabolic enzyme (DPYD) but may contribute to resistance as it favours the drug inactivation, in this case, the fluoropyrimidines [188], also contributing to increased toxicity. Another strategy that cancer cells can take to resist treatment is to decrease the concentration of the target enzyme. This was the case for the spheroids treated

with T3 and FOLFIRI, where the TOP1, target of SN-38 (the active metabolite of IRI) [194], is downregulated. Low TOP1 means less target enzyme, which means less benefit from the therapy [216,217] but more free drug and more side effects[367]. Altogether, these results clearly indicate that the presence of T3 during the formation of the spheroids contributed to phenotypic resistance to FOLFIRI *in vitro.* Still, if we extrapolate to an *in vivo* setting, T3 might be responsible for increased drug resistance and a magnification of IRI and 5-FU side effects. That is why the evaluation of the thyroid status should be routinely evaluated in chemotherapy-treated patients, as it is vital not only to know which patients will benefit from the therapy but also to prevent the exacerbation of the commonly known drugs' side effects.

Another distinct and interesting feature observed in the T3 FOLFIRI condition is the down-regulation of the cell cycle and the DNA damage response pathways. I mentioned many times that DPTs had the particularity of being slow-cycling or do not cycle at all and that DTPs have been found in many cancer types despite the type of therapy used (chemotherapy or targeted therapy) [164–166,168,176]. Notably, this goes in the same direction as a recent and elegant paper, linked to what we also observed in our RNA-seq analysis, which stated that cells treated with IRI and FOLFIRI entered a DPT state without selecting a pre-existing resistant population or an enrichment in CSC [165]. They observed rather a phenotypic resistance mechanism linked to a decreased cell cycle, mitosis and DNA repair [165]. This paper also connected the DTP state with increased autophagy and mTOR. Still, it is not the case in our T3 FOLFIRI condition, maybe simply because of the difference in the models (mice vs spheroids) or just because the presence of T3 allowed the spheroids to have the same phenotype without the requirement of modulating those pathways.

On the other hand, as upregulated gene ontology functions, we observed an adaptative thermogenesis mechanism that is taking place. THs are well known for modulating the thermogenesis and mobilising fat from the adipose tissue [240,252], which might be responsible for the huge metabolic remodelling of the spheroids. One striking result observed in the T3 FOLFIRI spheroids' differentially upregulated genes was the presence of the *OLFM4.* This gene is considered a SC marker in the normal human intestine and colon and is highly expressed in human CRC [22], although it is not expressed in the murine colon or not expressed at all in the Caco2 cell line we used to generate the spheroids. OLFM4 has been linked to chemoresistance and poor prognosis in pancreatic cancer [368], but this has not yet been explored in CRC. Additionally, it was interesting to observe an upregulation of histone modification genes like PHF8 and KDM3A. Indeed, epigenetic modulation is another form of phenotypic resistance that persister cells can acquire to overcome the treatment [167]; nevertheless, this has also been observed when analysing the upregulated genes in both treatments (FOLFOX and FOLFIRI).

Conversely, when we analysed the response of the spheroids to FOLFOX, regardless of the presence or not of T3, it did not seem to have any clear mechanism of phenotypic persistence to

the therapy. The spheroids appeared strongly affected and dying in both conditions. Morphologically they appeared dark and irregular, and when analysing the fold enrichment of our RNA-seq genes (regardless of the presence of T3), we could see that the higher upregulated enrichment is the activation of the apoptotic pathway which indicates that the spheroids are more sensitive to FOLFOX. The treatment with T3 is not giving any advantage in this case. Also, when we analysed the RNA-seq results, we did not observe any pathway or detoxification mechanism as observed for FOLFIRI. Instead, the response was more general, linking to a huge metabolic remodelling and the downregulation of several metabolic pathways. Indeed, especially for the T3 FOLFOX downregulated genes, there is a decrease in SC proliferation that seems to correspond mostly to a reduction in the molecular signals required for the maintenance of the SCs rather than a true downregulation of SC, but rather the reduction of proliferation signals. In addition to that, but independent of the T3 treatment, we could observe an increase in BMP4 and other differentiation signals implicated in the epithelial to mesenchymal transition. Other authors showed that T3 was responsive to the sensitisation to FOLFOX through an increase of BMP4 signals [294], and we observed this both in the presence and absence of T3. Because we did not see a phenotypic difference in the cultures and the RNA-seq did not point out any specific T3 related mechanism of persistence, we focused our studies on FOLFIRI. Even if we opted for this approach, the differences observed between the drugs may depend on the setting, model, cell line, and *in vivo*, where T3 could have a different effect

I would like to end this discussion with a personal thought. The conquest for new therapeutic agents to tackle cancer cells is passionate yet tricky. Pharmacology is an incredible field yet complex. Every day, many research groups try to find a new molecule, antibody, immunotherapy, targeted therapy, anything that can be as personalised as possible to give a good overall survival to the patients and a better life. At the same time, many other studies, including ours, analyze how the existing treatments fail due to resistance or persistence, trying to explain how it happens to find new ways of tackling the inefficacity to make them work again. For some time now, researchers are getting more and more interested in studying not only the tumour, with its heterogeneity, its mutations and complexity but are also starting to look beyond that, studying the microenvironment and all other signals (like hormones) that can impact the development of the tumour and thus the therapeutic response. Here, we focused on how the T3 can impact the CSC biology in CRC and confer the cells a phenotypic advantage that will allow cells to become DTPs and resist the chemotherapeutic treatment more easily than the cells that had not been exposed to T3. We showed that this advantage is particularly handy for the FOLFIRI treated cells as they are primed to eliminate the drug more easily. Although these are baby steps for the research in the field but very important for the improvement of the therapies and the patients' lives, I am convinced that this "humble" thesis paves the way for suggesting to incorporate the analysis of the thyroid status of patients in a routine before the choice of therapy. This would surely result in

a better response as the right patients will receive the correct treatment and help minimise preventable side effects.

Chapter 6: Conclusions and Perspectives

During this thesis, we were able to demonstrate, for the first time, the regulation of the *THRA* gene in a specific pathological context, the CRC. We showed using different cellular and molecular techniques that several pathways and transcription factors control the expression of the *THRA* gene in the context of CRC. In particular, we unveiled a complex regulatory loop between the Wnt pathway and TRα1. Indeed, the Wnt pathway can modulate the THRA promoter activity and TRα1 expression in the context of CRC. We also reinforced our previous work, showing that CRCs have a high TRα1 expression, which presents a heterogeneous expression pattern both inter-and intra-tumours.

Moreover, this higher expression and heterogeneity are clinically significant and relevant even more when CRC patients present altered TH levels and undergo a chemotherapeutic treatment. Indeed, an excess of THs, as we observed during this thesis, can affect the efficacy of the therapy. The response to the chemotherapeutic combination FOLFIRI can be altered, as T3 can induce a persistent phenotypic state characterised by increased drug detoxification, slowed metabolism, and proliferation arrest. However, it will also increase undesirable side effects. Thus, this work opens the way to rethinking the patients' clinical evaluation and how a patient with an altered thyroid status must be treated. A hyperthyroid patient will not benefit from treatment with FOLFIRI and will suffer from more side effects. Thus, the interest in evaluating the patient's thyroid status and the TRα1 levels in the tumours before even thinking about which treatment strategy should be used. Of course, epidemiological studies and a prospective study evaluating what happens in real life in patients will be needed to validate these observations. Still, it can be a starting point for practitioners to incorporate the evaluation of the thyroid status in their practice.

As perspectives for this thesis work and future directions, we want to get more in-depth into the involvement of the drug efflux pumps ABCB1 and ABCG2. We are performing studies using an inhibitor of both transporters, the elacridar. It will be evaluated by cytometry its impact on the survival of CTRL and T3 spheroids, treated or not with FOLFIRI. We will determine changes in the cell cycle, cell death, and the expression of ALDH coupled with ABCG2 expression. Moreover, we will evaluate the expression of the different markers linked to the metabolism and activity of IRI (TOP1, ABCB1 and ABCG2).

Additionally, we are about to launch an *in vivo* xenograft study where we will evaluate the impact of the T3 in response to chemotherapy in an *in vivo* model. The study will include two conditions, similar the ones used in the spheroids: a control group and a T3 group that will receive T3 in the drinking water. These two main groups will receive or not the FOLFIRI and tumours will be collected and analysed for histological analysis. This study will evaluate in a more integrated model the tumour growth and response to the treatment depending on their thyroid status (euthyroid or subclinical hyperthyroidism).

Bibliography

1. Levine, D. S. & Haggitt, R. C. Normal histology of the colon. *American Journal of Surgical Pathology* vol. 13 966–984 (1989).
2. Mescher, A. *Junqueira's Basic Histology: Text and Atlas, 12th Edition*. (McGraw-Hill Education, 2009).
3. Beumer, J. & Clevers, H. Cell fate specification and differentiation in the adult mammalian intestine. *Nat. Rev. Mol. Cell Biol.* (2020) doi:10.1038/s41580-020-0278-0.
4. Gehart, H. & Clevers, H. *Tales from the crypt: new insights into intestinal stem cells*. *Nature Reviews Gastroenterology and Hepatology* vol. 16 19–34 (Nature Publishing Group, 2019).
5. Cheng, H. & Leblond, C. P. Origin, differentiation and renewal of the four main epithelial cell types in the mouse small intestine I. Columnar cell. *Am. J. Anat.* **141**, 461–479 (1974).
6. Blachier, F., de Sá Resende, A., da Silva Fogaça Leite, G., Vasques da Costa, A. & Lancha Junior, A. H. Colon epithelial cells luminal environment and physiopathological consequences: impact of nutrition and exercise. *Nutrire* **43**, 1–9 (2018).
7. Potten, C. S. & Loeffler, M. Stem cells: attributes, cycles, spirals, pitfalls and uncertainties. Lessons for and from the crypt. *Development* **110**, 1001–1020 (1990).
8. Clevers, H. The Intestinal Crypt, A Prototype Stem Cell Compartment. *Cell* **154**, 274–284 (2013).
9. Van Der Flier, L. G. & Clevers, H. Stem cells, self-renewal, and differentiation in the intestinal epithelium. *Annual Review of Physiology* vol. 71 241–260 (2009).
10. Potten, C. S., Kovacs, L. & Hamilton, E. Continuous Labelling Studies on Mouse Skin and Intestine. *Cell Prolif.* **7**, 271–283 (1974).
11. Hendry, J. H. & Potten, C. S. Cryptogenic cells and proliferative cells in intestinal epithelium. *Int. J. Radiat. Biol.* **25**, 583–588 (1974).
12. Potten, C. S. Extreme sensitivity of some intestinal crypt cells to X and γ irradiation. *Nat. 1977 2695628* **269**, 518–521 (1977).
13. Barker, N., Bartfeld, S. & Clevers, H. Tissue-Resident Adult Stem Cell Populations of Rapidly Self-Renewing Organs. *Cell Stem Cell* **7**, 656–670 (2010).
14. Bjerknes, M. & Cheng, H. Clonal analysis of mouse intestinal epithelial progenitors. *Gastroenterology* **116**, 7–14 (1999).
15. Bjerknes, M. & Cheng, H. The stem-cell zone of the small intestinal epithelium. I. Evidence from paneth cells in the adult mouse. *Am. J. Anat.* **160**, 51–63 (1981).
16. Barker, N. *et al.* Identification of stem cells in small intestine and colon by marker gene Lgr5. *Nature* **449**, 1003–1007 (2007).
17. Sato, T. *et al.* Single Lgr5 stem cells build crypt-villus structures in vitro without a mesenchymal niche. *Nature* **459**, 262–265 (2009).
18. Nusse, R. & Clevers, H. Wnt/β-Catenin Signaling, Disease, and Emerging Therapeutic Modalities. *Cell* **169**, 985–999 (2017).
19. Clevers, H. Modeling Development and Disease with Organoids. *Cell* **165**, 1586–1597 (2016).
20. Muñoz, J. *et al.* The Lgr5 intestinal stem cell signature: Robust expression of proposed quiescent ′ +4′ cell markers. *EMBO J.* **31**, 3079–3091 (2012).
21. van der Flier, L. G. *et al.* Transcription Factor Achaete Scute-Like 2 Controls Intestinal Stem Cell Fate. *Cell* **136**, 903–912 (2009).

22. van der Flier, L. G., Haegebarth, A., Stange, D. E., van de Wetering, M. & Clevers, H. OLFM4 Is a Robust Marker for Stem Cells in Human Intestine and Marks a Subset of Colorectal Cancer Cells. *Gastroenterology* **137**, 15–17 (2009).

23. Yousefi, M., Li, L. & Lengner, C. J. Hierarchy and Plasticity in the Intestinal Stem Cell Compartment. *Trends in Cell Biology* vol. 27 753–764 (2017).

24. Tian, H. *et al.* A reserve stem cell population in small intestine renders Lgr5-positive cells dispensable. *Nature* **478**, 255 (2011).

25. Yan, K. S. *et al.* The intestinal stem cell markers Bmi1 and Lgr5 identify two functionally distinct populations. *Proc. Natl. Acad. Sci. U. S. A.* **109**, 466–471 (2012).

26. Metcalfe, C., Kljavin, N. M., Ybarra, R. & De Sauvage, F. J. Lgr5+ stem cells are indispensable for radiation-induced intestinal regeneration. *Cell Stem Cell* **14**, 149–159 (2014).

27. Barriga, F. M. *et al.* Mex3a Marks a Slowly Dividing Subpopulation of Lgr5+ Intestinal Stem Cells. *Cell Stem Cell* **20**, 801-816.e7 (2017).

28. Frau, C. *et al.* Deciphering the Role of Intestinal Crypt Cell Populations in Resistance to Chemotherapy. *Cancer Res.* **81**, 2730–2744 (2021).

29. Beumer, J. & Clevers, H. Regulation and plasticity of intestinal stem cells during homeostasis and regeneration. *Dev.* **143**, 3639–3649 (2016).

30. Bonis, V., Rossell, C. & Gehart, H. The Intestinal Epithelium – Fluid Fate and Rigid Structure From Crypt Bottom to Villus Tip. *Front. Cell Dev. Biol.* **9**, (2021).

31. Sangiorgi, E. & Capecchi, M. R. Bmi1 is expressed in vivo in intestinal stem cells. *Nat. Genet.* **40**, 915–920 (2008).

32. Montgomery, R. K. *et al.* Mouse telomerase reverse transcriptase (mTert) expression marks slowly cycling intestinal stem cells. *Proc. Natl. Acad. Sci. U. S. A.* **108**, 179–184 (2011).

33. Takeda, N. *et al.* Interconversion between intestinal stem cell populations in distinct niches. *Science (80-.).* **334**, 1420–1424 (2011).

34. Powell, A. E. *et al.* The pan-ErbB negative regulator lrig1 is an intestinal stem cell marker that functions as a tumor suppressor. *Cell* **149**, 146–158 (2012).

35. Yousefi, M. *et al.* Msi RNA-binding proteins control reserve intestinal stem cell quiescence. *J. Cell Biol.* **215**, 401–413 (2016).

36. Ayyaz, A. *et al.* Single-cell transcriptomes of the regenerating intestine reveal a revival stem cell. *Nature* **569**, 121–125 (2019).

37. Buczacki, S. J. A. *et al.* Intestinal label-retaining cells are secretory precursors expressing lgr5. *Nature* **495**, 65–69 (2013).

38. Meyer, A. R., Brown, M. E., McGrath, P. S. & Dempsey, P. J. Injury-Induced Cellular Plasticity Drives Intestinal Regeneration. *Cell. Mol. Gastroenterol. Hepatol.* **13**, 843–856 (2022).

39. Li, N., Nakauka-Ddamba, A., Tobias, J., Jensen, S. T. & Lengner, C. J. Mouse Label-Retaining Cells Are Molecularly and Functionally Distinct From Reserve Intestinal Stem Cells. *Gastroenterology* **151**, 298-310.e7 (2016).

40. Sheahan, B. J. *et al.* Epithelial Regeneration After Doxorubicin Arises Primarily From Early Progeny of Active Intestinal Stem Cells. *Cmgh* **12**, 119–140 (2021).

41. Van Es, J. H. *et al.* Dll1+ secretory progenitor cells revert to stem cells upon crypt damage. *Nat. Cell Biol.* **14**, 1099–1104 (2012).

42. Jadhav, U. *et al.* Dynamic Reorganization of Chromatin Accessibility Signatures during Dedifferentiation of Secretory Precursors into Lgr5+ Intestinal Stem Cells. *Cell Stem*

Cell **21**, 65-77.e5 (2017).

43. Tetteh, P. W. *et al.* Replacement of Lost Lgr5-Positive Stem Cells through Plasticity of Their Enterocyte-Lineage Daughters. *Cell Stem Cell* **18**, 203–213 (2016).

44. Tao, S. *et al.* Wnt activity and basal niche position sensitize intestinal stem and progenitor cells to DNA damage. *EMBO J.* **34**, 624–640 (2015).

45. Sphyris, N., Hodder, M. C. & Sansom, O. J. Subversion of niche-signalling pathways in colorectal cancer: What makes and breaks the intestinal stem cell. *Cancers (Basel).* **13**, 1–55 (2021).

46. Ohara, T. E., Colonna, M. & Stappenbeck, T. S. Adaptive differentiation promotes intestinal villus recovery. *Dev. Cell* (2022) doi:10.1016/J.DEVCEL.2021.12.012.

47. Bankaitis, E. D., Ha, A., Kuo, C. J. & Magness, S. T. Reserve Stem Cells in Intestinal Homeostasis and Injury. *Gastroenterology* **155**, 1348–1361 (2018).

48. Akazawa, C., Ishibashi, M., Shimizu, C., Nakanishi, S. & Kageyama, R. A mammalian helix-loop-helix factor structurally related to the product of Drosophila proneural gene atonal is a positive transcriptional regulator expressed in the developing nervous system. *J. Biol. Chem.* **270**, 8730–8738 (1995).

49. Beumer, J., Gehart, H. & Clevers, H. Enteroendocrine Dynamics - New Tools Reveal Hormonal Plasticity in the Gut. *Endocr. Rev.* **41**, 695 (2020).

50. Sato, T. *et al.* Paneth cells constitute the niche for Lgr5 stem cells in intestinal crypts. *Nature* **469**, 415–418 (2011).

51. Spit, M., Koo, B. K. & Maurice, M. M. Tales from the crypt: Intestinal niche signals in tissue renewal, plasticity and cancer. *Open Biol.* **8**, (2018).

52. Rodríguez-Colman, M. J. *et al.* Interplay between metabolic identities in the intestinal crypt supports stem cell function. *Nature* **543**, 424–427 (2017).

53. Yilmaz, Ö. H. *et al.* MTORC1 in the Paneth cell niche couples intestinal stem-cell function to calorie intake. *Nature* **486**, 490–495 (2012).

54. Beyaz, S. *et al.* High-fat diet enhances stemness and tumorigenicity of intestinal progenitors. *Nature* **531**, 53–58 (2016).

55. Kim, T. H., Escudero, S. & Shivdasani, R. A. Intact function of Lgr5 receptor-expressing intestinal stem cells in the absence of Paneth cells. *Proc. Natl. Acad. Sci. U. S. A.* **109**, 3932–3937 (2012).

56. Durand, A. *et al.* Functional intestinal stem cells after Paneth cell ablation induced by the loss of transcription factor Math1 (Atoh1). *Proc. Natl. Acad. Sci. U. S. A.* **109**, 8965–8970 (2012).

57. Parry, L., Young, M., Marjou, F. E. L. & Clarke, A. R. Evidence for a crucial role of Paneth cells in mediating the intestinal response to injury. *Stem Cells* **31**, 776–785 (2013).

58. Van Es, J. H. *et al.* Enteroendocrine and tuft cells support Lgr5 stem cells on Paneth cell depletion. *Proc. Natl. Acad. Sci. U. S. A.* **116**, 26599–26605 (2019).

59. Sasaki, N. *et al.* Reg4+ deep crypt secretory cells function as epithelial niche for Lgr5+ stem cells in colon. *Proc. Natl. Acad. Sci. U. S. A.* **113**, E5399–E5407 (2016).

60. Rothenberg, M. E. *et al.* Identification of a cKit+ colonic crypt base secretory cell that supports Lgr5+ stem cells in mice. *Gastroenterology* **142**, 1195-1205.e6 (2012).

61. Wang, Y. *et al.* Single-cell transcriptome analysis reveals differential nutrient absorption functions in human intestine. *J. Exp. Med.* **217**, (2020).

62. Sandow, M. J. & Whitehead, R. The Paneth cell. *Gut* **20**, 420 (1979).

63. Basak, O. *et al.* Induced Quiescence of Lgr5+ Stem Cells in Intestinal Organoids

Enables Differentiation of Hormone-Producing Enteroendocrine Cells. *Cell Stem Cell* **20**, 177-190.e4 (2017).

64. Beumer, J. *et al.* Enteroendocrine cells switch hormone expression along the crypt-to-villus BMP signalling gradient. *Nat. Cell Biol.* **20**, 909–916 (2018).
65. Banerjee, A., McKinley, E. T., Von Moltke, J., Coffey, R. J. & Lau, K. S. Interpreting heterogeneity in intestinal tuft cell structure and function. *J. Clin. Invest.* **128**, 1711–1719 (2018).
66. O'Leary, C. E., Schneider, C. & Locksley, R. M. Tuft cells – systemically dispersed sensory epithelia integrating immune and neural circuitry. *Annu. Rev. Immunol.* **37**, 47 (2019).
67. McCauley, H. A. & Guasch, G. Three cheers for the goblet cell: maintaining homeostasis in mucosal epithelia. *Trends Mol. Med.* **21**, 492–503 (2015).
68. Allaire, J. M. *et al.* Frontline defenders: Goblet cell mediators dictate host-microbe interactions in the intestinal tract during health and disease. *Am. J. Physiol. - Gastrointest. Liver Physiol.* **314**, G360–G377 (2018).
69. Wiese, K. E., Nusse, R. & van Amerongen, R. Wnt signalling: conquering complexity. *Development* **145**, dev165902 (2018).
70. Gregorieff, A. & Clevers, H. Wnt signaling in the intestinal epithelium: From endoderm to cancer. *Genes Dev.* **19**, 877–890 (2005).
71. Kretzschmar, K. & Clevers, H. Wnt/β-catenin signaling in adult mammalian epithelial stem cells. *Dev. Biol.* **428**, 273–282 (2017).
72. Merlos-Suárez, A. *et al.* The intestinal stem cell signature identifies colorectal cancer stem cells and predicts disease relapse. *Cell Stem Cell* **8**, 511–524 (2011).
73. Korinek, V. *et al.* Depletion of epithelial stem-cell compartments in the small intestine of mice lacking Tcf-4. *Nat. Genet.* **19**, 379–383 (1998).
74. Silva, J. *et al.* Promotion of Reprogramming to Ground State Pluripotency by Signal Inhibition. *PLOS Biol.* **6**, e253 (2008).
75. Berge, D. Ten *et al.* Embryonic stem cells require Wnt proteins to prevent differentiation to epiblast stem cells. *Nat. Cell Biol.* **13**, 1070–1077 (2011).
76. Pinto, D., Gregorieff, A., Begthel, H. & Clevers, H. Canonical Wnt signals are essential for homeostasis of the intestinal epithelium. *Genes Dev.* **17**, 1709–1713 (2003).
77. Hoffman, J., Kuhnert, F., Davis, C. R. & Kuo, C. J. Wnts as essential growth factors for the adult small intestine and colon. *Cell Cycle* vol. 3 552–555 (2004).
78. Kuhnert, F. *et al.* Essential requirement for Wnt signaling in proliferation of adult small intestine and colon revealed by adenoviral expression of Dickkopf-1. *Proc. Natl. Acad. Sci.* **101**, 266–271 (2004).
79. Fevr, T., Robine, S., Louvard, D. & Huelsken, J. Wnt/β-Catenin Is Essential for Intestinal Homeostasis and Maintenance of Intestinal Stem Cells. *Mol. Cell. Biol.* **27**, 7551–7559 (2007).
80. van Es, J. H. *et al.* A Critical Role for the Wnt Effector Tcf4 in Adult Intestinal Homeostatic Self-Renewal. *Mol. Cell. Biol.* **32**, 1918–1927 (2012).
81. Van de Wetering, M. *et al.* The β-catenin/TCF-4 complex imposes a crypt progenitor phenotype on colorectal cancer cells. *Cell* **111**, 241–250 (2002).
82. Powell, D. W., Pinchuk, I. V., Saada, J. I., Chen, X. & Mifflin, R. C. Mesenchymal cells of the intestinal lamina propria. *Annu. Rev. Physiol.* **73**, 213–237 (2011).
83. McCarthy, N., Kraiczy, J. & Shivdasani, R. A. Cellular and molecular architecture of the intestinal stem cell niche. *Nat. Cell Biol.* **22**, 1033–1041 (2020).

84. San Roman, A. K., Jayewickreme, C. D., Murtaugh, L. C. & Shivdasani, R. A. Wnt secretion from epithelial cells and subepithelial myofibroblasts is not required in the mouse intestinal stem cell niche in vivo. *Stem Cell Reports* **2**, 127–134 (2014).

85. Valenta, T. *et al.* Wnt Ligands Secreted by Subepithelial Mesenchymal Cells Are Essential for the Survival of Intestinal Stem Cells and Gut Homeostasis. *Cell Rep.* **15**, 911–918 (2016).

86. Collu, G. M., Hidalgo-Sastre, A. & Brennan, K. Wnt-Notch signalling crosstalk in development and disease. *Cell. Mol. Life Sci.* **71**, 3553–3567 (2014).

87. Fre, S. *et al.* Notch and Wnt signals cooperatively control cell proliferation and tumorigenesis in the intestine. *Proc. Natl. Acad. Sci. U. S. A.* **106**, 6309–6314 (2009).

88. Pellegrinet, L. *et al.* Dll1- and Dll4-Mediated Notch Signaling Are Required for Homeostasis of Intestinal Stem Cells. *Gastroenterology* **140**, 1230-1240.e7 (2011).

89. Fre, S. *et al.* Notch Lineages and Activity in Intestinal Stem Cells Determined by a New Set of Knock-In Mice. *PLoS One* **6**, e25785 (2011).

90. VanDussen, K. L. *et al.* Notch signaling modulates proliferation and differentiation of intestinal crypt base columnar stem cells. *Development* **139**, 488–497 (2012).

91. Yu, S. *et al.* Paneth Cell Multipotency Induced by Notch Activation following Injury. *Cell Stem Cell* **23**, 46-59.e5 (2018).

92. Suzuki, A., Sekiya, S., Gunshima, E., Fujii, S. & Taniguchi, H. EGF signaling activates proliferation and blocks apoptosis of mouse and human intestinal stem/progenitor cells in long-term monolayer cell culture. *Lab. Investig. 2010 9010* **90**, 1425–1436 (2010).

93. Biteau, B. & Jasper, H. EGF signaling regulates the proliferation of intestinal stem cells in Drosophila. *Development* **138**, 1045–1055 (2011).

94. Sancho, E., Batlle, E. & Clevers, H. SIGNALING PATHWAYS IN INTESTINAL DEVELOPMENT AND CANCER. *http://dx.doi.org.proxy.insermbiblio.inist.fr/10.1146/annurev.cellbio.20.010403.092805* **20**, 695–723 (2004).

95. Auclair, B. A., Benoit, Y. D., Rivard, N., Mishina, Y. & Perreault, N. Bone Morphogenetic Protein Signaling Is Essential for Terminal Differentiation of the Intestinal Secretory Cell Lineage. *Gastroenterology* **133**, 887–896 (2007).

96. Haramis, A. P. G. *et al.* De novo crypt formation and juvenile polyposis on BMP inhibition in mouse intestine. *Science* **303**, 1684–1686 (2004).

97. He, X. C. *et al.* BMP signaling inhibits intestinal stem cell self-renewal through suppression of Wnt-beta-catenin signaling. *Nat. Genet.* **36**, 1117–1121 (2004).

98. Qi, Z. *et al.* BMP restricts stemness of intestinal Lgr5+ stem cells by directly suppressing their signature genes. *Nat. Commun.* **8**, (2017).

99. Westendorp, B. F. *et al.* Indian Hedgehog Suppresses a Stromal Cell–Driven Intestinal Immune Response. *Cmgh* **5**, 67-82.e1 (2018).

100. van Dop, W. A. *et al.* Depletion of the Colonic Epithelial Precursor Cell Compartment Upon Conditional Activation of the Hedgehog Pathway. *Gastroenterology* **136**, 2195-2203.e7 (2009).

101. Mao, J., Kim, B. M., Rajurkar, M., Shivdasani, R. A. & McMahon, A. P. Hedgehog signaling controls mesenchymal growth in the developing mammalian digestive tract. *Development* **137**, 1721–1729 (2010).

102. Degirmenci, B., Valenta, T., Dimitrieva, S., Hausmann, G. & Basler, K. GLI1-expressing mesenchymal cells form the essential Wnt-secreting niche for colon stem cells. *Nature* **558**, 449–453 (2018).

103. Zacharias, W. J. *et al.* Hedgehog signaling controls homeostasis of adult intestinal smooth muscle. *Dev. Biol.* **355**, 152 (2011).

104. Van Dop, W. A. *et al.* Loss of Indian Hedgehog Activates Multiple Aspects of a Wound Healing Response in the Mouse Intestine. *Gastroenterology* **139**, 1665-1676.e10 (2010).

105. Moya, I. M. & Halder, G. Hippo–YAP/TAZ signalling in organ regeneration and regenerative medicine. *Nat. Rev. Mol. Cell Biol. 2018 204* **20**, 211–226 (2018).

106. Gregorieff, A., Liu, Y., Inanlou, M. R., Khomchuk, Y. & Wrana, J. L. Yap-dependent reprogramming of Lgr5+ stem cells drives intestinal regeneration and cancer. *Nat. 2015 5267575* **526**, 715–718 (2015).

107. Barry, E. R. *et al.* Restriction of intestinal stem cell expansion and the regenerative response by YAP. *Nat. 2012 4937430* **493**, 106–110 (2012).

108. Cai, J. *et al.* The Hippo signaling pathway restricts the oncogenic potential of an intestinal regeneration program. *Genes Dev.* **24**, 2383–2388 (2010).

109. Guillermin, O. *et al.* Wnt and Src signals converge on YAP-TEAD to drive intestinal regeneration. *EMBO J.* **40**, e105770 (2021).

110. Bray, F., Laversanne, M., Weiderpass, E. & Soerjomataram, I. The ever-increasing importance of cancer as a leading cause of premature death worldwide. *Cancer* **127**, 3029–3030 (2021).

111. Hanahan, D. & Weinberg, R. A. Hallmarks of cancer: The next generation. *Cell* **144**, 646–674 (2011).

112. Hanahan, D. Hallmarks of Cancer: New Dimensions. *Cancer Discov.* **12**, 31–46 (2022).

113. Wang, L. H., Wu, C. F., Rajasekaran, N. & Shin, Y. K. Loss of Tumor Suppressor Gene Function in Human Cancer: An Overview. *Cell. Physiol. Biochem.* **51**, 2647–2693 (2018).

114. Sung, H. *et al.* Global Cancer Statistics 2020: GLOBOCAN Estimates of Incidence and Mortality Worldwide for 36 Cancers in 185 Countries. *CA. Cancer J. Clin.* **71**, 209–249 (2021).

115. Fearon, E. R. & Vogelstein, B. A genetic model for colorectal tumorigenesis. *Cell* **61**, 759–767 (1990).

116. Rao, C. V & Yamada, H. Y. Genomic instability and colon carcinogenesis: from the perspective of genes. *Front. Oncol.* **3**, 130 (2013).

117. Fearon, E. R. Molecular genetics of colorectal cancer. *Annu. Rev. Pathol. Mech. Dis.* **6**, 479–507 (2011).

118. Batlle, E. & Clevers, H. Cancer stem cells revisited. *Nat. Med.* **23**, 1124–1134 (2017).

119. Clevers, H. The cancer stem cell: premises, promises and challenges. *Nat. Med.* **17**, 313—319 (2011).

120. Shih, I. M. *et al.* Top-down morphogenesis of colorectal tumors. *Proc. Natl. Acad. Sci.* **98**, 2640–2645 (2001).

121. Preston, S. L. *et al.* Bottom-up histogenesis of colorectal adenomas: Origin in the monocryptal adenoma and initial expansion by crypt fission. *Cancer Research* vol. 63 3819–3825 https://pubmed.ncbi.nlm.nih.gov/12839979/ (2003).

122. Chan, D. K. H. & Buczacki, S. J. A. *Tumour heterogeneity and evolutionary dynamics in colorectal cancer*. *Oncogenesis* vol. 10 1–9 (2021).

123. Radtke, F. & Clevers, H. Self-Renewal and Cancer of the Gut: Two Sides of a Coin. *Science (80-.).* **307**, 1904–1909 (2005).

124. Bijlsma, M. F., Sadanandam, A., Tan, P. & Vermeulen, L. Molecular subtypes in cancers of the gastrointestinal tract. *Nat. Rev. Gastroenterol. Hepatol.* **14**, 333–342 (2017).

125. Guinney, J. *et al.* The consensus molecular subtypes of colorectal cancer. *Nat. Med.* **21**, 1350–1356 (2015).

126. Nowell, P. C. The clonal evolution of tumor cell populations. *Science (80-.).* **194**, 23–28 (1976).

127. Ricci-Vitiani, L. *et al.* Identification and expansion of human colon-cancer-initiating cells. *Nature* **445**, 111–115 (2007).

128. O'Brien, C. A., Pollett, A., Gallinger, S. & Dick, J. E. A human colon cancer cell capable of initiating tumour growth in immunodeficient mice. *Nature* **445**, 106–110 (2007).

129. Dalerba, P. *et al.* Phenotypic characterization of human colorectal cancer stem cells. *Proc. Natl. Acad. Sci. U. S. A.* **104**, 10158–10163 (2007).

130. Zeuner, A., Todaro, M., Stassi, G. & De Maria, R. Colorectal cancer stem cells: From the crypt to the clinic. *Cell Stem Cell* **15**, 692–705 (2014).

131. Schwitalla, S. *et al.* Intestinal tumorigenesis initiated by dedifferentiation and acquisition of stem-cell-like properties. *Cell* **152**, 25–38 (2013).

132. Westphalen, C. B. *et al.* Long-lived intestinal tuft cells serve as colon cancer–initiating cells. *J. Clin. Invest.* **124**, 1283–1295 (2014).

133. Schepers, A. G. *et al.* Lineage tracing reveals Lgr5+ stem cell activity in mouse intestinal adenomas. *Science (80-.).* **337**, 730–735 (2012).

134. Schwitalla, S. *et al.* Intestinal tumorigenesis initiated by dedifferentiation and acquisition of stem-cell-like properties. *Cell* **152**, 25–38 (2013).

135. De Sousa E Melo, F. *et al.* A distinct role for Lgr5+ stem cells in primary and metastatic colon cancer. *Nat. 2017 5437647* **543**, 676–680 (2017).

136. Van Der Heijden, M. & Vermeulen, L. Stem cells in homeostasis and cancer of the gut. *Mol. Cancer* **18**, 66 (2019).

137. Barker, N. *et al.* Crypt stem cells as the cells-of-origin of intestinal cancer. *Nature* **457**, 608–611 (2009).

138. Drost, J. *et al.* Sequential cancer mutations in cultured human intestinal stem cells. *Nature* **521**, 43–47 (2015).

139. Lenos, K. J. *et al.* Stem cell functionality is microenvironmentally defined during tumour expansion and therapy response in colon cancer. *Nat. Cell Biol.* **20**, 1193–1202 (2018).

140. Yum, M. K. *et al.* Tracing oncogene-driven remodelling of the intestinal stem cell niche. *Nature* **594**, 442–447 (2021).

141. Vermeulen, L. *et al.* Defining stem cell dynamics in models of intestinal tumor initiation. *Science (80-.).* **342**, 995–998 (2013).

142. Snippert, H. J., Schepers, A. G., Van Es, J. H., Simons, B. D. & Clevers, H. Biased competition between Lgr5 intestinal stem cells driven by oncogenic mutation induces clonal expansion. *EMBO Rep.* **15**, 62 (2014).

143. Vermeulen, L. *et al.* Wnt activity defines colon cancer stem cells and is regulated by the microenvironment. *Nat. Cell Biol.* **12**, 468–476 (2010).

144. Flanagan, D. J. *et al.* NOTUM from Apc-mutant cells biases clonal competition to initiate cancer. *Nature* **594**, 430–435 (2021).

145. van Neerven, S. M. *et al.* Apc-mutant cells act as supercompetitors in intestinal tumour initiation. *Nature* **594**, 436–441 (2021).

146. Vermeulen, L. & Snippert, H. J. Stem cell dynamics in homeostasis and cancer of the intestine. *Nat. Rev. Cancer* **14**, 468–480 (2014).

147. Dow, L. E. *et al.* Apc restoration promotes cellular differentiation and reestablishes crypt homeostasis in colorectal cancer. *Cell* **161**, 1539 (2015).

148. Dunkin, D. *et al.* Intestinal epithelial Notch-1 protects from colorectal mucinous adenocarcinoma. *Oncotarget* **9**, 33536–33548 (2018).

149. Ternet, C. & Kiel, C. Signaling pathways in intestinal homeostasis and colorectal cancer: KRAS at centre stage. *Cell Commun. Signal. 2021 191* **19**, 1–22 (2021).

150. Jaeger, E. *et al.* Hereditary mixed polyposis syndrome is caused by a 40kb upstream duplication that leads to increased and ectopic expression of the BMP antagonist GREM1. *Nat. Genet.* **44**, 699 (2012).

151. Tomlinson, I. P. M. *et al.* Multiple Common Susceptibility Variants near BMP Pathway Loci GREM1, BMP4, and BMP2 Explain Part of the Missing Heritability of Colorectal Cancer. *PLoS Genet.* **7**, 1002105 (2011).

152. He, X. C. *et al.* BMP signaling inhibits intestinal stem cell self-renewal through suppression of Wnt-beta-catenin signaling. *Nat. Genet.* **36**, 1117–1121 (2004).

153. Voorneveld, P. W. *et al.* The BMP pathway either enhances or inhibits the Wnt pathway depending on the SMAD4 and p53 status in CRC. *Br. J. Cancer* **112**, 122 (2015).

154. Freeman, T. J. *et al.* Smad4-Mediated Signaling Inhibits Intestinal Neoplasia by Inhibiting Expression of β-Catenin. *Gastroenterology* **142**, 562 (2012).

155. Calon, A., Tauriello, D. V. F. & Batlle, E. *TGF-beta in CAF-mediated tumor growth and metastasis*. *Seminars in Cancer Biology* vol. 25 15–22 (2014).

156. Calon, A. *et al.* Stromal gene expression defines poor-prognosis subtypes in colorectal cancer. *Nat. Genet.* **47**, 320–329 (2015).

157. Tauriello, D. V. F. *et al.* TGFβ drives immune evasion in genetically reconstituted colon cancer metastasis. *Nat. 2018 5547693* **554**, 538–543 (2018).

158. Cray, P., Sheahan, B. J. & Dekaney, C. M. Secretory Sorcery: Paneth Cell Control of Intestinal Repair and Homeostasis. *Cell. Mol. Gastroenterol. Hepatol.* **12**, 1239–1250 (2021).

159. Kim, C. K., Yang, V. W. & Bialkowska, A. B. The Role of Intestinal Stem Cells in Epithelial Regeneration Following Radiation-Induced Gut Injury. *Curr. Stem Cell Reports* **3**, 320–332 (2017).

160. Richmond, C. A. *et al.* Dormant Intestinal Stem Cells Are Regulated by PTEN and Nutritional Status. *Cell Rep.* **13**, 2403–2411 (2015).

161. Regan, J. L. *et al.* RNA sequencing of long-term label-retaining colon cancer stem cells identifies novel regulators of quiescence. *iScience* **24**, 102618 (2021).

162. Russo, M., Sogari, A. & Bardelli, A. Adaptive Evolution: How Bacteria and Cancer Cells Survive Stressful Conditions and Drug Treatment. *Cancer Discov.* **11**, 1886–1895 (2021).

163. Balaban, N. Q., Merrin, J., Chait, R., Kowalik, L. & Leibler, S. Bacterial persistence as a phenotypic switch. *Science (80-.).* **305**, 1622–1625 (2004).

164. Sharma, S. V. *et al.* A Chromatin-Mediated Reversible Drug-Tolerant State in Cancer Cell Subpopulations. *Cell* **141**, 69–80 (2010).

165. Rehman, S. K. *et al.* Colorectal Cancer Cells Enter a Diapause-like DTP State to Survive Chemotherapy. *Cell* **184**, 226-242.e21 (2021).

166. Oren, Y. *et al.* Cycling cancer persister cells arise from lineages with distinct programs. *Nat. 2021 5967873* **596**, 576–582 (2021).

167. Shen, S., Vagner, S. & Robert, C. Persistent Cancer Cells: The Deadly Survivors. *Cell* **183**, 860–874 (2020).

168. Russo, M. *et al.* Adaptive mutability of colorectal cancers in response to targeted therapies. *Science (80-.).* **366**, 1473–1480 (2019).

169. Shaffer, S. M. *et al.* Rare cell variability and drug-induced reprogramming as a mode of cancer drug resistance. *Nature* **546**, 431–435 (2017).

170. Ramirez, M. *et al.* Diverse drug-resistance mechanisms can emerge from drug-tolerant cancer persister cells. *Nat. Commun.* **7**, (2016).

171. Marine, J. C., Dawson, S. J. & Dawson, M. A. Non-genetic mechanisms of therapeutic resistance in cancer. *Nat. Rev. Cancer* **20**, 743–756 (2020).

172. Leonce, C., Saintigny, P. & Ortiz-Cuaran, S. Cell-Intrinsic Mechanisms of Drug Tolerance to Systemic Therapies in Cancer. *Mol. Cancer Res.* **20**, 11–29 (2022).

173. Crucitta, S. *et al.* Treatment-driven tumour heterogeneity and drug resistance: Lessons from solid tumours. *Cancer Treatment Reviews* vol. 104 (2022).

174. Yabo, Y. A., Niclou, S. P. & Golebiewska, A. Cancer cell heterogeneity and plasticity: A paradigm shift in glioblastoma. *Neuro. Oncol.* (2021) doi:10.1093/NEUONC/NOAB269.

175. Rambow, F. *et al.* Toward Minimal Residual Disease-Directed Therapy in Melanoma. *Cell* **174**, 843-855.e19 (2018).

176. Marin-Bejar, O. *et al.* Evolutionary predictability of genetic versus nongenetic resistance to anticancer drugs in melanoma. *Cancer Cell* **39**, 1135-1149.e8 (2021).

177. Vasan, N., Baselga, J. & Hyman, D. M. A view on drug resistance in cancer. *Nature* **575**, 299–309 (2019).

178. Mimeault, M., Hauke, R. & Batra, S. K. Recent advances on the molecular mechanisms involved in the drug resistance of cancer cells and novel targeting therapies. *Clinical Pharmacology and Therapeutics* vol. 83 673–691 (2008).

179. Rang, H. P., Ritter, J. M., Flower, R. J. & Henderson, G. *Rang and Dales's Pharmacology*. (Elsevier, 2012).

180. Heidelberger, C. *et al.* Fluorinated Pyrimidines, A New Class of Tumour-Inhibitory Compounds. *Nat. 1957 1794561* **179**, 663–666 (1957).

181. Mohelnikova-Duchonova, B., Melichar, B. & Soucek, P. FOLFOX/FOLFIRI pharmacogenetics: the call for a personalized approach in colorectal cancer therapy. *World J. Gastroenterol.* **20**, 10316–10330 (2014).

182. Wolpin, B. M. & Mayer, R. J. Systemic Treatment of Colorectal Cancer. *Gastroenterology* **134**, 1296-1310.e1 (2008).

183. Van der Jeught, K., Xu, H.-C., Li, Y.-J., Lu, X.-B. & Ji, G. Drug resistance and new therapies in colorectal cancer. *World J. Gastroenterol.* **24**, 3834–3848 (2018).

184. Liang, Y. Y. *et al.* CETSA interaction proteomics define specific RNA-modification pathways as key components of fluorouracil-based cancer drug cytotoxicity. *Cell Chem. Biol.* **0**, (2021).

185. Bash-Imam, Z. *et al.* Translational reprogramming of colorectal cancer cells induced by 5-fluorouracil through a miRNA-dependent mechanism. *Oncotarget* **8**, 46219–46233 (2017).

186. Chalabi-Dchar, M. *et al.* A novel view on an old drug, 5-fluorouracil: an unexpected RNA modifier with intriguing impact on cancer cell fate. *NAR Cancer* **3**, (2021).

187. Diasio, R. B. & Harris, B. E. Clinical Pharmacology of 5-Fluorouracil. *Clinical Pharmacokinetics* vol. 16 215–237 (1989).

188. Van Kuilenburg, A. B. P., Meinsma, R. & Van Gennip, A. H. Pyrimidine degradation defects and severe 5-fluorouracil toxicity. in *Nucleosides, Nucleotides and Nucleic Acids*

vol. 23 1371–1375 (2004).

189. Thorn, C. F. *et al.* Pharm GKB summary: Fluoropyrimidine pathways. *Pharmacogenetics and Genomics* vol. 21 237–242 (2011).

190. Yuan, J. H. *et al.* Breast cancer resistance protein expression and 5-fluorouracil resistance. *Biomed. Environ. Sci.* **21**, 290–295 (2008).

191. Hagmann, W., Jesnowski, R., Faissner, R., Guo, C. & Löhr, J. M. ATP-binding cassette C transporters in human pancreatic carcinoma cell lines. *Pancreatology* **9**, 136–144 (2009).

192. Saltz, L. B. *et al.* Irinotecan plus Fluorouracil and Leucovorin for Metastatic Colorectal Cancer. *N. Engl. J. Med.* **343**, 905–914 (2000).

193. Parvez, M. M. *et al.* Quantitative investigation of irinotecan metabolism, transport, and gut microbiome activation. *Drug Metab. Dispos.* **49**, 683–693 (2021).

194. Fujita, K. I., Kubota, Y., Ishida, H. & Sasaki, Y. Irinotecan, a key chemotherapeutic drug for metastatic colorectal cancer. *World J. Gastroenterol.* **21**, 12234–12248 (2015).

195. Giacchetti, S. *et al.* Phase III multicenter randomized trial of oxaliplatin added to chronomodulated fluorouracil-leucovorin as first-line treatment of metastatic colorectal cancer. *J. Clin. Oncol.* **18**, 136–147 (2000).

196. de Gramont, A. *et al.* Leucovorin and fluorouracil with or without oxaliplatin as first-line treatment in advanced colorectal cancer. *J. Clin. Oncol.* **18**, 2938–2947 (2000).

197. Marsh, S. *et al.* Platinum pathway. *Pharmacogenetics and Genomics* vol. 19 563–564 (2009).

198. Rottenberg, S., Disler, C. & Perego, P. The rediscovery of platinum-based cancer therapy. *Nat. Rev. Cancer* **21**, 37–50 (2021).

199. Hurwitz, H. *et al.* Bevacizumab plus Irinotecan, Fluorouracil, and Leucovorin for Metastatic Colorectal Cancer. *N. Engl. J. Med.* **350**, 2335–2342 (2004).

200. Giantonio, B. J. *et al.* A phase II study of high-dose bevacizumab in combination with irinotecan, 5-fluorouracil, leucovorin, as initial therapy for advanced colorectal cancer: Results from the eastern cooperative oncology group study E2200. *Ann. Oncol.* **17**, 1399–1403 (2006).

201. Giantonio, B. J. *et al.* Bevacizumab in combination with oxaliplatin, fluorouracil, and leucovorin (FOLFOX4) for previously treated metastatic colorectal cancer: Results from the Eastern Cooperative Oncology Group Study E3200. *J. Clin. Oncol.* **25**, 1539–1544 (2007).

202. Goldberg, R. M., Venook, A. P. & Schilsky, R. L. Cetuximab in the treatment of colorectal cancer. *Clin. Adv. Hematol. Oncol.* **2**, (2004).

203. Vincenzi, B. *et al.* Cetuximab and irinotecan as third-line therapy in advanced colorectal cancer patients: A single centre phase II trial. *Br. J. Cancer* **94**, 792–797 (2006).

204. Messersmith, W. A. & Hidalgo, M. Panitumumab, a monoclonal anti-epidermal growth factor receptor antibody in colorectal cancer: Another one or the one? *Clin. Cancer Res.* **13**, 4664–4666 (2007).

205. Tabernero, J. *et al.* Encorafenib Plus Cetuximab as a New Standard of Care for Previously Treated BRAF V600E–Mutant Metastatic Colorectal Cancer: Updated Survival Results and Subgroup Analyses from the BEACON Study. *J. Clin. Oncol.* **39**, 273–284 (2021).

206. Briffa, R., Langdon, S. P., Grech, G. & Harrison, D. J. Acquired and Intrinsic Resistance to Colorectal Cancer Treatment. in *Colorectal Cancer - Diagnosis, Screening and Management* (IntechOpen, 2018). doi:10.5772/intechopen.70781.

207. Blondy, S. *et al.* 5-Fluorouracil resistance mechanisms in colorectal cancer: From classical pathways to promising processes. *Cancer Sci.* **111**, 3142–3154 (2020).

208. Rajal, A. G. *et al.* A non-genetic, cell cycle-dependent mechanism of platinum resistance in lung adenocarcinoma. *Elife* **10**, (2021).

209. Sazonova, E. V., Kopeina, G. S., Imyanitov, E. N. & Zhivotovsky, B. Platinum drugs and taxanes: can we overcome resistance? *Cell Death Discov.* **7**, (2021).

210. Shiokawa, D. *et al.* Slow-cycling cancer stem cells regulate progression and chemoresistance in colon cancer. *Cancer Res.* **80**, 4451–4464 (2021).

211. Luo, M., Yang, X., Chen, H. N., Nice, E. C. & Huang, C. Drug resistance in colorectal cancer: An epigenetic overview. *Biochim. Biophys. Acta - Rev. Cancer* **1876**, 188623 (2021).

212. Yang, C. *et al.* Histone methyltransferase and drug resistance in cancers. *J. Exp. Clin. Cancer Res.* **39**, 1–13 (2020).

213. Woolston, A. *et al.* Genomic and Transcriptomic Determinants of Therapy Resistance and Immune Landscape Evolution during Anti-EGFR Treatment in Colorectal Cancer. *Cancer Cell* **36**, 35-50.e9 (2019).

214. Touil, Y. *et al.* Colon cancer cells escape 5FU chemotherapy-induced cell death by entering stemness and quiescence associated with the c-Yes/YAP axis. *Clin. Cancer Res.* **20**, 837–846 (2014).

215. Bauzone, M. *et al.* Cross-talk between YAP and RAR-RXR drives expression of stemness genes to promote 5-FU resistance and self-renewal in colorectal cancer cells. *Mol. Cancer Res.* **19**, 612–622 (2021).

216. Ozawa, S., Miura, T., Terashima, J. & Habano, W. Cellular irinotecan resistance in colorectal cancer and overcoming irinotecan refractoriness through various combination trials including DNA methyltransferase inhibitors: a review. *Cancer Drug Resist.* **4**, 946–964 (2021).

217. Hammond, W. A., Swaika, A. & Mody, K. Pharmacologic resistance in colorectal cancer: A review. *Therapeutic Advances in Medical Oncology* vol. 8 57–84 (2016).

218. Montagut, C. *et al.* Identification of a mutation in the extracellular domain of the Epidermal Growth Factor Receptor conferring cetuximab resistance in colorectal cancer. *Nat. Med.* **18**, 221–223 (2012).

219. Robey, R. W. *et al. Revisiting the role of ABC transporters in multidrug-resistant cancer*. vol. 18 452–464 (Nature Publishing Group, 2018).

220. Davis, P. J. *et al.* Thyroid hormone and P-glycoprotein in tumor cells. *BioMed Research International* vol. 2015 (2015).

221. Nielsen, D. L., Palshof, J. A., Brünner, N., Stenvang, J. & Viuff, B. M. Implications of ABCG2 expression on irinotecan treatment of colorectal cancer patients: A review. *International Journal of Molecular Sciences* vol. 18 (2017).

222. Stacy, A. E., Jansson, P. J. & Richardson, D. R. Molecular Pharmacology of ABCG2 and its role in chemoresistance. *Molecular Pharmacology* vol. 84 655–669 (2013).

223. Feldt-Rasmussen, U., Effraimidis, G. & Klose, M. The hypothalamus-pituitary-thyroid (HPT)-axis and its role in physiology and pathophysiology of other hypothalamus-pituitary functions. *Mol. Cell. Endocrinol.* **525**, 111173 (2021).

224. Yen, P. M. Physiological and molecular basis of Thyroid hormone action. *Physiological Reviews* vol. 81 1097–1142 (2001).

225. Ortiga-Carvalho, T. M., Chiamolera, M. I., Pazos-Moura, C. C. & Wondisford, F. E. Hypothalamus-pituitary-thyroid axis. *Compr. Physiol.* **6**, 1387–1428 (2016).

226. Carvalho, D. P. & Dupuy, C. Thyroid hormone biosynthesis and release. *Mol. Cell. Endocrinol.* **458**, 6–15 (2017).

227. Sorrenti, S. *et al.* Iodine: Its Role in Thyroid Hormone Biosynthesis and Beyond. *Nutr. 2021, Vol. 13, Page 4469* **13**, 4469 (2021).

228. Bianco, A. C. & Kim, B. W. Deiodinases: Implications of the local control of thyroid hormone action. *J. Clin. Invest.* **116**, 2571–2579 (2006).

229. Dentice, M., Marsili, A., Zavacki, A., Larsen, P. R. & Salvatore, D. The deiodinases and the control of intracellular thyroid hormone signaling during cellular differentiation. *Biochimica et Biophysica Acta - General Subjects* vol. 1830 3937–3945 (2013).

230. Bianco, A. C. *et al.* Paradigms of Dynamic Control of Thyroid Hormone Signaling. *Endocr. Rev.* **40**, 1000–1047 (2019).

231. Kinne, A., Schülein, R. & Krause, G. Primary and secondary thyroid hormone transporters. *Thyroid Res.* **4**, S7 (2011).

232. Meyer Zu Schwabedissen, H. E. *et al.* Thyroid Hormones Are Transport Substrates and Transcriptional Regulators of Organic Anion Transporting Polypeptide 2B1. *Mol. Pharmacol.* **94**, 700–712 (2018).

233. Robinson-Rechavi, M., Garcia, H. E. & Laudet, V. *The nuclear receptor superfamily*. *Journal of Cell Science* vol. 116 585–586 (2003).

234. Evans, R. M. & Mangelsdorf, D. J. Nuclear receptors, RXR, and the big bang. *Cell* vol. 157 255–266 (2014).

235. Brent, G. A. Mechanisms of thyroid hormone action. *J. Clin. Invest.* **122**, 3035–3043 (2012).

236. Cheng, S. Y., Leonard, J. L. & Davis, P. J. Molecular aspects of thyroid hormone actions. *Endocrine Reviews* vol. 31 139–170 (2010).

237. Oetting, A. & Yen, P. M. New insights into thyroid hormone action. *Best Pract. Res. Clin. Endocrinol. Metab.* **21**, 193–208 (2007).

238. Mullur, R., Liu, Y. Y. & Brent, G. A. Thyroid hormone regulation of metabolism. *Physiol. Rev.* **94**, 355–382 (2014).

239. Hartong, R. *et al.* Delineation of three different thyroid hormone-response elements in promoter of rat sarcoplasmic reticulum Ca2+ ATPase gene. Demonstration that retinoid X receptor binds 5’ to thyroid hormone receptor in response element 1. *J. Biol. Chem.* **269**, 13021–13029 (1994).

240. Liu, Y. Y. & Brent, G. A. Thyroid hormone crosstalk with nuclear receptor signaling in metabolic regulation. *Trends in Endocrinology and Metabolism* vol. 21 166–173 (2010).

241. Sirakov, M. & Plateroti, M. The thyroid hormones and their nuclear receptors in the gut: From developmental biology to cancer. *Biochimica et Biophysica Acta - Molecular Basis of Disease* vol. 1812 938–946 (2011).

242. Koenig, R. J. *et al.* Inhibition of thyroid hormone action by a non-hormone binding c-erbA protein generated by alternative mRNA splicing. *Nature* **337**, 659–661 (1989).

243. Chassande, O. *et al.* Identification of Transcripts Initiated from an Internal Promoter in the c-erbAα Locus That Encode Inhibitors of Retinoic Acid Receptor-α and Triiodothyronine Receptor Activities. *Mol. Endocrinol.* **11**, 1278–1290 (1997).

244. Flamant, F. & Samarut, J. Thyroid hormone receptors: lessons from knockout and knock-in mutant mice. *Trends Endocrinol. Metab.* **14**, 85–90 (2003).

245. Modica, S. *et al.* The Intestinal Nuclear Receptor Signature With Epithelial Localization Patterns and Expression Modulation in Tumors. *Gastroenterology* **138**, 636-648.e12 (2010).

246. Sirakov, M., Kress, E., Nadjar, J. & Plateroti, M. Thyroid hormones and their nuclear receptors: New players in intestinal epithelium stem cell biology? *Cellular and Molecular Life Sciences* vol. 71 2897–2907 (2014).

247. Skah, S., Uchuya-Castillo, J., Sirakov, M. & Plateroti, M. The thyroid hormone nuclear receptors and the Wnt/β-catenin pathway: An intriguing liaison. *Dev. Biol.* **422**, 71–82 (2017).

248. Plateroti, M. *et al.* Functional Interference between Thyroid Hormone Receptor α (TRα) and Natural Truncated TRΔα Isoforms in the Control of Intestine Development. *Mol. Cell. Biol.* **21**, 4761–4772 (2001).

249. Harvey, C. B., Bassett, J. H. D., Maruvada, P., Yen, P. M. & Williams, G. R. The rat thyroid hormone receptor (TR) Δβ3 displays cell-, TR isoform-, and thyroid hormone response element-specific actions. *Endocrinology* **148**, 1764–1773 (2007).

250. Williams, G. R. Cloning and characterization of two novel thyroid hormone receptor beta isoforms. *Mol. Cell. Biol.* **20**, 8329–8342 (2000).

251. Ikeda, M., Rhee, M. & Chin, W. Thyroid hormone receptor monomer, homodimer, and heterodimer (with retinoid-X receptor) contact different nucleotide sequences in thyroid hormone response elements. *Endocrinology* **135**, 1628–1638 (1994).

252. Singh, B. K., Sinha, R. A. & Yen, P. M. Novel transcriptional mechanisms for regulating metabolism by thyroid hormone. *Int. J. Mol. Sci.* **19**, (2018).

253. Davis, P. J., Shih, A., Lin, H. Y., Martino, L. J. & Davis, F. B. Thyroxine Promotes Association of Mitogen-activated Protein Kinase and Nuclear Thyroid Hormone Receptor (TR) and Causes Serine Phosphorylation of TR. *J. Biol. Chem.* **275**, 38032–38039 (2000).

254. Glineur, C., Bailly, M. & Ghysdael, J. The c-erbAα-encoded thyroid hormone receptor is phosphorylated in its amino terminal domain by casein kinase II. *Oncogene* **4**, 1247–1254 (1989).

255. Liu, Y. Y. & Brent, G. A. Posttranslational Modification of Thyroid Hormone Nuclear Receptor by Sumoylation. *Methods Mol. Biol.* **1801**, 47–59 (2018).

256. Sánchez-Pacheco, A., Martínez-Iglesias, O., Méndez-Pertuz, M. & Aranda, A. Residues K128, 132, and 134 in the Thyroid Hormone Receptor-α Are Essential for Receptor Acetylation and Activity. *Endocrinology* **150**, 5143–5152 (2009).

257. Grøntved, L. *et al.* Transcriptional activation by the thyroid hormone receptor through ligand-dependent receptor recruitment and chromatin remodelling. *Nat. Commun.* **6**, 1–11 (2015).

258. Eckey, M., Moehren, U. & Baniahmad, A. Gene silencing by the thyroid hormone receptor. *Mol. Cell. Endocrinol.* **213**, 13–22 (2003).

259. Flamant, F. *et al.* Thyroid hormone signaling pathways: Time for a more precise nomenclature. *Endocrinology* **158**, 2052–2057 (2017).

260. Boyle, A. P. *et al.* High-Resolution Mapping and Characterization of Open Chromatin across the Genome. *Cell* **132**, 311 (2008).

261. Martin, N. P. *et al.* A Rapid Cytoplasmic Mechanism for PI3 Kinase Regulation by the Nuclear Thyroid Hormone Receptor, TRβ, and Genetic Evidence for Its Role in the Maturation of Mouse Hippocampal Synapses In Vivo. *Endocrinology* **155**, 3713 (2014).

262. Cao, X., Kambe, F., Moeller, L. C., Refetoff, S. & Seo, H. Thyroid Hormone Induces Rapid Activation of Akt/Protein Kinase B-Mammalian Target of Rapamycin-p70S6K Cascade through Phosphatidylinositol 3-Kinase in Human Fibroblasts. *Mol. Endocrinol.* **19**, 102–112 (2005).

263. Guigon, C. J., Zhao, L., Lu, C., Willingham, M. C. & Cheng, S. Regulation of β-Catenin

by a Novel Nongenomic Action of Thyroid Hormone β Receptor. *Mol. Cell. Biol.* **28**, 4598–4608 (2008).

264. Sirakov, M., Claret, L. & Plateroti, M. Thyroid Hormone Nuclear Receptor TRα1 and Canonical WNT Pathway Cross-Regulation in Normal Intestine and Cancer. *Front. Endocrinol. (Lausanne).* **12**, 1653 (2021).

265. Kalyanaraman, H. *et al.* Nongenomic Thyroid Hormone Signaling Occurs Through a Plasma Membrane Receptor. *Sci. Signal.* **7**, ra48 (2014).

266. Fu, L., Yin, J. & Shi, Y. B. Involvement of epigenetic modifications in thyroid hormone-dependent formation of adult intestinal stem cells during amphibian metamorphosis. *General and Comparative Endocrinology* vol. 271 91–96 (2019).

267. Tanizaki, Y., Bao, L., Shi, B. & Shi, Y. B. A Role of Endogenous Histone Acetyltransferase Steroid Hormone Receptor Coactivator 3 in Thyroid Hormone Signaling during Xenopus Intestinal Metamorphosis. *Thyroid* **31**, 692–702 (2021).

268. Davis, P. J., Goglia, F. & Leonard, J. L. Nongenomic actions of thyroid hormone. *Nat. Rev. Endocrinol.* **12**, 111–121 (2016).

269. Davis, P. J., Leonard, J. L., Lin, H.-Y., Leinung, M. & Mousa, S. A. Molecular Basis of Nongenomic Actions of Thyroid Hormone. in *Vitamins and Hormones* vol. 106 67–96 (Academic Press, 2018).

270. Ishizuya-Oka, A. How thyroid hormone regulates transformation of larval epithelial cells into adult stem cells in the amphibian intestine. *Mol. Cell. Endocrinol.* **459**, 98–103 (2017).

271. Kress, E., Rezza, A., Nadjar, J., Samarut, J. & Plateroti, M. The thyroid hormone receptor-α (TRα) gene encoding TRα1 controls deoxyribonucleic acid damage-induced tissue repair. *Mol. Endocrinol.* **22**, 47–55 (2008).

272. Sachs, L. M. & Buchholz, D. R. Insufficiency of thyroid hormone in frog metamorphosis and the role of glucocorticoids. *Front. Endocrinol. (Lausanne).* **10**, 287 (2019).

273. Shi, Y. B., Matsuura, K., Fujimoto, K., Wen, L. & Fu, L. Thyroid hormone receptor actions on transcription in amphibia: The roles of histone modification and chromatin disruption. *Cell and Bioscience* vol. 2 1–10 (2012).

274. Shi, Y. B. & Brown, D. D. The earliest changes in gene expression in tadpole intestine induced by thyroid hormone. *J. Biol. Chem.* **268**, 20312–20317 (1993).

275. Hasebe, T., Buchholz, D. R., Shi, Y. B. & Ishizuya-Oka, A. Epithelial-connective tissue interactions induced by thyroid hormone receptor are essential for adult stem cell development in the Xenopus laevis intestine. *Stem Cells* **29**, 154–161 (2011).

276. Hasebe, T., Fujimoto, K. & Ishizuya-Oka, A. Thyroid hormone-induced expression of Foxl1 in subepithelial fibroblasts correlates with adult stem cell development during Xenopus intestinal remodeling. *Sci. Rep.* **10**, 1–11 (2020).

277. Hasebe, T. *et al.* Thyroid Hormone-Induced Activation of Notch Signaling is Required for Adult Intestinal Stem Cell Development During Xenopus Laevis Metamorphosis. *Stem Cells* **35**, 1028–1039 (2017).

278. Hasebe, T., Fujimoto, K., Kajita, M. & Ishizuya-Oka, A. Thyroid hormone activates Wnt/β-catenin signaling involved in adult epithelial development during intestinal remodeling in Xenopus laevis. *Cell Tissue Res.* **365**, 309–318 (2016).

279. Ishizuya-Oka, A., Hasebe, T., Shimizu, K., Suzuki, K. & Ueda, S. Shh/BMP-4 signaling pathway is essential for intestinal epithelial development during Xenopus larval-to-adult remodeling. *Dev. Dyn.* **235**, 3240–3249 (2006).

280. Ishizuya-Oka, A. *et al.* Thyroid-hormone-dependent and fibroblast-specific expression of BMP-4 correlates with adult epithelial development during amphibian intestinal

remodeling. *Cell Tissue Res.* **303**, 187–195 (2001).

281. Kress, E. *et al.* Cooperation Between the Thyroid Hormone Receptor TRα1 and the WNT Pathway in the Induction of Intestinal Tumorigenesis. *Gastroenterology* **138**, 1863–1874 (2010).

282. Plateroti, M. *et al.* Involvement of T3Rα- and β-receptor subtypes in mediation of T3 functions during postnatal murine intestinal development. *Gastroenterology* **116**, 1367–1378 (1999).

283. Plateroti, M., Kress, E., Mori, J. I. & Samarut, J. Thyroid Hormone Receptor α1 Directly Controls Transcription of the β-Catenin Gene in Intestinal Epithelial Cells. *Mol. Cell. Biol.* **26**, 3204–3214 (2006).

284. Kress, E., Rezza, A., Nadjar, J., Samarut, J. & Plateroti, M. The frizzled-related sFRP2 gene is a target of thyroid hormone receptor α1 and activates β-catenin signaling in mouse intestine. *J. Biol. Chem.* **284**, 1234–1241 (2009).

285. Godart, M. *et al.* Murine intestinal stem cells are highly sensitive to modulation of the T3/TRα1-dependent pathway. *Dev.* **148**, dev194357 (2021).

286. Fraichard, A. *et al.* The T3Rα gene encoding a thyroid hormone receptor is essential for post-natal development and thyroid hormone production. *EMBO J.* **16**, 4412–4420 (1997).

287. Sirakov, M. *et al.* The thyroid hormone nuclear receptor TRα1 controls the Notch signaling pathway and cell fate in murine intestine. *Dev.* **142**, 2764–2774 (2015).

288. Gauthier, K. *et al.* Genetic analysis reveals different functions for the products of the thyroid hormone receptor alpha locus. *Mol. Cell. Biol.* **21**, 4748–4760 (2001).

289. Blitz, E. *et al.* Thyroid Hormones Regulate Goblet Cell Differentiation and Fgf19-Fgfr4 Signaling. *Endocrinol. (United States)* **162**, 1–13 (2021).

290. Uchuya-Castillo, J. *et al.* Increased expression of the thyroid hormone nuclear receptor TRa1 characterizes intestinal tumors with high Wnt activity. *Oncotarget* **9**, 30979–30996 (2018).

291. Lee, Y. S. *et al.* Thyroid Hormone Promotes β-Catenin Activation and Cell Proliferation in Colorectal Cancer. *Horm. Cancer* **9**, 156–165 (2018).

292. Peignon, G. *et al.* Complex interplay between β-catenin signalling and Notch effectors in intestinal tumorigenesis. *Gut* **60**, 166–176 (2011).

293. Rodilla, V. *et al.* Jagged1 is the pathological link between Wnt and Notch pathways in colorectal cancer. *Proc. Natl. Acad. Sci. U. S. A.* **106**, 6315–6320 (2009).

294. Catalano, V. *et al.* Activated thyroid hormone promotes differentiation and chemotherapeutic sensitization of colorectal cancer stem cells by regulating Wnt and BMP4 signaling. *Cancer Res.* **76**, 137–1244 (2016).

295. Krashin, E., Piekiełko-Witkowska, A., Ellis, M. & Ashur-Fabian, O. Thyroid hormones and cancer: A comprehensive review of preclinical and clinical studies. *Front. Endocrinol. (Lausanne).* **10**, 59 (2019).

296. Krashin, E., Piekiełko-Witkowska, A., Ellis, M. & Ashur-Fabian, O. Thyroid hormones and cancer: A comprehensive review of preclinical and clinical studies. *Front. Endocrinol. (Lausanne).* **10**, 59 (2019).

297. Wu, C. C. *et al.* Risk of cancer in long-term levothyroxine users: Retrospective population-based study. *Cancer Sci.* **112**, 2533–2541 (2021).

298. Liu, Y. C., Yeh, C. T. & Lin, K. H. Molecular functions of thyroid hormone signaling in regulation of cancer progression and anti-apoptosis. *International Journal of Molecular Sciences* vol. 20 (2019).

299. L'Heureux, A. *et al.* Association Between Thyroid Disorders and Colorectal Cancer Risk in Adult Patients in Taiwan. *JAMA Netw. Open* **2**, (2019).

300. Boursi, B., Haynes, K., Mamtani, R. & Yang, Y. X. Thyroid Dysfunction, Thyroid Hormone Replacement and Colorectal Cancer Risk. *JNCI J. Natl. Cancer Inst.* **107**, (2015).

301. Iishi, H., Tatsuta, M., Baba, M., Okuda, S. & Taniguchi, H. Enhancement by thyroxine of experimental carcinogenesis induced in rat colon by azoxymethane. *Int. J. Cancer* **50**, 974–976 (1992).

302. Wändell, P., Carlsson, A. C., Li, X., Sundquist, J. & Sundquist, K. Levothyroxine treatment is associated with an increased relative risk of overall and organ specific incident cancers - a cohort study of the Swedish population. *Cancer Epidemiol.* **66**, (2020).

303. Kuiper, J. G. *et al.* Levothyroxine use and the risk of colorectal cancer: a large population-based case-control study. *Endocr. Connect.* **1**, (2021).

304. Rennert, G., Rennert, H. S., Pinchev, M. & Gruber, S. B. A Case–Control Study of Levothyroxine and the Risk of Colorectal Cancer. *JNCI J. Natl. Cancer Inst.* **102**, 568–572 (2010).

305. Hellevik, A. I. *et al.* Thyroid function and cancer risk: A prospective population study. *Cancer Epidemiol. Biomarkers Prev.* **18**, 570–574 (2009).

306. Rose, D. P. & Davis, T. E. Plasma Thyronine Levels in Carcinoma of the Breast and Colon. *Arch. Intern. Med.* **141**, 1161–1164 (1981).

307. Dentice, M. *et al.* β-Catenin Regulates Deiodinase Levels and Thyroid Hormone Signaling in Colon Cancer Cells. *Gastroenterology* **143**, 1037–1047 (2012).

308. Lee, Y. S. *et al.* The combination of tetraiodothyroacetic acid and cetuximab inhibits cell proliferation in colorectal cancers with different K-ras status. *Steroids* **111**, 63–70 (2016).

309. Samuels, H. H., Stanley, F. & Casanova, J. Depletion of L-3,5,3'-Triiodothyronine and L-Thyroxine in Euthyroid Calf Serum for Use in Cell Culture Studies of the Action of Thyroid Hormone. *Endocrinology* **105**, 80–85 (1979).

310. Cao, Z. *et al.* Effects of Resin or Charcoal Treatment on Fetal Bovine Serum and Bovine Calf Serum. *http://dx.doi.org/10.3109/07435800903204082* **34**, 101–108 (2009).

311. Nana, A. W. *et al.* Tetrac downregulates β-catenin and HMGA2 to promote the effect of resveratrol in colon cancer. *Endocr. Relat. Cancer* **25**, 279–293 (2018).

312. Eichelbaum, M. Drug Metabolism in Thyroid Disease. *Clin. Pharmacokinet. 1976 15* **1**, 339–350 (2012).

313. Shenfield, G. M. Influence of thyroid dysfunction on drug pharmacokinetics. *Clin. Pharmacokinet.* **6**, 275–297 (1981).

314. Chen, D. W. *et al.* The inhibition of UDP-glucuronosyltransferases (UGTs) by tetraiodothyronine (T4) and triiodothyronine (T3). *Xenobiotica* **48**, 250–257 (2018).

315. Fujiwara, Y. *et al.* Hypothyroidism in patients with colorectal carcinoma treated with fluoropyrimidines. *Oncol. Rep.* **30**, 1802–1806 (2013).

316. Nishio, N., Katsura, T. & Inui, K.-I. I. Thyroid hormone regulates the expression and function of P-glycoprotein in Caco-2 cells. *Pharm. Res.* **25**, 1037–1042 (2008).

317. Kurose, K., Saeki, M., Tohkin, M. & Hasegawa, R. Thyroid hormone receptor mediates human MDR1 gene expression—Identification of the response region essential for gene expression. *Arch. Biochem. Biophys.* **474**, 82–90 (2008).

318. Burk, O. *et al.* The Impact of Thyroid Disease on the Regulation, Expression, and

Function of ABCB1 (MDR1/P Glycoprotein) and Consequences for the Disposition of Digoxin. *Clin. Pharmacol. Ther.* **88**, 685–694 (2010).

319. Siegmund, W. *et al.* Effect of levothyroxine administration on intestinal P-glycoprotein expression: Consequences for drug disposition*. *Clin. Pharmacol. Ther.* **72**, 256–264 (2002).

320. Drozdzik, M., Czekawy, I., Oswald, S. & Drozdzik, A. Intestinal drug transporters in pathological states: an overview. *Pharmacol. Reports* **72**, 1173–1194 (2020).

321. Mitin, T., Von Moltke, L. L., Court, M. H. & Greenblatt, D. J. Levothyroxine up-regulates P-glycoprotein independent of the pregnane X receptor. *Drug Metab. Dispos.* **32**, 779–782 (2004).

322. Begicevic, R. R. & Falasca, M. ABC Transporters in Cancer Stem Cells: Beyond Chemoresistance. *Int. J. Mol. Sci.* **18**, (2017).

323. Vesel, M. *et al.* ABCB1 and ABCG2 drug transporters are differentially expressed in non-small cell lung cancers (NSCLC) and expression is modified by cisplatin treatment via altered Wnt signaling. *Respir. Res.* **18**, (2017).

324. Chen, Y., Bieber, M. M. & Teng, N. N. H. Hedgehog signaling regulates drug sensitivity by targeting ABC transporters ABCB1 and ABCG2 in epithelial ovarian cancer. *Mol. Carcinog.* **53**, 625–634 (2014).

325. Singh, R. R. *et al.* ABCG2 is a direct transcriptional target of hedgehog signaling and involved in stroma-induced drug tolerance in diffuse large B-cell lymphoma. *Oncogene* **30**, 4874–4886 (2011).

326. Po, A. *et al.* Hedgehog-GLI signalling promotes chemoresistance through the regulation of ABC transporters in colorectal cancer cells. *Sci. Rep.* **10**, 1–14 (2020).

327. Nakanishi, T. *et al.* Novel 5′ Untranslated Region Variants of BCRP mRNA Are Differentially Expressed in Drug-Selected Cancer Cells and in Normal Human Tissues: Implications for Drug Resistance, Tissue-Specific Expression, and Alternative Promoter Usage. *Cancer Res.* **66**, 5007–5011 (2006).

328. Benoki, S., Yoshinari, K., Chikada, T., Imai, J. & Yamazoe, Y. Transactivation of ABCG2 through a novel cis-element in the distal promoter by constitutive androstane receptor but not pregnane X receptor in human hepatocytes. *Arch. Biochem. Biophys.* **517**, 123–130 (2012).

329. Ooe, H., Kon, J., Oshima, H. & Mitaka, T. Thyroid hormone is necessary for expression of constitutive androstane receptor in rat hepatocytes. *Drug Metab. Dispos.* **37**, 1963–1969 (2009).

330. Qatanani, M., Zhang, J. & Moore, D. D. Role of the Constitutive Androstane Receptor in Xenobiotic-Induced Thyroid Hormone Metabolism. *Endocrinology* **146**, 995–1002 (2005).

331. Yang, Y. C. S. H. *et al.* Role of thyroid hormone-integrin αvβ3-signal and therapeutic strategies in colorectal cancers. *J. Biomed. Sci.* **28**, 24 (2021).

332. Verga Falzacappa, C. *et al.* T3 preserves ovarian granulosa cells from chemotherapy-induced apoptosis. *J. Endocrinol.* **215**, 281–289 (2012).

333. López-Fontana, C. M. *et al.* Experimental hypothyroidism increases apoptosis in dimethylbenzanthracene-induced mammary tumors. *Oncol. Rep.* **30**, 1651–1660 (2013).

334. Lin, H.-Y. Y., Glinsky, G. V., Mousa, S. A. & Davis, P. J. Thyroid hormone and anti-apoptosis in tumor cells. *Oncotarget* **6**, 14735–14743 (2015).

335. Frau, C., Godart, M. & Plateroti, M. Thyroid hormone regulation of intestinal epithelial stem cell biology. *Mol. Cell. Endocrinol.* **459**, 90–97 (2017).

336. Giolito, M. V., Claret, L., Frau, C. & Plateroti, M. A Three-dimensional Model of

Spheroids to Study Colon Cancer Stem Cells. *JoVE* e61783 doi:doi:10.3791/61783.

337. Raha, D. *et al.* The cancer stem cell marker aldehyde dehydrogenase is required to maintain a drug-tolerant tumor cell subpopulation. *Cancer Res.* **74**, 3579–3590 (2014).

338. Sarkadi, B., Homolya, L., Szakács, G. & Váradi, A. Human multidrug resistance ABCB and ABCG transporters: Participation in a chemoimmunity defense system. *Physiological Reviews* vol. 86 1179–1236 (2006).

339. Desbats, M. A., Giacomini, I., Prayer-Galetti, T. & Montopoli, M. Metabolic Plasticity in Chemotherapy Resistance. *Frontiers in Oncology* vol. 10 281 (2020).

340. Dhimolea, E. *et al.* An Embryonic Diapause-like Adaptation with Suppressed Myc Activity Enables Tumor Treatment Persistence. *Cancer Cell* **39**, 240-256.e11 (2021).

341. Farge, T. *et al.* Chemotherapy Resistant Human Acute Myeloid Leukemia Cells are Not Enriched for Leukemic Stem Cells but Require Oxidative Metabolism. *Cancer Discov.* **7**, 716 (2017).

342. Denise, C. *et al. 5-Fluorouracil resistant colon cancer cells are addicted to OXPHOS to survive and enhance stem-like traits*. *Oncotarget* vol. 6 www.impactjournals.com/oncotarget (2015).

343. Lee, G. Y. *et al.* Stochastic acquisition of a stem cell-like state and drug tolerance in leukemia cells stressed by radiation. *Int. J. Hematol.* **93**, 27–35 (2011).

344. Auffinger, B. *et al.* Conversion of differentiated cancer cells into cancer stem-like cells in a glioblastoma model after primary chemotherapy. *Cell Death Differ.* **21**, 1119–1131 (2014).

345. Skowron, M. A. *et al.* Phenotype plasticity rather than repopulation from CD90/CK14+ cancer stem cells leads to cisplatin resistance of urothelial carcinoma cell lines. *J. Exp. Clin. Cancer Res.* **34**, (2015).

346. Nakazawa, N. *et al.* Thyroid hormone activated upper gastrointestinal motility without mediating gastrointestinal hormones in conscious dogs. *Sci. Reports 2021 111* **11**, 1–10 (2021).

347. Hays, M. T. Thyroid hormone and the gut. *Endocr. Res.* **14**, 203–224 (1988).

348. Fendler, A. *et al.* Inhibiting WNT and NOTCH in renal cancer stem cells and the implications for human patients. *Nat. Commun.* **11**, 1–16 (2020).

349. Huang, S. M. A. *et al.* Tankyrase inhibition stabilizes axin and antagonizes Wnt signalling. *Nature* **461**, 614–620 (2009).

350. Ying, Q. L. *et al.* The ground state of embryonic stem cell self-renewal. *Nature* **453**, 519–523 (2008).

351. Cancer Genome Atlas Network *et al.* Comprehensive molecular characterization of human colon and rectal cancer. *Nature* **487**, 330–337 (2012).

352. Barat, S. *et al.* Gamma-secretase inhibitor IX (GSI) impairs concomitant activation of notch and wnt-beta-catenin pathways in CD441 gastric cancer stem cells. *Stem Cells Transl. Med.* **6**, 819–829 (2017).

353. Borggrefe, T. *et al.* The Notch intracellular domain integrates signals from Wnt, Hedgehog, TGFβ/BMP and hypoxia pathways. *Biochim. Biophys. Acta - Mol. Cell Res.* **1863**, 303–313 (2016).

354. Krishnamurthy, N. & Kurzrock, R. Targeting the Wnt/beta-catenin pathway in cancer: Update on effectors and inhibitors. *Cancer Treat. Rev.* **62**, 50–60 (2018).

355. Berg, K. C. G. *et al.* Multi-omics of 34 colorectal cancer cell lines - a resource for biomedical studies. *Mol. Cancer* **16**, (2017).

356. Ahmed, D. *et al.* Epigenetic and genetic features of 24 colon cancer cell lines.

Oncogenesis **2**, e71 (2013).

357. Illouz, F., Braun, D., Briet, C., Schweizer, U. & Rodien, P. Endocrine side-effects of anti-cancer drugs: Thyroid effects of tyrosine kinase inhibitors. *European Journal of Endocrinology* vol. 171 R91–R99 (2014).

358. Illouz, F., Laboureau-Soares, S., Dubois, S., Rohmer, V. & Rodien, P. Tyrosine kinase inhibitors and modifications of thyroid function tests: A review. *Eur. J. Endocrinol.* **160**, 331–336 (2009).

359. Emmink, B. L. *et al.* Differentiated human colorectal cancer cells protect tumor-initiating cells from irinotecan. *Gastroenterology* **141**, 269–278 (2011).

360. Ochsner, S. A. & McKenna, N. J. No Dataset Left Behind: Mechanistic Insights into Thyroid Receptor Signaling Through Transcriptomic Consensome Meta-Analysis. *Thyroid* **30**, 621 (2020).

361. Timsit, Y. E. & Negishi, M. CAR and PXR: The Xenobiotic-Sensing Receptors. *Steroids* **72**, 231 (2007).

362. Maglich, J. M. *et al.* The nuclear receptor CAR is a regulator of thyroid hormone metabolism during caloric restriction. *J. Biol. Chem.* **279**, 19832–19838 (2004).

363. Tien, E. S., Matsui, K., Moore, R. & Negishi, M. The nuclear receptor constitutively active/androstane receptor regulates type 1 deiodinase and thyroid hormone activity in the regenerating mouse liver. *J. Pharmacol. Exp. Ther.* **320**, 307–313 (2007).

364. Basseville, A. *et al.* Irinotecan induces steroid and xenobiotic receptor (SXR) signaling to detoxification pathway in colon cancer cells. *Mol. Cancer* **10**, 1–12 (2011).

365. Allain, E. P., Rouleau, M., Lévesque, E. & Guillemette, C. Emerging roles for UDP-glucuronosyltransferases in drug resistance and cancer progression. *British Journal of Cancer* vol. 122 1277–1287 (2020).

366. Wei, J., Ye, X. & Liu, T. Toxicity magnification of irinotecan's toxicity by levothyroxine through inhibition of sn-38 glucuronidation. *Lat. Am. J. Pharm.* **33**, 1385–1388 (2014).

367. Gilbert, D. C., Chalmers, A. J. & El-Khamisy, S. F. Topoisomerase i inhibition in colorectal cancer: Biomarkers and therapeutic targets. *British Journal of Cancer* vol. 106 18–24 (2012).

368. Ohkuma, R. *et al.* High expression of olfactomedin-4 is correlated with chemoresistance and poor prognosis in pancreatic cancer. *PLoS One* **15**, (2020).

369. Bray, S. J. Notch signalling in context. *Nature Reviews Molecular Cell Biology* vol. 17 722–735 (2016).

370. Walther, A. *et al.* Genetic prognostic and predictive markers in colorectal cancer. *Nature Reviews Cancer* vol. 9 489–499 (2009).

371. Salvatore, D. Deiodinases and stem cells: an intimate relationship. *Journal of Endocrinological Investigation* vol. 41 59–66 (2018).

Annexe

Participation in an article

Murine intestinal stem cells are highly sensitive to modulation of the T3/TRα1 -dependent pathway

Matthias Godart [1], Carla Frau[1], Diana Farhat [1], *, **Maria Virginia Giolito [1],** *, Catherine Jamard[1], Clementine Le Nevé [1], Jean-Noel Freund[2], Luiz O. Penalva [3], Maria Sirakov[4] and Michelina Plateroti [1,] *,

1 Centre de Recherche en Cancé rologie de Lyon, INSERM U1052, CNRS UMR5286, Université de Lyon, Université Lyon 1, Centre Lé on Bérard, Département de la recherche, 69000 Lyon, France. 2 Université de Strasbourg, Inserm, IRFAC/UMR-S1113, FMTS, 67200 Strasbourg, France. 3 Children's Cancer Research Institute, University of Texas Health Science Center at San Antonio, San Antonio, TX 78229, USA. 4 Department of Biology and Evolution of Marine Organisms, Stazione Zoologica Anton Dohrn, Villa Comunale, 80121 Napoli, Italy. *Present address: Université de Strasbourg, Inserm, IRFAC/UMR-S1113, FMTS, 67200 Strasbourg, France. ‡Author for correspondence (michelina.plateroti@univ-lyon1.fr)

During my thesis, I had the opportunity to contribute to another project related to impact of the thyroid hormones (THs) and TRα1 on the murine intestinal stem cells. As we extensively view over the introduction of this thesis, the thyroid hormone T3 and its nuclear receptor TRα1 control gut development and homeostasis through the modulation of intestinal crypt cell proliferation. Despite increasing data, in-depth analysis of their specific action on intestinal stem cells is lacking. This project aimed then to study the control of intestinal stem cells dependent on THs and TRs in a physiological context using *in vivo* models, *ex vivo* organoids and molecular approaches led to the paper's publication below. Using ex vivo 3D organoid cultures and molecular techniques, we observed that short-term treatment with T3 induced a response linked to several T3 metabolising enzymes and transporters and a complex stem cell and progenitors gene signature. Moreover, when organoids were derived from mice carrying a specific TRα1 loss-of-function (either inducible or constitutive), they presented a low *ex vivo* development and an impaired stem cell activity. *In vivo* experiment where animals received a T3 treatment confirmed the positive action of the hormone on crypt cell proliferation and its action on the intestinal stem cells by modulating their number and the expression of their specific markers and the commitment of progenitors into lineage-specific differentiation.

© 2021. Published by The Company of Biologists Ltd | Development (2021) 148, dev194357. doi:10.1242/dev.194357

STEM CELLS AND REGENERATION

RESEARCH ARTICLE

Murine intestinal stem cells are highly sensitive to modulation of the T3/TRα1-dependent pathway

Matthias Godart[1], Carla Frau[1], Diana Farhat[1,*], Maria Virginia Giolito[1,*], Catherine Jamard[1], Clementine Le Nevé[1], Jean-Noel Freund[2], Luiz O. Penalva[3], Maria Sirakov[4] and Michelina Plateroti[1,*,‡]

ABSTRACT

The thyroid hormone T3 and its nuclear receptor TRα1 control gut development and homeostasis through the modulation of intestinal crypt cell proliferation. Despite increasing data, in-depth analysis on their specific action on intestinal stem cells is lacking. By using *ex vivo* 3D organoid cultures and molecular approaches, we observed early responses to T3 involving the T3-metabolizing enzyme Dio1 and the transporter Mct10, accompanied by a complex response of stem cell- and progenitor-enriched genes. Interestingly, specific TRα1 loss-of-function (inducible or constitutive) was responsible for low *ex vivo* organoid development and impaired stem cell activity. T3 treatment of animals *in vivo* not only confirmed the positive action of this hormone on crypt cell proliferation but also demonstrated its key action in modulating the number of stem cells, the expression of their specific markers and the commitment of progenitors into lineage-specific differentiation. In conclusion, T3 treatment or TRα1 modulation has a rapid and strong effect on intestinal stem cells, broadening our perspectives in the study of T3/TRα1-dependent signaling in these cells.

KEY WORDS: Intestinal stem cells, Organoids, Thyroid hormone, Thyroid hormone nuclear receptor

INTRODUCTION

The intestinal epithelium is structurally and functionally organized in a monostratified cell layer that, along a vertical axis, defines the crypts of Lieberkühn and the villi (van der Flier and Clevers, 2009). At the bottom of the crypts are self-renewing multipotent stem cells (SCs) and their rapidly amplifying daughter cells (Barker, 2014; Umar, 2010). Progenitor cells differentiate during their migration to the apex of villi and acquire their differentiated properties, becoming secretory and absorptive cells (Noah et al., 2011). This regulation is tightly controlled, given that the entire intestinal epithelium is renewed every 4-5 days in mammals (van der Flier and Clevers, 2009). The balance between SC self-renewal, progenitor proliferation and differentiation commitment in the crypts depends on the cross-regulation of several signaling pathways including Wnt, Hedgehog, Notch, BMP and thyroid hormones (Frau et al., 2017; Spit et al., 2018). In particular, Wnt and Notch activities are necessary for the maintenance of stem identity, and their dysregulation is a key determinant of cell differentiation engagement (Tian et al., 2015; van Es et al., 2005). It is worth noting that a high plasticity exists in the intestinal crypts and, in fact, different cell populations have been described, including the active SCs and cells with a potential to revert into an SC-like phenotype such as early progenitors or quiescent/slow cycling cells, also called reserve SCs (Gehart and Clevers, 2019; Li and Clevers, 2010). Active SCs expressing Lgr5 have been extensively studied and were identified as the cells responsible for continuous epithelial renewal (Barker et al., 2007), whereas the other SC-like populations including reserve SCs play a role in tissue repair upon injury and are mobilized following the loss of active SCs (Barker et al., 2010; Beumer and Clevers, 2016; Murata et al., 2020).

Importantly, we have previously demonstrated the key involvement of thyroid hormone (TH, namely T3 and T4)-induced signaling and TRα1 (T3 nuclear receptor)-induced signaling in intestinal development and homeostasis, through the control of Wnt and Notch activities (Kress et al., 2009, 2010; Sirakov et al., 2015). TRα1 is encoded by the *Thra* gene and it is the only bona fide T3 receptor transcribed by this gene that is able to bind both T3 and DNA (Brent, 2012). From a molecular point of view, thyroid hormone receptors (TRs) modulate the expression of target genes by binding to thyroid hormone response elements (TREs) present in regulatory regions of target genes. Upon T3 binding, TRs undergo a conformational change enabling activation or repression of the transcriptional machinery (Brent, 2012). TRα1 is specifically expressed in intestinal crypt cells (Kress et al., 2009, 2010), in which it acts as a direct activator of Wnt (Kress et al., 2009; Plateroti et al., 2006) and Notch pathways (Sirakov et al., 2015), as well as of cell proliferation (Kress et al., 2009, 2010; Uchuya-Castillo et al., 2018). These data are consistent with the phenotype described in TRα-knockout animals or in TRα1-overexpressing mice (Kress et al., 2009, 2010; Plateroti et al., 2001, 2006). The TRβ1 receptor, encoded by the *Thrb* gene, presents an expression profile restricted to the differentiated epithelial cells of the villi (Sirakov et al., 2014) and no overt function for this protein has been described in the intestine (Plateroti et al., 1999).

Even though many studies have described the major involvement of THs in intestinal postnatal development during amphibian metamorphosis and in SC emergence (Frau et al., 2017; Ishizuya-Oka et al., 2009; Shi et al., 2011), specific investigations in mammals are lacking. In our study, we took advantage of a collection of TRα-mutated models as well as *Lgr5*-EGFP-IRES-CreERT2 mice (Barker et al., 2007) to specifically analyze the SC compartment and its response to T3-dependent signaling *in vivo* and in *ex vivo* 3D organoids. Cellular and molecular analyses enabled us to establish a specific action of T3 on intestinal SCs and the pivotal role of TRα1 in this context.

[1]Centre de Recherche en Cancérologie de Lyon, INSERM U1052, CNRS UMR5286, Université de Lyon, Université Lyon 1, Centre Léon Bérard, Département de la recherche, 69000 Lyon, France. [2]Université de Strasbourg, Inserm, IRFAC/UMR-S1113, FMTS, 67200 Strasbourg, France. [3]Children's Cancer Research Institute, University of Texas Health Science Center at San Antonio, San Antonio, TX 78229, USA. [4]Department of Biology and Evolution of Marine Organisms, Stazione Zoologica Anton Dohrn, Villa Comunale, 80121 Napoli, Italy. *Present address: Université de Strasbourg, Inserm, IRFAC/UMR-S1113, FMTS, 67200 Strasbourg, France.

‡Author for correspondence (michelina.plateroti@univ-lyon1.fr)

M.V.G., 0000-0002-4888-7857; M.P., 0000-0003-0644-8837

Handling Editor: Gordon Keller
Received 22 June 2020; Accepted 8 March 2021

Development (2021) 148, dev194357. doi:10.1242/dev.194357

RESULTS

Molecular action of T3 on *ex vivo* 3D organoids

Previous studies have underlined the importance of T3 on intestinal proliferation and regulation of key signaling pathways via its nuclear receptor TRα1 both *in vivo* and in 2D primary cultures (Kress et al., 2009; Plateroti et al., 2006; Sirakov et al., 2015). We recently started employing in our research 3D primary intestinal epithelium organoid cultures, as they constitute an exquisite cellular *ex vivo* model to study SCs in the gut (Sato et al., 2009). We took advantage of this model, tested the response of organoids to 10^{-7} M T3-containing medium, which appeared to be the appropriated concentration for our studies (Fig. S1) and performed a kinetic analysis of T3 treatment over 24 h (Fig. 1). Although we did not notice any difference from a morphological point of view (Fig. 1A), we observed a very early response in the expression of *Dio1* and *Mct10* (also known as *Slc16a10*) mRNAs, a T3-metabolic enzyme and a TH transporter, respectively (Bianco and da Conceição, 2018; Groeneweg et al., 2017), which displayed significant upregulation in T3-treated organoids following 3 h of treatment (Fig. 1B). The T3-direct target gene *Jag1* was also upregulated upon T3 treatment (Fig. 1B), further confirming the efficacy of the treatment. Cyclin D1 (*Ccnd1*) was also upregulated after several hours of T3-treatment and remained significantly upregulated until the end of the experimental time-course (Fig. 1B), suggesting a positive regulation of cell proliferation. To verify this assumption, we performed EdU incorporation analysis and revealed proliferating cells by EdU labeling after 10 h and 24 h of T3 treatment. Although there was only a slight difference between control and T3 treatment at 10 h, at 24 h some organoids treated with T3 displayed an increased size and longer buddings where Edu-related proliferation was specifically restricted (Fig. 1C). Surprisingly, when we focused on the expression of SC markers we observed a complex scenario (Fig. 1B) with classical markers of active SCs such as *Lgr5*, *Olfm4* and *Ascl2* mRNA being significantly decreased in T3-treated organoids at 24 h. In parallel, markers considered to characterize facultative SCs, namely *Msi1*, *mTert* (*Tert*) and *Hopx* mRNAs were marginally or not affected (Fig. 1B). Of note, T3 treatment did not affect the expression of SC genes, proliferation-related markers or EdU labeling in $TR\alpha^{0/0}$ organoid cultures. *Dio1* and *Mct10* mRNAs were upregulated by T3 at later time points, possibly through TRβ1 (Amma et al., 2001) (Fig. S2).

Because of the intriguing results on SC markers, we then decided to perform a global analysis of RNA-seq on organoids maintained in control conditions or treated with T3 for 17 h, a time-point at which morphology remains unaffected but the molecular response to the hormone is clearly visible. We used statistical approaches to identify significant differentially expressed genes (DEGs) and retained only the genes presenting a $\log_2$ fold change>±0.5 and a *P*-value<0.05 (Table S1). The hierarchical clustering clearly grouped the genes according to culture conditions (Fig. 2A). Gene ontology (GO) analysis identified stress response and metabolism among the most relevant enriched biological functions (Fig. 2B,D). Molecular pathways that were significantly represented within the DEGs included retinoic acid signaling and xenobiotics (downregulated) as well as Toll-like receptor cascade and various transporter types (upregulated) (Fig. 2C,E). We also performed gene set enrichment analysis (GSEA) to compare our DEGs with genes preferentially expressed in SCs or in progenitor cells (Fig. 3A; Tables S2 and S3). The upregulated genes of our analysis were more significantly associated with a progenitor-type molecular signature (Fig. 3B; Fig. S3A; Tables S2 and S3), whereas the downregulated genes were more significantly associated with an SC molecular signature (Fig. 3C; Fig. S3B; Table S2). Bioinformatics analysis also revealed a network of functionally linked downregulated genes encoding SC markers and/or linked to SC biology (Fig. 3D). It is worth noting, however, that the molecular repertoire induced or repressed by T3 in organoids appears to be complex. Indeed, among upregulated genes associated with the SC signature, we observed the presence of the *Clu* (clusterin) gene (Fig. 3E; Table S2), which has recently been associated with a population of slow cycling/quiescent/revival intestinal SCs (Ayyaz et al., 2019). This suggests that an action on active SCs might be counterbalanced by a possible induction of a new population of SCs. In addition, this category of genes includes signaling molecules (*Tlr2*), genes involved in apoptosis (*Casp12*) or in molecule/ion transport (*Slc14a1*, *Slco3a1* and *Kcne3*). Among upregulated genes associated with a progenitor signature, we denoted proteins involved in retinol (*Rbp7*), TGFβ/BMP (*Tgfbi*) or Wnt (*Epha2*) signaling. Finally, we compared our dataset to DEGs described in laser microdissected crypts from pre-weaned TH-treated or untreated mice (Kress et al., 2009) (Table S4). Interestingly, a strong overlap of the two lists of DEGs was unveiled, which included several metabolism-linked genes, the proto-oncogene *cFos* (*Fos*), *Klf9*, a well-known direct T3-target gene (Denver and Williamson, 2009), and signaling molecules. Furthermore, three genes were inversely regulated by T3 in organoids in comparison with crypts, namely *Fgf1*, *Gcnt2* and *Notch1*, which are involved in cell signaling, cell fate and regulation of mucin expression, respectively (Chen et al., 2009; Danopoulos et al., 2017; Siebel and Lendahl, 2017).

This molecular analysis and comparison with previous studies indicate that 17 h of T3 treatment induces a 'thyroid shock' in organoids through a complex response that includes stress response, metabolic challenge and alteration of cell signaling. In addition, we identified a molecular signature of early T3-induced events, some of which displayed a clear overlap with previously described genes in intestinal crypts *in vivo*.

Growth characteristics of organoids upon T3 treatment

The previous results compelled us to investigate the effect of T3 on the kinetics of 3D organoid development and structuration (i.e. increasing size and number of buds) over time. We used *Lgr5*-EGFP-IRES-Cre^{ERT2} (hereafter designated as *Lgr5*-EGFP) mice in order to highlight and visualize Lgr5-expressing SCs (Barker et al., 2007). Freshly prepared crypts were cultured in control and 10^{-7} M T3-containing medium. As expected, we observed an increase in organoids displaying an augmented structural complexity in control condition, as illustrated by the growing size and number of buds appearing over time and a concomitant decrease in simple structured organoids (Fig. 4A,B; Fig. S4A). In T3-treated organoids, a multi-phasic response took place. First, we observed a decrease in the rate of spheres at day (D) 1 and D2 in parallel with the induction of complex structure formation (1-2 buds or more than 2 buds) until D3. This was followed by an almost stable percentage of less-complex organoids (1-2 buds) or their loss (more than 2 buds) after D3 (Fig. 4B; Fig. S4A). When we further analyzed the effects induced by T3 on organoids, we observed a change of morphology clearly visible from D4 onwards, with organoids displaying a larger central body and a decreased number of buds (Fig. 4A). Quantification of these parameters confirmed a significant increase in the central body in T3-treated compared with untreated organoids from D2 onwards. The number of buds significantly increased at D1, was unchanged at D2 but decreased at D3 and D4, whereas the total surface of the organoids showed no significant difference from control and T3 conditions at all time points analyzed (Fig. S4B). The growth of the organoids was

Development (2021) 148, dev194357. doi:10.1242/dev.194357

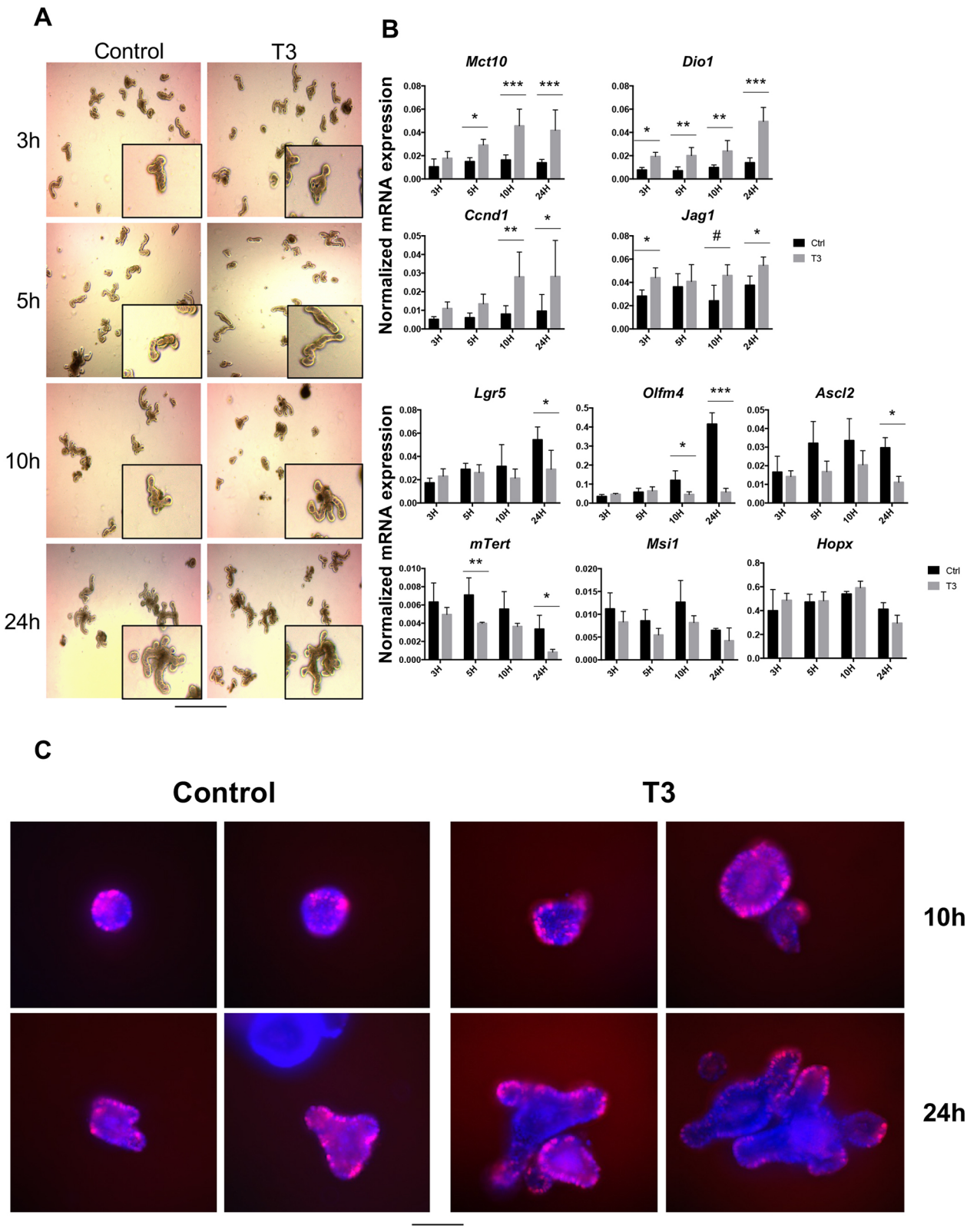

Fig. 1. Short-term response of organoids to T3. (A) Replicated wild-type organoids were cultured over 24 h in the absence (Control) or presence of 10^{-7} M T3, as indicated. The pictures were taken at different time points and are representative of three independent experiments, each conducted on six replicates. Insets show high magnification area of main image. (B) RT-qPCR experiments were performed at different time points, as indicated, to analyze the mRNA expression of the TH metabolizing enzyme *Dio1* and transporter *Mct10*; *Ccnd1* was used as a proliferative marker and *Jag1* as a direct T3-target gene. In addition, stem cell markers *Lgr5*, *Olfm4*, *Ascl2*, *mTert*, *Msi1* and *Hopx* were also analyzed. Histograms represent mean±s.d., n=4, after normalization with *Ppib*. *P<0.05, **P<0.01, ***P<0.001 compared with the respective control conditions. # indicates marginally significant (P=0.071) compared with the respective control conditions. (C) Proliferation analysis by EdU incorporation on organoids in the control condition or treated with T3 for 10 h or 24 h; in both cases EdU was added in the culture medium 2 h before ending the cultures. Images show merged EdU labeling (red) and nuclear staining (blue). Scale bars: 30 µm (A); 15 µm (A, insets); 7 µm (C).

Development (2021) 148, dev194357. doi:10.1242/dev.194357

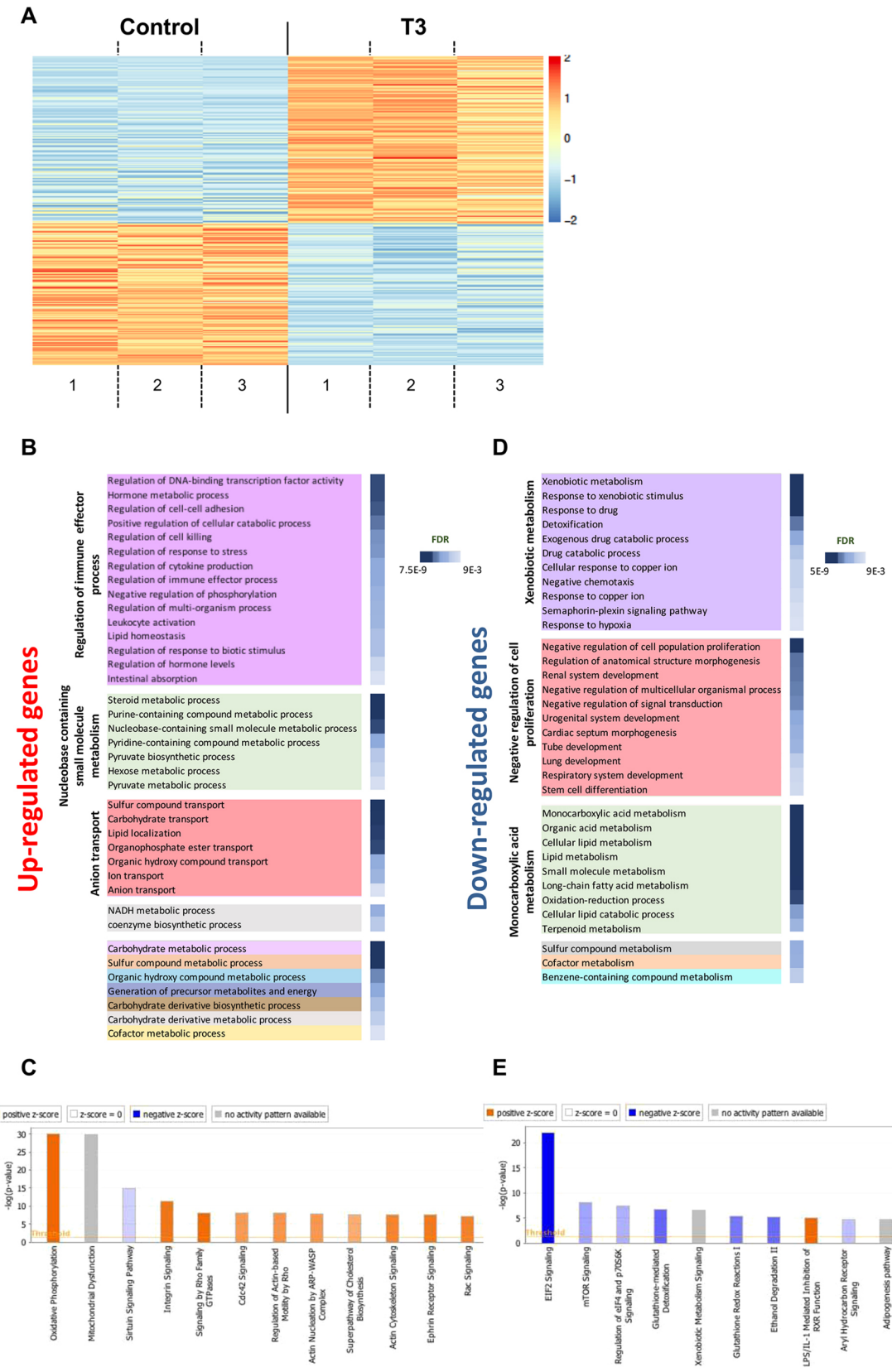

Fig. 2. Comparative transcription profile analysis of T3-treated organoids by RNA-seq. (A) Hierarchical clustering after RNA-seq enabled observation of the links between the organoid cultures in T3 or control conditions and to visualization of differentially expressed genes. In this clustering, the transcripts were grouped in two dendrograms, each of which represents a condition. Each line is a gene and each column is an RNA sample. Expression signal intensities are shown in red and blue, indicating high and low expression levels, respectively. (B,D) Gene Ontology (GO) terms enriched among genes showing increased (B) or decreased (D) expression upon T3 treatment. GO enriched terms are summarized using REViGO (Supek et al., 2011). (C,E) Ingenuity Pathway Analysis: bar charts show the most significant canonical pathways associated with the differentially-expressed increased (C) or decreased (E) genes.

Development (2021) 148, dev194357. doi:10.1242/dev.194357

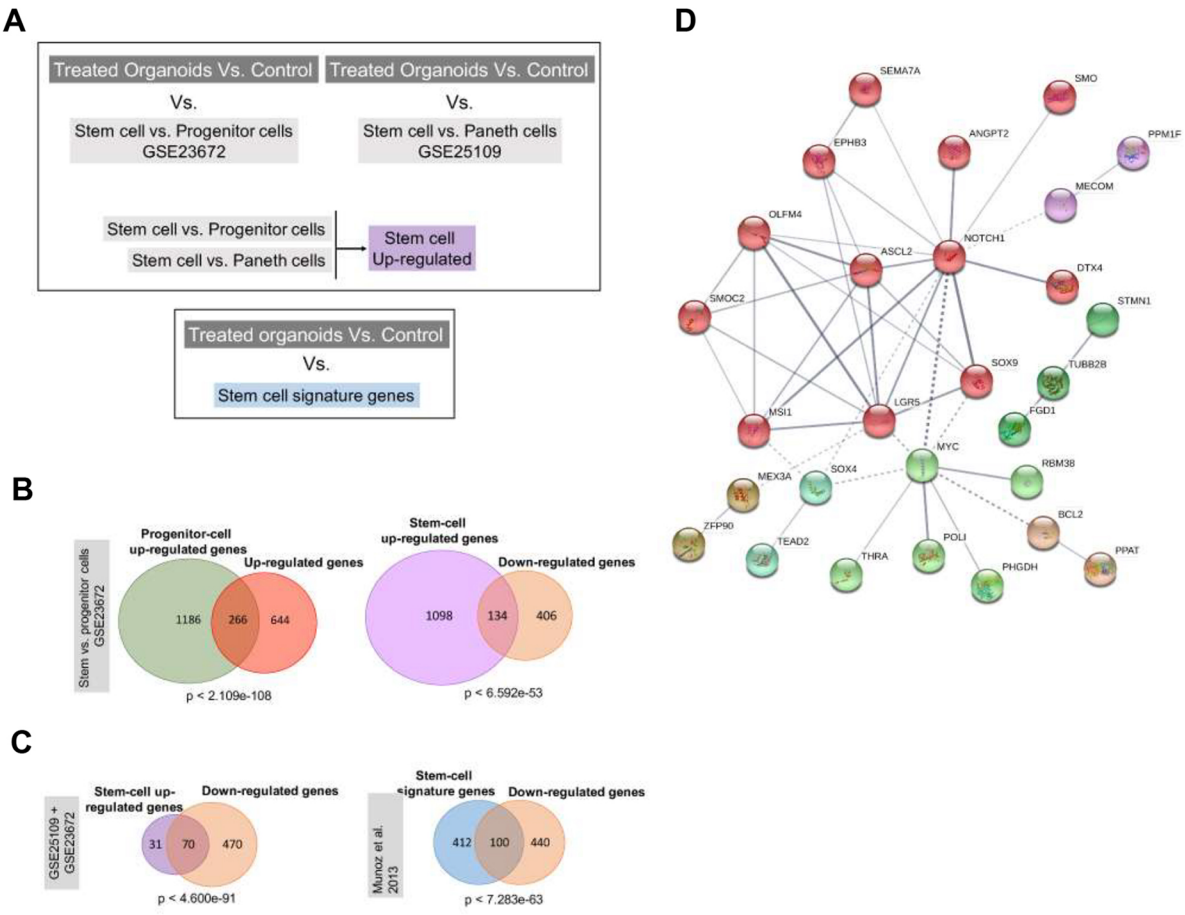

E

SC_UP	SC_Down	Prog_UP	Prog_Down
Clu	Aqp1	Rbp7	Reg3a
Greb1	Aqp4	Rbp2	Creb3l3
Wwtr1	Ces1d	Cx3cl1	Cyp2d26
Slc14a1	Hmgcs2	Mmp7	Aldh1a1
Slco3a1	Ephb3	Klf6	Adh4
Kcne3	Sfrp5	Abcg5	Adh1
Tlr2	Sema7a	Tgfbi	Cyp2c29
Tnfsf10	Fgfr4	Cdkn2b	Cyp4b1
Casp12	Lgr5	Epha2	Dll4
Esam	Olfm4	Id3	Abcc3

Fig. 3. Differentially-expressed genes and molecular signatures of intestinal crypt cell populations. (A) Diagram showing the comparison between different datasets to evaluate the changes in expression induced by T3 treatment. (B) Venn diagrams showing the overlaps between our dataset and GSE23672. The upregulated set in our analysis encompasses a large number of genes highly expressed in progenitor cells, whereas the downregulated set is similar to the gene set expressed in stem cells. (C) Venn diagrams showing the comparison between downregulated genes in our dataset and the 'stem cell' signatures. Hypergeometric test was conducted to define the significance of the overlap between groups. *P*-values show significance of overlap based on the number of expressed and altered genes. (D) Network of stem cell-related genes present in the downregulated set. Analysis was performed using String. Each colored cluster is defined by proteins (genes) showing strong functional associations between them. (E) Examples of genes up- or downregulated in our analysis associated with stem cell or progenitor signatures.

Development (2021) 148, dev194357. doi:10.1242/dev.194357

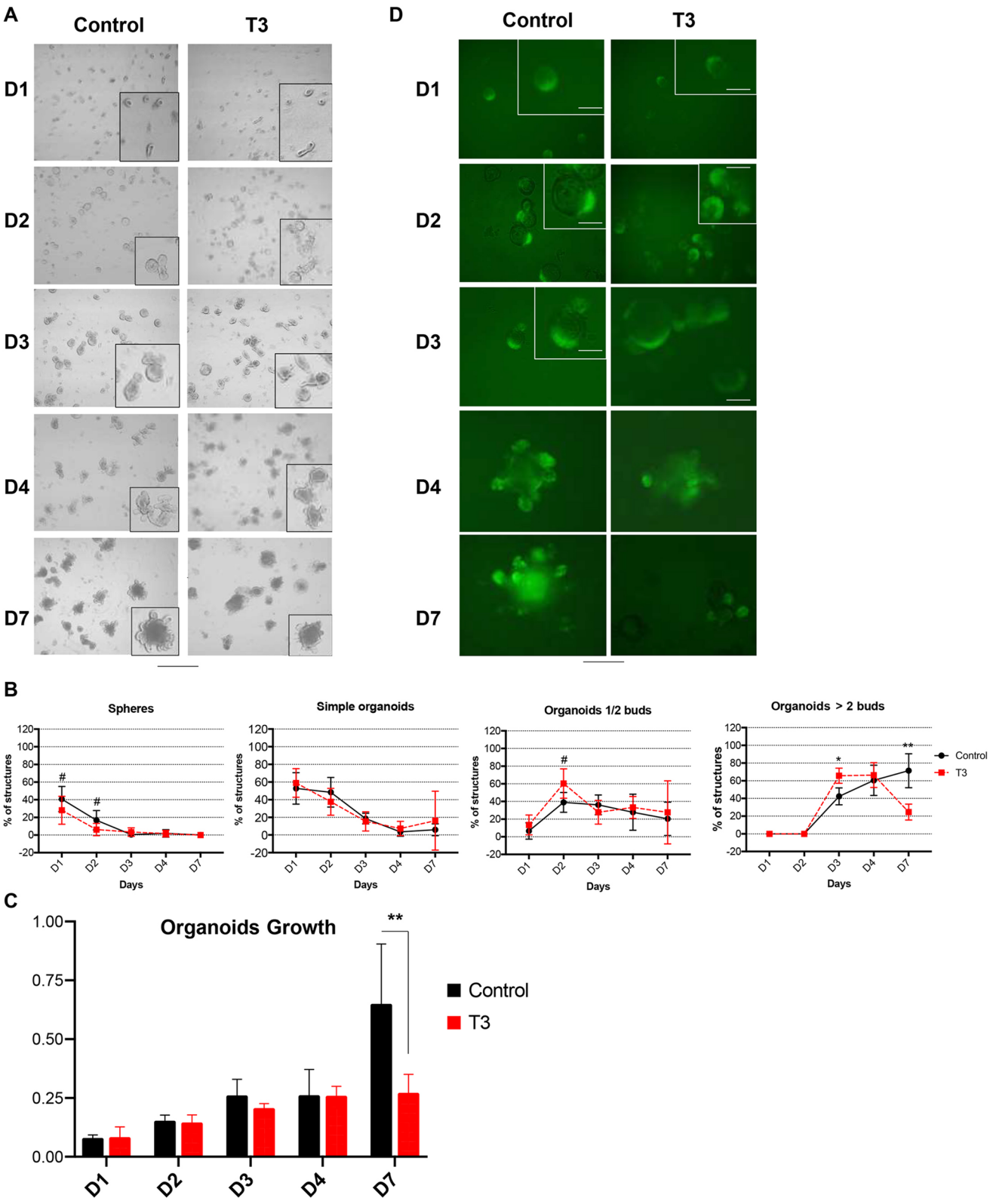

Fig. 4. Analysis of growth properties and features of cultured crypts. (A) Crypts were prepared from *Lgr5*-EGFP intestine and maintained in culture for several days in the absence (Control) or presence of 10^{-7} M T3 as indicated, allowing complex organoid development with increased number of buddings. Pictures were taken under an inverted microscope at the indicated days, and are representative of three/four independent experiments. (B) Graphs show the percentage of spheres, simple organoids, 1-2 bud organoids and more complex organoids (>2 buds) evaluated every day for 1 week. *n*=6. (C) Growth of organoids over time in culture, in control or T3 condition as indicated, analyzed using the WST-1 assay. *n*=12. (D) Live GFP fluorescence analysis of fresh *Lgr5*-EGFP organoids cultured in the presence or absence of T3 at indicated days in culture. Data are mean±s.d. **P*<0.05, ***P*<0.01 compared with the respective control conditions. #, marginally significant (spheres D1, *P*=0.052; spheres D2, *P*= 0.061; organoids 1/2 buds D2, *P*=0.06) compared with the respective control conditions. D, days in culture. Scale bars: 30 µm (A); 15 µm (A, insets); 10 µm (D); 5 µm (D, inset).

Development (2021) 148, dev194357. doi:10.1242/dev.194357

also monitored using the WST-1 Assay Reagent that quantifies cell proliferation and viability. Organoids treated with T3 at different time points showed a profile similar to that of the development of complex organoids, with a decreased growth at D7 compared with the respective untreated condition (Fig. 4C). Live fluorescence microscopy revealed GFP-positive cells from D1 to D7 in both control and T3 conditions (Fig. 4D). It is worth noting that from D1 to D3 the T3-treated organoids displayed more bud-like structures with a high number of GFP-positive cells (Fig. 4D). After a longer treatment time, we detected a clear decrease in both GFP intensity and GFP-positive cells (Fig. 4D, panel D7).

A parallel analysis of cell proliferation and cell death by immunofluorescence (IF) indicated a different patterning of KI67-positive cells at D2 compared with control organoids (Fig. 5A). Indeed, although in controls the proliferating cells were spread across the organoids (central and peripheral parts), in the T3-treated condition organoids presented a more evident zonal organization, with KI67-positive cells located within the emerging buds (Fig. 5A). These qualitative observations were confirmed by quantifying KI67-positive cells within the buds or outside the buds in both conditions (Fig. 5B). At D4, the control organoids had KI67-positive cells within the crypt-like structures, whereas this zone appeared to be reduced in the T3-treated condition (Fig. 5A). Indeed, the number of KI67-positive cells was more abundant in the buds in both conditions but it was significantly decreased in T3-treated organoids (Fig. 5B). Western blot (WB) analysis revealed that the levels of phospho-Histone H3, an indicator of actively cycling cells (Kim et al., 2017; Nielsen et al., 2013), were unchanged at D2 but reduced at D4 (Fig. 5C). Concomitantly, we observed that in the T3 condition, apoptosis increased at both time points as visualized by cleaved-caspase 3-positive cells within the lumen by IF (Fig. 5A) and by WB (Fig. 5C). The analysis of differentiation markers indicated no changes in the number of enterocytes, enteroendocrine and Paneth cells (Fig. 5D), but we saw a significant increase in mucus-producing goblet cells (Fig. 5E). Several markers of TH metabolism, cell proliferation and of SCs were also analyzed at the mRNA level, further supporting the overall phenotype induced by T3 (Fig. S5). Finally, to confirm that the T3 phenotype specifically depended on T3 and not on other hormones/metabolites or integrins (Davis et al., 2011; Hammes and Davis, 2015; Kalyanaraman et al., 2014), we also performed experiments by treating the organoids with T4, 3,3′-T2 (derived from degradation of T3 or T4) and Tetrac (an inhibitor of T3 or T4 binding to integrins). However, only T4 could recapitulate the T3 phenotype (Fig. S6), as expected by the presence and expression pattern of *Dio1* in the organoids and its action in metabolizing T4 to T3 (Bianco and da Conceição, 2018).

Taken together, these data show an advanced appearance of buddings in organoids upon T3 treatment during development *ex vivo*, indicating an accelerated turnover. The accelerated turnover, however, is responsible for a loss of SC and their engagement in secretory differentiation, in particular towards the goblet lineage.

The expression of a dominant negative TRα1 strongly affects organoid growth *ex vivo*

TRα1 has been shown to play a pivotal role in the intestinal crypt pathophysiology (Bao et al., 2019; Sirakov and Plateroti, 2011; Uchuya-Castillo et al., 2018). Using TRα1^{L400R} mice (hereafter designated as TRami), corresponding to a model of TRα1 loss-of-function (Quignodon et al., 2007), we analyzed the effects of inducing the TRα1 mutation on *ex vivo* 3D organoid growth and structuration. TRami animals were crossed with *Lgr5*-EGFP and *Rosa26*/*CAG*-floxed-STOP-tdTomato mice (hereafter named *Rosa*-Tomato) (Madisen et al., 2010) to generate tamoxifen-inducible triple transgenic TRami/*Lgr5*-EGFP/*Rosa*-Tomato animals, in which loss of TRα1 activity and expression of the Tomato fluorescent protein can be specifically induced in *Lgr5*-expressing crypt cells. Tamoxifen or corn oil (negative control) were injected *in vivo* into TRami/*Lgr5*-EGFP/*Rosa*-Tomato triple-transgenic animals and the intestine was recovered to perform crypt cultures and analyze organoid growth over time. The efficacy of the induction of the TRami allele by tamoxifen was validated by PCR on genomic DNA (Fig. S7A,B); no effect of tamoxifen was observed in TRami/Lgr5-WT organoids not expressing the inducible CRE protein (not shown). Live fluorescence microscopy confirmed the presence of double positive Tomato/GFP cells specifically in organoids from tamoxifen-injected mice compared with oil-injected control animals (Fig. S8A). As expected, organoids developed better in the oil/control condition, as evidenced by an increase in the number of organoids displaying several buds, a decrease in simple structured organoids (Fig. 6A,B) and the increased number of buds per organoid over the time in culture (Fig. 6C). Conversely, cultures from tamoxifen-induced TRami mice displayed a strong impairment in complex organoid formation (>2 buds) (Fig. 6A-C). Indeed, in this condition, most organoids remained at the stage of simple organoids or of organoids with 1-2 buds (Fig. 6B) and the number of buds per organoid was significantly decreased (Fig. 6C), strongly reflecting a negative impact of TRami induction on cell proliferation and eventually on SCs. Collectively, the expression of the dominant negative TRα1 specifically in Lgr5-expressing cells definitely demonstrated a key role for this nuclear receptor in intestinal progenitor and SC physiology.

Constitutive lack of TRα but not of TRβ decreases SC activity

Next, we further investigated intestinal SC activity depending on TRα1 expression and decided to use a constitutive knockout model. Indeed, in this model cells do not express TRα1, whereas in inducible models mosaic CRE expression (Barker et al., 2007) or inefficient recombination cannot be ruled out. We initially prepared fresh crypts from wild-type (WT) or TRα$^{0/0}$ animals and followed the kinetics of 3D organoid development and structuration over 7 days in culture (Fig. 7A-C). In WT cultures, we observed an increase in organoids displaying several buds and a concomitant decrease in simple structured organoids over the time-course of the experiment (Fig. 7A-C). TRα$^{0/0}$ crypt cultures showed a delay in development, whereas their growth profile indicated that simple structures were maintained for a longer period, with complex organoids forming more slowly (Fig. 7A-C). We also analyzed the number of buds per organoid at different time-points and observed that TRα$^{0/0}$ organoids presented a significantly lower number of buds at D4 and D7 compared with WT organoids (Fig. 7D). These phenotypes were specifically linked to TRα1, as experiments in TRβ$^{-/-}$ crypt cultures revealed results similar to those of WT cultures (Fig. 7A-D). This observation is not surprising given that *Thra* but not *Thrb* mRNA expression is enriched in SCs (Table S5). Finally, T3-treatment experiments in TRα$^{0/0}$ and TRβ$^{-/-}$ organoids validated the specific involvement of TRα1 (Fig. S9).

To further link the TRα1-dependent phenotype to stemness we then measured colony-forming efficacy, which represents the ability of SCs to self-renew and generate organoids at the single cell level (Sato et al., 2009; Yin et al., 2014). Before conducting colony-forming assays, we cultured WT or TRα$^{0/0}$ organoids for 2 days and then dissociated and recovered the single cells from each genotype. We then seeded 5000 cells per well and cultured organoids over 7 days. At D7 we counted the number of colonies formed in TRα$^{0/0}$

Development (2021) 148, dev194357. doi:10.1242/dev.194357

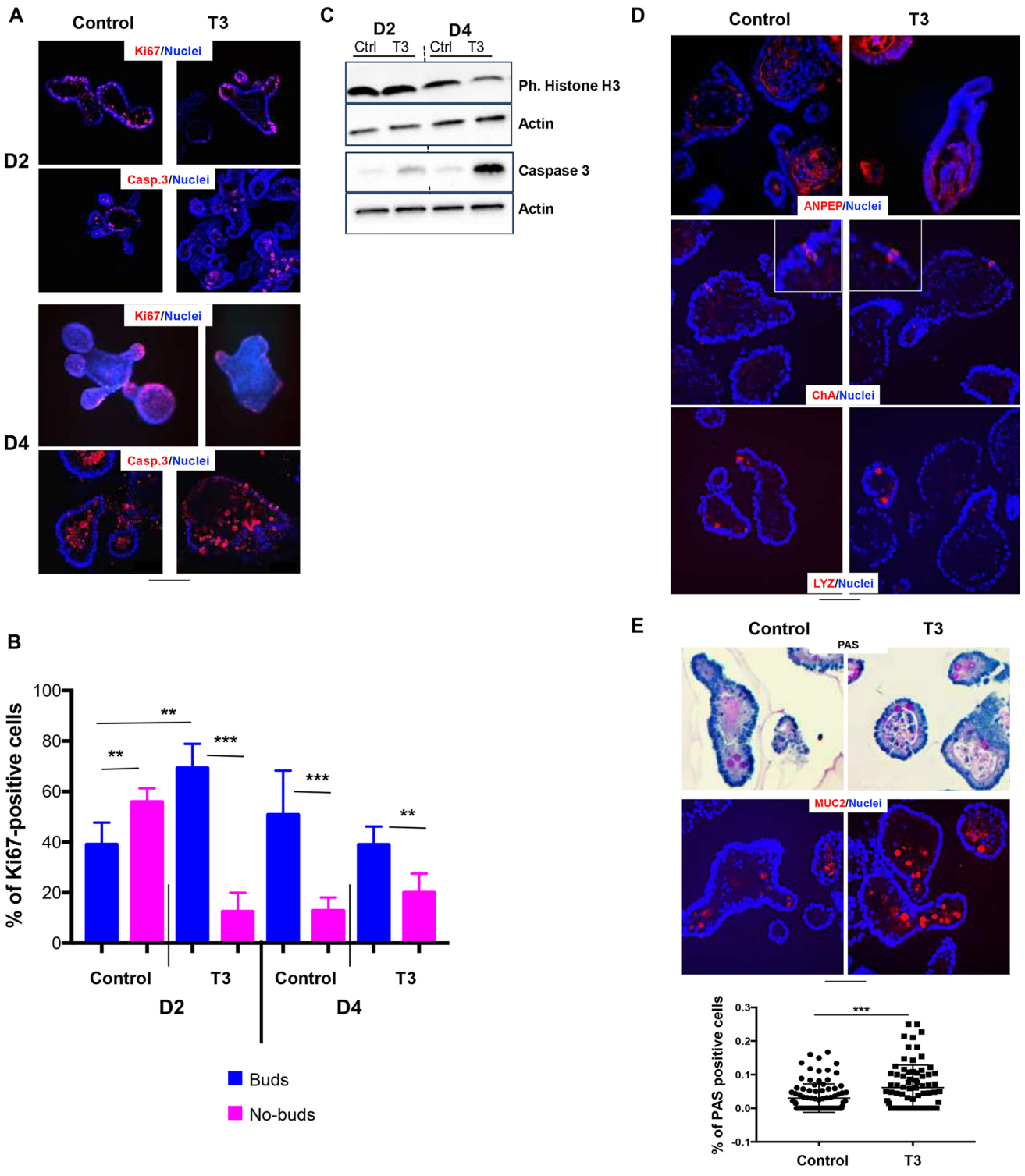

Fig. 5. Accelerated turnover and unbalanced differentiation in T3-treated organoids. (A) Ki67 and cleaved-caspase 3 immunolabeling of proliferating or apoptotic cells in organoids in control or T3 condition at day (D) 2 and D4. Images show merged specific immunolabeling (red) and nuclear staining (blue). Pictures are representative of three independent experiments. (B) Quantification of Ki67-positive cells in portions of organoids with buds or no-buds at D2 and D4 in control and T3-treated conditions, as indicated. (C) Western blot analysis of Histone H3, cleaved-caspase 3 levels in organoids in control or T3 condition at D2 and D4. Actin was used as the loading control. Pictures are representative of two independent experiments. (D) Analysis of differentiation markers in organoid paraffin sections in control or T3-treated conditions, as indicated, at D4. ANPEP (enterocytes), lysozyme (LYZ, Paneth cells) and chromogranin A (ChA, enteroendocrine cells) were analyzed by immunolabeling. The images show merged differentiation marker (red) and nuclear staining (blue). Pictures are representative of three independent experiments. (E) Analysis of mucus-producing goblet cell differentiation in organoids maintained in control or T3 conditions at D4. Upper panel shows mucus-producing cells stained with PAS or by immunolabeling with anti-MUC2 antibodies. Images show merged MUC2 (red) and nuclear staining (blue). Histograms in the lower panel summarize the quantification of PAS-positive cells in organoids depending on the culture condition. Approximately 50 organoids per condition were scored from pictures using the ImageJ software. Data are mean±s.d. ***P*<0.01, ****P*<0.001 compared to indicated conditions. D, days in culture. Scale bars: 20 µm (A); 10 µm (D,E); 5 µm (D, inset).

Development (2021) 148, dev194357. doi:10.1242/dev.194357

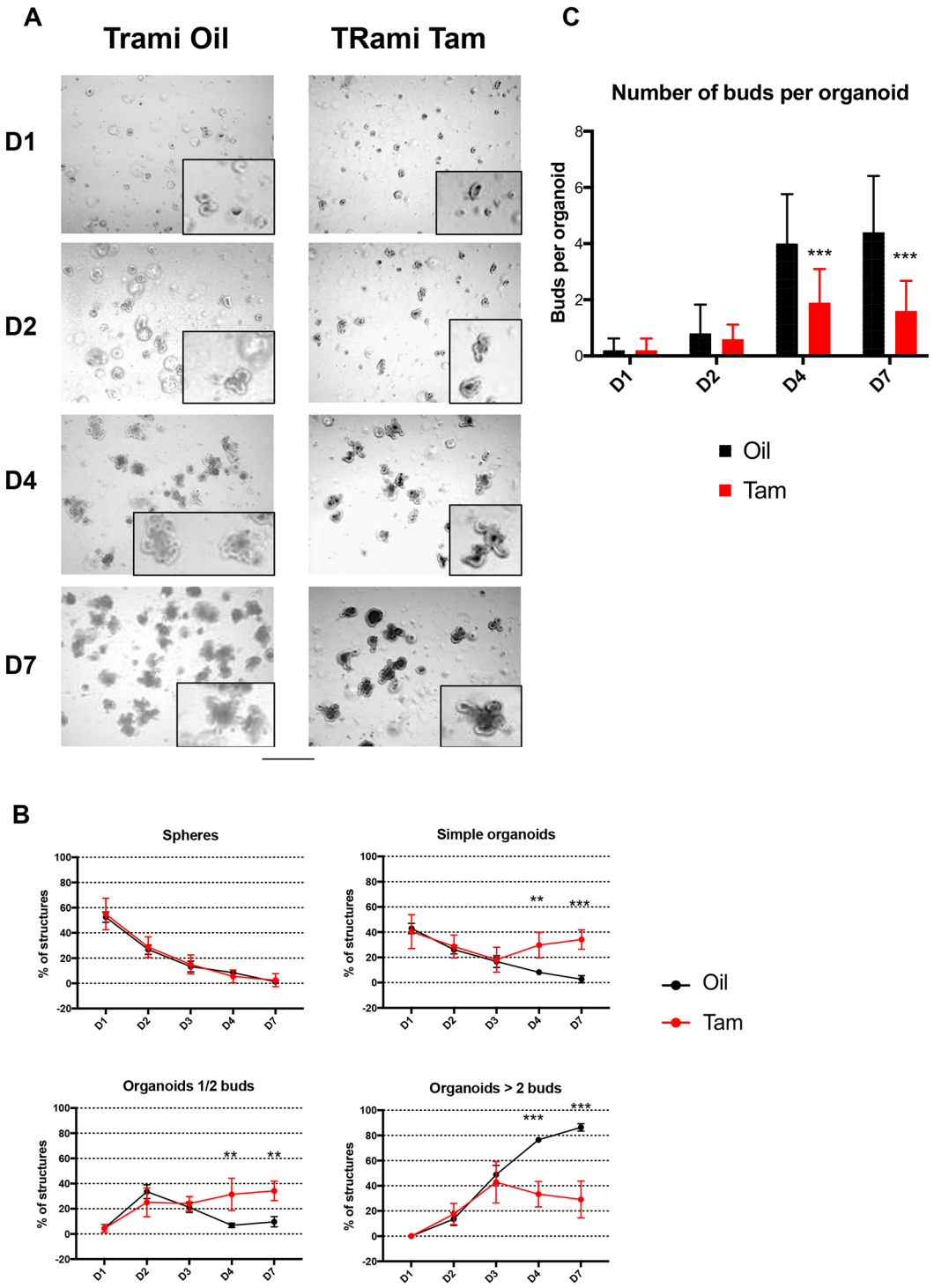

Fig. 6. Inducible dominant negative TRα1 expression has a negative effect on organoid development and structuration. (A) Time-course of fresh crypts isolated from TRami/*Lgr5*-EGFP/*Rosa*-Tomato injected with oil or tamoxifen (Tam) before sacrifice, as indicated. Crypts were cultured and developing structures were observed at day (D) 1, D2, D4 and D7 of culture. Pictures are representative of two independent experiments. The insets focus on representative organoids from each condition. (B) The number of simple structure (spheres) or organoids of increasing complexity (1 or 2 buds, more than 2 buds) were scored under the inverted microscope over 7 days of culture. *n*=6. (C) The number of buds per organoid were scored at different time points in the control and T3 condition. *n*=20. Data are mean±s.d. ***P*<0.01, ****P*<0.001. D, days in culture. Scale bars: 30 µm (A); 15 µm (A, insets).

compared with WT organoid cultures (Fig. 8A,B). As expected from *ex vivo* organoid developmental studies, $TR\alpha^{0/0}$ dissociated cultures had a strongly impaired capacity to generate new organoids, whereas no distinct phenotype was detected in $TR\beta^{-/-}$ colonies compared with WT cultures (Fig. 8A,B).

Impact of T3 on intestinal crypts *in vivo*

After defining the impact of T3 on intestinal SC biology in *ex vivo* organoids, we further characterized the relevance of our observations *in vivo*. For this aim, we treated *Lgr5*-EGFP animals with T3 *in vivo* and recovered the intestine 2 days after treatment. We analyzed the

Development (2021) 148, dev194357. doi:10.1242/dev.194357

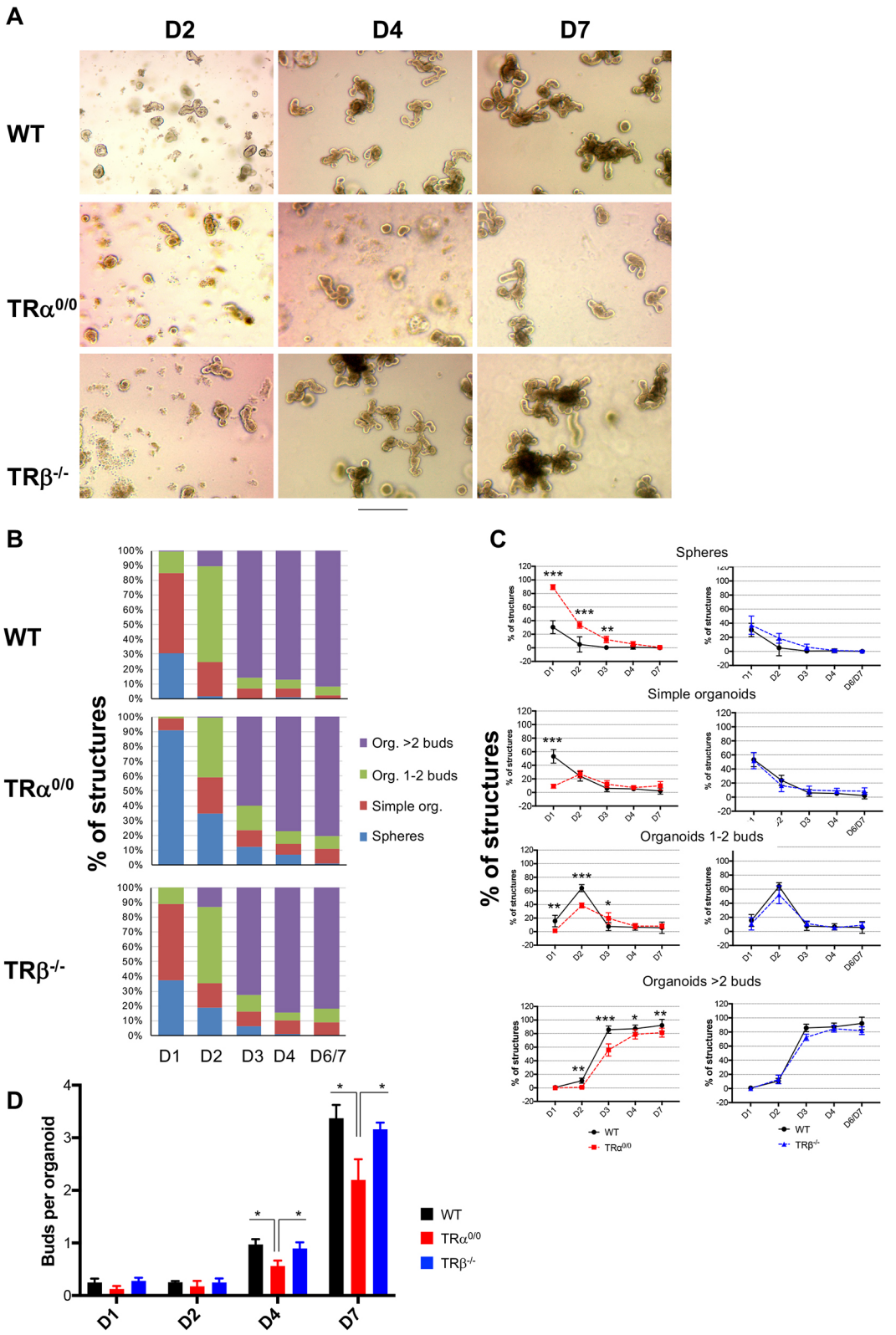

Fig. 7. Specific TRα-dependent action on organoid development. (A) Crypts were prepared from wild-type (WT), TR$\alpha^{0/0}$ and TR$\beta^{-/-}$ intestines and maintained in culture for several days, allowing complex organoid development. Pictures were taken under an inverted microscope at the indicated days, and are representative of three independent experiments. (B,C) Multilayered histograms (B) and graph lines (C) represent the mean±s.d., *n*=6, of each structure counted in the cultures from different genotypes. The number of simple structures (spheres) or organoids of increasing complexity (1 or 2 buds, more than 2 buds) were scored under the inverted microscope during 7 days of culture. **P*<0.05, ***P*<0.01, ****P*<0.001. (D) The number of buddings per organoid was scored at key time points in cultured organoids of different genotypes. Histograms represent mean±s.d., *n*=20. **P*<0.05 compared with WT and TR$\beta^{-/-}$ organoids. D, days in culture. Scale bar: 15 µm.

Development (2021) 148, dev194357. doi:10.1242/dev.194357

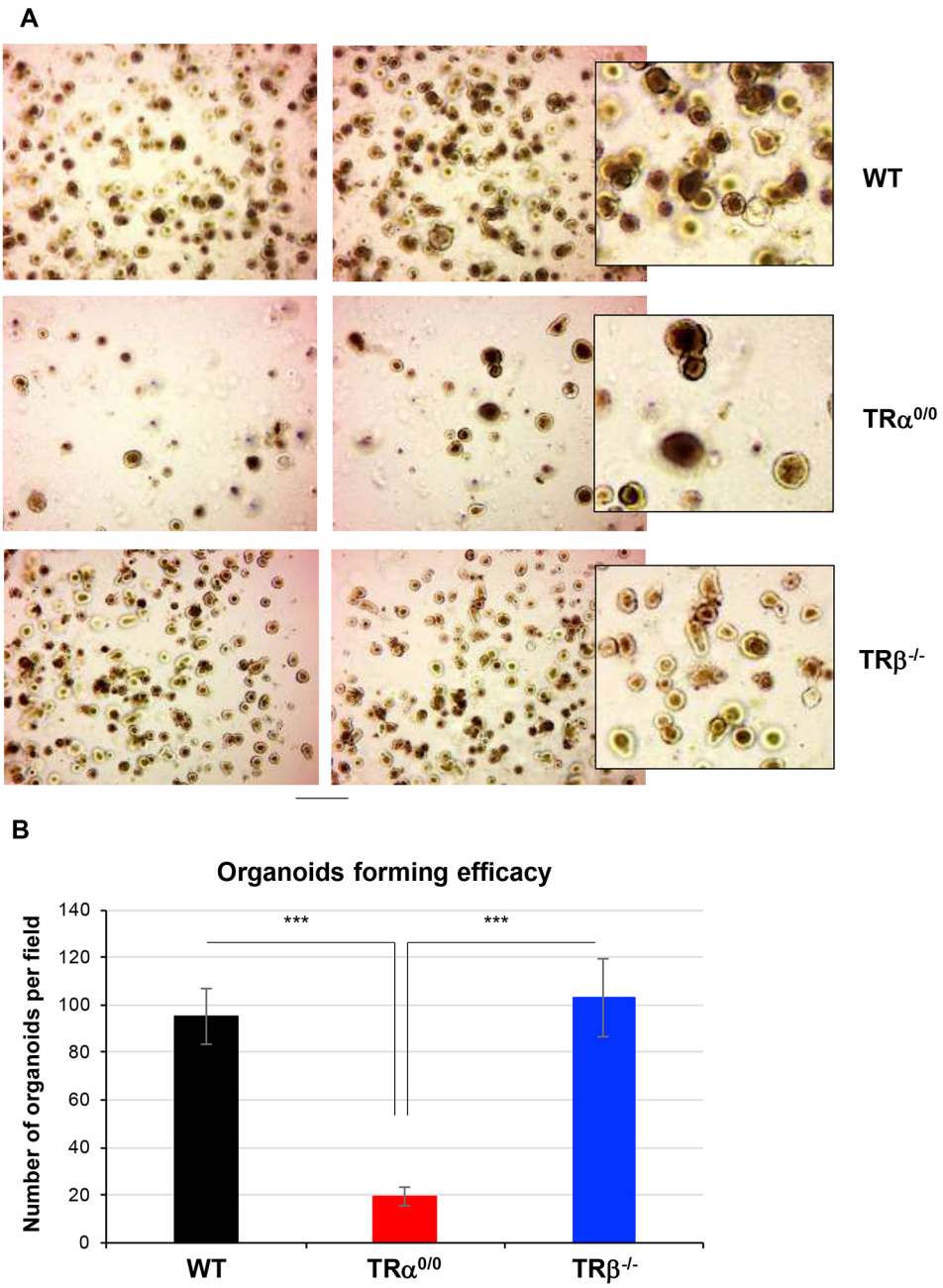

Fig. 8. Lack of TRα1 specifically affects stem cell activity. (A,B) Colony assay was performed on single cells dissociated from organoids and maintained for 2 days in culture. Then 5000 cells prepared from wild-type (WT), $TR\alpha^{0/0}$ or $TR\beta^{-/-}$ organoids were cultured in Matrigel. Pictures in A were taken on day 7. Pictures are representative of two independent experiments each conducted in four replicates. Histograms in B show the number of colonies formed in each condition after 7 days in culture. Data are mean±s.d., n=4. ***P<0.001. $TR\alpha^{0/0}$ compared to WT or $TR\beta^{-/-}$. Scale bar: 15 µm (A); 7 µm (A, insets).

proliferative and differentiation properties of the intestine by IF on sections. As expected from our previous studies (Kress et al., 2009; Plateroti et al., 2006), T3 treatment induced an increase in the number of PCNA-positive proliferating crypt cells (Fig. 9A). The analysis of differentiation markers indicated that T3 injection did not lead to an overt difference between T3-treated and untreated animals regarding enterocytes, enteroendocrine cells or mucus-producing goblet cells (Fig. 9B), whereas Paneth cells were significantly increased in T3-treated intestine (Fig. 9B). We also analyzed the GFP-positive or OLFM4-positive SCs in these same conditions by IF (Fig. 10A) and observed an expansion of the positive domain in the T3-treated condition. This result was reinforced by mRNA expression analysis of SC markers. Indeed, *Lgr5*, *Olfm4*, *Hopx* and *mTert* mRNAs displayed a higher level of expression in the T3 *versus* control condition, even if in the case of *mTert* the statistical significance was marginal (Fig. 10B). In addition, TH metabolism and transport (*Dio1* and *Mct10* mRNA expression) remained unaffected by T3 in animals *in vivo* (Fig. S10). Finally, GFP-positive cells were also analyzed by cytometry, but given the mosaic GFP expression in *Lgr5*-EGFP mice (Barker et al., 2007), the results were highly variable even within the same experimental group. Altogether, our observations in mice suggest a role for T3 in inducing an increase in crypt size and proliferation, as well as an increase in the pool of SCs and of Paneth cells.

DISCUSSION

Despite increasing data on the effect of altered TH levels or TRα1 expression on intestinal development and homeostasis in mammals, most of the knowledge gathered so far concerns intestinal progenitors, whereas specific analyses focusing on SC biology are lacking. Conversely, extensive research has been conducted on the T3-dependent role in inducing adult intestinal structuration and SC

Development (2021) 148, dev194357. doi:10.1242/dev.194357

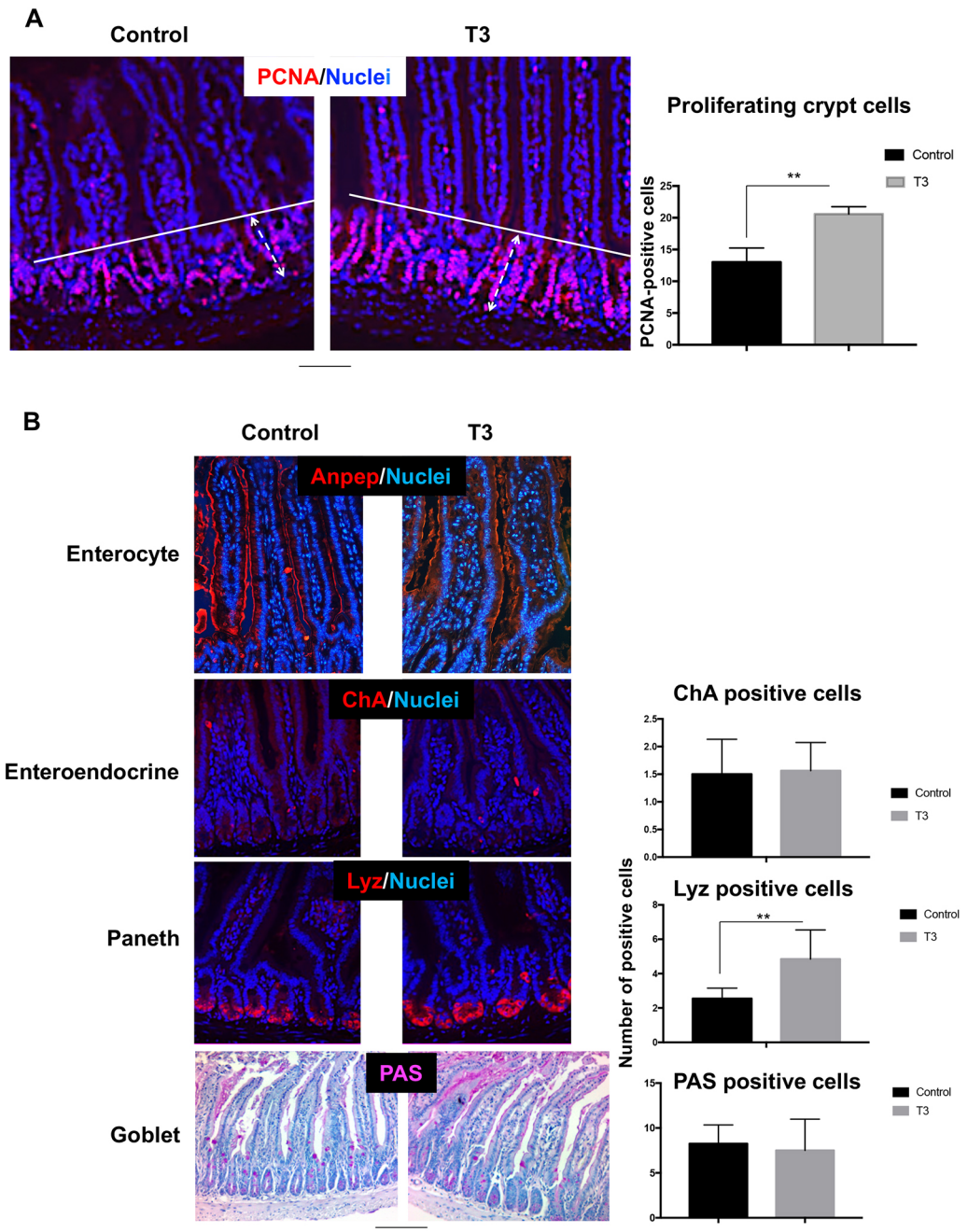

Fig. 9. Effect of T3 treatment *in vivo*. (A) Analysis of PCNA-positive proliferating cells in distal small intestinal sections from *Lgr5*-EGFP animals in control or T3 conditions. The images show merged PCNA (red) and nuclear staining (blue). Pictures are representative of three animals per condition. Quantification of PCNA-positive cells scored under a Zeiss imager microscope shown on right. The white lane delineates the PCNA-positive crypt compartment; the white dotted double-arrow indicates the crypt length. (B) Analysis of differentiation markers in distal small intestinal sections of control or T3-treated mice as indicated. ANPEP (enterocytes), lysozyme (LYZ, Paneth cells) and chromogranin A (ChA, enteroendocrine cells) were analyzed by immunolabeling. The images show merged differentiation marker (red) and nuclear staining (blue). Mucus-producing goblet cells were stained with PAS. Pictures are representative of three animals per condition. Quantification of positive cells for each differentiation marker scored under a Zeiss imager microscope shown on right. $^{**}P<0.01$, $n=30$. Scale bars: 10 µm (A, B, ANPEP, ChA, Lyz); 20 µm (PAS).

appearance in amphibians during metamorphosis (Frau et al., 2017; Ishizuya-Oka et al., 2009; Shi et al., 2011). Studies in mammals were hindered by a lack of cellular models to examine intestinal SCs. Indeed, discoveries relied exclusively on *in vivo* studies or on 2D primary cultures; these latter, however, presented multiple limitations, including the lack of vertical structuration of the epithelium and of cell hierarchy (Evans et al., 1994). These limitations became obsolete following the establishment of *ex vivo* 3D organoid cultures that represent a powerful tool to study SC self-renewal and multipotency properties (Sato et al., 2009). Thus, studies from the literature and our previous results strongly compelled us to analyze the effect of T3 treatment in intestinal organoids. We decided on the one hand to use a global approach to depict the molecular impact at the transcriptome level of T3 short-term treatment and, on the other hand, to follow the properties of organoid growth and structuration upon addition of T3. Both

Development (2021) 148, dev194357. doi:10.1242/dev.194357

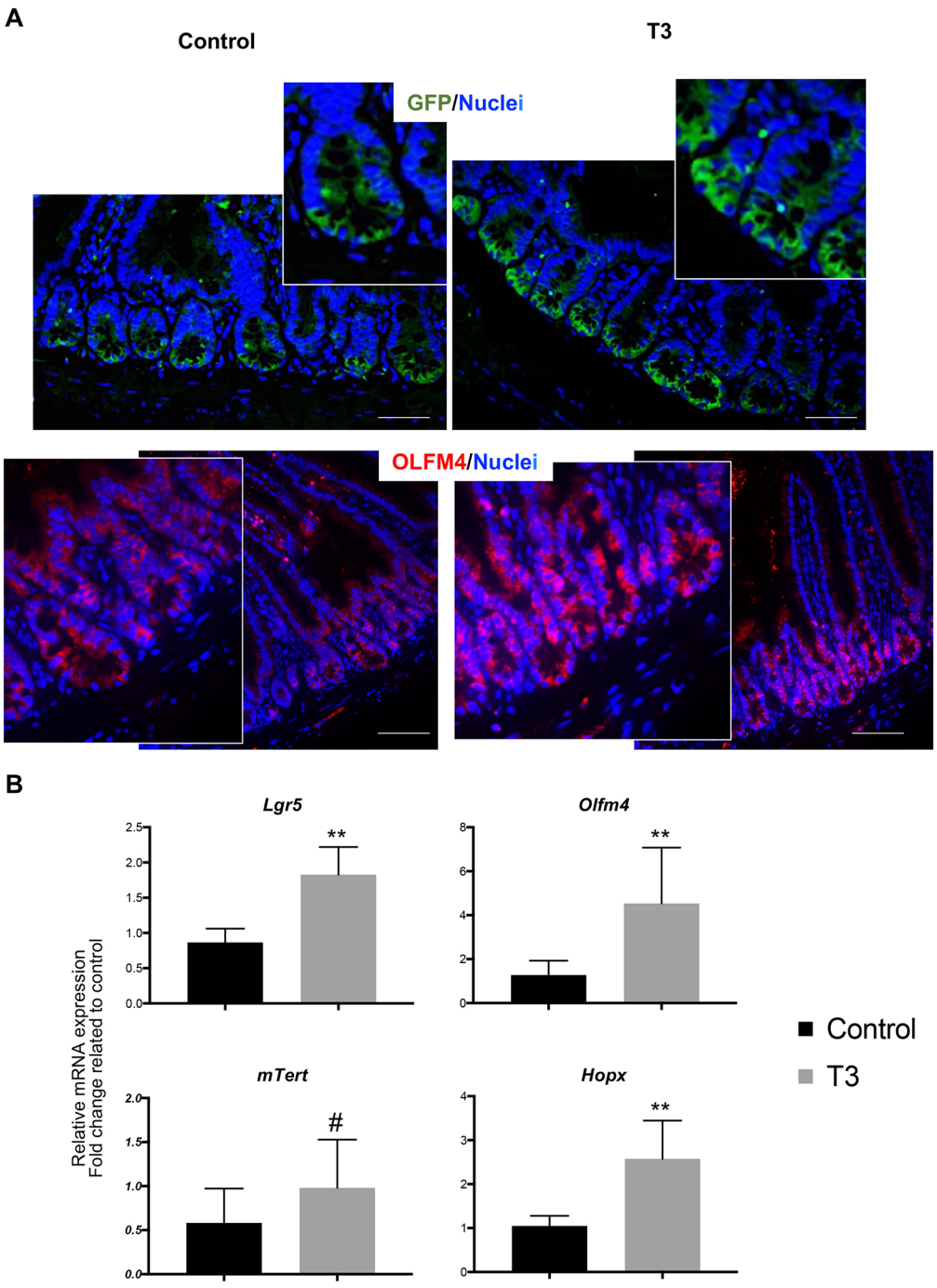

Fig. 10. Effect of T3 treatment on crypt stem cells *in vivo*. (A) Stem cells were analyzed in distal small intestinal sections of control or T3-treated mice by immunolabeling for GFP or OLFM4 expression. The images show merged GFP (green) or OLFM4 (red) and nuclear staining (blue). Pictures are representative of three different animals per condition. (B) RT-qPCR analysis of stem cell markers *Lgr5*, *Olfm4*, *Hopx* and *mTert* performed on RNA extracted from the distal small intestinal mucosa. Histograms represent mean±s.d., *n*=6, after normalization against *Ppib*. Data are represented as fold change relative to the control condition. ***P*<0.01. #, marginal significance (*P*=0.11). Scale bars: 10 µm for GFP; 5 µm, GFP insets; 15 µm for OLFM4; 7.5 µm for OLFM4 insets.

approaches were strongly informative and enabled us to define an early and complex response of SCs and progenitors to T3.

Molecular analyses revealed that the first clear-cut response to T3 signaling was at the level of SCs and we named it ‘thyroid shock’. Indeed, *Dio1* and *Mct10* mRNA expression were strongly upregulated at each time point analyzed, suggesting a cell defense mechanism in response to high T3 levels (i.e. DIO1 allows T3 degradation and MCT10 transporter regulates its efflux from the cells) (Bianco and da Conceição, 2018; Groeneweg et al., 2017). This response is reminiscent of that observed in the placenta to stop the entry of high TH levels into the bloodstream of embryos or of that of the nervous system during development in the case of hyperthyroidism (Bárez-López and Guadano-Ferraz, 2017; Patel et al., 2011). Regarding the transcriptome analysis, we observed that among the functions highly represented within the differentially regulated genes (up and down) were stress regulators, transporters and metabolism. For metabolism, in particular, it was evident that enzymes involved in energy metabolism, including glycolysis and lipid metabolism, were largely represented. This high metabolic response is in line with the function of T3 as a metabolic hormone (Cicatiello et al., 2018; Mullur et al., 2014) and with the phenotype observed at an early time point of T3 treatment, illustrated by an accelerated cell turnover. The stress response might be linked with the accelerated turnover and with the SC-associated phenotype. For a thorough comprehension at the level of cell populations, we compared the list of our T3-dependent DEGs with that defining SC

Development (2021) 148, dev194357. doi:10.1242/dev.194357

or progenitor gene signatures (Munoz et al., 2012; Sato et al., 2009). We observed that the genes upregulated in the T3 condition were more strongly and significantly associated with the progenitor-like signature than that of SCs. However, upregulated genes belonging to or described as markers of reserve/slow cycling/revival SCs were significantly associated with the SC gene signature. This result, together with the late phenotype of T3-treated organoids (i.e. attenuation of the GFP signal and/or decrease of the GFP-positive cells) strongly indicates that the progressive loss of active *Lgr5*-EGFP SCs might be counterbalanced by the activation and/or the mobilization of other highly plastic crypt cells. These features are commonly observed in animals *in vivo* as a consequence of an injury or of a stress inducing the loss of active SCs (Barker et al., 2010; Beumer and Clevers, 2016; Murata et al., 2020), but are not recapitulated in organoids. Indeed, an intestinal organoid, is a simplified mini-gut composed of the epithelium alone (Date and Sato, 2015) and is not able to overcome the loss of active SCs because the environment (epithelial cell types and culture medium) does not recapitulate all of the signals from the niche (Durand et al., 2012). It is thus not surprising that we observed an increase in reserve SCs markers (*Clu* or *Hopx*), which did not, however, result in an increase or an induction of SCs in response to continuous T3 treatment. Co-culture experiments including organoids and intestinal-derived fibroblasts will be instrumental to shed more light onto the T3-mediated phenotype and the signal exchanged. We expect mechanisms at work to be similar to those described in intestinal tadpole-derived epithelial monocultures or in co-cultured epithelium-mesenchymal tissues, in which T3 can have no/deleterious effects, or act as an inducer of the adult epithelium and the appearance of SCs, respectively (Ishizuya-Oka et al., 2009; Shi et al., 2011).

Lgr5-EGFP mice enabled us to specifically track and target the SCs (Barker et al., 2007) both *ex vivo* and *in vivo*. T3 treatment in organoids in the first 2 days induced faster organoid formation and cell proliferation. However, this increased turnover at longer T3 treatment times was responsible for increased cell death and unbalanced cell differentiation, in particular toward goblet cells. Although we did not focus specifically on the biological mechanisms involved, we can speculate that the induction of goblet cells in organoids could arise from altered Notch signaling in the presence of a milder or unaffected Wnt, as suggested by other studies (Gehart and Clevers, 2019; Spit et al., 2018; Yin et al., 2014). T3 treatment *in vivo* increased cell proliferation and also affected cell differentiation potential toward Paneth cells. This result strongly suggests that in animals *in vivo* T3 induces Paneth cell differentiation through an action on Wnt activity (reviewed by Skah et al., 2017). Importantly, Paneth cells constitute and participate in the SC niche, as they provide signals important for SC physiology (Gehart and Clevers, 2019; Spit et al., 2018; Yin et al., 2014). We then hypothesized and experimentally proved that in animals *in vivo* T3 induces an increase in the number of SCs and the expression of SC markers, according to the increased number of 'Paneth/niche cells'.

Taking into account similarities and differences between *in vivo* and in *ex vivo* settings, our data underline that T3 acts in an epithelial cell-autonomous manner by inducing an increase in cell proliferation, resulting in an amplification of the progenitor pool in both cases. However, as already commented, SC number and activity are differently affected by T3 when comparing the two systems. Indeed, complex cell interactions, including the presence of specific cell types as well as signals constituting the SC niche, are necessary for SC maintenance and activity (Gehart and Clevers, 2019; Spit et al., 2018; Yin et al., 2014). These signals are lacking or are lost in organoids treated with T3 for longer periods of time.

It is worth noting that the effect of T3 on intestinal epithelial crypt cells and on the self-renewal capacity of organoids (measured by the developmental characteristics and colony forming efficacy) is TRα1-dependent both *ex vivo* and *in vivo*, as $TR\alpha^{0/0}$ organoids have a lower stem cell capacity compared with WT and $TR\beta^{-/-}$ organoids. The induction of a dominant negative TRα1 protein was even more deleterious than complete TRα-gene loss. This is not surprising as constitutive knockout animals very often present an adaptive response to gene loss that can involve newly acquired functions of homologous genes, as previously described for the genes encoding retinoic acid nuclear receptors RAR (Benbrook et al., 2014) or for the Notch genes (Riccio et al., 2008). Redundancy, total or partial, has also been demonstrated in the case of TRα or TRβ knockout animals in several organs (Contreras-Jurado et al., 2011, 2014; Gullberg et al., 2002; Plateroti et al., 1999). We also observed that T3 treatment or TRα1 modulation *in vivo* resulted in a very similar intestinal crypt phenotype. Indeed, in addition to the direct correlation between TH or TRα1 levels and progenitor proliferation, we also observed a correlation with SC number and the expression of SC markers (Fig. 10; Fig. S11). However, TRα1-modulation gave rise to a stronger phenotype, probably owing to its effects on crypt epithelial cells exclusively, whereas T3 injections can target all the organism and have both direct and indirect effects. Moreover, we cannot completely rule out an involvement of TRβ in the T3 phenotype when considering that TRα1 is enriched in precursor cells, whereas TRβ is enriched in differentiated cells (Sirakov et al., 2014), possibly affecting the expression of genes in the differentiated compartment having, in turn, an effect on SCs.

In conclusion, our data on T3 and TRα1 on intestinal crypt SCs highlight complex and epithelial cell-autonomous as well as non-autonomous effects. On the one hand, TRα1 has a primary and direct effect on stem and progenitor cells and it is important for SC maintenance and biology. On the other hand, T3 plays a pleiotropic role that it is more complex to dissect. Indeed, our data underline that 3D organoids are a key model for dissecting early events occurring at the level of SCs, as well as progenitors, in a cell-autonomous manner. However, we should also take into account that the activity of SCs in both organogenesis and homeostasis is niche dependent (Gehart and Clevers, 2019; Spit et al., 2018; Yin et al., 2014). Hence, when studying changes occurring in proliferation, apoptosis and cell differentiation upon biological stimuli such as T3, the organoid system presents important limitations. Such limitations should, however, be overcome by the isolation and study of the various functions of T3 in specific cell populations by using a larger panel of appropriate markers or live-cell reporters. Finally, given that SCs have been clearly identified as the cells of origin of cancers in the intestine (Barker et al., 2009), new advances will help in the development of new tools in the field of precision medicine to target specific cell types, for which T3 has a pro-tumoral impact while preserving the other intestinal epithelial cell types.

MATERIALS AND METHODS

Animals and sample collection

We used male and female adult (2- to 4-month-old) *Lgr5*-EGFP-IRES-CreERT2 (*Lgr5*-EGFP) (Barker et al., 2007), $TR\alpha^{0/0}$ (Gauthier et al., 2001), $TR\beta^{-/-}$ (Gauthier et al., 1999) and TRami (Quignodon et al., 2007). Animals were maintained in a C57BL6/J genetic background. TRami mice were crossed with *Lgr5*-EGFP and *Rosa*-Tomato mice (Madisen et al., 2010) to generate tamoxifen-inducible triple transgenic mice. Animals were housed in the same animal facility and received standard mouse chow and

Development (2021) 148, dev194357. doi:10.1242/dev.194357

water *ad libitum*. All experiments were performed in compliance with the French and European guidelines for experimental animal studies and approved by the local committees 'Comités d'Éthique Ceccapp' (C2EA55), the Ministère de l'Enseignement Supérieur et de la Recherche Scientifique, Direction Générale de la Recherche et l'Innovation, Secrétariat 'Autorisation de projet' (agreement #13313-2017020210367606).

For T3 injections, a dose of 20 µg per 20 g body weight in 100 µl saline solution was used; mice were injected once a day for 2 days, controls received 100 µl of saline solution. Mice were sacrificed and intestinal samples were collected in 4% paraformaldehyde (PFA) or liquid nitrogen for paraffin embedding or molecular studies, respectively.

For tamoxifen injections, TRami mice received 100 µl of a 10 mg/ml solution in sunflower oil once a day for 5 days; controls received 100 µl of oil injections. After sacrifice, the intestine was removed for crypt preparation and organoid cultures or collected in 4% PFA or liquid nitrogen for paraffin embedding or molecular studies, respectively.

Isolation of small intestinal crypts, organoid cultures and treatments

Small intestine (from the proximal jejunum to the distal ileum) was harvested, washed with ice-cold 1× PBS, opened longitudinally to remove luminal content and finally cut into small pieces of 1-2 mm. Pieces of tissue were dynamically washed in ice-cold PBS at 4°C for 20 min. PBS was removed and fragments were incubated in a 2 mM EDTA/PBS solution for 30 min at 4°C. Fragments were then gently mixed with the pipette and the EDTA solution was removed. Intestinal fragments were dynamically washed in PBS and fragments were then shaken to dissociate crypts from the mesenchyme. Supernatant was recovered, giving rise to a crypt-enriched suspension. This suspension was centrifuged at 200 ***g*** for 3 min at 4°C and supernatant was removed. The crypt-enriched suspension was filtered through a 70 µm strainer and crypts were slowly centrifuged. Supernatant was removed and organoid culture medium was gently added to the crypt pellet. Finally, Matrigel matrix (Corning) was added to the crypt-medium solution at a 1:1 ratio and drops of 50 µl were then plated in 12-well plates. Finally, 900 µl of organoid culture medium was added to each well. Organoids were cultured at 37°C, 5% CO_2 in IntestiCult Organoid Growth Medium (Stemcell Technologies). Medium was changed every 4 days and organoids replicated approximately every 4/5 days. For replication, Matrigel-embedded organoids were grossly dissociated with a micropipette and fragments were recovered. The equivalent of four dissociated culture-drops were collected in tubes and the volume was adjusted to 5 ml with DMEM. Finally, organoids were mixed, centrifuged and pellets resuspended in Intesticult/Matrigel mix (1:1 volume) and plated in 50 µl drops, covered by 900 µl of culture medium in 12-well plates.

Organoid development studies over several days in culture were performed on freshly isolated crypt cultures. Live microscopy (bright-field or UV light) and counting of the different structures was carried out using a Zeiss AxioVert inverted microscope. For treatment experiments, T3 was used at a final concentration of 10^{-7} M in the culture medium; the stock solution (100×) was prepared in PBS containing 10% bovine serum albumin (BSA); 3,3′-T2 and tetraiodothyroacetic acid (Tetrac) were used at 10^{-7} M; T4 was used at 10^{-6} M (Merck-Sigma).

For proliferation studies, control or T3-treated organoids were incubated with 10 µM EdU solution (Click-it Plus Edu Assay Invitrogen, #C10636) for 2 h. After recovery, they were fixed in 4% PFA for 30 min, washed three times with PBS, for 5 min each, before adding 100 µl of 1× Click-it Plus permeabilization buffer to each sample for 15 min at room temperature. At the end of the permeabilization step, 500 µl of Click-it Plus reaction cocktail was added to each tube and samples were incubated for 30 min at room temperature, protected from light and in mild agitation. During the last 10 min of the reaction, 10 mg/ml of Hoechst was added to obtain a final dilution of 1:1000 in each tube. Finally, organoids were washed three times with PBS and mounted with Mowiol [6 g glycerol, 2.4 g mowiol 4-88, 6 ml H_2O, 12 ml Tris-Cl 0.2 M (pH 8.5) and 1% DABCO].

Growth analysis was performed at different time points in organoids cultured in 96-well round bottom plates. Metabolically active/living cells were analyzed by the tetrazolium salts reduction method (WST-1, Sigma-Aldrich) following the manufacturer's instructions (20 µl of WST-1 solution in 200 µl of culture medium from each well). The amount of formazan dye formed, directly correlated with the number of metabolically active cells in the culture, was measured using the CLARIOstar apparatus (BMG LABTech) at 450 nm.

For organoid colony assay experiments, organoids were recovered, incubated in Matrisperse (Corning) to eliminate the Matrigel, then incubated in TripLE express solution (Gibco, Thermo Fisher Scientific) at 37°C for 10 min and finally mechanically dissociated using a 1 ml pipette. Dissociation efficiency was directly monitored under the microscope. Cell suspensions were recovered in PBS, washed and filtered in a 40 µm strainer and 5000 single cells per 50 µl of Matrigel drop were plated onto 12-well plates.

Genomic DNA extraction and PCR analysis

Genomic DNA was extracted from TRami animals or organoids. CRE-mediated deletion was identified by PCR as described in Quignodon et al. (2007). Primers used were: b, 5′-GCCTTCTATCGCCTTCTTGACG; d, 5′-TCCACAGGTATCTCCAGACAGG; e, 5′-GATTCTTCTGGATTGTGC-GGCG.

RNA extraction and RTqPCR

Total RNA was extracted using the Nucleospin RNA Kit (Macherey-Nagel, Fisher Scientific). To remove contaminating genomic DNA (gDNA), DNase digestion was performed on all preparations. Reverse transcription (RT) was performed with the iScript reverse transcriptase (Bio-Rad) on total RNA according to the manufacturer's instructions. To further exclude gDNA contamination after RT we conducted a PCR in all preparations to amplify a housekeeping gene (*Hprt*) for which the primers are located on different exons of the corresponding gene. For qPCR approaches the SYBR qPCR Premix Ex Taq II (Tli RNaseH Plus, Takara) was used in a CFX connect apparatus (Bio-Rad). In each sample, specific mRNA expression was quantified using the ΔCt method and values normalized against *Ppib* levels. Primers are listed in Table S6.

Protein extraction and western blotting

Protein samples from organoids (50 µg per lane) were prepared with RIPA buffer as described in Uchuya-Castillo et al. (2018), separated by SDS-PAGE and transferred to PVDF membranes 0.2 µm (Bio-Rad). Membranes were blocked with TBS-Tween (Euromedex) supplemented with 5% non-fat milk before incubation with primary antibodies. This step was followed by incubation with HRP-conjugated secondary antibodies (Promega). The signal was analyzed using an enzymatic Clarity substrate detection kit (Bio-Rad) and image detection was performed using a Chemidoc XRS+ imaging system (Bio-Rad), according to manufacturer's protocol. All images were processed using the Image Lab software (Bio-Rad). Antibodies are listed in Table S7.

RNA-seq analysis

Sample preparation for sequencing

Triplicates of organoids maintained in control conditions or treated with 10^{-7} M T3 were prepared and processed by Active Motif RNA-seq service (www.activemotif.com). Steps included: isolation of total RNA; assessment of RNA quality/integrity using an Agilent Bioanalyzer; directional library generation and quality control of NGS library; next-generation sequencing using the Illumina platform (GEO accession number: GSE150697).

Sequencing and analyses

1. Read mapping – standard RNA-seq generates 42-nt sequence reads using Illumina NextSeq 500. The reads were mapped to the genome using the STAR algorithm with default settings (Dobin et al., 2013). Alignment information for each read is stored in the BAM format.
2. Fragment assignment – this process step is to count the number of reads (for single-end library) or fragments (for paired-end library) overlapping predefined genomic features of interest (e.g. genes). Only read pairs that had both ends aligned were counted. Read pairs that had their two ends mapping to different chromosomes or mapping to

the same chromosome but on different strands were discarded. We also required at least 25 bp overlapping bases in a fragment for read assignment. The gene annotations we used were obtained from Subread package (Liao et al., 2014). These annotations were originally from NCBI RefSeq database and then adapted by merging overlapping exons from the same gene to form a set of disjoint exons for each gene. Genes with the same Entrez gene identifiers were also merged into one gene (Liao et al., 2014).

3. Differential analysis – after obtaining the gene table containing the fragment (or read) counts of genes, differential analysis was performed to identify statistically significant differential genes using DESeq2 (Love et al., 2014). The following two pre-processing steps were used before differential calling. (1) Data normalization: DESeq2 expects an un-normalized count matrix of sequencing reads (for single-end RNA-seq) or fragments (for paired-end RNA-seq) for the DESeq2 statistical model to hold. The DESeq2 model internally corrects for library size using the median-of-ratios method (Love et al., 2014). The gene table obtained from fragment assignment was used as input to perform the DESeq2 differential test. (2) Filtering before multiple testing adjustment: after a differential test has been applied to each gene except the ones with zero counts, the *P*-value of each gene was calculated and needed to be further adjusted to control the number of false positives among all discoveries at a proper level. This procedure is known as multiple testing adjustment. During this process, DESeq2 by default filters out statistical tests (i.e. genes) that have low counts by a statistical technique called independent filtering. It uses the average counts of each gene (i.e. baseMean), across all samples, as its filter criterion, and it omits all genes with average normalized counts below a filtering threshold from multiple testing adjustment. This filtering threshold was automatically determined to maximize detection power (i.e. maximize the number of differential genes detected) at a specified false discovery rate (FDR).
4. Filtering criteria – DEGs were filters for shrunkenLog2FC >0.5 and adjusted *P*-value 0.05. The adjusted *P*-value was generated by Benjamini and Hochberg's FDR procedure and it is commonly used to evaluate statistical significance after multiple testing adjustment.

GO and pathway enrichment analysis

To classify the functions of DEGs, GO enrichment and Reactome pathway (Fabregat et al., 2016) analysis were performed using Panther (Mi et al., 2005) or Ingenuity Pathway Analysis (Ingenuity® Systems, www.ingenuity.com). For both analyses we considered terms to be significant if the FDR adjusted *P*-values were <0.05 and fold enrichment was >2.0. Furthermore, we used REViGO (Supek et al., 2011) to reduce redundancy of the enriched GO terms and visualize the semantic clustering of the identified top scoring terms. GSEA was performed using Enricher (Kuleshov et al., 2016) and with fast Gene Set Enrichment Analysis Package (version 1.9.7) implemented in R software. This analysis compared genes differentially expressed between T3-treated and control organoids and the Lgr5-GFP^{High} intestinal stem cell signature or Lgr5-GFP^{Low} progenitor signature as described previously (Munoz et al., 2012). Our dataset was compared with two studies (GSE23672 – stem cells versus progenitor cells; GSE25109 – stem cells versus Paneth cells) and to the stem cell gene signature defined by Munoz et al. (2012).

Gene interaction network analysis

In order to determine the association between genes in a given dataset, a protein-protein interaction network was constructed using the STRING database (v10) (Szklarczyk et al., 2015). The interactions were based on experimental evidence, co-occurrence and text-mining.

Immunofluorescence, histological staining and microscopy

For *in vivo* experiments, formalin-fixed paraffin-embedded (FFPE) sections (5 µm thickness) were used for indirect immunostaining. Briefly, the sections were processed to eliminate paraffin and then incubated with primary antibodies overnight at 4°C followed by incubation with fluorescent secondary antibodies (Alexa Fluor, Molecular Probes, 1:1000). All nuclei were counterstained with Hoechst (33342, Molecular Probes).

For *ex vivo* experiments, organoids were recovered and fixed in 3% PFA for 15 min at room temperature. They were then incubated in PBS/Triton 0.5% for 30 min, PBS/Triton 0.2%/BSA 1% for 30 min at room temperature. The solution was then discarded and primary antibodies were added at 4°C overnight. Organoids were rinsed in PBS and secondary antibodies were added for 4 h at room temperature. All nuclei were counterstained with Hoechst (33342, Molecular Probes) for 20 min. Finally, organoids were rinsed and mounted on glass slides. Antibodies are listed in Table S7. To label mucus-producing goblet cells, the paraffin sections were subjected to periodic acid-Schiff (PAS) staining as previously reported (Plateroti et al., 1999). Mucin-filled cells were stained in bright fuchsia.

Conventional bright-field and fluorescence microscopy was performed on a Right Zeiss AxioImager 2. All of the pictures were reproducibly modified using the ImageJ software (brightness/contrasts).

Statistical analysis

Results illustrated as histograms or line graphs represent the mean±s.d. Comparisons between groups were performed using a two-tailed unpaired Student's *t*-test; $P<0.05$ was considered to be statistically significant.

Acknowledgements

We are grateful to Manon Pratviel for her assistance with animal handling and care within the AniCan animal facility (Centre de Recherche en Cancérologie de Lyon; CRCL). We also acknowledge the imaging, cytometry and Anapath recherche small animal histology platforms (CRCL, Centre Léon Bérard). We are indebted to Anne Wierinckx and Joel Lachuer (ProfilExpert platform) for help with the bioinformatics analysis. Special thanks to Drs Elio Biffali and Pasquale De Luca as well as the Sequencing and Molecular Analyses Center personnel for their help in automated plate assembly and Real Time PCR runs at the Stazione Zoologica. We also thank Brigitte Manship for critical reading of the manuscript.

Competing interests

The authors declare no competing or financial interests.

Author contributions

Conceptualization: M.G., C.F., J.-N.F., L.O.P., M.S., M.P.; Methodology: M.G., C.F., M.V.G., C.J., C.L.N., M.S., M.P.; Validation: M.G., J.-N.F., M.S., M.P.; Formal analysis: L.O.P.; Investigation: M.G., C.F., D.F., M.V.G., C.J., C.L.N., L.O.P., M.S., M.P.; Resources: C.J., C.L.N.; Data curation: D.F., M.P.; Writing - original draft: M.G., C.F., J.-N.F., L.O.P., M.S., M.P.; Writing - review & editing: M.G., D.F., M.V.G., J.-N.F., L.O.P., M.S., M.P.; Visualization: D.F., M.V.G., M.P.; Supervision: M.P.; Funding acquisition: M.P.

Funding

The work was supported by the Département du Rhône de la Ligue Contre le Cancer (grant 172190), by the Fondation ARC pour la Recherche sur le Cancer (ARC) (grant PGA1201402000834), by the Fondation pour la Recherche Médicale (FRM) (Equipes FRM 2018, DEQ20181039598) and by the Institut National Du Cancer (PLBIO19-289). M.G. and M.V.G. received support from the FRM; C.F. received support from ARC and the Centre Léon Bérard.

Data availability

RNA-seq data have been deposited in GEO under accession number GSE150697.

References

Amma, L. L., Campos-Barros, A., Wang, Z., Vennström, B. and Forrest, D. (2001). Distinct tissue-specific roles for thyroid hormone receptors β and α1 in regulation of type 1 deiodinase expression. *Mol. Endocrinol.* **15**, 467-475. doi:10.1210/mend.15.3.0605

Ayyaz, A., Kumar, S., Sangiorgi, B., Ghoshal, B., Gosio, J., Ouladan, S., Fink, M., Barutcu, S., Trcka, D., Shen, J. et al. (2019). Single-cell transcriptomes of the regenerating intestine reveal a revival stem cell. *Nature* **569**, 121-125. doi:10.1038/s41586-019-1154-y

Bao, L., Roediger, J., Park, S., Fu, L., Shi, B., Cheng, S.-Y. and Shi, Y.-B. (2019). Thyroid hormone receptor alpha mutations lead to epithelial defects in the adult intestine in a mouse model of resistance to thyroid hormone. *Thyroid* **29**, 439-448. doi:10.1089/thy.2018.0340

Bárez-López, S. and Guadano-Ferraz, A. (2017). Thyroid hormone availability and action during brain development in rodents. *Front Cell Neurosci* **11**, 240. doi:10.3389/fncel.2017.00240

Barker, N. (2014). Adult intestinal stem cells: critical drivers of epithelial homeostasis and regeneration. *Nat. Rev. Mol. Cell Biol.* **15**, 19-33. doi:10.1038/nrm3721

Barker, N., van Es, J. H., Kuipers, J., Kujala, P., van den Born, M., Cozijnsen, M., Haegebarth, A., Korving, J., Begthel, H., Peters, P. J. et al. (2007). Identification of stem cells in small intestine and colon by marker gene Lgr5. *Nature* **449**, 1003-1007. doi:10.1038/nature06196

Barker, N., Ridgway, R. A., van Es, J. H., van de Wetering, M., Begthel, H., van den Born, M., Danenberg, E., Clarke, A. R., Sansom, O. J. and Clevers, H. (2009). Crypt stem cells as the cells-of-origin of intestinal cancer. *Nature* **457**, 608-611. doi:10.1038/nature07602

Barker, N., Bartfeld, S. and Clevers, H. (2010). Tissue-resident adult stem cell populations of rapidly self-renewing organs. *Cell Stem Cell* **7**, 656-670. doi:10.1016/j.stem.2010.11.016

Benbrook, D. M., Chambon, P., Rochette-Egly, C. and Asson-Batres, M. A. (2014). History of retinoic acid receptors. *Subcell. Biochem.* **70**, 1-20. doi:10.1007/978-94-017-9050-5_1

Beumer, J. and Clevers, H. (2016). Regulation and plasticity of intestinal stem cells during homeostasis and regeneration. *Development* **143**, 3639-3649. doi:10.1242/dev.133132

Bianco, A. C. and da Conceição, R. R. (2018). The Deiodinase Trio and Thyroid Hormone Signaling. *Methods Mol. Biol.* **1801**, 67-83. doi:10.1007/978-1-4939-7902-8_8

Brent, G. A. (2012). Mechanisms of thyroid hormone action. *J. Clin. Invest.* **122**, 3035-3043. doi:10.1172/JCI60047

Chen, G., Korfhagen, T. R., Xu, Y., Kitzmiller, J., Wert, S. E., Maeda, Y., Gregorieff, A., Clevers, H. and Whitsett, J. A. (2009). SPDEF is required for mouse pulmonary goblet cell differentiation and regulates a network of genes associated with mucus production. *J. Clin. Invest.* **119**, 2914-2924. doi:10.1172/JCI39731

Cicatiello, A. G., Di Girolamo, D. and Dentice, M. (2018). Metabolic effects of the intracellular regulation of thyroid hormone: old players, new concepts. *Front. Endocrinol.* **9**, 474. doi:10.3389/fendo.2018.00474

Contreras-Jurado, C., García-Serrano, L., Gómez-Ferrería, M., Costa, C., Paramio, J. M. and Aranda, A. (2011). The thyroid hormone receptors as modulators of skin proliferation and inflammation. *J. Biol. Chem.* **286**, 24079-24088. doi:10.1074/jbc.M111.218487

Contreras-Jurado, C., García-Serrano, L., Martínez-Fernández, M., Ruiz-Llorente, L., Paramio, J. M. and Aranda, A. (2014). Impaired hair growth and wound healing in mice lacking thyroid hormone receptors. *PLoS ONE* **9**, e108137. doi:10.1371/journal.pone.0108137

Danopoulos, S., Schlieve, C. R., Grikscheit, T. C. and Al Alam, D. (2017). Fibroblast growth factors in the gastrointestinal tract: twists and turns. *Dev. Dyn.* **246**, 344-352. doi:10.1002/dvdy.24491

Date, S. and Sato, T. (2015). Mini-gut organoids: reconstitution of the stem cell niche. *Annu. Rev. Cell Dev. Biol.* **31**, 269-289. doi:10.1146/annurev-cellbio-100814-125218

Davis, P. J., Davis, F. B., Mousa, S. A., Luidens, M. K. and Lin, H.-Y. (2011). Membrane receptor for thyroid hormone: physiologic and pharmacologic implications. *Annu. Rev. Pharmacol. Toxicol.* **51**, 99-115. doi:10.1146/annurev-pharmtox-010510-100512

Denver, R. J. and Williamson, K. E. (2009). Identification of a thyroid hormone response element in the mouse Krüppel-like factor 9 gene to explain its postnatal expression in the brain. *Endocrinology* **150**, 3935-3943. doi:10.1210/en.2009-0050

Dobin, A., Davis, C. A., Schlesinger, F., Drenkow, J., Zaleski, C., Jha, S., Batut, P., Chaisson, M. and Gingeras, T. R. (2013). STAR: ultrafast universal RNA-seq aligner. *Bioinformatics* **29**, 15-21. doi:10.1093/bioinformatics/bts635

Durand, A., Donahue, B., Peignon, G., Letourneur, F., Cagnard, N., Slomianny, C., Perret, C., Shroyer, N. F. and Romagnolo, B. (2012). Functional intestinal stem cells after Paneth cell ablation induced by the loss of transcription factor Math1 (Atoh1). *Proc. Natl. Acad. Sci. USA* **109**, 8965-8970. doi:10.1073/pnas.1201652109

Evans, G. S., Flint, N. and Potten, C. S. (1994). Primary cultures for studies of cell regulation and physiology in intestinal epithelium. *Annu. Rev. Physiol.* **56**, 399-417. doi:10.1146/annurev.ph.56.030194.002151

Fabregat, A., Sidiropoulos, K., Garapati, P., Gillespie, M., Hausmann, K., Haw, R., Jassal, B., Jupe, S., Korninger, F., McKay, S. et al. (2016). The Reactome pathway Knowledgebase. *Nucleic Acids Res.* **44**, D481-D487. doi:10.1093/nar/gkv1351

Frau, C., Godart, M. and Plateroti, M. (2017). Thyroid hormone regulation of intestinal epithelial stem cell biology. *Mol. Cell. Endocrinol.* **459**, 90-97. doi:10.1016/j.mce.2017.03.002

Gauthier, K., Chassande, O., Plateroti, M., Roux, J. P., Legrand, C., Pain, B., Rousset, B., Weiss, R., Trouillas, J. and Samarut, J. (1999). Different functions for the thyroid hormone receptors TRalpha and TRbeta in the control of thyroid hormone production and post-natal development. *EMBO J.* **18**, 623-631. doi:10.1093/emboj/18.3.623

Gauthier, K., Plateroti, M., Harvey, C. B., Williams, G. R., Weiss, R. E., Refetoff, S., Willott, J. F., Sundin, V., Roux, J.-P., Malaval, L. et al. (2001). Genetic analysis reveals different functions for the products of the thyroid hormone receptor α locus. *Mol. Cell. Biol.* **21**, 4748-4760. doi:10.1128/MCB.21.14.4748-4760.2001

Gehart, H. and Clevers, H. (2019). Tales from the crypt: new insights into intestinal stem cells. *Nat. Rev. Gastroenterol. Hepatol.* **16**, 19-34. doi:10.1038/s41575-018-0081-y

Groeneweg, S., Visser, W. E. and Visser, T. J. (2017). Disorder of thyroid hormone transport into the tissues. *Best Pract. Res. Clin. Endocrinol. Metab.* **31**, 241-253. doi:10.1016/j.beem.2017.05.001

Gullberg, H., Rudling, M., Saltó, C., Forrest, D., Angelin, B. and Vennström, B. (2002). Requirement for thyroid hormone receptor β in T3 regulation of cholesterol metabolism in mice. *Mol. Endocrinol.* **16**, 1767-1777. doi:10.1210/me.2002-0009

Hammes, S. R. and Davis, P. J. (2015). Overlapping nongenomic and genomic actions of thyroid hormone and steroids. *Best Practice Res. Clin. Endocrinol. Metab.* **29**, 581-593. doi:10.1016/j.beem.2015.04.001

Ishizuya-Oka, A., Hasebe, T., Buchholz, D. R., Kajita, M., Fu, L. and Shi, Y. B. (2009). Origin of the adult intestinal stem cells induced by thyroid hormone in Xenopus laevis. *FASEB J.* **23**, 2568-2575. doi:10.1096/fj.08-128124

Kalyanaraman, H., Schwappacher, R., Joshua, J., Zhuang, S., Scott, B. T., Klos, M., Casteel, D. E., Frangos, J. A., Dillmann, W., Boss, G. R. et al. (2014). Nongenomic thyroid hormone signaling occurs through a plasma membrane-localized receptor. *Sci. Signal.* **7**, ra48. doi:10.1126/scisignal.2004911

Kim, J.-Y., Jeong, H. S., Chung, T., Kim, M., Lee, J. H., Jung, W. H. and Koo, J. S. (2017). The value of phosphohistone H3 as a proliferation marker for evaluating invasive breast cancers: a comparative study with Ki67. *Oncotarget* **8**, 65064-65076. doi:10.18632/oncotarget.17775

Kress, E., Rezza, A., Nadjar, J., Samarut, J. and Plateroti, M. (2009). The frizzled-related sFRP2 gene is a target of thyroid hormone receptor α1 and activates β-catenin signaling in mouse intestine. *J. Biol. Chem.* **284**, 1234-1241. doi:10.1074/jbc.M806548200

Kress, E., Skah, S., Sirakov, M., Nadjar, J., Gadot, N., Scoazec, J. Y., Samarut, J. and Plateroti, M. (2010). Cooperation between the thyroid hormone receptor TRα1 and the WNT pathway in the induction of intestinal tumorigenesis. *Gastroenterology* **138**, 1863-1874.e1. doi:10.1053/j.gastro.2010.01.041

Kuleshov, M. V., Jones, M. R., Rouillard, A. D., Fernandez, N. F., Duan, Q., Wang, Z., Koplev, S., Jenkins, S. L., Jagodnik, K. M., Lachmann, A. et al. (2016). Enrichr: a comprehensive gene set enrichment analysis web server 2016 update. *Nucleic Acids Res.* **44**, W90-W97. doi:10.1093/nar/gkw377

Li, L. and Clevers, H. (2010). Coexistence of quiescent and active adult stem cells in mammals. *Science* **327**, 542-545. doi:10.1126/science.1180794

Liao, Y., Smyth, G. K. and Shi, W. (2014). featureCounts: an efficient general purpose program for assigning sequence reads to genomic features. *Bioinformatics* **30**, 923-930. doi:10.1093/bioinformatics/btt656

Love, M. I., Huber, W. and Anders, S. (2014). Moderated estimation of fold change and dispersion for RNA-seq data with DESeq2. *Genome Biol.* **15**, 550. doi:10.1186/s13059-014-0550-8

Madisen, L., Zwingman, T. A., Sunkin, S. M., Oh, S. W., Zariwala, H. A., Gu, H., Ng, L. L., Palmiter, R. D., Hawrylycz, M. J., Jones, A. R. et al. (2010). A robust and high-throughput Cre reporting and characterization system for the whole mouse brain. *Nat. Neurosci.* **13**, 133-140. doi:10.1038/nn.2467

Mi, H., Lazareva-Ulitsky, B., Loo, R., Kejariwal, A., Vandergriff, J., Rabkin, S., Guo, N., Muruganujan, A., Doremieux, O., Campbell, M. J., Kitano, H. and Thomas, P. D. (2005). The PANTHER database of protein families, subfamilies, functions and pathways. *Nucleic Acids Res.* **33**, D284-D288. doi:10.1093/nar/gki078

Mullur, R., Liu, Y.-Y. and Brent, G. A. (2014). Thyroid hormone regulation of metabolism. *Physiol. Rev.* **94**, 355-382. doi:10.1152/physrev.00030.2013

Munoz, J., Stange, D. E., Schepers, A. G., van de Wetering, M., Koo, B.-K., Itzkovitz, S., Volckmann, R., Kung, K. S., Koster, J., Radulescu, S. et al. (2012). The Lgr5 intestinal stem cell signature: robust expression of proposed quiescent '+4' cell markers. *EMBO J.* **31**, 3079-3091. doi:10.1038/emboj.2012.166

Murata, K., Jadhav, U., Madha, S., van Es, J., Dean, J., Cavazza, A., Wucherpfennig, K., Michor, F., Clevers, H. and Ramesh, A. et al. (2020). Ascl2-dependent cell dedifferentiation drives regeneration of ablated intestinal stem cells. *Cell Stem Cell* **26**, 377-390.e6. doi:10.1016/j.stem.2019.12.011

Nielsen, P. S., Riber-Hansen, R., Jensen, T. O., Schmidt, H. and Steiniche, T. (2013). Proliferation indices of phosphohistone H3 and Ki67: strong prognostic markers in a consecutive cohort with stage I/II melanoma. *Mod. Pathol.* **26**, 404-413. doi:10.1038/modpathol.2012.188

Noah, T. K., Donahue, B. and Shroyer, N. F. (2011). Intestinal development and differentiation. *Exp. Cell Res.* **317**, 2702-2710. doi:10.1016/j.yexcr.2011.09.006

Patel, J., Landers, K., Li, H., Mortimer, R. H. and Richard, K. (2011). Delivery of maternal thyroid hormones to the fetus. *Trends Endocrinol. Metab.* **22**, 164-170. doi:10.1016/j.tem.2011.02.002

Plateroti, M., Chassande, O., Fraichard, A., Gauthier, K., Freund, J. N., Samarut, J. and Kedinger, M. (1999). Involvement of T3Rα- and β-receptor subtypes in mediation of T3 functions during postnatal murine intestinal development. *Gastroenterology* **116**, 1367-1378. doi:10.1016/S0016-5085(99)70501-9

Plateroti, M., Gauthier, K., Domon-Dell, C., Freund, J.-N., Samarut, J. and Chassande, O. (2001). Functional interference between thyroid hormone receptor α (TRα) and natural truncated TRΔα isoforms in the control of intestine

development. *Mol. Cell. Biol.* **21**, 4761-4772. doi:10.1128/MCB.21.14.4761-4772.2001

Plateroti, M., Kress, E., Mori, J. I. and Samarut, J. (2006). Thyroid hormone receptor α1 directly controls transcription of the β-catenin gene in intestinal epithelial cells. *Mol. Cell. Biol.* **26**, 3204-3214. doi:10.1128/MCB.26.8.3204-3214.2006

Quignodon, L., Vincent, S., Winter, H., Samarut, J. and Flamant, F. (2007). A point mutation in the activation function 2 domain of thyroid hormone receptor α1 expressed after CRE-mediated recombination partially recapitulates hypothyroidism. *Mol. Endocrinol.* **21**, 2350-2360. doi:10.1210/me.2007-0176

Riccio, O., van Gijn, M. E., Bezdek, A. C., Pellegrinet, L., van Es, J. H., Zimber-Strobl, U., Strobl, L. J., Honjo, T., Clevers, H. and Radtke, F. (2008). Loss of intestinal crypt progenitor cells owing to inactivation of both Notch1 and Notch2 is accompanied by derepression of CDK inhibitors p27Kip1 and p57Kip2. *EMBO Rep.* **9**, 377-383. doi:10.1038/embor.2008.7

Sato, T., Vries, R. G., Snippert, H. J., van de Wetering, M., Barker, N., Stange, D. E., van Es, J. H., Abo, A., Kujala, P., Peters, P. J. et al. (2009). Single Lgr5 stem cells build crypt-villus structures in vitro without a mesenchymal niche. *Nature* **459**, 262-265. doi:10.1038/nature07935

Shi, Y.-B., Hasebe, T., Fu, L., Fujimoto, K. and Ishizuya-Oka, A. (2011). The development of the adult intestinal stem cells: Insights from studies on thyroid hormone-dependent amphibian metamorphosis. *Cell Biosci* **1**, 30. doi:10.1186/2045-3701-1-30

Siebel, C. and Lendahl, U. (2017). Notch signaling in development, tissue homeostasis, and disease. *Physiol. Rev.* **97**, 1235-1294. doi:10.1152/physrev.00005.2017

Sirakov, M. and Plateroti, M. (2011). The thyroid hormones and their nuclear receptors in the gut: from developmental biology to cancer. *Biochim. Biophys. Acta* **1812**, 938-946. doi:10.1016/j.bbadis.2010.12.020

Sirakov, M., Kress, E., Nadjar, J. and Plateroti, M. (2014). Thyroid hormones and their nuclear receptors: new players in intestinal epithelium stem cell biology? *Cell. Mol. Life Sci.* **71**, 2897-2907. doi:10.1007/s00018-014-1586-3

Sirakov, M., Boussouar, A., Kress, E., Frau, C., Lone, I. N., Nadjar, J., Angelov, D. and Plateroti, M. (2015). The thyroid hormone nuclear receptor TRα1 controls the Notch signaling pathway and cell fate in murine intestine. *Development* **142**, 2764-2774. doi:10.1242/dev.121962

Skah, S., Uchuya-Castillo, J., Sirakov, M. and Plateroti, M. (2017). The thyroid hormone nuclear receptors and the Wnt/β-catenin pathway: an intriguing liaison. *Dev. Biol.* **422**, 71-82. doi:10.1016/j.ydbio.2017.01.003

Spit, M., Koo, B. K. and Maurice, M. M. (2018). Tales from the crypt: intestinal niche signals in tissue renewal, plasticity and cancer. *Open Biol.* **8**, 180120. doi:10.1098/rsob.180120

Supek, F., Bošnjak, M., Škunca, N. and Šmuc, T. (2011). REVIGO summarizes and visualizes long lists of gene ontology terms. *PLoS ONE* **6**, e21800. doi:10.1371/journal.pone.0021800

Szklarczyk, D., Franceschini, A., Wyder, S., Forslund, K., Heller, D., Huerta-Cepas, J., Simonovic, M., Roth, A., Santos, A., Tsafou, K. P. et al. (2015). STRING v10: protein-protein interaction networks, integrated over the tree of life. *Nucleic Acids Res.* **43**, D447-D452. doi:10.1093/nar/gku1003

Tian, H., Biehs, B., Chiu, C., Siebel, C. W., Wu, Y., Costa, M., de Sauvage, F. J. and Klein, O. D. (2015). Opposing activities of Notch and Wnt signaling regulate intestinal stem cells and gut homeostasis. *Cell Rep* **11**, 33-42. doi:10.1016/j.celrep.2015.03.007

Uchuya-Castillo, J., Aznar, N., Frau, C., Martinez, P., Le Nevé, C., Marisa, L., Penalva, L. O. F., Laurent-Puig, P., Puisieux, A., Scoazec, J.-Y. et al. (2018). Increased expression of the thyroid hormone nuclear receptor TRα1 characterizes intestinal tumors with high Wnt activity. *Oncotarget* **9**, 30979-30996. doi:10.18632/oncotarget.25741

Umar, S. (2010). Intestinal stem cells. *Curr. Gastroenterol. Rep.* **12**, 340-348. doi:10.1007/s11894-010-0130-3

van der Flier, L. G. and Clevers, H. (2009). Stem cells, self-renewal, and differentiation in the intestinal epithelium. *Annu. Rev. Physiol.* **71**, 241-260. doi:10.1146/annurev.physiol.010908.163145

van Es, J. H., van Gijn, M. E., Riccio, O., van den Born, M., Vooijs, M., Begthel, H., Cozijnsen, M., Robine, S., Winton, D. J., Radtke, F. et al. (2005). Notch/γ-secretase inhibition turns proliferative cells in intestinal crypts and adenomas into goblet cells. *Nature* **435**, 959-963. doi:10.1038/nature03659

Yin, X., Farin, H. F., van Es, J. H., Clevers, H., Langer, R. and Karp, J. M. (2014). Niche-independent high-purity cultures of Lgr5+ intestinal stem cells and their progeny. *Nat. Methods* **11**, 106-112. doi:10.1038/nmeth.2737

Résumé et description du contenu de la thèse en français

Projet de thèse Giolito, Maria Virginia

Régulation et fonction du récepteur nucléaire des hormones thyroïdiennes TRα1 dans la biologie des cellules souches cancéreuses des cancers coliques

Contexte

Le cancer est l'une des principales causes de décès dans le monde, faisant de cette maladie non transmissible un problème de santé publique important dans le monde [1]. L'acquisition de caractéristiques tumorigènes peut se produire dans n'importe quelle cellule de l'organisme, quelle que soit son origine. La plupart des cancers de l'adulte proviennent des tissus épithéliaux en raison de leur renouvellement constant qui peut favoriser l'acquisition d'altérations génétiques. Dans le contexte de cette thèse, nous nous sommes intéressés particulièrement au cancer colorectal (CCR). Le CCR est la deuxième cause de décès dans le monde pour les cancers, malgré une forte implication des agences de santé publique pour le dépistage précoce de ce cancer[1].

Le développement du CCR résulte d'une acquisition et d'une accumulation progressives de mutations génétiques et d'altérations épigénétiques. La description classique de la carcinogenèse colorectale, la séquence adénome-carcinome et la tumorigenèse en plusieurs étapes ont bien été décrites dans les années 90 par Fearon et Vogelstein[2]. Premièrement, les tumeurs colorectales surviennent en raison de l'activation mutationnelle d'oncogènes couplée à une perte prédominante de gènes suppresseurs de tumeurs par inactivation mutationnelle. Deuxièmement, plusieurs mutations génétiques sont nécessaires pour former une tumeur maligne. Un faible taux de mutations suffit pour la tumorigenèse bénigne. Troisièmement, bien que les altérations génétiques se produisent souvent selon une séquence préférée, l'accumulation totale des changements, plutôt que leur ordre d'apparition, est responsable de la détermination des propriétés biologiques de la tumeur. Quatrièmement, dans certains cas, des mutations de gènes suppresseurs de tumeurs exercent un effet phénotypique même lorsqu'elles sont présentes à l'état hétérozygote ; ainsi, certains gènes suppresseurs de tumeurs peuvent ne pas être « récessifs » au niveau cellulaire[2]. Le CCR est un cancer présentant une fréquence élevée, généralement associé à une forte agressivité et avec un fort potentiel de rechute à la suite

des traitements actuellement utilisés. Par conséquent, une meilleure connaissance de sa biologie est nécessaire pour développer des thérapies plus efficaces.

L'intestin est un organe long composé de deux parties principales, l'intestin grêle et le côlon. Avec ses 6 m de long, l'intestin grêle humain supervise l'absorption efficace des nutriments. Parallèlement, le côlon est spécialisé dans la recapture de l'eau et des électrolytes et dans l'élimination des aliments et des déchets non digérés. L'intestin grêle et le côlon humains sont tous deux spécialisés dans la protection de l'organisme contre les xénobiotiques. L'intestin grêle est constitué de trois grandes parties anatomiques : le duodénum (env. 25 cm de long), qui est la partie la plus courte et la plus large, le jéjunum (env. 2,5 m de long) et enfin, l'iléon (env. 3,5 m de long). Entre l'iléon et le côlon, on trouve le caecum, et enfin on a le côlon, le rectum et le conduit anal qui composent le gros intestin. Le côlon lui-même se compose de quatre parties selon sa localisation anatomique, le côlon ascendant, le côlon transverse, le côlon descendant et le côlon sigmoïde[3,4].

L'épithélium intestinal a une structure particulière qui augmente la surface de contact, facilitant son rôle dans l'organisme. L'intestin grêle présente des saillies en forme de doigt dans la lumière, appelées villosités, et des invaginations dans la sous-muqueuse appelées cryptes de Lieberkühn[3–6]. Les villosités permettent d'augmenter la surface de contact avec les nutriments pour l'absorption et constituent le compartiment où se situent les cellules différenciées non plongeantes. En raison de ses fonctions d'absorption et d'élimination des xénobiotiques, il est constamment en contact avec des substances nocives qui peuvent favoriser davantage une transformation maligne. La longueur des villosités diminue du duodénum à l'iléon distal. Les cryptes se situent à la base de l'épithélium. Ils sont le site de localisation des cellules de Paneth, des cellules proliférantes: les cellules souches (CS) et un sous-ensemble de progéniteurs à prolifération rapide (également appelés cellules amplificatrices de transit (TA))[5,6]. En résumé, une CS nouveau-née se divisera asymétriquement pour s'auto-renouveler afin d'élargir le pool de CS et donner naissance à un sous-ensemble de TA progéniteurs qui migreront vers le haut tout en se différenciant en l'une des les lignées épithéliales spécialisées (entérocytes/colonocytes, cellules de Goblet, cellules de Paneth, cellules enteroendocrines, cellules de tuft ou cellules M)[5].

L'histologie du côlon est assez différente, des cryptes sont toujours présentes, sans pour autant avoir de villosités il est caractérisé comme étant un épithélium à surface cylindrique[7,8].

L'épithélium intestinal est l'un des tissus les plus intensément auto-reconstitués avec un renouvellement complet tous les cinq jours, cohérent avec la trajectoire complète d'une cellule souche de la base de la crypte jusqu'à l'extrémité des villosités[9]. Comme nous venons de voir, l'épithélium intestinal se caractérise par son renouvellement continu grâce à la présence de CS adultes multipotentes[5]. Leur bon fonctionnement assure la coordination des processus de prolifération, migration et différenciation dépendants des voies de signalisation Wnt, Notch et BMP. La dérégulation de ces mêmes voies est impliquée dans la tumorigenèse. Il est généralement admis que le CCR a pour origine le dysfonctionnement des CS, leur transformation en cellules souches cancéreuses (CSC) leur permettant alors d'acquérir des propriétés de cellules initiatrices de tumeurs. Ces propriétés des CSC sont à la base des rechutes tumorales et des disséminations pour former des métastases. Le concept de CSC est fortement soutenu par les observations effectuées sur des modèles murins et de biopsies de patients[10,11]. En vue de leurs caractéristiques, l'élimination des CSC est maintenant considérée comme une condition nécessaire à la réussite du traitement. Cependant, il est à noter qu'en parallèle de ces données montrant l'implication des CSC dans le développement tumoral, qu'ils existent des mécanismes plus complexes associés à des altérations génétiques et épigénétiques permettant à des cellules différenciées (non souches) d'acquérir, via un processus de plasticité cellulaire, des propriétés de CSC.

Particulièrement dans notre laboratoire nous sommes intéressés au rôle des hormones thyroïdiennes dans l'épithélium intestinal et dans le CCR. Notre laboratoire a contribué dans le domaine des hormones thyroïdiennes (HT) en étudiant l'importance du signal dépendant des HT sur le développement et l'homéostasie intestinale. Pour rappel, les HT sont synthétisées par la glande thyroïde dans un processus finement régule par l'axe hypothalamus-hypophyse-thyroïde[12]. La thyroïde synthétise deux hormones la L-thyroxine (T4) et la 3,5,3'-L-triidothyronine (T3) mais la production de T4 est environ 40 fois plus importante que celui de la T3. Les HT agissent via les récepteurs nucléaires des hormones thyroïdiennes TR, des facteurs de transcription modulés par l'hormone T3. La T3 et le récepteur TRα1 ont un rôle clé sur le développement et l'homéostasie de l'intestin grâce au contrôle de la prolifération des cellules des cryptes intestinales[13–15]. Plusieurs travaux au sein de l'équipe ont pu mettre en évidence un lien étroit entre les hormones thyroïdiennes et les CS intestinales. Premièrement, le traitement à la T3 dans un modèle *ex vivo* d'entéroïdes de souris mais aussi *in vivo*, induit l'augmentations des marqueurs des CS, tout en favorisant l'expansion de la crypte par l'augmentation des

cellules progenitrices[16]. Dans un second temps, des travaux sur des modèles murins mais aussi sur des tumeurs de patients, ont pu mettre en évidence une expression accrue de TRα1 au sein des CCR corrélée à une augmentation de l'activité de la voie Wnt[17]. Enfin, des études d'altération de l'expression de TRα1 dans la lignée cellulaire d'adénocarcinome colique humaine Caco2, ont pu non seulement confirmer que les niveaux de TRα1 permettait le contrôle de la voie Wnt, mais également que TRα1 jouait aussi un rôle dans la régulation de la prolifération et la migration cellulaires[17]. Dans l'ensemble, ces données suggèrent fortement l'implication de TRα1 dans la biologie des CSC, similaire à ce que nous avions précédemment observé dans les CS intestinales normales[16].

J'ai mentionné en amont que le CCR est généralement associé à une forte agressivité et avec un fort potentiel de rechute à la suite de l'acquisition de résistance aux traitements actuellement utilisés. Parmi les modalités de traitement systémique du CCR, la chimiothérapie a été la plus largement utilisée. Cependant, ces dernières années, les thérapies ciblées sont venues compléter les options thérapeutiques, notamment pour traiter le CCR métastatique. Depuis la fin des années 50, les fluoropyrimidines ont constitué l'épine dorsale des régimes chimio thérapeutiques du CCR avec le 5-fluorouracile (5-FU) comme agent le plus couramment utilisé[18]. L'ajout d'acide folique (aussi appelé leucovorine) (LV) au régime a montré des avantages sur la prévention des effets secondaires [19]. La seconde génération de régimes chimio thérapeutiques est apparue à la fin des années 90 avec l'avènement de deux agents cytotoxiques: l'oxaliplatine (OXA), un dérivé du platine, et l'irinotecan (IRI), un inhibiteur de la topoisomérase I[20–22]. Ainsi, l'association du 5-FU/LV avec l'oxaliplatine et l'irinotécan a donné lieu respectivement au traitement appelé FOLFOX et FOLFIRI. Plus tard, une triple combinaison, FOLFOXIRI, a également été proposée[23].

Au cours des deux dernières décennies, l'avènement d'anticorps monoclonaux ciblant la voie du facteur de croissance de l'endothélium vasculaire (VEGF) (bevacizumab) et la voie de l'EGFR (cetuximab et panitumumab) a fait progresser les thérapies pour le traitement du CCR métastatique en première ligne, bien que toujours associé à une chimiothérapie conventionnelle[22,24,25]. Chez les patients présentant des métastases hépatiques non résécables du CCR, la chimiothérapie systémique doublet ou triplet et la thérapie ciblée sont les thérapies de première ligne standard. Cependant, dans le CCR métastatique, l'utilisation d'inhibiteurs de point de contrôle immunitaire ciblant la mort

cellulaire programmée 1 (PD1) et son ligand 1 (PD-L1) et l'antigène cytotoxique des lymphocytes T-4 (CTLA-4) reste largement inefficace car seul un petit sous-ensemble de patients (4 à 5 %), hébergeant un système de réparation des mésappariements déficient/une instabilité élevée des microsatellites ou des mutations dans la sous-unité catalytique de la polymérase epsilon, peuvent en bénéficier[26]. La variabilité interindividuelle limite l'utilisation de la chimiothérapie pour traiter les cancers dus au développement de résistances thérapeutiques. Pour rappel, le foie est le principal site de métabolisation des médicaments anticancéreux. Par la suite, dans la tumeur et le TME, les transporteurs d'absorption/d'efflux de médicament modulent les niveaux intracellulaires du médicament ou de ses métabolites actifs (conjugués ou non conjugués)[27,28]. Ainsi, l'efficacité des médicaments anticancéreux dans les cellules tumorales dépend des concentrations efficaces, de la présence et de la quantité des cibles médicamenteuses au sein de la cellule[29]. La variabilité interpatient dû aux niveaux d'expression et d'activité enzymatique variable, jouant alors un rôle sur l'efficacité et la toxicité des médicaments anticancéreux[23,27,30].

Malgré les progrès réalisés, nous manquons encore d'informations détaillées sur la régulation de l'expression de TRα1, notamment dans les CCR, et son rôle dans la biologie des CSC et leur réponse aux chimiothérapies**.**

Dans ce contexte, les objectifs de ma thèse ont été :

(1) Analyser les mécanismes qui contrôlent l'expression du gène *THRA* (codant pour le récepteur TRα1) dans le cancer du côlon.

(2) Étudier la fonction de TRα1 dans les CSC, y compris leur maintien, leur différenciation et leur implication dans la résistance à la chimiothérapie.

Méthodes

Nous avons analysé l'activité du promoteur du gène THRA par des approches moléculaires et cellulaires (axe 1). Pour l'étude de la fonction de TRα1, nous avons utilisé des sphéroïdes tumoraux générés à partir de cellules Caco2, selon une méthodologie développée au cours de cette thèse[31]. Dans ce modèle nous avons évalué l'impact de l'altération des niveaux des HT ou de l'expression de TRα1 (axe 2) ainsi que la réponse aux chimiothérapie communément utilisées chez les patients atteints de CCR, notamment FOLFOX et FOLFIRI[20,32–34].

Résultats

Mécanismes moléculaires de la régulation du gène THRA

Cela fait plus de 50 ans que le gène THRA a été cloné et caractérisé comme un homologue du v-erbAgene, qui est impliqué dans les transformations néoplasiques conduisant à l'érythroleucémie aiguë et aux sarcomes[35,36], suggérant fortement son lien avec l'oncogenèse. Du fait de cette particularité, il était logique de supposer que TRα1, produit par ce locus, se comporte comme un oncogène. Il a également été supposé qu'un TRα1 muté au lieu de la forme WT peut avoir une fonction protumorale. En effet, certaines données ont décrit des mutations du gène THRA dans les cancers gastriques (essentiellement des délétions) 63X, et des modèles murins ont attribué des fonctions oncogènes au TRα1 muté 64,65XX. Cependant, des études récentes de notre laboratoire ont indiqué la fonction protumorale de WT TRα1 lorsqu'il est surexprimé dans l'intestin et le côlon de souris[37]. Des études dans des cohortes de CCR humains nous ont également permis d'établir la pertinence des observations de souris à la pathologie humaine[17]. Dans ce contexte, les régulations croisées entre TRα1 et la voie Wnt/β-caténine sont multiples. Dans le cas de la formation et de la progression tumorale, elles dépendent de mutations du gène suppresseur de tumeur Apc/APC [17,37]. En effet, le gène THRA est fréquemment surexprimé dans les sous-types moléculaires du CCR, en particulier dans le CMS2, caractérisé par un Wnt élevé[17]. Nous tenons à souligner que notre étude précédente a également montré son association significative avec CMS3, caractérisée par un statut métabolique élevé. Les différences entre les cohortes dans les analyses microarray vs RNA-seq et parmi les homologues normaux analysés peuvent expliquer l'écart. Une expression plus élevée de TRα1 était définitivement claire lors de l'examen de l'analyse IHC dans la TMA des CRC, où nous avons observé une forte augmentation de l'expression de TRα1 dans les tumeurs à tous les stades par rapport au côlon normal. Les résultats montrent également une grande hétérogénéité dans les parties tumorales et les cellules stromales exprimant fortement ou mal TRα1. En plus d'être régulé positivement dans les CRC dans l'intestin normal, TRα1 montre un schéma d'expression distinct qui suit le gradient des activités Wnt et Notch[15,37]. Cependant, ce qui détermine ce domaine d'expression spécifique était inconnu, et on ignorait également quels sont les effecteurs de son augmentation des CRC. Il convient de noter que seules quelques études ont analysé la base moléculaire de la régulation du gène THRA[38–41], et aucune n'a été réalisée dans le

contexte du cancer. Il s'agit de la première étude analysant les mécanismes de régulation de l'expression du gène THRA dans les CRC. Nous avons effectué une analyse *in silico* sur le promoteur THRA de 3 kb et avons montré des sites de liaison potentiels pour les facteurs de transcription impliqués dans l'homéostasie intestinale qui ont un impact sur la biologie de la CS/CSC et le développement du CRC, tels que TCF7L2 (voie Wnt), RBPJ (voie Notch) et CDX2 (identité des cellules épithéliales intestinales)[5,42,43]. Nous avons analysé l'implication de ces facteurs de transcription en utilisant un système rapporteur-luciférase permettant de suivre l'expression de THRA. Nous avons pu démontrer par ces analyses dans des lignées cellulaires du CCR que Wnt et CDX2 régulent positivement l'expression de THRA et que Notch régule négativement l'expression de THRA. Nous avons décidé d'approfondir dans nos études l'implication de la voie Wnt dans la régulation de THRA notamment parce que des études antérieures de notre équipe montraient que TRα1 était surexprimé dans les CCR et que TRα1 régulait l'expression de la β-catenin[17,37,44,45]. De ce fait, une analyse approfondie de la voie signalétique Wnt nous a permis de récapituler la régulation de la transcription de *THRA* et de l'expression de TRα1 par cette voie dans des lignées cellulaires d'adénocarcinome colique humain et des entéroïdes de souris. Particulièrement, nous avons pu montrer par une approche de précipitation de la chromatine (ChIP) que la β-catenin possède un domaine de fixation sur le promoteur de THRA au niveau des deux sites putatives TCF7L2 que nous avions trouvé dans nos analyses *in silico*. De plus, des mutations dans les deux sites de fixation pour la voie Wnt dans notre vecteur THRA-luciférase est accompagné d'une perte de transactivation de l'expression de ce dernier par la β -catenin et TCF/LEF. Compte tenu de nos résultats précédents sur le contrôle de la voie Wnt par TRα1, nos nouveaux résultats dévoilent une boucle de régulation complexe et une synergie entre ces signaux endocriniens et intrinsèques aux cellules épithéliales. Notre travail décrit, pour la première fois, la régulation du gène THRA dans des contextes cellulaires et tumoraux spécifiques. Ces résultats ont donné lieu à une publication scientifique Giolito et al. en cours de révision.

Action des hormones thyroïdiennes et de TRα1 sur la biologie des cellules souches cancéreuses

Les lignées cellulaires cancéreuses bidimensionnelles (2D) in vitro sont utilisées depuis longtemps et fournissent des informations précieuses sur le développement tumoral et les

mécanismes sous-jacents à l'efficacité des molécules thérapeutiques. Cependant, leur limitation concernant le manque d'hétérogénéités phénotypique et génétique trouvée dans les tumeurs d'origine est maintenant largement reconnue[46]. De plus, les nutriments, l'oxygène et les gradients de pH ne sont pas reproduits, pas plus que le microenvironnement tumoral, qui est important pour le maintien des différents types de cellules, y compris les CSC[46,47]. Plusieurs modèles tridimensionnels (3D) ont été développés pour aborder et reproduire expérimentalement la complexité et l'hétérogénéité des cancers afin de pallier ces principaux inconvénients. En utilisant une plaque de culture particulière, appelé Aggrewell 400, nous avons développé un nouveau modèle de sphéroïde à partir de la lignée cellulaire d'adénocarcinome colique humaine Caco2, qui permet d'obtenir des sphéroïdes de taille homogène et bien adapté pour l'étude des CSC[31]. Nous nous sommes demandés quel impact pourrait avoir les HT et la modulation de l'expression de TRα1 dans la formations des sphéroïdes et leur rôle possible sur l'expression des différents marqueurs incluant ceux des CS. En analysant la croissance des sphéroïdes au cours de la culture, nous avons pu observer que les HT et TRα1, permettent de stimuler leur croissance et qu'à l'inverse la perte de fonction du récepteur TRα1 est associée à une forte diminution de leur croissance. Il est important de noter que il avait déjà été démontré au sein de l'équipe que l'altération de l'expression de TRα1 dans des cellules Caco2 jouait un rôle dans la régulation de la prolifération et la migration cellulaires[17].

Dans un second temps nous avons pu déterminer par immunofluorescences et RTqPCR des marqueurs associés à ces changements de prolifération cellulaire dans les conditions où la T3 ou TRα1 étaient respectivement présente et exprimée. De manière intéressante, les HT agissent également comme un facteur de survie lorsque les sphéroïdes sont traités avec les combinaisons de chimiothérapies FOLFOX ou FOLFIRI. Nous avons analysé l'effet de ces chimiothérapies par différentes approches moléculaires et cellulaires, notamment par immunofluorescences et RTqPCR mais également par des analyses de cytométrie en flux. De plus, nous avons pu déterminer après une analyse de RNA Seq, que les mécanismes associés à cette résistance sont spécifiques et distincts aux différentes combinaisons de chimiothérapies (FOLFOX ou FOLFIRI). Nous avons pu aussi déterminer que les HT jouent un rôle important dans la détoxification de ces drogues, notamment du IRI grâce à la modification de l'expression des transporteurs d'efflux des drogues et d'autres enzymes liées à sa détoxification.

Discussion

Pendant ces travaux de thèse nous avons pu décrire pour la première fois la régulation du gène *THRA* dans un contexte cellulaire et tumoral spécifique. L'analyse des 3kb du promoteur *THRA* dans des lignées du CCR ont pu montrer une régulation positive de Wnt et CDX2 sur l'expression de THRA et qu'à l'inverse la voie Notch, quant à lui, régule négativement l'expression de THRA. Lors des travaux précédents de l'équipe il avait pu être mis en évidence un cross talk complexe entre TRα1 and la voie Wnt[13–15,48], sans pour autant mettre à jour le rôle clé de la β-catenin sur la régulation de l'expression de THRA/Thra. Lors de cette thèse, il a pu être mis en évidence qu'au sein des cellules de CCR qu'une activation de la voie Wnt par différentes approches résultait de l'augmentation de l'activité du promoteur de THRA. Dans un contexte physiologique, la stimulation de la voie Wnt par une mutation du gène APC dans des entéroïdes de souris est accompagnée par l'augmentation de l'expression de TRα1. Ces résultats sont à mettre en lien avec la littérature où il a pu être démontré dans un modèle *in vivo* que la surexpression de TRα1 dans l'épithélium intestinal couplé à la suractivation de la voie Wnt par mutation d'APC, induisaient une hyperprolifération et une hyperplasie au sein des cryptes. Cette synergie de l'augmentation de la voie Wnt et de TRα1 étant aussi corrélée à une croissance tumorale, une invasion tissulaire et une formation de métastases accrues. Deux points sont intéressants à souligner. Premièrement, qu'il a été démontré chez la souris et chez l'Homme le rôle de TRα1 sur l'inhibition de l'expression des protéines inhibitrices de la voie Wnt, notamment WIF1/Wif1, SOX17/Sox17 et FRZB/Frzb[1749]. Et deuxièmement, en lien plus direct avec ces travaux de thèse, le rôle possible du couple endocrine (TRα1) et signal cellulaire (voie Wnt) sur le développement d'un phénotype plus agressif soulignant leurs rôles possible sur l'acquisition et le maintien d'un phénotype CSC[37].

Dans la deuxième partie de cette thèse nous nous sommes focalisés sur le rôle des hormones thyroïdiennes et de son récepteur TRα1 dans la biologie des cellules souches cancéreuses et aussi sur leur implication dans la réponse aux chimiothérapies communément utilisées pour le traitement du CCR, notamment FOLFOX et FOLFIRI. Nous avons pu observer que lors de la formation des sphéroïdes dans les plaques Aggrewell, la présence des HT ou le gain de fonction de TRα1 permettent de stimuler la croissance des sphéroïdes tandis que la perte de fonction du récepteur TRα1 est associée à une forte diminution de leur croissance. La présence des HT lors de la croissance des

sphéroïdes favorise non seulement la croissance mais aussi, de manière intéressante, la survie lorsque les sphéroïdes sont traités avec les combinaisons de chimiothérapies FOLFOX ou FOLFIRI. Il est intéressant d'observer que la réponse à la chimiothérapie dans les sphéroïdes traités avec les HT est dépendante au type de combinaisons. Les sphéroïdes traités avec FOLFIRI, présentent notamment un avantage grâce à la modification de l'expression des transporteurs d'efflux des drogues et d'autres enzymes liées à la détoxification d'irinotecan et 5-FU, les HT favorisant alors l'acquisition d'une résistance phénotypique qui permettrait aux cellules d'éliminer plus facilement la drogue.

Conclusion et perspectives

Pour la première fois, nos travaux ont pu décrire la régulation du gène *THRA* dans un contexte cellulaire et tumoral spécifique. Nous avons également acquis des connaissances sur le comportement des cellules tumorales dépendantes des HT et de TRα1, et leur rôle dans leur réponse aux chimiothérapies**.** Ces derniers résultats ont une claire relevance en clinique et peuvent servir de base pour de futures études et pour l'incorporation du statut thyroïdien comme indicateur clinique de réponse aux traitements.

Bibliographie

1. Sung, H. *et al.* Global Cancer Statistics 2020: GLOBOCAN Estimates of Incidence and Mortality Worldwide for 36 Cancers in 185 Countries. *CA. Cancer J. Clin.* **71**, 209–249 (2021).
2. Fearon, E. R. & Vogelstein, B. A genetic model for colorectal tumorigenesis. *Cell* **61**, 759–767 (1990).
3. Levine, D. S. & Haggitt, R. C. Normal histology of the colon. *American Journal of Surgical Pathology* vol. 13 966–984 (1989).
4. Mescher, A. *Junqueira's Basic Histology: Text and Atlas, 12th Edition*. (McGraw-Hill Education, 2009).
5. Beumer, J. & Clevers, H. Cell fate specification and differentiation in the adult mammalian intestine. *Nat. Rev. Mol. Cell Biol.* (2020) doi:10.1038/s41580-020-0278-0.
6. Gehart, H. & Clevers, H. *Tales from the crypt: new insights into intestinal stem cells*. *Nature Reviews Gastroenterology and Hepatology* vol. 16 19–34 (Nature Publishing Group, 2019).
7. Cheng, H. & Leblond, C. P. Origin, differentiation and renewal of the four main epithelial cell types in the mouse small intestine I. Columnar cell. *Am. J. Anat.* **141**, 461–479 (1974).
8. Blachier, F., de Sá Resende, A., da Silva Fogaça Leite, G., Vasques da Costa, A. & Lancha Junior, A. H. Colon epithelial cells luminal environment and physiopathological consequences: impact of nutrition and exercise. *Nutrire* **43**, 1–9 (2018).

9. Potten, C. S. & Loeffler, M. Stem cells: attributes, cycles, spirals, pitfalls and uncertainties. Lessons for and from the crypt. *Development* **110**, 1001–1020 (1990).
10. Batlle, E. & Clevers, H. Cancer stem cells revisited. *Nat. Med.* **23**, 1124–1134 (2017).
11. Van Keymeulen, A. *et al.* Reactivation of multipotency by oncogenic PIK3CA induces breast tumour heterogeneity. **525**, 119–123 (2015).
12. Ortiga-Carvalho, T. M., Chiamolera, M. I., Pazos-Moura, C. C. & Wondisford, F. E. Hypothalamus-pituitary-thyroid axis. *Compr. Physiol.* **6**, 1387–1428 (2016).
13. Skah, S., Uchuya-Castillo, J., Sirakov, M. & Plateroti, M. The thyroid hormone nuclear receptors and the Wnt/β-catenin pathway: An intriguing liaison. *Dev. Biol.* **422**, 71–82 (2017).
14. Frau, C., Godart, M. & Plateroti, M. Thyroid hormone regulation of intestinal epithelial stem cell biology. *Mol. Cell. Endocrinol.* **459**, 90–97 (2017).
15. Sirakov, M., Kress, E., Nadjar, J. & Plateroti, M. Thyroid hormones and their nuclear receptors: New players in intestinal epithelium stem cell biology? *Cellular and Molecular Life Sciences* vol. 71 2897–2907 (2014).
16. Godart, M. *et al.* Murine intestinal stem cells are highly sensitive to modulation of the T3/TRα1-dependent pathway. *Dev.* **148**, dev194357 (2021).
17. Uchuya-Castillo, J. *et al.* Increased expression of the thyroid hormone nuclear receptor TRα1 characterizes intestinal tumors with high Wnt activity. *Oncotarget* **9**, 30979–30996 (2018).
18. Heidelberger, C. *et al.* Fluorinated Pyrimidines, A New Class of Tumour-Inhibitory Compounds. *Nat. 1957 1794561* **179**, 663–666 (1957).
19. Azwar, S., Seow, H. F., Abdullah, M., Jabar, M. F. & Mohtarrudin, N. Recent updates on mechanisms of resistance to 5-fluorouracil and reversal strategies in colon cancer treatment. *Biology (Basel).* **10**, 854 (2021).
20. Fujita, K. I., Kubota, Y., Ishida, H. & Sasaki, Y. Irinotecan, a key chemotherapeutic drug for metastatic colorectal cancer. *World J. Gastroenterol.* **21**, 12234–12248 (2015).
21. Fuchs, C., Mitchell, E. P. & Hoff, P. M. Irinotecan in the treatment of colorectal cancer. *Cancer Treatment Reviews* vol. 32 491–503 (2006).
22. Wolpin, B. M. & Mayer, R. J. Systemic Treatment of Colorectal Cancer. *Gastroenterology* **134**, 1296-1310.e1 (2008).
23. Mohelnikova-Duchonova, B., Melichar, B. & Soucek, P. FOLFOX/FOLFIRI pharmacogenetics: the call for a personalized approach in colorectal cancer therapy. *World J. Gastroenterol.* **20**, 10316–10330 (2014).
24. Goldberg, R. M., Venook, A. P. & Schilsky, R. L. Cetuximab in the treatment of colorectal cancer. *Clin. Adv. Hematol. Oncol.* **2**, (2004).
25. Hurwitz, H. *et al.* Bevacizumab plus Irinotecan, Fluorouracil, and Leucovorin for Metastatic Colorectal Cancer. *N. Engl. J. Med.* **350**, 2335–2342 (2004).
26. Van der Jeught, K., Xu, H.-C., Li, Y.-J., Lu, X.-B. & Ji, G. Drug resistance and new therapies in colorectal cancer. *World J. Gastroenterol.* **24**, 3834–3848 (2018).
27. de Man, F. M., Goey, A. K. L., van Schaik, R. H. N., Mathijssen, R. H. J. & Bins, S. Individualization of Irinotecan Treatment: A Review of Pharmacokinetics, Pharmacodynamics, and Pharmacogenetics. *Clinical Pharmacokinetics* vol. 57 1229–1254 (2018).
28. Hammond, W. A., Swaika, A. & Mody, K. Pharmacologic resistance in colorectal cancer: A review. *Therapeutic Advances in Medical Oncology* vol. 8

57–84 (2016).
29. Vasan, N., Baselga, J. & Hyman, D. M. A view on drug resistance in cancer. *Nature* **575**, 299–309 (2019).
30. Wei, J., Ye, X. & Liu, T. Toxicity magnification of irinotecan's toxicity by levothyroxine through inhibition of sn-38 glucuronidation. *Lat. Am. J. Pharm.* **33**, 1385–1388 (2014).
31. Giolito, M. V., Claret, L., Frau, C. & Plateroti, M. A Three-dimensional Model of Spheroids to Study Colon Cancer Stem Cells. *JoVE* e61783 doi:doi:10.3791/61783.
32. Parvez, M. M. *et al.* Quantitative investigation of irinotecan metabolism, transport, and gut microbiome activation. *Drug Metab. Dispos.* **49**, 683–693 (2021).
33. Giacchetti, S. *et al.* Phase III multicenter randomized trial of oxaliplatin added to chronomodulated fluorouracil-leucovorin as first-line treatment of metastatic colorectal cancer. *J. Clin. Oncol.* **18**, 136–147 (2000).
34. de Gramont, A. *et al.* Leucovorin and fluorouracil with or without oxaliplatin as first-line treatment in advanced colorectal cancer. *J. Clin. Oncol.* **18**, 2938–2947 (2000).
35. Thormeyer, D. & Baniahmad, A. The v-erbA oncogene (Review). *Int. J. Mol. Med.* **4**, 351–358 (1999).
36. Sap, J. *et al.* The c-erb-A protein is a high-affinity receptor for thyroid hormone. *Nature* **324**, 635–640 (1986).
37. Kress, E. *et al.* Cooperation Between the Thyroid Hormone Receptor TRα1 and the WNT Pathway in the Induction of Intestinal Tumorigenesis. *Gastroenterology* **138**, 1863–1874 (2010).
38. Laudet, V. *et al.* Genomic organization of the human thyroid hormone receptor α (c-erbA-1) gene. *Nucleic Acids Res.* **19**, 1105–1112 (1991).
39. Laudet, V., Hanni, C., Coll, J., Catzeflis, F. & Stehelin, D. Evolution of the nuclear receptor gene superfamily. *EMBO J.* **11**, 1003–1013 (1992).
40. Ishida, T., Yamauchi, K., Ishikawa, K. & Yamamoto, T. Molecular Cloning and Characterization of the Promoter Region of the Human c-erbAα Gene. *Biochem. Biophys. Res. Commun.* **191**, 831–839 (1993).
41. Vanacker, J. M., Bonnelye, E., Delmarre, C. & Laudet, V. Activation of the thyroid hormone receptor a gene promoter by the orphan nuclear receptor ERRα. *Oncogene* **17**, 2429–2435 (1998).
42. Spit, M., Koo, B. K. & Maurice, M. M. Tales from the crypt: Intestinal niche signals in tissue renewal, plasticity and cancer. *Open Biol.* **8**, (2018).
43. Freund, J. N., Domon-Dell, C., Kedinger, M. & Duluc, I. The Cdx-1 and Cdx-2 homeobox genes in the intestine. *Biochem. Cell Biol.* **76**, 957–969 (1998).
44. Plateroti, M. *et al.* Functional Interference between Thyroid Hormone Receptor α (TRα) and Natural Truncated TRΔα Isoforms in the Control of Intestine Development. *Mol. Cell. Biol.* **21**, 4761–4772 (2001).
45. Kress, E., Rezza, A., Nadjar, J., Samarut, J. & Plateroti, M. The frizzled-related sFRP2 gene is a target of thyroid hormone receptor α1 and activates β-catenin signaling in mouse intestine. *J. Biol. Chem.* **284**, 1234–1241 (2009).
46. Ferreira, L. P., Gaspar, V. M. & Mano, J. F. Design of spherically structured 3D in vitro tumor models -Advances and prospects. *Acta Biomater.* **75**, 11—34 (2018).
47. Kawai, S. *et al.* Three-dimensional culture models mimic colon cancer heterogeneity induced by different microenvironments. *Sci. Rep.* **10**, 3156

(2020).
48. Sirakov, M., Claret, L. & Plateroti, M. Thyroid Hormone Nuclear Receptor TRα1 and Canonical WNT Pathway Cross-Regulation in Normal Intestine and Cancer. *Front. Endocrinol. (Lausanne)*. **12**, 1653 (2021).
49. Silva, A.-L. *et al.* Boosting Wnt activity during colorectal cancer progression through selective hypermethylation of Wnt signaling antagonists. *BMC Cancer 2014 141* **14**, 1–10 (2014).

Université de Strasbourg

Maria Virginia GIOLITO

Régulation et fonction du récepteur nucléaire des hormones thyroïdiennes TRα1 dans la biologie des cellules souches cancéreuses des cancers coliques

École doctorale Sciences de la vie et de la santé | ED 414
Université de Strasbourg

Résumé

L'hormone thyroïdienne T3 et son récepteur nucléaire TRα1 contrôlent le développement et l'homéostasie intestinale via une action sur les cellules souches (CS) des cryptes intestinales. Le potentiel translationnel des études en modèles murins a été démontré chez des patients atteints de cancer colorectal (CCR), car l'expression accrue de TRα1 dans le CCR corrèle avec l'activité de la voie signalétique Wnt et un potentiel « souche » augmenté. Cependant, les bases moléculaires responsables de la régulation de l'expression de TRα1 et l'impact de la T3 et de TRα1 dans les CS cancéreuses (CSC) des CCR dans le CCR n'étaient pas connus.

Au cours de cette thèse, notre objectif était de :

(1) Analyser les mécanismes qui contrôlent l'expression de TRα1 dans les CCR et les CSC.

(2) Étudier la fonction de TRα1 dans la biologie des CSC, y compris leur maintenance, différenciation, et implication dans les mécanismes de chimiorésistance.

Mots clés : cellules souches, cancer colorectal, récepteur aux hormones thyroïdiennes alpha, chimiothérapie

Résumé en anglais

The thyroid hormone T3 and its nuclear receptor TRα1 control gut development and homeostasis via an action on the intestinal crypt stem cells (SC). The translational potential of the studies in mouse models has been proved in human colorectal cancer (CRC) patients as the increased TRα1 expression in CRC correlates with the activity of the Wnt pathway and with an increased "stem" potential. However, the molecular bases responsible for TRα1 expression regulation and the impact of T3 and TRα1 on cancer SC (CSC) biology were unknown.

During this thesis, we aimed to:

(1) Analyse the mechanisms that control THRA gene expression in colon cancer and CSCs.

(2) Study TRα1 in CSCs, including their maintenance, differentiation, and implication on drug resistance.

Keywords : stem cells, colorectal cancer, thyroid hormone receptor, chemotherapy